

Biosynthesis, Structure and Function of Protein Paucimannosylation in Human Neutrophils

Loke Ju Wen Ian

Bachelor of Science (Honours H1), Murdoch University



Department of Chemistry and Biomolecular Sciences
Faculty of Science and Engineering
Macquarie University, New South Wales, Australia

This thesis is presented for the degree of Doctor of Philosophy
in Chemistry and Biomolecular Sciences

February 2017

This thesis is dedicated in memory of
Professor Niels Borregaard, a passionate researcher and
haematologist in neutrophil biology

Table of Contents

| | |
|---|-------------|
| ABSTRACT..... | I |
| STATEMENT OF ORIGINALITY AND DECLARATION..... | III |
| ACKNOWLEDGEMENTS | V |
| LIST OF ORIGINAL PUBLICATIONS | IX |
| LIST OF PRESENTATIONS AND AWARDS..... | XI |
| SYMBOLS AND NOMENCLATURE..... | XIII |
| ABBREVIATIONS | XV |
| CHAPTER 1: GENERAL INTRODUCTION, THESIS OVERVIEW AND RESEARCH AIMS | 1 |
| 1.1 The human immune system | 3 |
| 1.1.1 Innate immunity and adaptive immunity | 3 |
| 1.2 Human haematopoiesis | 6 |
| 1.2.1 Lymphopoiesis | 8 |
| 1.2.2 Myelopoiesis | 8 |
| 1.2.3 Granulopoiesis | 8 |
| 1.2.4 Neutrophil granules and their associated granular proteins | 12 |
| 1.3 Neutrophil functions in innate immunity | 14 |
| 1.3.1 Neutrophil adhesion and transmigration | 15 |
| 1.3.2 Phagocytosis | 16 |
| 1.3.3 Formation of neutrophil extracellular traps | 17 |
| 1.3.4 Degranulation..... | 18 |
| 1.4 Protein glycosylation in humans | 20 |
| 1.4.1 Protein <i>N</i> -glycosylation | 20 |
| 1.4.2 <i>N</i> -glycoprotein synthesis..... | 24 |
| 1.5 Analytical approaches for structural characterisation of protein <i>N</i> -glycosylation..... | 27 |
| 1.5.1 Chromatographic separation of <i>N</i> -glycans released from proteins..... | 29 |
| 1.5.2 Chromatographic separation of protease-derived glycopeptides | 31 |
| 1.5.3 Mass spectrometric analysis of protein <i>N</i> -glycosylation | 33 |
| 1.5.4 Mass spectrometric analysis of intact glycoproteins | 38 |
| 1.6 Alterations in protein <i>N</i> -glycosylation during inflammation and infections | 40 |

| | |
|--|-----------|
| 1.7 Publication I: Emerging roles of protein mannosylation in inflammation and infection ... | 42 |
| 1.8 Thesis aims | 69 |
| CHAPTER 2: INITIAL OBSERVATION OF PAUCIMANNOSYLATED HUMAN NEUTROPHIL PROTEINS IN BACTERIAL COLONISED CYSTIC FIBROSIS SPUTUM | 71 |
| 2.1 Rationale | 73 |
| 2.2 Publication II: Human neutrophils secrete bioactive paucimannosidic proteins from azurophilic granules into pathogen-infected sputum | 75 |
| 2.3 Overview of main findings, conclusions and unresolved questions..... | 90 |
| CHAPTER 3: THE ROLE OF HEXOSAMINIDASES IN THE BIOSYNTHESIS OF PAUCIMANNOSIDIC <i>N</i>-GLYCOPROTEINS IN HUMAN NEUTROPHILS | 93 |
| 3.1 Rationale | 95 |
| 3.2 Introduction..... | 97 |
| 3.3 Materials and Methods | 98 |
| 3.3.1 Isolation of blood-derived human neutrophils for immunocytochemistry | 98 |
| 3.3.2 Immunocytochemistry | 99 |
| 3.3.3 <i>N</i> -glycan release of SD and healthy age-paired neutrophils..... | 100 |
| 3.3.4 Visualising glycoprotein features of neutrophil cell lysates via immunoblotting | 102 |
| 3.3.5 Culture conditions for HL-60 neutrophil-like cells | 103 |
| 3.3.6 <i>HEXA</i> and <i>HEXB</i> gene silencing | 103 |
| 3.3.7 Hexosaminidase activity assay | 103 |
| 3.3.8 Quantitative real-time polymerase chain reaction (qPCR)..... | 104 |
| 3.4 Results..... | 104 |
| 3.4.1 Immunocytochemistry of human neutrophils | 104 |
| 3.4.2 <i>N</i> -glycome profiling of neutrophils from a healthy donor and a SD patient..... | 107 |
| 3.5 Discussion..... | 117 |
| 3.5.1 Co-localisation of Hex A and paucimannosidic proteins in the azurophilic granules of resting neutrophils | 117 |
| 3.5.2 Aberrant <i>N</i> -glycosylation of neutrophils derived from a SD patient..... | 118 |
| 3.5.3 The biosynthetic trafficking of neutrophil paucimannosidic <i>N</i> -glycoproteins | 121 |

| | |
|--|------------|
| 3.5.4 Assessing the potential for siRNA-based <i>HEXA</i> and <i>HEXB</i> manipulation in HL-60 cells as a model for studying the biosynthesis and function of protein paucimannosylation | 122 |
| 3.6 Overview of main findings, conclusions and future directions | 125 |
| CHAPTER 4: SITE-SPECIFIC STRUCTURAL CHARACTERISATION OF THE N-GLYCOSYLATION OF HUMAN NEUTROPHIL CATHEPSIN G USING COMPLEMENTARY LC-MS/MS STRATEGIES..... | 127 |
| 4.1 Rationale | 129 |
| 4.2 Publication IV: Complementary LC-MS/MS-Based <i>N</i> -Glycan, <i>N</i> -Glycopeptide, and Intact <i>N</i> -Glycoprotein Profiling Reveals Unconventional Asn71-Glycosylation of Human Neutrophil Cathepsin G..... | 131 |
| 4.3 Overview of main findings, conclusions and future directions | 155 |
| CHAPTER 5: PAUCIMANNOSYLATION MODULATES THE INNATE IMMUNE FUNCTIONS OF HUMAN NEUTROPHIL ELASTASE ACROSS THE DISTINCT GRANULES OF HUMAN NEUTROPHILS | 159 |
| 5.1 Rationale | 161 |
| 5.2 Publication V: Paucimannose rich <i>N</i> -glycosylation of human neutrophil elastase modulates its immune function..... | 163 |
| 5.3 The <i>N</i> -glycome of purified neutrophil granule proteins using subcellular fractionation.. | 185 |
| 5.4 Materials and Methods..... | 186 |
| 5.4.1 Isolation of blood-derived human neutrophils for subcellular fractionation | 186 |
| 5.4.2 Disruption of neutrophils by nitrogen cavitation | 187 |
| 5.4.3 Four-layer Percoll density gradient separation | 187 |
| 5.4.4 Measurement of subcellular protein markers using immunoassays | 189 |
| 5.4.5 Percoll removal using ultra-centrifugation | 190 |
| 5.4.6 Deglycosylation and <i>N</i> -glycome analysis of azurophilic granule proteins..... | 192 |
| 5.5 Results..... | 192 |
| 5.5.1 Determining the purity of the isolated neutrophil granule proteins..... | 192 |
| 5.5.2 Characterisation of <i>N</i> -glycans of isolated proteins in the azurophilic granules | 197 |
| 5.5.3 Structural determination of paucimannosidic <i>N</i> -glycans of azurophilic granule origin | 198 |

| | |
|--|------------|
| 5.5.4 Structural determination of the complex <i>N</i> -sialo-glycans | 199 |
| 5.5.5 Protein paucimannosylation is not confined to the azurophilic granules | 201 |
| 5.6 Discussion..... | 202 |
| 5.7 Overview of main findings, conclusions and future directions | 206 |
| CHAPTER 6: <i>N</i>-GLYCOMICS INDICATES THAT PROTEIN PAUCIMANNOSESYLATION IS A MULTI-CELLULAR <i>N</i>-GLYCAN FEATURE IN INFLAMMATION, STEMNESS AND CANCER..... | 209 |
| 6.1 Rationale | 211 |
| 6.2 Introduction..... | 212 |
| 6.2 Materials and Methods | 214 |
| 6.2.1 Blood collection and isolation of blood-derived human white blood cells | 214 |
| 6.2.2 Isolation of platelets from buffy coats | 215 |
| 6.2.3 Isolation of total lymphocytes | 215 |
| 6.2.4 Isolation of neutrophils | 215 |
| 6.2.5 Determination of the purity, viability and morphology of the isolated cell populations | 216 |
| 6.2.6 Cell lysis | 216 |
| 6.2.7 <i>N</i> -glycan release, <i>N</i> -glycome profiling and <i>N</i> -glycan data analysis..... | 216 |
| 6.2.8 Other methods used for published data presented in this chapter | 217 |
| 6.3 Results..... | 217 |
| 6.3.1 Cell purity and morphology of isolated immune cells..... | 217 |
| 6.3.2 Whole cell <i>N</i> -glycome profiling of neutrophils, lymphocytes and platelets | 218 |
| 6.3.3 Expression of paucimannosylation in macrophages and alterations upon tuberculosis infection | 222 |
| 6.3.4 Expression and importance of paucimannosylation in A172 cells | 224 |
| 6.4 Discussion..... | 225 |
| 6.5 Overview of main findings, conclusions and future directions | 230 |
| CHAPTER 7: SUMMARY AND CONCLUSION..... | 233 |
| 7.1 Main summary | 235 |
| 7.2 The biosynthesis of paucimannosylated <i>N</i> -glycoproteins in human neutrophils | 239 |

| | |
|---|------------|
| 7.3 Structural characterisation of paucimannosylated azurophilic granule <i>N</i> -glycoproteins in neutrophils | 241 |
| 7.4 Functional aspects of paucimannosylation on HNE | 244 |
| 7.5 Protein paucimannosylation in other human cell types | 248 |
| 7.6 Concluding remarks | 250 |
| REFERENCES..... | 252 |
| APPENDICES..... | 299 |
| Appendix 1: Human ethics approvals | 301 |
| Appendix 2: Biosafety approvals | 304 |

Abstract

Asparagine (*N*)-linked glycosylation, a common post-translational modification of human proteins, is widely involved in molecular and cellular functions. Inflammation and infection are often associated with *N*-glycoprotein dysregulation. Truncated *N*-glycans consisting of GlcNAc₂Man₁₋₃Fuc₀₋₁, known as paucimannosylation, have previously been considered as an invertebrate-specific glyco-signature and are perceived to be negligible or arising from degradation in humans. However, emerging evidence indicates that protein paucimannosylation may play pivotal roles in human biology. Therefore, the presence and potential functions of protein paucimannosylation in the human *N*-glycoproteome remain controversial, warranting further investigation.

The granulated neutrophils are amongst the first responders to inflammation and pathogen infection during human innate immunity. Recently, protein paucimannosylation was encountered in pathogen-infected, neutrophil-rich sputum. This thesis extends from these initial findings by performing an in-depth molecular and (sub)cellular characterisation of the biosynthesis, structure and function of these unconventional glycoproteins in human neutrophils. LC-MS/MS-based glycomics, glycoproteomics and molecular glycobiological techniques were used to study human neutrophil-like cells (HL-60) and primary neutrophils isolated from healthy and β -hexosaminidase-deficient (Sandhoff disease; *HEXB*^{-/-}) individuals. The latter was diminished in paucimannosylated neutrophil proteins, shown to normally reside in dedicated azurophilic granules, suggesting the involvement of human hexosaminidases in the biosynthesis of paucimannosylation in human neutrophils.

Infection of HL-60 cells with *Pseudomonas aeruginosa* induced a virulence- and time-dependent secretion of paucimannosidic protein, indicating active degranulation of azurophilic granule proteins. Expression of paucimannose-rich human neutrophil elastase (HNE) on activated neutrophil cell surface and their interactions with α 1-antitrypsin and mannose binding lectin, demonstrated immunomodulatory roles of paucimannosylated glycoforms of HNE in neutrophil-mediated immune functions. Finally, protein paucimannosylation was found to be present in macrophages, lymphocytes, platelets and neuronal progenitor stem cells, suggesting wider functional roles of these glycoepitopes during physiological and pathological conditions. These findings detail and facilitate a deeper understanding of the unique *N*-glycoproteome of human neutrophils. This knowledge contributes to a greater appreciation of the biosynthesis, structure and function of paucimannosylated glycoproteins in neutrophil biology.

Statement of originality and declaration

I declare that the work described in this thesis is my own account of my research undertaken while I was a student for the doctorate degree in Chemistry and Biomolecular Sciences at Macquarie University, New South Wales, Australia. I certify that the content of this thesis entitled “Biosynthesis, Structure and Function of Protein Paucimannosylation in Human Neutrophils” has not previously been submitted for a higher degree nor has it been submitted as part of requirements for a degree to any other university or tertiary education institutions other than Macquarie University.

I also certify that this thesis is an original piece of research and it has been written by me. To the best of my knowledge, any help and assistances that I have received in my research work and all work performed by others, published or unpublished, have been duly acknowledged.

This is also to certify that I, Loke Ju Wen Ian, being a candidate for the degree of Doctor of Philosophy in Chemistry and Biomolecular Sciences, am aware of the policy of the University relating to the retention and use of higher degree theses as contained in the University’s Higher Research Thesis Preparation, Submission and Examination Policy. In light of this policy, I agree to allow a copy of my thesis to be deposited in the University Library for consultant, loan and photocopying forthwith.

Human ethics (approval number: 5201500409, HREC/08/RPAH/431 and X14-0074), biosafety (approval number: 5201500813) and biohazard (approval number: NIP041214BHA) approvals has been duly obtained to use human samples and genetically modified samples for research purposes only.

Loke Ju Wen Ian

Student number: 43079571

February 2017

Acknowledgements

I would like to thank my supervisors Dr. Morten Thaysen Andersen and Professor Nicki Packer for their unwavering guidance, support and trust in me during my PhD for the past four years. It has been a roller coaster ride of ups and downs, mixed emotions, anticipation, failures and successes. Both of you have not only made me a better scientist but also helped me build my confidence in myself while others had trampled on it previously. My PhD experience will not have been this exciting and fulfilling if I have not been given a chance to join the group. Dr. Morten, you have consistently inspired me through these years to challenge myself and to view and do research in ways that I have not imagined that I can do it myself. You have been an encouraging mentor to me and I thank you from the bottom of my heart. Professor Nicki, my sincere thanks and appreciation for introducing me to the world of sugars with your never-ending enthusiasm and passion for research. I would also like to express my heartfelt thanks to Professor Judi Homewood for believing in me and her assistance prior to the start of my PhD in the glyco group.

My profound appreciation and thanks to both past and present group member of the glyco group at Macquarie University including Christopher, Dr. Vignesh, Dr. Zeynep, Dr. Ling, Dr. Liisa, Dr. Arun, Dr. Manveen, Dr. Jodie, Dr. Matthew, Shazly, Dr. Merina, Dr. Chi-hung, Dr. Katherine, Wei, Dr. Robyn, Dr. Jenny, Sameera, Dr. Nima, Dr. Lindsay and Edward. I have always believed if one would to learn to walk, there must be a supportive individual or a group of individuals to teach and show him or her how to go about doing it. Therefore, my PhD journey would not have been complete without all the help and assistance from everyone in the glyco group. Thank you all for the constructive feedbacks, mind boggling brainstorming sessions and meetings and not to forget the willingness to help and accept me as part of the group. My sincere thanks and appreciation to Dr. Liisa for taking the time to teach me the skills to perform phlebotomy, it has been a wonderful and enriching experience to learn this to complement my knowledge in haematology. My special thanks also to Christopher for your infectious enthusiasm and passion for science, which have always motivated me when I am feeling down, especially when things don't go my way. You have been a supportive mate and I will always cherish and remember the hiking and eating trips that we, along with our partners, had during our free time.

It was the collaborators that have provided me the biological samples and access to expertise that completes my PhD experience and I would like to thank them. I would like to give my sincere thanks to the late Professor Niels Borregaard and his team of devoted researchers,

including Ms Charlotte Horn, who has assisted me in obtaining the neutrophil granule proteins. Having the opportunity to spend a few weeks in Professor Niels's laboratory at the University of Copenhagen, I am immensely grateful to him and Ms Charlotte for having me and sharing their expertise in isolating neutrophil granule proteins.

Research life at the university as a PhD student is not complete without the administrative staff of the department in supporting my candidature. My thanks to Catherine Wong, Jinxia Ke and Michelle Kang for their endless assistances with budgets, accounts, ordering and conference travels. I would also like to thank Joe from the faculty science store, you have been very patient and helpful in making my life easier at the department. My thanks to Ron Claassens, Marita Holley, Anthony Gurlica, Dr. Abidali and Dr. Alamgir for ensuring that we have a safe office and laboratory space to work in. I would also like to thank both Professor Helena Nevalainen and Professor Mark Molloy for their leadership in the department for the past years.

I would not have survived my PhD in Australia without the never-ending support and love from my partner, Serene Gwee. Dear, thank you for the love, comfort, encouragement and trust in me. Not to forgot all the household chores, cooking and errands that you have to undertake while I was busy at work. There is a quote: "Behind every successful man there is a successful woman" and I know you are the one who will always be there for me. I love you. A special thanks to the friends whom Serene and I had the opportunity to meet while in Australia; Heather Clift, Erin Lynch, Kelly Jacobs, Dr. Albert Lee, Stephanie, Maxinne and the HDR mentor volunteers who we have the honour to work with during my candidature. Also special thanks to my friends back in Singapore including Joseph, Nelson, Shun Xi, Kenny and Nicholas. Although we did not have much time to catch up, I am glad to have known you guys.

I am really blessed to have a very loving endearing and immensely supportive family. My sincere gratitude to my parents, thank you mom and dad for working tirelessly to support me and Irwin in our education and wellbeing. Both of you have sacrificed a lot and no words can describe my gratefulness to both of you. Without your support and patience over the last few years, this thesis would not have been possible. My apologies to mom, dad and Irwin for not have been with you all in Singapore for the past years during my PhD. Irwin, my apologies for not accompany you while you trotter through your collage and national service days but I know you miss me a lot. Thank you mom and dad for you endless and selfless love towards me and Irwin. Mom, thank you for all the love and prayers. Dad, thank you for been a role

model and supporting me in everything I do. I inspire to be like you when I start my own family in the future. In all, Irwin and I hope to be filial to both of you when both of you retire from the working world.

Finally, thanks to everyone who have helped me or teach me in one way. To me completing a PhD is not just looking forward towards the end of the road, it is the journey that matters the most and one that I will cherish for the rest of my life.

List of original publications

This thesis contains materials that has been published or have been submitted for review as listed below. My contributions in the individual publications are described in the respective chapters presented in this thesis.

- I **Loke, I.**, Kolarich, D., Packer, N.H., Thaysen-Andersen, M., 2016. Emerging roles of protein mannosylation in inflammation and infection. *Molecular Aspects of Medicine* 51, 31-55. doi:10.1016/j.mam.2016.04.004 (***Review article***)
- II Thaysen-Andersen, M., Venkatakrishnan, V., **Loke, I.**, Laurini, C., Diestel, S., Parker, B.L., Packer, N.H., 2015. Human neutrophils secrete bioactive paucimannosidic proteins from azurophilic granules into pathogen-infected sputum. *Journal of Biological Chemistry* 290 (14), 8789-8802. doi:10.1074/jbc.M114.631622 (***Research article***)
- III Pedersen, C., **Loke, I.**, Lorentzen, A., Wolf, S., Kamble, M., Kristensen, S., Munch, D., Radutoiu, S., Spillner, E., Roepstorff, P., Thaysen-Andersen, M., Stougaard, J., Dam, S. *N*-glycan maturation mutants in *Lotus japonicus* provide a novel tool for basic and applied glycoprotein research. *The Plant Journal*, in press. doi:10.1111/tpj.13570 (***Research article***)
- IV **Loke, I.**, Packer, N.H., Thaysen-Andersen, M., 2015. Complementary LC-MS/MS-Based *N*-Glycan, *N*-Glycopeptide, and Intact *N*-Glycoprotein Profiling Reveals Unconventional Asn71-Glycosylation of Human Neutrophil Cathepsin G. *Biomolecules* 5 (3), 1832-1854. doi:10.3390/biom5031832 (***Research article***)
- V **Loke, I.**, Østergaard, O., Heegaard N., Packer, N.H., Thaysen-Andersen, M. Paucimannose rich *N*-glycosylation of human neutrophil elastase modulates its immune function, *Molecular Cellular Proteomics*, in press. doi: 10.1074/mcp.M116.066746 (***Research article***)

- VI Hare, N.J., Lee, L.Y., **Loke, I.**, Britton, W.J., Saunders, B.M., Thaysen-Andersen, M., 2017. Mycobacterium tuberculosis Infection Manipulates the Glycosylation Machinery and the N-Glycoproteome of Human Macrophages and Their Microparticles. Journal of Proteome Research 16 (1), 247-263. doi:10.1021/acs.jproteome.6b00685 (***Research article***)
- VII Dahmen, A.C., Fergen, M.T., Laurini, C., Schmitz, B., **Loke, I.**, Thaysen-Andersen, M., Diestel, S., 2015. Paucimannosidic glycoepitopes are functionally involved in proliferation of neural progenitor cells in the subventricular zone. Glycobiology 25 (8), 869-880. doi:10.1093/glycob/cwv027 (***Research article***)

List of presentations and awards

International presentations (* Oral presentation)

1. **Loke, I.**^{*}, Venkatakrishnan, V., Packer, N.H., Thaysen-Andersen, M., The immunological role of paucimannosidic proteins in human neutrophils during Cystic Fibrosis, 11th Jenner Glycobiology and Medicine symposium, 19th – 21st April 2015, Paris, France.
2. **Loke, I.**, Packer, N.H., Thaysen-Andersen, M., The *N*-glycosylation of neutrophil cathepsin G and its role in the host innate immunity against *Pseudomonas aeruginosa*, 23th International Symposium on Glycoconjugates, 15th – 20th September 2015, Split, Croatia.
3. **Loke, I.**^{*}, Packer, N.H., Thaysen-Andersen, M., Immunological roles and the biosynthetic machinery of protein paucimannosylation in human neutrophils, 10th International Symposium on Glycosyltransferases, 19th – 20th June 2016, Toronto, Canada.

Domestic presentations (* Oral presentation)

1. **Loke, I.**^{*}, Venkatakrishnan, V., Packer, N.H., Thaysen-Andersen, M., The biosynthesis and immunological function of a novel type of protein N-glycosylation in human neutrophils, 2nd Proteomics and Beyond symposium, 12th November 2014, Macquarie University, Sydney, New South Wales, Australia.
2. **Loke, I.**, Packer, N.H., Thaysen-Andersen, M., Paucimannosylation in human neutrophils: Insights into the biosynthesis and immunological role of a novel type of protein glycosylation, 20th Lorne Proteomics symposium, 4th – 7th February 2015, Lorne, Victoria, Australia.
3. **Loke, I.**, Packer, N.H., Thaysen-Andersen, M., Neutrophil cathepsin G carries unusual truncated chitobiose core carbohydrate structures and its function in the host immune defence against *P. aeruginosa*. Chemical Proteomics symposium, 16th July 2015, Sydney, Australia.

4. **Loke, I.**^{*}, Packer, N.H., Thaysen-Andersen, M., Mapping the unusual *N*-glycosylation of neutrophil cathepsin G and its role in the host innate immunity against *P. aeruginosa*. Macquarie Biofocus research conference, 15th December 2015, Macquarie University, Sydney, Australia.
5. **Loke, I.**^{*}, Packer, N.H., Thaysen-Andersen, M., Probing human white blood cells for a novel type of protein *N*-glycosylation. 21th Lorne Proteomics symposium, 4th – 7th February 2016, Lorne, Victoria, Australia.

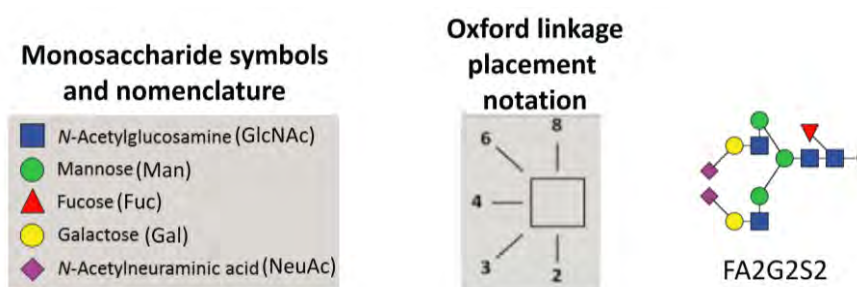
Awards

1. 2013 International Macquarie University Postgraduate Research Excellence Scholarship (iMQRS).
2. 2014 Australian Cystic Fibrosis Studentship Award (AUD\$15,000), Cystic Fibrosis Australia, New South Wales, Australia.
3. 2015 23th International Symposium on Glycoconjugates student Travel award (Euro€500), Split, Croatia.
4. 2015 Postgraduate Research Fund Award (AUD\$5,000), Macquarie University, Sydney, Australia.
5. 2016 21st Australian Proteomics Symposium Student Bursary (AUD\$150), Australian Proteomics Society, Sydney, Australia.
6. 2017 Global Young Scientist Summit Travel award (SGD\$1,000), Singapore.

Symbols and Nomenclature

Glycan nomenclature

All *N*-glycan chitobiose cores have two core *N*-acetyl-D-glucosamines (GlcNAc) with the exception of truncated chitobiose cores; F indicates a core α 1,6 fucose linked to the innermost GlcNAc; M_x, number (x) of mannose residue on core GlcNAc, A_x; number of antenna (GlcNAc) on the trimannosyl chitobiose core; A₂, biantennary with both GlcNAcs as β 1,2-linked; G_x, number (x) of β 1,4-linked galactose on the antenna; S_x, number (x) of sialic acid (*N*-acetyl-D-neuraminic acid) linked to galactose; The linkage type for sialic acid linkages, mannose arm linkages of the *N*-glycan trimannosyl core and other monosaccharide linkages are presented according to the angled Oxford linkage placement notation (Varki et al., 2015). The respective glycosidic linkages of the glycan structures in publication II, III, IV, V, VI, VII are represented not according to the Oxford linkage placement notation but are shown instead on each bond.



The glycan structures presented in this thesis are all created using GlycoWorkbench version 2.1 using Essentials of Glycobiology monosaccharide symbols and graphical representation of glycans (Varki et al., 2015) in compact and extended view and exported with reducing end indicator with the exception of publication II, III, IV, V, VI, VII where the reducing end is defined in the text unless otherwise stated.

Abbreviations

| | |
|----------------|--|
| 4-MU | 4-methylumbelliferone |
| A1AT | α 1-antitrypsin |
| APC | Antigen-presenting cells |
| AraC | Cytosine β -D-arabinofuranoside |
| Arg | Arginine |
| Asn | Asparagine |
| BCA | Bicinchoninic acid assay |
| BPI | Bactericidal/permeability-increasing protein |
| BSA | Bovine serum albumin |
| C/EBP α | CCAAT-enhancer binding protein alpha |
| CD | Cluster of differentiation |
| CDG | Congenital disorders of glycosylation |
| cDNA | Complementary Deoxyribonuclease |
| CF | Cystic Fibrosis |
| CFG | Consortium of functional glycomics |
| CID | Collision-induced dissociation |
| CLR | C-type lectin receptors |
| CRD | Carbohydrate recognition domain |
| DC | Dendritic cells |
| DMSO | Dimethyl sulphoxide |
| DTT | Dithiothreitol |

| | |
|--------|--|
| EDTA | Ethylenediaminetetraacetic acid |
| EIC | Extract ion chromatogram |
| ELISA | Enzyme-linked immunosorbent assays |
| EM | Electron microscopy |
| ENGase | Endo- β -N-acetylglucosaminidase |
| ER | Endoplasmic reticulum |
| ESI | Electrospray ionisation |
| ETD | Electron transfer dissociation |
| FA | Formic acid |
| FCS | Fetal calf serum |
| fMLP | N-formylmethionyl-leucyl-phenylalanine |
| Fuc | L-Fucose |
| FuT | Fucosyltransferase |
| Gal | D-Galactose |
| GalNAc | <i>N</i> -acetyl-D-galactosamine |
| GalT | Galactosyltransferase |
| GAPDH | Glyceraldehyde 3-phosphate dehydrogenase |
| Glc | D-Glucose |
| GlcNAc | <i>N</i> -acetyl-D-glucosamine |
| HBSS | Hanks' balanced salt solution |
| HCD | Higher energy collision dissociation |
| Hex A | β -N-acetylhexosaminidase A |
| Hex B | β -N-acetylhexosaminidase B |

| | |
|--------------|--|
| Hex C | β -N-acetylhexosaminidase C |
| Hex D | β -N-acetylhexosaminidase D |
| Hex S | β -N-acetylhexosaminidase S |
| HexNAc | N-acetylhexosamine |
| HILIC | Hydrophilic interaction liquid chromatography |
| HLA | Human leukocyte antigen |
| HNE | Human neutrophils elastase |
| HRP | Horse radish peroxidase |
| HSA | Human serum albumin |
| HSC | Haematopoietic stem cells |
| IAA | Iodoacetamide |
| ICC | Smart ion charge control |
| IT | Ion trap |
| ITAM | Immunoreceptor tyrosine-based activation motif |
| ITIM | Immunoreceptor tyrosine-based inhibition motif |
| LAMP | Lysosome-associated membrane glycoprotein |
| LC | Liquid chromatography |
| LC-MS/MS | Liquid chromatography tandem mass spectrometry |
| LPS | Lipopolysaccharides |
| LSD | Lysosomal storage diseases |
| LTQ | Linear ion trap quadrupole |
| Lys | Lysine |
| <i>M. tb</i> | <i>Mycobacterium tuberculosis</i> |

| | |
|-----------|--|
| M6P | Mannose-6-phosphate |
| MALDI-TOF | Matrix-assisted laser desorption/ionisation-Time of flight |
| Man | D-Mannose |
| MB | Myeloblast |
| MBL | Mannose binding lectin |
| MC | Myelocyte |
| MCC | Mander's co-localisation coefficient |
| miRNA | Micro ribonucleic acid |
| MM | Metamyelocyte |
| MMP-9 | Metalloproteinase 9 |
| MPO | Myeloperoxidase |
| mrCLR | Mannose recognising C-type lectin receptors |
| mRNA | Messenger ribonucleic acid |
| MS | Mass spectrometry |
| MS/MS | Tandem mass spectrometry |
| MUG | 4-methylumbelliferyl-2-acetamido- 2-deoxy- β -D-glucopyranoside |
| MUGS | 4-methylumbelliferyl-6-sulfo- N-acetyl- β -D-glucosaminide |
| nCG | Neutrophil cathepsin G |
| NETs | Neutrophil extracellular traps |
| NeuAc | <i>N</i> -acetyl-D-neuraminic acid |
| NGAL | neutrophil gelatinase-associated lipocalin |
| NK | Natural killer |

| | |
|----------|--|
| OST | Oligosaccharyltransferase |
| PAMP | Pathogen-associated molecular patterns |
| PBS | Phosphate buffered saline |
| PGC | Porous graphitised carbon |
| PM | Promyelocyte |
| PMA | Phorbol 12-myristate 13-acetate |
| PMSF | Phenylmethanesulfonyl fluoride |
| PNGase A | Peptide- <i>N</i> -glycosidase A |
| PNGase F | Peptide- <i>N</i> -glycosidase F |
| PR3 | Proteinase 3 |
| PSGL-1 | P selectin glycoprotein-1 |
| PTM | Post translational modifications |
| PVDF | Polyvinylidene fluoride |
| PVP | Polyvinylpyrrolidone |
| QTOF | Quadrupole-Time of flight |
| qPCR | Quantitative real-time polymerase chain reaction |
| ROS | Reactive oxygen species |
| RP | Reversed phase |
| RPMI | Roswell Park Memorial Institute medium |
| RT | Retention time |
| SD | Sandhoff disease |
| SDS-PAGE | Sodium dodecyl sulphate-polyacrylamide gel electrophoresis |

| | |
|-----------|--|
| Ser | Serine |
| shRNA | Short hairpin RNA |
| SiaT | Sialyltransferases |
| siRNA | Silencing induced ribonucleic acid |
| SNARE | Soluble N-ethylmaleimide-sensitive factor activating protein receptor |
| SPE | Solid phase extraction |
| TB | Tuberculosis |
| TBST | Tris buffered saline with tween 20 |
| TFA | Trifluoroacetic acid |
| Thr | Threonine |
| TSD | Tay-Sachs disease |
| vWF | Von Willibrand factor |
| ZIC-HILIC | Zwitterionic hydrophilic interaction liquid chromatography |

Chapter 1: General Introduction, Thesis Overview and Research Aims

This chapter aims to introduce and provide background information in light of the existing literature, current thinking and of the general methods and biological concepts used for the subsequent data chapters of this thesis. Central aspects of the human immune system, in particular innate immunity, are firstly covered. Human haematopoiesis is covered next, focusing on granulopoiesis and granulogenesis. Individual neutrophil granules will also be discussed in the context of their protein content (proteome) and the functions they undertaken during innate immunity. The main defence mechanisms utilising these granule proteins that enables neutrophils to mount an effective immune response against foreign pathogens are discussed next. As these granule proteins are mainly *N*-glycosylated, an introduction to protein *N*-glycosylation will be covered, followed by an introduction to the analytical methods used for characterising *N*-glycosylated proteins. In addition, alterations in protein *N*-glycosylation during pathological conditions will also be discussed, focusing on the emerging roles of protein mannosylation during inflammation and infection which will be presented as a review article.

Finally, an overview of the chapters and publications, together with the investigated topics covered in this thesis, will be presented towards the end of this chapter. The specific research aims presented in this thesis are also addressed at the end of this chapter.

1.1 The human immune system

Immunity refers to all mechanisms utilised by the body to protect against invading pathogens, foreign environmental agents or even compounds within the body that are potentially harmful to the human organism. These harmful self- and non-self agents can range from micro-organisms, chemicals, food, or even plant and animal products including cellular debris and biomolecules. The human immune system is divided into two major categories: innate immunity and adaptive immunity (**Figure 1**) (Yatim and Lakkis, 2015).

1.1.2 Innate immunity and adaptive immunity

Innate immunity begins from birth and consists of a range of physical and chemical barriers. The skin forms part of the physical barrier where it prevents microorganisms and foreign substances from penetrating into the underlying tissues. The low pH of sweat and sebaceous gland secretions, together with the anti-microbial effect of lysozymes, a potent glycoside hydrolase, also help in minimising invasion from foreign pathogens. In addition, soluble proteins in the blood circulation such as interferons and complement proteins contribute to

facilitate non-specific immune responses against viral and bacterial agents. Another important innate mechanism involves the mucous membranes of the gut and the respiratory tract. These mucous-membrane barriers trap microorganisms and help to contain infection due to their sticky nature. The “beating motion” generated by the ciliated epithelial cells that line the surfaces of these exposed tissues assists in preventing and suppressing inflammation by avoiding pathogenic growth and eliminating the microorganisms from the respiratory tract. Importantly, these protective mechanisms are assisted by phagocytes such as alveolar macrophages and neutrophils, which together form the cellular defence component of the innate immune system (Coico and Sunshine, 2009).

If an invading microorganism manages to penetrate the physical and chemical barriers, the body has developed several cellular defence mechanisms to combat this threat. In order to effectively distinguish between harmful foreign pathogens (“non-self”) from the body’s own cells and tissues (“self”), the innate immune system provides an immediate first line of defence as a non-specific response through the recognition of non-self antigens known as pathogen-associated molecular patterns (PAMPs) (Mahla et al., 2013). These antigenic molecules, which are often proteins, carbohydrates or lipid based, are recognised by toll-like receptors or lectin receptors, which are expressed by various immune cells such as dendritic cells (DCs), macrophages and neutrophils (Kawai and Akira, 2011). Lectin receptors or glycan binding lectins, are a group of carbohydrate binding proteins (Varki et al., 2009a). A subgroup family of the lectin receptors known as C-type lectin receptors (CLRs), is able to recognise carbohydrates via their carbohydrate recognition domains (CRDs) in the presence of calcium (Kerrigan and Brown, 2009). One of the sub-families of CLRs are the mannose recognising C-type lectin receptors (mrCLRs), which will be discussed in greater detail in the review article attached at the end of this chapter.

Facilitated by these receptors, the phagocytic cells ingest and kill invading pathogens and they form, as such, the interface between innate and adaptive immunity. For example, DCs and macrophages are professional antigen-presenting cells (APCs) that process foreign antigens and present them to B and T lymphocytes, which are involved in adaptive immunity. B and T lymphocytes are the major effector immune cells that direct a precise and tailored immune response through the production of antibodies (humoral immunity) or through the use of perforins released from CD8⁺ T cytotoxic cells upon activation by CD4⁺ T helper cells (cellular immunity) (Alberts, 2002). These protective mechanisms facilitate efficient extracellular killing of bacterial or virus infected cells through means of controlled cell death,

a process known as apoptosis. This mechanism is known to kill cancerous cells and several other unwanted, potentially harmful, cellular events in the human organism (Martinez-Lostao et al., 2015).

Compared to innate immunity, the adaptive immune response is a slower process, but it allows for the generation of immunological memory by B memory cells. This enables a faster immune response when the same pathogen is subsequently encountered by the host. However, the theory that this is a unique feature of the acquired immune system was recently challenged with the rather surprising finding of “memory-trained” innate immune cells (van der Meer et al., 2015). The immune responses generated by the innate and adaptive immunity have been traditionally viewed as separate entities but increasing evidence show that they do interact and complement each other (Bedoui et al., 2016). Collectively, these pieces of evidence demonstrate that the knowledge on the interactions between the innate and adaptive immune system are still poorly understood. This is particularly the case in the innate immune system, which has received lesser attention compared to the adaptive immune system.

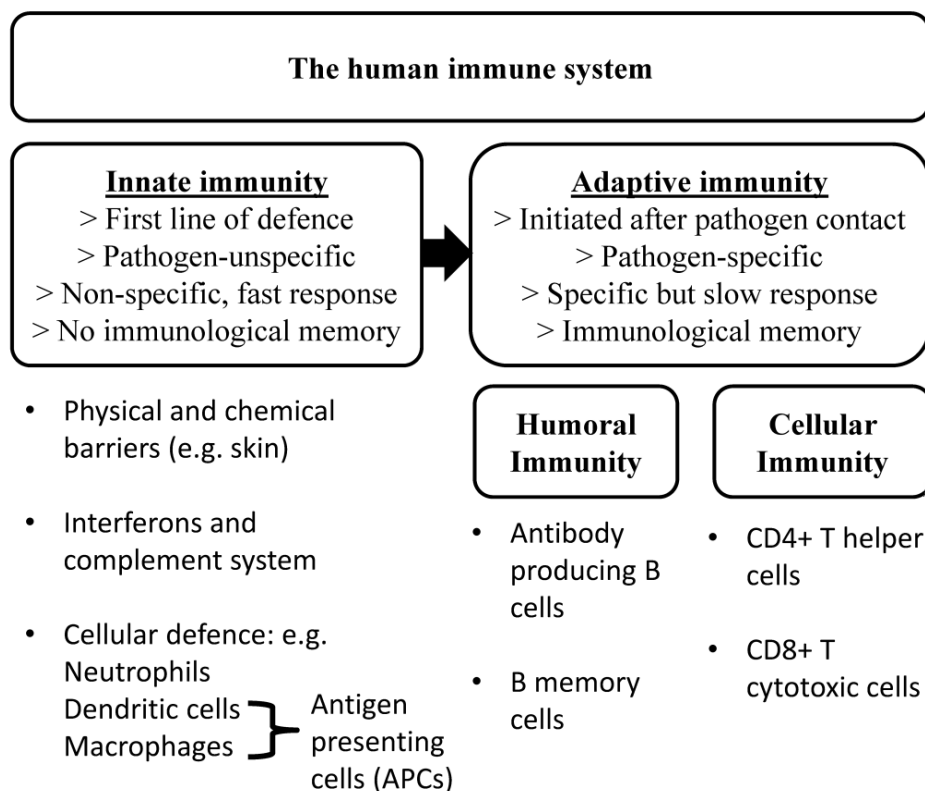


Figure 1. An overview and comparison on the classical differences between the innate and acquired immune system in humans as described in the literature. The various cells and molecular components involved in the respective immune system/processes are shown as well as their individual properties.

1.2 Human haematopoiesis

In humans, white blood cells, also known as leukocytes, from both the innate and adaptive immunity arms, arise from common pluripotent haematopoietic stem cells (HSCs) through a differentiation process called haematopoiesis (Yu and Scadden, 2016). These pluripotent HSCs residing in the bone marrow have the capacity to develop into more differentiated lines of blood cells (Coico and Sunshine, 2009). HSCs first differentiate into multipotent progenitors in the presence of a transcription factor known as CCAAT-enhancer binding protein alpha (C/EBP α) (Bjerregaard et al., 2003). From this point, these multipotent HSCs can further develop into common progenitor cells that are committed to a specific cell lineage. Two models for haematopoiesis have been proposed: The deterministic and stochastic theory (Kimmel, 2014; Rieger and Schroeder, 2012). In the deterministic (classical) theory, differentiation of HSCs is influenced by transcription factors and soluble growth factors in the micro-environment (bone marrow niche), that controls both the extent and direction of cell differentiation in a hierarchical manner (Ding et al., 2012; Sugiyama et al., 2006). Once differentiation has occurred, the cells are committed to produce only a single type of cell lineage and this state is known as unipotency (Coico and Sunshine, 2009).

There are three main cell lineages that the HSCs can differentiate into, namely the erythroid, lymphoid and the myeloid cells. The erythroid cells are oxygen carrying red blood cells (erythrocytes) while the lymphoid cell lineage is composed of B, T and natural killer (NK) cells that are formed during the lymphoid-specific differentiation route known as lymphopoiesis. The myeloid cell lineage includes the monocytes, macrophages, mast cells and DCs, together with the granulocytes which consist of the neutrophils, basophils and eosinophils. This ensemble of myeloid cells develops through myelopoiesis (Giebel and Punzel, 2008), and is intimately involved in facilitating a functional innate immune response (Gasteiger et al., 2016). Megakaryocytes also arise from the myeloid cell lineage; these cells differentiate and give rise to platelets through the process of thrombopoiesis. Platelets are classically known for their roles in blood coagulation (Clemetson, 2012) but have been recently shown to play equally important roles during innate immunity (Carestia et al., 2016).

In contrast, the stochastic theory proposes that HSCs differentiates to specific cell types by randomness (Abkowitz et al., 1996). This theory was supported by the observation of a subpopulation of HSCs differentiating into a committed cell type at a higher differentiation rate relative to the rest of the HSCs population. It was also shown that this subpopulation of

cells, in the presence of growth factors, was able to re-establish the original population of HSCs. This indicates that haematopoiesis is a stochastic and reversible process and not a unidirectional/hierarchical pathway of differentiation as proposed by the classical theory (Chang et al., 2008). To date, both theories continue to receive support.

Nevertheless, the presence of growth factors such as stem cell factors, interleukins and chemokines are important to regulate the proliferation and maturation of these cells (Ding et al., 2012; Poulos et al., 2013). Recently, microRNAs (miRNAs) were also suggested to regulate the proliferation of HSCs (Gentner et al., 2010). It appears that the differentiation and proliferation of HSCs are widely regulated by multiple players, but are tightly controlled in the bone marrow niche to avoid unwanted cell proliferation. The mechanisms for cellular differentiation into the myeloid and lymphoid lineages are further discussed below based on the classical theory (**Figure 2**).

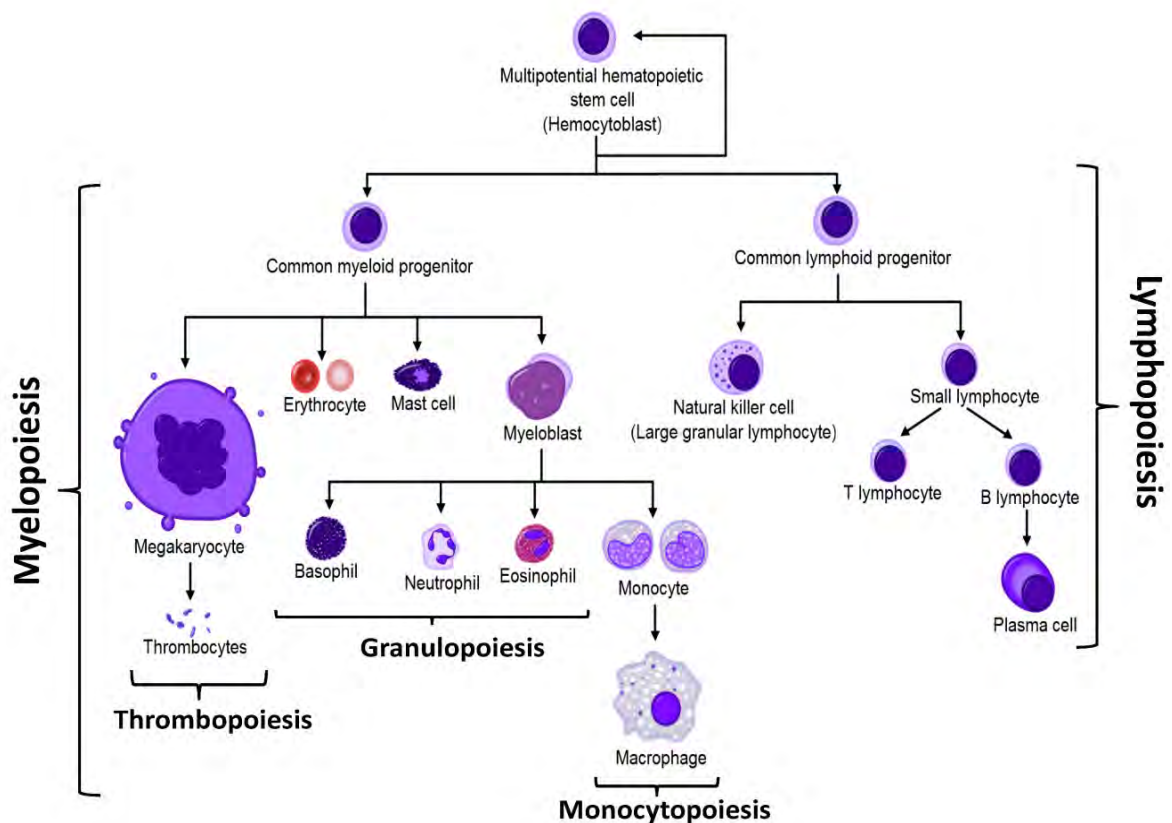


Figure 2. Human haematopoiesis. An overview of the complex network of human blood cell differentiation pathways showing the development of the different blood cells arising from HSCs and multipotency stem cells as described in the text. Image adapted and modified with permission from A. Raid from https://commons.wikimedia.org/wiki/File:Hematopoiesis_simple.svg

Chapter 1

1.2.1 Lymphopoiesis

The various differentiation stages in the respective hematopoietic cell lineages are characterised by the expression of cell surface markers, which can, amongst other techniques, be measured using flow cytometry (Giebel and Punzel, 2008; Mora-Jensen et al., 2011). Lymphoid progenitor cells arise from multipotent HSCs in the process known as lymphopoiesis. These progenitor cells lack the expression of lineage-specific antigens, low expression of stem cell associated antigen and c-kit, but they are highly positive for the interleukin-7 receptor α -chain (Kondo et al., 1997). Transcription factors such as Ikaros, Pax-5 factor and Gfi1 are important for lymphoid cell differentiation as gene mutations in these transcription factors have been associated with B cell lymphomas (Cobaleda et al., 2007; O'Brien et al., 2011; Suzuki et al., 2016).

1.2.2 Myelopoiesis

During myelopoiesis, myeloid cells are developed from common granulocyte-monocyte progenitor cells. Granulocytes are the major cell type forming this class of white blood cells, specifically the neutrophils, which are of particular relevance to this thesis. The differentiation route of these myeloid cells is similar to lymphopoiesis such that they are governed by the transcription factors C/EBP α and PU.1. Both C/EBP α and PU.1 were identified to be important for granulocyte maturation while Maf and Jun transcription factors were found to be important for monocyte development (Friedman, 2002). The proliferative state of differentiation begins in the granulocyte-monocyte progenitor cells in the presence of the granulocyte-monocyte colony stimulating factors. This is characterised by a high cell surface expression of the Fc γ receptor and cluster of differentiation (CD) 34, giving rise to either monocyte precursors known as monoblasts or granulocyte precursors known as myeloblasts (MB), respectively (Akashi et al., 2000). Further differentiation of monoblasts commit these cells to monocytes through monocytopoiesis while MB give rise to promyelocytes (PM), which are further differentiated into mature neutrophils through granulopoiesis (Lewis et al., 2006).

1.2.3 Granulopoiesis

Granulopoiesis is defined as the formation of granulocytes within the bone marrow, beginning from the differentiation of a MB to their respective myeloid cell lineage. As this thesis is primarily focused on neutrophils, the subsequent introduction and discussion on granulopoiesis will be restricted to human neutrophils in this chapter. The reader is directed to

other excellent reviews covering the development of other myeloid immune cells in greater details (Collin and Bigley, 2016; Geissmann et al., 2010) .

The development of mature neutrophils found in the blood circulation begins when the MB differentiates to form a PM. A round nucleus and the presence of azurophilic granules are characteristic morphological features of a PM (Borregaard, 1997). Several transcription genes and factors govern the neutrophil development in the bone marrow including Runx1, PU.1, C/EBP- α , - ϵ and Gfi1 (Bjerregaard et al., 2003; Theilgaard-Monch et al., 2005) . In addition, miRNAs such as miRNA-130a are one of the regulators of cell proliferation observed in MBs and PMs (Larsen et al., 2013). It should be noted that the expression of cell cycle proteins such as cyclin D2 is also important in regulating the cellular maturation of PMs to the more mature myelocytes (MCs) and metamyelocytes (MMs) (Klausen et al., 2004). The morphological characteristics of MMs are their kidney shaped nucleus. These maturation intermediates differentiate further to form band cells and segmented cells, which are classified as mature neutrophils (Lewis et al., 2006). In addition, the expression of transcription factors and cell cycle proteins fluctuates during the above described stages of neutrophil differentiation in the bone marrow. Eventually, mature neutrophils are generated and released into the blood circulation (Bjerregaard et al., 2003). This release into the circulation is aided by the presence of the granulocyte-colony stimulation factor, chemokine ligand 1 and 2 cytokines, which are recognised by chemokine-specific receptors expressed on the cell surface of mature neutrophils (Eash et al., 2010; Wengner et al., 2008).

Under steady state (non-alert) conditions, granulopoiesis of MB to mature neutrophils in the bone marrow takes around 14 days while the half-lives of terminally differentiated mature neutrophils in circulation is around 5 to 7 days (Dancey et al., 1976; Pillay et al., 2010). Neutrophils are often referred to as the first line of immune defence in the host and are among the first immune cells to arrive at the site of inflammation (Kruger et al., 2015). In response to severe infections, neutrophils can be readily generated and mobilised into circulation, a process termed emergency granulopoiesis, involving increased *de novo* synthesis of neutrophils as a result of enhanced proliferation of myeloid cells in the bone marrow (Devi et al., 2013; Manz and Boettcher, 2014).

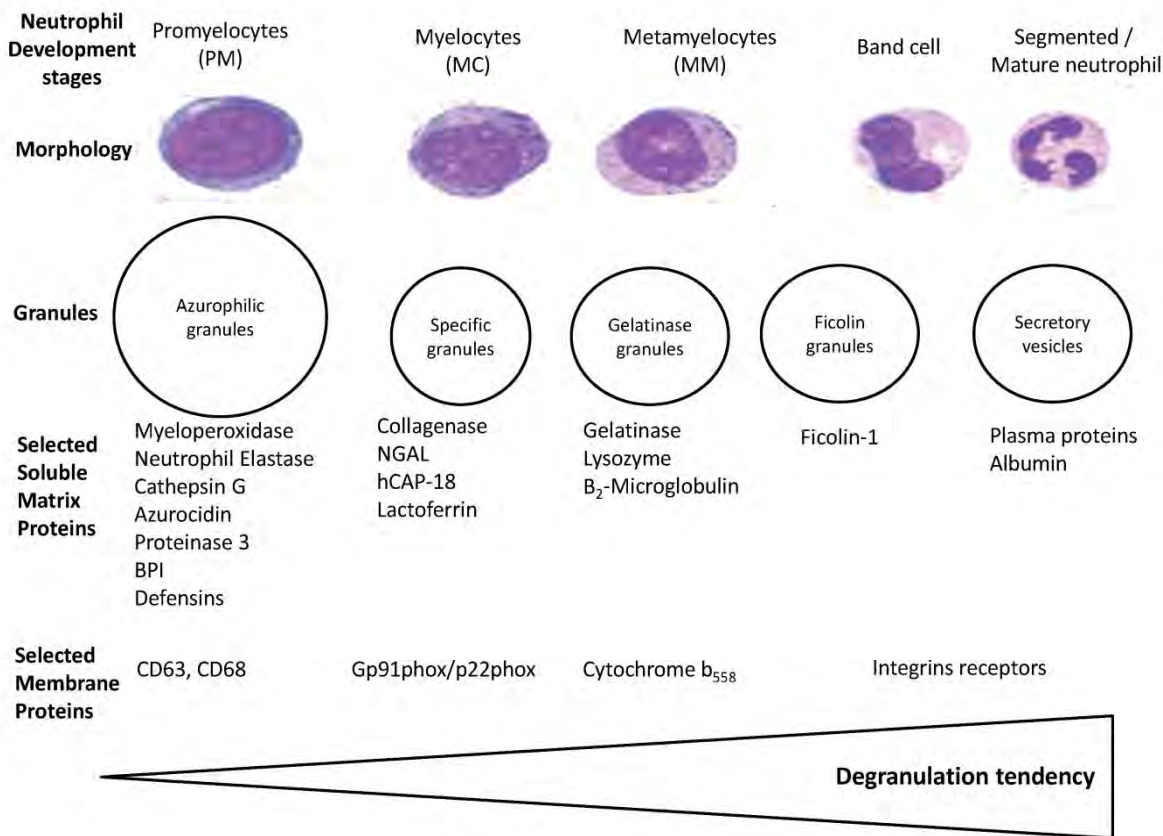


Figure 3. Formation of neutrophil granules in developing neutrophils found in the bone marrow. The respective morphologies and the production of the individual granules and their protein (membrane/soluble) constituents are shown over the various developmental stages of human neutrophils. The increasing degranulation tendency of the granules formed over the neutrophil development is shown i.e. secretory vesicles have a higher propensity for degranulation compared to the azurophilic granules. The neutrophil morphologies are reprinted from *Haematology: basic and principles*, 6th edition, Hoffman et al. © 2013, with permission from Elsevier (Hoffman, 2013).

Mature neutrophils are identified morphologically by their lobulated (drumstick-like) nucleus and the presence of cytoplasmic granules (Lewis et al., 2006). During neutrophil maturation from a MB to a segmented mature neutrophil, a spectrum of cytoplasmic granules are developed sequentially (Borregaard and Cowland, 1997). The formation of these neutrophil granules during bone marrow maturation (also known as granulogenesis) can be described as a continuum as shown in **Figure 3**. The azurophilic granules are the first to be produced at the PM stage, followed by the specific and gelatinase granules during the MC and MM/band cell stage. The secretory vesicles are the last to form when the cells are terminally differentiated as

segmented neutrophils. Similarly, the protein constituents (proteome) present in the individual granules are highly different due to the fluctuations and spatio-temporal regulation of the protein synthesis during neutrophil maturation in the bone marrow (Cowland and Borregaard, 2016). These complex processes, which generate a unique proteome “fingerprint” of the individual neutrophil compartments, are convincingly explained by the “targeting by timing” hypothesis (Borregaard and Cowland, 1997). Specifically, this hypothesis proposed that the granules are filled with different proteins synthesised during the time of their formation. Hence, granule proteins synthesised simultaneously will end up in the same granule. The hypothesis also proposed that there are no sorting motifs or tags on these granule proteins to direct them to the granules. The synthesised granule proteins are believed to arrive in the individual granules after exiting the endoplasmic reticulum (ER) - Golgi network (i.e. the secretory route) at various points through yet-to-be-determined mechanisms. This differential exit implies that the granule proteins may receive differential ER-Golgi processing, which is of particular interest with respect to the glycosylation process of these proteins that happens at that time. Furthermore, the sorting of the granule proteins was shown to be independent of the mannose-6-phosphate targeting pathway (Laura et al., 2016; Nauseef et al., 1992). Therefore, very little is known about the cellular and molecular sorting mechanisms of these proteins to these respective granules.

Interestingly, an early electron microscopy (EM) study by Bainton and colleagues showed that azurophilic granules formed during the PM stage buds off from the *cis*-Golgi, while the granules formed during the subsequent MC and MM stages exit from the *trans*-Golgi (Bainton and Farquhar, 1966). This landmark observation suggested that azurophilic granule proteins undergo different post-translational processing compared to granule proteins that are formed later in maturing neutrophils in the bone marrow e.g. proteins residing in the specific and gelatinase granules.

The “targeting by timing” hypothesis was proposed by Borregaard and co-workers based on the observation of the expression of selected granule marker proteins in isolated bone marrow neutrophils at successive stages of their maturation (Borregaard et al., 1995). It was validated by an induced expression of a specific granule protein, neutrophil gelatinase-associated lipocalin (NGAL) in the azurophilic granules of HL-60 cells, a neutrophil-like cell line widely used to study neutrophil biology (Le Cabec et al., 1996). Recently, correlations between the transcriptome of the granule proteins with the proteome of the subcellular fractionated granules isolated from neutrophils further supported the association between the time of

granule protein expression and their localisation in the various neutrophil granules (Clemmensen et al., 2014; Rorvig et al., 2013).

Although no studies have conclusively shown evidence that mature neutrophils do not produce granules while in circulation, the absence of mRNA coding for these granule proteins in circulating neutrophils suggests that granule proteins are only synthesised during maturation in the bone marrow under the control of transcriptional factors (Borregaard et al., 2001; Cowland and Borregaard, 1999).

1.2.4 Neutrophil granules and their associated granular proteins

As briefly introduced above and further elaborated on below, neutrophil granules are divided into multiple distinct subsets based on their appearance and protein contents. In addition, the various granule subsets also differ in their capacity to be exocytosed in response to stimulation (**Figure 3**). Granule exocytosis, also known as degranulation, was suggested to be mediated via compound exocytosis. These are a series of steps involving granule translocation towards the plasma membrane via actin remodelling and microtubule assembly. This is followed by tethering, docking and fusion of the granules into the plasma membrane that involves the Rab and soluble N-ethylmaleimide-sensitive factor activating protein receptor (SNARE) proteins (Lacy and Eitzen, 2008; Mollinedo et al., 2006). The heterotypic fusion of the granules with the plasma membrane of stimulated neutrophils serves to release the soluble granule proteins into the extracellular environment and present membrane-bound proteins on the cell surface of stimulated neutrophils (Borregaard and Cowland, 1997; Kuijpers et al., 1991). The differential degranulation capacity may be explained by granular differences in their sensitivity towards elevated calcium levels (Sengelov et al., 1993a). Secretory vesicles, which are the last granule subsets to form, are released first at the lowest level of calcium, followed by the gelatinase, specific and the azurophilic granules. The individual neutrophil granules and the proteins packaged in them are discussed below.

1.2.4.1 Azurophilic granules

The earliest-formed peroxidase-positive azurophilic granules are found in PMs and are named based on their affinity for the basic dye azure A (Lewis et al., 2006). The azurophilic granules can be further subdivided into the smaller defensin-poor granules, which are first formed, followed by the larger defensin-rich granules (Borregaard and Cowland, 1997). These granules abundantly display specific membrane proteins such as CD63 (Cham et al., 1994), CD68 (Saito et al., 1991) and carry an arsenal of soluble proteins that are anti-microbial and

proteolytic in nature, characteristics that are central to the biological functions of the neutrophils in general and the azurophilic granule in particular (Mitchell et al., 2008). One of the most abundant proteins stored in the azurophilic granules is myeloperoxidase (MPO), a heavily glycosylated catalytic enzyme that is involved in the conversion of hydrogen peroxide to hypochlorous acid upon granule fusion with the phagolysosomes. Phagolysosomes are intracellular compartments that are formed upon phagocytosis of foreign pathogens in neutrophils (Nordenfelt and Tapper, 2011). Anti-microbial proteins and peptides such as the bactericidal/permeability-increasing protein (BPI) and α -defensins are also important molecules stored within these granules. These proteins and peptides assist in host immune defence against gram-positive and gram-negative bacteria (Calafat et al., 2000; Ericksen et al., 2005; Faurschou et al., 2005).

In addition, key serine proteases such as human neutrophil elastase (HNE), neutrophil cathepsin G (nCG), proteinase 3 (PR3) and azurocidin are also glycosylated and located mainly in the azurophilic granule. Similarly, these potent hydrolytic enzymes are known to be effective in the protection against a broad range of bacteria. This is in part, due to their proteolytic activities and their highly positive charged arginine-rich protein surface (Belaouaj et al., 1998; Korkmaz et al., 2008; Miyasaki and Bodeau, 1992; Shafer et al., 1996; Shafer et al., 1991). Recently, a newly discovered serine protease known as neutrophil serine protease 4 was also found localised within the azurophilic granules (Perera et al., 2013), but its anti-microbial properties, if any, remain to be determined. The glycosylation of the above-mentioned serine proteases localised to the azurophilic granule will be one of the main foci in this thesis.

1.2.4.2 Specific, gelatinase and ficolin granules

Following the formation of the azurophilic granule, the peroxidase-negative specific and gelatinase granules are the next two granules to form in the developing neutrophils. The specific granules develop in the MCs and MMs stages and are defined based on their rich content of lactoferrin, an iron-binding protein with known anti-microbial activities. In addition, the specific granules also contain collagenase, NGAL and the human cathelicidin (hCAP-18) proteins that are essential for their anti-microbial activities (Kjeldsen et al., 1994; Sørensen et al., 1997; Yang et al., 2002). Unlike the azurophilic granules, the encapsulating membranes of the specific granules contain various adhesion receptors and subunits of the NADPH-oxidase complex, which are involved in the generation of the “respiratory-burst” in phagocytosing neutrophils (Avinash et al., 2014).

In contrast, the gelatinase granules are defined by their high levels of gelatinase matrix metalloproteinases known as metalloproteinase 9 (MMP-9) (Lominadze et al., 2005). MMP-9 is one of the hydrolytic proteases belonging to the zinc-metalloproteinase family that are capable of degrading extracellular matrix proteins such as collagen. The gelatinase granules are formed during the MM and band cell maturation stages in the bone marrow (Faurschou and Borregaard, 2003; Opdenakker et al., 2001). In addition, the membrane of gelatinase granules also contains subunits of the NADPH-oxidase complex such as Gp91phox/p22phox, cytochrome b₅₅₈ and integrins that are essential to assist with the adhesion processes of neutrophils in their migration towards the site of inflammation.

In addition to the specific and gelatinase granules, ficolin-1 containing granules were also shown to be synthesised in MCs, MMs and band cells using radiolabeled ficolin-1 proteins in isolated immature neutrophils developing in the bone marrow (Rorvig et al., 2009). These homopolymeric soluble ficolins are capable of binding to carbohydrates via their C-terminal fibrinogen-like domain and have been suggested to be involved in the lectin complement pathway (Lu et al., 2002).

1.2.4.3 Secretory vesicles

The secretory vesicles are the last major compartment to be produced in developing neutrophils. These compartments are known to have a high propensity for degranulation upon stimulation. Integrins receptors are found to be in abundance on the membrane of secretory vesicles, which was supported by the observation that these receptors are abundantly displayed by the plasma membrane of stimulated (degranulated) neutrophils (Calafat et al., 1993). However, it should be noted that secretory vesicles are not synthesised *in vivo* and are endocytic in nature as evident by their high abundance of albumin and other serum glycoproteins contained within the granule membrane (Borregaard et al., 1992). Thus, the proteome and the glycosylation of these proteins residing in this compartment do not adhere to the “targeting by timing” hypothesis as described above.

1.3 Neutrophil functions in innate immunity

In humans, 50-70% of circulating leukocytes are neutrophils. Mature neutrophils in circulation have an average diameter of 7-10 μm (Borregaard, 2015). As described above, neutrophils are one of the first innate immune cells to arrive at the sites of inflammation or infection in the body. Neutrophils in circulation can readily migrate and infiltrate into the

inflamed tissues such as the lung airways, which are particularly vulnerable to infections (Nicolas-Avila et al., 2017). Inflammation, characterised by the cardinal symptoms of pain, heat, redness, swelling and a loss of function (Tracy, 2006), is a vital mechanism to protect the body against harmful infections and detrimental cellular processes in the organism.

Upon receptor recognition of the PAMPs expressed by foreign microorganisms, tissue resident innate immune cells such as macrophages and DCs are activated, triggering the release of pro-inflammatory molecules such as tumour necrosis factor- α and interleukin-1. This results in the formation of an inflammatory condition that is characterised by localised blood vessel dilation and, in turn, an increase in the local blood flow and vessel permeability to facilitate the recruitment of immune cells such as neutrophils to the affected sites (Shen et al., 2013). Although these processes are highly effective in combatting infection and are highly beneficial to the host, it is important to stress that prolonged inflammation (such as the inflammation associated with chronic injury) may cause harm to surrounding tissues as demonstrated in various disease states (Headland and Norling, 2015). For example, if not controlled properly, recruited neutrophils have the potential to cause severe chronic inflammatory tissue damage due to their collection of anti-microbial and pro-inflammatory molecules present in the granules. This is often observed in diseases characterised by chronic neutrophil infiltration such as cystic fibrosis (CF) and atherosclerosis (Mantovani et al., 2011). As discussed below, the neutrophil granules and their proteins play important roles in various neutrophil functions.

1.3.1 Neutrophil adhesion and transmigration

A multi-step cascade of events occurs when neutrophils are recruited to the inflamed site in response to pro-inflammatory molecules such as interferon γ and tumor necrosis factors released by activated CD4⁺ T helper cells (Mantovani et al., 2011). This process is known as “homing”. The first step of neutrophil-homing involves the adhesion of circulating neutrophils to the endothelial cell layer. Upon activation by cytokines released by activated immune cells, the vascular endothelium up-regulates the expression of carbohydrate-recognising adhesion molecules such as P- and E-selectins on the luminal surface of the endothelial layer (McDonald et al., 2010). This enables the binding of P selectin glycoprotein-1 (PSGL-1) to carbohydrate ligands expressed on activated neutrophils. These interactions are crucial to facilitate the primary rolling contact with the activated endothelium (McEver et al., 1995; Moore et al., 1995). As the interactions between the endothelial layer and neutrophils become stronger, neutrophils start rolling along the endothelial walls. This interaction triggers

the mobilisation of the secretory vesicles and, thus, cell surface expression of integrin receptors to further strengthen the neutrophil-endothelial interactions. This eventually leads to neutrophil immobilisation and vascular tethering (Sperandio, 2006). In order for the neutrophils to migrate through the basement membrane and the interstitial tissues rich in type IV and type V collagen, the neutrophils undergo a process known as either transmigration or extravasation. This involves the release of the hydrolytic gelatinase enzymes from the gelatinase granules to degrade the extracellular matrix (Bakowski and Tschesche, 1992; Delclaux et al., 1996).

1.3.2 Phagocytosis

Upon reaching the inflamed tissues, one of the mechanism by which neutrophils fight microbial invaders is through the engulfment of the offending pathogen, also known as phagocytosis (Gordon, 2016). In order for phagocytosis to occur, neutrophils must be in direct physical contact with the pathogen. To do this, neutrophils are capable of migrating up a chemotactic concentration gradient to engage and internalise the pathogens by recognising complement opsonised particles via their complement or Fcγ receptors. In addition, neutrophils are capable of recognising bacteria expressing N-formylmethionyl-leucyl-phenylalanine (fMLP) through their fMLP receptors (Heit et al., 2008; Lee et al., 2011).

Upon phagocytosis of the pathogen, a lipid bilayer membrane enclosed vesicle containing the pathogen is formed known as the phagosome. In addition to Rab and SNARE proteins, lysosome-associated membrane glycoprotein (LAMP) proteins such as LAMP-1 and LAMP-2 were identified to be essential for the maturation of the phagosome that eventually will fuse with the hydrolytic low-pH lysosomes (Binker et al., 2007; Caron and Hall, 1998). Upon heterotypic organelle fusion of the phagosome with the lysosomes and later also with the azurophilic granules, an acidic phagolysosome containing different anti-microbial proteins derived from the azurophilic granules is formed. This compartment utilises both oxygen-dependent and independent mechanisms to kill the phagocytised pathogen within the phagolysosome (Greenberg and Grinstein, 2002).

In the oxygen-dependent mechanism also known as the “respiratory burst”, the production of reactive oxygen species (ROS) is attributed to the activity of the multi-component enzyme known as NADPH-oxidase. This enzyme, which consists of Gp91phox/p22phox, is responsible for generating superoxides that undergo dismutation to form hydrogen peroxide, a microbicidal compound (Hampton et al., 1998; Klebanoff, 2005). In addition, the fusion of

the MPO-rich azurophilic granules with the phagosome lumen and the conversion of hydrogen peroxidase by MPO, lead to the formation of hypochlorous acid, another potent anti-microbial species used by neutrophils to kill microorganisms (Klebanoff and Rosen, 1978). The importance of these generated ROS in mediating neutrophil anti-microbial defence is emphasised in patients suffering from chronic granulomatous disease who are highly susceptible to bacterial and fungal infections as a result of non-functional NADPH-oxidases (Segal et al., 2000).

In contrast, the oxygen-independent mechanism used by neutrophils relies on the stored repertoire of azurophilic granule proteins such as the serine proteases (e.g. HNE, nCG, azurocidin, introduced above), anti-microbial proteins and peptides (e.g. BPI and defensins) that are being delivered to the phagolysosome upon fusion. For example, HNE and nCG have been documented to kill and degrade phagocytised pathogens by exerting anti-microbial effects through the disruption of the microbial membranes effectively facilitated by their potent hydrolytic action (Hirche et al., 2008; Ines et al., 2011). However, these proteases are also active in a secondary mechanism in the immune response due to their so-called “bystander-effect” which is, for example, observed in pulmonary diseases. Left un-regulated, the serine proteases can cause severe lung damage, emphysema and a loss of function in maintaining lung fluid homeostasis in the airways due to excessive tissue and matrix degradation (Guyot et al., 2014; Le Gars et al., 2013). Thus, controlling the production, secretion and activity of these serine proteases are crucial to ensure a potent, efficient and protective immune response that is not harmful to the host.

1.3.3 Formation of neutrophil extracellular traps

Phagocytosis is a well-known defence mechanism of neutrophils against microorganisms. Formation of so-called neutrophil extracellular traps (NETs) is a more recent discovery that describes an additional strategy that neutrophils use to entrap micro-organisms in the extracellular environment to limit their infections (Yuen et al., 2016). NETs are networks of decondensed chromatin fibres that are decorated with azurophilic granule proteins such as MPO, serine proteases and anti-microbial peptides such as defensins. NETs are formed in a process known as netosis, a type of neutrophil cell death that differs from necrosis and apoptosis (Yousefi and Simon, 2016). The exact formation of NETs is still poorly understood, but various studies have proposed several factors and events that could lead to netosis, including the dependency of the NADPH oxidase to form ROS as initiators of NET formation (Björnsdóttir et al., 2015). In addition, the de-condensation of the neutrophil chromatin was

proposed to be mediated by the azurophilic granule-resident HNE and MPO as they relocate to the nucleus of stimulated neutrophils and degrade the core and linker histones (Metzler et al., 2014). The hyper-citrullination of the histone damages the nuclear membrane, leading to the mixing of the chromatin with the azurophilic granule proteins within the cell before they are released extracellularly (Zawrotniak and Rapala-Kozik, 2013). Interestingly, other myeloid cell types were also shown to form these extracellular traps, under the collective term known as etosis (Goldmann and Medina, 2012). Apart from immune defence, NETs have also been described to play roles in sterile conditions such as auto-immune diseases (Grayson and Kaplan, 2016; Kessenbrock et al., 2009). However, their roles in mediating neutrophil innate immunity remain controversial (Sørensen and Borregaard, 2016).

1.3.4 Degranulation

In addition to phagocytosis and NETs, another anti-microbial defence mechanism mediated by neutrophils is degranulation. Degranulation of the neutrophil granules can be rapidly induced by several stimulants such as fMLP and lipopolysaccharides (LPS) (Kjeldsen et al., 1992; Lollike et al., 1995; Sengelov et al., 1993b). *In vitro* studies have showed that the secretory vesicles, and the gelatinase and specific granules are more readily degranulated compared to the azurophilic granules in response to calcium stimuli (Fletcher and Seligmann, 1985; Neelakshi et al., 2007). Potent chemical stimulants such as phorbol 12-myristate 13-acetate (PMA) and actin filament disruptor compounds such as cytochalasin B and latrunculin B have been used to induce the degranulation of azurophilic granules in neutrophils (Mitchell et al., 2008). Azurophilic granules in neutrophils are known to be directed preferentially to the phagosomes to assist in pathogen killing and to a lesser extent, participate in more classical degranulation involving fusion with the plasma membrane (Tapper et al., 2002). The importance of degranulating neutrophil granules to mount an effective immune response against pathogenic infections was recently underscored in a study where the lack of degranulating neutrophil granule results in persistent *Yersinia pseudotuberculosis* infections (Taheri et al., 2016). In addition, the mechanisms centric to neutrophil degranulation have recently received more attention due to the recognised contributions of granular proteins towards protection against infectious diseases, including fungal infections and inflammatory diseases such as alcoholic cirrhosis (Boussif et al., 2016; Swamydas et al., 2016).

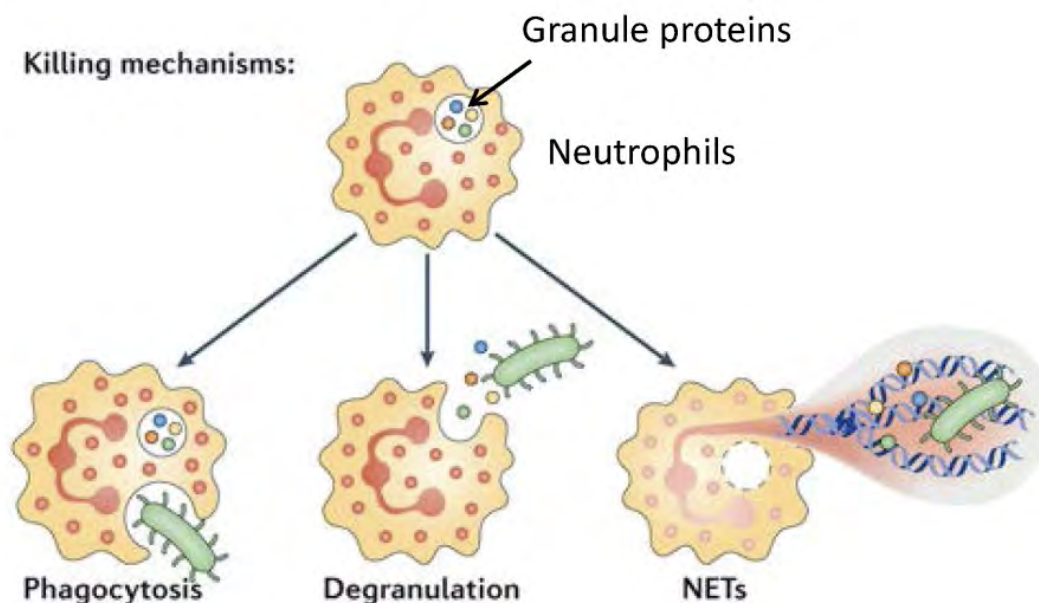


Figure 4. Illustration of the neutrophil killing mechanisms mediated by granule proteins. The three mechanisms that neutrophils utilise to fight infections with the help of granule proteins are shown (see text for details). Reprinted by permission from Macmillan Publisher Ltd: Nature Immunology Review © 2013 (Elzbieta and Paul, 2013)

Although powerful multi-omics technologies including genomics, transcriptomics and proteomics have enabled a better understanding of the various pathogen killing mechanisms mediated by the intracellular granule proteins of neutrophils (**Figure 4**), the structure and function of post translational modifications (PTMs) present in these neutrophil granule proteins remain severely understudied. This is the case not only at the single protein level, but also at the system-wide level. Given their well-known roles in mediating and modulating the host innate immunity, advancing our knowledge of the PTMs present on these granule proteins will allow a greater appreciation of their importance in neutrophil biology. Potential functions of the PTMs span a wide spectrum from changing the physicochemical properties of proteins, for example, in the modulation of the folding and stability of the granules proteins, to driving signalling cascades that may be more independent of their protein carriers. Unlike gene transcription, PTMs of proteins are template-free modifications of the polypeptide chain which are added and potentially processed further during protein translation (Varki et al., 2009b). As introduced below, one of the most common and the most complex type of PTMs on proteins is glycosylation, which is the main focus of this thesis.

1.4 Protein glycosylation in humans

Protein glycosylation is the co- and/or post-translational attachment of complex carbohydrates, sugars or oligosaccharides (hereafter collectively called glycans) to proteins. It is estimated that more than 50% of human proteins are glycosylated (Apweiler et al., 1999). This class of PTM, which utilises a significant amount of the energy of all human cells for the synthesis and regulation of glycoproteins, is known for playing diverse roles in human physiology (Moremen et al., 2012). Glycoproteins are predominantly found extracellularly, either tethered to the cell surface membrane or as secreted glycoproteins. In addition, some glycoproteins like the ones residing in neutrophil granules, discussed in this work are stored on the luminal side of the intracellular organelles that may be exposed to the extracellular environment under the appropriate conditions. Glycoproteins are divided into various classes depending on the attached glycan and the conjugation site of the polypeptide chain. Examples include *N*- and *O*-linked glycans, proteoglycans and glycosylphosphatidylinositol anchored proteins (Varki and Sharon, 2009).

Protein *N*-glycosylation is the addition of glycans attached to the nitrogen atoms of asparagine (Asn) residues found in a conserved consensus sequence (sequon). The sequon consists of Asn followed by any amino acid (X) except proline and ends with a serine (Ser) or threonine (Thr) (Asn-X-Ser/Thr, X ≠ Pro) (Kelleher and Gilmore, 2006; Opdenakker et al., 1993). In contrast, protein *O*-glycosylation is the addition of glycans linked to the oxygen atoms found in the hydroxyl groups of consensus-free predominantly Ser and Thr residues (Van den Steen et al., 1998). The building blocks forming the *N*- and *O*-linked glycans on human glycoproteins span a relative limited variety of neutral monosaccharides including the *N*-acetylhexosamines (HexNAc) i.e. *N*-acetyl-D-galactosamine (GalNAc) and *N*-acetyl-D-glucosamine (GlcNAc), the hexoses i.e. D-galactose (Gal), D-mannose (Man) and D-glucose (Glc), the deoxyhexose i.e. L-fucose (Fuc) and the acidic monosaccharide i.e. *N*-acetyl-D-neuraminic acid (NeuAc or sialic acid residues) (Stanley et al., 2009). Protein *N*-glycosylation is the main focus of this thesis and will be discussed further below.

1.4.1 Protein *N*-glycosylation

Protein *N*-glycosylation is an enzymatic process involving the addition and subsequent processing (removal and elongation) of complex glycans on proteins by the concerted actions of glycosyltransferases and glycosidases, in the presence of nucleotide sugar donors and their corresponding transporter molecules (Moremen et al., 2012). Under normal cellular

homeostasis, protein *N*-glycosylation has been shown to play important roles in various biological processes such as cell adhesion, cell proliferation, cell-cell communication and in mediating immunological responses (Varki, 2017). Alterations in protein *N*-glycosylation have been implicated in a wide spectrum of diseases such as congenital disorders of glycosylation (CDG) (Jaeken, 2010), immune disorders and cancer (Kizuka and Taniguchi, 2016), observations which further support the involvement of protein glycosylation in maintaining human health. Such alterations usually arise from enzymatic perturbations in the glycosylation machinery of the affected cells, but may similarly arise from variations in the other factors including the protein turnover and fluctuations in the level of nucleotide sugar donors.

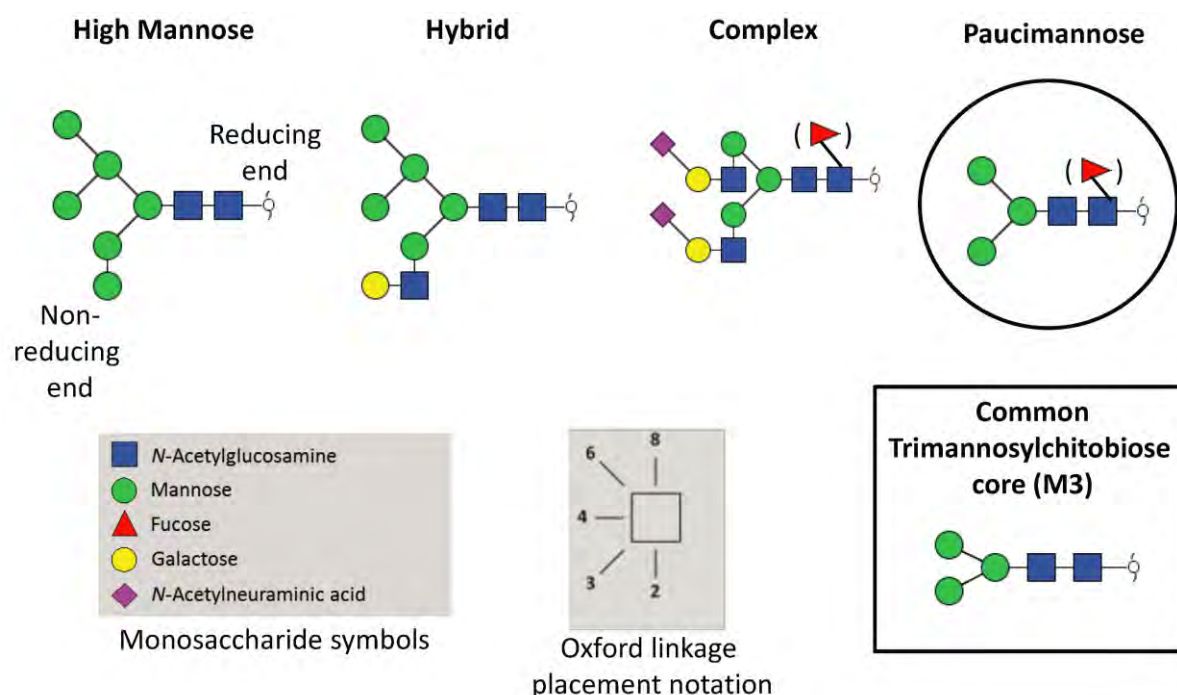


Figure 5. The main *N*-glycan types observed in humans. All *N*-glycans are based on the common trimannosyl-chitobiose core (M3, boxed) that may be decorated with different monosaccharide residues depending on the extent of glycan processing in the ER-Golgi apparatus secretory route. High mannose *N*-glycans containing a total of between five and nine Man residues are denoted as M5-M9 while hybrid *N*-glycans contain extended Man residues on the α 1,6 arm and a complex GlcNAc-based antenna linked to the α 1,3-mannose arm. Complex type *N*-glycans are characterised by the presence of GlcNAc residues on both the α 1,3- and α 1,6-mannose arms, which may be further extended with Gal, Fuc or sialic acid residues. Complex *N*-glycans can also exist as bi-, tri- and tetra-antennary structures. Paucimannose (circled) is a less reported truncated *N*-glycan type, which is the main focus of this thesis. This glycan class is unique since it consists of only the trimannosyl-chitobiose core or further truncated chitobiose core mannose-capped variants denoted M1(F)-M3(F). Both complex and paucimannosidic *N*-glycans may exist with or without core fucosylation in a α 1,6 linkage as shown in parentheses. Glycan structures are shown with reducing end indicator using monosaccharide symbols and conventions according to the Essentials of Glycobiology for symbol representation of glycan structures (Varki et al., 2015). Refer to “Symbols and Nomenclature” on page xiii for further information. The reducing end and non-reducing end terminals of the glycan structures are also indicated. Monosaccharide linkages are presented according to the angled Oxford linkage placement notation (Varki et al., 2015).

The structural commonality shared by all *N*-glycans conjugated to human glycoproteins is the trimannosyl-chitobiose core (Man α 1,6(Man α 1,3)Man β 1,4GlcNAc β 1,4GlcNAc β 1-Asn). This trimannosyl-chitobiose core structure is often further extended by a variety of monosaccharide residues to give rise to three main classes of human *N*-glycans (**Figure 5**): 1)

High mannose type *N*-glycans where only mannose residues are attached to the trimannosyl-chitobiose core, 2) Hybrid type *N*-glycans in which the Man α 1,6 arm of the core structure carries only mannose residues while the Man α 1,3 arm is GlcNAc modified and may be further extended by other monosaccharide residues including Gal and NeuAc residues, 3) Complex type *N*-glycans in which the core structure is modified by GlcNAc, on both the Man α 1,6 and Man α 1,3 arms and may receive further extension with, for example, Gal, GlcNAc and NeuAc. In addition, the complex and hybrid type *N*-glycans may be further modified by bisecting GlcNAc whereby a β 1,4-linked GlcNAc residue is attached to the β -Man of the trimannosyl-chitobiose core. Furthermore, the outer antennas and the chitobiose core of *N*-glycans can also be modified by Fuc, Gal and sialic acid residues as well as glycan PTMs i.e. *O*-acetylation, phosphorylation and sulfation (Stanley et al., 2009). The latter will not be covered further in this thesis. A fourth type of *N*-glycans known as the paucimannosidic *N*-glycans are well documented in invertebrates, in plants and in other lower organisms but have generally been considered to be absent and often regarded as degradation products or intermediates in vertebrates (Schachter, 2009; Zhang et al., 2003). However, paucimannosylation was recently indicated to be present in human bio-specimens (Dahmen et al., 2015; Everest-Dass et al., 2012). It is these unusual, rarely reported, paucimannosidic *N*-glycans in human neutrophils that are the main focus of study in this thesis.

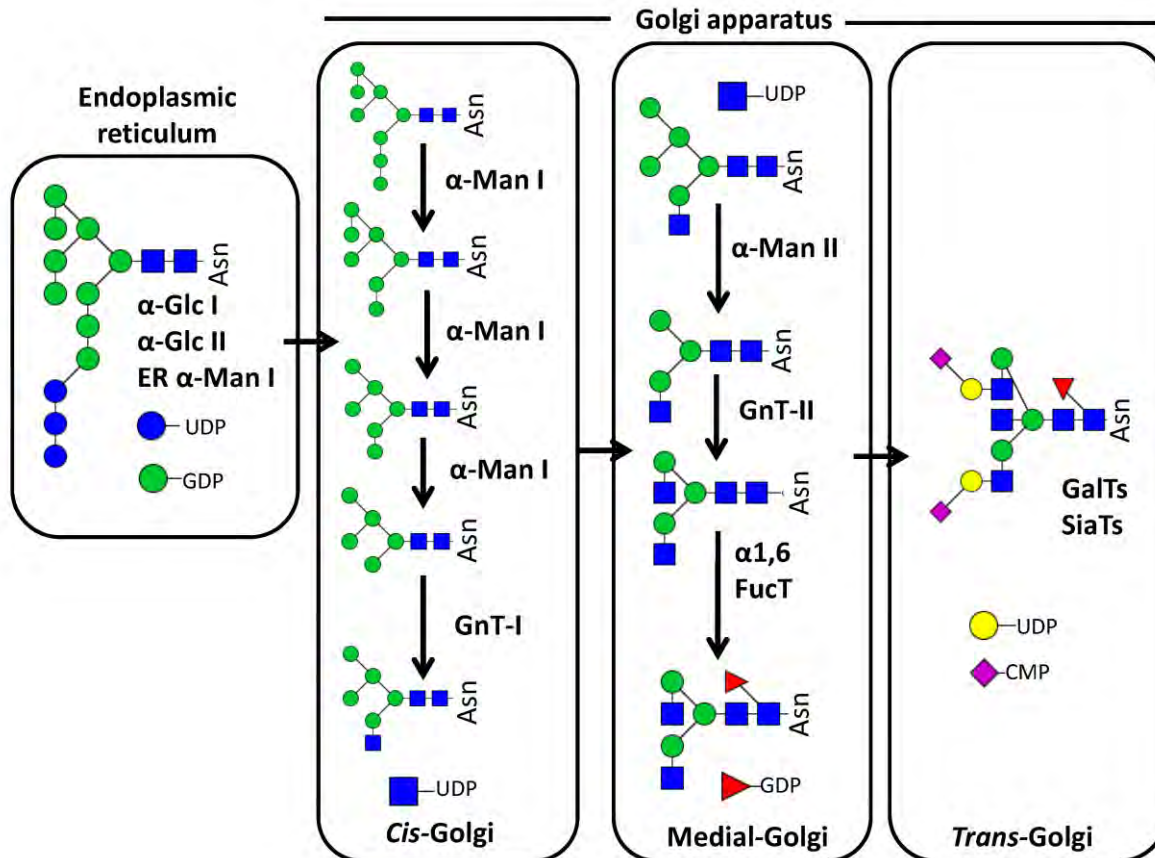


Figure 6. Protein *N*-glycosylation pathway in humans. The *N*-glycan precursor i.e. Glc₃Man₉GlcNAc₂ is transferred to the nascent protein from a lipid-linked carrier and then trimmed in the endoplasmic reticulum (ER) to remove the terminal Glc residues by ER glucosidase I (Glc I), allowing the chaperones calnexin and calreticulin to bind to the newly synthesised glycoprotein to promote proper folding of proteins (Hammond et al., 1994). The innermost Glc and Man residues are removed by α -Glc II and the ER-resident mannosidases before the processed glycoprotein is transported to the *cis*-, medial- and *trans*-Golgi for further trimming, elongation and branching of the *N*-glycan by the actions of the respective glycosyltransferases and a range of activated nucleotide sugar donors as indicated in the figure. This ordered maturation process allows for the generation of a diverse repertoire of *N*-glycans. The nucleotide sugar donors are required to be activated to a high energy donor form through kinase mediated reactions involving nucleoside triphosphates such as UDP, GDP and CMP.

1.4.2 *N*-glycoprotein synthesis

The biosynthesis of *N*-glycoproteins requires the enzymatic activity of a multitude of glycosyltransferases and glycosidases present in the ER and the Golgi apparatus found within eukaryotic cells (**Figure 6**). The process of protein *N*-glycosylation begins with the assembly

of common lipid-linked *N*-glycan precursors, Man₉GlcNAc₂ (M9), in the cytoplasmic side of the ER membrane and then later flipped into the ER lumen (Weerapana and Imperiali, 2006). This assembly process is finalised by the addition of Glc residues to the glycan precursor in the ER lumen, resulting in a Glc₃Man₉GlcNAc₂ precursor that is transferred “*en bloc*” as the common *N*-glycan to all *N*-glycoproteins. With only few exceptions to the rule (Gil et al., 2009), only the polypeptide consensus sequence motif (Asn-X-Ser/Thr, called a “sequon”) of the protein may receive *N*-glycans and this process is catalysed by the oligosaccharyltransferase (OST) complex (Aebi, 2013; Breitling and Aebi, 2013).

Once transferred to the protein backbone, the immature *N*-glycoprotein then undergoes further processing by exoglycosidases such as glucosidase I and II to remove the Glc residues at the non-reducing end of the M9 structure while the protein backbone folds to maturity. After ER-based trimming to the Man₈GlcNAc₂-Asn structure (M8), the glycoprotein is then sent to the *cis*-Golgi apparatus where further trimming of the Man residues takes place to give rise to the shorter forms of the high mannose structures (M5-M7) by the action of several Golgi α -mannosidases (Stanley, 2011). To generate the hybrid and complex type *N*-glycoproteins, GlcNAc residues are first transferred to the 3’Man arm of the Man₅GlcNAc₂Asn by the action of *N*-acetylglucosaminyltransferase-I (GlcNAcT-I or GnT-I) (Opdenakker et al., 1993; Varki, 1998). Frequently, α 1,6-linked fucosylation, also referred to as core fucosylation, is added to the innermost (reducing end) GlcNAc residue of the glycoprotein at this point by a dedicated α 1,6-fucosyltransferase encoded by the *FUT8* gene (Ihara et al., 2006). This is followed by further Man trimming to M3 and the action of GnT-II, GnT-IV and GnT-V present in the *cis*- and medial Golgi to allow further glycan elongation and branching of the structures that are mediated by the action of various galactosyltransferases (GalTs), fucosyltransferases (FuTs) and sialyltransferases (SiaTs) present in the latter part of the glycan processing cascade i.e. the medial and *trans*-Golgi (Stanley et al., 2009).

The elongation and branching of the complex type *N*-glycans may result in the formation of bi-, tri- and tetra-antennary structures by the enzymatic action of GnT-I to GnT-V. Further glycan diversity is generated through the addition of Fuc residues to the Gal or GlcNAc residues in the outer antennae in α 1,2-/ α 1,3- and α 1,4-linkages, giving rise to the so-called Lewis type antigens. The outer arm fucosylation is catalysed by α 1,2-/ α 1,3- and α 1,4-FUT. In addition, mature glycans are often terminated (or capped) with sialic acid residues that can be conjugated either in an α 2,3- or α 2,6-linkage to the penultimate Gal residues found at the non-reducing end of *N*-glycans by SiaTs (Stanley et al., 2009).

The stepwise enzymatic reactions of the *N*-glycoprotein biosynthesis describe how the three main types of *N*-glycans (high mannose, hybrid and complex type structures) are formed in humans. Glycoprotein micro-heterogeneity, the appearance of a glycoprotein in many similar glycoforms only structurally differing in their glycosylation, is a very common feature of protein *N*-glycosylation. The micro-heterogeneity is generated due to the fact that not all of these enzymatic reactions are going to completion and the fact that multiple glyco-enzymes are in direct competition with each other for the same glycan substrate. The biosynthetic glycoprotein processing described above can also be terminated at any of the above mentioned steps due to the lack of sufficient solvent site accessibility of the *N*-glycosylation sites (Thaysen-Andersen and Packer, 2012) as well as sterical hindrance from the more distal structural parts of the glycoprotein (Hang et al., 2015). In contrast, glycoprotein macro-heterogeneity, which refers to the fact that not all glycosylation sites are necessarily fully occupied by glycans, are driven by mechanisms early in the glycoprotein machinery involving the unfolded polypeptide chain and the OST complex (Zacchi and Schulz, 2015).

With the mechanisms described above, protein-specific glycosylation can arise whereby two proteins produced from the same cell at the same time can appear fundamentally different. In contrast, cell-specific glycosylation covering the well-established observations that different cells and even their subcellular compartments that generate and display different glycosylation features on their synthesised proteins, can arise due to spatio-temporal difference in their glycosylation machineries and other cellular and molecular factors (Lee et al., 2014a). Taken together, the fascinating features of the micro- and macro-heterogeneity of glycoproteins create unprecedented avenues for molecular complexity in the generation of glycoproteins, in particular for proteins carrying multiple glycans. This creates a magnitude of challenges for the analytical chemist aiming to understand the structure and ultimately, the function of this molecular micro-diversity.

Although the human protein *N*-glycosylation pathway has been well established for the three main types of *N*-glycoproteins (Schwarz and Aeby, 2011), the biosynthesis pathway of the unusual paucimannosidic *N*-glycoproteins in humans is still currently unknown. In this thesis, the biosynthetic machinery of paucimannosylation was investigated in human neutrophils. In order to understand how these modifications are synthesised, it is important to first characterise the *N*-glycan structures carried by neutrophil granule proteins and their exact attachment sites.

1.5 Analytical approaches for structural characterisation of protein *N*-glycosylation

The study of the entire set of *N*-glycans released from isolated glycoproteins or the entire repertoire of *N*-glycans present in a cell or an organism at a defined time and condition (jointly referred to as the “*N*-glycome”) is known as *N*-glycomics (Varki and Sharon, 2009). Researchers have often studied such system-wide features of the *N*-glycome utilising glycan-binding lectins or antibodies derived from plants and immunised animals, respectively, on glycan array type approaches or other visualisation techniques to map the presence of glycans motifs (Arthur et al., 2014; Monsigny et al., 1980; van Remoortere et al., 2003). These affinity-based methods have provided information on the type of glycan moieties present but they do not provide detailed information on the associated glycan structure. Furthermore, the recognition of the respective glycans using lectins is highly dependent on their binding affinity and the concentration and presentation of the carbohydrate ligands (Weis and Drickamer, 1996). In addition, antibodies utilised for glycan detection must also be highly specific toward their targets to avoid non-specific binding.

Substantial progress has been made in the development of alternative techniques in *N*-glycomics that has advanced our understanding on the structure of *N*-glycans and how the *N*-glycome is changing in various biological processes and diseases (Bhide and Colley, 2016; Stavenhagen et al., 2015a). As further elaborated below, with the advent of biological mass spectrometry (MS) in the eighties and its integration and implementation in proteomics in the early and late nineties (Hoffmann and Stroobant, 2007), liquid chromatography tandem mass spectrometry (LC-MS/MS) technologies have over the past decades matured to map, with precision and at reasonable speed, carbohydrates and even glycoconjugates (e.g. glycopeptides and glycolipids) at the system-wide level. However, *N*-glycomics does not, in itself, yield information about the glycan carrier molecule, the glycan attachment sites and the site occupancies of the *N*-glycan (Wuhrer et al., 2007). To complement *N*-glycomics, intact glycopeptides generated through “bottom-up” protease digestion are often the target analytes to provide a detailed site-specific glycosylation profile in order to obtain a holistic picture of the *N*-glycosylation profile on glycoproteins (Dalpathado and Desaire, 2008).

Unlike *N*-glycomics, which provides deep structural information of the *N*-glycans in a protein- and site-unspecific manner, glycopeptide analysis allows one to obtain information on the site-specific glycan monosaccharide composition (micro-heterogeneity) and the glycan

site occupancy (macro-heterogeneity), together with the relative abundance of the attached *N*-glycans carried by the glycoprotein being studied (Thaysen-Andersen and Packer, 2014). Such site-specific analyses are known as glycoproteomics when used to study the glycoproteome at the system-wide level (Bennun et al., 2016; Schumacher and Dodds, 2016; Thaysen-Andersen et al., 2016). Analytical glycoscientists have analysed intact glycoproteins using a “top-down” approach, allowing a more informative and complementary site-specific *N*-glycoprofile relative to the traditional “bottom-up” glycoprofiling based on glycopeptide analysis (Bourgoin-Voillard et al., 2014; Struwe et al., 2017; Thaysen-Andersen et al., 2015; Zoega et al., 2012). Although incredible powerful, the workflows and techniques for characterising intact glycoproteins (and even glycopeptides) remain relatively immature compared to *N*-glycomics (Chandler and Costello, 2016; Thaysen-Andersen et al., 2016). Nevertheless, glycan-, glycopeptide- and intact glycoprotein-based analyses should ideally be conducted in parallel in glycoprotein characterisation workflows to provide complementary and in-depth site-specific information on the glycoprotein of interest as emphasised in a recent inter-laboratory study (Leymarie et al., 2013).

Currently, the use of LC coupled to a MS has become the gold standard for *N*-glycomics (Jensen et al., 2012) and *N*-glycopeptide analyses (Parker et al., 2016). The separation power of the LC, together with the information of the mass of the analyte and its substituents provided by the mass spectrometer through MS/MS, has enabled LC-MS/MS to become the preferred analytical technique in many biochemistry laboratories around the world. For analytical glycoscience, LC-MS/MS has allowed for the confident identification and the relative quantitation of *N*-glycan structures and their glycosylation site attachment, derived from a single glycoprotein or from a complex glycoprotein mixture. Due to the versatility and inherent strength of LC-MS/MS, many other questions in structural glycobiology can be addressed using this technique. For example, the study of potential glycan biomarkers for cancer malignancies (Kizuka and Taniguchi, 2016; Lee et al., 2014b; Sethi et al., 2015) or for the characterisation of therapeutic immunoglobulin IgG antibodies in biotechnology industries (Abès and Teillaud, 2010; Reusch et al., 2013), have greatly benefited from the use of LC-MS/MS. Chromatographic separation of the *N*-glycans and *N*-glycopeptides are often required before they are detected using MS, in particular when samples of great molecular complexity are analysed. Importantly, the molecular retention behaviour on the LC column may additionally provide crucial structural information about the target analyte. In the following sections, LC-MS/MS analytical approaches utilised for the separation and detection

of *N*-glycans and *N*-glycopeptides performed in this thesis are discussed further below. Only LC-MS/MS topics relevant to the data presented in this thesis are introduced. The reader is directed to other excellent reviews for a more thorough introduction to mass spectrometry-based analysis of protein glycosylation (Khoo, 2014; Liu et al., 2014).

1.5.1 Chromatographic separation of *N*-glycans released from proteins

In *N*-glycomics, *N*-glycans are released enzymatically from glycoproteins using a recombinant hydrolase, peptide-*N*-glycosidase F (PNGase F), from *Flavobacterium meningosepticum* (Trimble and Tarentino, 1991). This process is also known as de-*N*-glycosylation and PNGase F is a widely used enzyme for de-glycosylation due to its ability to release the common *N*-glycan types such as high mannose, hybrid, and complex without any quantitative bias. PNGase F hydrolases the amide bond between the reducing end GlcNAc and Asn residues which forms the attachment site of the *N*-glycan. Upon cleavage, the previously glycan-bound Asn is deamidated, yielding a free aspartic acid residue. However, PNGase F has been documented to require an intact chitobiose core attached to the Asn in order for efficient de-*N*-glycosylation to occur (Chu, 1986). As discussed in the later chapters of this thesis, this structural requirement is a severe limitation and a potentially significant concern when considering the discovery of the ultra-truncated chitobiose core type (e.g. GlcNAc β Asn and Fuc α 1,6GlcNAc β Asn) *N*-glycans conjugated to intact bioactive neutrophil proteins. *N*-glycomics of samples containing such unusual *N*-glycan structures may be negatively impacted by the use of PNGase F by compromising the completion of the *N*-glycan release. In addition, PNGase F is also insensitive towards plant and insect glycoproteins carrying α 1,3-, as opposed to the human α 1,6-linked core fucosylation (Tretter et al., 1991). In this case, the related peptide-*N*-glycosidase A (PNGase A) typically derived from almonds has been used to effectively release and subsequently characterise plant- and insect-based *N*-glycans in an unbiased manner (Dam et al., 2013).

Following de-glycosylation, the released *N*-glycans can either be left in a free form for downstream analysis or chemically treated in various ways prior to analysis including 1) sodium borohydride (NaBH₄)-based reduction of the reducing end to alditols, 2) reductive amination involving reducing-end derivatisation with various fluorophores or alternative chemical groups that have other beneficial physicochemical properties such as enhanced ionisation or LC retention, and finally 3) permethylation of all the free hydroxyl groups of the glycans to allow for improved chromatographic separation and detection via ultra-violet or MS for improved *N*-glycan identification and characterisation (Lamari et al., 2003; Leymarie

et al., 2013). A range of LC methods have been developed and used successfully for the separation of released *N*-glycans such as hydrophilic interaction liquid chromatography (HILIC) (Vreeker and Wuhrer, 2017; Wuhrer et al., 2009), high pH anion exchange chromatography (Guignard et al., 2005), reversed-phase (RP) chromatography (Stavenhagen et al., 2015b) and size exclusion chromatography (Ziegler and Zaia, 2006). In addition to these somewhat more established approaches, porous graphitised carbon (PGC), the principal LC method used for *N*-glycomics analysis in this thesis, has also gained traction in recent years for the characterisation of released *N*-glycans (Kolarich et al., 2015; Ruhaak et al., 2014).

The biggest advantage of using PGC over other stationary phases is its ability to separate non-derivatised *N*-glycan isomers with high structural resolution (Pabst and Altmann, 2008). PGC has showed good retention capability towards polar as well as hydrophobic compounds, but the exact mechanisms of this mixed-mode retention behaviour and how it applies to the elution pattern of *N*-glycans are questions still not fully understood (Buszewski and Noga, 2012). Nonetheless, PGC provides separation of *N*-glycan based on their primary, secondary and tertiary structures; even subtle structural differences such as the anomericity (α -/ β -) of a single glycosidic bond can provide shape-based discrimination in PGC, which is an effective way to separate isomeric (i.e. same monosaccharide composition and same mass with different monosaccharide linkages) and isobaric (i.e same monosaccharide composition and same mass with different branch extensions) structures (Giuseppe et al., 2013; Pabst et al., 2007). For example, different sialyl-linkages can easily be differentiated from each other using PGC-LC: α 2,6-linked sialo-glycans are known to elute before the same structure terminating with α 2,3-sialylation (Jensen et al., 2012). Separation of the isomers arising from α 1,3- and α 1,6- mannosyl differences as often seen in the high mannose type structures can also be achieved using PGC-LC (Pabst et al., 2012).

Therefore, it is clear that isomeric and isobaric *N*-glycans directly influence their PGC elution behaviour and allows a retention pattern to be created that is highly reproducible. This has allowed the generation of a PGC retention time “library” of the most common types of *N*-glycans, which facilitates a rapid and confident identification of observed structures by correlation of the PGC retention times to the *N*-glycans in the library (Hitchen and Dell, 2006; Pabst et al., 2007). Coupled with the molecular mass determination of MS and the sequencing features of MS/MS, PGC-LC-MS/MS is a powerful analytical technique that allows the *N*-glycan structures to be elucidated with confidence. Therefore, PGC-LC-MS/MS was the

chosen chromatographic method used in this thesis for the separation and detection of *N*-glycans.

1.5.2 Chromatographic separation of protease-derived glycopeptides

Prior to MS and MS/MS acquisition, suitable (i.e. MS-friendly) glycopeptides need to be generated to ensure optimal LC-MS/MS separation and detection. As commonly used in conventional proteomics, trypsin is favoured as a proteolytic enzyme over other proteases due to its low cost, high activity and specificity towards arginine (Arg) and lysine (Lys) residues at the C-terminus (Leymarie et al., 2013; Wührer et al., 2005). The Arg and Lys cleavage site specificity is convenient since these basic amino acid residues appear with the appropriate frequency in human proteins to typically facilitate the generation of peptides of ~10-40 amino acid residues in length that are ideally suited for LC-MS/MS. In addition, trypsin is also usually capable of accessing their proteolytic sites even in the presence of large branched and bulky *N*-glycans occupying nearby Asn sites although some steric hindrance, in particular when *N*-glycans are core fucosylated, has been observed (Deshpande et al., 2010). The specific cleavage of trypsin also allows the generation of appropriately cationic-charged tryptic peptides and therefore enhances their ionisation efficiency for MS detection (Wührer et al., 2007). It should be noted that other specific proteases such as Asp-N and Lys-C may also be used alone or in conjunction with trypsin, to produce suitable glycopeptide fragments for specific glycoproteins of interest (Gadgil et al., 2006). Furthermore, non-specific proteases such as pronase and chymotrypsin have also been used to obtain small MS-friendly populations of glycopeptide fragments, but at the cost of introducing peptide heterogeneity into the samples which unnecessarily increase the analyte complexity (Zhu and Desaire, 2015).

C₁₈ RP-LC is the most common type of chromatographic separation method used in *N*-glycopeptide analysis, due to its superior peak capacity for glycopeptides compared to other LC separation techniques such as HILIC (Kolarich et al., 2012). It also enables better resolution by the introduction of new column packing technologies achieving near-zero dead volumes and capacity for extremely low flow rates to yield narrow elution windows of glycopeptides, thereby providing high detection sensitivity (Thaysen-Andersen and Packer, 2014).

In RP-LC, the retention mechanism of peptides is based on the hydrophobicity of the analysed peptides. Peptide elution is typically achieved with a gradient of an increasing concentration

of organic solvent such as acetonitrile, in the presence of acidifiers and ion pairing agents such as formic acid (FA) or trifluoroacetic acid (TFA) at low concentrations (Gong, 2015). Therefore, hydrophilic peptides are poorly retained on these stationary phases and are the first to be eluted. *N*-glycopeptides that share a common peptide moiety, but differ in their conjugated *N*-glycan, elute close together in clusters. The non-glycosylated peptide variant, being a bit more hydrophobic due to the missing *N*-glycan, typically elute a few minutes later. In addition, the significant degree of localised hydrophilicity of the conjugated glycan is attributed to its large number of free hydroxyl groups.

It is also this common property of all *N*-glycopeptides, displaying a localised hydrophilicity that enables the selective enrichment of *N*-glycopeptides from the relatively hydrophobic non-glycosylated peptides on HILIC stationary phases. Glycopeptide enrichment is important prior to LC-MS/MS-based peptide analysis due to the sub-stoichiometry of the glycopeptides and the fact that their MS signals are suppressed relative to the non-glycosylated peptides (Stavenhagen et al., 2013). The use of HILIC, which involves a broad spectrum of stationary and mobile phases (Gama et al., 2012) for the enrichment of *N*-glycopeptide, has been instrumental in the sample preparation and the maturation of the glycoproteomics workflow (Huang et al., 2016; Parker et al., 2013).

In general, the retention mechanism of all HILIC variants can be described as being primarily driven by hydrophilic partitioning of the glycopeptides into the watery layer positioned around the hydrophilic solid phase. In the presence of highly hydrophilic solvents such as water, the partitioned/retained glycopeptides can be competitively eluted (Thaysen-Andersen et al., 2011). In this thesis, zwitterionic HILIC (ZIC-HILIC) was chosen to enrich glycopeptides generated from the protease digestion of neutrophil granule proteins. Solid phase extraction (SPE) formats of ZIC-HILIC columns were used in an off-line manner during sample preparation in this thesis rather than the on-line approach (Di Palma et al., 2011).

Another advantage of performing glycopeptide enrichment or peptide depletion is to overcome the higher ionisation efficiencies of non-glycosylated peptides over glycosylated peptides (Stavenhagen et al., 2013). With LC-MS/MS, the micro-heterogeneity of the enriched glycopeptides can often relatively be determined on a single glycoprotein level. However, it should be noted that prior enrichment should not be performed if information on the site-specific glycan occupancy is required since both glycosylated and non-glycosylated

peptides are needed to be present, in their original ratios, in order to obtain macro-heterogeneity information on the *N*-glycosylation sites on the glycoprotein.

1.5.3 Mass spectrometric analysis of protein *N*-glycosylation

In combination with the off-line fractionation using ZIC-HILIC SPE and on-line separation using RP-LC-MS/MS approaches discussed above, MS is widely used for the analysis of both *N*-glycans and *N*-glycopeptides (Patrie et al., 2013). The use of MS in the analysis of protein *N*-glycosylation not only accurately provides the molecular masses of the *N*-glycans and *N*-glycopeptides, it also provides valuable information to assign their detailed structures based on their fragment ion patterns. In a typical MS experiment, charged analyte ions are generated in the ion source that are then introduced into the mass spectrometer where they are separated based on their mass-to-charge ratio (m/z). The m/z of the ions are then measured by the conversion of electrical signals produced by the ions by a detector into corresponding mass spectra consisting of the m/z ratio of the charged ions on the horizontal axis and their signal intensities on the vertical axis. Due to the extreme complexity and volume, such mass spectral data are nowadays typically viewed and processed in semi- or fully- automated workflows using advanced computer software (Bern et al., 2012; Loziuk et al., 2017). However, as further discussed later, the slow maturation of the glycosciences relative to other fields in biochemistry and molecular biology has meant that, glyco-informatics is trailing somewhat behind after comparative areas such as proteomics, which, in turn, still leaves a significant amount of manual annotation of glyco-mass spectra to the user.

The “soft” ionisation methods such as electrospray ionisation (ESI) are typically used for biomolecules including *N*-glycans, *N*-glycopeptides and glycoproteins to maintain the molecular integrity in the ionisation process (Bousfield et al., 2015; Ho et al., 2003; Joanne et al., 2007). The application of an electrical field to a capillary found in the MS instrument generates charged droplets as solvent containing the analytes are passed through at low flow rates. These charged droplets, in the presence of an inert gas such as nitrogen at atmospheric pressure and high temperature, shrink in size and thus, allow them to enter the mass spectrometer as desolvated charged gas phase ions (Hoffmann and Stroobant, 2007). Although the positive ionisation polarity mode has been used for *N*-glycan analysis, negative ionisation polarity mode is often preferred as it produces more informative cross-ring and glycosidic fragment cleavage products compared to positive ionisation (Harvey, 2005b). An informative MS/MS fragment profile allows detailed structural characterisation of the released *N*-glycans provided that the spectrum can be interpreted. In contrast, positive ionisation is preferred for

MS analysis of glycopeptides due to the superior ionisation of tryptic glycopeptides in this polarity mode (Wuhrer et al., 2005). The positive ionisation mode also allows the abundance of related glycopeptides sharing the same peptide moiety to be estimated based on their relative signal strength in ESI-MS (Leymarie et al., 2013; Thaysen-Andersen et al., 2009).

As the charged gas phase ions enter the mass spectrometer, they are separated based on their m/z ratio in the mass analyser. In this thesis, mass spectrometers consisting of various mass analysers with different separation principles have been utilised e.g. 3D ion trap (IT), quadrupole (Q) time-of-flight (TOF), linear ion trap quadrupole (LTQ) and Orbitrap analysers were all used to provide mass information of the analytes of interest. However, the mass of the molecular ion alone usually does not provide sufficient information to allow the analytical chemist to determine the detailed structure of the compound in question. This is particularly true for *N*-glycan or *N*-glycopeptide analysis, where the presence of multiple isomeric and isobaric structures frequently make the structural elucidation significantly more challenging than other biomolecules.

In order to identify the monosaccharide compositions, linkages, and branching features of *N*-glycans and to determine the glycopeptide sequence and its attached glycan moiety, MS/MS fragmentation is required in conjunction with an accurate mass of the glyco-analyte (Everest-Dass et al., 2013b; Wuhrer et al., 2007). The ionised molecule of interest, also known as the precursor ion, is isolated in the mass spectrometer and may be collided by inert gas molecules such as helium or nitrogen in the low pressure vacuum environment of the collision cell. Such collisions generate heat energy, which is transferred to and distributed across the analyte as vibrational energy, facilitating cleavage at the “weakest” points of the molecule. Similar to the precursor ion, the accurate m/z of the generated fragment ions (also known as product ions) are detected in the mass analyser. The multiple fragmentation (or dissociation) methods utilised in this thesis for *N*-glycan and *N*-glycopeptide analysis will be discussed below.

For *N*-glycan analysis, collision-induced dissociation (CID) was the fragmentation method of choice in this thesis. During CID fragmentation of *N*-glycans, cleavage of the glycosidic bonds and cross-ring fragmentation have been reported (Harvey, 2005a, b, c; Harvey et al., 2008). The nomenclature of the glycan fragments formed as proposed by Domon and Costello has been well integrated in the literature (Domon and Costello, 1988) (**Figure 7**). Briefly, the glycan fragments generated containing the non-reducing end of the glycan are described as A, B and C ions while the fragment ions containing the reducing end are described as X, Y and Z

depending on which chemical bond of the glycan is broken. Other more exotic glycan fragments including the D-type ions also exists and can indeed be very prominent and useful.

As briefly mentioned above, *N*-glycans fragmented under negative ionisation mode generally produce more informative fragment signatures compared to positive ionisation mode, which may help to distinguish hard-to-identify isomers of reduced *N*-glycans (Harvey, 2005a, b). For example, the identification of a unique D ion (m/z 979) or a D-18 ion (m/z 961) during MS/MS fragmentation signifies the presence of a terminal sialylated antennae on the α 1,6-Man arm (Everest-Dass et al., 2013a). Thus, the PGC-LC retention times, precursor ion mass and the CID-MS/MS fragmentation data allow confident characterisation of released and reduced *N*-glycans. In addition, supporting online databases and tools that assist in the process of structural elucidation of glycans are available. For example, UniCarb-KB (Campbell et al., 2014b), GlycoMod (Cooper et al., 2001) and Glycoworkbench (Ceroni et al., 2008).

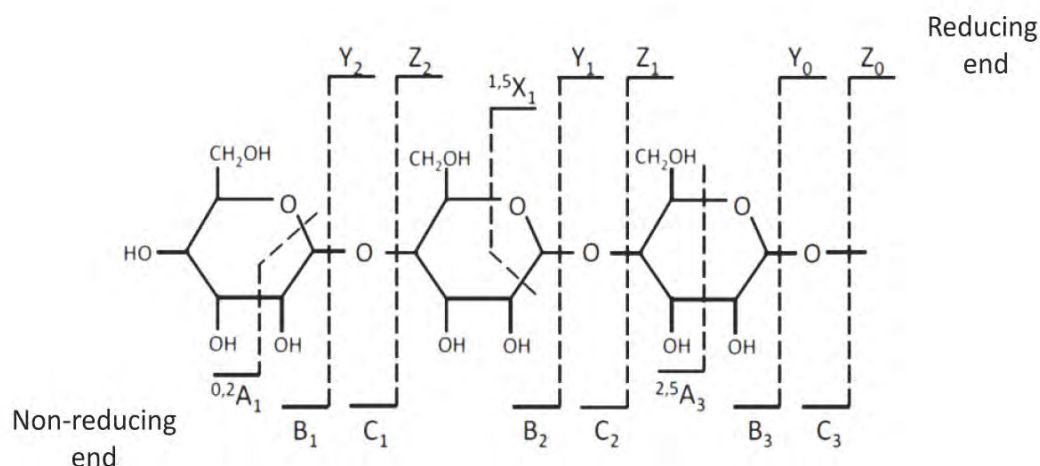


Figure 7. Nomenclature of the fragment (product) ions of a linear glycan as proposed by Domon and Costello (Domon and Costello, 1988). A- and X-type ions denote fragments formed upon cross-ring cleavages; The B, C, Y, Z ions denote fragments formed by glycosidic bond cleavages. The subscripts of the B/C and Y/Z ion series denote the number of monosaccharide residues numbered from the non-reducing and reducing end.

Although data analysis and the annotation of the obtained MS/MS *N*-glycan spectra have made significant progress in terms of software and database availability for automated analysis (Loziuk et al., 2017; Yu et al., 2016), the structural characterisation of intact glycopeptides is still highly dependent on manual mass spectral analysis by expert users.

Similar to the fragmentation of *N*-glycans, CID fragmentation can also be applied to *N*-glycopeptide analysis, which is typically recorded in the positive ionisation mode. CID-based fragmentation of *N*-glycopeptides is dominated by Y-type ions and diagnostic oxonium ions as well as low mass B-type ions in the MS/MS spectra. Diagnostic oxonium ions are the product ions arising from the cleavage of the glycosidic bonds linking the respective monosaccharide residues with charge retention found at the lower *m/z* region (Conboy and Henion, 1992; Huddleston et al., 1993). These characteristic ions allow identification of intact glycopeptides in the MS/MS spectra following CID fragmentation. The glycopeptide fragments ions follow the same Domon and Costello nomenclature (Domon and Costello, 1988). These ions arise from cleavage of the relatively weak glycosidic bonds between the monosaccharide residues due to the low energy potential of CID. When performed in an ion trap, this dissociation mode is referred to as resonance activation CID or more simply IT-CID. Cleavage of the peptide backbone of glycopeptides is not usually observed under IT-CID (Hogan et al., 2005).

Fragment spectra containing *N*-glycopeptides may be crudely classified by the observation of low molecular mass diagnostic oxonium ions such as HexNAc (m/z 204.1), NeuAc (m/z 292.1), Hex-HexNAc (m/z 366.1) and NeuAc-Hex-HexNAc (m/z 657.2). In addition, higher molecular mass fragment ions (peptide plus glycan fragments, Y-type ions) generated from the cleavage of the glycosidic bonds and charge retention of the peptide provides additional hints of the spectra, corresponding to a “true” glycopeptide (Wuhrer et al., 2007). These features allow the identification of the monosaccharide composition of the attached *N*-glycan carried by the respective glycopeptide. It should be mentioned that higher energy collision dissociation (HCD) fragmentation, a variant of CID performed on Orbitrap and LTQ type instruments in dedicated collision cells, has also been applied successfully for the MS/MS analysis of *N*-glycopeptides (Singh et al., 2012). In addition to their better mass accuracy and resolution, one of the benefits associated with HCD of *N*-glycopeptides is that the low mass diagnostic ions are very intense and readily detectable due to the slightly higher fragmentation energy and avoidance of the low mass cut-off (so-called “1/3 rule”) observed with the use of regular IT-CID.

Unfortunately, the use of neither CID nor HCD fragmentation can provide sufficient peptide backbone information of the glycopeptides in order to pinpoint the attachment site of the glycan. The use of electron transfer dissociation (ETD) MS/MS was shown to generate additional and indeed orthogonal structural peptide information when applied to glycopeptides. In ETD MS/MS, fragmentation is facilitated by the transfer of electrons carried by so-called reactants such as fluoranthene to the positively charged amino acid residues of the (glyco)peptide (Scholten et al., 2011). Importantly, the attached glycan moiety has been demonstrated to remain conjugated and intact during ETD-MS/MS (Alley et al., 2009; Trinidad et al., 2013). Therefore, utilising both CID- and/or HCD- and ETD-MS/MS fragmentation, which can be performed either in an alternating fashion in the same analysis or in separate LC-MS/MS runs, is an approach to achieve a more complete characterisation of a glycopeptide. This includes providing information on the glycan structure (typically monosaccharide composition, sequence and topology) and the micro-heterogeneity of *N*-glycosylation sites that can be provided by CID-/HCD- fragmentation. In contrast, ETD-MS/MS allows the provision of information on the peptide sequence and the glycosylation site occupied by the respective *N*-glycan structures (Conboy and Henion, 1992; Hogan et al., 2005; Ma et al., 2016). The limitation of using these multiple dissociation modes in an alternating fashion is that fewer precursor ions can be selected for fragmentation in a given

LC-MS/MS run due to a longer duty cycle and therefore, giving a lesser coverage of the glycoproteome present in the analyte of interest. Alternatively, multiple LC-MS/MS runs with separate fragmentation modes can be acquired at the expense of sample sensitivity and longer instrument time usage.

1.5.4 Mass spectrometric analysis of intact glycoproteins

Although the analysis of *N*-glycosidase released *N*-glycans and trypsin-digested glycopeptides are able to provide the micro- and macro-heterogeneity of *N*-glycosylated glycoproteins, glycoproteins can also be directly analysed by MS without the need for digestion (Heck, 2008; Yang et al., 2017). This approach, also known as top-down MS, involves the introduction of intact glycoproteins into the MS via direct infusion without any chromatography or through chromatographic separation, either under denaturing conditions or non-denaturing conditions (native). Native conditions are generally preferred compared to denaturing conditions as the use of detergents or organic solvents can disrupt the tertiary and quaternary structures of (glyco)proteins, leading to a loss of spatial protein information including protein-protein and protein-ligand interactions upon protein denaturation (Yang et al., 2017). Glycoproteins are known to consist of an ensemble of structurally-related glycoforms as a result of their variation in glycosylation site occupancies (macro-heterogeneity), and attached glycan structures (micro-heterogeneity) arising from the incomplete and competing actions of a myriad of glycosylation enzymes present in the Golgi apparatus (Stanley, 2011). It should be noted that the macro- and micro-heterogeneity diversity is not limited to a single glycoprotein but rather the total pool of glycoproteins present within the sample of interest. In contrast to the bottom-up approach, native MS is able to provide a more complete picture of the entire ensemble of glycoforms of a glycoprotein, which is particularly important to obtain for glycoproteins carrying multiple occupied glycosylation sites conjugated with different glycans and to interrogate any potential “cross-talk” between the glycosylation status of the glycoprotein and other PTMs. Such information cannot be obtained by glycopeptide analysis. Therefore, native MS provides a more detailed and holistic description of the macro- and micro-heterogeneity of glycoproteins. All these are made possible with high mass accuracy/high resolution ESI-QTOF-MS (Heck and Van Den Heuvel, 2004; Thaysen-Andersen et al., 2015) or the recently introduced high-resolution hybrid and tribrid Orbitrap (e.g. Fusion Lumos Orbitrap, Thermo Scientific) MS instruments (Gault et al., 2015) and ion-mobility (e.g. Vion IMS QTOF, Waters) MS instruments (Struwe et al., 2017). This is coupled with their ability to perform CID- or ETD/HCD-MS/MS which

are now increasingly able to ionise, accurately measure and sequence intact glycoproteins to provide a more accurate global distribution of these observed glycoforms. Spatial information of the glycoprotein conformation and glycoprotein-glycoprotein interactions can also be obtained through native MS with little prior sample handling.

During native MS analysis, glycoproteins maintain their folded structures in the gas phase and this limits the accumulation of charged protons to basic amino acid residues present on their surfaces during the ESI process. Therefore, intact glycoproteins analysed under native conditions on average, have lower charge state ions compared to the ions of denaturing glycoproteins where they generally take on higher charge states (Leney and Heck, 2017). As a result, glycoproteins takes on a narrower charge state distribution and the centre of the charge envelopes shift towards a higher m/z region under native MS. This enables a larger space between the adjacent charge state ions, allowing these charge state ions to be separated and resolved from the significant mass distribution arising from the highly heterogeneous glycosylation of glycoproteins. More importantly, this results in a less congested mass spectrum in native MS, allowing a higher signal:noise ratio to enhance the detection of low-abundance glycoforms upon deconvolution. Deconvolution is defined as the process where the original mass spectrum from the total signal intensity of multiple charge state envelopes of the analyte are processed by advanced algorithms to obtain a non-charged single molecular mass (in Daltons) in order to simplify data interpretation and identify the molecular ion(s). Deconvolution algorithms such as maximum entropy were described previously in early biological ESI-based MS (Reinhold and Reinhold, 1992), but are constantly being further developed and refined (Liu et al., 2010). In contrast to native MS, signal ions in a narrower m/z window under denaturing MS conditions creates undesirable overlapping of charge state ions, making it impossible to resolve the spectrum.

The use of native MS for the study of intact *N*-glycoproteins has been successfully applied to *N*-glycoproteins with one or two occupied glycosylation sites such as monoclonal antibodies (Rosati et al., 2013) and chicken ovalbumin (Yang et al., 2013). More complex and highly heterogeneous glycosylated proteins are still extremely challenging for native MS analysis due to the presence of overlapping glycoforms in the mass spectrum (Unpublished observations). Glycoprotein-regulated interactions such as antibody-antigen complexes (Dyachenko et al., 2015) or glycoprotein complexes involved in complement activation (Franc et al., 2017) have also been reported. However, there are still significant limitations to native MS profiling of intact glycoproteins. Currently, top-down glycoprotein analysis is of

low-throughput and is highly dependent on the ionisation potential and the stability of the analyte of interest. Furthermore, the exact stereochemistry of a glycan, including its glycosidic linkages cannot be determined through native MS. Thus, it is not possible to distinguish between the isobaric hexoses such as Glc, Gal and Man and the amino sugars such as GlcNAc and GalNAc moieties because of their identical molecular mass (Catherman et al., 2014; Larsen et al., 2006). Therefore, native MS, at this moment, is most suitable as an additional level of glyco-analysis, serving as a complementary tool in addition to the more established methodologies involving the analysis of *N*-glycans and *N*-glycopeptides derived from the glycoprotein of interest.

1.6 Alterations in protein *N*-glycosylation during inflammation and infections

The established MS-based methods described above have enabled protein-specific as well as cell- and tissue-wide investigations to map the alterations of protein *N*-glycosylation during inflammatory conditions, such as cancer malignancies and auto-immune diseases. For example, LC-MS/MS based glycopeptides analysis has identified that the surfaces of cancer cells display increased protein sialylation relative to normal cells and that this altered glyco-phenotype is associated with an increase in the enzymatic activities of sialyltransferases (Warren et al., 1972). Cancer-specific changes in the sialyl-linkages were also observed on cancer glycoproteins (Kaprio et al., 2015; Lee et al., 2014b). In addition to sialylation, an increase in fucosylated *N*-glycans was also observed in breast cancer tumours (Goetz et al., 2009). Furthermore, a decrease in terminal galactosylation on the immunoglobulin IgG was associated with the rheumatoid arthritis (Abès and Teillaud, 2010).

In addition to the inflammatory diseases, alterations in protein *N*-glycosylation were also observed in infectious diseases. For example, a decrease in protein sialylation and a range of other associated changes in the *N*-glycosylation have been suggested to promote chronic *P. aeruginosa* lung infections in CF patients (van Heeckeren et al., 2004; Venkatakrisnan et al., 2015). Furthermore, *Trypanosoma cruzi* infections have also been documented to alter the protein sialylation of human cell surface proteins by transferring α 2,3-linked sialic acid from the host cell surface sialo-glycoconjugates to terminal Gal residues on the parasite surface glycoconjugates. The transfer of sialylation onto the parasite surface was found to be mediated by a unique trans-sialidase and this process was suggested to play a role in the

invasion of the parasite into the host, resulting in Chagas' disease (Colli, 1993; Nardy et al., 2016).

As described above, it is evident that the *N*-glycosylation of proteins is often altered in inflammation and infection. However, protein sialylation, fucosylation and galactosylation have mostly been the focus of these studies while protein mannosylation has received relatively less attention. In fact, it appears that mannose; an abundant monosaccharide residue found in high mannose and paucimannosidic *N*-glycans and in other glycoconjugates, generally has been overlooked or disregarded as a potentially important glycoepitope in the human repertoire of glycan features. Furthermore, knowledge on the role of protein paucimannosylation in humans is equally sparse. However, as detailed below in **Publication I**, there is an increasing volume of evidence in the literature documenting the important roles played by these glycoepitopes during inflammatory and infectious diseases. The presence and involvement of mannosyl as important glycoepitopes in human innate immunity, their potential interactions and functional consequence with mannose recognising receptors are discussed in this review article (**Publication I**). The main findings and conclusions derived from the review are briefly discussed following the attached publication, as well as the specific research aims and the experimental overview of this thesis.

1.7 Publication I: Emerging roles of protein mannosylation in inflammation and infection

Publication: Loke, I., Kolarich, D., Packer, N.H., Thaysen-Andersen, M., 2016. Emerging roles of protein mannosylation in inflammation and infection. *Molecular Aspects of Medicine* 51, 31-55. doi:10.1016/j.mam.2016.04.004

Reprinted from *Molecular Aspects of Medicine*, 51, Loke I., Kolarich, D., Packer, N.H., Thaysen-Andersen, M., Emerging roles of protein mannosylation in inflammation and infection, 31-55, © 2016, with permission from Elsevier.

Author contributions: IL, DK and MTA wrote the paper. IL, DK, MTA and NHP reviewed and edited the paper.

Specifically, my supervisor, Dr. Morten Thaysen-Andersen and I were responsible for the concept, design and preparation of the manuscript. I prepared all the sections, while Dr. Daniel Kolarich contributed to the section on the interaction of mrCLRs and mannosylated glycoconjugate ligands during allergy.



Contents lists available at ScienceDirect

Molecular Aspects of Medicine

journal homepage: www.elsevier.com/locate/mam

Review

Emerging roles of protein mannosylation in inflammation and infection

Ian Loke ^a, Daniel Kolarich ^b, Nicolle H. Packer ^a, Morten Thaysen-Andersen ^{a,*}^a Department of Chemistry and Biomolecular Sciences, Macquarie University, Sydney, NSW 2109, Australia^b Department of Biomolecular Systems, Max Planck Institute of Colloids and Interfaces, 14424 Potsdam, Germany

ARTICLE INFO

Article history:

Received 21 January 2016

Revised 5 April 2016

Accepted 10 April 2016

Available online 13 April 2016

Keywords:

Mannose

Paucimannosylation

Inflammation

Infection

C-type lectin

Glycoprotein

ABSTRACT

Proteins are frequently modified by complex carbohydrates (glycans) that play central roles in maintaining the structural and functional integrity of cells and tissues in humans and lower organisms. Mannose forms an essential building block of protein glycosylation, and its functional involvement as components of larger and diverse α -mannosidic glycoepitopes in important intra- and intercellular glycoimmunological processes is gaining recognition. With a focus on the mannose-rich asparagine (*N*-linked) glycosylation type, this review summarises the increasing volume of literature covering human and non-human protein mannosylation, including their structures, biosynthesis and spatiotemporal expression. The review also covers their known interactions with specialised host and microbial mannose-recognising C-type lectin receptors (mrCLRs) and antibodies (mrAbs) during inflammation and pathogen infection. Advances in molecular mapping technologies have recently revealed novel immuno-centric mannose-terminating truncated *N*-glycans, termed paucimannosylation, on human proteins. The cellular presentation of α -mannosidic glycoepitopes on *N*-glycoproteins appears tightly regulated; α -mannose determinants are relative rare glycoepitopes in physiological extracellular environments, but may be actively secreted or leaked from cells to transmit potent signals when required. Simultaneously, our understanding of the molecular basis on the recognition of mannosidic epitopes by mrCLRs including DC-SIGN, mannose receptor, mannose binding lectin and mrAb is rapidly advancing, together with the functional implications of these interactions in facilitating an effective immune response during physiological and pathophysiological conditions. Ultimately, deciphering these complex mannose-based receptor–ligand interactions at the detailed molecular level will significantly advance our understanding of immunological disorders and infectious diseases, promoting the development of future therapeutics to improve patient clinical outcomes.

© 2016 Elsevier Ltd. All rights reserved.

Chemical compounds studied in this article: D-Mannose (PubChem CID: 18950) Mannose α 1,3-Mannose (PubChem CID: 3476988)

Abbreviations: 3D, three-dimensional; ANCA, anti-neutrophilic cytoplasmic antibodies; APC, antigen-presenting cell; ASCA, anti-*Saccharomyces cerevisiae* antibodies; Asn, asparagine; CD, cluster of differentiation; CLR, C-type lectin receptor; CRC, colorectal cancer; CRD, carbohydrate recognition domain; Cys, cysteine; DAMP, damage-associated molecular pattern; DC, dendritic cell; DC-SIGN(R), dendritic cell-specific intercellular adhesion molecule-3-grabbing non-integrin (related); DCIR, dendritic cell immunoreceptor; ER, endoplasmic reticulum; Fc γ R, Fc gamma receptor; Fc ϵ R1, Fc epsilon receptor type 1; FL, follicular lymphoma; Fuc, fucose; FVIII, factor VIII; Gal, galactose; GalNAc, *N*-acetylgalactosamine; Glc, glucose; GlcNAc, *N*-acetylglucosamine; GPI, glycosylphosphatidylinositol; HA, hemagglutinin; HIV, human immunodeficiency virus; ITAM/ITIM, immunoreceptor tyrosine-based activating/inhibiting motif; *K*_a, dissociation constant; LAMP-2, lysosomal-associated membrane protein 2; LPS, lipopolysaccharide; Man, mannose; ManLAM, mannose-capped lipoarabinomannan; MASP, MBL-associated serine protease; MBL, mannose-binding lectin; mDC, myeloid dendritic cells; Mincle, macrophage inducible C-type lectin; MR, mannose receptor; mrAb, mannose-recognising antibody; mrCLR, mannose-recognising C-type lectin receptor; Mtb, *Mycobacterium tuberculosis*; NeuAc, *N*-acetylneuraminic acid; NF- κ B, nuclear factor kappa-light-chain-enhancer of activated B cells; PAMP, pathogen-associated molecular pattern; pDC, plasmacytoid dendritic cells; PRR, pattern recognition receptor; Ser, serine; SLE, systemic lupus erythematosus; SP-A/D, surfactant protein A/D; TB, tuberculosis; Thr, threonine; TLR, toll-like receptor; UTI, urinary tract infection.

* Corresponding author: Biomolecular Frontiers Research Centre, Department of Chemistry and Biomolecular Sciences, Macquarie University, Sydney, NSW 2109, Australia. Tel.: +61 2 9850 7487; fax: +61 2 9850 6192.

E-mail address: morten.andersen@mq.edu.au (M. Thaysen-Andersen).

<http://dx.doi.org/10.1016/j.mam.2016.04.004>

0098-2997/© 2016 Elsevier Ltd. All rights reserved.

Contents

| | |
|---|----|
| 1. Introduction | 32 |
| 2. Structural diversity and spatiotemporal expression of protein mannosylation | 33 |
| 2.1. Mannose is a central component of protein N-glycosylation | 33 |
| 2.2. Human high mannose glycoproteins | 33 |
| 2.3. Non-human mannosidic N-glycosylation | 35 |
| 2.4. Paucimannosidic glycoproteins | 35 |
| 3. Mannosidic epitope recognition by specialised human C-type lectin receptors | 36 |
| 3.1. DC-derived mrCLRs | 36 |
| 3.1.1. DC-SIGN and DC-SIGNR | 37 |
| 3.1.2. DCIR | 38 |
| 3.1.3. MR | 38 |
| 3.2. Langerhans cell-derived mrCLRs | 39 |
| 3.2.1. Langerin | 39 |
| 3.3. Macrophage-derived mrCLRs | 39 |
| 3.3.1. Dectin-2 | 39 |
| 3.3.2. Mincle | 39 |
| 3.4. Soluble mrCLRs-collectins | 39 |
| 3.4.1. MBL | 39 |
| 3.4.2. SP-A and SP-D | 40 |
| 3.4.3. Other soluble mannose-recognising collectins | 40 |
| 4. Importance of mrCLRs-mannose interactions in inflammation and pathogenic infection | 40 |
| 4.1. Sterile (non-pathogenic) inflammation | 40 |
| 4.1.1. Cancer | 41 |
| 4.1.2. Haematological and vascular disorders | 41 |
| 4.1.3. Allergy | 42 |
| 4.1.4. Autoimmunity | 43 |
| 4.2. Pathogenic infections | 43 |
| 4.2.1. Bacterial and fungal infections | 43 |
| 4.2.2. Viral infections | 44 |
| 4.2.3. Mannose-recognising antibodies | 45 |
| 5. Conclusion and future perspectives | 45 |
| Acknowledgements | 46 |
| References | 46 |

1. Introduction

Protein glycosylation is a common post-translational modification involving the addition of complex carbohydrates (glycans) to specific amino acid residues of polypeptides. Protein glycosylation modulates important intra- and intercellular processes critical in maintaining cellular homeostasis (Ohtsubo and Marth, 2006; Varki et al., 2009) and plays central roles in protein folding and activity (Moremen et al., 2012; Xu and Ng, 2015a), in developmental processes (Haltiwanger and Lowe, 2004) and in pathogen–host interactions (Kreisman and Cobb, 2012; Venkatakrishnan et al., 2013). The normally tightly controlled glycosylation process is often dysregulated in pathologies e.g. cancer (Christiansen et al., 2014), inflammation (Scott and Patel, 2013), Alzheimer's disease (Schedin-Weiss et al., 2014), multiple sclerosis (Grigorian et al., 2012) and cystic fibrosis (Venkatakrishnan et al., 2015).

Protein glycosylation is mediated by highly specific enzymes in the cellular machinery. This “template-free” biosynthetic apparatus generates glycan structural diversity comprising different monosaccharide compositions, anomericity/linkage types (α or β) and topologies (branched or linear) that reflect the physiology of the cell at the time of biosynthesis (Rini et al., 2009). Consequently, glycopro-

teins commonly display extensive heterogeneity by appearing as a spectrum of closely related glycoforms (Cohen and Varki, 2010). Humans use a limited number of glycan building blocks for protein glycosylation including, but not limited to, D- α /D- β -mannose (Man), D- α -glucose (Glc), L- α -fucose (Fuc), D- β -galactose (Gal), D- α /D- β -N-acetylglucosamine (GlcNAc), D- α -N-acetylgalactosamine (GalNAc) and sialic acids e.g. D- α -N-acetylneuraminic acid (NeuAc) (Varki and Sharon, 2009). In particular, terminal monosaccharide residues are functionally important due to their exposed position, spatial flexibility and ability to form multivalent clusters (Cohen and Varki, 2014; Peterson et al., 2013). Glycoepitopes are recognised by two classes of receptors, glycan-binding proteins (lectins/adhesins) and glycan-binding antibodies.

Excellent reviews have summarised the important immune-modulatory roles of galactose, sialic acid and N-acetylglucosamine epitopes in human inflammation (Crocker et al., 2007; Johnson et al., 2013; Margreet and Geert-Jan, 2013; Rabinovich and Toscano, 2009; Schnaar, 2016). Mannose forms various α -anomeric epitopes on human and non-human glycoproteins, however, contributions of protein mannosylation to inflammatory and infection processes have received less attention. Motivated by an increasing volume of recent literature documenting the

presence and involvement of mannose as vital glycoepitopes in diverse areas of human immunity, this review first summarises the current understanding of the structural diversity and spatiotemporal presentation of human and non-human protein mannosylation, then covers the molecular recognition by host and microbial mannose-recognising C-type lectin receptors (mrCLRs) and antibodies (mrAbs), and finally, discusses the functional consequences of such interactions in the context of inflammation and infection.

2. Structural diversity and spatiotemporal expression of protein mannosylation

This review focuses on asparagine (Asn) (*N*-linked) glycosylation in humans, a type of protein glycosylation that uses mannose as a central building block (Stanley et al., 2009). Due to limited literature, tryptophan (*C*-linked) mannosylation (Furmanek and Hofsteenge, 2000; Ihara et al., 2015) will not be covered. Due to space constraints, the less investigated serine (Ser)/threonine (Thr) (*O*-linked) α -mannosylation (Lommel and Strahl, 2009; Praissman and Wells, 2014) and GPI anchors (Ferguson et al., 2009), identified in higher and lower organisms, are only discussed *en passant* although they are also being described as displaying potentially functional mannosidic cores (Wells, 2013). *N*-linked glycoproteins form an abundant and structurally diverse class of glycoconjugates that is discussed here with a strictly mannose-centric focus. Readers are encouraged to consult supporting literature for a broader introduction to protein *N*-glycosylation (Freeze, 2013; Moremen et al., 2012; Stanley et al., 2009).

2.1. Mannose is a central component of protein *N*-glycosylation

Mammalian *N*-glycosylation is largely restricted to Asn-Xxx-Ser/Thr/Cys (Xxx \neq Pro) consensus sequences (Aebi, 2013). Protein *N*-glycans share a common trimannosyl-chitobiose core (Man α 1.3(Man α 1.6)Man β 1.4GlcNAc β 1.4GlcNAc β Asn). All *N*-glycoproteins are biosynthesised in the secretory pathway in the endoplasmic reticulum (ER) and Golgi compartments of the cell by the transfer of immature glycan precursors (Glc₃Man₉GlcNAc₂) to Asn residues in the consensus sequences of yet-to-be folded proteins. These glycan precursors assist in the protein folding prior to or during the release of the three terminal Glc residues from the non-reducing (distal) glycan end (Aebi et al., 2010), albeit this mechanism is still debated (Duus et al., 2009; Mollegaard et al., 2011). Subsequently, *N*-glycoproteins may be secreted directly as relatively unprocessed high mannose type structures i.e. Man₅₋₉GlcNAc₂ (M5–M9), Fig. 1A,B. The protein *N*-glycans can then be processed further into the partially mannose-terminating hybrid type and then to complex *N*-glycans, where the mannosidic epitopes of the trimannosyl-chitobiose core are sterically masked by other terminal monosaccharide residues. Lack of further processing of the high mannose structures can be the result of restricted glycosylation site accessibility (Thaysen-Andersen and Packer, 2012) and/or limited glycosylation enzyme activity or substrate availability (Stanley et al., 2009). Interestingly, all mannose residues of *N*-glycans have been

found to be α -anomers (i.e. α 1,2/3/6) except for the β 1,4-linked mannose residue conjugated to the chitobiose core, Fig. 1C.

2.2. Human high mannose glycoproteins

High mannose glycans make up a large proportion of the human *N*-glycome, but are unevenly distributed across the glycoproteome and reside in spatiotemporally restricted locations. We recently showed that human cells, despite having a shared biosynthetic machinery that processes all *N*-glycoproteins expressed at any given time, generate subcellular-specific *N*-glycosylation signatures (Lee et al., 2014a). It has been generalised that high mannose glycoproteins are relatively infrequently secreted and present on cell surface membranes in healthy viable cells (Stanley et al., 2009). The reduced mannosylation of secreted glycoproteins was correlated with higher glycosylation site accessibility (Lee et al., 2014a) or with their altered macroheterogeneity (Lohse et al., 2015; Zacchi and Schulz, 2015), allowing processing of the conjugated glycans beyond the high mannose series. Recently, studies of human lung fibroblasts showed a similar enrichment of high mannose glycoproteins in the ER and on cell membranes (Takakura et al., 2015). An abundance of high mannose glycans, particularly M8 and M9 structures, was also identified on the cell membrane of human embryonic stem cells (An et al., 2012). Thus, it appears that α -mannosidic glycoepitopes in the form of high mannose glycoproteins are expressed on cell membranes but are predominantly intracellular signatures in normally differentiated and viable cells. This agrees with the known intracellular functions of high mannose type glycosylation including lysosomal trafficking via the mannose-6-phosphate receptor (Varki and Kornfeld, 2009) and the targeting of misfolded glycoproteins for degradation (Spiro, 2004). Furthermore, mannosidic *N*-glycans are well-conserved on specific sites of several important serum immunoglobulins such as IgM and IgE, suggesting their involvement in modulating the host immune response (Arnold et al., 2005; Moh et al., 2016; Shade et al., 2015). Finally, it has been suggested that leaking high mannose glycoproteins may constitute 'danger signals' during cellular damage e.g. necrosis where mrCLRs expressed on immune cells can recognise them to mount an appropriate immune response (Lee et al., 2014a; Rachmilewitz, 2010). Other researchers have echoed that mannosidic epitopes should be considered as molecular entities that can initiate an effective anti-inflammatory response e.g. during acute lung injury (Xu et al., 2015), but argued against their role as 'danger signals' (Gazi and Martinez-Pomares, 2009). The capacity of cells to reproducibly attach little processed high mannose glycans at specific protein sites, whereas other sites, even on the same protein, consistently receive complex glycans is fascinating and suggests that specific functions are associated with these features (Thaysen-Andersen and Packer, 2012). Furthermore, it is now recognised that free unconjugated *N*-glycans, some of which are known to be highly mannosylated, are present in the ER, lysosome and cytosol of human cells (Harada et al., 2015). Although evidence points to functions mainly involving recycling of these free *N*-glycans and their monosaccharide constituents in the

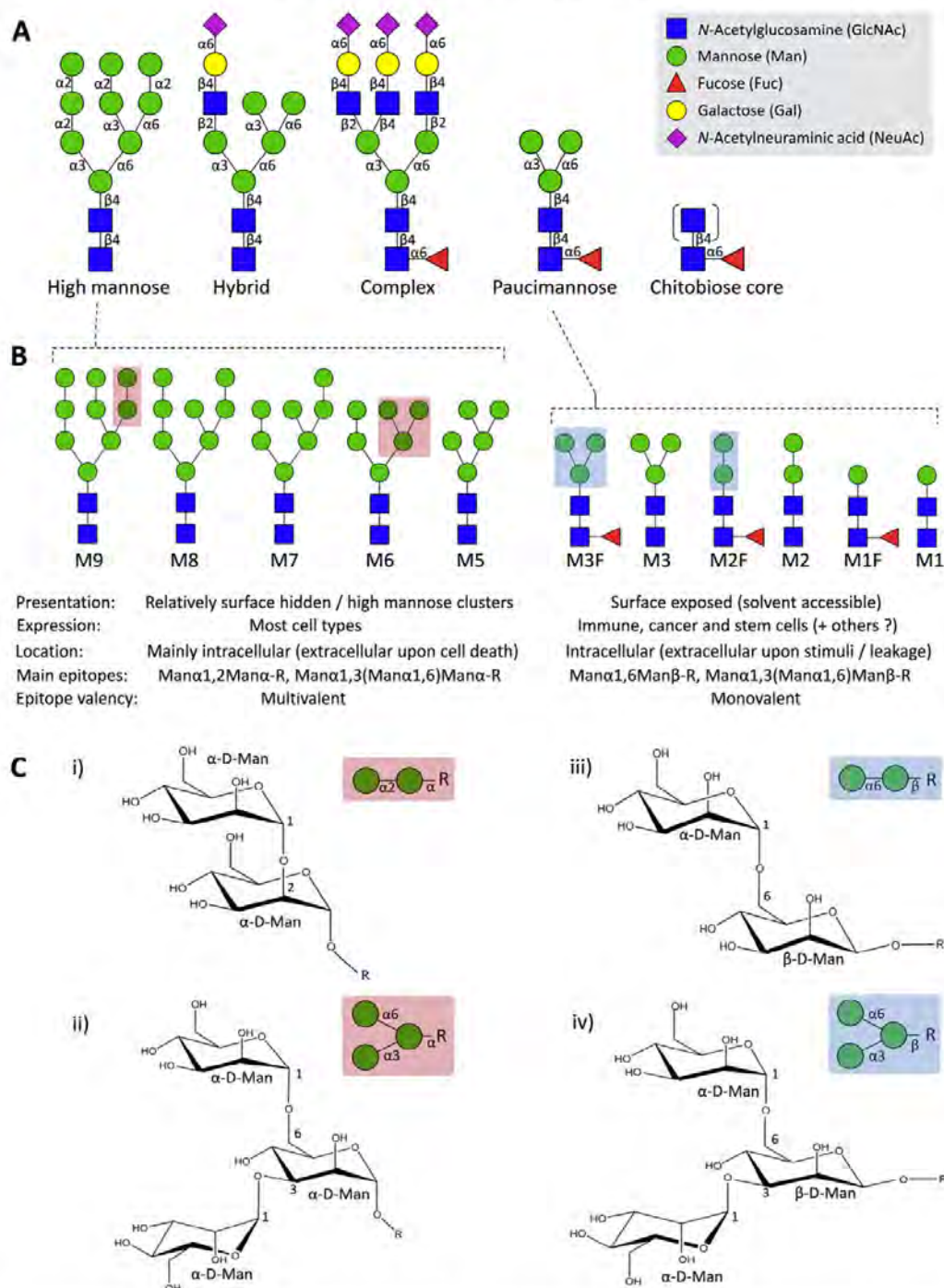


Fig. 1. Mannose is an essential building block of human *N*-glycosylation. (A) High mannose and paucimannose form two mannose-terminating *N*-glycan classes (see insert for key to monosaccharide symbols, which are presented as the recommended nomenclature for depicting glycans (Varki et al., 2015)). (B) Multiple glycan structures comprise each class i.e. high mannose (M5–M9) and paucimannose (M1–M3F). The general characteristics of the high mannosidic and paucimannosidic glycoproteins as derived from supporting literature (see main text) are summarised including their spatial presentation, cellular expression, location and the nature of their epitopes. (C) Chemical representation of the main glycoepitopes of (i–ii) high mannosidic i.e. Man α 1,2Man α -R and Man α 1,3(Man α 1,6)Man α -R (red shading) and (iii–iv) paucimannosidic i.e. Man α 1,6Man β -R and Man α 1,3(Man α 1,6)Man β -R (blue shading) glycoproteins.

synthesis of nucleotide sugars used in glycoprotein biogenesis, a fraction of the free glycans are known to leave the cell and appear in bodily fluids including the urine (Xia et al., 2013). However, it is unclear whether free mannosidic *N*-glycans can react with specific mCLRs in the extracellular environment and their precise role in immunological processes, if any, remains to be determined.

2.3. Non-human mannosidic *N*-glycosylation

Mannosylated *N*-glycans are not exclusive to mammals. High mannose glycoproteins are common and essential features of fungi (Cummings and Doering, 2009). For example, *Saccharomyces cerevisiae* and *Candida albicans* produce *N*-glycans with mannose-rich antennas consisting of repeating α 1,6-mannose units with branched α 1,2/3-mannosyl residues extending from a common core (Hykkolari et al., 2016; Loibl and Strahl, 2013; Shibata et al., 1995). In addition, yeast mannans are branched α 1,2/3/6-mannose-rich polysaccharides found in abundance in the cell wall (Masuoka, 2004) that appear to be critical for fungal viability and pathogenicity towards humans (Ernst and Prill, 2001; Strahl-Bolsinger et al., 1999). The less studied *O*-mannosylation was recently identified to also be a feature of yeast glycoproteins (Halim et al., 2015). Outside the fungi kingdom, high mannose and paucimannosidic glycoproteins were identified in eggs of the parasites, *Schistosoma mansoni* and *S. japonicum*, that are often found in the water of developing countries with poor sanitation (Khoo et al., 1997). These mannosylated glycoproteins are responsible for intestinal schistosomiasis in humans (Grimes et al., 2015). The majority of known plant and insect allergen glycoproteins also carry high amounts of high mannose and paucimannose type *N*-glycans (Kolarich and Altmann, 2000; Kolarich et al., 2005, 2006; Lauer et al., 2004; Westphal et al., 2003). These glycans have been shown to mediate allergen protein uptake by dendritic cells (DCs), indicating that these structures could play an important role in development of allergic diseases (Barrett et al., 2009; Deslée et al., 2002). Apart from *Campylobacter jejuni* that appears devoid of mannose in its *N*-glycoproteome (Karlyshev et al., 2005; Nichollas et al., 2014; Scott et al., 2014), little is known about mannose in the context of bacterial *N*-glycosylation. In the viral world, human viruses including human deficiency virus (HIV) and influenza A, use the host glycosylation machinery to produce human-like *N*-glycosylation on their envelope proteins including clusters of high mannosylation (Behrens et al., 2016; Mir-Shekari et al., 1997). As described below, these mannose-rich epitope clusters are functionally important for the viral transmission and survival and may serve as therapeutic targets.

2.4. Paucimannosidic glycoproteins

Driven by technology advances in glycoproteomics mass spectrometry (Parker et al., 2013, 2015; Thaysen-Andersen and Packer, 2014; Thaysen-Andersen et al., 2016), we recently discovered an unconventional form of α - and β -mannose epitope-rich human *N*-glycosylation, known as

protein paucimannosylation, in sputum from inflamed and bacteria-infected individuals (Thaysen-Andersen et al., 2015; Venkatakrishnan et al., 2015). The truncated mannoseterminating human paucimannosidic structures spanned the monosaccharide compositions of $\text{Man}_{1-3}\text{GlcNAc}_2\text{Fuc}_{0-1}$ (M1–M3F) with a prevalence of one of the M2F isomers i.e. $\text{Man}\alpha 1,6\text{Man}\beta 1,4\text{GlcNAc}\beta 1,4(\text{Fuc}\alpha 1,6)\text{GlcNAc}\beta \text{Asn}$, Fig. 1B. Previously, paucimannosidic *N*-glycosylation was thought to be restricted to invertebrates and plants, and although these structures were found to be important in development and in other life-essential processes, their exact biological function(s) in these organisms are yet to be understood (Schachter, 2009).

Importantly, the human sputum paucimannosidic glycans were found to be conjugated to intact proteins, demonstrating that these truncated *N*-glycoproteins are not degradation products for the purpose of salvaging monosaccharides (Loke et al., 2015; Thaysen-Andersen et al., 2015). Subsequently, we showed that some of the paucimannose *N*-glycans were truncated even further to present the chitobiose core type (i.e. $\text{GlcNAc}_{1-2}\text{Fuc}_{0-1}$) on the proteins whilst retaining intact protein activity and function (Kondo et al., 2010; Loke et al., 2015). A biosynthetic pathway involving the timely expression of β -hexosaminidases and α -mannosidases was proposed to explain the generation of paucimannosidic glycoproteins. The azurophilic granules of human neutrophils were identified as the (sub)cellular origins of paucimannosylation in inflamed sputum (Thaysen-Andersen et al., 2015); these granules are known to be readily mobilised and the granular content presented on the cell surface or secreted into the extracellular environment upon neutrophil activation (Nauseef and Borregaard, 2014). In support of this observation, multiple proteins that are known to be localised in the azurophilic granules of human neutrophils, including myeloperoxidase, cathepsin G, proteinase 3 and azurocidin (Loke et al., 2015; Olczak and Watorek, 2002; Van Antwerpen et al., 2010; Zoega et al., 2012), were isolated and shown to carry paucimannosidic glycans. Several other studies have demonstrated that protein paucimannosylation is also a signature of preeclampsia (Robajac et al., 2015), cancer (Balog et al., 2012; Lee et al., 2014b; Sethi et al., 2014) and “stemness” in humans (Dahmen et al., 2015; Zipser et al., 2012). Interestingly, paucimannosidic epitopes are presented on exposed glycosylation sites on proteins, unlike their spatially more hidden high mannose type counterparts (Thaysen-Andersen et al., 2015). This solvent exposed position suggests that paucimannosidic epitopes may present as suitable ligands for the mCLRs. In contrast to high mannose epitopes, the literature is to the best of our knowledge devoid of any examples of clusters of paucimannosylation on individual glycoproteins. However, known paucimannosidic proteins i.e. neutrophil elastase, proteinase 3, cathepsin G have been reported to be abundantly enriched on the plasma membrane of human neutrophils after activation, which may result in local “cluster-like effects” of paucimannosidic epitopes on the neutrophil cell surface (Campbell and Owen, 2007; Campbell et al., 2000; Hajjar et al., 2008). The accessible nature and the spatiotemporal expression of paucimannosylation in the extracellular environment under certain physiological conditions may be features that

immune cells and perhaps other cell types utilise to communicate within the immune system.

3. Mannosidic epitope recognition by specialised human C-type lectin receptors

Given their ubiquitous nature, high abundance, structural diversity and energetically demanding spatiotemporal regulation, it is not surprising that mannoseylated glycoproteins have been found to participate in essential cellular functions in human physiology (van Kooyk and Rabinovich, 2008; Xu and Ng, 2015b). Secreted and cell-surface glycoproteins facing the extracellular environment are ideally located to facilitate cell–cell communication by engaging in host–host or host–pathogen interactions. Naturally, this requires that the exposed glycoepitopes are recognised with the appropriate specificity and sensitivity. Immune cells express a group of pattern recognition receptors (PRR), such as toll-like receptors (TLR), to sense host cell-derived damage associated molecular pattern (DAMP) and pathogen associated molecular pattern (PAMP) ligands (Zhang and Mosser, 2008). It is still not known if mannosidic epitopes contribute as DAMPs and PAMPs. Another important group of receptors involved in mediating immune recognition are known as the C-type lectin receptors (CLRs).

CLRs are considered as endocytic lectin receptors that recognise a wide repertoire of ‘self’ (host) and ‘non-self’ (foreign) glycoepitopes. Their main function is the endocytosis of the bound glycoconjugates (glycoproteins and glycolipids alone, or as whole intact cells) and the presentation of their fragments for recognition by specific adaptive immune cells such as lymphocytes (Weis et al., 1998). Thus, CLRs do not mediate immune recognition by themselves, but instead assist the adaptive immune cells in detecting important epitopes (Biedron et al., 2015). It should be noted that some CLRs are not endocytic, but instead are considered as PRRs (Richardson and Williams, 2014); however, this view is still controversial (Jozefowski, 2015). Lectins inherently recognise glycoepitopes with relatively low affinity (millimolar–micromolar K_d), but the binding strength can be enhanced by orders of magnitude by means of multivalency, generating high avidity (nanomolar–picomolar K_d) glycan–protein interactions (Menon et al., 2009; Mitchell et al., 2001; van Liempt et al., 2006). Most CLRs are transmembrane or secreted calcium-dependent or independent lectins, sharing primary and secondary structural homology of their carbohydrate recognition domains (CRD) (Drickamer and Taylor, 2015; Zelensky and Gready, 2005). However, harbouring one or more CRDs does not necessarily permit glycan recognition (Hurtado et al., 2004) since other structural features could affect the ligand binding (Drickamer, 1992). Two broad groups of CLRs are expressed on innate immune cells; type I CLRs display an extracellular N-terminus and multiple CRDs and type II CLRs comprise an extracellular C-terminus and a single CRD (Cambi and Figdor, 2003). CLRs are organised in oligomeric configurations to increase their avidity towards multivalent glycan ligands (Appelmelk et al., 2003; Lee and Lee, 2000).

Most mrCLRs contain a common CRD-localised Glu-Pro-Asn (EPN) motif. Due to structural similarity, mrCLRs also

recognise fucose and GlcNAc containing epitopes in addition to mannosidic glycoepitopes (Figdor et al., 2002; Nagae et al., 2016; Wu and Sampson, 2014). The molecular mechanisms of mannose binding by mrCLRs are driven by van der Waals forces and hydrogen bonding between the hydroxyls of the terminal mannose residue(s) and the amino acid residues in the CRD. Ca^{2+} ions are mandatory ligands in the conserved calcium recognition sites of calcium-dependent CLRs, serving the purpose of forming coordinated bonds with the interacting glycan and stabilising the glycan binding site (Gabius et al., 2011; Weis and Drickamer, 1996). Furthermore, the orientation of the glycan relative to the CLRs and the glycan ligand multivalency are critical factors in mediating potent CRD binding (Drickamer, 1999). MrCLRs are abundantly expressed on “front-line” innate immune cells such as DCs and macrophages and as soluble receptors in tissues and blood; human mrCLRs are here reviewed with special attention to their tissue/cellular-origins and their molecular basis of mannose recognition. It is stressed that many mrCLRs are expressed by multiple cell-types and that the herein used classification is a simplified representation. It should also be noted that apart from mannoseylated epitopes, mrCLRs also recognise other glycans displaying terminal fucose or GlcNAc epitopes that, in turn, may add to their diverse immunological functions. The functional consequences of the mannosidic presentation and recognition in inflammation and pathogen infection are subsequently discussed.

3.1. DC-derived mrCLRs

Human blood DCs are important antigen-presenting cells (APCs) in peripheral blood and tissues arising from hematopoietic progenitors in the bone marrow (Lee et al., 2015). There are two major subtypes of blood DCs in humans, the myeloid DCs (mDCs) and plasmacytoid DCs (pDCs), which are classified according to their surface antigens (Ziegler-Heitbrock et al., 2010). mDCs that reside in the thymus, spleen and lymph nodes are termed resident lymphoid organ DCs, and mDCs that reside in the peripheral tissues and migrate to lymph nodes are known as migratory DCs (Villadangos and Schnorrer, 2007). Adding to the complexity, activated monocytes that differentiate into migratory DCs *in vivo* during inflammatory conditions are called inflammatory DCs (Qu et al., 2004; Segura and Amigorena, 2013). pDCs are found predominately in the blood circulation and in peripheral lymphoid tissues such as the tonsils and lymph nodes under normal physiological conditions (Haniffa et al., 2013). Both mDCs and pDCs are of low abundance (~1% of mononuclear cells) in blood circulation, but they contribute significantly to the innate immune response (Lombardi et al., 2015). DC-derived mrCLRs are often studied utilising *in vitro* monocyte-derived DCs (Sallusto and Lanzavecchia, 1994) or mouse DCs (Mildner and Jung, 2014) that are better characterised than human DCs (Villadangos and Shortman, 2010). In this review, ‘DC’ refers to human blood DCs unless otherwise stated.

DCs express various surface mrCLRs allowing them to sample host and foreign mannosidic ligands in the extracellular environment and react with a broad range of pathogens to induce inflammation (Hortz et al., 2013). Upon

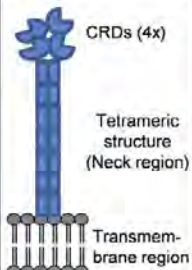
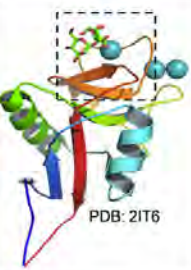

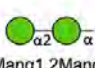
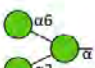
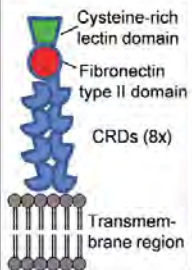


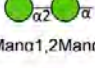
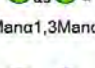

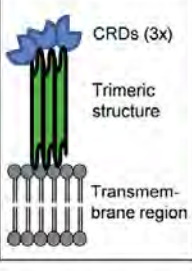

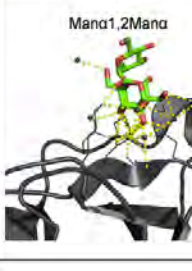
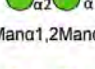
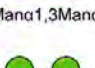
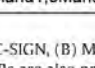
| mrCLR (CD type) [type] | Schematic molecular structure | Overall structural fold of CRD | CRD (zoom/rotated, glycan-CRD interaction in yellow) | Mannosidic epitope recognition |
|---|---|---|--|--|
| A DC- SIGN (CD209) [II] |  <p>CRDs (4x)</p> <p>Tetrameric structure (Neck region)</p> <p>Transmembrane region</p> |  <p>PDB: 2IT6</p> |  <p>Manα1,2Manα</p> |  <p>Manα1,2Manα-R</p>  <p>Manα1,3(Manα1,6)Manα-R</p> |
| B MR (CD206) [I] |  <p>Cysteine-rich lectin domain</p> <p>Fibronectin type II domain</p> <p>CRDs (8x)</p> <p>Transmembrane region</p> |  <p>PDB: 1FWU</p> |  <p>3-SO-Galβ1,4(Fuca1,3)GlcNAc</p> |  <p>Manα1,2Manα-R</p>  <p>Manα1,3Manα-R</p>  <p>Manα1,6Manα-R</p> |
| C Langerin (CD207) [II] |  <p>CRDs (3x)</p> <p>Trimeric structure</p> <p>Transmembrane region</p> |  <p>PDB: 3P5F</p> |  <p>Manα1,2Manα</p> |  <p>Manα1,2Manα-R</p>  <p>Manα1,3Manα-R</p>  <p>Manα1,6Manα-R</p> |

Fig. 2. Structural features of human mrCLRs. The schematic and 3D structure of key human endocytic mrCLRs i.e. (A) DC-SIGN, (B) MR and (C) Langerin with a focus on illustrating the CRD–ligand interaction. The main mannosidic epitopes recognised by the individual mrCLRs are also presented. Monosaccharide symbols are presented as recommended previously (Varki et al., 2015). The 3D structures were generated with crystal structural data obtained from Protein Data Bank (PDB IDs indicated) using the PyMOL Molecular Graphics System, Version 1.7.4, Schrödinger LLC.

internalisation of antigens by pinocytosis, DCs mature as they migrate to the draining lymph nodes where they process both exogenous and endogenous antigens and present them to CD8+ or CD4+ cytotoxic T cells via major histocompatibility complex classes I and II, respectively (Neefjes and Ovaa, 2013; Robinson et al., 2006). Hence, the DC activity bridges between self-tolerance and the induction of host immune response, by distinguishing self and non-self antigens through their PRRs and mrCLRs, such as the dendritic cell-specific intercellular adhesion molecule-3-grabbing non-integrin (DC-SIGN).

3.1.1. DC-SIGN and DC-SIGNR

The human DC-specific DC-SIGN (CD209) (UniProtKB accession number: Q9NNX6), a type II mrCLR, is involved in many aspects of immunity including the mediation of HIV type 1 infections where its function was first investigated

(Geijtenbeek et al., 2000b). The single flexible CRD of DC-SIGN, Fig. 2A recognises high mannose, more specifically the trimannosyl (Man α 1,3(Man α 1,6)Man α -R) and Man α 1,2Man α -R epitopes, as well as the fucosylated trisaccharide Lewis type antigens. Paucimannosidic glycans showed higher DC-SIGN reactivity using flow cytometry compared to glycan array assessments (van Liempt et al., 2006), suggesting that high glycan epitope density, cell surface expression and multivalency are pivotal to confer binding of paucimannosidic glycans to DC-SIGN. Interestingly, X-ray crystallography has revealed that optimal binding to DC-SIGN is dependent on the α -anomericity of the central mannose residue in trimannosyl epitopes, Fig. 1C (Feinberg et al., 2001). This may explain the stronger binding of high mannose (that has a central α -anomeric mannose) than paucimannosidic (that has a central β -anomeric mannose) epitopes (van Liempt et al., 2006). Although DC-SIGN has

a higher fucose affinity relative to mannose per monosaccharide entity, the binding avidity becomes significantly higher (low millimolar range) with increasing mannosyl valency (Mitchell et al., 2001). This higher avidity is partially facilitated by the configuration of the neck region of the tetrameric DC-SIGN, Fig. 2A (Feinberg et al., 2005, 2007; Menon et al., 2009). X-ray crystallography and binding affinity studies have also demonstrated that the disaccharyl Man α 1,2Man α -R epitopes of high mannose type structures in humans and some pathogenic organisms directly interact with the CRD of DC-SIGN (Cambal et al., 2008; Guo et al., 2004; Torrelles et al., 2012).

DC-SIGN is a transmembrane receptor without immunoreceptor tyrosine-based activating (ITAM) or inhibiting (ITIM) motifs (Sancho and Reis e Sousa, 2012). This means that DC-SIGN functions predominantly by endocytosing bound ligands and presenting them to T cells. However, DC-SIGN also acts as a signalling receptor upon binding of mannosidic ligands by triggering a downstream association with a signalosome that phosphorylates Raf-1, a protein kinase that regulates and promotes the activation of nuclear factor kappa-light-chain-enhancer of activated B cells (NF- κ B). The NF- κ B activation factor leads ultimately to a prolonged inflammatory response. Interestingly, fucosylated DC-SIGN ligands did not mediate Raf-1-based signalling, indicating unique mannosidic epitope recognition of DC-SIGN or a mannose-dependent functional response by the immune-modulatory TLRs (Geijtenbeek and Gringhuis, 2009). DC-SIGN also promotes cell-cell interactions with endothelial cells to support DC transmigration to inflammatory sites (Geijtenbeek et al., 2000a; van Gisbergen et al., 2005b). While DC-SIGN is mainly expressed on DCs, the homologous DC-SIGN related (DC-SIGNR) (CD299) (UniProtKB accession number: Q9H2X3), a type II mCLR, is predominately expressed in liver sinusoidal endothelial cells, in lymph node sinuses and in the placenta, but at lower levels compared to DC-SIGN. In addition, DC-SIGNR acts primarily as an attachment factor and does not participate in endocytosis or cell signalling (Pohlmann et al., 2001). The tetrameric DC-SIGNR has a similar ligand binding profile as DC-SIGN (Feinberg et al., 2001; Mitchell et al., 2001).

3.1.2. DCIR

Another transmembrane type II mCLR, the human DC immunoreceptor (DCIR) (UniProtKB accession number: Q9UMR7), is the only ITIM-containing CLR identified in humans. In addition, DCIR deviates from other relatives by displaying a CRD-localised Glu-Pro-Ser (EPS) motif instead of the more conserved EPN motif. DCIR is widely expressed in DCs and macrophages (Sancho and Reis e Sousa, 2012). The exact role of DCIR in the immune response is still unclear, but it appears to inhibit the activation of *in vitro* differentiated DCs under inflammation and pathogenic invasion (Hutter et al., 2014). Qualitatively through a solid phase fluorescence binding assay, DCIR was demonstrated to recognise similar ligands as DC-SIGN including the disaccharyl Man α 1,2Man α -R epitopes (Lee et al., 2011). Interestingly, an occupied N-glycosylation site in the CRD reduces the overall binding capacity of DCIR and may fine-tune the ligand affinity by glycan-glycan interactions (Bloem

et al., 2013). It should be noted that DCIR also has high affinity towards sulphated Lewis A ligands (Bloem et al., 2014) and can present antigens to CD8+ T cells *in vitro* (Klechevsky et al., 2010). The 3D structure of human DCIR was recently reported (Nagae et al., 2016).

3.1.3. MR

The endocytic mannose receptor (MR) (CD206) (UniProtKB accession number: P22897) is part of the MR family comprising other CLR including phospholipase A2, Endo180 and DEC205 (Taylor et al., 2005). MR is a calcium-dependent type I transmembrane mCLR consisting of eight extracellular CRD with a tyrosine-based motif in the cytoplasmic tail, Fig. 2B. Although commonly known as the “macrophage mannose receptor”, MR is also widely expressed in other cell types including *in vitro* monocyte-derived DCs, hepatic endothelial and Kupffer cells (Kerrigan and Brown, 2009; Sondergaard et al., 2014). The CRD 4 and 5 of MR bind to high mannose N-glycans as well as to glycans containing fucose, GlcNAc and sulphate residues (East and Isacke, 2002). The glycan ligand binding is calcium-dependent, creating a loop in the CRD that acts as a pH sensor (Taylor et al., 1992). This mechanism mediates a pH-dependent release of the ligands during endocytosis, specifically facilitating a release of MR-bound mannosidic ligands into the weakly acidic intracellular endosomal compartments (Mullin et al., 1997). Interestingly, the binding characteristics of MR were, similarly to DCIR, shown to be affected by the presence of a CRD-localised N-glycan; the lack of terminal sialylation of the CRD N-glycan reduced the binding of mannosylated ligands. However, the exact mechanism for this intriguing relationship was not delineated (Su et al., 2005). In a similar study, it was observed that the binding of mannosidic ligands to MR aids its oligomerisation (Lai et al., 2009). The 3D structure of MR has been solved (Feinberg et al., 2000; Liu et al., 2000) and confirms that the cysteine-rich domain is also capable of binding to sulphated GalNAc glycans on pituitary hormones, thus demonstrating the wide specificity of MR as an endocytic lectin receptor (Fiete et al., 1998). Surprisingly, binding of dimannosyl epitopes to the CRD 4 of MR was not observed, which was attributed to the artificial conditions used to generate the crystal structure. Of interest, calcium-independent binding of mannosidic epitopes to the cysteine-rich domain was also reported, suggesting that MR binding to mannosidic epitopes may be mediated by both the CRD and the cysteine-rich domain (Lai et al., 2009). Based on a comparison of the recognition sites of CRD 4 of MR and rat mannose-binding lectin (MBL)-A, it was predicted that MR, upon calcium-binding, recognises Man α 1,6Man α -R epitopes (Feinberg et al., 2000; Mullin et al., 1994).

Ligand bound MR mediates clathrin-dependent endocytosis of extracellular ligands and, after processing, eventually transports their fragments back to the cell surface for presentation to T helper cells (Martinez-Pomares, 2012). The tyrosine binding motif of MR is responsible for the delivery of mannosylated ligands to the early endosomes for sorting and clearance (Schweizer et al., 2000). It was suggested that MR displays both *cis* and *trans* binding modes mediating phagocytosis independent of other receptors or signal molecules (Kerrigan and Brown, 2009). However, the

role of MR as a phagocytic receptor is still debated (Esparza et al., 2015; Heinsbroek et al., 2008; Le Cabec et al., 2005). Finally, in mice, the membrane-bound MR undergoes metalloproteinase-based proteolysis generating soluble MR (Martinez-Pomares et al., 1998), which still recognises mannosylated and sulphated glycans (Su et al., 2005). Since the membrane-bound and soluble MRs have similar ligand binding profiles, MRs may serve other functions including decoy mechanisms in addition to targeting exogenous antigens for cellular presentation.

3.2. Langerhans cell-derived mrCLRs

Langerhans cells are a subset of specialised cells distinct from DCs that reside in the epidermis and the mucosa epithelium and contain large cytoplasmic organelles known as Birbeck granules. The functions of Langerhans cells resemble the DC functions, but are unique since the Birbeck granules are used as recycling endosomal compartments for antigen presentation to naive T cells after the migration to the lymph nodes (Valladeau et al., 2000).

3.2.1. Langerin

Langerin (CD207) (UniProtKB accession number: Q9UJ71) is a type II calcium-dependent endocytic transmembrane mrCLR with a single CRD specifically expressed in Langerhans cells. Langerin possesses an intracellular proline-rich motif and an extracellular neck region that mediates a trimer formation, Fig. 2C. The langerin CRD recognises and preferentially binds high mannosidic glycans (Stambach and Taylor, 2003). The trimeric configuration of langerin may be an important structural feature to promote binding since it proposedly interacts in a multivalent manner with mannosidic epitopes to enhance its binding avidity (Chatwell et al., 2008). As evidence for this, monomeric langerin showed weak mannosidic binding affinity compared to trimeric langerin (Stambach and Taylor, 2003). However, the multivalent binding mechanism of langerin is still debated (Feinberg et al., 2011). X-ray crystallography documented that the ligand profile of langerin is, similar to DC-SIGN, centred around the favourable recognition and binding of the $\text{Man}\alpha 1,2\text{Man}\alpha\text{-R}$ epitope by the CRD (Feinberg et al., 2011).

3.3. Macrophage-derived mrCLRs

The phagocytic macrophages are important APCs in the human innate immune system. Similar to DCs, they form the link between the innate and adaptive immune system. The dectin-2 cluster of PRRs, consisting of dectin-2 and macrophage inducible C-type lectin (Mincle), forms a small subset of non-endocytic calcium-dependent mrCLRs expressed predominantly in macrophages, and also in *in vitro* monocyte-derived DCs, neutrophils and B and T lymphocytes (Loures et al., 2015; Richardson and Williams, 2014).

3.3.1. Dectin-2

Human dectin-2 (UniProtKB accession number: Q6EIG7), a type II mrCLR with a single CRD, showed relatively high affinity for high mannose N-glycans and *S. cerevisiae* cell wall-derived α -mannans (McGreal et al., 2006). Dectin-2

has no cytoplasmic signalling motif, making it incapable of participating in antigen uptake (Robinson et al., 2009). The cell surface location of dectin-2 requires it to associate with an ITAM-containing Fc γ R, which enables it to induce a downstream cytokine-driven inflammatory response. The dectin-2–Fc γ R interaction-induced signal also promotes endocytosis of mannosylated glycoconjugates of *C. albicans* through a spleen tyrosine kinase (Syk)-mediated intracellular signalling pathway. Eventually this results in various pro-inflammatory cellular responses such as cytokine release and formation of reactive oxygen species in the phagolysosomes of macrophages (Mocsai et al., 2010; Sato et al., 2006). To date, the 3D structure of human dectin-2 remains unresolved.

3.3.2. Mincle

Human Mincle (UniProtKB accession number: Q9ULY5) is a transmembrane type II mrCLR consisting of a single CRD. Similar to dectin-2, Mincle activates cellular processes via Fc γ R-coupling. The cell surface expression of Mincle, which is induced by activated TLRs (Lee et al., 2011), was shown on peritoneal macrophages, *in vitro* differentiated macrophages, mDCs and inflammatory DCs (Graham et al., 2012; Matsumoto et al., 1999). Mincle displays mannose-based binding characteristics, most notably to polyvalent $\alpha 1,2$ -linked mannosidic epitopes and more broadly also to high mannose glycans (Wells et al., 2008; Zhu et al., 2013). The 3D structure of Mincle was recently reported, revealing a shallow hydrophobic region adjacent to the CRD for binding of mannosylated proteins and lipids (Furukawa et al., 2013).

3.4. Soluble mrCLRs-collectins

Collectins form a group of soluble type II (single CRD) mrCLRs containing collagen-like regions. Collectins function as PRRs by binding and agglutinating surface-expressed mannosidic glycans on bacteria, mycobacteria, viruses and fungi (Ip et al., 2009). Examples of well-studied human collectins include mannose-binding lectin (MBL) and surfactant proteins A and D (SP-A/D). Collectins are organised into trimeric, tetrameric or higher multimeric structures with appropriate spacing between the CRDs to allow multivalent ligand binding (Sheriff et al., 1994; Weis and Drickamer, 1994). The collectin CRDs are configured to enable high nanomolar binding strength to extended mannosidic glycan clusters present on the surface of microbial pathogens (Kjaer et al., 2013; Lu et al., 1990).

3.4.1. MBL

The hepatocyte-derived MBL (UniProtKB accession number: P11226) circulates at ~ 200 ng/mL in healthy individuals, but levels are elevated during infections (Gunn et al., 2012). Human MBL circulates as a trimer, but can form higher oligomers (tetra- to hexamers) in “bouquet-like” structures with higher avidity towards mannose-, GlcNAc- and fucose-containing glycans (Iobst et al., 1994; Turner, 2003). The oligomerisation thus allows MBL to regulate its binding characteristics (Teillet et al., 2005). Limited knowledge of the exact ligand binding profile of human MBL is available (Mazumder and Mukhopadhyay, 2012; Sheriff et al., 1994), but the homologous rat MBL-A was shown to

recognise Man α 1,2/3/6Man-R epitopes and high mannose type N-glycans based on X-ray crystallography studies (Lee and Lee, 1997; Ng et al., 1996, 2002; Weis et al., 1991). Interestingly, Man α 1,6-R epitopes are central components of human paucimannosidic and high mannose glycoconjugates (see Fig. 1A–B) suggesting, by homology, their recognition by human MBL. Indeed, we recently showed *in vitro* binding, albeit relatively weak in nature, of paucimannosidic and high mannose glycoconjugates to monomeric human MBL (Thaysen-Andersen et al., 2015). Furthermore, MBL has been proposed to clear aggregated antigen-free, highly mannoseylated, human serum IgM (Arnold et al., 2005). The 3D structure of rat MBL-A showed that the free 3- and 4-hydroxyl groups of terminal D- α -mannose in branched high mannose ligands are critical for CRD interaction in the presence of Ca²⁺ (Jobst et al., 1994; Weis et al., 1992). Upon glycan ligand binding, MBL changes conformation and activates the lectin complement pathway by stimulating the MBL-associated serine proteases (MASPs). The MASPs initiate a cleavage cascade of complement factors, which produce the opsonic C3b complement fragments that coat pathogens for removal by phagocytic macrophages (Endo et al., 2006), thereby promoting clearance of both foreign pathogens and apoptotic/necrotic host cells (Nauta et al., 2003).

3.4.2. SP-A and SP-D

The SP-A and SP-D (UniProtKB accession number: Q8IWL2 and P35247, respectively) collectins are mainly secreted into the alveolar space by type II alveolar and Clara cells (Lu et al., 2002). Both SP-A/D bind mannosidic ligands, but unlike MBL, they do not activate the complement system. Instead, SP-A and SP-D act as opsonins by facilitating phagocytosis by alveolar macrophages (Kerrigan and Brown, 2009). Crystal structures of SP-A/D revealed spatial differences in their neck domains, which may help to explain their different recognition profiles of lipopolysaccharides (LPS) from gram-negative bacteria (Veldhuizen et al., 2011). While SP-D interacts mainly with the mannose-rich components of O-linked polysaccharides (Sahly et al., 2002), SP-A binds GlcNAc epitopes of the lipid A component of LPS (Van Iwaarden et al., 1994). Differences in the amino acid residues flanking the CRD binding site of SP-A/D were shown to contribute to the preferential interaction of SP-D with high mannose type glycans (Crouch et al., 2006).

3.4.3. Other soluble mannose-recognising collectins

Various other soluble collectins have been identified in human serum i.e. CL-11/CL-K1 (UniProtKB accession number: Q9BWP8) (kidney) and CL-12/CL-P1 (UniProtKB accession number: Q5KU26) (placenta) (Degen and Thiel, 2013; Hansen et al., 2010). CL-11 was described to be functionally similar to MBL (involved in complement activation) and also showed interaction with high mannoseylated and fucosylated structures. In contrast, CL-12 recognises β 1,3-glucan, a fungal cell wall component, in a calcium-independent manner (Ma et al., 2015). Finally, recombinant bovine CL-43 collectins were found to recognise mannoseylated and fucosylated ligands (Hansen and Holmskov, 2002) and have been proposed as potential inhibitors of viral influenza infections

(Hartshorn et al., 2002); however, the direct human protein homologue remains to be identified.

In summary, many tangible examples are now available in the literature documenting the recognition of endogenous and exogenous mannosidic epitopes by a range of specialised human mrCLRs in diverse parts of the innate immune system. In general, the high avidity mrCLR–ligand interactions are achieved by the recognition of spatially organised mannosidic glycoepitope clusters on the surface of pathogens and on host cells/proteins by the CRD of the often oligomeric mrCLRs (Cohen, 2015). While mannosidic glycoproteins appear to undergo tight spatio-temporal regulation, other immune-stimulating glycoepitopes including galactosyl, sialyl and N-acetylglucosaminyl glycoepitopes are more constitutively secreted and expressed on cell surfaces (Lee et al., 2014a; Rachmilewitz, 2010; Stanley et al., 2009). Consequently, it may be speculated that the immune activation provided by these more ubiquitous extracellular glycoepitopes are dependent to a larger extent on a strict regulation of their specific receptors e.g. siglecs and galectins in order to only yield immune signals when strictly required in conditions involving inflammation and infection.

Interestingly, recent findings indicate that certain mrCLRs such as DC-SIGN assemble into microdomains (lipid rafts) on the cell surface, which create nanoclusters displaying a higher level “oligomerisation” that can further modulate the ligand binding profile (Gablus et al., 2015; Garcia-Parajo et al., 2014). The “low affinity, high avidity” binding mechanism of mrCLRs demonstrates that not only the nature of the monosaccharide, but also the ligand density, local orientation and solvent accessibility are factors determining the qualitative and quantitative recognition of mannosidic ligands and the cellular functional response (Dam and Brewer, 2010; Hyakumura et al., 2015; Mitchell et al., 2001).

4. Importance of mrCLRs–mannose interactions in inflammation and pathogenic infection

The expression and regulation of CLRs by a wide spectrum of immune cells and the physiology-dependent cellular presentation of protein glycosylation signatures are mechanisms that are now recognised to modulate the immune response (Lyons et al., 2015; Margreet and Geert-Jan, 2013). As discussed below through representative examples, the literature harbours accumulating evidence on the involvement of protein mannosylation in critical inflammatory and infection processes. With these examples, we aim to illustrate the significance of protein mannosylation expression and recognition under specific physiological conditions. Readers are reminded that protein–glycan interactions and the immune signals they transmit are often very complex in nature and may involve multiple recognition receptors and signal pathways (van Kooyk and Rabinovich, 2008). In addition to mannoseylated epitopes, other glycosidic or even polypeptide epitopes may contribute in an inhibitory or stimulating manner to the immune response.

4.1. Sterile (non-pathogenic) inflammation

Acute inflammation is often characterised by a rapid increase in vascular permeability and influx of innate immune

cells to inflammatory sites (Coico and Sunshine, 2009). The trigger, in the absence of pathogen infections, may be various sterile stimuli such as tissue injury, ischaemia or exogenous toxins and chemicals (Rock et al., 2010). If not resolved, such inflammatory responses can lead to chronic inflammation and tissue damage that are characteristic events underpinning several human diseases including cancer.

4.1.1. Cancer

Common characteristics of all cancers are the rapid cell growth leading to cell invasion and metastasis to other body parts (Fuster and Esko, 2005). Due to the altered cell physiology, cancerous transformations are inherently accompanied by aberrant glycosylation signatures that may assist in the diagnosis, staging and surveillance of cancer (Christiansen et al., 2014). As an example, glycoproteins isolated from the serum of breast cancer patients showed a positive correlation between the levels of high mannoseylation and the tumour burden (de Leoz et al., 2011). In addition, increased levels of high mannoseylated glycoproteins were found in both invasive and non-invasive breast cancer cells (Goetz et al., 2009) and mannoseylated glycoforms were expressed directly on the epithelial growth factor receptor, a glycoprotein considered as a strong tumour marker (Johns et al., 2005; Nicholson et al., 2001). Large cohorts of paired breast cancerous and adjacent non-tumorigenic tissues have convincingly demonstrated high mannose-rich glycan signatures (particular M8) in tumours (Liu et al., 2013b). Similarly, deep *N*-glycome profiling of paired colorectal cancer (CRC) and adjacent healthy tissues showed high mannose-rich cancer associated profiles (Sethi et al., 2015), which has been further documented in many other cancers including tissues and fluids from colon cancer (Saeland et al., 2012), ovarian cancer (Anugraham et al., 2014), lung adenocarcinoma (Ruhaak et al., 2015), pancreatic cancer (Park et al., 2015), gastric cancer (Ozcan et al., 2014) and in various cancer cell lines (Holst et al., 2015; Sethi et al., 2014). The cancer-specific association with high mannose type glycosylation has been attributed to the premature secretion of glycoproteins from the secretory pathway, perhaps due to the rapid growth rate of cancer cells, resulting in less *N*-glycan processing to complex and hybrid structures and therefore, an accumulation of high mannose glycoproteins secreted into the extracellular milieu (de Leoz et al., 2011; Sethi et al., 2015). We have also shown a correlation between lower *N*-glycan processing and high glycoprotein secretion rates in breast cancer cells (Lee et al., 2014a). Finally, some of the high mannose epitopes seen in cancer tissues and body fluids may arise from the leakage of intracellular (ER/Golgi) glycoproteins from dying cells.

Elevation in the expression of paucimannosidic epitopes has also been observed in CRC tumour tissues. Specifically, the amount of paucimannosylation, such as the level of the M1F *N*-glycans with terminal β 1,4-linked mannose, was found to be increased during the progression of CRC (Balog et al., 2012; Kaprio et al., 2015; Serhi et al., 2015). The protein profiling of CRC tumour tissues indicated a neutrophil-rich tumour microenvironment suggesting significant neutrophil infiltration and contribution to the molecular profile of CRC (Sethi et al., 2015). Indeed, neutrophilic in-

filtration in CRC has been described and correlated with favourable patient outcome (Hirt et al., 2013). The expression of high mannose and paucimannosidic glycoproteins in cancer tissues, originating from both immune cells and epithelial cancer cells, suggest their functional relevance in the cancer environment, but their functions remain undescribed. Importantly, the expression of soluble DC-SIGN and DC-SIGNR in the serum of colon cancer patients was found to reflect the clinical patient outcome, suggesting the functional involvement of these mCLRs (Jiang et al., 2014). Furthermore, serum MBL levels in CRC patients were correlated with patient survival (Swierczko et al., 2013). Finally, the presence of MR-expressing regulatory type 2 macrophages in CRC was also correlated with metastatic tumour progression (Algars et al., 2012). Although it is tempting to speculate on mannose-based binding and effector functions of these soluble mCLRs in cancer, they were also found to display high reactivity towards Lewis-type epitopes in the investigated systems (Nonaka et al., 2014; van Gisbergen et al., 2005a), further emphasising the complexity of the involvement of protein glycosylation in tumourigenic processes.

Considering that cancer is associated with an increased mannose "load" and elevated levels of soluble mCLRs, it seems reasonable to suggest that protein mannoseylation expression and recognition may play important roles in the regulation of cancer processes including cancer cell adhesion, migration and signalling. However, the exact role(s) of protein mannoseylation in mediating tumour development, immunosurveillance and eliciting anti-tumour immune responses are still poorly understood, underscoring the difficulty in unravelling the mechanisms buried in the competing anti- and pro-inflammatory processes inherent to cancer development and progression, that, when understood, will undoubtedly aid in the design of cancer therapeutics (Pinho and Reis, 2015; Yan et al., 2015). As proof-of-concept, several mannose-based cancer therapeutics have been recently reported and tested *in vitro*, but awaiting clinical testing, including mannoseylated chitosan for prostate tumour immunotherapy (Yao et al., 2013), mannoseylated radiotracers for cancer staging (Azad et al., 2015) and anti-tumourigenic mannose-recognising plant lectins (Liu et al., 2008).

4.1.2. Haematological and vascular disorders

The importance of protein mannoseylation was demonstrated in follicular lymphoma (FL), which is characterised by an accumulation of mutated clonal germinal centre B cells (Limpens et al., 1995). IgM on the surface of these FL B cells carries high mannose glycans at the antigen-binding site. The light chain high mannoseylated IgM interacted with MBL, DC-SIGN and MR that are over-expressed in myeloid cells within the FL tumour microenvironment (Farinha et al., 2005). It was suggested that these interactions promote the growth of FL B cells (pro-tumoural activity) by mediating the intracellular signalling and facilitating cytokine-based recruitment of tumour-associated macrophages (Amin et al., 2015; Coelho et al., 2010; Linley et al., 2015; Radcliffe et al., 2007). The binding and signalling cascades were attenuated by blocking DC-SIGN and MR with mannoseylated epitopes, thereby validating the involvement of high

mannose glycans in the binding of IgM to these mCLRs and in the downstream effector functions. Such protein–glycan interactions illustrate viable therapeutical avenues if similar compounds that selectively antagonise the receptor binding can be designed. Protein mannosylation also plays an important role in haemophilia A, in which patients are characterised by a partial or complete deficiency in the coagulation factor VIII (FVIII). Replacement therapy with recombinant human FVIII is currently administered to patients to treat bleeding tendencies and to restore normal vascular haemostasis (Morfini et al., 2013). However, allo-antibodies directed against FVIII (anti-FVIII antibodies) in treated patients have resulted in unwanted refractory responses (Ehrenforth et al., 1992). High mannose glycans were identified on two *N*-glycosylation sites of recombinant human FVIII (Hironaka et al., 1992; Medzihradsky et al., 1997) and the production of anti-FVIII antibodies was attributed to the presence of these high mannose glycans. The glycans were recognised by the MR on *in vitro* monocyte-derived DCs, resulting in the subsequent T cell activation and production of anti-FVIII antibodies (Dasgupta et al., 2007). Interestingly, von Willebrand factor, a FVIII chaperone, inhibited the FVIII–MR interactions (Dasgupta et al., 2007). This example demonstrates that mCLRs on APCs are promoting immunogenic or “tolerogenic” features. The immunogenicity of FVIII in haemophilia A patients has been recently reviewed (Hartholt et al., 2015; Lai et al., 2015).

Immune cell infiltration into inflamed tissues is a first-line inflammatory response and a characteristic feature of early atherosclerosis (Galkina and Ley, 2009). The circulating immune cells follow a cascade of tethering, rolling, adhesion, and finally, transmigration to the inflamed tissues by interaction with endothelial cells (Kelly et al., 2007). Activated aortic endothelial cells abundantly express high mannose epitopes potentiating the recruitment of monocytes during atherogenesis. In addition, activated endothelial cells in coronary arteries preferentially express high mannose ICAM-1 (Scott et al., 2012, 2013). As discussed above, high mannose glycoproteins are typically rare epitopes in a “healthy” (non-alert) extracellular environment (Rachmilewitz, 2010). As another line of evidence for the involvement of mannosylated glycans in leukocyte transmigration, cytokine inhibition reduced the mannosylation of endothelial surfaces, which, in turn, attenuated the monocyte extravasation (Chacko et al., 2011). The exact interaction partners and their binding mechanisms were not determined, but lectin staining of endothelial vascular tissues using concanavalin A indicated that trimannosidic epitopes are the recognition ligands for a yet-to-be-determined mCLR (García-Vallejo et al., 2006). Of direct relevance, the presence of MBL was identified in mice with early aortic lesions (Matthijssen et al., 2009) and mannose-recognising DCs were the main cellular features of athero-predisposed areas of human aorta (Bobryshev, 2010). Adding to the growing list of immune-regulatory functions, protein mannosylation, thus, also serves as “signposts” to direct and regulate the trafficking and homing of leukocytes to inflammatory sites (Scott and Patel, 2013). Other lectin receptors including L- and E-selectin, which have affinities towards fucose-, galactose-, GalNAc- and sialic acid-containing glycans such

as sialyl-Lewis^x expressed on activated leukocytes and endothelial cells, respectively, also play important roles in the homing of leukocytes to sites of inflammation, underscoring the complexity involved in ligand–receptor interactions (Lowe, 2003). Any synergistic effects of these sialic acid-centric ligand receptors and the mCLRs in mediating leukocyte trafficking remains unknown.

4.1.3. Allergy

Recently, mannosidic *N*-glycans were reported to mediate mast cell activation via IgE antibodies (Plomp et al., 2014). With six occupied *N*-glycosylation sites, human IgE is a highly glycosylated Ig in the antibody family. Despite its low serum levels and short half-life, IgE mediates highly life threatening anaphylactic reactions due to its association with the Fc epsilon receptor type 1 (FcεRI) on mast cells during an allergic reaction e.g. pollen. This mechanism is considered to be the cause of some inflammatory diseases including asthma (Lee and Vadas, 2011). Interestingly, a single glycosylation site of human IgE (Asn394) carrying high mannose *N*-glycans was found to be essential for the initiation of anaphylaxis. Genetic deletion of this glycosylation site as well as enzymatic removal of the mannosidic *N*-glycans abrogated the IgE–FcεRI interaction and prevented mast cell degranulation (Shade et al., 2015). This observation emphasises the importance of performing site-specific glycoprofiling of glycoproteins to advance our understanding of the functional role(s) of protein glycosylation (Thaysen-Andersen and Packer, 2014; Thaysen-Andersen et al., 2016; Wu et al., 2015). It also suggests that mannosidic *N*-glycans are specifically located on IgE to serve a role in initiating anaphylaxis, however, the specific role(s) of IgE mannosylation is still being debated (Bantleon et al., 2016). Dust mite allergens (Der f 1 and Der p 1) are also causative factors of asthma. Dectin-2 and MR on monocyte-derived DCs, together with soluble SP-A/D collectins, were shown to recognise mannosylated Der f 1 and Der p 1 allergens thereby contributing to the pathogenesis of asthma (Al-Ghoul et al., 2012; Barrett et al., 2009; Deslée et al., 2002). Paucimannosylated proteins were also reported in the allergy-associated innate immune cells including eosinophils (Eriksson et al., 2007) that have the similar capacity as neutrophils to undergo degranulation (Woschnagg et al., 2009). Although the potential interactions of the eosinophil-derived paucimannosidic glycoproteins with mCLRs remain to be further investigated in the context of allergy, these observations support the notion that paucimannosylation may have a functional role in eliciting allergic reactions. Finally, protein mannosylation may also play a role in food allergies against nuts and legumes. For example, the major peanut allergen Ara h 1 was identified to be a ligand of DC-SIGN and acts as an adjuvant for T helper type 2 cell activation (Shreffler et al., 2006). Interestingly, Ara h 1 and the homologous convicillin storage protein 2 in *Lotus japonicus* have been found to carry exclusively high mannose and paucimannosidic *N*-glycans (Al-Ghoul et al., 2012; Dam et al., 2013; Kolarich and Altmann, 2000), suggesting a direct or indirect role of plant protein mannosylation in eliciting human food allergies.

4.1.4. Autoimmunity

Autoimmune diseases such as systemic lupus erythematosus (SLE) arise from the dysregulation of self-tolerance. The immune system incorrectly generates auto-antibodies against the host itself, resulting in the formation of immune complexes and cellular/tissue damage via complement activation. Mannose-based autoimmunity was illustrated in mutant mice expressing high mannose-rich proteins due to a lack of the Golgi α -mannosidase II responsible for the formation of complex and hybrid *N*-glycans (Chui et al., 1997; Roth et al., 2010). These mice displayed SLE-like symptoms and renal dysfunction (Chui et al., 2001), presumably induced by the increased expression of high mannose and paucimannosidic glycoproteins in kidney and red blood cells (Green et al., 2007; Hashii et al., 2009). Given the ability of mannosylated glycans to interact with mCLRs (e.g. MBL and DC-SIGN) (Sancho and Reis e Sousa, 2012), deficiency in α -mannosidase II may trigger a mannose-based self-intolerance, resulting in a chronic SLE-like inflammatory response. It was further proposed that GlcNAc-capped *N*-glycans masking the immunogenic mannosidic epitopes are protective mechanisms against self-recognition (Chui et al., 2001). In short, considering their dynamic expression and recognition in the immune system, it is likely that mannosylated glycoepitopes play central roles in autoimmunity (Maverakis et al., 2015). Dissecting the complexity of these ligand–receptor interactions may open therapeutic avenues, not only for autoimmune disorders, but also to resolve unwanted sterile and pathogen-induced inflammatory conditions.

4.2. Pathogenic infections

Human immunity involves two inter-dependent components: the innate and adaptive immune system. The innate immunity provides the front line defence against foreign pathogens and modulates the adaptive immune response that arrives as a second, more targeted, response to the present threat. Innate immune cells including neutrophils, monocytes, DCs and macrophages are specialised in capturing and engulfing micro-organisms, releasing cytokines and activating adaptive immune cells thereby collectively promoting inflammation. Unlike sterile inflammation, pathogenic infections rarely become chronic provided that a timely and sufficiently strong host immune response is established. Intriguingly, pathogens have evolved to express host-like glycoepitopes that they use as host attachment factors or as a means to evade the host immune system through molecular mimicry (Netea et al., 2015; van Kooyk and Geijtenbeek, 2003). Conversely, humans use glycoepitope decoys to avoid pathogen infection by means of ligand (glycan) competition (Kreisman and Cobb, 2012). Although displaying many of the same mannosidic epitopes (Man α 1,2/3/6Man-R) and even larger mannose substructures, the pathogenic glycoepitopes are mostly presented on *O*-linked mannosidic scaffolds rather than on the common core of the human *N*-glycans.

4.2.1. Bacterial and fungal infections

The *Mycobacterium tuberculosis* (Mtb) bacterium demonstrates unique survival and infection traits in lung alveolar

macrophages, leading to tuberculosis (TB) (Russell, 2011). Infected individuals are often asymptomatic during an extended latent phase due to an inhibited adaptive immune response. Hence, innate immune cells such as neutrophils and macrophages are considered key players in combating TB (Hare et al., 2015; Hilda et al., 2015). Excellent reviews describe the immune-regulation in macrophages during Mtb infections (Amaral et al., 2015; Rajaram et al., 2014). In particular, the mannose-containing glycoconjugates in the cell envelope of Mtb have received significant interest. Amongst other prevalent lipomannan and manno-proteins, the mannose-capped lipoarabinomannan (ManLAM) is an abundant envelope-expressed mannose-containing lipoglycan of Mtb (Kallenius et al., 2015; Torrelles et al., 2012). The ManLAM core consists of α -mannan and α -arabinan whereas α 1,2-linked mono- to trimannosyl epitopes are exposed on the non-reducing end (Kolattukudy et al., 1997; Schlesinger et al., 1994). These mannose ‘caps’ interact with MR (Schlesinger et al., 1996) and DC-SIGN (Geijtenbeek et al., 2002; Maeda et al., 2003) on macrophages and DCs, respectively. Dectin-2 and soluble mCLRs also recognise ManLAM (Scordo et al., 2015; Yonekawa et al., 2014). Interestingly, Mtb shows strain-specific length and configuration of the ManLAMs, differences that are recognised by the host immune system and add complexity to the TB pathogenesis (Maeda et al., 2003).

Mannose on the Mtb surface has also been described to contribute to the bacterial survival processes within macrophages e.g. by inhibiting the fusion of the phagolysosomes and antimicrobial lysosomal vacuoles (Kang et al., 2005; Rajaram et al., 2011). This mechanism increases the Mtb replication rate and accelerates the cell death of the macrophages (McCarthy et al., 2005; Patterson et al., 2003; Torrelles et al., 2009). Mannosidic epitopes do not influence the host immune response in other *Mycobacterium* (non-Mtb) variants (Appelmek et al., 2008), suggesting species/strain-specific surface mannosylation or unique mannose-based pathogenic mechanisms of Mtb. It was hypothesised that the Man α 1,2Man α -R epitopes coating virulent Mtb create high avidity ligands for host mCLRs to promote latent TB infections (Torrelles and Schlesinger, 2010). In support of this hypothesis, *O*-mannosidic epitopes expressed by Mtb were demonstrated to contribute to host virulence (Liu et al., 2013a; Smith et al., 2014). By utilising the mannose-centric disease mechanism of Mtb, ManLAM-mimicking multivalent mannodendrimers have been synthesised and found to prevent acute lung inflammation in mice, but its efficacy towards TB prevention in humans still needs to be assessed (Blattes et al., 2013).

Mannans and mannoproteins are also found in the fungal cell wall of *C. albicans*. The protective mechanisms of host CLRs against *C. albicans* were recently reviewed (Netea et al., 2015). *C. albicans* strains deficient in these mannose-based components showed altered virulence and immune-recognition by host mCLRs i.e. DC-SIGN (Cambi et al., 2008; Te Riet et al., 2015), Mincle (Bugarcic et al., 2008) and dectin-2 (Sato et al., 2006). However, it was concluded that induction of the inflammatory response was not solely dependent on the mannosidic epitopes and mCLRs, but rather involved multiple pathways of fungal *N*- and *O*-glycan recognition (Netea et al., 2006; van der Graaf et al., 2005),

emphasising the importance of engaging multiple PRRs to initiate an efficient host immune response.

Adding to the complexity, pathogen infections also involve interactions between host protein mannosylation and microbial lectins, so-called adhesins. As prime examples, the pathogenic bacteria, *Escherichia coli* and *Pseudomonas aeruginosa*, causing urinary tract infections (UTI) (Mulvey et al., 2000) and cystic fibrosis (Davies, 2002; Venkatakrishnan et al., 2015), respectively, possess adhesins that enable colonisation of host tissue by binding to mannosidic epitopes. Specifically, the type I fimbriae adhesin FimH protein (UniProtKB accession number: P08191) expressed by *E. coli* binds to terminal epitopes of high mannose and paucimannosidic glycans conjugated to uroplakin Ia residing on the surface of urothelial cells using catch bond binding mechanisms (Bouckaert et al., 2006; Sauer et al., 2016; Taganna et al., 2011; Wellens et al., 2008). Remarkably, urinary SP-A/D collectins were recently reported to inhibit the growth of uropathogenic *E. coli* *in vitro*, underscoring the important protective roles of soluble mCLRs (Hu et al., 2015). Similarly, *P. aeruginosa* relies on its α -mannose- and α -fucose-binding PA-III (*LecB*) (UniProtKB accession number: Q9HYN5, currently unreviewed entry) for the attachment to lung airways (Tielker et al., 2005). Comparable binding strengths of mannosidic and fucosylated ligands by PA-III were observed using glycan arrays; however, thermodynamic studies using modified monosaccharides suggested that fucosylated ligands are strongly preferred over mannosidic epitopes by PA-III, displaying high avidity binding (micromolar K_d) (Marotte et al., 2007; Sabin et al., 2006). These glycan (host)–adhesin (pathogen) interactions are examples of efficient mannose-based mechanisms that pathogens use for adherence to the host as the first step towards establishing infections. Uromodulin, a major high mannose-containing glycoprotein excreted in the urine, shows protective effects against UTI by competing with the binding of *E. coli* FimH to uroplakin Ia (Pak et al., 2001). Interestingly, changes in mannosylation of uromodulin were observed in pregnant women (Smagula et al., 1990; Van Rooijen et al., 2001), however, it remains to be investigated if the pregnancy-associated changes elicit enhanced or reduced protection towards UTI. In addition, glycan–glycan interactions of pathogenic bacteria such as *Salmonella typhimurium* and *Haemophilus influenzae* to mannosidic host epitopes were recently shown using glycan arrays. This suggests that glycan–glycan interactions also play important roles in pathogen–host interactions in addition to the adhesion-mediated infection strategy (Day et al., 2015). Finally, exciting developments of mannose-centric drug delivery systems and anti-adhesive therapies tested *in vitro* and *in vivo* to combat pathogenic infections such as UTI (Bouckaert et al., 2013; Mydock-McGrane et al., 2015; Pichl et al., 2015) and cystic fibrosis (Hauck et al., 2013) have been recently reported. Dietary α -mannose was also found to be beneficial towards limiting the UTI burden in clinical trials (Kranjcec et al., 2014), illustrating the multiple areas in which mannose can contribute to human health.

4.2.2. Viral infections

Viruses notoriously hijack the host protein and glycosylation machinery enabling them to produce virions

(virus particles) with human-like surface glycosylation. Essential viral functions including host entry and egress are inherently dependent on the glycosylation pattern of key viral envelope proteins e.g. hemagglutinin (HA) and neuraminidase expressed by the influenza virus (Klenk et al., 2002). For immune-evasion, glycosylation serves the purpose of masking antigenic epitopes of HA enabling viruses to prevent host recognition and antibody-mediated immune response (Vigerust and Shepherd, 2007).

The HIV envelope protein, gp120, consists of densely packed high mannose glycans organised into large mannosidic patches on the surface of the proteins located on the virus. Such patches generate glycan shields that efficiently prevent elimination of the virus by viral-directed neutralising antibodies (Bonomelli et al., 2011; Botos and Wlodawer, 2005). These intricate protective mechanisms contribute to the HIV antigenic drift allowing the virus to continue to evade the immune system. DCs assist in neutralising HIV infections by binding the highly mannosylated surface of virus particles and simultaneously utilise DC-SIGN and DCIR to mediate the transmission of virus particles to CD4+ T helper cells by their recognition of high mannosylated gp120 (Geijtenbeek and Gringhuis, 2009; Jin et al., 2014). The HIV further exploits the host by inducing apoptosis of DCs while concurrently enhancing their own viral replication rate (Fanibunda et al., 2011; Mason and Tarr, 2015; Sondergaard et al., 2014). Other viruses (e.g. measles and influenza A) also express high mannose glycans on their virion surface proteins and similarly utilise DC-SIGN for cell entry and transinfection of T helper cells (Mesman et al., 2012; Santiago et al., 2010; Tate et al., 2014). Considering its mannose-reactivity, it was not too surprising that SP-D was predicted to interact with high mannosylated glycosylation sites of HA on influenza A virus (Khatri et al., 2016). Soluble MBL was also shown to bind high mannosylated gp120 of HIV (Hart et al., 2002). Furthermore, human Langerhans cells also capture HIV through langerin and degrade them by internalisation into the Birbeck granules (de Witte et al., 2007) as described above.

The glycoprofile of HIV gp120 and the intrinsic mannose patch have been accurately characterised (Doores et al., 2010; Scanlan et al., 2007). These efforts enabled the development of anti-glycan vaccines, such as the broad neutralising antibody, 2G12, that targets the high mannose glycans, specifically Man α 1,2Man α -R epitopes of M7–M9, on HIV gp120 (Sanders et al., 2002). Subsequent developments used shared gp120 glycosidic and polypeptide epitopes to produce efficacious neutralising antibodies (i.e. PGT128) (Pejchal et al., 2011). Since HIV can add and delete glycosylation sites on gp120 in response to selection pressure, resistance to broad neutralising antibodies was predicted (Moore et al., 2012). However, these broad neutralising antibodies seem to tolerate changes in the intrinsic mannose patch of gp120 with limited impact on their efficacy, suggesting that it is a stable antigenic target (Pritchard et al., 2015). Alternatively, multivalent glycodendrimers and mannose-based glycomimetics have been designed to prevent the transmission of HIV to T helper cells by blocking the DC-SIGN-based uptake of HIV (Garcia-Vallejo et al., 2013; Obermajer et al., 2011; Varga et al., 2014). Taken together, it appears that viruses better than many other species can present and constantly

manipulate protein mannosylation on their surface to facilitate a successful co-existence with the host.

4.2.3. Mannose-recognising antibodies

The prognostic serological markers, anti-neutrophilic cytoplasmic antibodies (ANCA) and anti-*Saccharomyces cerevisiae* antibodies (ASCA) are mannose-recognising antibodies (mrAbs), capable of accurately diagnosing Crohn's disease and ulcerative colitis (Sandborn, 2004; Sendid et al., 1996). ASCA may be raised against the yeast mannan-cell wall (branched α 1,2/3/6-linked mannose-rich polysaccharides). Recently, anti-mannobioside carbohydrate antibodies reactive to Man α 1,3Man α -R epitopes were developed to complement these ASCA and showed high predictive value for Crohn's disease (Vandewalle-El Khoury et al., 2008). In addition, mrAbs against the mannosidic glycoprotein 2 on microfold cells in intestinal Peyer's patches were utilised for the diagnosis of Crohn's disease (Yu and Lowe, 2009). Furthermore, pauci-immune focal necrotising glomerulonephritis, a severe autoimmune inflammatory disease, was shown to involve ANCA directed against paucimannosylated human LAMP-2 residing in the azurophilic and specific granules of neutrophils (Kain et al., 2008; Thaysen-Andersen et al., 2015), but the nature of the reactive epitopes is still debated (Kain and Rees, 2013; Roth et al., 2012). The pathogenicity of ANCA-associated glomerulonephritis was proposed to be partly related to the binding and inactivation of antimicrobial proteins secreted by human neutrophils upon degranulation, including the paucimannosylated myeloperoxidase and proteinase 3 (Couser and Johnson, 2015; Ravnsborg et al., 2010; Zoega et al., 2012). Additionally, ANCA may cause increased and unwanted activation of neutrophils resulting in tissue injury due to the downstream pro-inflammatory response. The reacting ANCA epitopes remain to be specified, but evidence points to partial glycan-(mannose)-based recognition motifs.

In addition to the self-recognising ANCA, the literature also describes many examples of host-derived mrAbs resulting from pathogenic infections. For example, mice infected with the paucimannose- and high mannose-containing *S. mansoni* parasite produced mrAbs reactive against the paucimannosidic trimannosyl epitope, indicating that such epitopes are immunogenic in mice (Khoo et al., 1997). However, anti-paucimannosidic antibodies were not produced in *Schistosoma*-infected patients implying that the parasitic glycoepitopes were not sufficiently immunogenic, or not present in sufficient quantities, to trigger a B cell-based antibody response in humans (van Remoortere et al., 2003). The mouse-derived anti-paucimannosidic antibodies reacted towards human liver and cerebellum glycoproteins, indicating the abundance of endogenous human paucimannosylation and perhaps thereby providing a possible explanation as to the absent immune response upon this parasitic infection (van Remoortere et al., 2003). Another anti-paucimannosidic antibody (Mannitou) raised against leech glycans and similarly recognises the paucimannosidic trimannosidic epitope was used to study the expression of paucimannosylation in mouse tissues, human cancer tissues and adult pancreatic stem cells and it was suggested that paucimannosidic epitopes are oncofetal antigens in mammals (Zipser et al., 2012). Subsequently,

paucimannosidic epitopes were shown to be involved in the propagation of mouse neural progenitor cells, human glioblastoma cells and macrophages (Dahmen et al., 2015). Supported by molecular structural analysis (Thaysen-Andersen et al., 2015; Venkatakrishnan et al., 2015), these findings substantiate that protein paucimannosylation is a recurring feature of mammalian protein glycosylation, arguing their classification as a separate under-reported type of protein N-glycosylation.

5. Conclusion and future perspectives

The literature summarised in this review provides accumulated support for the notion that mannosidic glycoepitopes play important roles in the initiation, progression, and the resolution of inflammation and pathogenic infections. Tangible examples document the importance of mannosidic glycoepitopes as exogenous and endogenous ligands that cells express in a spatiotemporally-regulated manner and, further, demonstrate their interactions with a range of mrCLRs and mrAbs expressed by various host immune cells as well as by pathogens.

In addition to inflammation and infection-centric processes, which were the focus of this review, recent findings also point to a functional involvement of mannosidic epitopes in fertility (Olejnik et al., 2015; Tecle and Gagneux, 2015) and many other physiological and pathophysiological conditions such as the congenital disorders of glycosylation (Henner and Cabalzar, 2015; Zhang et al., 2015). The use of mannose as a clinical supplement in the treatment of these conditions was also recently described (Sharma et al., 2014). Exceeding the scope of this review, it could be speculated that mannose structures play even wider roles in inflammation and infection in the context of antimicrobial activity: a quick search in the chemical database SciFinder (Chemical Abstracts Service) revealed ~140 α -mannose-containing small molecules, many of which are natural products displaying potential antimicrobial activity. However, for the majority of the compounds, the antimicrobial and immune-stimulating activities and any mannose-dependent mode-of-action remain to be appropriately tested and confirmed.

In summary, recent advances in 'omics' technologies and glycobiology have increased our structural and functional knowledge of the spectrum of biomolecular and cellular signatures associated with inflammation and pathogenic infection in human and representative model systems. Nonetheless, it seems reasonable to suggest that we are merely beginning to decode the multiple and diverse roles served by glycosylated ligands, including mannose-based structures, and their receptors in maintaining immunological homeostasis (Garcia-Vallejo et al., 2015). Being a major structural and functional building block of N-glycoproteins, mannose clearly serves other roles than just being a source of nutrition in humans (Ichikawa et al., 2014). The intra-, inter- and extracellular roles of protein mannosylation, represented predominantly by the spatiotemporally-regulated high mannose and paucimannosidic glycoproteins in humans, appear to span a wide spectrum and is complicated further by being strongly context-dependent. Multidisciplinary approaches appear to be rewarded, or

indeed required, as we enhance our understanding of the exact roles of protein mannosylation and how they interrelate with the recognition of other important glycoepitopes in inflammation and infection. Lessons learned along this journey are feeding into basic science, translational research and therapeutic developments in the extended network of immune-related diseases in the field of glycoimmunology.

Acknowledgements

I.L., D.K., N.H.P. and M.T.-A. wrote the review. I.L. was supported by an international Macquarie University Research Scholarship (iMQRES) and an Australian Cystic Fibrosis postgraduate studentship. M.T.-A. was supported by a Fellowship from the Cancer Institute NSW, Australia (grant number 13/ECF/1-02) and a Macquarie University Research Development Grant (MQRDG). D.K. is supported by the Max Planck Society and European Union, "Glycoproteomics", grant number PCIG09-GA-2011-293847. Serene Gwee is thanked for proof-reading the review.

References

- Aebi, M., 2013. N-linked protein glycosylation in the ER. *Biochim. Biophys. Acta* 1833 (11), 2430–2437. doi:10.1016/j.bbamcr.2013.04.001.
- Aebi, M., Bernasconi, R., Clerc, S., Molinari, M., 2010. N-glycan structures: recognition and processing in the ER. *Trends Biochem. Sci.* 35 (2), 74–82. doi:10.1016/j.tibs.2009.10.001.
- Al-Ghoul, A., Johal, R., Sharquie, I.K., Emara, M., Harrington, H., Shakib, F., et al., 2012. The glycosylation pattern of common allergens: the recognition and uptake of Der p 1 by epithelial and dendritic cells is carbohydrate dependent. *PLoS ONE* 7 (3), e33929. doi:10.1371/journal.pone.0033929.
- Algars, A., Irjala, H., Vaitinen, S., Huhtinen, H., Sundstrom, J., Salmi, M., et al., 2012. Type and location of tumor-infiltrating macrophages and lymphatic vessels predict survival of colorectal cancer patients. *Int. J. Cancer* 131 (4), 864–873. doi:10.1002/ijc.26457.
- Amaral, E.P., Lasunskaja, E.B., D'Imperio-Lima, M.R., 2015. Innate immunity in tuberculosis: how the sensing of mycobacteria and tissue damage modulates macrophage death. *Microbes Infect.* doi:10.1016/j.micinf.2015.09.005.
- Amin, R., Mourcin, F., Uhel, F., Pangault, C., Ruminy, P., Dupre, L., et al., 2015. DC-SIGN expressing macrophages trigger activation of mannosylated IgM B-cell receptor in follicular lymphoma. *Blood* doi:10.1182/blood-2015-04-640912.
- An, H.J., Gip, P., Kim, J., Wu, S., Park, K.W., McVaugh, C.T., et al., 2012. Extensive determination of glycan heterogeneity reveals an unusual abundance of high mannose glycans in enriched plasma membranes of human embryonic stem cells. *Mol. Cell. Proteomics* 11 (4), M111.010660. doi:10.1074/mcp.M111.010660.
- Anugraham, M., Jacob, F., Nixdorf, S., Everest-Dass, A.V., Heinzlmann-Schwarz, V., Packer, N.H., 2014. Specific glycosylation of membrane proteins in epithelial ovarian cancer cell lines: glycan structures reflect gene expression and DNA methylation status. *Mol. Cell. Proteomics* 13 (9), 2213–2232. doi:10.1074/mcp.M113.037085.
- Appelmek, B.J., van Die, I., van Vliet, S.J., Vandenbroucke-Grauls, C.M.J.E., Geijtenbeek, T.B.H., van Kooyk, Y., 2003. Cutting edge: carbohydrate profiling identifies new pathogens that interact with dendritic cell-specific ICAM-3-grabbing integrin on dendritic cells. *J. Immunol.* 170 (4), 1635–1639. doi:10.4049/jimmunol.170.4.1635.
- Appelmek, B.J., den Dunnen, J., Driessen, N.N., Ummels, R., Pak, M., Nigou, J., et al., 2008. The mannose cap of mycobacterial liparabinomannan does not dominate the mycobacterium-host interaction. *Cell. Microbiol.* 10 (4), 930–944. doi:10.1111/j.1462-5822.2007.01097.x.
- Arnold, J.N., Wormald, M.R., Suter, D.M., Radcliffe, C.M., Harvey, D.J., Dwek, R.A., et al., 2005. Human serum IgM glycosylation: identification of glycoforms that can bind to mannan-binding lectin. *J. Biol. Chem.* 280 (32), 29080–29087. doi:10.1074/jbc.M504528200.
- Azad, A.K., Rajaram, M.V.S., Metz, W.L., Cope, F.O., Blue, M.S., Vera, D.R., et al., 2015. γ -Tilmanocept, a new radiopharmaceutical tracer for cancer sentinel lymph nodes, binds to the mannose receptor (CD206). *J. Immunol.* doi:10.4049/jimmunol.1402005.
- Balog, C.L., Stavenhagen, K., Fung, W.L., Koeleman, C.A., McDonnell, L.A., Verhoeven, A., et al., 2012. N-glycosylation of colorectal cancer tissues: a liquid chromatography and mass spectrometry-based investigation. *Mol. Cell. Proteomics* 11 (9), 571–585. doi:10.1074/mcp.M111.011601.
- Bantleon, F., Wolf, S., Seismann, H., Dam, S., Lorentzen, A., Mische, M., et al., 2016. Human IgE is efficiently produced in glycosylated and biologically active form in lepidopteran cells. *Mol. Immunol.* 72, 49–56. doi:10.1016/j.molimm.2016.02.013.
- Barrett, N.A., Maekawa, A., Rahman, O.M., Austen, K.F., Kanaoka, Y., 2009. Dectin-2 recognition of house dust mite triggers cysteinyl leukotriene generation by dendritic cells. *J. Immunol.* 182 (2), 1119–1128. doi:10.4049/jimmunol.182.2.1119.
- Behrens, A.-J., Vasiljevic, S., Pritchard, L.K., Harvey, D.J., Andev, R.S., Krumm, S.A., et al., 2016. Composition and antigenic effects of individual glycan sites of a trimeric HIV-1 envelope glycoprotein. *Cell Rep.* doi:10.1016/j.celrep.2016.02.058.
- Biedron, R., Konopinski, M.K., Marcinkiewicz, J., Jozefowski, S., 2015. Oxidation by neutrophils-derived HOCl increases immunogenicity of proteins by converting them into ligands of several endocytic receptors involved in antigen uptake by dendritic cells and macrophages. *PLoS ONE* 10 (4), e0123293. doi:10.1371/journal.pone.0123293.
- Blattes, E., Vercellone, A., Eutamene, H., Turrin, C.O., Theodorou, V., Majoral, J.P., et al., 2013. Mannodendrimers prevent acute lung inflammation by inhibiting neutrophil recruitment. *Proc. Natl. Acad. Sci. U.S.A.* 110 (22), 8795–8800. doi:10.1073/pnas.1221708110.
- Bloem, K., Vuist, I.M., van der Plas, A.J., Knippels, L.M., Garssen, J., Garcia-Vallejo, J.J., et al., 2013. Ligand binding and signaling of dendritic cell immunoreceptor (DCIR) is modulated by the glycosylation of the carbohydrate recognition domain. *PLoS ONE* 8 (6), e66266. doi:10.1371/journal.pone.0066266.
- Bloem, K., Vuist, I.M., van den Berk, M., Klaver, E.J., van Die, I., Knippels, L.M., et al., 2014. DCIR interacts with ligands from both endogenous and pathogenic origin. *Immunol. Lett.* 158 (1–2), 33–41. doi:10.1016/j.imlet.2013.11.007.
- Bobyryshev, Y.V., 2010. Dendritic cells and their role in atherogenesis. *Lab. Invest.* 90 (7), 970–984. doi:10.1038/labinvest.2010.94.
- Bonomelli, C., Doores, K.J., Dunlop, D.C., Thaney, V., Dwek, R.A., Burton, D.R., et al., 2011. The glycan shield of HIV is predominantly oligomannose independently of production system or viral clade. *PLoS ONE* 6 (8), e23521. doi:10.1371/journal.pone.0023521.
- Botos, I., Wlodawer, A., 2005. Proteins that bind high-mannose sugars of the HIV envelope. *Prog. Biophys. Mol. Biol.* 88 (2), 233–282. doi:10.1016/j.pbiomolbio.2004.05.001.
- Bouckaert, J., Mackenzie, J., de Paz, J.L., Chipwaza, B., Choudhury, D., Zavialov, A., et al., 2006. The affinity of the FimH fimbrial adhesin is receptor-driven and quasi-independent of Escherichia coli pathotypes. *Mol. Microbiol.* 61 (6), 1556–1568. doi:10.1111/j.1365-2958.2006.05352.x.
- Bouckaert, J., Li, Z., Xavier, C., Almant, M., Caveliers, V., Lahoutte, T., et al., 2013. Heptyl alpha-D-mannosides grafted on a beta-cyclodextrin core to interfere with Escherichia coli adhesion: an in vivo multivalent effect. *Chemistry (Easton)* 19 (24), 7847–7855. doi:10.1002/chem.201204015.
- Bugarcic, A., Hitchens, K., Beckhouse, A.G., Wells, C.A., Ashman, R.B., Blanchard, H., 2008. Human and mouse macrophage-inducible c-type lectin (micle) bind candida albicans. *Glycobiology* 18 (9), 679–685. doi:10.1093/glycob/cwn046.
- Cambi, A., Figdor, C.G., 2003. Dual function of c-type lectin-like receptors in the immune system. *Curr. Opin. Cell Biol.* 15 (5), 539–546. doi:10.1016/j.cel.2003.08.004.
- Cambi, A., Netea, M.G., Mora-Montes, H.M., Gow, N.A., Hato, S.V., Lowman, D.W., et al., 2008. Dendritic cell interaction with candida albicans critically depends on n-linked mannan. *J. Biol. Chem.* 283 (29), 20590–20599. doi:10.1074/jbc.M709334200.
- Campbell, E.J., Owen, C.A., 2007. The sulfate groups of chondroitin sulfate- and heparan sulfate-containing proteoglycans in neutrophil plasma membranes are novel binding sites for human leukocyte elastase and cathepsin G. *J. Biol. Chem.* 282 (19), 14645–14654. doi:10.1074/jbc.M608346200.
- Campbell, E.J., Campbell, M.A., Owen, C.A., 2000. Bioactive proteinase 3 on the cell surface of human neutrophils: quantification, catalytic activity, and susceptibility to inhibition. *J. Immunol.* 165 (6), 3366–3374.
- Chacko, B.K., Scott, D.W., Chandler, R.T., Patel, R.P., 2011. Endothelial surface n-glycans mediate monocyte adhesion and are targets for anti-inflammatory effects of peroxisome proliferator-activated receptor

- gamma ligands. *J. Biol. Chem.* 286 (44), 38738–38747. doi:10.1074/jbc.M111.247981.
- Chatwell, L., Holla, A., Kaufer, B.B., Skerra, A., 2008. The carbohydrate recognition domain of langerin reveals high structural similarity with the one of DC-SIGN but an additional, calcium-independent sugar-binding site. *Mol. Immunol.* 45 (7), 1981–1994. doi:10.1016/j.molimm.2007.10.030.
- Christiansen, M.N., Chik, J., Lee, L., Anugraham, M., Abrahams, J.L., Packer, N.H., 2014. Cell surface protein glycosylation in cancer. *Proteomics* 14 (4–5), 525–546. doi:10.1002/pmic.201300387.
- Chui, D., Oh-Eda, M., Liao, Y.F., Panneerselvam, K., Lal, A., Marek, K.W., et al., 1997. Alpha-mannosidase-II deficiency results in dyserythropoiesis and unveils an alternate pathway in oligosaccharide biosynthesis. *Cell* 90 (1), 157–167. doi:10.1016/S0092-8674(00)80322-0.
- Chui, D., Sellakumar, G., Green, R.S., Sutton-Smith, M., McQuistan, T., Marek, K.W., et al., 2001. Genetic remodeling of protein glycosylation in vivo induces autoimmune disease. *Proc. Natl. Acad. Sci. U.S.A.* 98 (3), 1142–1147. doi:10.1073/pnas.98.3.1142.
- Coelho, V., Krysov, S., Ghaemmaghami, A.M., Emara, M., Potter, K.N., Johnson, P., et al., 2010. Glycosylation of surface Ig creates a functional bridge between human follicular lymphoma and microenvironmental lectins. *Proc. Natl. Acad. Sci. U.S.A.* 107 (43), 18587–18592. doi:10.1073/pnas.1009388107.
- Cohen, M., 2015. Notable aspects of glycan-protein interactions. *Biomolecules* 5 (3), 2056–2072. doi:10.3390/biom5032056.
- Cohen, M., Varki, A., 2010. The sialome—far more than the sum of its parts. *OMICS* 14 (4), 455–464. doi:10.1089/omi.2009.0148.
- Cohen, M., Varki, A., 2014. Modulation of glycan recognition by clustered saccharide patches. *Int. Rev. Cell Mol. Biol.* 308, 75–125. doi:10.1016/B978-0-12-800097-7.00003-8.
- Coico, R., Sunshine, G., 2009. *Immunology: A Short Course*, sixth ed. John Wiley, New Jersey.
- Couser, W.G., Johnson, R.J., 2015. What is myeloperoxidase doing in ANCA-associated glomerulonephritis? *Kidney Int.* 88 (5), 938–940. doi:10.1038/ki.2015.259.
- Crocker, P.R., Paulson, J.C., Varki, A., 2007. Siglecs and their roles in the immune system. *Nat. Rev. Immunol.* 7 (4), 255–266. doi:10.1038/nri2056.
- Crouch, E., McDonald, B., Smith, K., Cafarella, T., Seaton, B., Head, J., 2006. Contributions of phenylalanine 335 to ligand recognition by human surfactant protein d: ring interactions with sp-d ligands. *J. Biol. Chem.* 281 (26), 18008–18014. doi:10.1074/jbc.M601749200.
- Cummings, R.D., Doering, T.L., 2009. Fungi. In: Varki, A., Cummings, R.D., Esko, J.D., Freeze, H.H., Stanley, P., Bertozzi, C.R., et al. (Eds.), *Essentials of Glycobiology*, second ed. Cold Spring Harbor, New York, pp. 309–320.
- de Leon, M.L., Young, L.J., An, H.J., Kronewitter, S.R., Kim, J., Miyamoto, S., et al., 2011. High-mannose glycans are elevated during breast cancer progression. *Mol. Cell. Proteomics* 10 (1), M110.002717. doi:10.1074/mcp.M110.002717.
- de Witte, L., Nabatov, A., Pion, M., Fluittsma, D., de Jong, M.A., de Grijl, T., et al., 2007. Langerin is a natural barrier to HIV-1 transmission by langerhans cells. *Nat. Med.* 13 (3), 367–371. doi:10.1038/nm1541.
- Dahmen, A.C., Fergen, M.T., Laurini, C., Schmitz, B., Loke, I., Thaysen-Andersen, M., et al., 2015. Paucimannosidic glycoepitopes are functionally involved in proliferation of neural progenitor cells in the subventricular zone. *Glycobiology* 25 (8), 869–880. doi:10.1093/glycob/cwv027.
- Dam, S., Thaysen-Andersen, M., Stenkjaer, E., Lorentzen, A., Roepstorff, P., Packer, N.H., et al., 2013. Combined n-glycome and n-glycoproteome analysis of the lotus japonicus seed globulin fraction shows conservation of protein structure and glycosylation in legumes. *J. Proteome Res.* 12 (7), 3383–3392. doi:10.1021/pr400224s.
- Dam, T.K., Brewer, C.F., 2010. Lectins as pattern recognition molecules: the effects of epitope density in innate immunity. *Glycobiology* 20 (3), 270–279. doi:10.1093/glycob/cwp186.
- Dasgupta, S., Navarrete, A.M., Bayry, J., Delignat, S., Wootla, B., Andre, S., et al., 2007. A role for exposed mannose in presentation of human therapeutic self-proteins to CD4+ T lymphocytes. *Proc. Natl. Acad. Sci. U.S.A.* 104 (21), 8965–8970. doi:10.1073/pnas.0702120104.
- Davies, J.C., 2002. *Pseudomonas aeruginosa* in cystic fibrosis: pathogenesis and persistence. *Paediatr. Respir. Rev.* 3 (2), 128–134. doi:10.1016/S1526-0550(02)00003-3.
- Day, C.J., Tran, E.N., Semchenko, E.A., Tram, G., Hartley-Tassell, L.E., Ng, P.S., et al., 2015. Glycan:glycan interactions: high affinity biomolecular interactions that can mediate binding of pathogenic bacteria to host cells. *Proc. Natl. Acad. Sci. U.S.A.* doi:10.1073/pnas.1421082112.
- Degen, S.E., Thiel, S., 2013. Humoral pattern recognition and the complement system. *Scand. J. Immunol.* 78 (2), 181–193. doi:10.1111/sji.12070.
- Deslée, G., Charbonnier, A.S., Hammad, H., Angyalosi, G., Tillie-Leblond, I., Mantovani, A., et al., 2002. Involvement of the mannose receptor in the uptake of der p 1, a major mite allergen, by human dendritic cells. *J. Allergy Clin. Immunol.* 110 (5), 763–770. doi:10.1067/mai.2002.129121.
- Doores, K.J., Bonomelli, C., Harvey, D.J., Vasiljevic, S., Dwek, R.A., Burton, D.R., et al., 2010. Envelope glycans of immunodeficiency viruses are almost entirely oligomannose antigens. *Proc. Natl. Acad. Sci. U.S.A.* 107 (31), 13800–13805. doi:10.1073/pnas.1006498107.
- Drickamer, K., 1992. Engineering galactose-binding activity into a c-type mannose-binding protein. *Nature* 360 (6400), 183–186. doi:10.1038/360183a0.
- Drickamer, K., 1999. C-type lectin-like domains. *Curr. Opin. Struct. Biol.* 9 (5), 585–590. doi:10.1016/S0959-440X(99)00009-3.
- Drickamer, K., Taylor, M.E., 2015. Recent insights into structures and functions of c-type lectins in the immune system. *Curr. Opin. Struct. Biol.* 34, 26–34. doi:10.1016/j.sbi.2015.06.003.
- Duus, K., Sandhu, N., Jorgensen, C.S., Hansen, P.R., Steino, A., Thaysen-Andersen, M., et al., 2009. Interaction of the chaperone calreticulin with proteins and peptides of different structural classes. *Protein Pept. Lett.* 16 (11), 1414–1423.
- East, L., Isacke, C.M., 2002. The mannose receptor family. *Biochim. Biophys. Acta* 1572 (2–3), 364–386. doi:10.1016/S0304-4165(02)00319-7.
- Ehrenforth, S., Kreuz, W., Scharrer, J., Linde, R., Funk, M., Gungor, T., et al., 1992. Incidence of development of factor VIII and factor IX inhibitors in haemophiliacs. *Lancet* 339 (8793), 594–598. doi:10.1016/0140-6736(92)90874-3.
- Endo, Y., Takahashi, M., Fujita, T., 2006. Lectin complement system and pattern recognition. *Immunobiology* 211 (4), 283–293. doi:10.1016/j.jimbio.2006.01.003.
- Eriksson, J., Woschnagg, C., Fernvik, E., Venge, P., 2007. A SELDI-TOF MS study of the genetic and post-translational molecular heterogeneity of eosinophil cationic protein. *J. Leukoc. Biol.* 82 (6), 1491–1500. doi:10.1189/jlb.0507272.
- Ernst, J.F., Prill, S.K., 2001. O-glycosylation. *Med. Mycol.* 39 (Suppl. 1), 67–74. doi:10.1080/mmy.39.1.67.74.
- Esparza, M., Palomares, B., García, T., Espinosa, P., Zenteno, E., Mancilla, R., 2015. Pst-S1, the 38-kDa mycobacterium tuberculosis glycoprotein, is an adhesin, which binds the macrophage mannose receptor and promotes phagocytosis. *Scand. J. Immunol.* 81 (1), 46–55. doi:10.1111/sji.12249.
- Fanibunda, S.E., Modi, D.N., Gokral, J.S., Bandivdekar, A.H., 2011. HIV gp120 binds to mannose receptor on vaginal epithelial cells and induces production of matrix metalloproteinases. *PLoS ONE* 6 (11), e28014. doi:10.1371/journal.pone.0028014.
- Farinha, P., Masoudi, H., Skinnider, B.F., Shumansky, K., Spinelli, J.J., Gill, K., et al., 2005. Analysis of multiple biomarkers shows that lymphoma-associated macrophage (LAM) content is an independent predictor of survival in follicular lymphoma (FL). *Blood* 106 (6), 2169–2174. doi:10.1182/blood-2005-04-1565.
- Feinberg, H., Park-Snyder, S., Kolkar, A.R., Heise, C.T., Taylor, M.E., Weis, W.I., 2000. Structure of a c-type carbohydrate recognition domain from the macrophage mannose receptor. *J. Biol. Chem.* 275 (28), 21539–21548. doi:10.1074/jbc.M002366200.
- Feinberg, H., Mitchell, D.A., Drickamer, K., Weis, W.I., 2001. Structural basis for selective recognition of oligosaccharides by DC-SIGN and DC-SIGNR. *Science* 294 (5549), 2163–2166. doi:10.1126/science.1066371.
- Feinberg, H., Guo, Y., Mitchell, D.A., Drickamer, K., Weis, W.I., 2005. Extended neck regions stabilize tetramers of the receptors DC-SIGN and DC-SIGNR. *J. Biol. Chem.* 280 (2), 1327–1335. doi:10.1074/jbc.M409925200.
- Feinberg, H., Castelli, R., Drickamer, K., Seeberger, P.H., Weis, W.I., 2007. Multiple modes of binding enhance the affinity of DC-SIGN for high mannose n-linked glycans found on viral glycoproteins. *J. Biol. Chem.* 282 (6), 4202–4209. doi:10.1074/jbc.M609689200.
- Feinberg, H., Taylor, M.E., Razi, N., McBride, R., Knirel, Y.A., Graham, S.A., et al., 2011. Structural basis for langerin recognition of diverse pathogen and mammalian glycans through a single binding site. *J. Mol. Biol.* 405 (4), 1027–1039. doi:10.1016/j.jmb.2010.11.039.
- Ferguson, M.A.J., Kinoshita, T., Hart, G.W., 2009. Glycosylphosphatidylinositol anchors. In: Varki, A., Cummings, R.D., Esko, J.D., Freeze, H.H., Stanley, P., Bertozzi, C.R., et al. (Eds.), *Essentials of Glycobiology*, second ed. Cold Spring Harbor (NY), New York, pp. 143–162.
- Piet, D.J., Beranek, M.C., Baenziger, J.U., 1998. A cysteine-rich domain of the “mannose” receptor mediates GalNAc-4-SO4 binding. *Proc. Natl. Acad. Sci. U.S.A.* 95 (5), 2089–2093.
- Figdor, C.G., van Kooyk, Y., Adema, G.J., 2002. C-type lectin receptors on dendritic cells and Langerhans cells. *Nat. Rev. Immunol.* 2 (2), 77–84. doi:10.1038/nri723.

- Freeze, H.H., 2013. Understanding human glycosylation disorders: biochemistry leads the charge. *J. Biol. Chem.* 288 (10), 6936–6945. doi:10.1074/jbc.R112.429274.
- Furmanek, A., Hofsteenge, J., 2000. Protein c-mannosylation: facts and questions. *Acta Biochim. Pol.* 47 (3), 781–789.
- Furukawa, A., Kamishikiryo, J., Mori, D., Toyonaga, K., Okabe, Y., Toji, A., et al., 2013. Structural analysis for glycolipid recognition by the c-type lectins mincle and MCL. *Proc. Natl. Acad. Sci. U.S.A.* 110 (43), 17438–17443. doi:10.1073/pnas.1312649110.
- Fuster, M.M., Esko, J.D., 2005. The sweet and sour of cancer: glycans as novel therapeutic targets. *Nat. Rev. Cancer* 5 (7), 526–542. doi:10.1038/nrc1649.
- Gabius, H.-J., Kaltner, H., Kopitz, J., André, S., 2015. The glycobiology of the CD system: a dictionary for translating marker designations into glycan/lectin structure and function. *Trends Biochem. Sci.* 40 (7), 360–376. doi:10.1016/j.tibs.2015.03.013.
- Gabius, H.J., Andre, S., Jimenez-Barbero, J., Romero, A., Solis, D., 2011. From lectin structure to functional glycomics: principles of the sugar code. *Trends Biochem. Sci.* 36 (6), 298–313. doi:10.1016/j.tibs.2011.01.005.
- Galkina, E., Ley, K., 2009. Immune and inflammatory mechanisms of atherosclerosis. *Annu. Rev. Immunol.* 27, 165–197. doi:10.1146/annurev.immunol.021908.132620.
- Garcia-Parajo, M.F., Cambi, A., Torreno-Pina, J.A., Thompson, N., Jacobson, K., 2014. Nanoclustering as a dominant feature of plasma membrane organization. *J. Cell Sci.* 127 (Pt 23), 4995–5005. doi:10.1242/jcs.146340.
- Garcia-Vallejo, J.J., Van Dijk, W., Van Het Hof, B., Van Die, I., Engelse, M.A., Van Hinsbergh, V.W., et al., 2006. Activation of human endothelial cells by tumor necrosis factor- α results in profound changes in the expression of glycosylation-related genes. *J. Cell. Physiol.* 206 (1), 203–210. doi:10.1002/jcp.20458.
- Garcia-Vallejo, J.J., Koning, N., Ambrosini, M., Kalay, H., Vuist, I., Sarraimi-Forooshani, R., et al., 2013. Glycoclusters prevent HIV transmission via DC-SIGN on dendritic cells. *Int. Immunol.* 25 (4), 221–233. doi:10.1093/intimm/dxs115.
- Garcia-Vallejo, J.J., Bloem, K., Knippels, L.M., Garssen, J., van Vliet, S.J., van Kooyk, Y., 2015. The consequences of multiple simultaneous c-type lectin-ligand interactions: DCIR alters the endo-lysosomal routing of DC-SIGN. *Front. Immunol.* 6, 87. doi:10.3389/fimmu.2015.00087.
- Gazi, U., Martinez-Pomares, L., 2009. Influence of the mannose receptor in host immune responses. *Immunobiology* 214 (7), 554–561. doi:10.1016/j.imbio.2008.11.004.
- Geijtenbeek, T.B., Gringhuis, S.L., 2009. Signalling through c-type lectin receptors: shaping immune responses. *Nat. Rev. Immunol.* 9 (7), 465–479. doi:10.1038/nri2569.
- Geijtenbeek, T.B., Krooshoop, D.J., Bleijs, D.A., van Vliet, S.J., van Duijnhoven, G.C., Grabovsky, V., et al., 2000a. DC-SIGN-ICAM-2 interaction mediates dendritic cell trafficking. *Nat. Immunol.* 1 (4), 353–357. doi:10.1038/79815.
- Geijtenbeek, T.B., Kwon, D.S., Torensma, R., van Vliet, S.J., van Duijnhoven, G.C., Middel, J., et al., 2000b. DC-SIGN, a dendritic cell-specific HIV-1-binding protein that enhances trans-infection of T cells. *Cell* 100 (5), 587–597. doi:10.1016/S0092-8674(00)80694-7.
- Geijtenbeek, T.B.H., van Vliet, S.J., Koppel, E.A., Sanchez-Hernandez, M., Vandenbroucke-Grauls, C.M.J.E., Appelmek, B., et al., 2002. Mycobacteria target DC-SIGN to suppress dendritic cell function. *J. Exp. Med.* 197 (1), 7–17. doi:10.1084/jem.2002.1229.
- Goetz, J.A., Mechref, Y., Kang, P., Jeng, M.H., Novotny, M.V., 2009. Glycomic profiling of invasive and non-invasive breast cancer cells. *Glycoconj. J.* 26 (2), 117–131. doi:10.1007/s10719-008-9170-4.
- Graham, L.M., Gupta, V., Schafer, G., Reid, D.M., Kimberg, M., Dennehy, K.M., et al., 2012. The c-type lectin receptor CLEC4E (CLEC4D) is expressed by myeloid cells and triggers cellular activation through Syk kinase. *J. Biol. Chem.* 287 (31), 25964–25974. doi:10.1074/jbc.M112.384164.
- Green, R.S., Stone, E.L., Tenno, M., Lehtonen, E., Farquhar, M.G., Marth, J.D., 2007. Mammalian n-glycan branching protects against innate immune self-recognition and inflammation in autoimmune disease pathogenesis. *Immunity* 27 (2), 308–320. doi:10.1016/j.immuni.2007.06.008.
- Grigorian, A., Mkhikian, H., Li, C.F., Newton, B.L., Zhou, R.W., Demetriou, M., 2012. Pathogenesis of multiple sclerosis via environmental and genetic dysregulation of n-glycosylation. *Semin. Immunopathol.* 34 (3), 415–424. doi:10.1007/s00281-012-0307-y.
- Grimes, J.E., Croll, D., Harrison, W.E., Utzinger, J., Freeman, M.C., Templeton, M.R., 2015. The roles of water, sanitation and hygiene in reducing schistosomiasis: a review. *Parasit. Vectors* 8, 156. doi:10.1186/s13071-015-0766-9.
- Gunn, B.M., Morrison, T.E., Whitmore, A.C., Blevins, L.K., Hueston, L., Fraser, R.J., et al., 2012. Mannose binding lectin is required for alphavirus-induced arthritis/myositis. *PLoS Pathog.* 8 (3), e1002586. doi:10.1371/journal.ppat.1002586.
- Guo, Y., Feinberg, H., Conroy, E., Mitchell, D.A., Alvarez, R., Blixt, O., et al., 2004. Structural basis for distinct ligand-binding and targeting properties of the receptors DC-SIGN and DC-SIGNR. *Nat. Struct. Mol. Biol.* 11 (7), 591–598. doi:10.1038/nsmb784.
- Hajjar, E., Mihajlovic, M., Witko-Sarsat, V., Lazaridis, T., Reuter, N., 2008. Computational prediction of the binding site of proteinase 3 to the plasma membrane. *Proteins* 71 (4), 1655–1669. doi:10.1002/prot.21853.
- Halim, A., Larsen, L.S., Neubert, P., Joshi, H.J., Petersen, B.L., Vakhrushev, S.Y., et al., 2015. Discovery of a nucleocytoplasmic o-mannose glycoproteome in yeast. *Proc. Natl. Acad. Sci. U.S.A.* doi:10.1073/pnas.1511743112.
- Haltiwanger, R.S., Lowe, J.B., 2004. Role of glycosylation in development. *Annu. Rev. Biochem.* 73, 491–537. doi:10.1146/annurev.biochem.73.011303.074043.
- Haniffa, M., Collin, M., Ginhoux, F., 2013. Ontogeny and functional specialization of dendritic cells in human and mouse. *Adv. Immunol.* 120, 1–49. doi:10.1016/B978-0-12-417028-5.00001-6.
- Hansen, S., Holmskov, U., 2002. Lung surfactant protein d (sp-d) and the molecular diverted descendants: conglutinin, CL-43 and CL-46. *Immunobiology* 205 (4–5), 498–517. doi:10.1078/0171-2985-00150.
- Hansen, S., Selman, L., Palaniyar, N., Ziegler, K., Brandt, J., Kliem, A., et al., 2010. Collectin 11 (CL-11, CL-K1) is a MASP-1/3-associated plasma collectin with microbial-binding activity. *J. Immunol.* 185 (10), 6096–6104. doi:10.4049/jimmunol.1002185.
- Harada, Y., Hirayama, H., Suzuki, T., 2015. Generation and degradation of free asparagine-linked glycans. *Cell. Mol. Life Sci.* 72 (13), 2509–2533. doi:10.1007/s00018-015-1881-7.
- Hare, N.J., Chan, B., Chan, E., Kaufman, K.L., Britton, W.J., Saunders, B.M., 2015. Microparticles released from mycobacterium tuberculosis-infected human macrophages contain increased levels of the type I interferon inducible proteins including ISG15. *Proteomics* 15 (17), 3020–3029. doi:10.1002/pmic.201400610.
- Hart, M.L., Saifuddin, M., Uemura, K., Bremer, E.C., Hooker, B., Kawasaki, T., et al., 2002. High mannose glycans and sialic acid on gp120 regulate binding of mannose-binding lectin (MBL) to HIV type 1. *AIDS Res. Hum. Retroviruses* 18 (17), 1311–1317. doi:10.1089/088922202320886352.
- Hartsholt, R.B., Peyron, I., Voorberg, J., 2015. Hunting down factor VIII in the immunopeptidome. *Cell. Immunol.* doi:10.1016/j.cellimm.2015.11.001.
- Hartshorn, K.L., Holmskov, U., Hansen, S., Zhang, P., Meschi, J., Mogues, T., et al., 2002. Distinctive anti-influenza properties of recombinant collectin 43. *Biochem. J.* 366 (Pt 1), 87–96. doi:10.1042/BJ20011868.
- Hashii, N., Kawasaki, N., Itoh, S., Nakajima, Y., Kawanishi, T., Yamaguchi, T., 2009. Alteration of n-glycosylation in the kidney in a mouse model of systemic lupus erythematosus: relative quantification of n-glycans using an isotope-tagging method. *Immunology* 126 (3), 336–345. doi:10.1111/j.1365-2567.2008.02898.x.
- Hauck, D., Joachim, I., Frommeyer, B., Varrot, A., Philipp, B., Moller, H.M., et al., 2013. Discovery of two classes of potent glycomimetic inhibitors of pseudomonas aeruginosa LecB with distinct binding modes. *ACS Chem. Biol.* 8 (8), 1775–1784. doi:10.1021/cb400371r.
- Heinsbroek, S.E., Taylor, P.R., Martinez, F.O., Martinez-Pomares, L., Brown, G.D., Gordon, S., 2008. Stage-specific sampling by pattern recognition receptors during candida albicans phagocytosis. *PLoS Pathog.* 4 (11), e1000218. doi:10.1371/journal.ppat.1000218.
- Hennet, T., Cabalzar, J., 2015. Congenital disorders of glycosylation: a concise chart of glycolysis dysfunction. *Trends Biochem. Sci.* 40 (7), 377–384. doi:10.1016/j.tibs.2015.03.002.
- Hilda, J.N., Narasimhan, M., Das, S.D., 2015. Mycobacterium tuberculosis strains modify granular enzyme secretion and apoptosis of human neutrophils. *Mol. Immunol.* doi:10.1016/j.molimm.2015.09.019.
- Hironaka, T., Furukawa, K., Esmon, P.C., Fournel, M.A., Sawada, S., Kato, M., et al., 1992. Comparative study of the sugar chains of factor VIII purified from human plasma and from the culture media of recombinant baby hamster kidney cells. *J. Biol. Chem.* 267 (12), 8012–8020.
- Hirt, C., Eppenberger-Castori, S., Sconocchia, G., Iezzi, G., Tornillo, L., Terracciano, L., et al., 2013. Colorectal carcinoma infiltration by myeloperoxidase-expressing neutrophils is associated with favorable prognosis. *Oncotarget* 2 (10), e25990. doi:10.4161/onci.25990.
- Holst, S., Deuss, A.J., van Pelt, G.W., van Vliet, S.J., Garcia-Vallejo, J.J., Koeleman, C.A., et al., 2015. N-glycosylation profiling of colorectal cancer cell lines reveals association of fucosylation with differentiation and CDX1/villin mRNA expression. *Mol. Cell. Proteomics* doi:10.1074/mcp.M115.051235.
- Hottz, E.D., Oliveira, M.F., Nunes, P.C., Nogueira, R.M., Valls-de-Souza, R., Da Poian, A.T., et al., 2013. Dengue induces platelet activation,

- mitochondrial dysfunction and cell death through mechanisms that involve DC-SIGN and caspases. *J. Thromb. Haemost.* 11 (5), 951–962. doi:10.1111/jth.12178.
- Hu, F., Ding, G., Zhang, Z., Gatto, L.A., Hawgood, S., Poulain, F.R., et al., 2015. Innate immunity of surfactant proteins a and d in urinary tract infection with uropathogenic *Escherichia coli*. *Innate Immun.* doi:10.1177/1753425915609973.
- Hurtado, C., Granja, A.G., Bustos, M.J., Nogal, M.L., Gonzalez de Buitrago, G., de Yébenes, V.G., et al., 2004. The c-type lectin homologue gene (EP153R) of African swine fever virus inhibits apoptosis both in virus infection and in heterologous expression. *Virology* 326 (1), 160–170. doi:10.1016/j.virol.2004.05.019.
- Hutter, J., Eriksson, M., Johannsen, T., Klopffleisch, R., von Smolinski, D., Gruber, A.D., et al., 2014. Role of the c-type lectin receptors MCL and DCIR in experimental colitis. *PLoS ONE* 9 (7), e103281. doi:10.1371/journal.pone.0103281.
- Hyakumura, M., Walsh, R., Thaysen-Andersen, M., Kingston, N.J., La, M., Lu, L., et al., 2015. Modification of asparagine-linked glycan density for the design of hepatitis b virus virus-like particles with enhanced immunogenicity. *J. Virol.* 89 (22), 11312–11322. doi:10.1128/JVI.01123-15.
- Hykolari, A., Eckmair, B., Voglmeir, J., Jin, C., Yan, S., Vanbeselae, J., et al., 2016. More than just oligomannose: an n-glycomic comparison of penicillium species. *Mol. Cell. Proteomics* 15 (1), 73–92. doi:10.1074/mcp.M115.055061.
- Ichikawa, M., Scott, D.A., Losfeld, M.-E., Freeze, H.H., 2014. The metabolic origins of mannose in glycoproteins. *J. Biol. Chem.* 289 (10), 6751–6761. doi:10.1074/jbc.M113.544064.
- Ihara, Y., Inai, Y., Ikezaki, M., Matsui, I.-S.L., Manabe, S., Ito, Y., 2015. C-mannosylation: modification on tryptophan in cellular proteins. In: Taniguchi, N., Endo, T., Hart, G.W., Seeberger, P.H., Wong, C.-H. (Eds.), *Glycoscience: Biology and Medicine*. pp. 1091–1099. <http://dx.doi.org/10.1007/978-4-431-54841-6_67>; 978-4-431-54841-6 (Online), ISBN: 978-4-431-54840-9 (Print), Springer Date: 20 October 2014.
- Iobst, S.T., Wormald, M.R., Weis, W.I., Dwek, R.A., Drickamer, K., 1994. Binding of sugar ligands to Ca²⁺-dependent animal lectins. I. analysis of mannose binding by site-directed mutagenesis and NMR. *J. Biol. Chem.* 269 (22), 15505–15511.
- Ip, W.K., Takahashi, K., Ezekowitz, R.A., Stuart, L.M., 2009. Mannose-binding lectin and innate immunity. *Immunol. Rev.* 230 (1), 9–21. doi:10.1111/j.1600-065X.2009.00789.x.
- Jiang, Y., Zhang, C., Chen, K., Chen, Z., Sun, Z., Zhang, Z., et al., 2014. The clinical significance of DC-SIGN and DC-SIGNR, which are novel markers expressed in human colon cancer. *PLoS ONE* 9 (12), e114748. doi:10.1371/journal.pone.0114748.
- Jin, W., Li, C., Du, T., Hu, K., Huang, X., Hu, Q., 2014. DC-SIGN plays a stronger role than DCIR in mediating HIV-1 capture and transfer. *Virology* 458–459, 83–92. doi:10.1016/j.virol.2014.04.016.
- Johns, T.G., Mellman, I., Cartwright, G.A., Ritter, G., Old, L.J., Burgess, A.W., et al., 2005. The antitumor monoclonal antibody 806 recognizes a high-mannose form of the EGF receptor that reaches the cell surface when cells over-express the receptor. *FASEB J.* doi:10.1096/fj.04-1766fje.
- Johnson, J.L., Jones, M.B., Ryan, S.O., Cobb, B.A., 2013. The regulatory power of glycans and their binding partners in immunity. *Trends Immunol.* 34 (6), 290–298. doi:10.1016/j.it.2013.01.006.
- Jozefowski, S., 2015. The danger model: questioning an unconvincing theory. *Immunol. Cell Biol.* doi:10.1038/icb.2015.68.
- Kain, R., Rees, A.J., 2013. What is the evidence for antibodies to LAMP-2 in the pathogenesis of ANCA associated small vessel vasculitis? *Curr. Opin. Rheumatol.* 25 (1), 26–34. doi:10.1097/BOR.0b013e32835b4f8f.
- Kain, R., Exner, M., Brandes, R., Ziebmayer, R., Cunningham, D., Alderson, C.A., et al., 2008. Molecular mimicry in pauci-immune focal necrotizing glomerulonephritis. *Nat. Med.* 14 (10), 1088–1096. doi:10.1038/nm.1874.
- Kallenius, G., Correia-Neves, M., Buteme, H., Hamasur, B., Svenson, S.B., 2015. Lipoarabinomannan, and its related glycolipids, induce divergent and opposing immune responses to mycobacterium tuberculosis depending on structural diversity and experimental variations. *Tuberculosis (Edinb.)* doi:10.1016/j.tube.2015.09.005.
- Kang, P.B., Azad, A.K., Torrelles, J.B., Kaufman, T.M., Beharka, A., Tibesar, E., et al., 2005. The human macrophage mannose receptor directs mycobacterium tuberculosis lipoarabinomannan-mediated phagosome biogenesis. *J. Exp. Med.* 202 (7), 987–999. doi:10.1084/jem.20051239.
- Kaprio, T., Satomaa, T., Heiskanen, A., Hokke, C.H., Deelder, A.M., Mustonen, H., et al., 2015. N-glycomic profiling as a tool to separate rectal adenomas from carcinomas. *Mol. Cell. Proteomics* 14 (2), 277–288. doi:10.1074/mcp.M114.041632.
- Karlyshev, A.V., Ketley, J.M., Wren, B.W., 2005. The campylobacter jejuni glycome. *FEMS Microbiol. Rev.* 29 (2), 377–390. doi:10.1016/j.femsre.2005.01.003.
- Kelly, M., Hwang, J.M., Kubes, P., 2007. Modulating leukocyte recruitment in inflammation. *J. Allergy Clin. Immunol.* 120 (1), 3–10. doi:10.1016/j.jaci.2007.05.017.
- Kerrigan, A.M., Brown, G.D., 2009. C-type lectins and phagocytosis. *Immunobiology* 214 (7), 562–575. doi:10.1016/j.imbio.2008.11.003.
- Khatri, K., Klein, J.A., White, M.R., Grant, O.C., Leymarie, N., Woods, R.J., et al., 2016. Integrated omics and computational glycobiology reveal structural basis for influenza A virus glycan microheterogeneity and host interactions. *Mol. Cell. Proteomics* doi:10.1074/mcp.M116.058016.
- Khoo, K.H., Chatterjee, D., Caulfield, J.P., Morris, H.R., Dell, A., 1997. Structural mapping of the glycans from the egg glycoproteins of *Schistosoma mansoni* and *Schistosoma japonicum*: identification of novel core structures and terminal sequences. *Glycobiology* 7 (5), 663–677.
- Kjaer, T.R., Thiel, S., Andersen, G.R., 2013. Toward a structure-based comprehension of the lectin pathway of complement. *Mol. Immunol.* 56 (4), 413–422. doi:10.1016/j.molimm.2013.05.007.
- Klechevsky, E., Flamar, A.L., Cao, Y., Blanck, J.P., Liu, M., O'Bar, A., et al., 2010. Cross-priming CD8+ T cells by targeting antigens to human dendritic cells through DCIR. *Blood* 116 (10), 1685–1697. doi:10.1182/blood-2010-01-264960.
- Klenk, H.D., Wagner, R., Heuer, D., Wolff, T., 2002. Importance of hemagglutinin glycosylation for the biological functions of influenza virus. *Virus Res.* 82 (1–2), 73–75. doi:10.1016/S0168-1702(01)00389-6.
- Kolarich, D., Altmann, F., 2000. N-glycan analysis by matrix-assisted laser desorption/ionization mass spectrometry of electrophoretically separated nonmammalian proteins: application to peanut allergen Ara h 1 and olive pollen allergen Ole e 1. *Anal. Biochem.* 285 (1), 64–75. doi:10.1006/abio.2000.4737.
- Kolarich, D., Leonard, R., Hemmer, W., Altmann, F., 2005. The n-glycans of yellow jacket venom hyaluronidases and the protein sequence of its major isoform in *Vespa vulgaris*. *FEBS J.* 272 (20), 5182–5190. doi:10.1111/j.1742-4658.2005.04841.x.
- Kolarich, D., Altmann, F., Sunderasan, E., 2006. Structural analysis of the glycoprotein allergen Hev b 4 from natural rubber latex by mass spectrometry. *Biochim. Biophys. Acta* 1760 (4), 715–720. doi:10.1016/j.bbagen.2005.11.012.
- Kolattukudy, P.E., Fernandes, N.D., Azad, A.K., Fitzmaurice, A.M., Sirakova, T.D., 1997. Biochemistry and molecular genetics of cell-wall lipid biosynthesis in mycobacteria. *Mol. Microbiol.* 24 (2), 263–270.
- Kondo, A., Thaysen-Andersen, M., Hjerno, K., Jensen, O.N., 2010. Characterization of sialylated and fucosylated glycopeptides of beta2-glycoprotein I by a combination of HILIC LC and MALDI MS/MS. *J. Sep. Sci.* 33 (6–7), 891–902. doi:10.1002/jssc.200900802.
- Kranjcek, B., Papes, D., Altarac, S., 2014. D-mannose powder for prophylaxis of recurrent urinary tract infections in women: a randomized clinical trial. *World J. Urol.* 32 (1), 79–84. doi:10.1007/s00345-013-1091-6.
- Kreisman, L.S., Cobb, B.A., 2012. Infection, inflammation and host carbohydrates: a glyco-evasion hypothesis. *Glycobiology* 22 (8), 1019–1030. doi:10.1093/glycob/cws070.
- Lai, J., Bernhard, O.K., Turville, S.G., Harman, A.N., Wilkinson, J., Cunningham, A.L., 2009. Oligomerization of the macrophage mannose receptor enhances gp120-mediated binding of HIV-1. *J. Biol. Chem.* 284 (17), 11027–11038. doi:10.1074/jbc.M809698200.
- Lai, J.D., Georgescu, M.T., Hough, C., Lillicrap, D., 2015. To clear or to fear: an innate perspective on factor VIII immunity. *Cell. Immunol.* doi:10.1016/j.cellimm.2015.10.011.
- Lauer, I., Foetisch, K., Kolarich, D., Ballmer-Weber, B.K., Conti, A., Altmann, F., et al., 2004. Hazelnut (*Corylus avellana*) vicilin Cor a 11: molecular characterization of a glycoprotein and its allergenic activity. *Biochem. J.* 383 (Pt 2), 327–334. doi:10.1042/bj20041062.
- Le Cabec, V., Emorine, L.J., Toesca, I., Cougoule, C., Maridonneau-Parini, I., 2005. The human macrophage mannose receptor is not a professional phagocytic receptor. *J. Leukoc. Biol.* 77 (6), 934–943. doi:10.1189/jlb.1204705.
- Lee, J., Breton, G., Oliveira, T.Y., Zhou, Y.J., Aljoufi, A., Puhr, S., et al., 2015. Restricted dendritic cell and monocyte progenitors in human cord blood and bone marrow. *J. Exp. Med.* 212 (3), 385–399. doi:10.1084/jem.20141442.
- Lee, J.K., Vadas, P., 2011. Anaphylaxis: mechanisms and management. *Clin. Exp. Allergy* 41 (7), 923–938. doi:10.1111/j.1365-2222.2011.03779.x.
- Lee, L.Y., Lin, C.H., Fanayan, S., Packer, N.H., Thaysen-Andersen, M., 2014a. Differential site accessibility mechanistically explains subcellular-specific n-glycosylation determinants. *Front. Immunol.* 5, 404. doi:10.3389/fimmu.2014.00404.

- Lee, L.Y., Thaysen-Andersen, M., Baker, M.S., Packer, N.H., Hancock, W.S., Fanayan, S., 2014b. Comprehensive n-glycome profiling of cultured human epithelial breast cells identifies unique secretome n-glycosylation signatures enabling tumorigenic subtype classification. *J. Proteome Res.* 13 (11), 4783–4795. doi:10.1021/pr500331m.
- Lee, R.T., Lee, Y.C., 1997. Difference in binding-site architecture of the serum-type and liver-type mannose-binding proteins. *Glycoconj. J.* 14 (3), 357–363.
- Lee, R.T., Lee, Y.C., 2000. Affinity enhancement by multivalent lectin-carbohydrate interaction. *Glycoconj. J.* 17 (7–9), 543–551. doi:10.1023/A:1011070425430.
- Lee, R.T., Hsu, T.L., Huang, S.K., Hsieh, S.L., Wong, C.H., Lee, Y.C., 2011. Survey of immune-related, mannose/fucose-binding c-type lectin receptors reveals widely divergent sugar-binding specificities. *Glycobiology* 21 (4), 512–520. doi:10.1093/glycob/cwq193.
- Limpens, J., Stad, R., Vos, C., de Vlaam, C., de Jong, D., van Ommen, G.J., et al., 1995. Lymphoma-associated translocation (t(14;18)) in blood B cells of normal individuals. *Blood* 85 (9), 2528–2536.
- Linley, A., Krysov, S., Ponzoni, M., Johnson, P.W., Packham, G., Stevenson, F.K., 2015. Lectin binding to surface Ig variable regions provides a universal persistent activating signal for follicular lymphoma cells. *Blood* 126 (16), 1902–1910. doi:10.1182/blood-2015-04-640805.
- Liu, C.F., Tonini, L., Malaga, W., Beau, M., Stella, A., Bouyssi, D., et al., 2013a. Bacterial protein-o-mannosylating enzyme is crucial for virulence of mycobacterium tuberculosis. *Proc. Natl. Acad. Sci. U.S.A.* 110 (16), 6560–6565. doi:10.1073/pnas.1219704110.
- Liu, X., Nie, H., Zhang, Y., Yao, Y., Maitikabili, A., Qu, Y., et al., 2013b. Cell surface-specific n-glycan profiling in breast cancer. *PLoS ONE* 8 (8), e72704. doi:10.1371/journal.pone.0072704.
- Liu, Y., Chirino, A.J., Misulovin, Z., Leteux, C., Feizi, T., Nussenzweig, M.C., et al., 2000. Crystal structure of the cysteine-rich domain of mannose receptor complexed with a sulfated carbohydrate ligand. *J. Exp. Med.* 191 (7), 1105–1116. doi:10.1084/jem.191.7.1105.
- Liu, Z., Liu, B., Zhang, Z.T., Zhou, T.T., Bian, H.J., Min, M.W., et al., 2008. A mannose-binding lectin from *Sophora flavescens* induces apoptosis in HeLa cells. *Phytomedicine* 15 (10), 867–875. doi:10.1016/j.phymed.2008.02.025.
- Lohse, S., Meyer, S., Meulenbroek, L.A., Jansen, J.H., Nederend, M., Kretschmer, A., et al., 2015. An anti-EGFR IgA that displays improved pharmacokinetics and myeloid effector cell engagement in vivo. *Cancer Res.* doi:10.1158/0008-5472.CAN-15-1232.
- Loibl, M., Strahl, S., 2013. Protein o-mannosylation: what we have learned from baker's yeast. *Biochim. Biophys. Acta* 1833 (11), 2438–2446. doi:10.1016/j.bbamcr.2013.02.008.
- Loke, I., Packer, N.H., Thaysen-Andersen, M., 2015. Complementary LC-MS/MS-based n-glycan, n-glycopeptide, and intact n-glycoprotein profiling reveals unconventional Asn71-glycosylation of human neutrophil cathepsin G. *Biomolecules* 5 (3), 1832–1854. doi:10.3390/biom5031832.
- Lombardi, V.C., Khaiboullina, S.F., Rizvanov, A.A., 2015. Plasmacytoid dendritic cells, a role in neoplastic prevention and progression. *Eur. J. Clin. Invest.* 45 (Suppl. 1), 1–8. doi:10.1111/eci.12363.
- Lommel, M., Strahl, S., 2009. Protein o-mannosylation: conserved from bacteria to humans. *Glycobiology* 19 (8), 816–828. doi:10.1093/glycob/cwp066.
- Loures, F.V., Rohm, M., Lee, C.K., Santos, E., Wang, J.P., Specht, C.A., et al., 2015. Recognition of *Aspergillus fumigatus* hyphae by human plasmacytoid dendritic cells is mediated by dectin-2 and results in formation of extracellular traps. *PLoS Pathog.* 11 (2), e1004643. doi:10.1371/journal.ppat.1004643.
- Lowe, J.B., 2003. Glycan-dependent leukocyte adhesion and recruitment in inflammation. *Curr. Opin. Cell Biol.* 15 (5), 531–538. doi:10.1016/j.cceb.2003.08.002.
- Lu, J., Teh, C., Kishore, U., Reid, K.B., 2002. Collectins and ficolins: sugar pattern recognition molecules of the mammalian innate immune system. *Biochim. Biophys. Acta* 1572 (2–3), 387–400. doi:10.1016/S0304-4165(02)00320-3.
- Lu, J.H., Thiel, S., Wiedemann, H., Timpl, R., Reid, K.B., 1990. Binding of the pentamer/hexameric forms of mannan-binding protein to zymosan activates the proenzyme C1r2C1s2 complex, of the classical pathway of complement, without involvement of C1q. *J. Immunol.* 144 (6), 2287–2294.
- Lyons, J.J., Milner, J.D., Rosenzweig, S.D., 2015. Glycans instructing immunity: the emerging role of altered glycosylation in clinical immunology. *Front. Pediatr.* 3, 54. doi:10.3389/fped.2015.00054.
- Ma, Y.J., Hein, E., Munthe-Fog, L., Skjoedt, M.O., Bayarri-Olmos, R., Romani, L., et al., 2015. Soluble collectin-12 (CL-12) is a pattern recognition molecule initiating complement activation via the alternative pathway. *J. Immunol.* doi:10.4049/jimmunol.1500493.
- Maeda, N., Nigou, J., Herrmann, J.L., Jackson, M., Amara, A., Lagrange, P.H., et al., 2003. The cell surface receptor DC-SIGN discriminates between mycobacterium species through selective recognition of the mannose caps on lipaarabinomannan. *J. Biol. Chem.* 278 (8), 5513–5516. doi:10.1074/jbc.C200586200.
- Margreet, A.W., Geert-Jan, B., 2013. Adaptive immune activation: glycosylation does matter. *Nat. Chem. Bio.* 9 (12), 776–784. doi:10.1038/nchembio.1403.
- Marotte, K., Sabin, C., Preville, C., Moume-Pymbock, M., Wimmerova, M., Mitchell, E.P., et al., 2007. X-ray structures and thermodynamics of the interaction of PA-III from *Pseudomonas aeruginosa* with disaccharide derivatives. *ChemMedChem* 2 (9), 1328–1338. doi:10.1002/cmdc.200700100.
- Martinez-Pomares, L., 2012. The mannose receptor. *J. Leukoc. Biol.* 92 (6), 1177–1186. doi:10.1189/jlb.0512231.
- Martinez-Pomares, L., Mahoney, J.A., Kaposzt, R., Linehan, S.A., Stahl, P.D., Gordon, S., 1998. A functional soluble form of the murine mannose receptor is produced by macrophages in vitro and is present in mouse serum. *J. Biol. Chem.* 273 (36), 23376–23380. doi:10.1074/jbc.273.36.23376.
- Mason, C.P., Tarr, A.W., 2015. Human lectins and their roles in viral infections. *Molecules* 20 (2), 2229–2271. doi:10.3390/molecules20022229.
- Masuoka, J., 2004. Surface glycans of *Candida albicans* and other pathogenic fungi: physiological roles, clinical uses, and experimental challenges. *Clin. Microbiol. Rev.* 17 (2), 281–310. doi:10.1128/cmr.17.2.281-310.2004.
- Matsumoto, M., Tanaka, T., Kaisho, T., Sanjo, H., Copeland, N.G., Gilbert, D.J., et al., 1999. A novel LPS-inducible c-type lectin is a transcriptional target of NF-IL6 in macrophages. *J. Immunol.* 163 (9), 5039–5048.
- Matthijssen, R.A., de Winther, M.P., Kuipers, D., van der Made, I., Weber, C., Herias, M.V., et al., 2009. Macrophage-specific expression of mannose-binding lectin controls atherosclerosis in low-density lipoprotein receptor-deficient mice. *Circulation* 119 (16), 2188–2195. doi:10.1161/circulationaha.108.830661.
- Maverakis, E., Kim, K., Shimoda, M., Gershwin, M.E., Patel, F., Wilken, R., et al., 2015. Glycans in the immune system and the altered glycan theory of autoimmunity: a critical review. *J. Autoimmun.* 57, 1–13. doi:10.1016/j.jaut.2014.12.002.
- Mazumder, P., Mukhopadhyay, C., 2012. Conformations, dynamics and interactions of di-, tri- and pentamannoside with mannose binding lectin: a molecular dynamics study. *Carbohydr. Res.* 349, 59–72. doi:10.1016/j.carres.2011.11.021.
- McCarthy, T.R., Torrelles, J.B., MacFarlane, A.S., Katarczak, M., Kutzbach, B., Desjardins, L.E., et al., 2005. Overexpression of mycobacterium tuberculosis manB, a phosphomannomutase that increases phosphatidylinositol mannoside biosynthesis in mycobacterium smegmatis and mycobacterial association with human macrophages. *Mol. Microbiol.* 58 (3), 774–790. doi:10.1111/j.1365-2958.2005.04862.x.
- McGreal, E.P., Rosas, M., Brown, G.D., Zamze, S., Wong, S.Y., Gordon, S., et al., 2006. The carbohydrate-recognition domain of dectin-2 is a c-type lectin with specificity for high mannose. *Glycobiology* 16 (5), 422–430. doi:10.1093/glycob/cwj077.
- Medzhradszky, K.F., Besman, M.J., Burlingame, A.L., 1997. Structural characterization of site-specific n-glycosylation of recombinant human factor VIII by reversed-phase high-performance liquid chromatography-electrospray ionization mass spectrometry. *Anal. Chem.* 69 (19), 3986–3994. doi:10.1021/ac970372z.
- Menon, S., Rosenberg, K., Graham, S.A., Ward, E.M., Taylor, M.E., Drickamer, K., et al., 2009. Binding-site geometry and flexibility in DC-SIGN demonstrated with surface force measurements. *Proc. Natl. Acad. Sci. U.S.A.* 106 (28), 11524–11529. doi:10.1073/pnas.0901783106.
- Mesman, A.W., de Vries, R.D., McQuaid, S., Duprex, W.P., de Swart, R.L., Geijtenbeek, T.B., 2012. A prominent role for DC-SIGN+ dendritic cells in initiation and dissemination of measles virus infection in non-human primates. *PLoS ONE* 7 (12), e49573. doi:10.1371/journal.pone.0049573.
- Mildner, A., Jung, S., 2014. Development and function of dendritic cell subsets. *Immunity* 40 (5), 642–656. doi:10.1016/j.immuni.2014.04.016.
- Mir-Shekari, S.Y., Ashford, D.A., Harvey, D.J., Dwek, R.A., Schulze, I.T., 1997. The glycosylation of the influenza A virus hemagglutinin by mammalian cells. A site-specific study. *J. Biol. Chem.* 272 (7), 4027–4036.
- Mitchell, D.A., Fadden, A.J., Drickamer, K., 2001. A novel mechanism of carbohydrate recognition by the c-type lectins DC-SIGN and DC-SIGNR. subunit organization and binding to multivalent ligands. *J. Biol. Chem.* 276 (31), 28939–28945. doi:10.1074/jbc.M104565200.
- Mocsai, A., Ruland, J., Tybulewicz, V.L., 2010. The SYK tyrosine kinase: a crucial player in diverse biological functions. *Nat. Rev. Immunol.* 10 (6), 387–402. doi:10.1038/nri2765.

- Moh, E.S., Lin, C.H., Thaysen-Andersen, M., Packer, N.H., 2016. Site-specific n-glycosylation of recombinant pentameric and hexameric human IgM. *J. Am. Soc. Mass Spectrom.* doi:10.1007/s13361-016-1378-0.
- Mollegaard, K.M., Duus, K., Traeholt, S.D., Thaysen-Andersen, M., Liu, Y., Palma, A.S., et al., 2011. The interactions of calreticulin with immunoglobulin G and immunoglobulin Y. *Biochim. Biophys. Acta* 1814 (7), 889–899. doi:10.1016/j.bbapap.2011.03.015.
- Moore, P.L., Gray, E.S., Wibmer, C.K., Bhiman, J.N., Nonyane, M., Sheward, D.J., et al., 2012. Evolution of an HIV glycan-dependent broadly neutralizing antibody epitope through immune escape. *Nat. Med.* 18 (11), 1688–1692. doi:10.1038/nm.2985.
- Moremen, K.W., Tiemeyer, M., Nairn, A.V., 2012. Vertebrate protein glycosylation: diversity, synthesis and function. *Nat. Rev. Mol. Cell Biol.* 13 (7), 448–462. doi:10.1038/nrm3383.
- Morfini, M., Coppola, A., Franchini, M., Di Minno, G., 2013. Clinical use of factor VIII and factor IX concentrates. *Blood Transfus.* 11 (Suppl. 4), s55–s63. doi:10.2450/2013.0105.
- Mullin, N.P., Hall, K.T., Taylor, M.E., 1994. Characterization of ligand binding to a carbohydrate-recognition domain of the macrophage mannose receptor. *J. Biol. Chem.* 269 (45), 28405–28413.
- Mullin, N.P., Hitchen, P.G., Taylor, M.E., 1997. Mechanism of Ca²⁺ and monosaccharide binding to a c-type carbohydrate-recognition domain of the macrophage mannose receptor. *J. Biol. Chem.* 272 (9), 5668–5681. doi:10.1074/jbc.272.9.5668.
- Mulvey, M.A., Schilling, J.D., Martinez, J.J., Hultgren, S.J., 2000. Bad bugs and beleaguered bladders: interplay between uropathogenic *Escherichia coli* and innate host defenses. *Proc. Natl. Acad. Sci. U.S.A.* 97 (16), 8829–8835. doi:10.1073/pnas.97.16.8829.
- Mydock-McGrane, L.K., Cusumano, Z.T., Janerka, J.W., 2015. Mannose-derived FimH antagonists: a promising anti-virulence therapeutic strategy for urinary tract infections and Crohn's disease. *Expert Opin. Ther. Pat.* doi:10.1517/13543776.2016.1131266.
- Nagae, M., Ikeda, A., Hanashima, S., Kojima, T., Matsumoto, N., Yamamoto, K., et al., 2016. Crystal structure of human dendritic cell inhibitory receptor (DCIR) C-type lectin domain reveals the binding mode with n-glycan. *FEBS Lett.* doi:10.1002/1873-3468.12162.
- Nauseef, W.M., Borregaard, N., 2014. Neutrophils at work. *Nat. Immunol.* 15 (7), 602–611. doi:10.1038/ni.2921.
- Nauta, A.J., Raaschou-Jensen, N., Roos, A., Daha, M.R., Madsen, H.O., Borrias-Essers, M.C., et al., 2003. Mannose-binding lectin engagement with late apoptotic and necrotic cells. *Eur. J. Immunol.* 33 (10), 2853–2863. doi:10.1002/eji.200323888.
- Neefjes, J., Ovaa, H., 2013. A peptide's perspective on antigen presentation to the immune system. *Nat. Chem. Biol.* 9 (12), 769–775. doi:10.1038/nchembio.1391.
- Netea, M.G., Gow, N.A., Munro, C.A., Bates, S., Collins, C., Ferwerda, G., et al., 2006. Immune sensing of *Candida albicans* requires cooperative recognition of mannans and glucans by lectin and Toll-like receptors. *J. Clin. Invest.* 116 (6), 1642–1650. doi:10.1172/JCI27114.
- Netea, M.G., Joosten, L.A., van der Meer, J.W., Kullberg, B.J., van de Veerdonk, F.L., 2015. Immune defence against candida fungal infections. *Nat. Rev. Immunol.* 15 (10), 630–642. doi:10.1038/nri3897.
- Ng, K.K., Drickamer, K., Weis, W.I., 1996. Structural analysis of monosaccharide recognition by rat liver mannose-binding protein. *J. Biol. Chem.* 271 (2), 663–674. doi:10.1074/jbc.271.2.663.
- Ng, K.K., Kolatkar, A.R., Park-Snyder, S., Feinberg, H., Clark, D.A., Drickamer, K., et al., 2002. Orientation of bound ligands in mannose-binding proteins. Implications for multivalent ligand recognition. *J. Biol. Chem.* 277 (18), 16088–16095. doi:10.1074/jbc.M200493200.
- Nichollas, E.S., Marzook, N.B., Joel, A.C., Nestor, S., Morten, T.-A., Steven, P.D., et al., 2014. Comparative proteomics and glycoproteomics reveal increased n-linked glycosylation and relaxed sequon specificity in *Campylobacter jejuni* NCTC11168 O. *J. Proteome Res.* 13 (11), 5136–5150. doi:10.1021/pr5005554.
- Nicholson, R.L., Gee, J.M., Harper, M.E., 2001. EGFR and cancer prognosis. *Eur. J. Cancer* 37 (Suppl. 4), S9–S15. doi:10.1016/S0959-8049(01)00231-3.
- Nonaka, M., Imaeda, H., Matsumoto, S., Yong Ma, B., Kawasaki, N., Mekara, E., et al., 2014. Mannan-binding protein, a c-type serum lectin, recognizes primary colorectal carcinomas through tumor-associated Lewis glycans. *J. Immunol.* 192 (3), 1294–1301. doi:10.4049/jimmunol.1203023.
- Obermayer, N., Sattin, S., Colombo, C., Bruno, M., Svajger, U., Anderluh, M., et al., 2011. Design, synthesis and activity evaluation of mannose-based DC-SIGN antagonists. *Mol. Divers.* 15 (2), 347–360. doi:10.1007/s11030-010-9285-y.
- Ohtsubo, K., Marth, J.D., 2006. Glycosylation in cellular mechanisms of health and disease. *Cell* 126 (5), 855–867. doi:10.1016/j.cell.2006.08.019.
- Olczak, M., Watorek, W., 2002. Structural analysis of n-glycans from human neutrophil azurocidin. *Biochem. Biophys. Res. Commun.* 293 (1), 213–219. doi:10.1016/S0006-291X(02)00201-2.
- Olejnik, B., Jarzab, A., Kratz, E.M., Zimmer, M., Gamian, A., Ferens-Sieczkowska, M., 2015. Terminal mannose residues in seminal plasma glycoproteins of infertile men compared to fertile donors. *Int. J. Mol. Sci.* 16 (7), 14933–14950. doi:10.3390/ijms160714933.
- Ozcan, S., Barkauskas, D.A., Renee Ruhaak, L., Torres, J., Cooke, C.L., An, H.J., et al., 2014. Serum glycan signatures of gastric cancer. *Cancer Prev. Res. (Phila)* 7 (2), 226–235. doi:10.1158/1940-6207.CAPR-13-0235.
- Pak, J., Pu, Y., Zhang, Z.T., Hastly, D.L., Wu, X.R., 2001. Tamm-horsfall protein binds to type 1 fimbriated *Escherichia coli* and prevents *E. coli* from binding to uroplakin Ia and Ib receptors. *J. Biol. Chem.* 276 (13), 9924–9930. doi:10.1074/jbc.M008610200.
- Park, H.M., Hwang, M.P., Kim, Y.W., Kim, K.J., Jin, J.M., Kim, Y.H., et al., 2015. Mass spectrometry-based n-linked glycomic profiling as a means for tracking pancreatic cancer metastasis. *Carbohydr. Res.* 413, 5–11. doi:10.1016/j.carres.2015.04.019.
- Parker, B.L., Thaysen-Andersen, M., Solis, N., Scott, N.E., Larsen, M.R., Graham, M.E., et al., 2013. Site-specific glycan-peptide analysis for determination of n-glycoproteome heterogeneity. *J. Proteome Res.* 12 (12), 5791–5800. doi:10.1021/pr400783j.
- Parker, B.L., Thaysen-Andersen, M., Fazakerley, D.J., Holliday, M., Packer, N.H., James, D.E., 2015. Terminal galactosylation and sialylation switching on membrane glycoproteins upon TNF- α -induced insulin resistance in adipocytes. *Mol. Cell. Proteomics* doi:10.1074/mcp.M115.054221.
- Patterson, J.H., Waller, R.F., Jeevarajah, D., Billman-Jacobe, H., McConville, M.J., 2003. Mannose metabolism is required for mycobacterial growth. *Biochem. J.* 372 (Pt 1), 77–86. doi:10.1042/BJ20021700.
- Pejchal, R., Doores, K.J., Walker, L.M., Khayat, R., Huang, P.S., Wang, S.K., et al., 2011. A potent and broad neutralizing antibody recognizes and penetrates the HIV glycan shield. *Science* 334 (6059), 1097–1103. doi:10.1126/science.1213256.
- Peterson, R., Cheah, W.Y., Grinyer, J., Packer, N., 2013. Glycoconjugates in human milk: protecting infants from disease. *Glycobiology* 23 (12), 1425–1438. doi:10.1093/glycob/cwt072.
- Pichl, C.M., Feilhauer, S., Schwaigerlehner, R.M., Gabor, F., Wirrh, M., Neusch, L., 2015. Glycan-mediated uptake in urothelial primary cells: perspectives for improved intravesical drug delivery in urinary tract infections. *Int. J. Pharm.* 495 (2), 710–718. doi:10.1016/j.jipharm.2015.09.017.
- Pinho, S.S., Reis, C.A., 2015. Glycosylation in cancer: mechanisms and clinical implications. *Nat. Rev. Cancer* 15 (9), 540–555. doi:10.1038/nrc3982.
- Plom, R., Hensbergen, P.J., Rombouts, Y., Zauner, G., Dragan, I., Koeleman, C.A., et al., 2014. Site-specific n-glycosylation analysis of human immunoglobulin e. *J. Proteome Res.* 13 (2), 536–546. doi:10.1021/pr400714w.
- Pohlmann, S., Soilleux, E.J., Baribaud, F., Leslie, G.J., Morris, L.S., Trowsdale, J., et al., 2001. DC-SIGN, a DC-SIGN homologue expressed in endothelial cells, binds to human and simian immunodeficiency viruses and activates infection in trans. *Proc. Natl. Acad. Sci. U.S.A.* 98 (5), 2670–2675. doi:10.1073/pnas.051631398.
- Praissman, J.L., Wells, L., 2014. Mammalian o-mannosylation pathway: glycan structures, enzymes, and protein substrates. *Biochemistry* 53 (19), 3066–3078. doi:10.1021/bi500153y.
- Pritchard, L.K., Spencer, D.I., Royle, L., Bonomelli, C., Seabright, G.E., Behrens, A.J., et al., 2015. Glycan clustering stabilizes the mannose patch of HIV-1 and preserves vulnerability to broadly neutralizing antibodies. *Nat. Commun.* 6, 7479. doi:10.1038/ncomms8479.
- Qu, C., Edwards, E.W., Tacke, F., Angeli, V., Llodra, J., Sanchez-Schmitz, G., et al., 2004. Role of CCR8 and other chemokine pathways in the migration of monocyte-derived dendritic cells to lymph nodes. *J. Exp. Med.* 200 (10), 1231–1241. doi:10.1084/jem.20032152.
- Rabinovich, G.A., Toscano, M.A., 2009. Turning 'sweet' on immunity: galectin-glycan interactions in immune tolerance and inflammation. *Nat. Rev. Immunol.* 9 (5), 338–352. doi:10.1038/nri2536.
- Rachmilewitz, J., 2010. Glycosylation: an intrinsic sign of "danger". *Self Nonself* 1 (3), 250–254. doi:10.4161/self.1.3.12330.
- Radcliffe, C.M., Arnold, J.N., Suter, D.M., Wormald, M.R., Harvey, D.J., Royle, L., et al., 2007. Human follicular lymphoma cells contain oligomannose glycans in the antigen-binding site of the B-cell receptor. *J. Biol. Chem.* 282 (10), 7405–7415. doi:10.1074/jbc.M602690200.
- Rajaram, M.V., Ni, B., Morris, J.D., Brooks, M.N., Carlson, T.K., Bakthavachalu, B., et al., 2011. Mycobacterium tuberculosis lipomannan blocks TNF biosynthesis by regulating macrophage MAPK-activated protein kinase 2 (MK2) and microRNA miR-125b. *Proc. Natl. Acad. Sci. U.S.A.* 108 (42), 17408–17413. doi:10.1073/pnas.1112660108.

- Rajaram, M.V., Ni, B., Dodd, C.E., Schlesinger, L.S., 2014. Macrophage immunoregulatory pathways in tuberculosis. *Semin. Immunol.* 26 (6), 471–485. doi:10.1016/j.smim.2014.09.010.
- Ravnsborg, T., Houen, G., Hojrup, P., 2010. The glycosylation of myeloperoxidase. *Biochim. Biophys. Acta* 1804 (10), 2046–2053. doi:10.1016/j.bbapap.2010.07.001.
- Richardson, M.B., Williams, S.J., 2014. MCL and mincle: c-type lectin receptors that sense damaged self and pathogen-associated molecular patterns. *Front. Immunol.* 5, 288. doi:10.3389/fimmu.2014.00288.
- Rini, J., Esko, J., Varki, A., 2009. Glycosyltransferases and glycan-processing Enzymes. In: Varki, A., Cummings, R.D., Esko, J.D., Freeze, H.H., Stanley, P., Bertozzi, C.R., et al. (Eds.), *Essentials of Glycobiology*, second ed. Cold Spring Harbor, New York, pp. 63–74.
- Robajac, D., Vanhooren, V., Masnikosa, R., Miković, Ž., Mandić, V., Libert, C., et al., 2015. Preeclampsia transforms membrane N-glycome in human placenta. *Exp. Mol. Pathol.* doi:10.1016/j.yexmp.2015.11.029.
- Robinson, M.J., Sancho, D., Slack, E.C., LeibundGut-Landmann, S., Reis e Sousa, C., 2006. Myeloid C-type lectins in innate immunity. *Nat. Immunol.* 7 (12), 1258–1265. doi:10.1038/ni1417.
- Robinson, M.J., Osorio, F., Rosas, M., Freitas, R.P., Schweighoffer, E., Gross, O., et al., 2009. Dectin-2 is a Syk-coupled pattern recognition receptor crucial for Th17 responses to fungal infection. *J. Exp. Med.* 206 (9), 2037–2051. doi:10.1084/jem.20082818.
- Rock, K.L., Latz, E., Ontiveros, F., Kono, H., 2010. The sterile inflammatory response. *Annu. Rev. Immunol.* 28, 321–342. doi:10.1146/annurev-immunol-030409-101311.
- Roth, A.J., Brown, M.C., Smith, R.N., Badhwar, A.K., Parente, O., Chung, H., et al., 2012. Anti-LAMP-2 antibodies are not prevalent in patients with antineutrophil cytoplasmic autoantibody glomerulonephritis. *J. Am. Soc. Nephrol.* 23 (3), 545–555. doi:10.1681/asn.2011030273.
- Roth, J., Zuber, C., Park, S., Jang, I., Lee, Y., Kysela, K.G., et al., 2010. Protein N-glycosylation, protein folding, and protein quality control. *Mol. Cells* 30 (6), 497–506. doi:10.1007/s10059-010-0159-z.
- Ruhaak, L.R., Taylor, S.L., Stroble, C., Nguyen, U.T., Parker, E.A., Song, T., et al., 2015. Differential n-glycosylation patterns in lung adenocarcinoma tissue. *J. Proteome Res.* 14 (11), 4538–4549. doi:10.1021/acs.jproteome.5b00255.
- Russell, D.G., 2011. Mycobacterium tuberculosis and the intimate discourse of a chronic infection. *Immunol. Rev.* 240 (1), 252–268. doi:10.1111/j.1600-065X.2010.00984.x.
- Sabin, C., Mitchell, E.P., Pokorna, M., Gautier, C., Utile, J.P., Wimmerova, M., et al., 2006. Binding of different monosaccharides by lectin PA-III. from *Pseudomonas aeruginosa*: thermodynamics data correlated with x-ray structures. *FEBS Lett.* 580 (3), 982–987. doi:10.1016/j.febslet.2006.01.030.
- Saeland, E., Belo, A.I., Mongera, S., van Die, I., Meijer, G.A., van Kooyk, Y., 2012. Differential glycosylation of MUC1 and CEACAM5 between normal mucosa and tumour tissue of colon cancer patients. *Int. J. Cancer* 131 (1), 117–128. doi:10.1002/ijc.26354.
- Sahly, H., Ofek, I., Podschun, R., Brade, H., He, Y., Ullmann, U., et al., 2002. Surfactant protein d binds selectively to klebsiella pneumoniae lipopolysaccharides containing mannose-rich o-antigens. *J. Immunol.* 169 (6), 3267–3274. doi:10.4049/jimmunol.169.6.3267.
- Sallusto, F., Lanzavecchia, A., 1994. Efficient presentation of soluble antigen by cultured human dendritic cells is maintained by granulocyte/macrophage colony-stimulating factor plus interleukin 4 and downregulated by tumor necrosis factor alpha. *J. Exp. Med.* 179 (4), 1109–1118.
- Sancho, D., Reis e Sousa, C., 2012. Signaling by myeloid c-type lectin receptors in immunity and homeostasis. *Annu. Rev. Immunol.* 30, 491–529. doi:10.1146/annurev-immunol-031210-101352.
- Sandborn, W.J., 2004. Serologic markers in inflammatory bowel disease: state of the art. *Rev. Gastroenterol. Disord.* 4 (4), 167–174.
- Sanders, R.W., Venturi, M., Schiffner, L., Kalyanaraman, R., Katinger, H., Lloyd, K.O., et al., 2002. The mannose-dependent epitope for neutralizing antibody 2G12 on human immunodeficiency virus type 1 glycoprotein gp120. *J. Virol.* 76 (14), 7293–7305. doi:10.1128/JVI.76.14.7293-7305.2002.
- Santiago, C., Celma, M.L., Stehle, T., Casasnovas, J.M., 2010. Structure of the measles virus hemagglutinin bound to the CD46 receptor. *Nat. Struct. Mol. Biol.* 17 (1), 124–129. doi:10.1038/nsmb.1726.
- Sato, K., Yang, X.L., Yude, T., Chung, J.S., Wu, J., Luby-Phelps, K., et al., 2006. Dectin-2 is a pattern recognition receptor for fungi that couples with the Fc receptor gamma chain to induce innate immune responses. *J. Biol. Chem.* 281 (50), 38854–38866. doi:10.1074/jbc.M606542200.
- Sauer, M.M., Jakob, R.P., Eras, J., Baday, S., Eris, D., Navarra, G., et al., 2016. Catch-bond mechanism of the bacterial adhesin FimH. *Nat. Commun.* 7, 10738. doi:10.1038/ncomms10738.
- Scanlan, C.N., Offer, J., Zitzmann, N., Dwek, R.A., 2007. Exploiting the defensive sugars of HIV-1 for drug and vaccine design. *Nature* 446 (7139), 1038–1045. doi:10.1038/nature05818.
- Schachter, H., 2009. Paucimannose n-glycans in *Caenorhabditis elegans* and *Drosophila melanogaster*. *Carbohydr. Res.* 344 (12), 1391–1396. doi:10.1016/j.carres.2009.04.028.
- Schedin-Weiss, S., Winblad, B., Tjernberg, L.O., 2014. The role of protein glycosylation in Alzheimer disease. *FEBS J.* 281 (1), 46–62. doi:10.1111/febs.12590.
- Schlesinger, L.S., Hull, S.R., Kaufman, T.M., 1994. Binding of the terminal mannosyl units of lipoarabinomannan from a virulent strain of mycobacterium tuberculosis to human macrophages. *J. Immunol.* 152 (8), 4070–4079.
- Schlesinger, L.S., Kaufman, T.M., Iyer, S., Hull, S.R., Marchiando, L.K., 1996. Differences in mannose receptor-mediated uptake of lipoarabinomannan from virulent and attenuated strains of mycobacterium tuberculosis by human macrophages. *J. Immunol.* 157 (10), 4568–4575.
- Schnaar, R.L., 2016. Glycobiology simplified: diverse roles of glycan recognition in inflammation. *J. Leukoc. Biol.* doi:10.1189/jlb.3R10116-021R.
- Schweizer, A., Stahl, P.D., Rohrer, J., 2000. A di-aromatic motif in the cytosolic tail of the mannose receptor mediates endosomal sorting. *J. Biol. Chem.* 275 (38), 29694–29700. doi:10.1074/jbc.M000571200.
- Scordo, J.M., Knoell, D.L., Torrelles, J.B., 2015. Alveolar epithelial cells in mycobacterium tuberculosis infection: active players or innocent bystanders? *J. Innate Immun.* doi:10.1159/000439275.
- Scott, D.W., Patel, R.P., 2013. Endothelial heterogeneity and adhesion molecules n-glycosylation: implications in leukocyte trafficking in inflammation. *Glycobiology* 23 (6), 622–633. doi:10.1093/glycob/cwt014.
- Scott, D.W., Chen, J., Chacko, B.K., Traylor, J.G., Jr., Orr, A.W., Patel, R.P., 2012. Role of endothelial n-glycan mannose residues in monocyte recruitment during atherosclerosis. *Arterioscler. Thromb. Vasc. Biol.* 32 (8), e51–e59. doi:10.1161/atvbaha.112.253203.
- Scott, D.W., Dunn, T.S., Ballester, M.E., Litovsky, S.H., Patel, R.P., 2013. Identification of a high-mannose ICAM-1 glycoform: effects of ICAM-1 hypoglycosylation on monocyte adhesion and outside in signaling. *Am. J. Physiol. Cell Physiol.* 305 (2), C228–C237. doi:10.1152/ajpcell.00116.2013.
- Scott, N.E., Marzook, N.B., Cain, J.A., Solis, N., Thaysen-Andersen, M., Djordjevic, S.P., et al., 2014. Comparative proteomics and glycoproteomics reveal increased n-linked glycosylation and relaxed sequon specificity in *Campylobacter jejuni* NCTC11168 O. *J. Proteome Res.* 13 (11), 5136–5150. doi:10.1021/pr5005554.
- Segura, E., Amigorena, S., 2013. Inflammatory dendritic cells in mice and humans. *Trends Immunol.* 34 (9), 440–445. doi:10.1016/j.it.2013.06.001.
- Sendid, B., Colombel, J.F., Jacquinet, P.M., Faille, C., Fruit, J., Cortot, A., et al., 1996. Specific antibody response to oligomannosidic epitopes in Crohn's disease. *Clin. Diagn. Lab. Immunol.* 3 (2), 219–226.
- Sethi, M.K., Thaysen-Andersen, M., Smith, J.T., Baker, M.S., Packer, N.H., Hancock, W.S., et al., 2014. Comparative n-glycan profiling of colorectal cancer cell lines reveals unique bisecting GlcNAc and alpha-2,3-linked sialic acid determinants are associated with membrane proteins of the more metastatic/aggressive cell lines. *J. Proteome Res.* 13 (1), 277–288. doi:10.1021/pr400861m.
- Sethi, M.K., Kim, H., Park, C.K., Baker, M.S., Paik, Y.K., Packer, N.H., et al., 2015. In-depth n-glycome profiling of paired colorectal cancer and non-tumorigenic tissues reveals cancer-, stage- and EGFR-specific protein n-glycosylation. *Glycobiology* 25 (10), 1064–1078. doi:10.1093/glycob/cwv042.
- Shade, K.T., Platzter, B., Washburn, N., Mani, V., Bartsch, Y.C., Conroy, M., et al., 2015. A single glycan on IgE is indispensable for initiation of anaphylaxis. *J. Exp. Med.* 212 (4), 457–467. doi:10.1084/jem.20142182.
- Sharma, V., Ichikawa, M., Freeze, H.H., 2014. Mannose metabolism: more than meets the eye. *Biochem. Biophys. Res. Commun.* 453 (2), 220–228. doi:10.1016/j.bbrc.2014.06.021.
- Sheriff, S., Chang, C.Y., Ezekowitz, R.A., 1994. Human mannose-binding protein carbohydrate recognition domain trimerizes through a triple alpha-helical coiled-coil. *Nat. Struct. Biol.* 1 (11), 789–794. doi:10.1038/nsb1194-789.
- Shibata, N., Ikuta, K., Imai, T., Satoh, Y., Satoh, R., Suzuki, A., et al., 1995. Existence of branched side chains in the cell wall mannans of pathogenic yeast, *Candida albicans*. structure-antigenicity relationship between the cell wall mannans of *Candida albicans* and *Candida parapsilosis*. *J. Biol. Chem.* 270 (3), 1113–1122. doi:10.1074/jbc.270.3.1113.

- Shreffler, W.G., Castro, R.R., Kucuk, Z.Y., Charlop-Powers, Z., Grishina, G., Yoo, S., et al., 2006. The major glycoprotein allergen from arachis hypogaea, Ara h 1, is a ligand of dendritic cell-specific ICAM-grabbing nonintegrin and acts as a Th2 adjuvant in vitro. *J. Immunol.* 177 (6), 3677–3685. doi:10.4049/jimmunol.177.6.3677.
- Smagula, R.M., Van Halbeek, H., Decker, J.M., Muchmore, A.V., Moody, C.E., Sherblom, A.P., 1990. Pregnancy-associated changes in oligomannose oligosaccharides of human and bovine uromodulin (Tamm-horsfall glycoprotein). *Glycoconj. J.* 7 (6), 609–624.
- Smith, G.T., Sweredoski, M.J., Hess, S., 2014. O-linked glycosylation sites profiling in mycobacterium tuberculosis culture filtrate proteins. *J. Proteomics* 97, 296–306. doi:10.1016/j.jprot.2013.05.011.
- Sondergaard, J.N., Vinner, L., Brix, S., 2014. Natural mannosylation of HIV-1 gp120 imposes no immunoregulatory effects in primary human plasmacytoid dendritic cells. *Mol. Immunol.* 59 (2), 180–187. doi:10.1016/j.molimm.2014.02.009.
- Spiro, R.G., 2004. Role of n-linked polymannose oligosaccharides in targeting glycoproteins for endoplasmic reticulum-associated degradation. *Cell. Mol. Life Sci.* 61 (9), 1025–1041. doi:10.1007/s00018-004-4037-8.
- Stambach, N.S., Taylor, M.E., 2003. Characterization of carbohydrate recognition by langerin, a c-type lectin of langerhans cells. *Glycobiology* 13 (5), 401–410. doi:10.1093/glycob/cwg045.
- Stanley, P., Schachter, H., Taniguchi, N., 2009. N-Glycans. In: Varki, A., Cummings, R.D., Esko, J.D., Freeze, H.H., Stanley, P., Bertozzi, C.R., et al. (Eds.), *Essentials of Glycobiology*, second ed. Cold Spring Harbor (NY), New York, pp. 101–114.
- Strahl-Bolsinger, S., Gentzsch, M., Tanner, W., 1999. Protein o-mannosylation. *Biochim. Biophys. Acta* 1426 (2), 297–307. doi:10.1016/S0304-4165(98)00131-7.
- Su, Y., Bakker, T., Harris, J., Tsang, C., Brown, G.D., Wormald, M.R., et al., 2005. Glycosylation influences the lectin activities of the macrophage mannose receptor. *J. Biol. Chem.* 280 (38), 32811–32820. doi:10.1074/jbc.M503457200.
- Swierko, A.S., Kilpatrick, D.C., Cedzynski, M., 2013. Mannan-binding lectin in malignancy. *Mol. Immunol.* 55 (1), 16–21. doi:10.1016/j.molimm.2012.09.005.
- Taganna, J., de Boer, A.R., Wührer, M., Bouckaert, J., 2011. Glycosylation changes as important factors for the susceptibility to urinary tract infection. *Biochem. Soc. Trans.* 39 (1), 349–354. doi:10.1042/BST0390349.
- Takakura, D., Tada, M., Kawasaki, N., 2015. Membrane glycoproteomics of fetal lung fibroblasts using LC/MS. *Proteomics* doi:10.1002/pmic.201500003.
- Tate, M.D., Job, E.R., Deng, Y.M., Gunalan, V., Maurer-Stroh, S., Reading, P.C., 2014. Playing hide and seek: how glycosylation of the influenza virus hemagglutinin can modulate the immune response to infection. *Viruses* 6 (3), 1294–1316. doi:10.3390/v6031294.
- Taylor, M.E., Bezouska, K., Drickamer, K., 1992. Contribution to ligand binding by multiple carbohydrate-recognition domains in the macrophage mannose receptor. *J. Biol. Chem.* 267 (3), 1719–1726.
- Taylor, P.R., Gordon, S., Martinez-Pomares, L., 2005. The mannose receptor: linking homeostasis and immunity through sugar recognition. *Trends Immunol.* 26 (2), 104–110. doi:10.1016/j.it.2004.12.001.
- Te Riet, J., Reinieren-Beeren, I., Figdor, C.G., Cambi, A., 2015. AFM force spectroscopy reveals how subtle structural differences affect the interaction strength between candida albicans and DC-SIGN. *J. Mol. Recognit.* 28 (11), 687–698. doi:10.1002/jmr.2481.
- Tecle, E., Gagneux, P., 2015. Sugar-coated sperm: unraveling the functions of the mammalian sperm glycocalyx. *Mol. Reprod. Dev.* 82 (9), 635–650. doi:10.1002/mrd.22500.
- Teillet, F., Dublet, B., Andrieu, J.P., Gaboriaud, C., Arlaud, G.J., Thielens, N.M., 2005. The two major oligomeric forms of human mannan-binding lectin: chemical characterization, carbohydrate-binding properties, and interaction with MBL-associated serine proteases. *J. Immunol.* 174 (5), 2870–2877. doi:10.4049/jimmunol.174.5.2870.
- Thaysen-Andersen, M., Packer, N.H., 2012. Site-specific glycoproteomics confirms that protein structure dictates formation of n-glycan type, core fucosylation and branching. *Glycobiology* 22 (11), 1440–1452. doi:10.1093/glycob/cws110.
- Thaysen-Andersen, M., Packer, N.H., 2014. Advances in LC-MS/MS-based glycoproteomics: getting closer to system-wide site-specific mapping of the n- and o-glycoproteome. *Biochim. Biophys. Acta* 1844 (9), 1437–1452. doi:10.1016/j.bbapap.2014.05.002.
- Thaysen-Andersen, M., Venkatakrishnan, V., Loke, I., Laurini, C., Diestel, S., Parker, B.L., et al., 2015. Human neutrophils secrete bioactive paucimannosidic proteins from azurophilic granules into pathogen-infected sputum. *J. Biol. Chem.* 290 (14), 8789–8802. doi:10.1074/jbc.M114.631622.
- Thaysen-Andersen, M., Packer, N.H., Schulz, B.L., 2016. Maturing glycoproteomics technologies provide unique structural insights into the N-glycoproteome and its regulation in health and disease. *Mol. Cell. Proteomics* doi:10.1074/mcp.O115.057638.
- Tielker, D., Hacker, S., Loris, R., Strathmann, M., Wingender, J., Wilhelm, S., et al., 2005. Pseudomonas aeruginosa lectin LecB is located in the outer membrane and is involved in biofilm formation. *Microbiology* 151 (Pt 5), 1313–1323. doi:10.1099/mic.0.27701-0.
- Torrelles, J.B., Schlesinger, L.S., 2010. Diversity in mycobacterium tuberculosis mannose cell wall determinants impacts adaptation to the host. *Tuberculosis (Edinb.)* 90 (2), 84–93. doi:10.1016/j.tube.2010.02.003.
- Torrelles, J.B., Desjardin, L.E., MacNeil, J., Kaufman, T.M., Kutzbach, B., Knaup, R., et al., 2009. Inactivation of mycobacterium tuberculosis mannose-6-phosphate 6-phosphotransferase pimB reduces the cell wall lipopolysaccharide and lipomannan content and increases the rate of bacterial-induced human macrophage cell death. *Glycobiology* 19 (7), 743–755. doi:10.1093/glycob/cwp042.
- Torrelles, J.B., Sieling, P.A., Zhang, N., Keen, M.A., McNeil, M.R., Belisle, J.T., et al., 2012. Isolation of a distinct mycobacterium tuberculosis mannose-capped lipopolysaccharide isoform responsible for recognition by CD1b-restricted T cells. *Glycobiology* 22 (8), 1118–1127. doi:10.1093/glycob/cws078.
- Turner, M.W., 2003. The role of mannose-binding lectin in health and disease. *Mol. Immunol.* 40 (7), 423–429. doi:10.1016/S0161-5890(03)00155-X.
- van der Graaf, C.A., Netea, M.G., Verschuuren, L., van der Meer, J.W., Kullberg, B.J., 2005. Differential cytokine production and toll-like receptor signaling pathways by candida albicans blastoconidia and hyphae. *Infect. Immun.* 73 (11), 7458–7464. doi:10.1128/IAI.73.11.7458-7464.2005.
- van Gisbergen, K.P., Aarnoudse, C.A., Meijer, G.A., Geijtenbeek, T.B., van Kooyk, Y., 2005a. Dendritic cells recognize tumor-specific glycosylation of carcinoembryonic antigen on colorectal cancer cells through dendritic cell-specific intercellular adhesion molecule-3-grabbing nonintegrin. *Cancer Res.* 65 (13), 5935–5944. doi:10.1158/0008-5472.can-04-4140.
- van Gisbergen, K.P., Sanchez-Hernandez, M., Geijtenbeek, T.B., van Kooyk, Y., 2005b. Neutrophils mediate immune modulation of dendritic cells through glycosylation-dependent interactions between Mac-1 and DC-SIGN. *J. Exp. Med.* 201 (8), 1281–1292. doi:10.1084/jem.20041276.
- van Kooyk, Y., Geijtenbeek, T.B., 2003. DC-SIGN: escape mechanism for pathogens. *Nat. Rev. Immunol.* 3 (9), 697–709. doi:10.1038/nri1182.
- van Kooyk, Y., Rabinovich, G.A., 2008. Protein-glycan interactions in the control of innate and adaptive immune responses. *Nat. Immunol.* 9 (6), 593–601. doi:10.1038/nri.203.
- van Liemp, E., Bank, C.M., Mehta, P., Garcia-Vallejo, J.J., Kwar, Z.S., Geyer, R., et al., 2006. Specificity of DC-SIGN for mannose- and fucose-containing glycans. *FEBS Lett.* 580 (26), 6123–6131. doi:10.1016/j.febslet.2006.10.009.
- van Remoortere, A., Bank, C.M., Nyame, A.K., Cummings, R.D., Deelder, A.M., van Die, I., 2003. Schistosoma mansoni-infected mice produce antibodies that cross-react with plant, insect, and mammalian glycoproteins and recognize the truncated biantennary n-glycan Man3GlcNAc2-R. *Glycobiology* 13 (3), 217–225. doi:10.1093/glycob/cwg025.
- Valladeau, J., Ravel, O., Dezutter-Dambuyant, C., Moore, K., Kleijmeer, M., Liu, Y., et al., 2000. Langerin, a novel c-type lectin specific to langerhans cells, is an endocytic receptor that induces the formation of birbeck granules. *Immunity* 12 (1), 71–81. doi:10.1016/S1074-7613(00)80160-0.
- Van Antwerpen, P., Slomianny, M.-C.C., Boudjeltia, K.Z., Delporte, C., Faid, V., Calay, D., et al., 2010. Glycosylation pattern of mature dimeric leukocyte and recombinant monomeric myeloperoxidase: glycosylation is required for optimal enzymatic activity. *J. Biol. Chem.* 285 (21), 16351–16359. doi:10.1074/jbc.M109.089748.
- Van Iwaarden, J.F., Pikaar, J.C., Storm, J., Brouwer, E., Verhoef, J., Oosting, R.S., et al., 1994. Binding of surfactant protein A to the lipid A moiety of bacterial lipopolysaccharides. *Biochem. J.* 303 (Pt 2), 407–411.
- Van Rooijen, J.J., Hermentin, P., Kamerling, J.P., Vliegthart, J.F., 2001. The patterns of the complex- and oligomannose-type glycans of uromodulin (Tamm-horsfall glycoprotein) in the course of pregnancy. *Glycoconj. J.* 18 (7), 539–546. doi:10.1023/A:1019644413639.
- Vandewalle-El Khoury, P., Colombel, J.F., Joossens, S., Standaert-Vitse, A., Collot, M., Halfvarson, J., et al., 2008. Detection of antisynthetic mannoside antibodies (ASigmaMA) reveals heterogeneity in the ASCA response of Crohn's disease patients and contributes to differential diagnosis, stratification, and prediction. *Am. J. Gastroenterol.* 103 (4), 949–957. doi:10.1111/j.1572-0241.2007.01648.x.

- Varga, N., Sutkeviciute, I., Ribeiro-Viana, R., Berzi, A., Ramdasi, R., Daghetti, A., et al., 2014. A multivalent inhibitor of the DC-SIGN dependent uptake of HIV-1 and dengue virus. *Biomaterials* 35 (13), 4175–4184. doi:10.1016/j.biomaterials.2014.01.014.
- Varki, A., Kornfeld, S., 2009. P-type lectins. In: Varki, A., Cummings, R.D., Esko, J.D., Freeze, H.H., Stanley, P., Bertozzi, C.R., et al. (Eds.), *Essentials of Glycobiology*, second ed. Cold Spring Harbor, New York, pp. 425–438.
- Varki, A., Sharon, N., 2009. Historical background and overview. In: Varki, A., Cummings, R.D., Esko, J.D., Freeze, H.H., Stanley, P., Bertozzi, C.R., et al. (Eds.), *Essentials of Glycobiology*, second ed. Cold Spring Harbor, New York, pp. 1–22.
- Varki, A., Freeze, H.H., Vacquier, V.D., 2009. Glycans in development and systemic physiology. In: Varki, A., Cummings, R.D., Esko, J.D., Freeze, H.H., Stanley, P., Bertozzi, C.R., et al. (Eds.), *Essentials of Glycobiology*, second ed. Cold Spring Harbor, New York, pp. 531–536.
- Varki, A., Cummings, R.D., Aebi, M., Packer, N.H., Seeberger, P.H., Esko, J.D., et al., 2015. Symbol nomenclature for graphical representations of glycans. *Glycobiology* 25 (12), 1323–1324. doi:10.1093/glycob/cwv091.
- Veldhuizen, E.J., van Eijk, M., Haagsman, H.P., 2011. The carbohydrate recognition domain of collectins. *FEBS J.* 278 (20), 3930–3941. doi:10.1111/j.1742-4658.2011.08206.x.
- Venkatakrishnan, V., Packer, N.H., Thaysen-Andersen, M., 2013. Host mucin glycosylation plays a role in bacterial adhesion in lungs of individuals with cystic fibrosis. *Expert Rev. Respir. Med.* 7 (5), 553–576. doi:10.1586/17476348.2013.837752.
- Venkatakrishnan, V., Thaysen-Andersen, M., Chen, S.C., Nevalainen, H., Packer, N.H., 2015. Cystic fibrosis and bacterial colonization define the sputum n-glycosylation phenotype. *Glycobiology* 25 (1), 88–100. doi:10.1093/glycob/cwv092.
- Vigerust, D.J., Shepherd, V.L., 2007. Virus glycosylation: role in virulence and immune interactions. *Trends Microbiol.* 15 (5), 211–218. doi:10.1016/j.tim.2007.03.003.
- Villadangos, J.A., Schnorrer, P., 2007. Intrinsic and cooperative antigen-presenting functions of dendritic-cell subsets in vivo. *Nat. Rev. Immunol.* 7 (7), 543–555. doi:10.1038/nri2103.
- Villadangos, J.A., Shortman, K., 2010. Found in translation: the human equivalent of mouse CD8+ dendritic cells. *J. Exp. Med.* 207 (6), 1131–1134. doi:10.1084/jem.20100985.
- Weis, W.I., Drickamer, K., 1994. Trimeric structure of a c-type mannose-binding protein. *Structure* 2 (12), 1227–1240. doi:10.1016/S0969-2126(94)00124-3.
- Weis, W.I., Drickamer, K., 1996. Structural basis of lectin-carbohydrate recognition. *Annu. Rev. Biochem.* 65, 441–473. doi:10.1146/annurev.bi.65.070196.002301.
- Weis, W.I., Crichton, G.V., Murthy, H.M., Hendrickson, W.A., Drickamer, K., 1991. Physical characterization and crystallization of the carbohydrate-recognition domain of a mannose-binding protein from rat. *J. Biol. Chem.* 266 (31), 20678–20686.
- Weis, W.I., Drickamer, K., Hendrickson, W.A., 1992. Structure of a c-type mannose-binding protein complexed with an oligosaccharide. *Nature* 360 (6400), 127–134. doi:10.1038/360127a0.
- Weis, W.I., Taylor, M.E., Drickamer, K., 1998. The c-type lectin superfamily in the immune system. *Immunol. Rev.* 163, 19–34. doi:10.1111/j.1600-065X.1998.tb01185.x.
- Wellens, A., Garofalo, C., Nguyen, H., Van Gerven, N., Slattegard, R., Hernalsteens, J.P., et al., 2008. Intervening with urinary tract infections using anti-adhesives based on the crystal structure of the FimH-oligomannose-3 complex. *PLoS ONE* 3 (4), e2040. doi:10.1371/journal.pone.0002040.
- Wells, C.A., Salvage-Jones, J.A., Li, X., Hitchens, K., Butcher, S., Murray, R.Z., et al., 2008. The macrophage-inducible c-type lectin, mincle, is an essential component of the innate immune response to candida albicans. *J. Immunol.* 180 (11), 7404–7413. doi:10.4049/jimmunol.180.11.7404.
- Wells, L., 2013. The o-mannosylation pathway: glycosyltransferases and proteins implicated in congenital muscular dystrophy. *J. Biol. Chem.* 288 (10), 6930–6935. doi:10.1074/jbc.R112.438978.
- Westphal, S., Kolarich, D., Foetisch, K., Lauer, I., Altmann, F., Conti, A., et al., 2003. Molecular characterization and allergenic activity of Lyc e 2 (beta-fructofuranosidase), a glycosylated allergen of tomato. *Eur. J. Biochem.* 270 (6), 1327–1337.
- Woschnagg, C., Rubin, J., Venge, P., 2009. Eosinophil cationic protein (ECP) is processed during secretion. *J. Immunol.* 183 (6), 3949–3954. doi:10.4049/jimmunol.0900509.
- Wu, G., Hitchen, P.G., Panico, M., North, S.J., Barbouche, M.R., Biner, D., et al., 2015. Glycoproteomic studies of IgE from a novel hyper IgE syndrome linked to PGM3 mutation. *Glycoconj. J.* doi:10.1007/s10719-015-9638-y.
- Wu, L., Sampson, N.S., 2014. Fucose, mannose, and beta-n-acetylglucosamine glycopolymers initiate the mouse sperm acrosome reaction through convergent signaling pathways. *ACS Chem. Biol.* 9 (2), 468–475. doi:10.1021/cb400550j.
- Xia, B., Asif, G., Arthur, L., Pervaiz, M.A., Li, X., Liu, R., et al., 2013. Oligosaccharide analysis in urine by MALDI-TOF mass spectrometry for the diagnosis of lysosomal storage diseases. *Clin. Chem.* 59 (9), 1357–1368. doi:10.1373/clinchem.2012.201053.
- Xu, C., Ng, D.T., 2015a. Glycosylation-directed quality control of protein folding. *Nat. Rev. Mol. Cell Biol.* doi:10.1038/nrm4073.
- Xu, C., Ng, D.T., 2015b. O-mannosylation: the other glycan player of ER quality control. *Semin. Cell Dev. Biol.* 41, 129–134. doi:10.1016/j.semcdb.2015.01.014.
- Xu, X.-L., Zhang, P., Shen, Y.-H., Li, H.-Q., Wang, Y.-H., Lu, G.-H., et al., 2015. Mannose prevents acute lung injury through mannose receptor pathway and contributes to regulate PPAR γ and TGF- β 1 level. *Int. J. Clin. Exp. Pathol.* 8 (6), 6214–6224.
- Yan, H., Kamiya, T., Suabjakyoung, P., Tsuji, N.M., 2015. Targeting c-type lectin receptors for cancer immunity. *Front. Immunol.* 6, 408. doi:10.3389/fimmu.2015.00408.
- Yao, W., Peng, Y., Du, M., Luo, J., Zong, L., 2013. Preventative vaccine-loaded mannose-modified chitosan nanoparticles intended for nasal mucosal delivery enhance immune responses and potent tumor immunity. *Mol. Pharm.* 10 (8), 2904–2914. doi:10.1021/mp4000053.
- Yonekawa, A., Saijo, S., Hoshino, Y., Miyake, Y., Ishikawa, E., Suzukawa, M., et al., 2014. Dectin-2 is a direct receptor for mannose-capped liparabinomannan of mycobacteria. *Immunity* 41 (3), 402–413. doi:10.1016/j.immuni.2014.08.005.
- Yu, S., Lowe, A.W., 2009. The pancreatic zymogen granule membrane protein, GP2, binds Escherichia coli type 1 fimbriae. *BMC Gastroenterol.* 9, 58. doi:10.1186/1471-230X-9-58.
- Zacchi, L.F., Schulz, B.L., 2015. N-glycoprotein macroheterogeneity: biological implications and proteomic characterization. *Glycoconj. J.* doi:10.1007/s10719-015-9641-3.
- Zelenky, A.N., Greedy, J.E., 2005. The c-type lectin-like domain superfamily. *FEBS J.* 272 (24), 6179–6217. doi:10.1111/j.1742-4658.2005.05031.x.
- Zhang, W., James, P.M., Ng, B.G., Li, X., Xia, B., Rong, J., et al., 2015. A novel n-tetrasaccharide in patients with congenital disorders of glycosylation including asparagine-linked glycosylation protein 1, phosphomannomutase 2, and phosphomannose isomerase deficiencies. *Clin. Chem.* doi:10.1373/clinchem.2015.243279.
- Zhang, X., Mosser, D.M., 2008. Macrophage activation by endogenous danger signals. *J. Pathol.* 214 (2), 161–178. doi:10.1002/path.2284.
- Zhu, L.L., Zhao, X.Q., Jiang, C., You, Y., Chen, X.P., Jiang, Y.Y., et al., 2013. C-type lectin receptors dectin-3 and dectin-2 form a heterodimeric pattern-recognition receptor for host defense against fungal infection. *Immunity* 39 (2), 324–334. doi:10.1016/j.immuni.2013.05.017.
- Ziegler-Heitbrock, L., Ancuta, P., Crowe, S., Dalod, M., Graub, V., Hart, D.N., et al., 2010. Nomenclature of monocytes and dendritic cells in blood. *Blood* 116 (16), e74–e80. doi:10.1182/blood-2010-02-258558.
- Zipser, B., Bello-DeOcampo, D., Diestel, S., Tai, M.H., Schmitz, B., 2012. Mannin monoclonal antibody uniquely recognizes paucimannose, a marker for human cancer, stemness, and inflammation. *J. Carbohydr. Chem.* 31 (4–6), 504–518. doi:10.1080/07328303.2012.661112.
- Zoega, M., Ravnsborg, T., Hojrup, P., Houen, G., Schou, C., 2012. Proteinase 3 carries small unusual carbohydrates and associates with alpha-defensins. *J. Proteomics* 75 (5), 1472–1485. doi:10.1016/j.jprot.2011.11.019.

Mr Ian Loke currently holds an international Macquarie University Research Excellence scholarship and the Cystic Fibrosis Australia Studentship award at Macquarie University, Sydney, Australia. He obtained his bachelor degree with first class honours in biomedical science and molecular biology in 2010 from Murdoch University. He is currently pursuing a PhD in Chemistry and Biomolecular Sciences under the supervision of Dr Morten Thaysen-Andersen and Professor Nicole H. Packer at Macquarie University. His current research is conducted in the area of human paucimannosylation, with a strong focus on understanding its influence in human neutrophils and the host's innate immune system.

Daniel Kolarich became fascinated with glycobiology and mass spectrometry during his undergraduate studies in Vienna. During his PhD with Professor Friedrich Altmann and his post-doctoral work with Professor Nicole H. Packer at Macquarie University in Sydney, Australia where he worked intensively on glycopeptide oriented glycoproteomics of human glycoproteins and plant/insect glycoprotein allergens. In late 2010, he joined the Department of Biomolecular Systems headed by Professor Peter H. Seeberger in Potsdam, Germany as a group leader. He has established his

own research group focusing on glycomics and glycoproteomics techniques for investigating the role glycosylation plays in health and disease.

Professor Nicki Packer has had a varied career in biomolecular research. She was part of the team that established the Australian Proteome Analysis Facility (APAF) and co-founded Proteome Systems Limited, an Australian biotechnology company. She is now Professor of Glycoproteomics and Director of Macquarie University Biomolecular Frontiers Research Centre. She has gained international profile by linking glycomics with proteomics and bioinformatics to determine biological function. Her research interests are now in the structure, function, informatics and application of glycans as molecular markers, particularly in their role in cancer, imaging and microbial infection.

Morten Thaysen-Andersen obtained his PhD in Protein Chemistry in 2009 from University of Southern Denmark under Professor Peter Højrup before undertaking postdoctoral research in Glycobiology at Macquarie University, Sydney, Australia under Professor Nicolle Packer. As a Cancer Institute NSW fellow, he now heads a research team in Analytical Glycobiology at Macquarie University, focusing on understanding how glycosylation affects protein function in complex biological systems including inflammation, cancer, and pathogenic–host interactions. His group develops and utilises mass spectrometry-based technologies for the accurate molecular mapping of glycoproteins (glycomics/glycoproteomics), and molecular and cellular assays to investigate the glycoprotein structure/function relationships in human diseases.

To **summarise** the main findings and conclusions of the literature review; there is an increasing amount of evidence in the literature documenting the contribution of protein mannosylation during inflammation and infection. Protein mannosylation also appears to be regulated spatially and temporally during these conditions and has the capacity to interact with mrCLRs. These interactions are likely to have functional consequences that could influence or facilitate the immunological response during physiological or pathophysiological conditions.

The work presented in this thesis builds on the initial observation of protein paucimannosylation in bacterial colonised CF sputum. These less reported paucimannosidic *N*-glycans were found to be carried by proteins residing in the azurophilic granules of human neutrophils (**Chapter 2, Publication II**). Protein paucimannosylation has over the past decades been considered as a glyco-signature of invertebrates and repeatedly been reported to be absent or negligible in human bio-specimens. As such, the presence of human protein paucimannosylation is still highly controversial and debated in the glycobiology community. The biosynthesis of these paucimannosylated proteins driven by the highly active β -*N*-acetylhexosaminidases (hexosaminidases) has been well documented in lower invertebrates. However, their biosynthetic machinery in humans is still currently unknown.

To extend the findings of paucimannosylated proteins in the azurophilic granules of neutrophils, a detailed LC-MS/MS characterisation of the *N*-glycosylated azurophilic granule-resident proteins, specifically two important azurophilic granule proteins, nCG and HNE, was performed since a deep structural elucidation is often required before the functional roles and biosynthetic pathways of glycoproteins can be assessed. In order to provide an overview of the aims of this thesis, the various aspects of protein paucimannosylation investigated and the related chapters and publications are summarised in **Figure 8**.

1.8 Thesis aims

The overall aims of this thesis are:

1. To determine the biosynthetic machinery underpinning protein paucimannosylation in human neutrophils. Specifically,
 - i. To determine if and how human β -hexosaminidases are involved in the generation of protein paucimannosylation in human neutrophils (**Chapter 2 to 3, Publication II and Publication III**).
2. To investigate the protein *N*-glycosylation profile and the function of protein paucimannosylation displayed by neutrophil azurophilic granule proteins. Specifically,
 - i. To structurally characterise the protein *N*-glycosylation profile of nCG (**Chapter 4, Publication IV**).
 - ii. To structurally characterise the protein *N*-glycosylation of HNE and the role of site-specific paucimannosylation on HNE in its modulatory contributions towards innate immunity (**Chapter 5, Publication V**).
 - iii. To characterise the *N*-glycome and compare the degree of paucimannosylation and other *N*-glycans types in the neutrophil azurophilic granules relative to other neutrophil granule compartments using subcellular fractionation (**Chapter 5**).
3. To determine the expression of protein paucimannosylation in various immune- and non-immune cell populations. Specifically,
 - i. To characterise the *N*-glycome and compare the degree of paucimannosylation and other *N*-glycan types in immune cell populations such as lymphocytes, platelets and macrophages (**Chapter 6, Publication VI**).
 - ii. To characterise the *N*-glycome and the degree of paucimannosylation and other *N*-glycan types in neuronal cells during cellular development in the brain (**Chapter 6, Publication VII**).

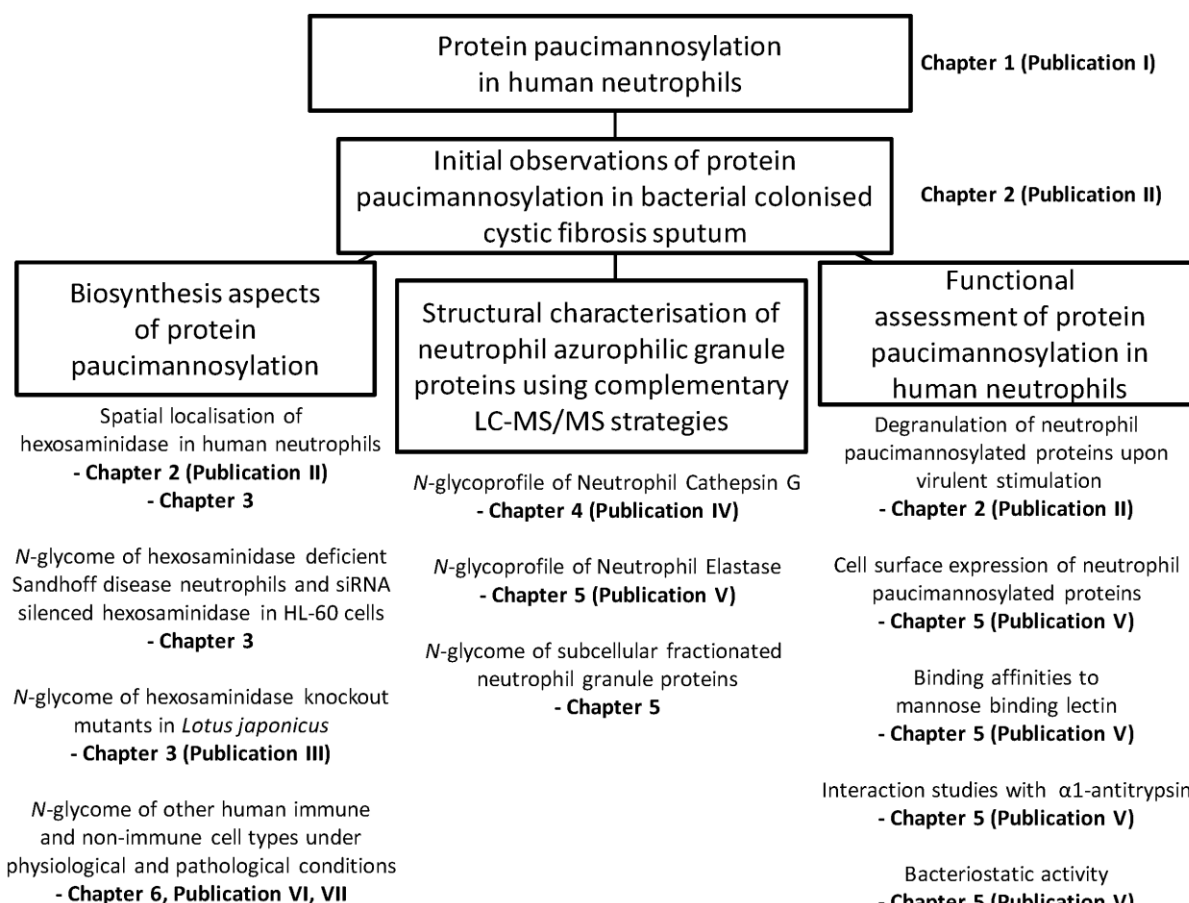


Figure 8. Thesis overview. The corresponding chapters and publications underpinning the three main pillars of protein paucimannosylation in human neutrophils investigated in this thesis (i.e. biosynthesis, structure and function) are indicated.

Chapter 2: Initial observation of paucimannosylated human neutrophil proteins in bacterial colonised cystic fibrosis sputum

2.1 Rationale

Paucimannosidic *N*-glycans are defined with the general monosaccharide composition (Man)₁₋₃(Fuc)₀₋₁(GlcNAc)₂. Paucimannosidic *N*-glycans are part of the usual glycan repertoire of invertebrates such as nematodes (Schachter, 2009; Zhang et al., 2003), and insects (Altmann et al., 1995) and are carried by plant proteins (Vitale and Chrispeels, 1984). Their presence has repeatedly been described to be absent or negligible in mammals including human bio-specimens (Gutternigg et al., 2007; Schachter and Boulianne, 2011) and, if observed from these origins, is often perceived as a degradation product of *N*-glycoproteins. However, recent ‘omics-type literature have suggested their presence in mammalian specimens obtained from various physiological states. For example, in inflammation (Hashii et al., 2009; Pegg et al., 2016; Robajac et al., 2016), cancer (Balog et al., 2012; Sethi et al., 2014; Shah et al., 2015) and also during normal cellular homeostasis (Everest-Dass et al., 2012; Parker et al., 2013; Trinidad et al., 2013). However, human protein paucimannosylation remains, on the whole, rather controversial and largely unstudied.

In this chapter, we present the initial finding of these less investigated paucimannosidic *N*-glycans in the sputum of CF patients infected with *Pseudomonas aeruginosa* and other pathogenic bacteria common to inflamed lungs. In-depth structural analyses of the paucimannosidic *N*-glycans utilising both glycomics and glycoproteomics technologies were performed. We demonstrated that these unconventional structures were carried predominantly by azurophilic granule-resident neutrophil proteins and that these paucimannosylated proteins can be degranulated from human resting neutrophils upon virulent stimulation.

The presence of paucimannosylated proteins in lower invertebrates are attributed to the high enzymatic activities of β -hexosaminidases. In humans, β -hexosaminidases were mainly reported to be present in the acidic lysosomes and are known to be the homodimeric hexosaminidase B (Hex B), hexosaminidase S (Hex S) or heterodimeric hexosaminidase A (Hex A) enzymes, depending on the pairing of the α and β subunits (Hex A, $\alpha\beta$; Hex B, $\beta\beta$; Hex S, $\alpha\alpha$). Specifically, the subcellular localisation of Hex A, in the azurophilic granules within human neutrophils was investigated. The presence of other glycosidases and other hydrolytic enzymes (e.g. α -/ β -mannosidases) were also investigated in human neutrophils. The results and conclusions presented in this chapter, of which I was a significant contributor (see author contributions below), represent the first observation of protein paucimannosylation from human neutrophils in inflamed and infected micro-environments.

Chapter 2

This work provided the structural foundation, biosynthetic and functional hypotheses, as well as the main motivation for my further investigation of protein paucimannosylation in human neutrophils. It also provided the inspiration to study the roles of paucimannosylation in the immune functions of neutrophils during inflammation and pathogen infections, which are described in the subsequent chapters of this thesis.

2.2 Publication II: Human neutrophils secrete bioactive paucimannosidic proteins from azurophilic granules into pathogen-infected sputum

Publication: Thaysen-Andersen, M., Venkatakrishnan, V., **Loke, I.**, Laurini, C., Diestel, S., Parker, B.L., Packer, N.H., 2015. Human neutrophils secrete bioactive paucimannosidic proteins from azurophilic granules into pathogen-infected sputum. *Journal of Biological Chemistry* 290 (14), 8789-8802. doi:10.1074/jbc.M114.631622

This research was originally published in *Journal of Biological Chemistry*. Thaysen-Andersen, M., Venkatakrishnan, V., Loke, I., Laurini, C., Diestel, S., Parker, B.L., Packer, N.H. Human neutrophils secrete bioactive paucimannosidic proteins from azurophilic granules into pathogen-infected sputum. *Journal of Biological Chemistry*. 2015; 290 (14), 8789-8802. © the American Society for Biochemistry and Molecular Biology.

Supplementary Materials are available in the enclosed DVD.

Author contributions: Conception of hypothesis and study – MTA and VV, experimental design – MTA, VV and **IL**, data collection and analysis – MTA, VV, **IL** and CL, manuscript preparation – MTA, VV, **IL**, and NP, editing and reviewing – MTA, BP, **IL**, SD and NP.

Specifically, I was responsible for the design, data collection and interpretation of the immunoblotting experiment of CF sputum proteins with a paucimannose-reactive antibody, Mannitou (**Publication II, Figure 1D**), the immunocytochemistry experiments of differentiated HL-60 neutrophil-like cells with antibodies recognising MPO and Hex A (**Publication II, Figure 4G**) and the pathogen-induced paucimannosidic protein secretion experiment involving differentiated HL-60 cells and the stimulation with multiple strains of *P. aeruginosa* (**Publication II, Figure 5A**).

Human Neutrophils Secrete Bioactive Paucimannosidic Proteins from Azurophilic Granules into Pathogen-Infected Sputum^{*S}

Received for publication, December 15, 2014, and in revised form, January 21, 2015. Published, JBC Papers in Press, February 2, 2015, DOI 10.1074/jbc.M114.631622

Morten Thaysen-Andersen^{†1}, Vignesh Venkatakrishnan[‡], Ian Loke[‡], Christine Laurini[§], Simone Diestel[§], Benjamin L. Parker[†], and Nicolle H. Packer[†]

From the [†]Department of Chemistry and Biomolecular Sciences, Macquarie University, Sydney, New South Wales-2109, Australia, the [‡]Institute of Nutrition and Food Sciences, University of Bonn, Bonn 53113, Germany, and the [§]Diabetes and Obesity Program, Garvan Institute of Medical Research, Sydney, New South Wales-2010, Australia

Background: Protein paucimannosylation is considered an important invertebrate- and plant-specific glycoepitope.

Results: Azurophilic granule-specific human neutrophil proteins from pathogen-infected sputum displayed significant core-fucosylated paucimannosylation generated by maturation- and granule-specific β -hexosaminidase A and were preferentially secreted from non-lysosomal origins into sputum upon *P. aeruginosa* stimulation.

Conclusion: Human neutrophils produce, store, and selectively secrete bioactive paucimannosidic proteins.

Significance: This work will aid in understanding the function(s) of human paucimannosylation in glycoimmunology.

Unlike plants and invertebrates, mammals reportedly lack proteins displaying asparagine (N)-linked paucimannosylation (mannose_{1–3}fucose_{0–1}N-acetylglucosamine₂Asn). Enabled by technology advancements in system-wide biomolecular characterization, we document that protein paucimannosylation is a significant host-derived molecular signature of neutrophil-rich sputum from pathogen-infected human lungs and is negligible in pathogen-free sputum. Five types of paucimannosidic N-glycans were carried by compartment-specific and inflammation-associated proteins of the azurophilic granules of human neutrophils including myeloperoxidase (MPO), azurocidin, and neutrophil elastase. The timely expressed human azurophilic granule-resident β -hexosaminidase A displayed the capacity to generate paucimannosidic N-glycans by trimming hybrid/complex type N-glycan intermediates with relative broad substrate specificity. Paucimannosidic N-glycoepitopes showed significant co-localization with β -hexosaminidase A and the azurophilic marker MPO in human neutrophils using immunocytochemistry. Furthermore, promyelocyte stage-specific expression of genes coding for paucimannosidic proteins and biosynthetic enzymes indicated a novel spatio-temporal biosynthetic route in early neutrophil maturation. The absence of bacterial exoglycosidase activities and paucimannosidic N-glycans excluded exogenous origins of paucimannosylation. Paucimannosidic proteins from isolated and sputum neutrophils were preferentially secreted upon inoculation with virulent *Pseudomonas aeruginosa*. Finally, paucimannosidic proteins displayed affinities to mannose-binding lectin, suggesting immune-related functions of paucimannosylation in activated human neutrophils. In conclusion, we are the first to document that human neutrophils produce, store and, upon activation, selectively secrete bioactive

paucimannosidic proteins into sputum of lungs undergoing pathogen-based inflammation.

Asparagine (N)-linked glycosylation adds unprecedented structural and functional heterogeneity to polypeptide chains by the covalent attachment of oligosaccharides (hereafter called glycans) to motif-specific asparagine residues. Although advances in glycobiology and analytical glycoscience continually improve the understanding of protein N-glycosylation, the structure-function relationships of most protein glycoforms remain unknown. Dysregulation of protein N-glycosylation by the deletion or modulation of its diverse intra- and extracellular functions is a common cause and/or effect of numerous pathologies (1, 2). Our understanding of the conserved mammalian N-glycosylation as a structural and functional modulator of proteins is most critically built on the principles of the well described glycoprotein biosynthetic machinery (3). The defined complex and dynamic enzymatic biosynthesis of glycoproteins in the secretory pathway produces three well recognized N-glycan classes that are abundantly displayed on mammalian proteins, i.e. high mannose, hybrid, and complex type, all of which are based on a common trimannosylated chitobiose core (2).

Contrary to this dogma, several recent glycomics-based studies indicate that a fourth type of protein N-glycosylation, referred to as paucimannosylation, with monosaccharide compositions less than or equal to the N-glycan trimannosylchitobiose core, i.e. mannose(Man)_{1–3}fucose(Fuc)_{0–1}N-acetylglucosamine(GlcNAc)₂, is present in mammals. These structures do not correspond to the defined N-glycan types nor can their synthesis be described by established mammalian biosynthetic pathways. To date, mammalian protein paucimannosylation has been suggested to be present in (i) human buccal epithelial cells (4), (ii) human colorectal cancer epithelial cells and tissue (5–7), (iii) kidney tissue from mice suffering from systemic

^{*} This work was supported by the Australian Research Council Super Science Program (FS110200026).

^S This article contains supplemental Fig. 1 and Tables 1–3.

[†] Funded by an Early Career Fellowship, Cancer Institute NSW. To whom correspondence should be addressed. Tel.: 61-2-9850-7487; Fax: 61-2-9850-6192; E-mail: morten.andersen@mq.edu.au.

Human Paucimannosylation Structure, Function, and Biosynthesis

lupus erythematosus (8), (iv) mouse embryonic neural stem cells (9), and (v) rat brain (10). In addition, we recently indicated the presence of paucimannosylation in pathogen-infected sputum derived from individuals with cystic fibrosis (CF)² and upper respiratory tract infection (URTI) (11). Importantly, these observations were all based on molecular profiling of *N*-glycans released from cell/tissue-derived proteins and thus disregarded the protein carrier identities. Consequently, exogenous origin(s) of paucimannosylation could not be ruled out. Mammalian paucimannosylation was supported by immunohistochemistry and immunocytochemistry of selected human and murine tissues and cells using paucimannose-reactive antibodies (12–14). In general, however, mammals including human and mice have usually been reported to lack protein paucimannosylation (15–21). As such, human paucimannosylation remains controversial in the context of our current understanding of mammalian glycobiology.

Outside the vertebrate subphylum, invertebrates such as *Caenorhabditis elegans* (16, 18, 22–24) and *Drosophila melanogaster* (15, 17, 25, 26), plants (27), and other “lower” organisms (28) abundantly produce protein paucimannosylation. Paucimannose synthesis in these species is facilitated by high β -*N*-acetylhexosaminidase activity, allowing partial suppression of the complex *N*-glycan biosynthetic route. Although the exact functions and effector mechanisms still remain elusive, the *N*-glycosylation of the paucimannose-rich *C. elegans* and *D. melanogaster* has been associated with roles in the immune response against bacterial pathogens (19) and the organism lifespan (21).

Here, we present unequivocal evidence that paucimannosylation is also a significant host-derived molecular signature of sputum proteins from pathogen-infected human lungs. Enabled by recent developments in system-wide biomolecular detection, we document that inflammation-associated proteins, localizing to the azurophilic granules of human neutrophils, abundantly display paucimannosylation. In line with their presence in specific micro-environments that are central to inflammation and pathogen infection, we confirm that the timely expressed human azurophilic granule-resident β -hexosaminidase A (Hex A) enzymatically facilitates the generation of protein paucimannosylation by trimming hybrid/complex type *N*-glycan intermediates using a machinery, which is formed during early myeloid maturation, and functionally associate paucimannosidic proteins with roles in innate immunity upon secretion from activated human neutrophils.

EXPERIMENTAL PROCEDURES

Sputum and Bacteria Origin/Handling—Saliva-free whole sputum (>1 ml/donor) was sampled with informed consent

from individuals with ($n = 5$) or without ($n = 4$) CF by non-invasive expectoration at Westmead Hospital, Sydney, Australia (see Ref. 11 for donor data). Two of the non-CF individuals were diagnosed with URTI and two were diagnosed with pathogen-free pneumonia or chronic obstructive pulmonary disease. The sputum of the seven pathogen-positive individuals was infected primarily by mucoid/non-mucoid *Pseudomonas aeruginosa*, but also *Aspergillus fumigatus*, *Staphylococcus aureus*, and *Streptococcus pneumoniae* were identified. *P. aeruginosa* laboratory wound (PAO1) and CF sputum (PASS1–4) strains were isolated and cultured (Table 1). Sputum from all donors showed inflammation characteristics ($>1 \times 10^{10}$ polymorphonuclear cells/l sputum). Soluble proteins were isolated from washed sputum plugs (whole sputum) as described (11). In brief, sputum proteins were reduced, and alkylated and intact cells, cellular debris, and insoluble mucins/proteins were removed by centrifugation. The concentration of soluble sputum proteins was measured (Direct Detect, Millipore) and normalized prior to biomolecular characterization.

Origin and Isolation of Human Neutrophils—Resting human neutrophils were isolated to high purity from healthy blood donors as described (29, 30). In brief, the neutrophils were isolated using dextran sedimentation ($1 \times g$), hypotonic lysis of erythrocytes, and centrifugation in a Ficoll-Paque gradient. Resting neutrophils were resuspended in a Krebs-Ringer phosphate buffer and counted. Neutrophils were pelleted ($4,000 \times g$, 5 min), and proteins were extracted by cell lysis (6 M urea, 0.1% (w/v) SDS).

Handling of Human Neutrophil-like Cells—Human promyelocytic leukemia cells (HL-60, ATCC CCL-240) were differentiated (5–6 days, 1.3% (v/v) DMSO, Sigma) to meta/band/segmented neutrophil-like cells. HL-60 cells were cultured (RPMI 1640, Gibco, 10% fetal bovine serum, 2 mM L-glutamine, and 50 units/ml penicillin and 50 μ g/ml streptomycin) at 37 °C under 5% CO₂. High differentiation efficiencies (>50%) were obtained as assessed by morphology of Wright-Giemsa stained cells (see below). Cells were washed in PBS before use.

LC-MS/MS-based *N*-Glycome Characterization—*N*-Glycans were released by 2–5 units of *N*-glycosidase F (PNGase F, *Flavobacterium meningosepticum*, Roche Applied Science)/10 μ g of proteins (37 °C, 10–12 h) of protein extracts from sputum, human neutrophils, neutrophil-like cells, and *P. aeruginosa* as described (31) (see supplemental Table 1 for details of sample handling and data acquisition of all LC-MS/MS *N*-glycome experiments). The resulting *N*-glycans (and *N*-glycan reference compounds, Dextra Laboratories) were profiled in their hydroxylated state after porous graphitized carbon (PGC) solid phase extraction desalting (31) using PGC-LC (Hypercarb, Thermo Scientific, 5 μ m; 180 μ m \times 10 cm; pore size: 250 Å) (LC: Ultimate 3000, Dionex) collision-induced dissociation negative ion MS/MS (HCT three-dimensional ion trap, Bruker Daltonics or LTQ-XL, Agilent).

LC-MS/MS-based Proteome and Glycoproteome Profiling—The CF sputum proteome and *N*-glycoproteome were mapped following a crude fractionation on 4–12% SDS-PAGE (fractions 1–5: 65–100, 50–65, 35–50, 20–35, and 5–20 kDa, respectively). The fractions were digested individually in 20 μ l of 50 mM NH₄HCO₃ (aq), pH 7.8, using porcine trypsin (Pro-

² The abbreviations used are: CF, cystic fibrosis; GM1, Gal β 1,3GalNAc β 1,4(NeuAca2,3)Gal β 1,4Glc β -ceramide; GM2, GalNAc β 1,4(NeuAca2,3)-Gal β 1,4Glc β -ceramide; GM3, NeuAca2,3Gal β 1,4Glc β -ceramide; Hex A, β -hexosaminidase A; HCD, higher-energy collisional dissociation; LAMP, lysosome-associated membrane protein; Man, mannose; MBL, mannose-binding lectin; MPO, myeloperoxidase; NE, neutrophil elastase; PGC, porous graphitized carbon; PMA, phorbol myristate acetate; URTI, upper respiratory tract infection; ER, endoplasmic reticulum; DMSO, dimethyl sulfoxide; aq, aqueous.

Human Paucimannosylation Structure, Function, and Biosynthesis

mega, 50 ng/ μ l, 8 h, 37 °C). The resulting peptide mixtures were used for proteome and glycoproteome mapping. *N*-Glycopeptides were de-*N*-glycosylated using 3 units of *N*-glycosidase F/fraction (12 h, 37 °C) and desalted prior to proteomics or enriched in their intact form using hydrophilic interaction liquid chromatography solid phase extraction prior to *N*-glycoproteomics as described (32). All fractions were analyzed individually using C₁₈ LC-Orbitrap Elite-MS/MS (Thermo Scientific) with higher-energy collision-induced dissociation (HCD) and collision-induced dissociation MS/MS fragmentation as described (10) (see supplemental Tables 2–3 for details of sample handling and data acquisition of all LC-MS/MS proteome and glycoproteome experiments).

LC-MS/MS Data Handling—*N*-Glycans were manually characterized using (i) molecular mass, PGC-LC retention time, and *de novo* MS/MS sequencing, and (ii) MS/MS spectral and PGC-LC retention time matching to reference compounds (Dextra Laboratories). Proteome HCD-MS/MS data were searched separately against UniProt *Homo sapiens* and *P. aeruginosa* PAO1 (Mascot v2.4). *N*-Glycoproteome *m/z* 204.08-filtered HCD-MS/MS spectra were searched against a targeted sputum proteome and *N*-glycome database (Byonic™ v1.2, Protein Metrics) (10). Protein identifications were filtered to 1% false discovery rate. *N*-Glycopeptide identifications (≥ 4 b/y-ions in HCD-MS/MS) were validated using collision-induced dissociation-MS/MS (see supplemental Fig. 1 for *N*-glycopeptide annotation). Accurate MS-based relative quantitation of proteins, *N*-glycans, and *N*-glycopeptides was performed (33).

Western Blotting of Paucimannosidic Proteins—Paucimannosidic proteins derived from sputum were visualized using paucimannose-recognizing Mannitox IgM (12) (undiluted concentration, 8–10 h) and HRP-conjugated anti-mouse IgM (Life Technologies) (1:3000, 1 h) on SDS-PAGE-separated sputum proteins (10 μ g) transferred to nitrocellulose membranes (Bio-Rad). HRP chemiluminescent substrates (Millipore) were used in a ChemiDoc MP system (Bio-Rad).

Substrate Specificity of Hex A—The substrate specificity of human Hex A (Sf 21 baculovirus-derived, R&D Systems, >95% purity and >1.2 nmol/min/ μ g of 4-methylumbelliferyl-*N*-acetyl- β -D-glucosaminide activity) was assessed by monitoring the exoglycosidase activity on complex (Dextra Laboratories) and hybrid (chicken ovalbumin, Sigma) *N*-glycans and GM1–3 (Matreya LLC, Pleasant Gap, PA) using positive ion MALDI time-of-flight MS (MicroFlex, Bruker Daltonics) or negative ion PGC-LC-MS/MS (above). Digestion was performed in 100 mM sodium citrate, 250 mM NaCl (aq), pH 4.5 (25:1 substrate/enzyme molar ratio, 0–108 h, 37 °C, gentle agitation). 10:1 substrate/enzyme molar ratios were used after 18 h to drive the reaction further.

Sequence Homology of Hex A—The sequence homology of human Hex A (α/β) to hexosaminidases from paucimannose-rich organisms was assessed using EMBOSS Needle.

Subcellular Localization of Neutrophilic Proteins—The subcellular localizations were established using granule-specific proteome libraries of human neutrophils (34) to classify identified sputum proteins and by immunocytochemistry of DMSO-differentiated, fixed (4% (v/v) formaldehyde), and membrane-permeabilized (0.5% (v/v) Triton X-100 in PBS (aq),

20 min, 25 °C) HL-60 cells plated on 0.02% (v/v) polylysine-coated coverslips using the following antibodies: mouse anti-human myeloperoxidase (MPO) IgG (1:2000), rabbit anti-human Hex A IgG (1:500) (Santa Cruz Biotechnology), the paucimannose-recognizing Mannitox IgM (undiluted concentration) (12), goat anti-mouse IgG Alexa Fluor 546 (1:400), and goat anti-rabbit IgG Alexa Fluor 488 (1:400). Nuclei were DAPI-stained. Images were taken using Olympus FV-1000 and Zeiss LSM510 MetaUV confocal microscopes. Co-localization was evaluated semi-quantitatively via iMaris (Bitplane) using Manders' coefficient of six representative cells (35).

Bacterial Exoglycosidase Activity Assay—Bacterial α -sialidase, β -galactosidase, α -fucosidase, β -hexosaminidase, and α -mannosidase activities were assessed by monitoring the *N*-glycan profiles (above) of bovine fetuin, human IgG, and bovine ribonuclease B (Sigma) with and without inoculation of *P. aeruginosa* PAO1 and PASS1–3 (10^5 bacterial/ μ g of protein, 12 h, 37 °C).

Temporal Gene Expression of Paucimannosidic Proteins and Enzymes—Maturation stage-specific expression of genes coding for paucimannosidic biosynthetic enzymes and proteins was investigated using a transcriptional profile of terminal granulocytic human neutrophil differentiation following bone marrow and peripheral blood collection from healthy individuals and granulocyte isolation using density gradient centrifugation and immune-magnetic sorting (GEO accession number GSE19556, platform GPL96). The promyelocytic and myelocytic expression levels of genes coding for putative paucimannosidic enzymes, i.e. *HEXA* (ID 215155_at/201765_s_at), *HEXB* (201944_at), *MAN2A2* (219999_at), *MAN2B2* (214703_s_at), and *MANBA* (203778_at), and proteins, i.e. *AZU1* (214575_s_at), *MPO* (203949_at), *CD63* (200663_at), and *LAMP2* (200821_at/203042_at/203041_s_at) were represented as a -fold change relative to levels in mature resting human neutrophils.

Pathogen-induced Paucimannosidic Protein Secretion—Pathogen-induced secretion of paucimannosidic proteins was monitored by inoculating DMSO-differentiated HL-60 cells (1–3 h, 37 °C, $n = 3$) and neutrophil-rich pathogen-free whole sputum (8 h, 37 °C, $n = 4$) with and without *P. aeruginosa* PAO1 and PASS1. *N*-Glycan profiling (above) was performed on acetone-precipitated proteins (80% (v/v), 8 h) secreted into the culture medium (1:100 HL-60:bacteria cell ratio). For sputum neutrophils, 10^5 bacteria/ μ g of whole sputum was used. Bacteria were estimated based on optical density (assuming A_{600} : 0.2 ~ 7.8 $\times 10^7$ CFU/ml). Bacteria and HL-60 co-cultures were performed in serum- and antibiotics-free RPMI 1640 media (37 °C, 5% CO₂, gentle agitation). Cell counts and viabilities were monitored using an electronic cell counter (Bio-Rad) and trypan blue exclusion. Phorbol myristate acetate (PMA) treatment (200 nM, 1–3 h, 37 °C) of HL-60 cells served as activation controls. HL-60 morphology was monitored using Wright-Giemsa-stained smears prepared with a Cytospin centrifuge (Shandon).

MBL Binding Assay—Binding of paucimannosidic proteins derived from pathogen-positive sputum and commercially sourced *N*-glycans (Dextra Laboratories) to agarose-conjugated mannose-binding lectin (MBL) (Thermo Scientific) was assessed in 300 μ l of 20 mM CaCl₂, 1.25 M NaCl, 10 mM Tris-

Human Paucimannosylation Structure, Function, and Biosynthesis

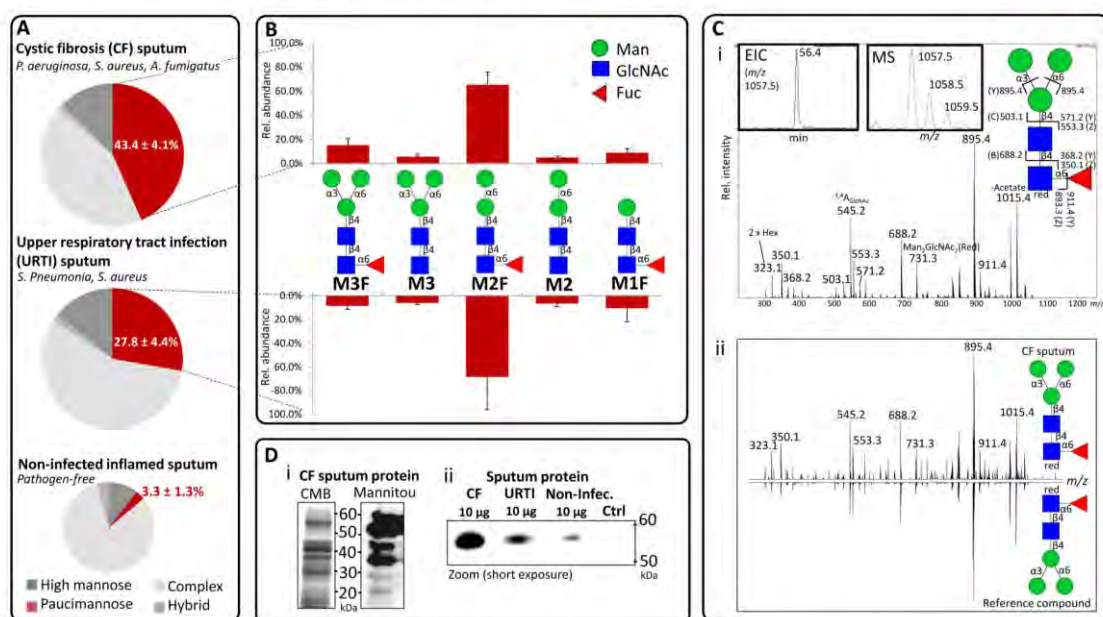


FIGURE 1. Paucimannosylation is an abundant glycopeptide of proteins derived from pathogen-infected sputum. A, N-glycan type distribution of sputum proteins from pathogen-infected individuals with CF (top) and URTI (middle) and pathogen-free individuals with other inflammatory lung conditions (bottom) (red; total proportion of paucimannosylation of the entire N-glycome) (see Ref. 11 for sputum donor-specific data). B, distribution of paucimannosidic N-glycans released from proteins derived from pathogen-infected sputum (see inset for nomenclature). Rel. abundance, relative abundance. C, example of structural confirmation of a paucimannosidic N-glycan (M3F) using LC-MS/MS for (panel i) *de novo* sequencing and (panel ii) spectral matching to a well characterized reference compound (see supplemental Table 1); red refers to a NaBH₄-reduced N-glycan reducing end. EIC, extracted-ion chromatogram; Rel. intensity, relative intensity. D, the paucimannose-recognizing Mannitox antibody was highly reactive toward CF sputum proteins (panel i). CF and URTI sputum proteins (zoom of 50–60-kDa region, short exposure) were more reactive toward Mannitox relative to proteins derived from pathogen-free sputum (panel ii). CMB, Coomassie blue; Non-infec., non-infected; Ctrl, negative control. For all data: mean \pm S.D.

HCl (aq), pH 7.4, in a ratio of 1 nmol of analyte to 100 μ l of washed MBL-agarose slurry (12 h, 4 $^{\circ}$ C, end-over-end rotation). The unbound fractions were collected for separate analysis after centrifugation. MBL-agarose beads were washed twice in 500 μ l of binding buffer. Bound analytes were eluted with 300 μ l of 2 mM EDTA, 1.25 M NaCl, 10 mM Tris-HCl (aq), pH 7.4 (8 h, 25 $^{\circ}$ C, end-over-end rotation). Paucimannosidic proteins and N-glycans in the MBL unbound and bound fractions were glycoprofiled using PGC-LC-MS/MS after glycan release/clean-up (see explicit description above).

Statistics—The significance of the individual experiments was assessed by one- or two-tailed Student's *t* tests where *p* less than 0.05 was chosen as the minimum acceptable level of confidence to support a rejection of the proposed null hypothesis, *e.g.* difference of two means. In general, tests fulfilling the minimum confidence level of significance were indicated by *; stronger confidence was indicated by ** and ***. The sample number (*n*) is given for the individual experiments. Data points are presented as a mean, and error is presented as S.D. or S.E.

RESULTS

Paucimannosylation, the Fourth Type of Human N-Glycosylation—Among other N-glycan alterations, we recently suggested that inflamed pathogen-infected sputum of individuals with CF and URTI displayed paucimannose-rich N-glycome

signatures (43.4 \pm 4.1 and 27.8 \pm 4.4%, respectively) relative to sputum from pathogen-free, but neutrophil-positive, lungs of individuals suffering from pneumonia and chronic obstructive pulmonary disease (3.3 \pm 1.3%, *p* = 2.7–9.7 \times 10^{−3}) (11) (as summarized in Fig. 1A). Mucoid/non-mucoid *P. aeruginosa*, *A. fumigatus*, *S. pneumoniae*, and *S. aureus* were identified in the pathogen-infected paucimannose-rich sputum (Table 1), illustrating a pathogen species-unspecific link to paucimannosylation.

Herein, we undertake a thorough investigation of this indication of human protein paucimannosylation by performing in-depth spatio-temporal analyses of the structure, function, and biosynthesis of paucimannosidic proteins in neutrophil-rich sputum from pathogen-infected individuals, isolated blood-derived human neutrophils, and neutrophil-like cells (HL-60). The detailed structures and distribution of five chromatographically pure paucimannosidic N-glycans (M1F, M2, M2F, M3, and M3F) were determined in pathogen-infected sputum (Fig. 1B). M2F (Man α 1,6Man β 1,4GlcNAc β 1,4(Fuca α 1,6)GlcNAc) was consistently the most abundant paucimannosidic N-glycan; the corresponding α 1,3-isomer of M2F (and M2) was absent. The detailed N-glycan characterization was facilitated by *de novo* MS/MS sequencing and by spectral and PGC-LC retention time matching to paucimannosidic reference compounds (Fig. 1C, see supplemental Table 1 for supporting N-glycome data). Although M0F *per se* does not fall under our definition of pauci-

TABLE 1
Overview of isolated and cultured *P. aeruginosa* strains used in the study

| <i>P. aeruginosa</i> strain | Tissue origin | Patient origin ^a | Strain origin | Type | Biofilm formation ^b | Genome known |
|-----------------------------|---------------|-----------------------------|---------------|-------------------|--------------------------------|------------------|
| PAO1 | Wound | NA ^c | Laboratory | Non-mucoid | Yes | Yes |
| PASS1 | Sputum | CF5 | Clinical | Mucoid | Yes | Yes ^d |
| PASS2 | Sputum | CF1 | Clinical | Mucoid | No | Yes ^d |
| PASS3 | Sputum | CF2 | Clinical | Non-mucoid | Yes | Yes ^d |
| PASS4 | Sputum | CF4 | Clinical | Mucoid/Non-mucoid | Yes | Yes ^d |

^a See Ref. 11 for de-identified sputum donor information.
^b Determined on a flow cell system on LB and minimal media with glucose (data not shown).
^c NA, not applicable.
^d Recently genome-sequenced and functionally characterized by Prof. Ian Paulson, Macquarie University, Sydney, Australia (unpublished).

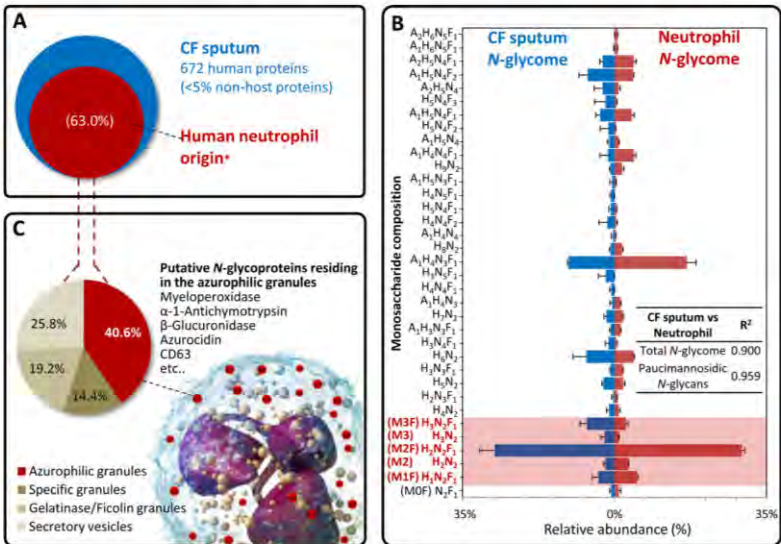


FIGURE 2. Pathogen-infected sputum and human neutrophils share biomolecular characteristics. A, similar proteomes from CF sputum (blue) and human neutrophils (red) (*, see Ref. 34). B, near identical N-glycomes of proteins derived from CF sputum (blue) and blood-derived resting human neutrophils (red) (mean \pm S.D.) (see inset for correlation, R^2); A, NeuAc; H, Hex; N, GlcNAc; F, fucose. C, the granular distribution of predicted N-glycoproteins identified in CF sputum using neutrophilic granule libraries (34) shows that the putative glycoproteins (when not considering their type of N-glycosylation) localize to all four main compartments of the human neutrophil, but preferentially to the azurophilic granules (red) (see supplemental Tables 1 and 2 for more). Graphics modified and used with permission from Blausen Medical (Blausen Gallery 2014).

mannosylation, the presence of this paucimannosidic-related structure was confirmed in the CF sputum. Trace levels of the truncated M1, M0, (Fuca1,6)GlcNAc, or single GlcNAc residues may have been present below the detection limit or not released efficiently by N-glycosidase F. In support of these observations, Western blotting using the paucimannose-reactive Mannitox antibody showed high reactivity to CF and URTI sputum proteins (Fig. 1D).

Possible exogenous bacterial origins of the abundant paucimannosylation in sputum were ruled out by the absence of paucimannosidic N-glycan signatures of proteomes obtained from isolated and cultured laboratory wound (PAO1) and CF (PASS1–2) *P. aeruginosa* strains. In addition, no significant α -sialidase, β -galactosidase, β -hexosaminidase, α -fucosidase, and α -mannosidase activities were detected in any of the investigated *P. aeruginosa* strains using a series of digestion assays with well characterized glycoproteins displaying a spectrum of glycoepitopes and LC-MS/MS N-glycan profiling, thus confirming that sputum

paucimannosylation does not result from exogenous *P. aeruginosa* exoglycosidase activities.

Granule-specific Paucimannosylation of Human Neutrophil Proteins—LC-MS/MS-based proteome mapping of CF sputum revealed the protein characteristics of significant leukocytes, e.g. abundance of MPO, neutrophil elastase (NE), eosinophil peroxidase, lactoferrin, catalase, and aminopeptidase N (see supplemental Table 2 for supporting proteome data). The neutrophil-specific proteome (as predicted from a relatively unique transcriptional profile of human neutrophils among other immune cell types (36)) was significantly represented in the CF sputum proteome (63% of 672 human proteins) (34) (Fig. 2A), which was supported by morphology-based identification by microscopy of sputum neutrophils (data not shown). Exogenous bacterial proteins were negligible in the CF sputum proteome, i.e. *P. aeruginosa* proteins constituted <2% of the sputum proteome. Further evidence supporting strong neutrophilic molecular signatures in sputum was obtained by the near identical N-glycomes of CF sputum proteins and blood-derived

Human Paucimannosylation Structure, Function, and Biosynthesis

TABLE 2

Human paucimannosidic proteins and their relative glycoform distribution identified in pathogen-infected sputum using glycoproteomics

| Protein | UniProt | Asn site | $\Sigma_{\text{pauc}} (\%)$ | Paucimannosidic glycans (%) | | | | |
|------------------------------|---------|----------|-----------------------------|-----------------------------|------|------|------|-----|
| | | | | M3F | M3 | M2F | M2 | M1F |
| MPO | P05164 | 323 | 63.0 | 13.5 | 3.9 | 39.9 | 5.6 | 0.2 |
| | | 355 | 0.6 | | 0.6 | | | |
| β -Glucuronidase | P08236 | 483 | 69.5 | 67.3 | | 2.2 | | |
| LAMP2 | P13473 | 58 | 100 | 73.0 | | 11.1 | 2.1 | |
| | | 356 | 100 | | | 100 | | |
| NE | P08246 | 88 | 100 | | | | 100 | |
| LAMAN | O00754 | 692 | 100 | | 100 | | | |
| Azurocidin | P20160 | 171 | 100 | | | 100 | | |
| CEACAM6 | P40199 | 197 | 100 | | 13.0 | | 87.0 | |
| CD63 | P08962 | 130 | 100 | 100 | | | | |
| CREG1 | O75629 | 160 | 67.0 | | 7.5 | | 59.5 | |
| α -1-Antichymotrypsin | P01011 | 186 | 100 | | 100 | | | |
| | | 271 | 100 | | | | 100 | |
| Aspartylglucosaminidase | P20933 | 38 | 54.1 | | 20.2 | | | |
| γ -Glutamyl hydrolase | Q92820 | 203 | 73.6 | | 20.2 | | 34.0 | |
| NGAL ^a | P80188 | 85 | 0.2 | 0.1 | | | 53.3 | |
| Phospholipase B-like 1 | Q6P4A8 | 71 | 10.2 | | 10.2 | | | |
| | | 366 | 44.0 | | 44.0 | | | |
| α -1-Antitrypsin | P01009 | 271 | 100 | | 100 | | | |
| Ig α -2 chain C | P01877 | 205 | 1.6 | 1.6 | | | | |
| Ig μ chain C | P01871 | 46 | 7.7 | 7.7 | | | | |
| UPF0762 protein C6orf58 | Q6P5S2 | 69 | 3.1 | | 3.1 | | | |

^a NGAL, neutrophil gelatinase-associated lipocalin.

human neutrophil proteins ($R^2 = 0.90$); in particular, strong correlation of the paucimannosidic *N*-glycans ($R^2 = 0.96$) was observed (Fig. 2B).

Utilizing sequon-based (NX(T/S), $X \neq P$) prediction of *N*-glycosylation and published granule proteome libraries of human neutrophils (34), the putative *N*-glycoproteins of CF sputum were shown to localize to all four main subcellular granular compartments of the human neutrophil, *i.e.* azurophilic, specific, gelatinase/ficolin granules, and secretory vesicles. However, significant proportions of the *N*-glycoproteome ($\sim 40\%$) resided in the azurophilic granule (Fig. 2C).

Unequivocal evidence for human protein paucimannosylation in pathogen-infected sputum and its granule specificity was generated by system-wide mapping of intact glycopeptides using our recently developed glycoproteomics technology (10). Site-specific paucimannosylation was identified on 18 abundant proteins (23 *N*-sites, 35 unique *N*-glycopeptides) of the total of 30 human *N*-glycoproteins identified in CF sputum (36 *N*-sites, 115 unique *N*-glycopeptides), quantitatively covering $\sim 20\%$ of the CF sputum proteome (Table 2, see also supplemental Table 3 and supplemental Fig. 1 for supporting glycoproteome data). By overlaying these data onto granule proteome libraries of human neutrophils (34), paucimannosylation was found to be highly enriched in the azurophilic granules ($p = 2.3 \times 10^{-4}$) relative to the other three main compartments of the neutrophil (Fig. 3, A and E). High mannose and complex type *N*-glycoproteins displaying β -galactosylation, Lewis type fucosylation, and α -sialylation localized predominantly to the other granules (Fig. 3, B–E). These observations were supported by partial co-localization of the azurophilic marker MPO and paucimannosidic epitopes in DMSO-differentiated human neutrophil-like cells using immunocytochemistry (data not shown).

Spatio-temporal Paucimannose Generation by Human β -Hex A—The biosynthetic mechanisms of human paucimannosylation were investigated. We have previously shown that *N*-glycan processing and the solvent accessibility of

N-glycosylation sites on maturely folded proteins are closely correlated (37). The identified paucimannosidic *N*-glycosylation sites on sputum proteins were found to be significantly more accessible than the spatially hidden high mannose sites ($p = 8.0 \times 10^{-4}$) showing solvent accessibilities similar to the highly processed complex sites (Fig. 4A), indicating that paucimannosylation results from significant exoglycosidase processing of the solvent-exposed *N*-glycan structures. No specific sequence recognition motifs for the paucimannosidic *N*-glycosylation sites were evident as assessed by a frequency plot.

In paucimannose-rich invertebrates, hexosaminidases are required for the removal of the β 1,2-GlcNAc residue on the 3'-mannose arm to form paucimannosidic structures (28). The α and β subunits of the heterodimeric human Hex A showed high sequence similarities to hexosaminidases of such organisms, in particular to *C. elegans* Hex A (53.8 and 52.9%) and *Arabidopsis thaliana* Hex1–3 (49.1 and 47.9%) (Fig. 4B). *In vitro* incubation of human Hex A with β 1,2-GlcNAc-terminating *N*-glycan substrates, at physiologically realistic conditions, *i.e.* enzyme/substrate ratio, temperature, and organelle-like pH, generated M3F, albeit at low enzymatic rates (Fig. 4C). Furthermore, β 1,2-GlcNAc-terminating afucosylated complex and hybrid type *N*-glycans and β 1,4-GalNAc-terminating GM2 glycolipids were found to be acceptable Hex A substrates (Fig. 4D). Hex A showed no activity on β 1,2-GlcNAc-terminating *N*-glycan substrates when proximal antennas carried β 1,4-galactosylation or β 1,4-bisecting GlcNAcylation (Fig. 4E).

Partial co-localization of human Hex A and paucimannosidic glycoepitopes as evaluated by immunocytochemistry of DMSO-differentiated human neutrophil-like cells supported the involvement of Hex A in paucimannose production (Fig. 4F). Azurophilic granule residence of human Hex A was indicated by moderate/strong co-localization of Hex A with the azurophilic marker MPO (Fig. 4G). This was supported by proteomics-based identifications of α and β subunits of Hex A in isolated azurophilic granules of human neutrophils (34, 38).

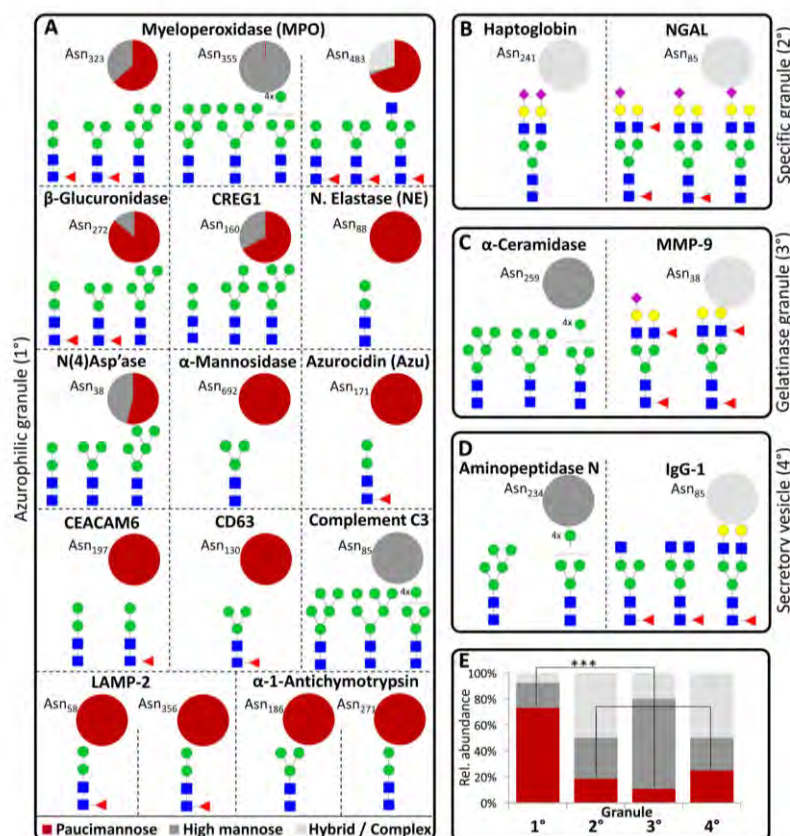


FIGURE 3. **Paucimannosylation is carried by proteins localizing to the azurophilic granules of human neutrophils.** A–D, the granular classification (34) of the characterized site-specific glycoproteomes of the CF sputum glycoproteome confirms that azurophilic proteins are the main carriers of paucimannosylation (A), whereas proteins localizing to the specific granules (B), gelatinase/ficolin granules (C), and secretory vesicles (D) display predominantly hybrid and complex *N*-glycosylation. Proteins carrying the under-processed high mannose type *N*-glycosylation localize to all compartments (see supplemental Table 3 for more information). NGAL, neutrophil gelatinase-associated lipocalin. E, the granule *N*-glycan type distribution as derived from the *N*-glycoproteomics data confirms that paucimannosylation is highly enriched in the azurophilic granules (primary, 1°) relative to other neutrophilic compartment (secondary-quaternary granules/vesicle, 2–4°) (***, $p < 0.001$). Rel. abundance, relative abundance.

High expression of the genes coding for the putative paucimannosidic enzymes, e.g. *HEXA* and *HEXB* (coding for β -hexosaminidase subunit α and β , respectively, which together hydrolyze β -GlcNAc- and α -GalNAc-terminating glycoconjugates), and for paucimannosidic proteins, e.g. *MPO* and *AZU1* (coding for MPO and azurocidin, respectively) in promyelocytes, indicated assembly of the synthetic machinery for paucimannosylation (but not necessarily the complete biosynthetic generation of paucimannosidic proteins), early in the bone marrow maturation (Fig. 4H). M3(F) truncation to M2(F), M1(F), and M0(F) may be facilitated by human α - and β -mannosidases previously identified in the azurophilic granules of human neutrophils (34, 38); promyelocytic stage-specific expression of the corresponding mannosidase genes, i.e. *MAN2A2/MAN2B2* (coding for α -mannosidases, which hydrolyze terminal α 1,3/6-linked mannoses) and *MANBA* (coding for β -mannosidase, which hydrolyzes terminal β -linked mannoses), was indeed observed. Taken together, we propose a new granule- and maturation-specific

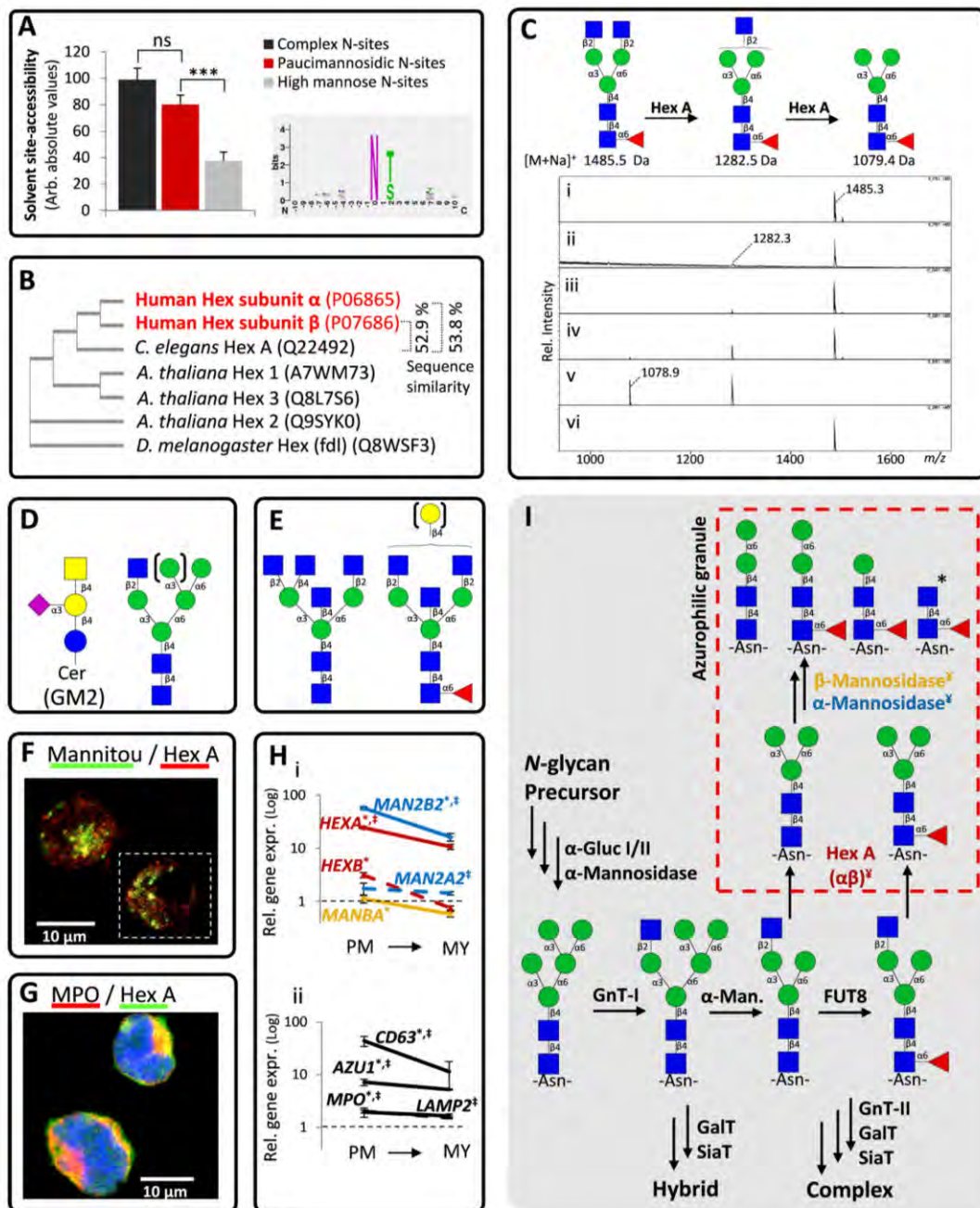
assembly of the biosynthetic machinery for human protein paucimannosylation in the azurophilic granules during early myeloid maturation of neutrophil precursors in the bone marrow (Fig. 4I).

Pathogen-induced Secretion of Paucimannosidic Proteins—Pathogen-induced secretion of paucimannosidic proteins was observed *in vitro* from DMSO-differentiated neutrophil-like HL-60 cells (Fig. 5A, top). *P. aeruginosa* PAO1 and PASS1 induced a time-dependent (1 h versus 3 h, $p = 1.8 \times 10^{-3}$) release of paucimannosidic proteins, preferentially M2F glycoforms (Fig. 5A, bottom), into the culture medium. Upon *P. aeruginosa* inoculation, the total levels of paucimannosylation were consistently above the unchallenged secretion levels ($p = 5.4 \times 10^{-3}$ to 5.0×10^{-5}); less elevation of the paucimannosylation levels was observed when the neutrophil-like HL-60 cells were activated with PMA ($p < 0.05$, 1 h versus 3 h). The unchanged morphology and cell counts of PAO1-challenged (1 h) neutrophils and PMA-activated neutrophils relative to the resting level suggested active secretion of paucimanno-

Human Paucimannosylation Structure, Function, and Biosynthesis

sidic proteins from viable cells by degranulation mechanisms. However, reduced cell numbers and viability after prolonged bacteria inoculation (2–3 h), in particular with the virulent CF-derived PASS1 strain, indicated that paucimannosidic proteins may, in part, be released into the culture

media upon cell death under these conditions. Interestingly, only PASS1 inoculation induced significant secretion (but not M2F-specific secretion) of paucimannosidic proteins into neutrophil-rich pathogen-free sputum ($31.9\% \pm 8.4\%$) relative to the unchallenged counterpart ($9.4\% \pm 2.7\%$, $p = 2.2 \times 10^{-2}$, $n = 4$) (Fig. 5B).



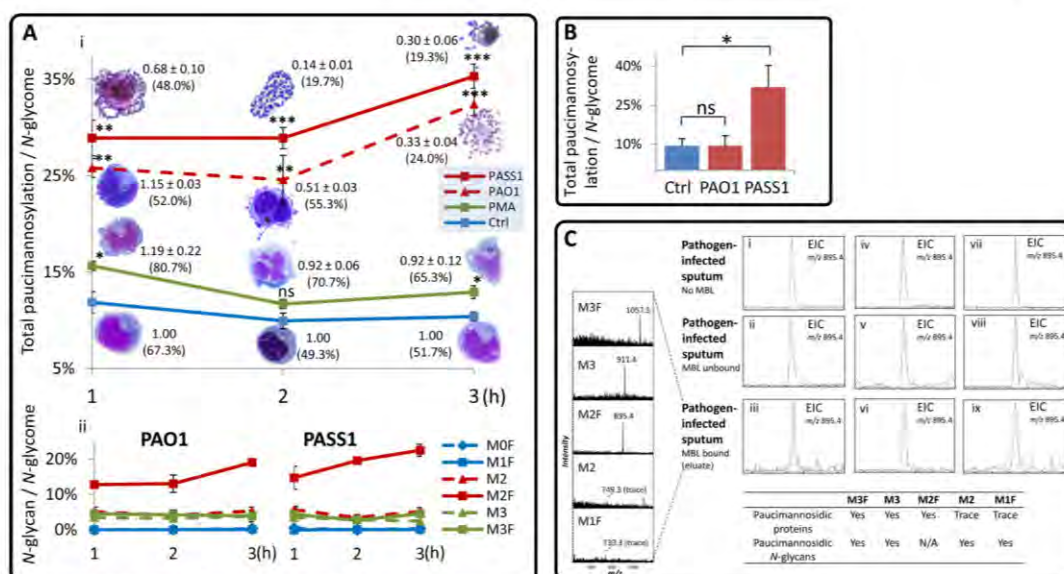


FIGURE 5. Multiple functions of paucimannosidic proteins in neutrophil biology. A, inoculation and incubation of laboratory wound (PAO1, broken red line) and virulent CF (PASS1, red line) *P. aeruginosa* strains and PMA activation (green line) of DMSO-differentiated HL-60 cells showing induced secretion of paucimannosidic proteins as measured by the degree of total paucimannosylation of the entire N-glycome in the culture medium relative to unchallenged DMSO-differentiated HL-60 cells (control, blue line) (top panel). Representative morphologies of Wright-stained neutrophils, total cell counts (normalized to control), and cell viabilities (in %) are presented for the individual time points. M2F-specific secretion in response to the bacterial inoculation was observed (bottom panel) ($n = 3$ for all time points and conditions). Although M0F *per se* does not fall under our definition of paucimannosylation, this paucimannosidic-related structure was included because it was observed in the HL-60 N-glycome. ns, not significant. B, PASS1-specific induction of paucimannosidic protein secretion in inflamed (neutrophil-rich) pathogen-free sputum ($n = 4$ for all conditions). C, all five paucimannosidic glycoepitopes displayed on sputum proteins have affinities to MBL (M2 and M1F were observed at low abundance in sputum) (left spectra). The abundant M2F (extracted ion chromatogram of m/z 895.4) found in CF sputum (top panels, i, iv, and vii) was present in the MBL unbound (middle panels, ii, v, and viii) and bound (eluted) fractions (bottom panels, iii, vi, and ix). Lower, table providing overview of MBL affinities for paucimannosidic proteins derived from CF sputum and commercially sourced paucimannosidic N-glycans (Dextra Laboratories) (M2F was not available). EIC, extracted-ion chromatogram; N/A, not applicable. For all A and B panels: mean \pm S.E., *, $p < 0.05$; **, $p < 0.01$; ***, $p < 0.001$.

Binding of Paucimannosidic Proteins to Mannose Receptors— Potential involvement of protein paucimannosylation in complement activation was assessed by evaluating the binding capacity of paucimannosidic glycoepitopes to MBL. All paucimannosidic glycoforms carried by the CF sputum proteins showed affinities to MBL (Fig. 5C). Isolated paucimannosidic N-glycans from commercial sources showed similar binding behavior. However, the significant presence of paucimannosidic glycoforms in the MBL unbound fractions indicated low binding affinities or MBL saturation under the assayed condi-

tions. High mannose-containing bovine ribonuclease B did not bind to MBL, whereas free high mannose N-glycans showed significant affinities (data not shown).

DISCUSSION

Augmenting established glycobiology (15–21), we here, for the first time, demonstrate that humans also produce bioactive paucimannosidic proteins similar to lower organisms such as nematodes, insects, and plants (15, 16, 26, 28) (see Fig. 6 for overview of our findings). However, in contrast to lower organ-

FIGURE 4. Human Hex A facilitates paucimannosidic N-glycan generation. A, glycosylation sites carrying paucimannosidic N-glycans, which are not sequon-constrained beyond the conventional NX(S/T) glycosylation motifs (shaded, inset), are significantly more accessible than the spatially hidden high mannose N-glycans (**, $p < 0.001$, mean \pm S.E.) when compared with published data (37), implying steric access of these glycoepitopes to exoglycosidase processing. ns, not significant. B, subunit α and β of human Hex A show high sequence homology to hexosaminidases from paucimannose-rich organisms. C, human Hex A can generate M3F *in vitro* from a complex N-glycan intermediate as monitored by MALDI-MS following (i) 0 h (no treatment), (ii) 6 h, (iii) 18 h, (iv) 90 h, (v) 108 h of Hex A incubation and (vi) 108 h without enzyme (control). Rel. intensity, relative intensity. D and E, Hex A also acts on hybrid N-glycan intermediates and ganglioside GM2, but shows no activity toward β 1,2-GlcNAc-containing structures displaying bisecting β 1,4-GlcNAc or β 1,4-galactose residues on proximal antennae. Cer, ceramide. F, partial co-localization (yellow) of paucimannosidic epitopes as detected by the paucimannose-reactive Mannitox (green) and human Hex A (red) antibodies in DMSO-differentiated HL-60 cells supports the involvement of Hex A in paucimannose generation (inset is a neutrophil-like cell from a separate field with the same scale and exposure). G, moderate/strong co-localization (yellow) of the human azurophilic marker MPO (red) and Hex A (green) in differentiated neutrophil-like HL-60 (multi-lobular nuclei in blue). H, temporal gene expression data (GSE19556) of enzymes putatively related to human paucimannosylation including HEXA (red), HEXB (broken red), MAN2A2 (blue), MAN2B2 (broken blue), and MANBA (green) (panel i) and paucimannosidic proteins including AZU1, MPO (broken line), CD63, and LAMP2 (panel ii) in promyelocytes (PM) relative to myelocytes (MY) and mature (resting) neutrophils (normalized to 1, indicated by broken line). Mean \pm S.D., $p < 0.05$ (*, PM versus MY; †, PM versus resting neutrophil). Rel. gene expr., relative gene expression. I, proposed biosynthetic route of protein paucimannosylation in azurophilic granules of maturing human promyelocytes. The enzymes putatively responsible for the generation of paucimannosidic proteins are presented in the same color scheme as in panel H. ‡, paucimannose biosynthetic enzymes previously identified in the azurophilic granules of human neutrophils (34, 38). *, although M0F *per se* does not fall under our definition of paucimannosidic type structures, it is included here because this paucimannosidic-related structure was observed in pathogen-infected sputum.

Human Paucimannosylation Structure, Function, and Biosynthesis

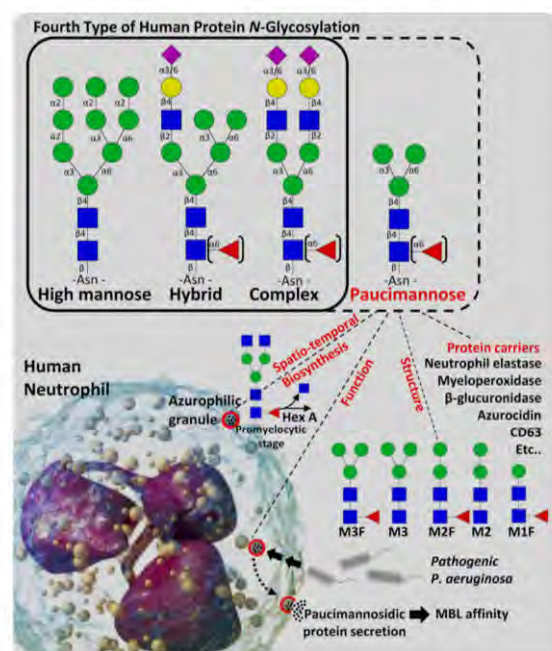


FIGURE 6. Structure, biosynthesis, and function of paucimannosylation as a fourth type of protein *N*-glycosylation in human neutrophils. Shown is a schematic overview illustrating in a simplified form the main findings of this work in terms of structure (*N*-glycan species and protein carriers), temporal, and spatial aspects of the biosynthetic route, as well as the functions of protein paucimannosylation in the human neutrophil. As such, protein paucimannosylation constitutes a new and fourth type of human *N*-glycosylation in addition to the established high mannose, hybrid, and complex type *N*-glycans. Graphics modified and used with permission from Blausen Medical (Blausen Gallery 2014).

isms where paucimannosylation is generated in the classical ER-Golgi secretory pathway and constitute a ubiquitous class of structures in the *N*-glycome repertoire, humans appear to use a non-classical ER-Golgi-granule pathway to produce paucimannosidic proteins. Irrespective of this diverted (organelle-specific) and time-demanding hydrolytic route, we argue that the abundance of paucimannosylation in infected sputum and the presentation of these structures on intact and functionally bioactive proteins support their classification as a fourth *N*-glycan type (in addition to high mannose, hybrid, and complex type) in neutrophil-rich environments central to inflammation and infection.

The discovery of this alternate type of human *N*-glycosylation, as exemplified in pathogen-infected sputum, was enabled by recent analytical developments in system-wide characterization of protein glycosylation (10, 31). Protein paucimannosylation was found to be abundant in sputum from inflamed pathogen-infected lungs irrespective of lung disease/condition, infecting microorganism, gender, age, and antibiotic treatment. Pathogen-free sputum, although derived from neutrophil-rich lungs (39), displayed negligible amounts of protein paucimannosylation. This implies that human protein paucimannosylation is neither genotype-specific, microbe-specific, nor disease-specific, but rather a general molecular feature common to

inflamed micro-environments of hosts undergoing pathogenic attack.

Five human paucimannosidic *N*-glycans were found to be carried by 18 abundant human sputum proteins that localized specifically to the azurophilic granules of the multi-compartmentalized human neutrophil (40). Neutrophilia is well established in CF and other respiratory conditions including URTL, featuring high proportion (>95%), counts (>10⁷ cells/g of sputum), and viability (>70%) of neutrophils in sputum (41). Strong support of paucimannosidic subcellular-specific localization in azurophilic granules and the proposed association between sputum protein paucimannosylation and neutrophil activation by pathogens comes from the observation that purified neutrophil proteins, including human MPO (42, 43), proteinase 3 (PR3) (44), azurocidin (45), Hex B (46), and bovine α -mannosidase (47), which localize to azurophilic granules (34), were previously shown to carry monosaccharide compositions corresponding to paucimannosidic *N*-glycans. Our glycoproteomics data indicate that sputum glycoproteins localizing to the specific and gelatinase granules and secretory vesicles in human neutrophils carried preferentially complex and high mannose *N*-glycans, suggesting a compartment-specific production and storage of paucimannosidic proteins in azurophilic granules. Highly similar *N*-glycosylation profiles of pathogen-infected sputum and neutrophil proteins, including the paucimannosidic profiles, further supported the neutrophilic origin of paucimannosylation and are congruent with studies indicating mammalian paucimannosylation in cancer and systemic lupus erythematosus (5, 7, 8, 12), which are neutrophil-rich pathologies. The neutrophil *N*-glycosylation profile in our study resembles a previously reported human neutrophil *N*-glycan profile (48) in which the low mass paucimannosidic structures however were not reported. The biosynthetically intriguing mono-antennary sialo-*N*-glycans (NeuAc₁Gal₁Man₃GlcNAc₃Fuc₀₋₁) were abundant in the neutrophil and CF sputum *N*-glycomes, but did not appear to be directly related to the azurophilic granule-specific paucimannosylation based on their attachment to proteins localizing to other neutrophil granules (supplemental Fig. 1).

The fact that paucimannosidic *N*-glycans are carried by highly solvent-accessible sites on sputum proteins suggests that they are derived from extensive exoglycosidase processing (37). The high solvent accessibilities also explain the prevalence (>85%) of the accessibility-dependent α 1,6-(core) fucosylation on the paucimannosidic *N*-glycans. High core fucosylation, in turn, implies that the paucimannosidic biosynthetic route involves *N*-glycan intermediates displaying terminal β 1,2-GlcNAcylation, a substrate requirement for fucosyltransferase 8 (49). This implies again that paucimannose generation follows the initial synthesis of *cis*-Golgi-localized fucosylated hybrid/complex glycan intermediates.

Hexosaminidases are highly expressed in paucimannose-rich organisms including *C. elegans*, *D. melanogaster*, and plants (21). We observed high sequence homology of the α and β subunits of the heterodimeric human Hex A to these hexosaminidases in line with a previous study (20). In addition, the specific identification of human Hex A α/β subunits in azurophilic granules of neutrophils (34, 38) and our immunocyto-

Human Paucimannosylation Structure, Function, and Biosynthesis

chemistry data showing partial co-localization of both human Hex A and paucimannosidic glycoepitopes with an azurophilic granule marker (MPO) in differentiated neutrophil-like HL-60 cells together support the Hex A-driven compartment-specific paucimannosylation pathway proposed herein. The capacity of Hex A to generate paucimannosidic *N*-glycans *in vitro* from biosynthetic intermediates at realistic physiological conditions, albeit at low enzymatic rates, also confirms this relationship. The similarities of primary (66.5% sequence similarity) (data not shown) and higher structural levels of α and β subunits of Hex A (50, 51) suggest that the homodimeric Hex B ($\beta\beta$) and Hex S ($\alpha\alpha$) isoenzymes may also be able to catalyze paucimannosylation. The relative broad substrate specificity of hexosaminidases to both β -GlcNAc-terminating and α -GalNAc-terminating glycoconjugates (52), together with the low activity observed here, may evolutionarily be more beneficial than high enzyme activity considering the prolonged storage of Hex A and glycoprotein substrates in the azurophilic granules: from the compartment assembly early in the neutrophil maturation in the bone marrow (40) over blood circulation averaging 5 days (53), to transmigration and mobilization via degranulation mechanisms at the inflammatory site. The relative efficiency of Hex A-driven paucimannosylation of membrane, *e.g.* lysosome-associated membrane protein 2 (LAMP2) and soluble *e.g.* NE proteins and any co-factor requirements for optimal paucimannosidic protein generation as reported for GM2 ganglioside degradation by Hex A (54), await further investigation.

Assembly of the paucimannose generating azurophilic granules and its molecular components early during myeloid maturation in the bone marrow was supported by the temporal gene expression of paucimannosidic proteins and putative paucimannose biosynthetic enzymes in promyelocytes in excellent agreement with previous studies (55, 56). Gene set enrichment analysis (57) revealed a high gene expression of paucimannosidic proteins in isolated blood leukocytes from *S. pneumoniae*-infected (but not *S. aureus*, *Escherichia coli*, and influenza A virus-infected) individuals (9-fold enrichment, $p = 3.4 \times 10^{-3}$) relative to healthy individuals, suggesting that the assembly of the paucimannose biosynthetic machinery in neutrophil precursors can be shifted from the bone marrow to the blood circulation via infection-dependent "left shifts."

The "targeted-by-timing biosynthesis" hypothesis mechanistically explaining the formation of the granule-specific proteomes in neutrophils (34, 40, 58) is congruent with our observation of compartment-specific *N*-glycosylation; the majority of all glycoproteins trafficking through the *N*-glycosylation machinery at the promyelocytic stage of the neutrophil development are directed to the azurophilic granules by vesicles budding from the *cis*-Golgi without reaching the late *N*-glycan maturation stage, *e.g.* β -galactosylation and α -sialylation in the *trans*-Golgi network (59). As expected, proteins localizing to the specific (and other) granules, which are synthesized exclusively in the myelocyte and more mature stages of the neutrophil development by vesicles budding off from the *trans*-Golgi network (58, 59), displayed complex type *N*-glycosylation. This subcellular-specific *N*-glycosylation is further supported by the absence of human α -sialidases and β -galactosidases in azurophilic granules (34, 38), which suggest that Hex A does not

function in concert with other outer-arm exoglycosidases and may explain why the sterically protected GlcNAc-terminating *N*-glycans are unacceptable substrates for human Hex A. This fascinating feature of compartment-specific *N*-glycosylation is not unique to neutrophils (60).

The further trimming of the paucimannosidic glycoforms by human α -mannosidases appears to be linkage-specific as shown by the specific generation of the α 1,6-linked mannose-terminating M2F and M2 isomers (see supplemental Table 1). This agrees well with the exclusive presence of the α 1,6-mannose isomer of M2F and M2 previously reported on neutrophil-derived human proteins (45) and the preferential hydrolysis of α 1,3-linked mannosides by human α -mannosidase (61). Human β -mannosidase may be responsible for yielding amannosylated di- (M0) or tri- (M0F) saccharides. The detection of α - and β -mannosidases in isolated azurophilic granules (34, 38) and the promyelocyte-specific expression of genes coding for the corresponding mannosidases support their association with protein paucimannosylation. By overlaying our observations on the existing map of the mammalian *N*-glycosylation machinery (3), we propose a new spatio-temporal restricted biosynthetic route enabling paucimannosylation of human neutrophil proteins (Fig. 4f).

Azurophilic granules of human neutrophils share some functional and molecular commonalities with the glycoprotein-degrading lysosome, yet the two compartments are separate entities as displayed by their unique proteomes as well as by the mobile characteristics of azurophilic granules as secretory components (59, 62). In addition, bidirectional lysosomal glycoprotein degradation is facilitated by a suite of exoglycosidases and proteases, leaving the released and partially degraded *N*-glycans without the reducing-end β -GlcNAc and α 1,6-fucose residues (61), contrary to the paucimannosidic *N*-glycans and indeed the *N*-glycoproteins identified in this study. Together this indicates that protein paucimannosylation in pathogen-infected sputum is of non-lysosomal origin. The absence of significant co-localization of paucimannosidic glycoepitopes and several established lysosomal and ER/Golgi markers in other paucimannose-positive human cells further supported a non-lysosomal/ER/Golgi-based paucimannose synthesis.³ As such, we argue that protein paucimannosylation in the azurophilic compartment of the human neutrophil should not be perceived as a degradation product aimed to salvage monosaccharides and amino acids, but rather as a cellular mechanism to generate an arsenal of releasable biomolecules displaying unique glycoepitopes and activities.

Sorting of proteins to storage granules is not unique to neutrophils, but seems to occur by mechanisms common to all cells (59). Intrigued by the temporal and compartment-specific biosynthetic route for paucimannosylation in neutrophils proposed here, we are investigating whether paucimannosylation is unique to neutrophils or common across cell types. We have recently reported that cultured human colon and breast cancer epithelial cells produce paucimannosidic epitopes (6, 60), albeit in lower quantities (typically less than 15–20% of the total

³ A. C. Dahmen, M. T. Fergen, C. Laurini, B. Schmitz, I. Loke, M. Thaysen-Anderesen, and S. Diestel, submitted for publication.

Human Paucimannosylation Structure, Function, and Biosynthesis

N-glycome), supporting a possible oncofetal antigen potential of paucimannosylation (12) and the possible molecular and functional similarity of neutrophils and epithelial cells (58). However, the lack of azurophilic granules in epithelial cells implies that production, storage, and secretion of paucimannosidic proteins may be facilitated by other mechanisms in these systems.

Containing an ensemble of bioactive molecules, including antimicrobial peptides and proteases, the azurophilic granule is the microbicidal compartment of the neutrophil (62, 63). Thus, the azurophil-specific localization of protein paucimannosylation in neutrophils is potentially of high biological significance. It has been established that azurophilic granules are mobilized as the last compartment upon phagocytosis (40, 62, 63), emptying their soluble content into the phagolysosome and the extracellular environment to combat invading pathogens (40). The virulence-specific release of paucimannosidic proteins into sputum upon *P. aeruginosa* stimulation indicates an infection-dependent mobilization of azurophilic granules, aspects we are currently investigating by bacterial genome sequencing and proteomics. The importance of granule mobilization for innate immunity is well illustrated in the Chediak-Higashi syndrome where immobile azurophilic granules reduce the host response to pathogens (64). The induced secretion of paucimannosidic proteins from neutrophils presented here indicates that, as reported (40, 62), granules fuse not only with the phagolysosome, but also with the plasma membrane upon activation.

The strong neutrophilic association with the paucimannosidic proteins observed in sputum from pathogen-infected inflamed lungs prompted us to investigate possible functional aspects of human paucimannosylation, *i.e.* lectin-based recognition by the immune system via mannose-receptor interactions. Mannose-terminating glycoconjugates are infrequent in the extracellular environment of healthy human cells/tissues (60), but such determinants from internal membranes or granules may be exposed under specific cellular conditions, *e.g.* immature ER-resident glycoepitopes were shown to be exposed in apoptotic cells serving as “eat me” signals for macrophage-based clearance (65). Exposure of α - and β -mannose determinants on solvent-accessible glycosylation sites such as those presented by paucimannosidic proteins may be a unique feature to enable molecular and cellular communication of activated neutrophils via mannose receptors in the micro-environment by mechanisms of active secretion (degranulation) of paucimannosidic proteins or by release upon cell death (39). The abundant paucimannosidic determinants found in infected sputum may also arise from the release of granular contents into neutrophil extracellular traps (NETs) via the activation and NETosis of polymorphonuclear cells (66). We have demonstrated binding of paucimannosidic proteins and *N*-glycans to MBL; however, the exact roles of paucimannosylation in the downstream complement activation clearly need further investigation. In addition, paucimannosidic binding to other lectins including the macrophage mannose receptors (CD206 and CD280) and dendritic C type lectins (*e.g.* CD209, CD299, and CD303) may provide avenues for the neutrophils to communicate with other immune cells (67). Opportunistic pathogens may also recognize exposed mannosidic determinants as

an avenue for host adherence, *e.g.* *E. coli* fimbrial FimH adhesin shows high affinity for high mannose type as well as paucimannosidic *N*-glycans (68, 69).

In addition, bacteriostatic and bactericidal effects of the paucimannose-rich neutrophilic proteins NE, azurocidin, and cathepsin G have previously been reported (70). We are currently investigating the functional role of the carbohydrate moieties on these human paucimannosidic proteins in the context of bacterial killing and growth inhibition.

Finally, we speculate that paucimannosylation may carry out modulatory roles in the generation and/or recognition of anti-neutrophil cytoplasmic autoantibodies by masking or presenting immunogenic epitopes on the anti-neutrophil cytoplasmic autoantibody-typic and paucimannose-rich LAMP2, PR3, MPO, and NE (71). As such, it becomes clear that paucimannosylation may be linked to multiple diverse functional roles in the micro-environments where paucimannosidic proteins appear to be enriched following neutrophil activation, *i.e.* in phagolysosomes (39, 62), microvesicles/ectosomes (72) and neutrophil extracellular traps (73).

In conclusion, we document that human neutrophils produce, store, and selectively secrete bioactive paucimannosidic proteins into sputum of lungs undergoing pathogen-based inflammation and infection. We show that the azurophilic granules of neutrophils are the biosynthetic “venues” and that human hexosaminidases are the enzymatic “facilitators” of this fourth type of human protein *N*-glycosylation. In line with established neutrophil biology, we propose that paucimannosidic proteins are targeted to the azurophilic granule “by timing” rather than by selective sorting in the early bone marrow maturation of developing myeloid cells. The rather narrow temporal and spatial nature of paucimannosidic proteins in micro-environments surrounding inflammation, and in response to pathogen infection, suggests specialized biomolecular immune functions and may explain how protein paucimannosylation to date has remained under the radar in human glycobiology.

Acknowledgments—Dr. Niclas Karlsson, University of Gothenburg, Sweden, and Dr. Sharon Chen, Westmead Hospital, Sydney, Australia are thanked for donating isolated human neutrophils and sputum, respectively. Dr. Ardeshir Armirkhani, Jodie Abrahams, Dr. Robert Parker, and Dr. Mark Molloy are thanked for glycomics and proteomics assistance. Debra Birch and Nicole Vella are thanked for microscopy assistance. Dr. Marshall Bern is thanked for technical assistance with automated glycopeptide identification using Byonic™. Members of the Australian Research Council Super Science Program at Macquarie University are thanked for fruitful discussions.

Note Added in Proof—Fig. 4F did not indicate that the images of the neutrophil-like HL-60 cells were obtained from separate fields in the version of this article that was published on February 2, 2015 as a Paper in Press. This error has been corrected.

REFERENCES

1. Freeze, H. H. (2013) Understanding human glycosylation disorders: biochemistry leads the charge. *J. Biol. Chem.* **288**, 6936–6945
2. Moremen, K. W., Tiermeyer, M., and Nairn, A. V. (2012) Vertebrate protein glycosylation: diversity, synthesis and function. *Nat. Rev. Mol. Cell*

Human Paucimannosylation Structure, Function, and Biosynthesis

- Biol.* **13**, 448–462
3. Aeby, M. (2013) N-linked protein glycosylation in the ER. *Biochim. Biophys. Acta* **1833**, 2430–2437
 4. Everest-Dass, A. V., Jin, D., Thaysen-Andersen, M., Nevalainen, H., Kolarich, D., and Packer, N. H. (2012) Comparative structural analysis of the glycosylation of salivary and buccal cell proteins: innate protection against infection by *Candida albicans*. *Glycobiology* **22**, 1465–1479
 5. Balog, C. I., Stavenhagen, K., Fung, W. L., Koelerman, C. A., McDonnell, L. A., Verhoeven, A., Mesker, W. E., Tollenaar, R. A., Deelder, A. M., and Wührer, M. (2012) N-Glycosylation of colorectal cancer tissues: a liquid chromatography and mass spectrometry-based investigation. *Mol. Cell. Proteomics* **11**, 571–585
 6. Sethi, M. K., Thaysen-Andersen, M., Smith, J. T., Baker, M. S., Packer, N. H., Hancock, W. S., and Fanayan, S. (2014) Comparative N-glycan profiling of colorectal cancer cell lines reveals unique bisecting GlcNAc and α -2,3-linked sialic acid determinants are associated with membrane proteins of the more metastatic/aggressive cell lines. *J. Proteome Res.* **13**, 277–288
 7. Joosten, C. E., Cohen, L. S., Ritter, G., Batt, C. A., and Shuler, M. L. (2004) Glycosylation profiles of the human colorectal cancer A33 antigen naturally expressed in the human colorectal cancer cell line SW1222 and expressed as recombinant protein in different insect cell lines. *Biotechnol. Prog.* **20**, 1273–1279
 8. Hashii, N., Kawasaki, N., Itoh, S., Nakajima, Y., Kawanishi, T., and Yamaguchi, T. (2009) Alteration of N-glycosylation in the kidney in a mouse model of systemic lupus erythematosus: relative quantification of N-glycans using an isotope-tagging method. *Immunology* **126**, 336–345
 9. Yagi, H., Saito, T., Yanagisawa, M., Yu, R. K., and Kato, K. (2012) Lewis X-carrying N-glycans regulate the proliferation of mouse embryonic neural stem cells via the Notch signaling pathway. *J. Biol. Chem.* **287**, 24356–24364
 10. Parker, B. L., Thaysen-Andersen, M., Solis, N., Scott, N. E., Larsen, M. R., Graham, M. E., Packer, N. H., and Cordwell, S. J. (2013) Site-specific glycan-peptide analysis for determination of N-glycoproteome heterogeneity. *J. Proteome Res.* **12**, 5791–5800
 11. Venkatakrishnan, V., Thaysen-Andersen, M., Chen, S. C., Nevalainen, H., and Packer, N. H. (2015) Cystic fibrosis and bacterial colonization define the sputum N-glycosylation phenotype. *Glycobiology* **25**, 88–100
 12. Zipser, B., Bello-DeOcampo, D., Diestel, S., Tai, M. H., and Schmitz, B. (2012) Mannitox monoclonal antibody uniquely recognizes paucimannose, a marker for human cancer, stemness, and inflammation. *J. Carbohydr. Chem.* **31**, 504–518
 13. van Remoortere, A., Bank, C. M., Nyame, A. K., Cummings, R. D., Deelder, A. M., and van Die, I. (2003) *Schistosoma mansoni*-infected mice produce antibodies that cross-react with plant, insect, and mammalian glycoproteins and recognize the truncated biantennary N-glycan Man3GlcNAc2-R. *Glycobiology* **13**, 217–225
 14. Kaprio, T., Satomaa, T., Heiskanen, A., Hokke, C. H., Deelder, A. M., Mustonen, H., Hagström, I., Carpen, O., Saarinen, I., and Haglund, C. (2015) N-Glycomic profiling as a tool to separate rectal adenomas from carcinomas. *Mol. Cell. Proteomics* **14**, 277–288
 15. Sarkar, M., Leventis, P. A., Silvescu, C. I., Reinhold, V. N., Schachter, H., and Boulianne, G. L. (2006) Null mutations in *Drosophila* N-acetylglucosaminyltransferase I produce defects in locomotion and a reduced life span. *J. Biol. Chem.* **281**, 12776–12785
 16. Schachter, H. (2009) Paucimannose N-glycans in *Caenorhabditis elegans* and *Drosophila melanogaster*. *Carbohydr. Res.* **344**, 1391–1396
 17. Altmann, F., Staudacher, E., Wilson, I. B., and März, L. (1999) Insect cells as hosts for the expression of recombinant glycoproteins. *Glycoconj. J.* **16**, 109–123
 18. Zhang, W., Cao, P., Chen, S., Spence, A. M., Zhu, S., Staudacher, E., and Schachter, H. (2003) Synthesis of paucimannose N-glycans by *Caenorhabditis elegans* requires prior actions of UDP-N-acetyl-D-glucosamine: α -3-D-mannoside β 1,2-N-acetylglucosaminyltransferase I, α 3,6-mannosidase II and a specific membrane-bound β -N-acetylglucosaminidase. *Biochem. J.* **372**, 53–64
 19. Shi, H., Tan, J., and Schachter, H. (2006) N-Glycans are involved in the response of *Caenorhabditis elegans* to bacterial pathogens. *Methods Enzymol.* **417**, 359–389
 20. Guttering, M., Kretschmer-Lubich, D., Paschinger, K., Rendic, D., Hader, J., Geier, P., Ranftl, R., Jantsch, V., Lochrit, G., and Wilson, I. B. (2007) Biosynthesis of truncated N-linked oligosaccharides results from non-orthologous hexosaminidase-mediated mechanisms in nematodes, plants, and insects. *J. Biol. Chem.* **282**, 27825–27840
 21. Schachter, H., and Boulianne, G. (2011) Life is sweet! A novel role for N-glycans in *Drosophila* lifespan. *Fly* **5**, 18–24
 22. Altmann, F., Fabini, G., Ahorn, H., and Wilson, I. B. (2001) Genetic model organisms in the study of N-glycans. *Biochimie* **83**, 703–712
 23. Cipollo, I. F., Costello, C. E., and Hirschberg, C. B. (2002) The fine structure of *Caenorhabditis elegans* N-glycans. *J. Biol. Chem.* **277**, 49143–49157
 24. Haslam, S. M., Gens, D., Morris, H. R., and Dell, A. (2002) The glycomes of *Caenorhabditis elegans* and other model organisms. *Biochem. Soc. Symp.* **117**, 117–134
 25. Altmann, F., Schwihla, H., Staudacher, E., Glössl, J., and März, L. (1995) Insect cells contain an unusual, membrane-bound β -N-acetylglucosaminidase probably involved in the processing of protein N-glycans. *J. Biol. Chem.* **270**, 17344–17349
 26. Léonard, R., Rendic, D., Rabouille, C., Wilson, I. B., Pr  at, T., and Altmann, F. (2006) The *Drosophila fused lobes* gene encodes an N-acetylglucosaminidase involved in N-glycan processing. *J. Biol. Chem.* **281**, 4867–4875
 27. Dam, S., Thaysen-Andersen, M., Stenkj  r, E., Lorentzen, A., Roepstorff, P., Packer, N. H., and Stougaard, J. (2013) Combined N-glycome and n-glycoproteome analysis of the *Lotus japonicus* seed globulin fraction shows conservation of protein structure and glycosylation in legumes. *J. Proteome Res.* **12**, 3383–3392
 28. Schiller, B., Hykollari, A., Yan, S., Paschinger, K., and Wilson, I. B. (2012) Complicated N-linked glycans in simple organisms. *Biol. Chem.* **393**, 661–673
 29. Jin, C., Ekvall, A. K., Bylund, J., Bj  rkman, L., Estrella, R. P., Whitelock, J. M., Eisler, T., Bokarewa, M., and Karlsson, N. G. (2012) Human synovial lubricin expresses sialyl Lewis x determinant and has L-selectin ligand activity. *J. Biol. Chem.* **287**, 35922–35933
 30. Boyum, A., L  vhaug, D., Tresland, L., and Nordlie, E. M. (1991) Separation of leucocytes: improved cell purity by fine adjustments of gradient medium density and osmolality. *Scand. J. Immunol.* **34**, 697–712
 31. Jensen, P. H., Karlsson, N. G., Kolarich, D., and Packer, N. H. (2012) Structural analysis of N- and O-glycans released from glycoproteins. *Nat. Protoc.* **7**, 1299–1310
 32. M  ysling, S., Palmisano, G., H  rj  r, P., and Thaysen-Andersen, M. (2010) Utilizing ion-pairing hydrophilic interaction chromatography solid phase extraction for efficient glycopeptide enrichment in glycoproteomics. *Anal. Chem.* **82**, 5598–5609
 33. Leymarie, N., Griffin, P. J., Jonscher, K., Kolarich, D., Orlando, R., McComb, M., Zaia, J., Aguilan, J., Alley, W. R., Altmann, F., Ball, L. E., Basumallick, L., Bazemore-Walker, C. R., Behnen, H., Blank, M., Brown, K. J., Bunz, S. C., Cairo, C. W., Cipollo, I. F., Daneshfar, R., Desaire, H., Drake, R. R., Go, E. P., Goldman, R., Gruber, C., Halim, A., Hathout, Y., Hensbergen, P. J., Horn, D. M., Hurum, D., J  bs, W., Larson, G., Ly, M., Mann, B. F., Marx, K., Mechref, Y., Meyer, B., M  glinger, U., Neus   , C., Nilsson, I., Novotny, M. V., Ny  l  w  dhe, J. O., Packer, N. H., Pompach, P., Reiz, B., Resemann, A., Rohrer, J. S., Ruthenbeck, A., Sanda, M., Schulz, J. M., Schweiger-Hufnagel, U., Sihlbom, C., Song, E., Staples, G. O., Suckau, D., Tang, H., Thaysen-Andersen, M., Viner, R. I., An, Y., Valmu, L., Wada, Y., Watson, M., Windwarder, M., Whittall, R., W  hrer, M., Zhu, Y., and Zou, C. (2013) Interlaboratory study on differential analysis of protein glycosylation by mass spectrometry: the ABRF Glycoprotein Research Multi-Institutional Study 2012. *Mol. Cell. Proteomics* **12**, 2935–2951
 34. R  rvig, S., Østergaard, O., Heegaard, N. H., and Borregaard, N. (2013) Proteome profiling of human neutrophil granule subsets, secretory vesicles, and cell membrane: correlation with transcriptome profiling of neutrophil precursors. *J. Leukoc. Biol.* **94**, 711–721
 35. Zinchuk, V., Wu, Y., and Grossenbacher-Zinchuk, O. (2013) Bridging the gap between qualitative and quantitative colocalization results in fluorescence microscopy studies. *Sci. Rep.* **3**, 1365
 36. Abbas, A. R., Baldwin, D., Ma, Y., Ouyang, W., Gurney, A., Martin, F.,

Human Paucimannosylation Structure, Function, and Biosynthesis

- Fong, S., van Lookeren Campagne, M., Godowski, P., Williams, P. M., Chan, A. C., and Clark, H. F. (2005) Immune response *in silico* (IRIS): immune-specific genes identified from a compendium of microarray expression data. *Genes Immun.* **6**, 319–331
37. Thaysen-Andersen, M., and Packer, N. H. (2012) Site-specific glycoproteomics confirms that protein structure dictates formation of *N*-glycan type, core fucosylation and branching. *Glycobiology* **22**, 1440–1452
38. Lominadze, G., Powell, D. W., Luerman, G. C., Link, A. J., Ward, R. A., and McLeish, K. R. (2005) Proteomic analysis of human neutrophil granules. *Mol. Cell. Proteomics* **4**, 1503–1521
39. Nauseef, W. M., and Borregaard, N. (2014) Neutrophils at work. *Nat. Immunol.* **15**, 602–611
40. Borregaard, N. (2010) Neutrophils, from marrow to microbes. *Immunity* **33**, 657–670
41. Jayaram, L., Labiris, N. R., Efthimiadis, A., Valchos-Mayer, H., Hargreave, F. E., and Freitag, A. P. (2007) The efficiency of sputum cell counts in cystic fibrosis. *Can Respir. J.* **14**, 99–103
42. Ravnsborg, T., Houen, G., and Højrup, P. (2010) The glycosylation of myeloperoxidase. *Biochim. Biophys. Acta* **1804**, 2046–2053
43. Van Antwerpen, P., Slomianny, M. C., Boudjeltia, K. Z., Delporte, C., Faïd, V., Calay, D., Rousseau, A., Moguilevsky, N., Raes, M., Vanhamme, L., Furtmüller, P. G., Obinger, C., Vanhaeverbeek, M., Nève, J., and Michalski, J. C. (2010) Glycosylation pattern of mature dimeric leukocyte and recombinant monomeric myeloperoxidase: glycosylation is required for optimal enzymatic activity. *J. Biol. Chem.* **285**, 16351–16359
44. Zoega, M., Ravnsborg, T., Højrup, P., Houen, G., and Schou, C. (2012) Proteinase 3 carries small unusual carbohydrates and associates with α -defensins. *J. Proteomics* **75**, 1472–1485
45. Olczak, M., and Watorek, W. (2002) Structural analysis of *N*-glycans from human neutrophil azurocidin. *Biochem. Biophys. Res. Commun.* **293**, 213–219
46. Schuette, C. G., Weisgerber, J., and Sandhoff, K. (2001) Complete analysis of the glycosylation and disulfide bond pattern of human β -hexosaminidase B by MALDI-MS. *Glycobiology* **11**, 549–556
47. Faïd, V., Evjen, G., Tollersrud, O. K., Michalski, J. C., and Morelle, W. (2006) Site-specific glycosylation analysis of the bovine lysosomal α -mannosidase. *Glycobiology* **16**, 440–461
48. Babu, P., North, S. J., Jang-Lee, J., Chalabi, S., Mackerness, K., Stowell, S. R., Cummings, R. D., Rankin, S., Dell, A., and Haslam, S. M. (2009) Structural characterisation of neutrophil glycans by ultra sensitive mass spectrometric glycomics methodology. *Glycoconj. J.* **26**, 975–986
49. Paschinger, K., Staudacher, E., Stemmer, U., Fabini, G., and Wilson, I. B. (2005) Fucosyltransferase substrate specificity and the order of fucosylation in invertebrates. *Glycobiology* **15**, 463–474
50. Lemieux, M. J., Mark, B. L., Cherney, M. M., Withers, S. G., Mahuran, D. J., and James, M. N. (2006) Crystallographic structure of human β -hexosaminidase A: interpretation of Tay-Sachs mutations and loss of G_{M2} ganglioside hydrolysis. *J. Mol. Biol.* **359**, 913–929
51. Mark, B. L., Mahuran, D. J., Cherney, M. M., Zhao, D., Knapp, S., and James, M. N. (2003) Crystal structure of human β -hexosaminidase B: understanding the molecular basis of Sandhoff and Tay-Sachs disease. *J. Mol. Biol.* **327**, 1093–1109
52. Hepbildikler, S. T., Sandhoff, R., Kolzer, M., Proia, R. L., and Sandhoff, K. (2002) Physiological substrates for human lysosomal β -hexosaminidase S. *J. Biol. Chem.* **277**, 2562–2572
53. Pillay, J., den Braber, I., Vrsekooop, N., Kwast, L. M., de Boer, R. J., Borghans, J. A., Tesselaar, K., and Koenderman, L. (2010) *In vivo* labeling with $^3\text{H}_2\text{O}$ reveals a human neutrophil lifespan of 5.4 days. *Blood* **116**, 625–627
54. Meier, E. M., Schwarzmann, G., Fürst, W., and Sandhoff, K. (1991) The human G_{M2} activator protein. A substrate specific cofactor of β -hexosaminidase A. *J. Biol. Chem.* **266**, 1879–1887
55. Martinelli, S., Urosevic, M., Daryadel, A., Oberholzer, P. A., Baumann, C., Fey, M. F., Dummer, R., Simon, H. U., and Yousefi, S. (2004) Induction of genes mediating interferon-dependent extracellular trap formation during neutrophil differentiation. *J. Biol. Chem.* **279**, 44123–44132
56. Theilgaard-Mönch, K., Jacobsen, L. C., Borup, R., Rasmussen, T., Bjerregaard, M. D., Nielsen, F. C., Cowland, J. B., and Borregaard, N. (2005) The transcriptional program of terminal granulocytic differentiation. *Blood* **105**, 1785–1796
57. Ramilo, O., Allman, W., Chung, W., Mejias, A., Ardura, M., Glaser, C., Wittkowski, K. M., Piqueras, B., Banchereau, J., Palucka, A. K., and Chaussabel, D. (2007) Gene expression patterns in blood leukocytes discriminate patients with acute infections. *Blood* **109**, 2066–2077
58. Borregaard, N., Sørensen, O. E., and Theilgaard-Mönch, K. (2007) Neutrophil granules: a library of innate immunity proteins. *Trends Immunol.* **28**, 340–345
59. Borregaard, N., and Cowland, J. B. (1997) Granules of the human neutrophilic polymorphonuclear leukocyte. *Blood* **89**, 3503–3521
60. Lee, L. Y., Lin, C. H., Fanayan, S., Packer, N. H., and Thaysen-Andersen, M. (2014) Differential site accessibility mechanistically explains subcellular-specific *N*-glycosylation determinants. *Front. Immunol.* **5**, 404
61. Winchester, B. (2005) Lysosomal metabolism of glycoproteins. *Glycobiology* **15**, 1R–15R
62. Witko-Sarsat, V., Rieu, P., Descamps-Latscha, B., Lesavre, P., and Halbwachs-Mecarelli, L. (2000) Neutrophils: molecules, functions and pathophysiological aspects. *Lab. Invest.* **80**, 617–653
63. Lacy, P. (2006) Mechanisms of degranulation in neutrophils. *Allergy Asthma Clin. Immunol.* **2**, 98–108
64. Kjeldsen, L., Calafat, J., and Borregaard, N. (1998) Giant granules of neutrophils in Chediak-Higashi syndrome are derived from azurophilic granules but not from specific and gelatinase granules. *J. Leukoc. Biol.* **64**, 72–77
65. Bilyy, R. O., Shkandina, T., Tomin, A., Muñoz, L. E., Franz, S., Antonyuk, V., Kit, Y. Y., Zirngibl, M., Fürnrohr, B. G., Janko, C., Lauber, K., Schiller, M., Schett, G., Stoika, R. S., and Herrmann, M. (2012) Macrophages discriminate glycosylation patterns of apoptotic cell-derived microparticles. *J. Biol. Chem.* **287**, 496–503
66. Schauer, C., Janko, C., Munoz, L. E., Zhao, Y., Kienhöfer, D., Frey, B., Lell, M., Manger, B., Rech, J., Naschberger, E., Holmdahl, R., Krenn, V., Harrer, T., Jeremic, I., Bilyy, R., Schett, G., Hoffmann, M., and Herrmann, M. (2014) Aggregated neutrophil extracellular traps limit inflammation by degrading cytokines and chemokines. *Nat. Med.* **20**, 511–517
67. Galli, S. J., Borregaard, N., and Wynn, T. A. (2011) Phenotypic and functional plasticity of cells of innate immunity: macrophages, mast cells and neutrophils. *Nat. Immunol.* **12**, 1035–1044
68. Taganna, J., de Boer, A. R., Wuhrer, M., and Bouckaert, J. (2011) Glycosylation changes as important factors for the susceptibility to urinary tract infection. *Biochem. Soc. Trans.* **39**, 349–354
69. Bouckaert, J., Mackenzie, J., de Paz, J. L., Chipwaza, B., Choudhury, D., Zavalov, A., Mannerstedt, K., Anderson, I., Piérard, D., Wyns, L., Seeberger, P. H., Oscarson, S., De Greve, H., and Knight, S. D. (2006) The affinity of the FimH fimbrial adhesin is receptor-driven and quasi-independent of *Escherichia coli* pathotypes. *Mol. Microbiol.* **61**, 1556–1568
70. Miyasaki, K. T., Bodeau, A. L., and Flemmig, T. F. (1991) Differential killing of *Actinobacillus actinomycetemcomitans* and *Capnocytophaga* spp. by human neutrophil granule components. *Infect. Immun.* **59**, 3760–3767
71. Kain, R., Exner, M., Brandes, R., Ziebertmayr, R., Cunningham, D., Alderson, C. A., Davidovits, A., Raab, I., Jahn, R., Ashour, O., Spitzauer, S., Sunder-Plassmann, G., Fukuda, M., Klemm, P., Rees, A. J., and Kerjaschki, D. (2008) Molecular mimicry in pauci-immune focal necrotizing glomerulonephritis. *Nat. Med.* **14**, 1088–1096
72. Timár, C. I., Lorincz, A. M., Csépanyi-Kömi, R., Vályi-Nagy, A., Nagy, G., Buzás, E. I., Iványi, Z., Kittel, A., Powell, D. W., McLeish, K. R., and Ligeti, E. (2013) Antibacterial effect of microvesicles released from human neutrophilic granulocytes. *Blood* **121**, 510–518
73. Brinkmann, V., Reichard, U., Goosmann, C., Fauler, B., Uhlemann, Y., Weiss, D. S., Weinrauch, Y., and Zychlinsky, A. (2004) Neutrophil extracellular traps kill bacteria. *Science* **303**, 1532–1535

2.3 Overview of main findings, conclusions and unresolved questions

Main findings and conclusions

- Paucimannosidic *N*-glycans ($\text{Man}_{1-3}\text{Fuc}_{0-1}\text{GlcNAc}_2$) were observed in bacteria-colonised neutrophil-rich sputum of patients with respiratory conditions and were found to be carried predominately by the azurophilic granule proteins of human neutrophils.
- From our current knowledge of the glycan degradation pathways, the observations indicated that protein paucimannosylation in human neutrophils is not a degradation product as evidenced by their conjugation to intact sputum peptides and proteins as evaluated using LC-MS/MS and paucimannose-reactive antibodies.
- The major paucimannosidic *N*-glycan observed in the *N*-glycome of human neutrophils was the α 1,6-mannose capped structure (M2F). In addition, an unusual sialo-glycan (FA1G1S1) was also observed in inflamed sputum. Both of these unusual *N*-glycan structures will be investigated in subsequent chapters.
- Paucimannosidic proteins were readily degranulated from stimulated human neutrophils in response to virulent stimuli, suggestive of their potential protective role in neutrophils to combat pathogen infections.
- Paucimannosylated *N*-glycans and proteins demonstrated binding capacity to mannose binding lectin (MBL), a specialised mannose receptor present in inflamed lungs, suggesting the importance of protein paucimannosylation in innate immunity.
- The two human hexosaminidase subunits α and β forming the heterodimeric Hex A ($\alpha\beta$ -subunit), showed high protein sequence homology to the hexosaminidases of paucimannosidic rich organisms, further suggesting the involvement of human Hex A in the generation of human paucimannosylation.
- Genes encoding for enzymes forming the paucimannosylation machinery and the azurophilic granule-specific proteins receiving paucimannosylation were highly expressed in the promyelocytic stage of neutrophils. This indicates that the biosynthetic apparatus for paucimannosidic *N*-glycoproteins is assembled during early neutrophil development in the bone marrow.

- Human Hex A *in vitro* generated paucimannosidic *N*-glycans from complex *N*-glycan intermediates, albeit at a low enzyme kinetic rate. This builds further support for the involvement of this glycosidase in the generation of protein paucimannosylation.
- Human Hex A co-localised with paucimannosidic proteins in the azurophilic granule compartment of resting HL-60 neutrophil-like cells, supporting the involvement of Hex A in the biosynthesis of paucimannosidic *N*-glycoproteins in human neutrophils.

Unresolved questions

- The role of hexosaminidases in the biosynthesis of paucimannosidic *N*-glycoproteins in invertebrates is well established, but their involvement in the biosynthesis of paucimannosidic *N*-glycoproteins *in vivo* in human neutrophils remain unresolved. This aspect will be investigated in **Chapter 3** in this thesis.
- Human neutrophil proteins were shown to carry paucimannosidic *N*-glycans in this chapter, but no significant structural depth was achieved from this system-wide study design. Subsequent chapters in this thesis (**Chapter 4** and **5**) are focused on the deep structural and functional characterisation of some key paucimannosylated glycoproteins from human neutrophils described in this chapter, including the potent serine proteases; nCG and HNE.
- The exact function of paucimannosidic proteins and their contribution towards innate immunity remains unknown. However, this chapter showed that paucimannosylated proteins residing in the azurophilic granule in resting neutrophils can be degranulated and bind to specialised receptors in the extracellular environment. The specific roles of paucimannosylation of HNE will be investigated further in **Chapter 5** of this thesis.
- Neutrophils are part of the wide spectrum of white blood cells arising from myelopoiesis. Protein paucimannosylation in other myeloid and lymphoid immune cells such as platelets and lymphocytes will be investigated in **Chapter 6** of this thesis.

Chapter 3: The role of hexosaminidases in the biosynthesis of paucimannosidic *N*-glycoproteins in human neutrophils

3.1 Rationale

The constitutive production of paucimannosidic *N*-glycoproteins in lower organisms including the invertebrates and plants is well documented, and has been described to be highly dependent on the action of a series of (de)glycosylation enzymes. For example, the glycosyltransferase I (GnT-1), α 1,3/6-mannosidase II and the hexosaminidases within the lumen of the Golgi apparatus (Schachter and Boulianne, 2011). This arrangement of the glycosylation machinery renders these lower organisms able to synthesise large amounts of paucimannosidic *N*-glycoproteins instead of forming the more elongated complex type *N*-glycoproteins typically observed in mammals (Schachter, 2009). The presence of hexosaminidases in human milk (Dudzik et al., 2008) and in immune cells (Casal et al., 2005) has been reported previously. However, the ability of these hydrolases to generate paucimannosidic *N*-glycoproteins within the biosynthetic machinery of human cells has not yet been determined.

In **Chapter 2**, we showed that the human hexosaminidase subunit α and β have protein sequence similarity with the hexosaminidases of multiple paucimannosidic-rich organisms such as the Hex A of *Caenorhabditis elegans*. The co-localisation of human Hex A with azurophilic granule-resident proteins in human promyelocytic leukaemia HL-60 (neutrophil-like) cells was demonstrated. This observation, together with the observation that human Hex A was found to be able to generate paucimannosidic *N*-glycans *in vitro*, suggested that human hexosaminidases may also be involved in the biosynthesis of human paucimannosylation in neutrophils *in vivo*.

Building on these initial observations, the presence and location of hexosaminidases, specifically the Hex A heterodimeric variant ($\alpha\beta$ -subunit), were here first investigated in human neutrophils purified from whole blood by immunocytochemistry. Neutrophils from a *HEXB*^{-/-} individual suffering from a rare lysosomal storage disease, Sandhoff disease (SD), were then investigated through the use of *N*-glycomics and immunoblotting to assess the *N*-glycome in human neutrophils without functional hexosaminidases, relative to healthy neutrophils. The findings from this study were also recapitulated in the legume, *Lotus japonicus*, where hexosaminidase-knockout mutants were investigated as described in **Publication III** attached as supplementary materials enclosed in the DVD. Finally, siRNA-based *HEXA* and *HEXB* silencing of HL-60 cells was performed as a proof-of-concept study, to assess the susceptibility of these neutrophil-like cells to undergo gene manipulation and to test the capacity to modulate the paucimannose-centric glyco-enzymes in this model system.

Chapter 3

This proof-of-concept study facilitates the use of this model system to validate the involvement of Hex A and B in the synthesis of human paucimannosylation in neutrophils and to study the function of protein paucimannosylation in the future.

In this chapter, my supervisor, Dr. Morten Thaysen-Andersen and I were responsible for the study design, data collection and interpretation of the immunocytochemistry of healthy human neutrophils and the *N*-glycome profiling of human neutrophils purified from a SD patient and an age-paired healthy control. The siRNA-based knockdown experiments, data collection and interpretation were performed in collaboration with Dr. Zeynep Sumer-Bayraktar, using hexosaminidase enzyme activity assays and immunoblotting protocols which I implemented and validated.

3.2 Introduction

Hexosaminidases (EC 3.2.1.52) are a class of glycoside hydrolases present in lower organisms such as invertebrates and plants as well as in all higher species including mammals (Mahuran, 1999). This class of hydrolases is responsible for the removal of terminal non-reducing end β -linked GlcNAc and GalNAc residues from various glycoconjugates such as glycoproteins, glycolipids and non-conjugated (free) *N*-glycans (Lemieux et al., 2006). In the *Arabidopsis* genus, the vacuolar hexosaminidase hydrolase, HEXO1, is the main enzyme responsible for the generation of paucimannosidic *N*-glycoproteins that predominately localise in the vacuole of plant cells (Strasser et al., 2007). In mammals, hexosaminidases were mainly reported to be present in the acidic lysosomes and are known to be homo- or hetero-dimeric enzymes depending on the pairing of the α and β subunits (Hex A, $\alpha\beta$; Hex B, $\beta\beta$; Hex S, $\alpha\alpha$). The α and β subunits are encoded by *HEXA* and *HEXB*, respectively (Korneluk et al., 1986). Hex A and Hex B are the major functional hexosaminidase isoenzymes that are relatively well studied in the context of lysosomal storage diseases (LSD) such as Tay-Sachs (TSD) and SD. These diseases are inherited pathologies where the patients lack functional Hex A and Hex B isoenzymes due to mutations in the coding genes for the α and β subunits, respectively. These isoenzymes are clearly critical in the breakdown of gangliosides, in particular in the glycolipid-rich brain, by hydrolysing GM2 gangliosides in neuronal lysosomes to ensure proper neurological development (Matsuoka et al., 2011; Meier et al., 1991). In contrast, Hex S isoenzymes are the minor labile forms that are active in SD but not in TSD individuals. Hex S have also been shown to be involved in the catabolism of glycosaminoglycans in the absence of Hex B (Hepbaldikler et al., 2002).

Although the functional roles of Hex A and Hex B have been well studied in LSD, only few studies have reported on the involvement of Hex A and Hex B in the synthesis and/or degradation of *N*-glycoproteins in human cells including neutrophils. Early studies reported the presence of Hex A/B in the promyelocytic leukemic neutrophil-like cells (Casal et al., 2003; Emiliani et al., 1990a). Treatment of these cells with dimethyl sulfoxide (DMSO) was observed to promote the *in vitro* differentiation and development of these cells to a higher maturation stage which is thought to resemble developing myelocytes. The abundance and activities of Hex A and Hex B were greatly elevated during differentiation (Emiliani et al., 1990c). Altered Hex A and Hex B expression and their activity profiles were also reported in leukemic neutrophils when compared to normal neutrophils (Orlacchio et al., 1986). These

studies suggest that both the Hex A and Hex B may be important in the early cellular and functional development of neutrophils in the bone marrow.

The azurophilic granules within neutrophils are the initial compartments to be synthesised in the bone marrow during the promyelocytic stage of myelopoiesis (Borregaard et al., 2007). Paucimannosidic proteins were suggested to be enriched in these azurophilic granules (**Chapter 2**). Given the importance of Hex A and Hex B in the development of neutrophils, it is important to understand their involvement in the spatio-temporal synthesis of paucimannosidic *N*-glycoproteins residing predominantly in the azurophilic granules.

In this chapter, the localisation of Hex A in human neutrophils, the *N*-glycome profile and therefore the degree of paucimannosylation of neutrophils isolated from a SD patient and an age-paired healthy donor were determined. A pilot study assessing the utility of siRNA to reduce the *HEXA* and *HEXB* gene expression in neutrophil-like cells *in vitro* was also performed as a proof-of-concept of genetically manipulating hexosaminidases. This is to facilitate future studies to investigate the function and the involvement of these isoenzymes in the synthesis of paucimannosidic *N*-glycoproteins.

3.3 Materials and Methods

3.3.1 Isolation of blood-derived human neutrophils for immunocytochemistry

Human resting neutrophils were isolated from the peripheral blood of a single healthy adult male donor after informed consent was obtained. The collection, handling and biomolecular analysis of healthy human neutrophils were approved by the Human Research Ethics Committee at Macquarie University, Sydney, Australia (Reference no. 5201500409). Neutrophils were isolated from 40 ml freshly drawn blood collected in EDTA anti-coagulant tubes. The neutrophils were isolated by laying 20 ml of peripheral blood on top of polymorphprep separation media (Axis Shield, Norway) in a 1:1 ratio in a 50 ml falcon tube at room temperature. A polymorphprep density gradient was chosen, rather than a dextran/ficoll density gradient, since the former has been shown to give a high isolation yield and purity of resting neutrophils (Zhou et al., 2012). Layered blood was centrifuged at 550g for 35 min at 20°C with no brakes using a swing bucket centrifuge (Sigma-Aldrich). After centrifugation, the plasma and the buffy coat were carefully removed using a disposable Pasteur pipette. The neutrophil layer, located on top of the red blood cell layer was transferred

to a fresh 15 ml falcon tube. 5 ml cold sterile filtered 0.9% (v/v) sodium chloride and 5 ml cold sterile filtered high purity (MilliQ) water was added to restore tonicity. Cells were centrifuged for 6 min at 400g, 4°C with brakes and the supernatant was removed. Cell pellet was resuspended in cold sterile filtered MilliQ water and vortexed for 30 s to lyse the remaining erythrocytes. After hypotonic lysis, neutrophils were centrifuged again for 6 min at 400g, 4°C with brakes and resuspended in sterile filtered Hanks' balanced salt solution (HBSS) (5.4 mM KCl, 0.3 mM Na₂HPO₄, 0.4 mM KH₂PO₄, 4.2 mM NaHCO₃, 137 mM NaCl, 5.6 mM D-(+)-glucose, pH 7.4). Neutrophil counts and viabilities were determined using a Muse cell analyser (Merck-Millipore, Australia). The neutrophil population purity was estimated based on Wright-Giemsa stained cells prepared using a cytospin centrifuge (Thermo Scientific). Upon isolation, the neutrophils were used immediately for immunocytochemistry experiments.

3.3.2 Immunocytochemistry

Purified human neutrophils were cyto-centrifuged on 99% (v/v) ethanol/1% (v/v) hydrochloric acid-cleaned glass coverslips (12 mm diameter) using a cytospin centrifuge (Thermo Scientific, Australia). Coverslips were then placed in a 12 well cell culture plate and fixed with 300 µl of 4% (v/v) paraformaldehyde for 15 min at room temperature. Coverslips were then washed three times with 1x phosphate buffered saline (PBS). Membrane permeabilisation was performed with 300 µl 0.2% (v/v) Triton X-100 in 1x PBS for 10 min at room temperature. Coverslips were washed three times with 1x PBS before blocking was performed with 10% (v/v) fetal calf serum (FCS) in 1x PBS for 1 h at room temperature. Following blocking, the coverslips were stained overnight at 4°C with rabbit IgG anti-human Hex A (1:300), mouse IgG anti-human myeloperoxidase (1:2000), mouse IgG anti-human CD63 (1:300) (all from Santa Cruz Biotechnology, U.S.A) or paucimannose-recognising Mannitou IgM (undiluted concentration, kind gift from Dr. Simone Diestel, University of Bonn, Bonn, Germany) primary antibodies. Mannitou has been shown previously to be reactive towards paucimannosidic *N*-glycans (Zipser et al., 2012). After overnight incubation, washes with 1x phosphate buffered saline (PBS) were performed three times on the coverslips with occasional shaking at 5 min interval to remove unbound antibodies before secondary antibodies compatible with the corresponding host-specific primary antibodies (as described above) was applied using goat anti-rabbit IgG Alexa Fluor 488 (1:400), goat anti-mouse IgG Alexa Fluor 546 (1:400) or goat anti-mouse IgM Alexa Fluor 488 (all from Life Technologies, Australia) for 1 h at room temperature. Washes with 1x PBS were performed three times

directly on the coverslips to remove unbound antibodies. Coverslips were mounted on 99% (v/v) ethanol/1% (v/v) hydrochloric acid-cleaned glass slides using Prolong Gold antifade mountant with double stranded DNA (dsDNA)-specific DAPI (Life Technologies). Images were taken using Olympus FV-1000. Co-localisation was evaluated semi-quantitatively with iMaris (Bitplane, Germany) using Mander's co-localisation coefficients (Dunn et al., 2011). The specificity of anti-Hex A antibodies was validated by immunoblotting using recombinant human Hex A (R & D Systems, Australia).

3.3.3 *N*-glycan release of SD and healthy age-paired neutrophils

Protein extracts derived from isolated neutrophils from a two year old SD infant and a four year old (age-paired) healthy donor were kindly provided by Prof. Meral Ozguc, Hacettepe University, Turkey with ethics approval and patient consent obtained at the clinic. Neutrophils were isolated using Histopaque (Density: 1.077 g/ml, Sigma-Aldrich) and 3% (v/v) dextran (Sigma Aldrich) in 0.15 M sodium chloride. Protein extracts were obtained by cell lysis of the purified neutrophils in lysis buffer (10 mM Tris, 300 mM NaCl, 2 mM EDTA, 0.5% (v/v) Triton X-100, pH 7.4) supplemented with protease inhibitors (Roche). The total protein concentrations were determined using bicinchoninic acid assay (BCA) (Thermo Scientific), which were used to normalise the amount of protein for the de-*N*-glycosylation experiments. Proteins disulphide bonds were reduced with 10 mM dithiothreitol (DTT) (final concentration) at 56°C for 45 min and alkylated with iodoacetamide (IAA) at room temperature in the dark for 30 min. *N*-glycans were released from immobilised proteins as previously described (Jensen et al., 2012). Approximately 20 µg reduced and alkylated protein extract was dot blotted on ethanol activated polyvinylidene fluoride (PVDF) membranes and left overnight to dry to ensure maximum protein adhesion. The membrane was stained with Direct blue 71 (Sigma-Aldrich) to enable visualisation and accurate excision of the protein spots for enzymatic *N*-glycan release in a flat bottom 96-well plate. To prevent non-specific binding of *N*-glycosidase F, the excised membrane spots were blocked with 1% (w/v) polyvinylpyrrolidone (PVP) 40 and washed with water before application of the enzyme. *N*-glycans were released by overnight incubation with *N*-glycosidase F (3 U in 10 µl water) at 37°C. Released *N*-glycans were recovered in Eppendorf tubes (Eppendorf) after sonication of the 96-well plate for 5 min. The wells were later washed two times with water and all wash fractions were pooled. Samples were incubated with 100 mM ammonium acetate, pH 5 at room temperature for 1 h to remove the glycosylamines from the reducing terminus of the *N*-

glycosidase F released glycans to allow for quantitative reduction as described below and then dried in a vacuum centrifuge. *N*-glycans from bovine fetuin (Sigma-Aldrich) were used as positive controls to test the glycan release and subsequent glycan purification protocol.

3.3.3.1 Reduction and desalting of *N*-glycans

The dried glycans were reduced to alditols with 0.5 M NaBH₄ in 50 mM KOH for 3 h at 50°C. Reactions were quenched by adding 2 µl glacial acetic acid. Desalting of reduced *N*-glycans was performed using AG 50W X8 strong cation exchange resin (200-400 mesh) (Bio-Rad) (30 µl bed volume) packed in C18 stage tips (Merck-Millipore) and dried in a vacuum centrifuge. Samples were washed three times with 100% (v/v) methanol (analytical grade) to evaporate residual borate.

3.3.3.2 *N*-glycan clean up

The dried samples were reconstituted with water and subjected to PGC-SPE manually packed on top of C18 stage tips (Merck-Millipore) before the downstream analysis by LC-MS/MS. The desalted glycans were eluted from the PGC-SPE tips using 40% (v/v) acetonitrile containing 0.05% (v/v) TFA. The eluate fractions were dried in a vacuum centrifuge, kept at -20°C and only redissolved in 10 µl of MilliQ water just before LC-MS/MS analysis.

3.3.3.3 PGC LC-MS/MS of *N*-glycans

The purified *N*-glycans were separated by capillary PGC (Hypercarb KAPPA capillary column, 180 µm inner diameter x 100 mm length, 5 µm particle size, 200 Å, Thermo Scientific, Australia) using an Agilent 1260 Infinity HPLC instrument. The glycan separation was carried out over a linear gradient of 0-45% (v/v) acetonitrile/10 mM ammonium bicarbonate for 85 min at a constant flow rate of 2 µl/min. Glycans were ionised using ESI and detected using a 3D (Paul) IT mass spectrometer (LC/MSD Trap XCT Plus Series 1100, Agilent Technologies, Australia). The full scan acquisition range was kept constant at *m/z* 200-2,200 in negative ionisation polarity mode. Data-dependent acquisition was enabled where the top three most abundant precursors in each full scan spectrum were selected for MS/MS using resonance activation CID fragmentation. CID was performed with smart fragmentation (start/end amplitude 30-200%) at 1.0 V and an isolation window of 4 Th with a maximum accumulation time of 200 ms. Smart ion charge control (ICC) was enabled with a smart parameter setting target of *m/z* 900. ESI was performed using a capillary voltage of +3.2 kV, a nitrogen drying gas flow of 6 l/min at 325°C, and a nitrogen-based nebuliser pressure of

12 psi. Dynamic exclusion was inactivated over the entire LC-MS/MS acquisition. The mass spectrometer was calibrated using a tune mix (Agilent Technologies) and the mass accuracy of the precursor and product ions were typically better than 0.5 Da.

3.3.3.4 Data analysis of released *N*-glycans

The glycan structures were analysed using Bruker DataAnalysis software version 4.0 (Bruker Daltonics, Germany). Throughout the thesis chapters, characterisation of the individual *N*-glycans was based on the monoisotopic precursor mass, glycan fragment ions in the corresponding CID-MS/MS spectra were annotated according to the nomenclature by Domon and Costello (Domon and Costello, 1988) and their retention time (RT) on PGC. We have extensive in-house knowledge of the PGC-LC retention patterns for reduced *N*-glycans and this parameter is often used as a powerful orthogonal identifier in addition to MS and MS/MS (Everest-Dass et al., 2013a; Harvey, 2005c; Stadlmann et al., 2008). Throughout the thesis chapters, the *N*-glycans are depicted according to the established symbol nomenclature and conventions based on the Essentials of Glycobiology (Varki et al., 2015).

3.3.4 Visualising glycoprotein features of neutrophil cell lysates via immunoblotting

Protein extracts derived from neutrophil lysates (~10 µg) were separated on a 4-12% sodium dodecyl sulphate-polyacrylamide gel electrophoresis (SDS-PAGE) under reducing conditions (Life Technologies). The gel separated proteins were transferred to a PVDF membrane (Bio-Rad) for immunoblotting with Trans-Blot Turbo (Bio-Rad), blocked with 3% (w/v) bovine serum albumin (BSA) in Tris buffered saline with 0.1% (v/v) Tween 20 (TBST) for 1 h at room temperature. The membrane was then incubated overnight with paucimannose-recognising IgM (called “Mannitou”) primary antibodies at 4°C. Mannitou is reactive towards paucimannosidic *N*-glycans (Zipser et al., 2012). The membrane was washed three times with TBST to remove unbound antibodies. Horse radish peroxidase (HRP)-conjugated anti-mouse IgM (1:3000) was applied to the membrane for 1 h at room temperature. Washes were performed with TBST and visualisation was performed using the chemiluminescence channel on the ChemiDoc MP system (Bio-Rad) upon application of the HRP chemiluminescent substrate (Bio-Rad). Glyceraldehyde 3-phosphate dehydrogenase (GAPDH) was used as a control for equal protein loading.

3.3.5 Culture conditions for HL-60 neutrophil-like cells

HL-60 cells isolated from an acute promyelocytic leukaemia patient (Gallagher et al., 1979) was obtained from the American Type Culture Collection (ATCC) (ATCC CCL-240). The cells were mycoplasma-free as evaluated using MycoAlert mycoplasma detection kit (Lonza). Cells were grown in Roswell Park Memorial Institute (RPMI) medium supplemented with 2 mM L-glutamine without FCS and phenol red (Life Technologies) in a humidified incubator equilibrated with 5% (v/v) CO₂ at 37°C. Cells were washed two times in supplemented RPMI medium before transfection.

3.3.6 *HEXA* and *HEXB* gene silencing

Undifferentiated HL-60 cells (4×10^5 cells) were transfected using commercially prepared siRNA targeting exon 7 of *HEXA* (AM16708) and exon 3 and 4 of *HEXB* (AM16708) (All from Life Technologies). The siRNA probes were used at various quantities (75 pmol, 100 pmol and 150 pmol) on either pre-plated or non-pre-plated cells. Lipofectamine 3000 or siPORT (all from Life Technologies) were used as transfection reagents. siRNA transfection-free control cells undergoing the same treatment were included to test the transfection efficiency. The pre-plated cells were transfected for 24 h after pre-plating in 24 well cell culture plates. The medium (~700 µl) was removed prior to the addition of the transfection reagents in supplemented RPMI. Alternatively, the transfection reagents were added directly to the non-pre-plated cells. Cells were incubated in a humidified incubator equilibrated with 5% (v/v) CO₂ at 37°C during transfection and were harvested 48 h post transfection.

3.3.7 Hexosaminidase activity assay

Protein extracts were obtained from harvested cells using a lysis buffer (10 mM Tris, 300 mM NaCl, 2 mM EDTA, 0.5% (v/v) Triton X-100, pH 7.4) supplemented with a cocktail of protease inhibitors (Roche). The activity assay was adopted from a published protocol (Wendeler and Sandhoff, 2009), but was slightly modified. In short, 15 µl of protein extract (~1 µg) was incubated with 30 µl pre-warmed 4-methylumbelliferyl-2-acetamido-2-deoxy-β-D-glucopyranoside (MUG) or 4-methylumbelliferyl-6-sulfo-N-acetyl-β-D-glucosaminide (MUGS) (All from Merck Millipore) for 30 min at 37°C in phosphate citrate buffer. The reactions were stopped by the addition of 0.25 M glycine carbonate stop buffer, pH 10. Recombinant Hex A and Hex B proteins (RnD Systems) were used as positive controls for the hexosaminidase activity and to ensure that reagents and the protocols were working. The release of 4-methylumbelliferone (4-MU) upon MUG/MUGS-based hydrolysis was quantified using a fluorometer plate reader (BMG Technologies) with an excitation at 360 nm

and emission at 450 nm. The release of fluorogenic 4-MU was determined by comparison to a premade standard curve performed using a known amount of 4-MU standards (Sigma-Aldrich) after blank correction to the stop buffer.

3.3.8 Quantitative real-time polymerase chain reaction (qPCR)

The specificity of the qPCR amplification of *HEXA* and *HEXB* genes in non-transfected HL-60 cells with the designed primers shown in Supplementary Materials, Table S1 enclosed in the DVD, was assessed using melting curve analysis. Total RNA was purified from the cells using an RNA isolation kit (Bioline) according to the manufacturer's instructions and was quantified using a Nanodrop spectrophotometer (Thermo Scientific) at $A_{260\text{nm}}/280\text{nm}$. cDNA synthesis was performed using Tetro cDNA synthesis kit (Bioline) according to the manufacturer's instructions. qPCR and melting curves were performed using SensiFAST SYBR green (Bioline) on a LightCycler 480 (Roche) using the designed primers with the following conditions: 95°C for 5 min equilibration followed by 95°C for 15 s, 60°C for 30 s and 72°C for 30 s repeated for 40 cycles.

3.4 Results

The initial observations indicated co-localisation of human Hex A and MPO, an azurophilic granule protein marker, in DMSO-differentiated HL-60 myeloid leukaemia cells, which resemble mature human neutrophils morphologically and functionally (**Chapter 2**). Immunocytochemistry also revealed the co-localisation of paucimannosidic proteins and human Hex A in these neutrophil-like cells. These observations in conjunction with the known involvement of hexosaminidases in paucimannose-rich lower organisms suggested that human Hex A is involved in the biosynthesis of protein paucimannosylation in human neutrophils. However, differentiated HL-60 is a promyelocytic leukaemia cell line cultured *in vitro* and these cells may not reflect the actual *in vivo* physiology and behaviour of healthy human neutrophils maturing in the bone marrow and in the blood circulation upon full maturation.

3.4.1 Immunocytochemistry of human neutrophils

In order to assess the presence of Hex A in healthy human neutrophils, peripheral blood neutrophils were isolated from whole blood of a healthy male adult donor by density gradient separation followed by immunocytochemistry using antibodies with reactivity towards human Hex A, MPO, CD63 and paucimannosidic glycoepitopes (Zipser et al., 2012). The resulting signals were then evaluated quantitatively in a spatial manner to estimate the degree of co-

localisation of the proteins and glycoepitopes of interest within the multiple compartments of human neutrophil. The immunocytochemistry demonstrated some co-localisation of human Hex A (green) and human MPO (red) as shown by the existence of yellow pixels (**Figure 1A**). MPO is a well-established azurophilic granule protein in resting neutrophils (Okada et al., 2015). More quantitative co-localisation analysis using the so-called Mander's co-localisation coefficient (MCC) revealed a moderate degree of co-localisation of Hex A and MPO with an MCC of 0.82 ± 0.07 . MCC values of 1 are indicative of perfect co-localisation between two analytes. To further support this observation, resting neutrophils were stained with antibodies directed towards Hex A (green) and CD63 (red), another azurophilic granule marker that is well documented to be highly expressed on the luminal side of the membrane of azurophilic granules (Calafat et al., 2000) (**Figure 1B**). Semi-quantitative co-localisation analysis demonstrated a moderate-to-high co-localisation of Hex A and CD63 yielding an MCC of 0.94 ± 0.02 . Moderate co-localisation was also observed when resting neutrophils were stained with paucimannose-recognising antibodies Mannitou (green) and human Hex A (red) as demonstrated by the MCC of 0.91 ± 0.05 (**Figure 1C**). These observations indicated that human Hex A and the paucimannosidic proteins reside in azurophilic granules within resting human neutrophils. The potential localisation of these analytes in other neutrophil granules awaits further investigation.

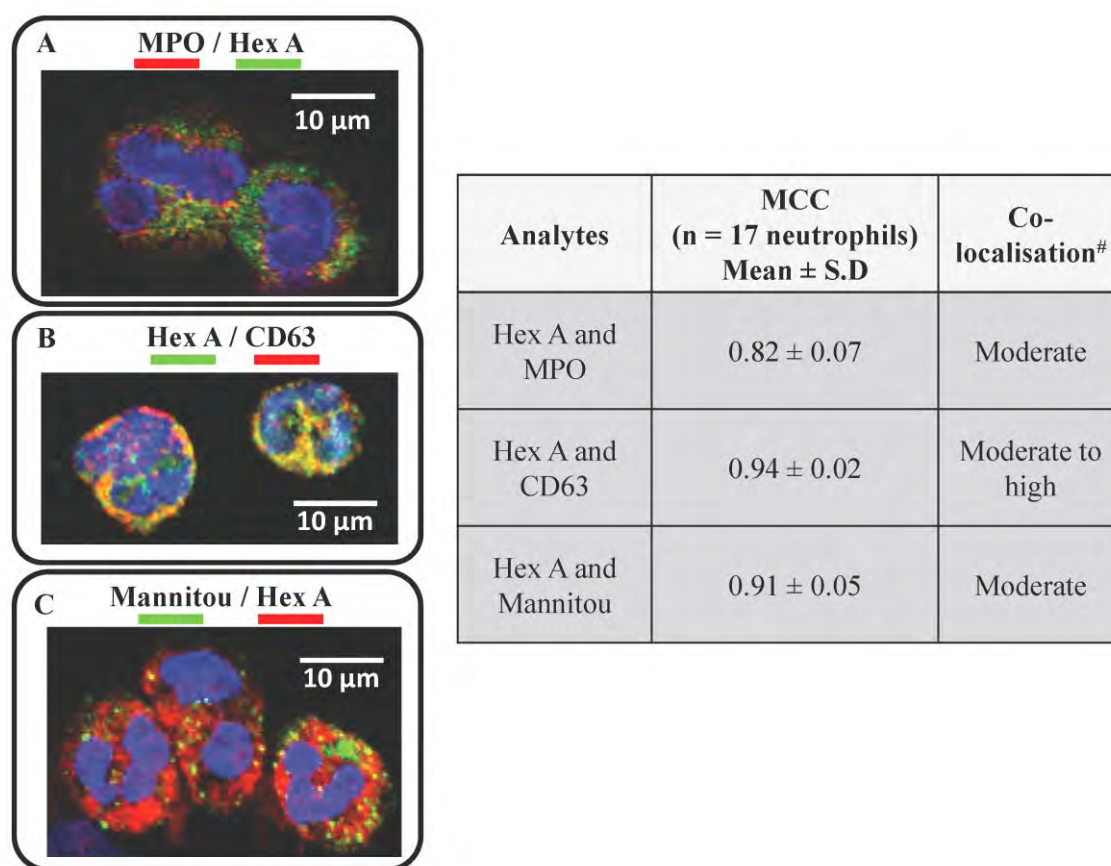


Figure 1. Immunocytochemistry of resting neutrophils from a healthy human donor was performed to assess the subcellular location of Hex A and paucimannosylated proteins in the azurophilic granule. Representative image of neutrophils stained with (A) anti-human myeloperoxidase (MPO) (red) and anti-human Hex A (green), (B) anti-human Hex A (green) and anti-human CD63 (red), and (C) anti-paucimannose (Mannitou) (green) and anti-human Hex A (red) antibodies. The characteristic nuclei of the human resting neutrophils were stained with DAPI (blue). The scale bar represents 10 µm. The table shows the MCCs of the assessed analytes. MCC values of 1 indicate perfect co-localisation (data points are given as mean MCC ± S.D, n = 17 neutrophils). # The degree of co-localisation for each of these analytes was estimated as a more qualitative measure (Zinchuk et al., 2013).

Having confirmed the subcellular location of Hex A in resting neutrophils, the enzymatic capacity of this hydrolase to generate paucimannosidic *N*-glycoproteins in neutrophils was investigated next. SD patients harbour gene mutations in the *HEXB* gene, resulting in defects in the β-subunits required for the formation and catalytic activity of both the Hex A (αβ) and Hex B (ββ) isoenzymes (Mahuran, 1999). The lack of any significant Hex A and Hex B catalytic activity has been described to result in an accumulation of GM2 gangliosides, in particular in the glycolipid-rich brain. Patients have been found to display severe neurological abnormalities that cause mental retardation and early death (Kobayashi et al., 1992).

However, the degree of protein paucimannosylation present in the neutrophils of these patients has not yet been reported. Neutrophils isolated from SD patients are, as such, ideal to study the contribution of Hex A and Hex B in the generation of paucimannosylated *N*-glycoproteins as both isoenzymes are inactive. To assess the degree of paucimannosylation in SD neutrophils, we were fortunate to obtain protein extracts of circulating neutrophils from a two year old infantile SD patient genotyped with an intronic mutation of *HEXB* (IVS11+5G>A) and from a four year old healthy individual which was included in the study as an age-paired control. This *HEXB* mutation resulted in a homozygous null-functional genotype (*HEXB*^{-/-}) as confirmed by a negligible total Hex A and Hex B enzyme activity in the SD patient relative to the healthy donor (*HEXB*^{-/-} patient: Hex A, 45 nmol/h/mg; Hex B, 40 nmol/h/mg; healthy control: 1223 nmol/h/mg). The *N*-glycans were released from these total protein lysates and then analysed using *N*-glycomics.

3.4.2 *N*-glycome profiling of neutrophils from a healthy donor and a SD patient

The *N*-glycans from proteins of neutrophil lysates were released using *N*-glycosidase F and the glycans were analysed using PGC-LC-ESI-CID-MS/MS (**Figure 2**). The monosaccharide compositions, the glycosidic linkages, branching and other structural features of the observed glycans were assigned based on manual interpretation of the PGC-LC retention, MS and MS/MS data based on the identification of diagnostic fragmentation ions (Everest-Dass et al., 2013a; Harvey, 2005a, b, c). Some structural aspects were inferred based on the established knowledge of human *N*-glycosylation and the biosynthetic relatedness between the observed glycoforms (Aebi, 2013; Winchester, 2005) as well as from previous observations made from the previous *N*-glycome profiling of purified neutrophil lysates and inflamed/pathogen-positive sputum (**Chapter 2**).

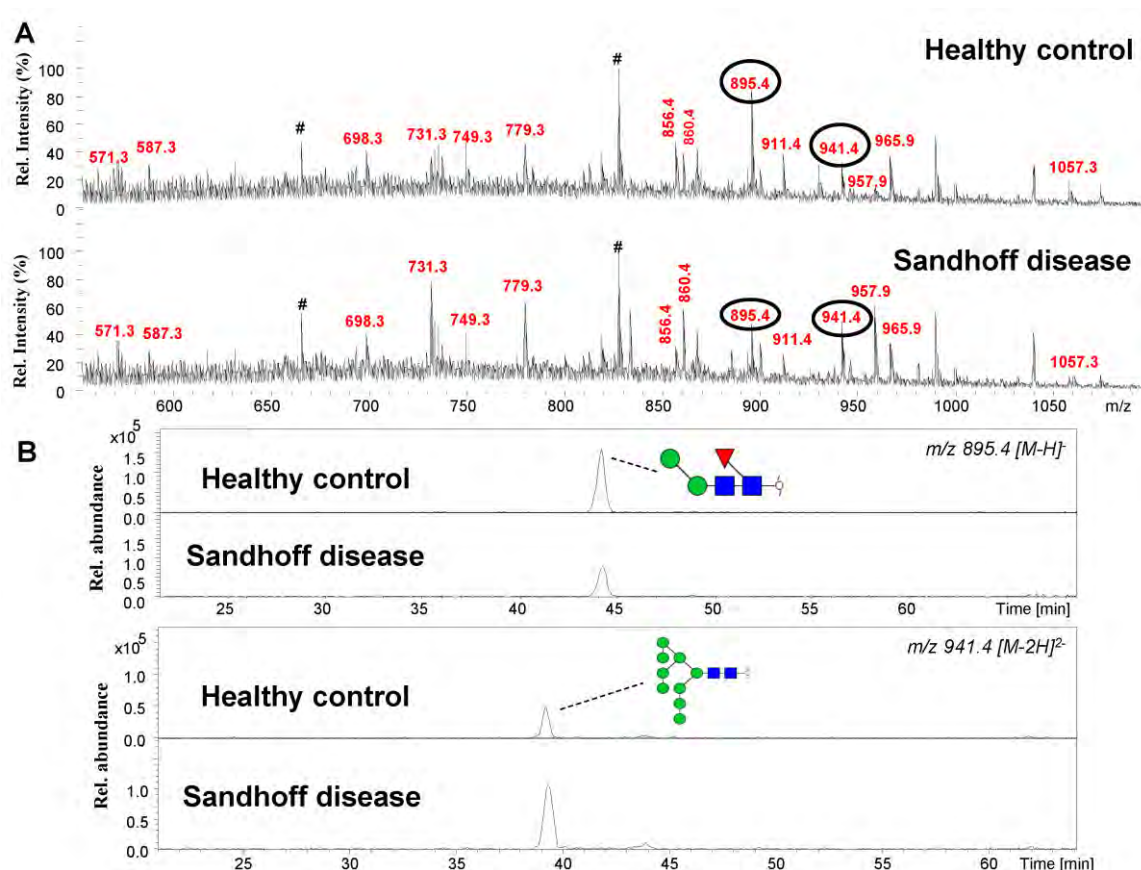


Figure 2. (A) Representative PGC-LC negative ion MS profiles of the *N*-glycans released from neutrophil lysates of a healthy donor (top spectrum) and a SD patient (bottom spectrum). Precursor masses highlighted in bold and red corresponded to the *N*-glycans that were altered in SD relative to the healthy donor neutrophils. # denotes contaminant peaks. (B) Representative extracted ion chromatograms (EICs) of the precursor masses circled in panel A demonstrating the quantitative differences of the M2F paucimannosidic (top EICs) and M9 high mannose isomers (bottom EICs) between healthy donors and SD neutrophils. Intensity scales were normalised between samples to directly show the quantitative differences. Details of the glycan structures and the relative abundances of the observed *N*-glycan types are shown in Table 1 and Figure 3.

Table 1. Overview of the structural assignments and relative abundances of *N*-glycans released from the whole neutrophil lysates of a healthy donor and a SD patient.

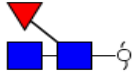
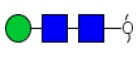
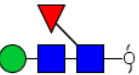

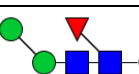
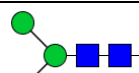

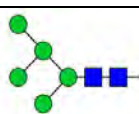
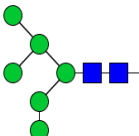
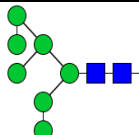
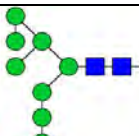
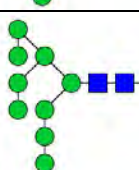
| Glycan type, short-hand nomenclature and proposed structures of observed <i>N</i> -glycans | | Observed mass (<i>m/z</i>) | | Relative abundance (%) | |
|--|---|------------------------------|-------------------------------|--|--|
| | | [<i>M-H</i>] ¹⁻ | [<i>M-2H</i>] ²⁻ | Healthy age-paired donor (<i>n</i> = 3 technical replicates, mean ± S.D) | SD patient (<i>n</i> = 3 technical replicates, mean ± S.D) |
| Truncated chitobiose core / Paucimannose | M0F  | 571.3 | | 4.8 ± 0.7 | 3.8 ± 0.1 |
| | M1  | 587.3 | | 1.4 ± 0.2 | 0.8 ± 0.1 |
| | M1F  | 733.3 | | 4.4 ± 0.2 | 4.2 ± 0.2 |
| | M2  | 749.3 | | 4.6 ± 0.2 | 2.4 ± 0.1 |
| | M2F  | 895.5 | | 20.0 ± 0.8 | 6.8 ± 0.5 |
| | M3  | 911.4 | | 3.8 ± 0.2 | 0.9 ± 0.1 |
| | M3F  | 1057.3 | | 2.0 ± 0.3 | 0.3 ± 0.1 |
| High Mannose | M5  | 1235.6 | | 3.1 ± 0.2 | 1.8 ± 1.3 |
| | M6  | | 698.3 | 5.8 ± 0.6 | 6.0 ± 0.8 |
| | M7  | | 779.4 | 6.9 ± 1.0 | 8.0 ± 0.4 |
| | M8  | | 860.4 | 5.3 ± 1.4 | 11.6 ± 0.9 |
| | M9  | | 941.4 | 6.0 ± 1.4 | 10.8 ± 1.8 |

Table 1 (Continued). Overview of the structural assignments and relative abundances of *N*-glycans released from the whole neutrophil lysates of a healthy donor and a SD patient.

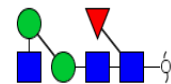
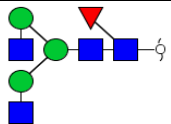
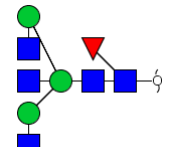
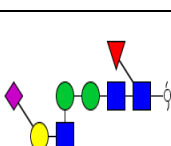
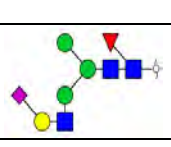
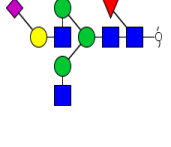
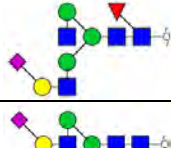
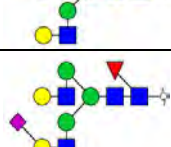

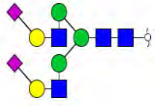
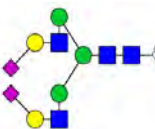
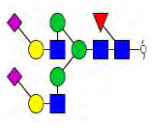
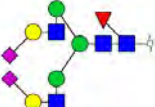
| Glycan type, short-hand nomenclature and proposed structures of observed <i>N</i> -glycans | | Observed mass (<i>m/z</i>) | | Relative abundance (%) | |
|--|---|------------------------------|----------------------|--|--|
| | | [M-H] ¹⁻ | [M-2H] ²⁻ | Healthy age-paired donor (n = 3 technical replicates, mean ± S.D) | SD patient (n = 3 technical replicates, mean ± S.D) |
| Complex | M2F + (GlcNAc)  | 1098.6 | | 0.4 ± 0.1 | 6.5 ± 0.7 |
| | M3F + (GlcNAc) ₂  | | 731.3 | 4.0 ± 1.4 | 9.2 ± 0.3 |
| | Bisecting core fucosylated  | | 832.9 | 3.3 ± 3.0 | 6.0 ± 0.8 |
| | Bimannosyl-chitobiose core monoantennary core fucosylated monosialylated  | | 775.3 | 1.0 ± 0.2 | 0.7 ± 0.1 |
| | FA1G1S1  | | 856.4 | 7.4 ± 0.6 | 2.9 ± 0.3 |
| | FA2G1S1  | | 957.9 | | 6.7 ± 0.4 |
| | FA2G1S1  | | | | 1.7 ± 0.2 |
| | A2G2S1  | | 965.9 | 5.0 ± 0.6 | 2.8 ± 1.2 |
| | FA2G2S1  | | 1038.9 | 2.6 ± 0.7 | 3.3 ± 0.2 |

Table 1 (Continued). Overview of the structural assignments and relative abundances of *N*-glycans released from the whole neutrophil lysates of a healthy donor and a SD patient.

| Glycan type, short-hand nomenclature and proposed structures of observed <i>N</i> -glycans | | | Observed mass (m/z) | | Relative abundance (%) | |
|--|---------|--|-------------------------|---------------|---|---|
| | | | $[M-H]^{-1}$ | $[M-2H]^{-2}$ | Healthy age-paired donor ($n = 3$ technical replicates, mean \pm S.D) | SD patient ($n = 3$ technical replicates, mean \pm S.D) |
| Complex | A2G2S2 |  | | 1111.5 | 6.6 \pm 0.4 | 2.1 \pm 0.1 |
| | A2G2S2 |  | | | 0.7 \pm 0.8 | 0.3 \pm 0.2 |
| | FA2G2S2 |  | | 1184.5 | 0.8 \pm 0.1 | 0.7 \pm 0.5 |
| | FA2G2S2 |  | | | 0.1 \pm 0.1 | 0.4 \pm 0.3 |

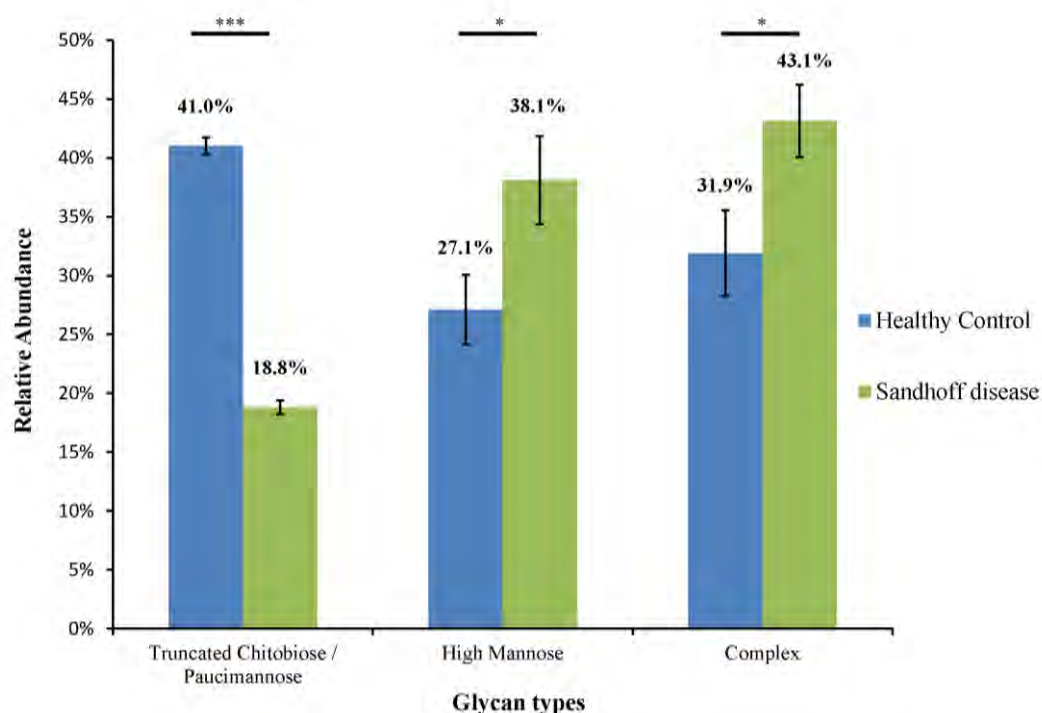


Figure 3. Relative abundance of the three *N*-glycan types identified in neutrophils isolated from a healthy donor and a SD patient (mean \pm S.D, $n = 3$ technical replicates). * denotes $P < 0.05$, *** denotes $P < 0.001$ using two-tailed paired student's T tests.

Paucimannosidic, high mannose and complex type *N*-glycans were observed spanning 22 monosaccharide compositions and a total of 27 *N*-glycan structures. The relative abundances of the observed *N*-glycans were estimated based on their relative EIC peak areas from a triplicate *N*-glycan release and analysis ($n = 3$) from neutrophils from an infant SD patient and an age-paired healthy donor, **Table 1**. The distribution of the three *N*-glycan types is summarised in **Figure 3**. In the neutrophils from the healthy donor, truncated chitobiose core and paucimannosidic *N*-glycans were the most abundant structures (41.0%), followed by complex (31.9%) and high mannose (27.1%) type structures. The M2F paucimannosidic *N*-glycan was the most abundant glycan within the class of paucimannosidic structures (~20% of the total *N*-glycome). Even distribution of the high mannose glycoforms (i.e. M5 – M9) were observed while the presence of an unusual sialo-glycan complex type structure (FA1G1S1) carrying $\alpha 2,6$ -linked sialic acid residues appeared to be highly abundant within the class of complex structures (~7.4% of the total *N*-glycome).

The class of truncated chitobiose/paucimannosidic *N*-glycans were significantly reduced in SD neutrophils (18.8%) compared to the healthy donor (41.0%) ($P < 0.001$). Specifically, the

chitobiose structure M0F and paucimannosidic structures with or without α 1,6 core fucosylation i.e. M1(F) - M3(F) were all observed to be significantly reduced in the SD patient relative to the healthy control ($P < 0.05$). The high mannose type structures were significantly higher in SD (38.1%) compared to healthy donor neutrophils (27.1%) ($P < 0.05$). The complex *N*-glycans were also significantly more abundant in SD compared to healthy neutrophils ($P < 0.05$). The higher relative abundance of these structures could be attributed to the altered abundance of the GlcNAc-capped biosynthetic precursors for the paucimannosidic structures i.e. M2F(GlcNAc) and M3F(GlcNAc)₂, **Table 1**. These precursors were considered as complex type structures in this study as these intermediates *per se* do not fall under the definition of paucimannosidic or high mannose structures. The complex type FA2G1S1 observed in SD neutrophils was absent in the healthy neutrophils. In addition, the FA1G1S1 and A2G2S2 isomers appeared in significantly lower levels in SD relative to healthy neutrophils ($P < 0.05$). These complex type structures are discussed further in the following sections.

To confirm these glycomics-based observations, immunoblotting was performed with a paucimannose-recognising antibody, Mannitou, which has reactivity towards paucimannosidic epitopes (Zipser et al., 2012). **Figure 4** shows the immunoblot of the cell lysates of healthy and SD neutrophils probed with Mannitou. The chemiluminescence revealed an intense staining of a single protein band (70-80 kDa) in the healthy neutrophil lysate. Protein bands at similar molecular masses were also observed in the SD neutrophil lysates, but at a much lower (~12 fold) intensity after equal protein loading in the gel lanes. The loading control utilising antibodies towards a housekeeping protein, GAPDH, that was not expected to be altered in SD, revealed the presence of a single protein band at ~37 kDa, consistent with the molecular mass of GAPDH. The similar intensity of the GAPDH bands validated the equal protein loading across the gel lanes.

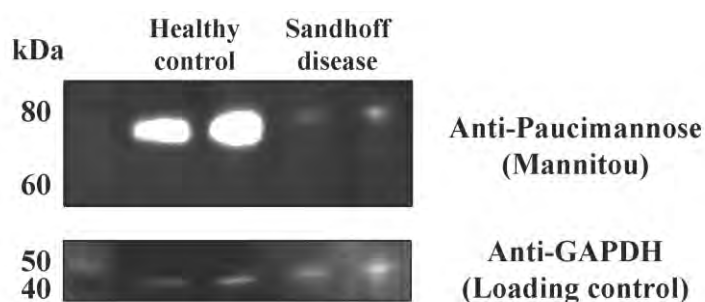


Figure 4. Immunoblot of protein extracts of neutrophils of a healthy donor and a SD patient probed with anti-paucimannose (Mannitou) (upper gel region) and anti-GAPDH antibodies (lower gel region). Samples were analysed in duplicate lanes and visualised using chemiluminescence.

Paucimannosylation in human neutrophils has been observed in bacterial-colonised inflamed sputum and in other inflammatory and even cancerous conditions as we have summarised in the literature review (**Chapter 1, Publication I**). Thus, human paucimannosylation in neutrophils was hypothesised to be functionally involved in innate immunity (**Chapter 2**). The downstream functional consequences of hexosaminidase deficient neutrophils with respect to their abilities to mount an effective immune response were studied. Specifically, attempts were made to manipulate the genes encoding the hexosaminidases using siRNA in order to use the *HEXA/HEXB* silenced neutrophil-like cells for functional studies. The siRNA-based silencing of *HEXA/HEXB* of HL-60 cells was assessed using a hexosaminidase activity assay as a proxy to determine successful gene manipulation.

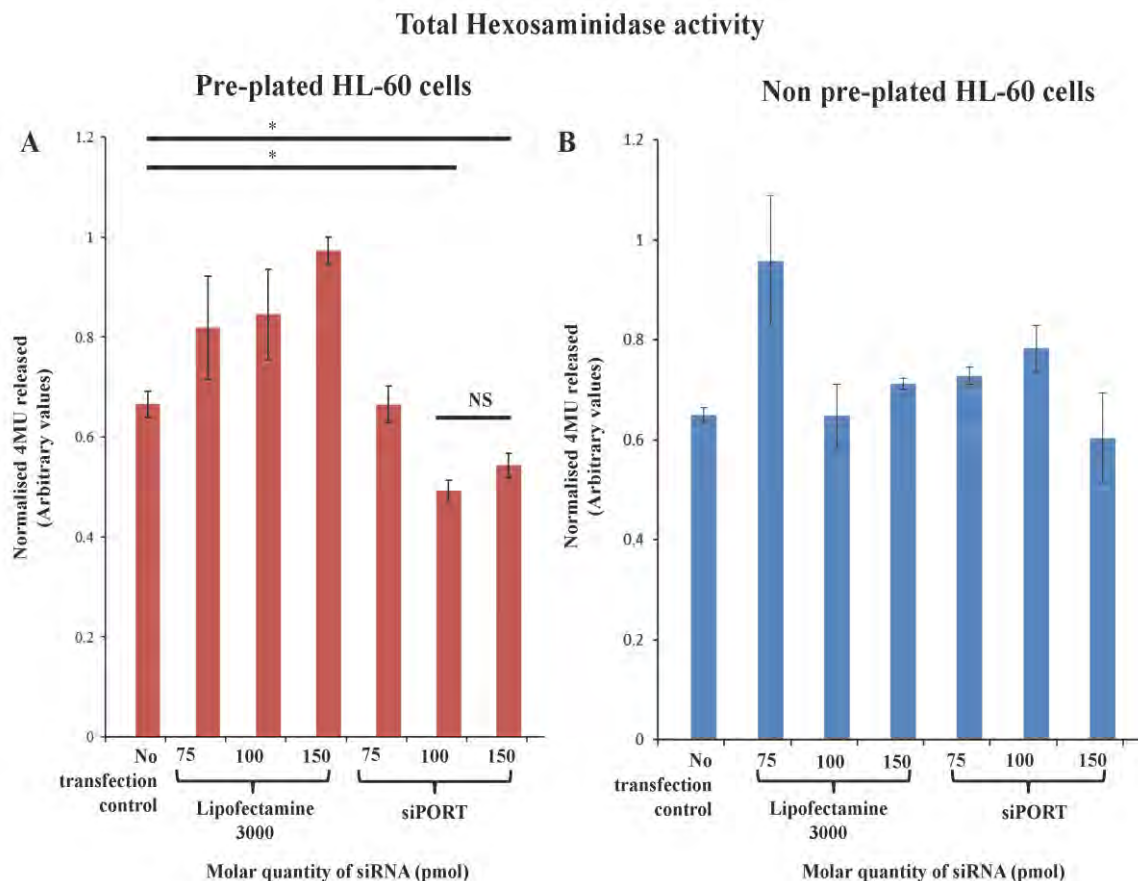


Figure 5. Total hexosaminidase activity of pre-plated (**A**) and non-pre-plated (**B**) HL-60 cells transfected with siRNA targeting both *HEXA* and *HEXB*. Various quantities of siRNA were tested i.e. 75 pmol, 100 pmol and 150 pmol using either lipofectamine 3000 or siPORT as the transfection reagent. The level of fluorogenic 4-MU was used as a proxy for the total hexosaminidase activity based on the hydrolysis of MUG substrates added to the cell lysates. The specific activity of total hexosaminidases activity was not assessed here. Data points are plotted as mean \pm S.E.M, $n = 3$ technical replicates. NS denotes not significant, * denotes $P < 0.05$.

3.4.3 siRNA-based silencing of *HEXA* and *HEXB* in HL-60 cells

The siRNA-based *HEXA* and *HEXB* knockdown in neutrophil-like cells was attempted as a proof-of-concept experiment on pre-plated and non-pre-plated HL-60 cells using different transfection strategies. Specifically, the use of two different transfection reagents, lipofectamine 3000 and siPORT in various quantities i.e. 75 pmol, 100 pmol and 150 pmol were compared. To assess if *HEXA* and *HEXB* expressions were successfully reduced, hexosaminidase enzyme assays using MUG (which measures total hexosaminidase A and B activity) and MUGS (which measures Hex A and Hex S activity) substrates were used. These substrates are commonly used for fast and convenient diagnosis of GM2 gangliosidosis (Wendeler and Sandhoff, 2009). As these substrates are enzymatically hydrolysed, the fluorogenic 4-MU is released, which can be detected fluorometrically using a spectrophotometer (Hepbildikler et al., 2002). Both Hex A and Hex B are able to degrade the neutral MUG substrate while only Hex A and the minor isoenzyme Hex S are able to hydrolyse the negative charged (sulphated) MUGS substrate.

As shown in **Figure 5B**, non-pre-plated HL-60 cells transfected using lipofectamine 3000 and siPORT did not result in a significant reduction of the hexosaminidase activity as evaluated by the 4-MU release measured 48 h post transfection. The level of 4-MU release was not altered significantly at the higher dosage of siRNA i.e. 150 pmol. This indicates that the total hexosaminidase activity of these cells was not altered with the introduction of the siRNA using both transfection reagents in the non-pre-plated cells.

Similarly, the lipofectamine 3000 transfected cells also did not display a reduction in the 4-MU release at 75 pmol, 100 pmol and 150 pmol siRNA within the pre-plated cells (**Figure 5A**). However, significant reduction in 4-MU release was observed for the pre-plated cells using siPORT with 100 pmol and 150 pmol siRNA ($P < 0.05$). This suggests a lower total hexosaminidase activity (total Hex A and Hex B activity) and that transfection of siRNA into the cells are optimal at these conditions.

To confirm the reduction of *HEXA* within pre-plated cells, a MUGS assay was used to assess the Hex A activity. **Figure 6** shows the Hex A activity of pre-plated HL-60 cells transfected with siPORT at 100 pmol and 150 pmol siRNA targeting both *HEXA* and *HEXB*. This demonstrated a decreased level of 4-MU relative to the non-transfected control when using 100 pmol siRNA, but this reduction was found not to be statistically significant. In contrast, the use of 150 pmol siRNA demonstrated a significant reduction in 4-MU relative to the non-

transfected control and the use of 100 pmol siRNA ($P < 0.05$). Taken together, these observations demonstrated a proof-of-concept of the ability to suppress the Hex A and Hex B expression and/or enzyme activity using 150 pmol of siRNA in neutrophil-like cells.

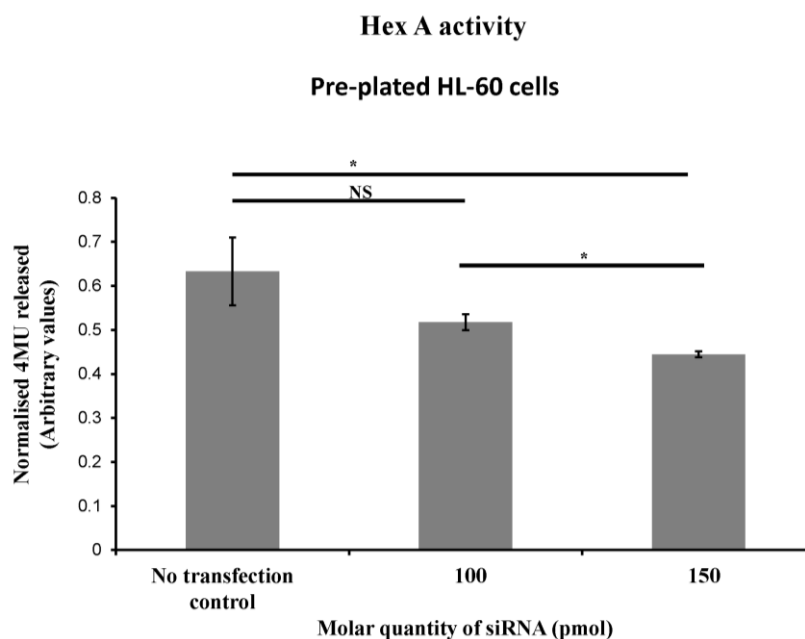


Figure 6. Hex A activity of pre-plated HL-60 cells transfected with siRNA targeting both *HEXA* and *HEXB* at 100 pmol and 150 pmol using siPORT transfection reagent. The level of fluorogenic 4-MU was measured as a proxy for the Hex A activity based on the hydrolysis of MUGS substrates added to cell lysates. The specific activity of Hex A was not assessed here. Data points are plotted as mean \pm S.E.M, $n = 3$ technical replicates. NS denotes not significant, * denotes $P < 0.05$.

3.5 Discussion

3.5.1 Co-localisation of Hex A and paucimannosidic proteins in the azurophilic granules of resting neutrophils

The presence of hexosaminidases in the neutrophil-rich environment of bacteria-infected and inflamed sputum and in neutrophil-like cells was shown in **Chapter 2**. However, the ability of these hydrolases to generate paucimannosidic *N*-glycoproteins in human neutrophils *in vivo* was not directly assessed in this initial investigation. In order to investigate this relationship, the co-localisation of the hexosaminidases and the paucimannosidic proteins in human neutrophils was assessed here. Specifically, the co-localisation of Hex A, the azurophilic markers (MPO and CD63) and paucimannosylated glycoproteins were investigated in peripheral blood isolated human neutrophils. Although visual inspection of the immunocytochemistry images revealed co-localisation of Hex A and MPO, CD63 and paucimannosylated glycoproteins, this readout is largely qualitative in nature and may be

somewhat misleading due to the limitation in the optical microscopy diffraction resolution relative to the much smaller size of the molecules of interest (Zinchuk et al., 2007). To allow a more quantitative measure of the co-localisation, MCC was also utilised as a measure for spatial association/proximity of two analytes within the cells. MCCs were chosen since these values are independent of the background pixels in the stained z stack within the confocal images. Unlike another established measure for co-localisation such as the Pearson's co-localisation coefficient, MCC is less prone to being artificially inflated due to the background pixels, leading to a higher accuracy in the estimates of the degree of co-localisation (Oheim and Li, 2007).

A moderate co-localisation of Hex A, MPO and paucimannosylated proteins were observed based on the MCC values. In addition, a moderate to high co-localisation of Hex A and CD63 was also observed based on the MCC values. During the promyelocytic stage of neutrophil development in the bone marrow, the genes encoding these proteins have been documented to be highly expressed in neutrophils and stored within the azurophilic granules (Rorvig et al., 2013) (see also **Chapter 2**). The strong gene expression of *HEXA*, *HEXB*, *MPO* and *CD63* at this developmental stage aligns well with the co-localisation results, indicating that these proteins are localised together within the azurophilic granules. The *in vitro* ability of human Hex A to produce paucimannosylated proteins has been shown (**Chapter 2**). The observation of Hex A co-localising spatially with MPO and paucimannosylated proteins further supports the involvement of Hex A in the generation of protein paucimannosylation. To ensure the specificity of the anti-human Hex A antibodies utilised in this study, Hex A antibodies was validated by immunoblotting with recombinant human Hex A and results shows good specificity (see **Supplementary Material, Figure S1 in the enclosed DVD**). All these observations increase the confidence on the notion that Hex A is responsible for the generation of protein paucimannosylation and that it resides within the azurophilic granule of human neutrophils.

3.5.2 Aberrant *N*-glycosylation of neutrophils derived from a SD patient

Cell lysates of purified neutrophils from an infantile SD patient was obtained to investigate the enzymatic capacity of the hexosaminidases to generate paucimannosidic *N*-glycoprotein. SD patients carry deleterious mutations in *HEXB*, the gene coding for the β subunit forming part of the dimeric Hex A ($\alpha\beta$) and Hex B ($\beta\beta$). In this study, the *N*-glycome of neutrophils purified from a homozygous *HEXB* deficient individual with clinically diagnosed SD was

analysed relative to an age-paired healthy donor. PGC-LC-ESI-CID-MS/MS showed that the relative abundance of the paucimannosidic type *N*-glycans was significantly lower in SD neutrophils (18.8%) in comparison to healthy donor neutrophils (41.0%). This glycome alteration supports the importance of this hexosaminidase subunit in the production of paucimannosidic *N*-glycoproteins. The enzymatic impairment of both Hex A and Hex B was reflected in the negligible total hexosaminidase activity. The relationship of the β subunit to protein paucimannosylation was further strengthened by the accumulation of GlcNAc-capped biosynthetic precursor glycans in SD neutrophils.

Interestingly, the build-up of these biosynthetic precursor intermediates also resulted in an increase of the high mannose structures, particularly the M7-M9 structures. This showed that a downstream manipulation of the biosynthetic machinery can indirectly impact the early stages of the *N*-glycoprotein synthesis. These observations demonstrated the inability of impaired Hex A and Hex B to act efficiently on their substrates and therefore leading to an accumulation of these early high mannose precursor structures in the *N*-glycosylation pathway.

Furthermore, the reduced paucimannosidic *N*-glycoprotein synthesis and the concomitant accumulation of high mannose in hexosaminidase-deficient human neutrophils were also recapitulated in a separate study where we generated hexosaminidase-knockout mutants i.e. *HEXO1* and *HEXO2* in the widely studied legume *Lotus japonicus* (see **Supplementary Material, Publication III in the enclosed DVD**). Remarkably, reduced growth and impaired development of this model plant system were observed phenotypically in these mutants, but were not found to be lethal despite the fact that paucimannosylation is a constitutive *N*-glycosylation expressed in *Lotus japonicas* (Dam et al., 2013).

The functional consequences on the reduced synthesis of paucimannosidic *N*-glycoproteins in SD neutrophils remain unknown and would be an interesting aspect to study in the future. TSD individuals with *HEXA* gene mutations have been reported to confer resistance towards *Mycobacterium tuberculosis* (*M. tb*) infection, but the molecular mechanisms driving this protection are still elusive (Ingrid et al., 2008). As to how SD individuals and their neutrophils respond to infectious diseases also remain to be investigated. The findings described here underscore the importance of the hexosaminidases in maintaining a functional mammalian and plant *N*-glycosylation pathway, and indicated that hexosaminidases may also be involved in other non-biosynthetically related functions.

The unusual monoantennary FA1G1S1 and the disialylated biantennary A2G2S2 glycans were observed to be suppressed in SD neutrophils relative to healthy donor neutrophils. These glycans were previously observed in the neutrophil-rich CF sputum and in isolated healthy neutrophils (**Chapter 2**). The significant reduction of these complex type glycans was somewhat surprising as the lack of functional hexosaminidases should not alter this part of the *N*-glycosylation machinery (Stanley et al., 2009). However, a reduction in the abundance of sialylated biantennary structures has been reported in the cerebrospinal fluid of a patient with GM2 gangliosidosis (Barone et al., 2016), which mirrors the observations described here.

Interestingly, the unusual FA1G1S1 has also been reported in stomach cancer-derived cell lines and mouse embryonic fibroblasts (Huang et al., 2015; Tadashi et al., 2002). How these structures were synthesised and their functional relevance in SD neutrophils remain to be investigated. The exoglycosidases such as sialidase or galactosidase might play important roles in the production of FA1G1S1 through catabolic reactions targeting just a single antenna. However, these isomers could also be generated in a stepwise manner through anabolic reactions of the single observed antenna on the 3' Man arm by specific glycosyltransferases, giving rise to these unusual glycoconjugates.

It is important to note that there is still residual presence of paucimannosidic *N*-glycoproteins in SD neutrophils. This observation suggests that in addition to Hex A and Hex B, there may be another hexosaminidase that process non-reducing end GlcNAc-capped structures into paucimannosidic glycoproteins. A human hexosaminidase, hexosaminidase C (Hex C) may be a candidate to generate paucimannosidic proteins in the absence of Hex A and Hex B. However, this enzyme was only shown to cleave *O*-linked GlcNAc from synthetic glycopeptides and other substrates, and not GlcNAc residues of *N*-linked glycoproteins (Gao et al., 2001). Another human hexosaminidase, hexosaminidase D (Hex D), was recently characterised and might play a role in the biosynthesis of paucimannosidic proteins (Gutternigg et al., 2009). It should be noted that both Hex C and Hex D were identified to reside in the nucleocytoplasmic region of mammalian cells and not in the lumen of human neutrophil granules. Although Hex S ($\alpha\alpha$) is lower in abundance in SD and its synthesis is not affected by non-functional β subunit in affected patients (Emiliani et al., 1990b), there could also be compensatory activities conferred by Hex S to generate paucimannosidic proteins. The functional and biological significance of the Hex C and Hex D remain to be resolved in the biosynthesis of paucimannosidic proteins in the absence of functional Hex A and Hex B.

3.5.3 The biosynthetic trafficking of neutrophil paucimannosidic *N*-glycoproteins

The biosynthetic trafficking route of paucimannosylated proteins in human neutrophils is still unknown. The current understanding of the human *N*-glycosylation pathway (Aebi et al., 2010; Stanley et al., 2009) does not allow for an explanation of these truncated chitobiose/paucimannosidic *N*-glycoproteins. Based on the glycomics- and glycoproteomics-based observations presented in this thesis, it may be suggested that the paucimannosidic *N*-glycoproteins are generated, after exiting the ER, by detouring from the conventional downstream Golgi-based processing in the biosynthetic machinery in developing neutrophils. The high core fucosylation indicate that the paucimannosidic glycoproteins undergo essential processing in the *cis*- and medial-Golgi apparatus via β -linked GlcNAc capped intermediates (catalysed by GnT-I, α 1,3/6-mannosidases II and α 1,6-FuTs) before they may be sequestered into the azurophilic granule for hydrolase-driven truncation by Hex A/B and the α -/ β -mannosidases (**Figure 7**). This hypothesis is in agreement with the “targeting by timing” hypothesis proposed by Borregaard and co-workers suggesting that all (glyco)proteins produced at the promyelocyte stage of the myeloid development are targeted to the azurophilic granule (Borregaard and Cowland, 1997). It also agrees well with the observation by Bainton and colleagues showing that azurophilic granule proteins formed during the promyelocytic stage buds off from the *cis*-Golgi (Bainton and Farquhar, 1966). In addition, the absence of α -sialidase, α -fucosidase and β -galactosidase in the proteome datasets of the azurophilic granules (Lominadze et al., 2005; Rorvig et al., 2013) further suggests that, paucimannosidic glycoproteins are generated from immature complex type glycan intermediates and not from more mature fully extended sialo-glycoproteins sequestered late in the biosynthetic machinery. It also implies that paucimannosidic proteins are not sequestered to the azurophilic granules by specific sequence motifs or other molecular signals intrinsic to these proteins.

It is worth mentioning at this point that later in this thesis (**Chapter 5**) where I will be describing that paucimannosylation of the intact bioactive HNE surprisingly was found not to be an exclusive feature of the azurophilic granules in neutrophils. HNE appears to be present in other granules of human neutrophil, albeit at a lower abundance. This suggests that an alternative biosynthetic route in addition to the one hypothesised above may exist. Such alternative pathway(s) may explain the residual levels of paucimannosidic glycoproteins in SD neutrophils. Therefore, the biosynthetic route of paucimannosidic glycoproteins remains to be studied in greater details in the future.

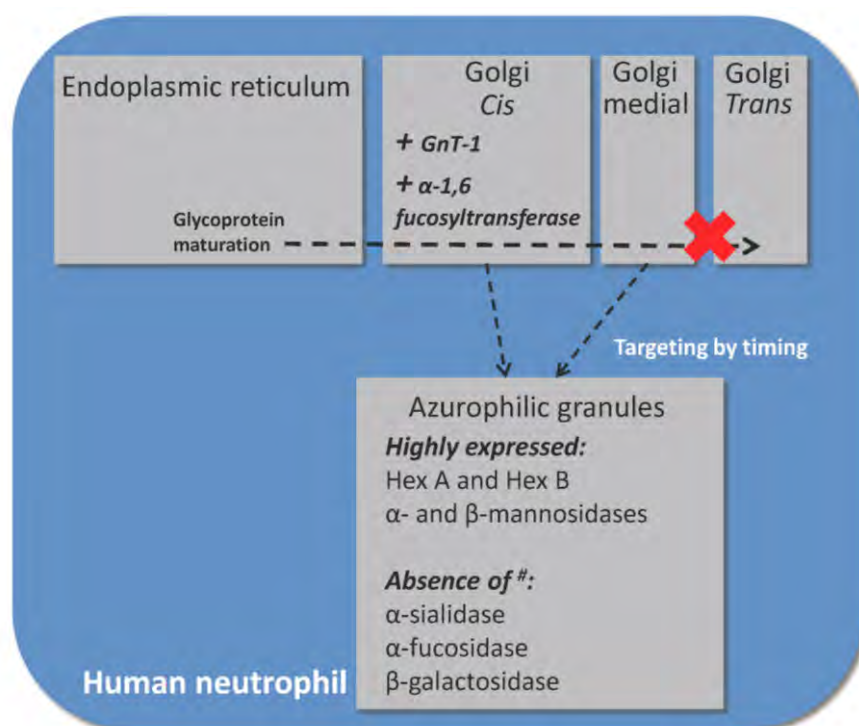


Figure 7. Proposed biosynthetic pathway of paucimannosidic *N*-glycoproteins in developing human neutrophils. The data indicate that the *N*-glycoproteins exit the ER in a regular manner and are then lightly processed in the cis- and medial-Golgi, before they are sequestered and truncated by the hexosaminidases and mannosidases in the azurophilic granules. This suggested pathway aligns with the “targeting by timing” hypothesis (Borregaard and Cowland, 1997). # Proteomics data suggested that sialidases, fucosidases and galactosidases are not abundantly present in the azurophilic granules (Lominadze et al., 2005; Rorvig et al., 2013).

3.5.4 Assessing the potential for siRNA-based *HEXA* and *HEXB* manipulation in HL-60 cells as a model for studying the biosynthesis and function of protein paucimannosylation

The efficient delivery of siRNA into cells is a major challenge in siRNA-based gene manipulation experiments and time-consuming optimisation is often required before cells are transfected at sufficient efficiency (Cheng et al., 2011). This proof-of-concept study was no different; only after extensive optimisation was significant siRNA-based reduction of the *HEXA* and *HEXB* expression achieved using relative high amounts (150 pmol) siRNA with siPORT in pre-plated undifferentiated HL-60 cells. Relative efficient transfection has been reported previously using pre-plated cells (Dalby et al., 2004), in agreement with the results presented here. The usage of lipofectamine 3000 was previously reported to yield poor transfection efficiencies due to its cytotoxic effects. This was attributed to the formation of fewer intracellular vesicles containing the target siRNA with lipofectamine 3000 relative to

other commercially available transfection reagents (Spagnou et al., 2004). Thus, these might explain the poor transfection efficiencies of lipofectamine 3000 on HL-60 neutrophil-like cells. Apart from the use of enzyme activity assays, qPCR can also be utilised to assess the gene expression of *HEXA* and *HEXB* in these siPORT-transfected cells. To this end, qPCR primers were designed and tested in non-transfected HL60 cells in a preliminary proof-of-concept study. Melting curve analysis revealed that the designed primers were specific as shown by the presence of a single melting curve peak, suggesting that a single, pure amplicon spanning the exons of *HEXA* and *HEXB* was produced, respectively (see **Supplementary Materials, Figure S2 and Table S1 in the enclosed DVD** for more information). This shows that the qPCR amplification is specific with these designed primers and that the running conditions are optimal. The use of qPCR-based readouts should be tested and carried out more systemically in the future to monitor and validate the silence-induced knockdown of *HEXA* and *HEXB* expression presented in this chapter.

In order to determine the functional outcome of siRNA-silenced hexosaminidases and its influence on neutrophil immune functions, functional primary neutrophils should be utilised. However, purified primary neutrophils are short lived once they are isolated *ex vivo* (Dancey et al., 1976). Therefore, HL-60 neutrophil-like cells were utilised here as an initial proof-of-concept transfection model as these cells are immortal (Birnie, 1988) and have functional capacities similar to *ex vivo* purified neutrophils upon DMSO differentiation (Collins et al., 1978; Newburger et al., 1979). However, DMSO differentiation of HL-60 cells requires five to seven days (Emiliani et al., 1990b) and the use of siRNA might not be sufficient to effectively knockdown *HEXA* and *HEXB* to assess the contribution of hexosaminidases towards the generation of paucimannosidic proteins. This is because siRNA-based silencing of genes is a transient gene knockdown technique and has been shown to be less effective on rapidly dividing cells over extended period of time (Bartlett and Davis, 2006).

Therefore, the use of a more stable gene manipulation technique in the future might be more suitable for knocking down *HEXA* and *HEXB* in HL-60 cells. Techniques for stable gene manipulation include the use of short hairpin RNA (shRNA) and the use of lentivirus or adenovirus vectors for effective integration of shRNA into the cell for stable expression and long term gene knockdown (Brummelkamp et al., 2002). However, these techniques might introduce unwanted mutagenic effects or trigger antiviral immunological response in the transfected HL-60 cells. Recently, the CRISPR/Cas9 method was used to knockout glycosylation genes in HL-60 cells such as the β 1,2 GlcNAc transferase (MGAT1) in order to

assess the glycan contribution towards neutrophil trafficking and adhesion during inflammation (Stolfa et al., 2016). This method could also be used in the future to provide a more stable gene knockout to assess the contribution of hexosaminidases towards the generation of paucimannosidic proteins. The immunological outcomes of a stable and long term gene knockout of *HEXA* and *HEXB* can also be more effectively studied subsequently in DMSO differentiated HL-60 cells.

In conclusion, the optimised protocol described above will be useful for future transfection-based gene manipulation studies of undifferentiated HL-60 cells, allowing the study of the function of *HEXA* and *HEXB* gene products and consequently, the lack of functional hexosaminidases and its influence on the immune response facilitated by neutrophils.

3.6 Overview of main findings, conclusions and future directions

Main findings and conclusions

- The heterodimeric Hex A was found to reside within the azurophilic granule compartment of resting human neutrophils as shown by the co-localisation of Hex A with the azurophilic protein markers MPO and CD63.
- Co-localisation of human Hex A with paucimannosylated proteins in resting human neutrophils and the high sequence homology of human Hex A to the hexosaminidases of known paucimannose-rich organisms indicated that human Hex is involved in the enzymatic generation of paucimannosidic *N*-glycoproteins in human neutrophils.
- Neutrophils of a *HEXB*^{-/-} SD patient displaying dysfunctional β subunit and thus lack of any hexosaminidase activity showed reduced paucimannosylation and concomitantly an accumulation of intermediate complex type structures relative to a healthy individual as demonstrated using *N*-glycomics and immunoblotting. This implies that Hex A ($\alpha\beta$) and/or Hex B ($\beta\beta$) isoenzymes are important in the synthesis of paucimannosidic *N*-glycoproteins.
- Significant levels of paucimannosidic *N*-glycoproteins were still observed in SD neutrophils which suggested compensation mechanisms of alternative glycosidases e.g. Hex S ($\alpha\alpha$) or an alternative yet-to-be-understood pathway involved in paucimannosidic *N*-glycoprotein synthesis.

Future directions

- The *HEXA* and/or *HEXB* genes of pre-plated undifferentiated HL-60 cells were successfully silenced using siRNA and siPORT as a transfection reagent as demonstrated by the reduction in total hexosaminidase and Hex A activity. This provides proof-of-concept that the hexosaminidases can be genetically manipulated in neutrophil-like cells and, thus, that this model system can use to assess the functional relevance of the Hex enzymes and protein paucimannosylation in the future.
- The use of qPCR to assess the gene expression of *HEXA* and *HEXB* would be a straightforward approach to validate these silence-induced knockdown observations. The designed primers and proof-of-concept of utilising qPCR to assess *HEXA* and *HEXB* gene expression was demonstrated, but such qPCR-based readouts should be carried out more systemically in the future.

- The *N*-glycome and the *N*-glycoproteome of the *HEXA* and *HEXB* manipulated HL-60 cells should be determined in the future to investigate the structural and functional impact of the dysfunctional Hex A and B with respect to protein paucimannosylation.
- The spatial co-localisation of Hex A with other granule markers such as NGAL and gelatinase that are characteristic of specific and gelatinase granule respectively should be determined in the future using immunocytochemistry.
- The spatial co-localisation of Hex B with azurophilic granule markers such as MPO and CD63, along and other granule markers such as NGAL and gelatinase should be determined in the future using immunocytochemistry.
- The temporal co-localisation of Hex A and Hex B with paucimannosidic proteins could be investigated in the future using live cell imaging to monitor for potential interactions with their substrates.
- It is desired that neutrophils and potentially other immune cells and/or bodily fluids from a much larger cohort of SD and TSD patients, coupled with relevant healthy donors, should be investigated in the future to validate the findings described in this chapter. Similar to the experiments described herein, the use of glycomics, glycoproteomics and immunocytochemistry are instrumental technologies in order to assess the contribution of Hex A and Hex B in the generation of protein paucimannosylation. The reduced protein paucimannosylation in SD/TSD specimens also represents a unique opportunity to study the functional consequences of paucimannosidic proteins in immunity and infection.

**Chapter 4: Site-specific structural characterisation
of the *N*-glycosylation of human neutrophil
cathepsin G using complementary LC-MS/MS
strategies**

4.1 Rationale

In the initial observation of protein paucimannosylation in human neutrophils derived from bacterial-colonised CF sputum, azurophilic granule glycoproteins such as MPO, HNE and azurocidin were identified to carry paucimannosidic *N*-glycans using LC-MS/MS based glycomics and glycoproteomics (**Chapter 2**). However, only partial structural information was obtained of these key neutrophilic proteins. HNE and azurocidin are part of the serine protease family that have been documented to be essential for the anti-microbial activities of human neutrophils, particularly during phagocytosis, degranulation and the formation of NETs (Borregaard and Cowland, 1997; Faurschou and Borregaard, 2003). Another serine protease that is part of this family, nCG, was identified in the CF sputum proteome, but the micro- and macro-heterogeneity of the glycosylation of nCG comprising of a single *N*-glycosylation site, was not documented.

Although the use of PGC-LC-ESI-MS/MS based glycomics is a powerful tool to provide qualitative (i.e. monosaccharide composition, topology and glycosidic linkages of isomeric glycans) and quantitative (i.e. relative glycan abundance) structural information as introduced in **Chapter 3**, this analytical platform does not provide information about the carrier protein and the specific attachment sites of each glycan. Furthermore, the glycosylation site occupancies of the attached *N*-glycans are lost by the use of this method alone (Leymarie et al., 2013). Site-specific structural characterisation of glycoproteins is important to understand the structural and functional relevance of protein glycosylation (Panico et al., 2016; Sumer-Bayraktar et al., 2016). In addition, spatial and temporal cellular changes have been known to alter the site-specific glycosylation of proteins during diseases and in altered physiological conditions (Hulsmeier et al., 2016; Shade et al., 2015).

In this chapter, I will focus on the use of three complementary LC-MS/MS approaches to profile, at high structural resolution, a selected neutrophil *N*-glycoprotein of particular interest. Specifically, three structural levels of nCG from resting human neutrophils were analysed including *N*-glycosidase F-released *N*-glycans, chymotrypsin-generated *N*-glycopeptides and intact glycoprotein. This facilitated, for the first time, a deep characterisation of the site-specific *N*-glycosylation of nCG. More importantly, this structural information facilitates future investigation of the functional role of nCG *N*-glycosylation. In addition, the complementary methods were also used to study the

structure/function relationship of the *N*-glycosylation of another serine protease, HNE (**Chapter 5**).

N-glycan analysis revealed a high abundance of paucimannosidic *N*-glycans. Surprisingly, the *N*-glycopeptide analysis qualitatively and quantitatively deviated from the glycome data and indicated that further truncated chitobiose core type structures i.e. GlcNAc β Asn and Fuc α 1,6GlcNAc β Asn, were abundantly expressed on nCG. The presence of paucimannosidic *N*-glycans (M1, M1F, M2) and lower abundance complex structures, including the unusual sialo-glycan FA1G1S1 were observed. Intact nCG glycoform profiling agreed well with the *N*-glycopeptide analysis, thereby confirming the distribution of glycans on nCG. These observations highlight the importance of performing complementary LC-MS/MS strategies to validate the *N*-glycosylation profile of glycoproteins, in particular when unusual glycans are being studied. More importantly, the data presented in this chapter also illustrates the need to consider these unconventional glycans as being an integral part of the human glyco-repertoire and, thus, to include these truncated structures when using dedicated search engines such as UniCarb-KB or Byonic for glycomics and glycoproteomics based experiments. This will facilitate further system-wide explorations of these exciting novel glycan classes in human cells and tissues.

4.2 Publication IV: Complementary LC-MS/MS-Based *N*-Glycan, *N*-Glycopeptide, and Intact *N*-Glycoprotein Profiling Reveals Unconventional Asn71-Glycosylation of Human Neutrophil Cathepsin G

Publication: Loke, I., Packer, N.H., Thaysen-Andersen, M., 2015. Complementary LC-MS/MS-Based *N*-Glycan, *N*-Glycopeptide, and Intact *N*-Glycoprotein Profiling Reveals Unconventional Asn71-Glycosylation of Human Neutrophil Cathepsin G. *Biomolecules* 5 (3), 1832-1854. doi:10.3390/biom5031832

Supplementary Materials are available in the enclosed DVD.

Author contributions: Conception of study and experimental design – IL and MTA, data collection and analysis – IL, data interpretation and extraction of conclusions, – IL and MTA, manuscript preparation – IL and MTA, manuscript editing and review – IL, NP and MTA.

Article

Complementary LC-MS/MS-Based *N*-Glycan, *N*-Glycopeptide, and Intact *N*-Glycoprotein Profiling Reveals Unconventional Asn71-Glycosylation of Human Neutrophil Cathepsin G

Ian Loke, Nicolle H. Packer and Morten Thaysen-Andersen *

Department of Chemistry and Biomolecular Sciences, Macquarie University, North Ryde, Sydney 2109, Australia; E-Mails: ian.loke@students.mq.edu.au (I.L.); nicki.packer@mq.edu.au (N.H.P.)

* Author to whom correspondence should be addressed; E-Mail: morten.andersen@mq.edu.au; Tel.: +61-2-9850-7487; Fax: +61-2-9850-6192.

Academic Editor: Hans Vliegthart

Received: 9 June 2015 / Accepted: 6 August 2015 / Published: 12 August 2015

Abstract: Neutrophil cathepsin G (nCG) is a central serine protease in the human innate immune system, but the importance of its *N*-glycosylation remains largely undescribed. To facilitate such investigations, we here use complementary LC-MS/MS-based *N*-glycan, *N*-glycopeptide, and intact glycoprotein profiling to accurately establish the micro- and macro-heterogeneity of nCG from healthy individuals. The fully occupied Asn71 carried unconventional *N*-glycosylation consisting of truncated chitobiose core (GlcNAc β : 55.2%; Fuc α 1,6GlcNAc β : 22.7%), paucimannosidic *N*-glycans (Man β 1,4GlcNAc β 1,4GlcNAc β : 10.6%; Man β 1,4GlcNAc β 1,4(Fuc α 1,6)GlcNAc β : 7.9%; Man α 1,6Man β 1,4GlcNAc β 1,4GlcNAc β : 3.7%, trace level of Man α 1,6Man β 1,4GlcNAc β 1,4(Fuc α 1,6)GlcNAc β), and trace levels of monoantennary α 2,6- and α 2,3-sialylated complex *N*-glycans. High-resolution/mass accuracy LC-MS profiling of intact nCG confirmed the Asn71-glycoprotein profile and identified two C-terminal truncation variants at Arg243 (57.8%) and Ser244 (42.2%), both displaying oxidation of solvent-accessible Met152. Asn71 appeared proximal (~19 Å) to the active site of nCG, but due to the truncated nature of Asn71-glycans (~5–17 Å) we questioned their direct modulation of the proteolytic activity of the protein. This work highlights the continued requirement of using complementary technologies to accurately profile even relatively simple glycoproteins and illustrates important challenges associated with the analysis of unconventional protein *N*-glycosylation. Importantly, this study now facilitates investigation of the functional role of nCG Asn71-glycosylation.

Keywords: neutrophil; cathepsin G; *N*-glycan; glycopeptide; glycoprotein; chitobiose; paucimannose; *N*-acetylglucosamine; glycomics; azurophilic granule

1. Introduction

Neutrophil cathepsin G (nCG) is an important serine protease produced and stored predominately in the azurophilic granules of resting human neutrophils [1]. Facilitated by its proteolytic and anti-microbial activities [2], nCG is a key player in multiple physiological and pathophysiological processes e.g., innate immune defense against pathogens [3], vascular homeostasis [4], and inflammatory response [5].

The nascent polypeptide chain of nCG (255 amino acid residues, ~28 kDa) is matured partly by the removal of an N-terminal signal- and pro-peptide and by a C-terminal cleavage at Ser244-Phe245 (unprocessed nCG polypeptide chain numbering hereafter) (Figure 1a) [6,7]. The crystal structure of nCG shows the catalytic triad characteristic of serine proteases forming the active site of the protein at His64, Asp108, and Ser201 [8]. The protein structure, catalytic activity, and function of nCG as a serine protease in the human immune system have been thoroughly reviewed [9,10]. It was established that nCG forms three intra-molecular disulfide bonds and presents a single potential asparagine (*N*)-linked glycosylation site at Asn71 [11].

Although the *N*-glycosylation of nCG has been studied previously, the micro- and macro-heterogeneity of nCG remain incompletely understood. Utilizing nuclear magnetic resonance, the presence of a biantennary disialylated complex and paucimannosidic *N*-glycans have been documented [12]. However, the distribution of the Asn71-glycoforms, glycosylation site occupancy, and presence of other post-translational modifications (PTMs) on nCG were not described. Knowledge of any potential involvement of Asn71-glycosylation in the function of nCG is similarly sparse: to our knowledge there is only a single *in vitro* study using a mutated nCG variant lacking the Asn71-glycosylation site, indicating that glycosylation at this site is not essential for the biosynthesis, stability, post-translational enzymatic activation, and granule sorting of nCG [13]. Nonetheless, Asn71-glycosylation may still play an important role in the function of nCG. In order to understand the influence of *N*-glycosylation on protein function, it is essential to accurately map the glycan structures and their distribution in a site-specific manner.

We recently identified the presence of an under-reported class of truncated human *N*-glycoproteins in neutrophil-rich and bacteria-infected sputum [14,15]. This so-called paucimannosylation of proteins is defined by the presence of a complete or partial trimannosyl-chitobiose *N*-linked core with the general monosaccharide composition *N*-acetylglucosamine(GlcNAc)₂mannose(Man)₁₋₃fucose(Fuc)₀₋₁. Notably, these unusual glycoepitopes were found to be carried in abundance by proteins localizing to the azurophilic granules of neutrophils, including the bioactive myeloperoxidase, azurocidin, and neutrophil elastase (NE). We suggested that paucimannosylation may play crucial modulatory roles in the human innate immune system. Thus, detailing the exact *N*-glycosylation of nCG, which is also a known azurophilic granule protein [16], will facilitate further insights into the function of the unusual compartment-specific *N*-glycosylation of neutrophil proteins.

To this end, we here use complementary liquid chromatography-tandem mass spectrometry (LC-MS/MS) technologies available in modern glycoscience to show that nCG carries unexpected Asn71-glycosylation, including truncated chitobiose cores, and paucimannosidic and monoantennary monosialylated complex glycans. Documenting the Asn71-glycosylation and its relationship to other PTMs of the polypeptide chain of nCG advances our understanding of its molecular heterogeneity, and will enable more exact structure-function studies. Importantly, this study demonstrates the continued requirement for utilizing an array of analytical technologies to perform accurate and confident structural characterization of human *N*-glycoproteins carrying unconventional carbohydrates.

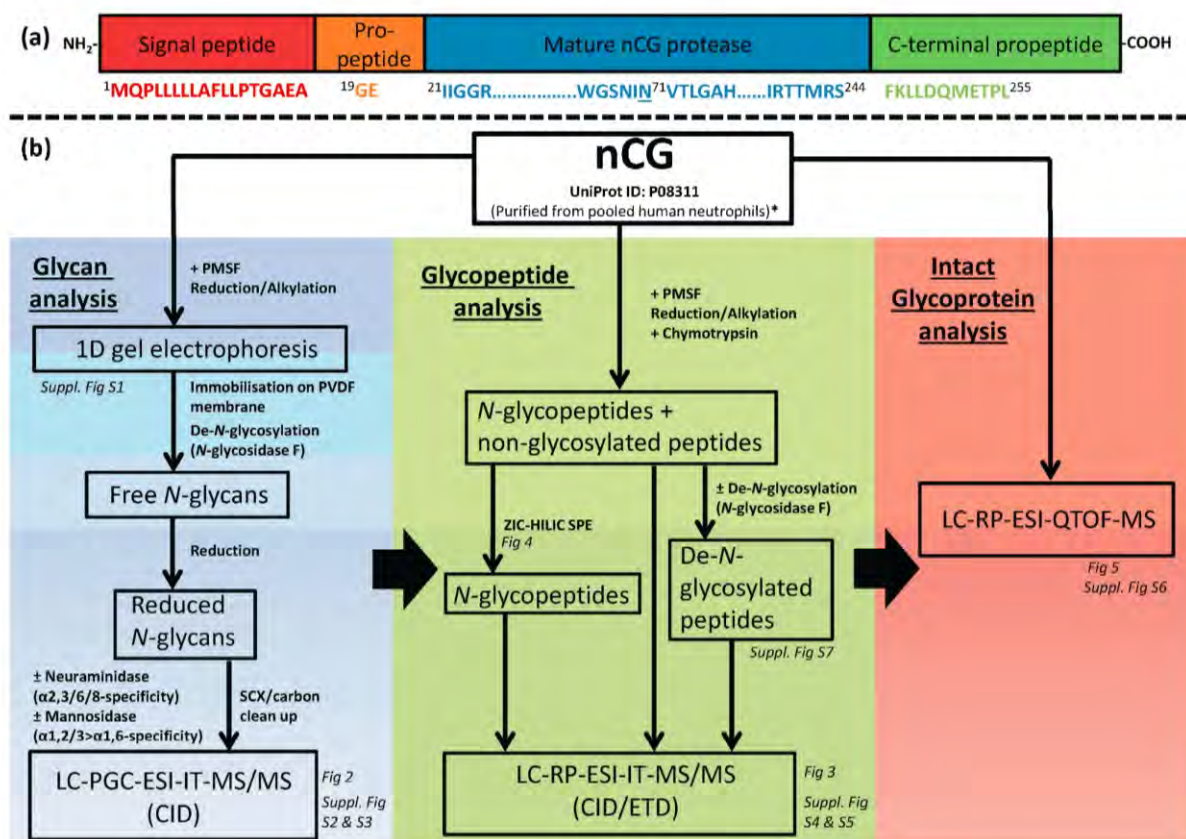


Figure 1. (a) Diagram showing the protein sequence of full length nCG consisting of a signal peptide, propeptide, the protease sequence, and a C-terminal propeptide. Numbering is based on the unprocessed nCG polypeptide chain; (b) Experimental workflow outlining the characterization of nCG *N*-glycoproteomic. The LC-MS/MS-centric experiments were divided into the three investigated analyte levels *i.e.*, *N*-glycans, *N*-glycopeptides, and intact glycoprotein. The relevant figures presenting the structural information extracted from the different analyses are indicated. * Other interfering human neutrophil glycoproteins of significant abundance were detected in the investigated protein preparation *i.e.*, azurocidin and neutrophil elastase (NE).

2. Results and Discussion

2.1. Design of Study—Three Analysis Levels were Used to Complete the nCG Glycoprofiling

Multiple LC-MS/MS-based approaches were utilized to achieve a deep site-specific structural characterization of nCG *N*-glycosylation (Figure 1b). These complementary techniques comprised the analysis of *N*-glycosidase F-released *N*-glycans, chymotrypsin-generated *N*-glycopeptides, and intact nCG. Porous graphitized carbon (PGC) LC electrospray ionization (ESI) resonance activation collision induced dissociated (CID) MS/MS is a well-documented technology to characterize reduced, underivatized *N*-glycans released from glycoproteins [17–22]. Such information-rich analysis provides the detailed structure of the individual *N*-glycans, their isomers, and their relative distribution, albeit in a protein and site-unspecific manner. The reduced *N*-glycan alditols released from nCG were analyzed in negative ion polarity, allowing for simultaneous detection of neutral and acidic glycans [23]. Parallel treatments with multiple exoglycosidases *i.e.*, α 2,3/6/8-linkage unspecific and α 2,3-linkage-specific sialidases and (α 1,2/3 > α 1,6) mannosidase were used together with the PGC-LC-MS/MS glycan profiling retention data and the established pathway knowledge of human *N*-glycosylation [14,24] to define the indicated terminal monosaccharide residues and their glycosidic linkages.

The site-specific *N*-glycosylation analysis was carried out on a reversed phase (RP) LC-MS/MS ion trap platform by identifying Asn71-glycopeptides. nCG was treated with phenylmethanesulfonyl fluoride (PMSF) to prevent autolysis (Figure S1). Asn71-glycopeptides falling into an MS-friendly mass range (<4 kDa) were achieved using chymotrypsin digestion rather than using conventional trypsin digestion. Orthogonal CID and electron transfer dissociation (ETD) glycopeptide fragmentation, as previously described [25–28], facilitated knowledge of the glycosylation site, occupancy level, and site-specific distribution of Asn71-glycans. Zwitterionic hydrophilic interaction liquid chromatography (ZIC-HILIC)-based solid phase extraction (SPE) was employed to enrich for, and enhance the stoichiometry of, nCG *N*-glycopeptides, and to reduce the suppression effect of non-glycosylated peptides [29–31]. Although exoglycosidase treatment may be performed on the glycopeptide level to confirm the site-specific glycan linkages [32], this was not performed in this study.

Finally, intact nCG glycoprotein was profiled using high-resolution/high mass accuracy quadrupole time-of-flight (QTOF) LC-ESI-MS, generating a more holistic qualitative and quantitative picture of the connectivity of all PTMs displayed by the nCG polypeptide chain [33].

2.2. *N*-Glycome Profiling Indicates Unconventional nCG *N*-Glycosylation

The *N*-glycome profiling was performed on PMSF-treated nCG isolated to single gel band purity as assessed by protein staining to minimize the risk of *N*-glycan contributions from interfering glycoproteins (Figure S1). However, as later demonstrated, the single gel band of the commercially prepared nCG turned out to contain multiple contaminating glycoproteins, illustrating that the risk of contamination may be reduced by SDS-PAGE separation, but cannot be eliminated completely. PGC-LC-MS/MS of *N*-glycans released from this gel band revealed an abundance of five paucimannosidic *N*-glycans (individual structures hereafter called M1, M1F, M2, M2F, and M3F, where M denotes the mannosylated chitobiose core (GlcNAc β 1,4GlcNAc β) and F denotes α 1,6-core fucosylation) and lower

called M0F) and monoantennary complex sialo-*N*-glycans (Figure 2a). The specific linkages and branching configurations of the *N*-glycans were deduced from their monoisotopic masses, relative PGC-LC retention times, presence of diagnostic and other B-/C-/Y-/Z- and cross ring fragment ions (Figures S2 and S3 and Table S1) as previously described [21,34–36], and their response to specific exoglycosidase digestions [35]. *De novo* resonance activation (ion trap) CID-MS/MS sequencing, as well as the matching of ion trap CID-MS/MS spectra and the relative PGC-LC retention time to glycan reference compounds, were also performed to confirm the mannose arm linkage configurations of the paucimannosidic structures (Figure 2b).

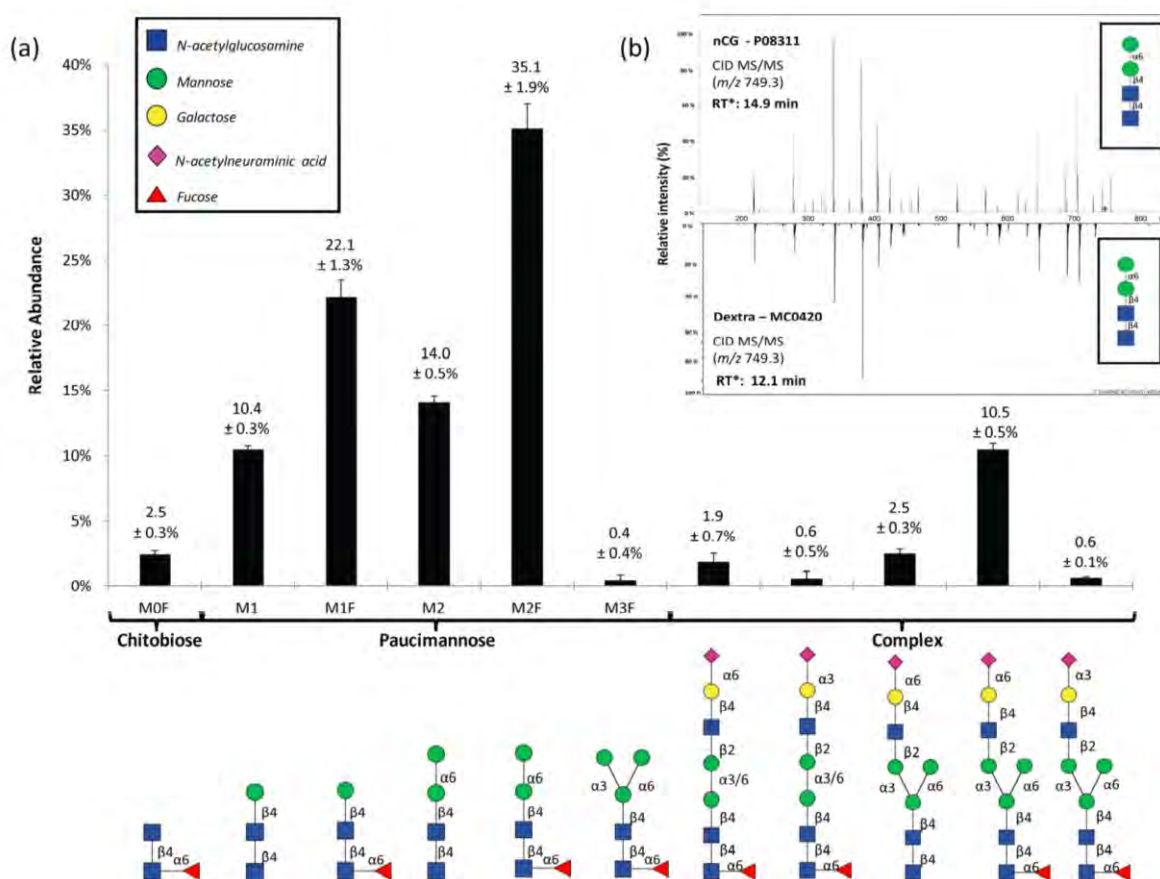


Figure 2. (a) The PGC-LC-MS/MS-based *N*-glycome profiling revealed 11 *N*-glycans comprising chitobiose core, paucimannosidic, and complex type *N*-glycans. The structures, linkages, and relative abundances of the individual *N*-glycans are illustrated. Data points are plotted as mean \pm SD, $n = 3$. Symbols are used according to the Consortium for Functional Glycomics / Essentials of Glycobiology notation (see insert). All *N*-glycans were observed in their reduced (alditol) form; (b) CID-MS/MS and PGC-LC retention time (* calculated relative to M3F in each profile) matching of the paucimannosidic M2 to an identical glycan reference compound was performed. See Figure S3 for *de novo* CID-MS/MS characterization of all observed *N*-glycans analyzed under negative ionization polarity.

The M2F α 1,6-isomer of nCG was the most abundant *N*-glycan, in agreement with our recent *N*-glycome profiles of isolated human neutrophils and neutrophil-rich pathogen-infected sputum [14,15]. The corresponding α 1,3-isomers of M2 and M2F were absent, in line with previous observations made in azurophilic granule proteins derived from human neutrophils [15,24] and the known preferential hydrolysis of α 1,3-linked mannose of M3(F) by human α -D-mannosidase in the biosynthetic machinery [37]. Protein paucimannosylation has recently been indicated to exist in human cells and tissues other than neutrophils e.g., in inflammation and cancer [38–40]. Due to their abundance and presence on intact proteins in human neutrophils [24,41,42], we recently suggested that paucimannosylation is not simply a degradation product but should be considered as a separate non-conventional type of expressed human *N*-glycoproteins in addition to the more conventional high mannose, hybrid, and complex type glycoproteins [15].

Interestingly, the monoantennary complex *N*-glycans carrying an intact core-fucosylated trimannosyl-chitobiose core were found to display both α 2,6- and α 2,3-linked sialylation on the 3'-mannose arm, while the single non-core fucosylated monoantennary complex *N*-glycan was exclusively α 2,6-sialylated. The less abundant related mannose-truncated (bimannosyl-chitobiose core) complex *N*-glycans carried both α 2,6- and α 2,3-linked sialylation on the 3'- or 6'-mannose arm, in agreement with previous studies reporting the presence of these unconventional monoantennary complex *N*-glycans on neutrophil proteins [24,43]. These structures did not contain the intact common trimannosyl-chitobiose cores typically found in mammalian *N*-glycans, illustrating that it may be relevant to include such unconventional structures (or the corresponding monosaccharide compositions) when using search engines (e.g., Byonic) for glycomics/glycoproteomics experiments. Upon consultation of an established glycan structure database (*i.e.*, UniCarbKB), we noticed that monoantennary core-truncated *N*-glycans have not yet been deposited. We ensured that artificial generation of these truncated structures by any contaminating glycosidase activity during the *N*-glycosidase F based *N*-glycan release was ruled out by performing parallel treatment and analysis of a number of model glycoproteins (*i.e.*, fetuin, ovalbumin, and RNase B) subjected to identical conditions as for nCG. However, further characterization is still needed to confirm the structure, function, and (sub)cellular origin of these unconventional species.

2.3. Site-Specific Asn71-Glycopeptide Profiling Uncovers Single GlcNAc β and Fuca1,6GlcNAc β on nCG and Reveals Significant Presence of Other Interfering *N*-Glycoproteins

RP-LC-CID/ETD MS/MS of the unenriched chymotryptic peptide mixture of nCG facilitated the identification of five abundant glycoforms of the Asn71-glycopeptide GSNINVTL, including the attachment of single GlcNAc β ($55.2\% \pm 3.5\%$) and Fuca1,6GlcNAc β ($22.7 \pm 4.9\%$) structures (Figure 3a,b). Other lower abundant chymotryptic Asn71-glycopeptide variants were also observed carrying the same set of *N*-glycans *i.e.*, the GSNINV peptide (see Figure S4 and Table S2). Surprisingly, these abundant Asn71-glycoforms did not reflect the *N*-glycome relative distribution, probably due to the lack of PGC-LC retention of mono- and di-saccharides [20] and the resistance to digestion by *N*-glycosidase F of the truncated chitobiose core type structures [44]. GlcNAc β Asn- and Fuca1,6GlcNAc β Asn-glycosylation has been suggested to be present in the mouse synaptosomes and liver [45,46], as well as in mammalian cell lines [47] and invertebrates [48,49], but remains an under-reported and under-investigated class of *N*-glycans as they have previously been assumed to be non-functional degradation products.

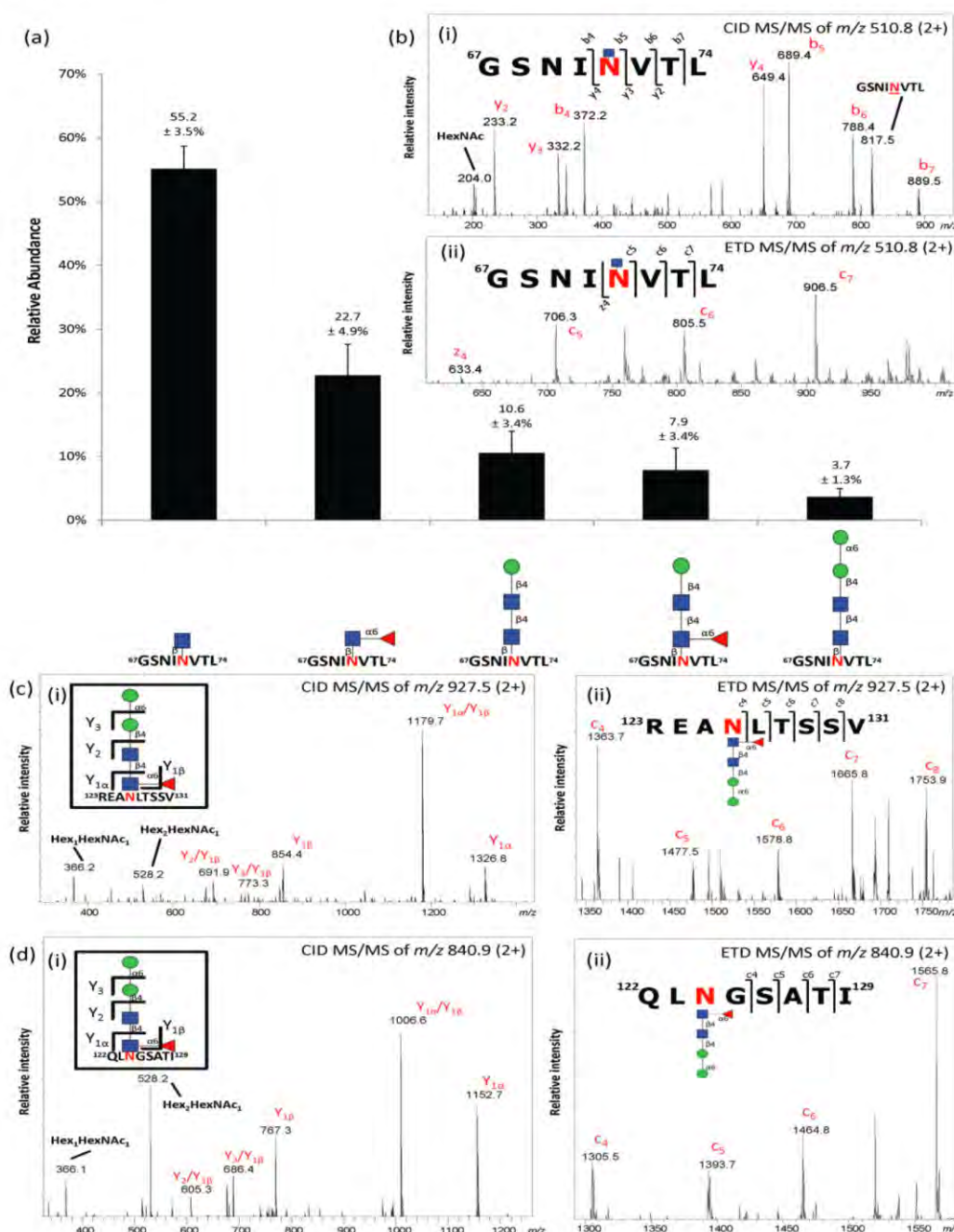


Figure 3. (a) Profiling of unenriched chymotryptic Asn71-glycopeptides derived from nCG in positive ionization polarity. Data points are plotted as mean ± SD, $n = 3$; (b) (i) CID- and (ii) ETD-MS/MS of the predominant chymotryptic GlcNAc β Asn71-glycopeptide variant (GSNINVT L); (c,d) (i) CID- and (ii) ETD-MS/MS of the chymotryptic M2F-containing *N*-glycopeptide originating from the interfering neutrophil proteins *i.e.*, (c) azurocidin and (d) NE covering the *N*-glycosylation sites Asn126 and Asn124, respectively. See Figure S4 for glycopeptides covering other observed sites of azurocidin and NE. See also Table 1 for summary of all observed glycoforms of the three *N*-glycoproteins identified in the protein preparation.

Table 1. Semi-quantitative overview of the site-specific *N*-glycosylation of human nCG, azurocidin and NE observed in this study. “xxxx” denotes glycoforms of high abundance, “xxx” glycoforms of intermediate abundance, “xx” glycoforms of low abundance and “x” trace (non-quantifiable) glycoform abundance.

| <i>N</i> -glycan Structure | nCG | Azurocidin | | NE | |
|--|-------|------------|--------|--------|--------|
| | Asn71 | Asn126 | Asn171 | Asn124 | Asn173 |
| GlcNAc β | xxxx | | | | |
| Fuca1,6GlcNAc β | xxxx | | | | |
| Man β 1,4GlcNAc β 1,4GlcNAc β (M1) | xxx | | | | |
| Man β 1,4GlcNAc β 1,4(Fuca1,6) GlcNAc β (M1F) | xxx | | xx | | |
| Man α 1,6Man β 1,4GlcNAc β 1,4 GlcNAc β (M2) | xxx | | | | |
| Man α 1,6Man β 1,4GlcNAc β 1,4 (Fuca1,6)GlcNAc β (M2F) | x | xxxx | xxxx | xxxx | xxxx |
| Trimannosyl-chitobiose core monoantennary core fucosylated α 2,6-monosialylated | x | | | | |
| Trimannosyl-chitobiose core monoantennary core fucosylated α 2,3-monosialylated | x | | | | |
| Trimannosyl-chitobiose core monoantennary α 2,6-monosialylated | x | | | | |
| Bimannosyl-chitobiose core monoantennary core fucosylated α 2,6-monosialylated | x | | | | |
| Bimannosyl-chitobiose core monoantennary core fucosylated α 2,3-monosialylated | x | | | | |

Importantly, paucimannosylation (M1, M1F, M2) corresponded to only ~20% of the total Asn71-glycopeptides derived from nCG. The glycopeptide profiling also indicated that nCG carried no or a negligible amount of M0F, M2F, and complex structures, all of which appeared at relatively high abundance in the released *N*-glycome. Comparable ionization response factors were estimated for the population of the glycopeptide species carrying the neutral chitobiose core and paucimannose glycans when analyzed in positive polarity MS [30]. This was supported by their similar LC elution window *i.e.*, 39 ± 1 min, giving them approximately equal solvent conditions for the ionization. However, the sialylated monoantennary complex *N*-glycopeptides were likely under-represented in the positive ion polarity used for the glycopeptide analysis relative to the neutral glycopeptides carrying the paucimannose, chitobiose core, and single GlcNAc β variants [30], possibly also creating a slight bias towards the sialoglycans in the glycomic profile obtained in negative ion polarity mode. This discrepancy was also explained by the identification of M1F and, in particular, M2F glycopeptides on two *N*-glycosylation sites of azurocidin (Asn126 and Asn171) and NE (Asn124 and Asn173) (Figure 3c–d). Hence, it became evident that nCG was not isolated to absolute purity and that the interfering azurocidin and NE had dramatically skewed the *N*-glycomic profile towards a more paucimannose-rich profile. The presence of nCG, azurocidin, and NE observed may relate to their similar nature and physicochemical properties, including their common storage compartment in the neutrophil azurophilic granules, similar protein mass (27–29 kDa), and high isoelectric points (pI 10–12) [9,50,51]. The presence of M2F glycoforms on azurocidin and NE has been reported previously [12,24].

2.4. ZIC-HILIC SPE Enrichment of nCG N-Glycopeptides Favors Complex Glycoforms

Chymotryptic glycopeptides were enriched using ZIC-HILIC SPE to target the nCG Asn71-glycopeptides carrying the missing glycan structures that were observed in the *N*-glycome, *i.e.*, M0F and complex *N*-glycans. This approach identified the Asn71-glycopeptide (GSNI~~N~~VTL) carrying the core fucosylated monosialylated complex *N*-glycan with an intact trimannosyl-chitobiose core in the retained ZIC-HILIC fraction (Figure 4a). Interestingly, however, the paucimannosidic and truncated chitobiose core structures carried by the nCG, azurocidin, and NE glycopeptides were, in contrast, identified in the non-retained fraction (Figure 4b). This indicates a requirement of a minimum degree of local hydrophilicity to enable ZIC-HILIC retention, which did not appear to be provided by the paucimannosidic *N*-glycans on these peptides. We have previously reported that M2 and M2F peptides are, at least in part, retained on ZIC-HILIC SPE when using identical stationary and mobile phase conditions *i.e.*, 1% (v/v) trifluoroacetic acid (TFA) as an ion pairing agent [15]. This indicates that the nature of the individual peptide carriers (as well as the mobile and stationary phases [52,53]) significantly influences the ZIC-HILIC retention behavior of these lowly hydrophilic truncated *N*-glycans attached to peptides.

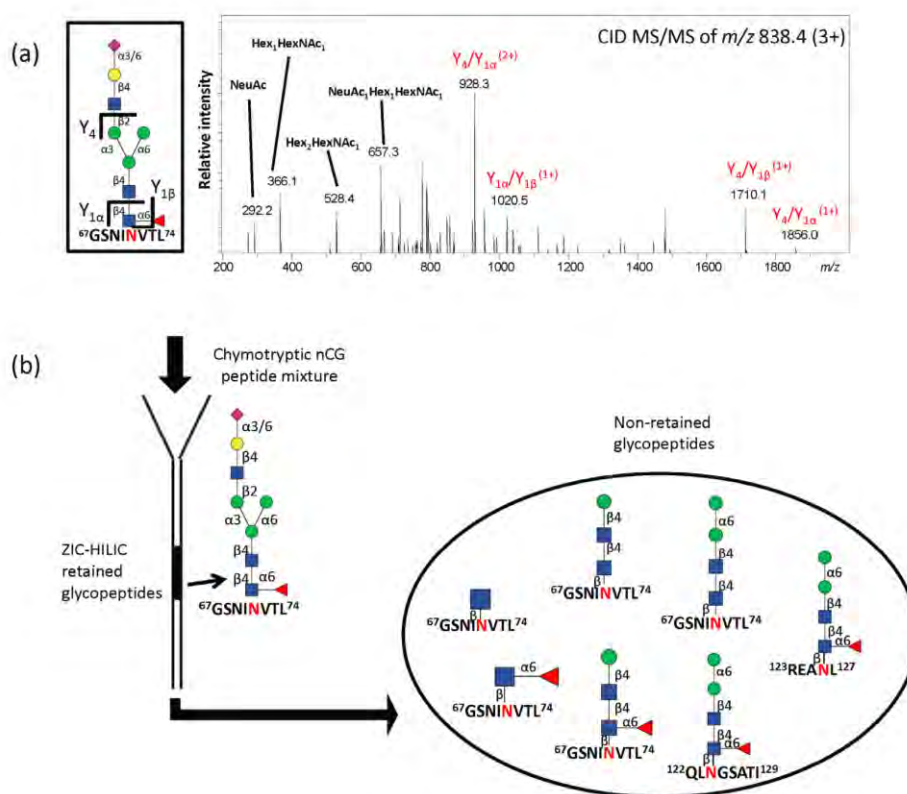


Figure 4. (a) RP-LC-CID-MS/MS confirming the structure of the single Asn71-glycopeptide of nCG retained on ZIC-HILIC SPE; (b) Schematic illustration showing the population of non-retained chymotryptic *N*-glycopeptides, *i.e.*, Asn71, Asn126, and Asn124 containing glycopeptides of nCG, azurocidin, and NE, respectively, using ZIC-HILIC SPE for glycopeptide enrichment. All glycopeptides were identified by CID- and ETD-MS/MS.

2.5. Intact nCG Profiling Maps the Asn71-Glycosylation and Other PTMs

The discrepancy between the *N*-glycome and Asn71-glycopeptide analysis was further investigated by profiling intact nCG using high-resolution/mass accuracy QTOF LC-ESI-MS. Several nCG glycoforms were observed including the truncated chitobiose cores (GlcNAc β and Fuc α 1,6GlcNAc β), paucimannosidic *N*-glycans (M1, M1F, M2, and M2F) and complex structures corresponding to the monoantennary sialylated *N*-glycans (Figure 5a). Interestingly, two C-terminal truncation variants of nCG displaying similar *N*-glycosylation were observed at different relative abundances *i.e.*, the Arg243-(61.9%) and the Ser244-(38.1%) terminating nCG. This was supported by the constant mass deviation of the multiple MS signal pairs ($\Delta m = +87$ Da) corresponding to the additional serine residue of the Ser244-variant and the accurate match of the theoretical and experimentally observed isotopic distribution of nCG. The two nCG truncated isoforms were validated at the peptide level by the identification and relative quantitation of the C-terminal $^{238}\text{IRTTMR}^{243}$ ($57.8\% \pm 1.1\%$) and $^{238}\text{IRTTMRS}^{244}$ ($42.2\% \pm 1.1\%$) peptides from the chymotryptic digest (Figure 5b). The Ser244 C-terminal of nCG has been documented before [7,54], but this is, to the best of our knowledge, the first time the additional Arg243 C-terminal on nCG has been defined and quantified.

The intact protein measurements also confirmed that nCG displayed no other modifications except for a single complete oxidation ($\Delta m = +16$ Da). The oxidation was localized to Met152 as confirmed by chymotryptic peptide analysis (see Figure S5). The high degree of oxidation of Met152 was supported by its high solvent accessibility (NACCESS score: 123.5) relative to the other more inaccessible methionine residues on the maturely folded nCG (*i.e.*, Met35 NACCESS score: 5.1, Met110 NACCESS score: 0, Met242 NACCESS score: 27.1). Oxidation of methionine residues of nCG has been reported to be modulated by myeloperoxidase as a mechanism to regulate the proteolytic activity of nCG [55]. The peptide analysis also confirmed that specific glutamine (Gln163) and asparagine (Asn208) residues were found to be deamidated. The deamidation may have been introduced naturally within the cell upon biosynthesis or artificially due to sample handling and/or during the MS/MS analysis [56]. The intact nCG glycoprofile accurately reflected the analysis of the Asn71-glycopeptide profile ($R^2 = 0.96$) rather than the *N*-glycan profile that was influenced by the presence of the other interfering neutrophil glycoproteins ($R^2 = 0.38$), thereby validating the correct Asn71-glycoprofile of nCG (Figure 5c). In a previous study by Watorek and coworkers, M2F and biantennary disialylated complex *N*-glycans were the only structures documented on nCG [12]. However, we did not observe biantennary disialylated complex *N*-glycans in our analysis, possibly due to differences in purification and the applied analytical methods. Table 1 provides a semi-quantitative overview of the site-specific *N*-glycosylation of nCG, azurocidin, and NE observed in this study.

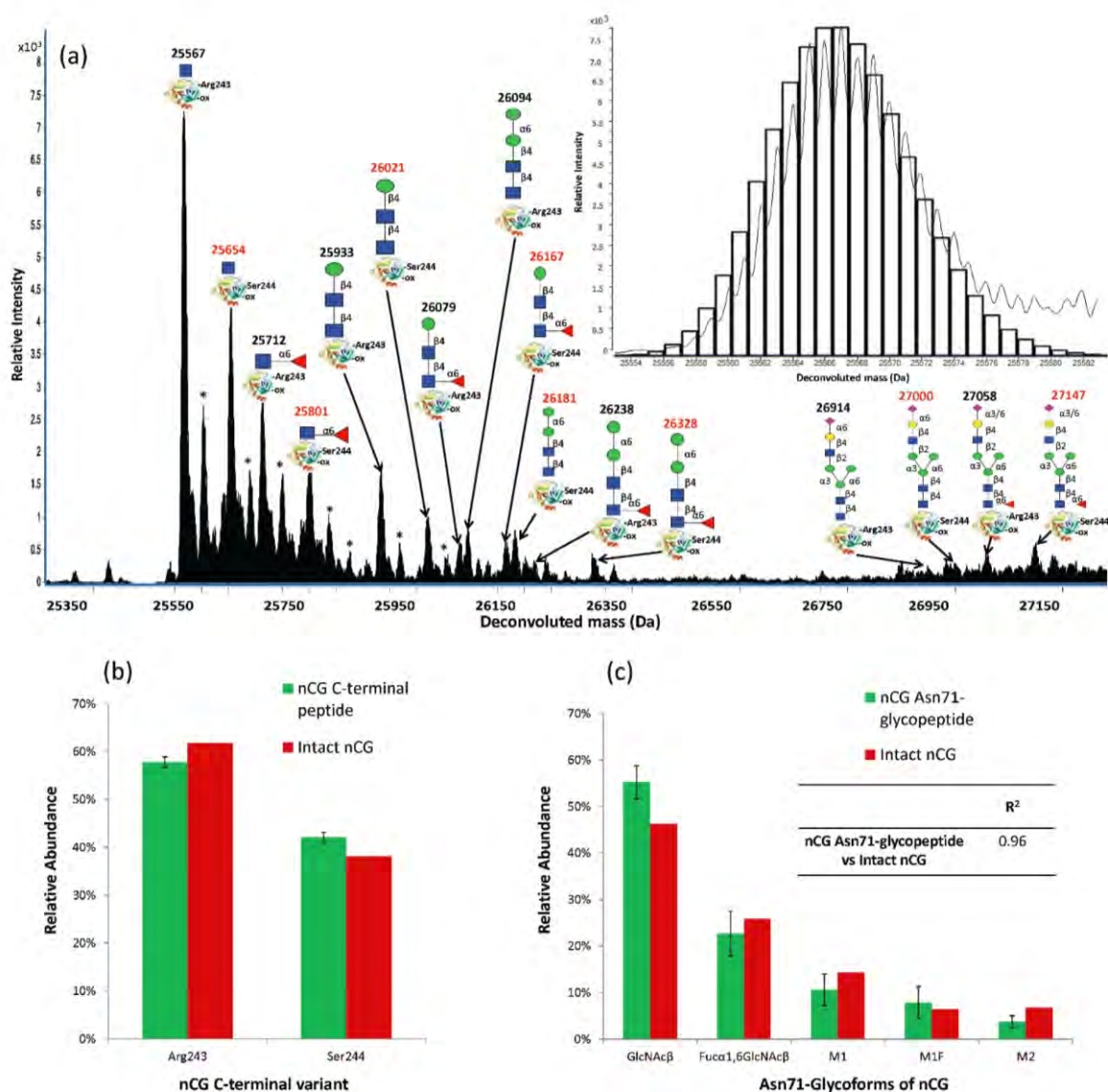


Figure 5. (a) QTOF LC-ESI-MS glycoprofiling of intact nCG at relative low fragmentor potential (200 V). The deconvoluted (average, apex) masses and structures of the individual nCG glycoforms are illustrated on the two C-terminal truncation variants of the protein (Arg243- and Ser244-C-terminal nCG variants in black and red, respectively). “-ox” denotes Met152 oxidation. * denotes adduct formation. Insert: Example of the accurate match of the theoretical (black bars) and the observed isotopic distribution of the Arg243-terminating and Asn71-GlcNAc β and Met152-oxidation containing nCG; (b) The ratio of nCG Arg243- and Ser244-truncation variants was confirmed at the peptide level; (c) The similar nCG Asn71-glycopeptide and intact nCG glycoform profile, as evaluated by the high correlation coefficient (R^2), confirmed the relative distribution of the Asn71-glycans. The trace Asn71-glycoforms were not included in this quantitative comparison. Data points are plotted as mean \pm SD, $n = 3$.

2.6. Establishing Asn71 Occupancy Level and N-Glycosidase F-Resistant Glycoforms of nCG

Initially, intact nCG was profiled under high fragmentor potential (>300 V), which suggested that a significant proportion of the nCG molecules appeared without a conjugated Asn71-glycan (Figure S6). Various fragmentor voltages were applied (150–400 V) to determine if the non-glycosylated nCG variants were indeed MS artefacts caused by in-source/post-source fragmentation due to the relative high fragmentor potential, rather than being naturally occurring proteoforms. It was observed that under milder MS conditions (200 V), the non-glycosylated nCG variants were absent. The complete Asn71-glycosylation site occupancy and the glycoform distribution were validated by excellent agreement of the intact glycoprotein and glycopeptide profiles (described above). We have previously validated that *N*-glycopeptides undergo no detectable fragmentation under the regular LC-ESI-MS/MS acquisition conditions and no non-glycosylated chymotryptic Asn71-peptides were observed in the chymotryptic peptide mixture, suggesting full occupancy of Asn71. Non-glycosylated peptides have been previously documented to ionize preferentially over the larger *N*-glycosylated peptides [30], thereby excluding a potential bias towards the glycosylated nCG in this evaluation. Site occupancy can also typically be evaluated using the non-glycosylated to de-*N*-glycosylated peptide ratio after *N*-glycosidase F treatment, due to the more similar ionization properties of these two species [30]. However, it was observed that the GlcNAc β and Fuc α 1,6GlcNAc β carbohydrate moieties were not removed from the peptide carriers by *N*-glycosidase F even under favorable enzyme concentrations, while, as expected, the paucimannosidic and complex *N*-glycans were completely removed from the same peptide during this treatment (see Figure S7). The *N*-glycosidase F-resistance of truncated chitobiose cores, which has been reported previously [44], not only excludes the possibility of performing the site occupancy based on the non- to de-*N*-glycosylated peptide ratio, but also masks these truncated structures in the regular *N*-glycosidase F-based *N*-glycome profiles.

2.7. The Proximal, but Short, Asn71-Glycans are not Obstructing the Active Site of nCG

Consulting a high-resolution three-dimensional (3D) structure of nCG [8] revealed that although Asn71 is proximal to the active site of nCG (~19 Å), the conjugated *N*-glycans are unlikely to interfere directly with the catalytic activity of the protein due to their truncated nature (e.g., the height of GlcNAc β is ~5 Å and M2 is ~17 Å) (see Figure 6). Only the low abundant elongated monoantennary complex sialo-*N*-glycans (height: ~27 Å) would theoretically be able to sterically interfere with the accessibility to the active site (see Figure S8). However, the presence of a bulky protein surface domain separating the Asn71-glycosylation site and the active site, and the fact that Asn71-conjugated *N*-glycans appear to be pointing away from the active site when using the default torsion angles to assess its presentation on the protein surface, makes any such interference unlikely. It was previously concluded that Asn71-glycosylation is not essential for the enzymatic activation and granule sorting of nCG [13]. Thus, the potential modulatory roles of Asn71-glycosylation on the nCG activity, its structural conformation, or any protein-independent functions of the carbohydrate moiety remain to be determined.

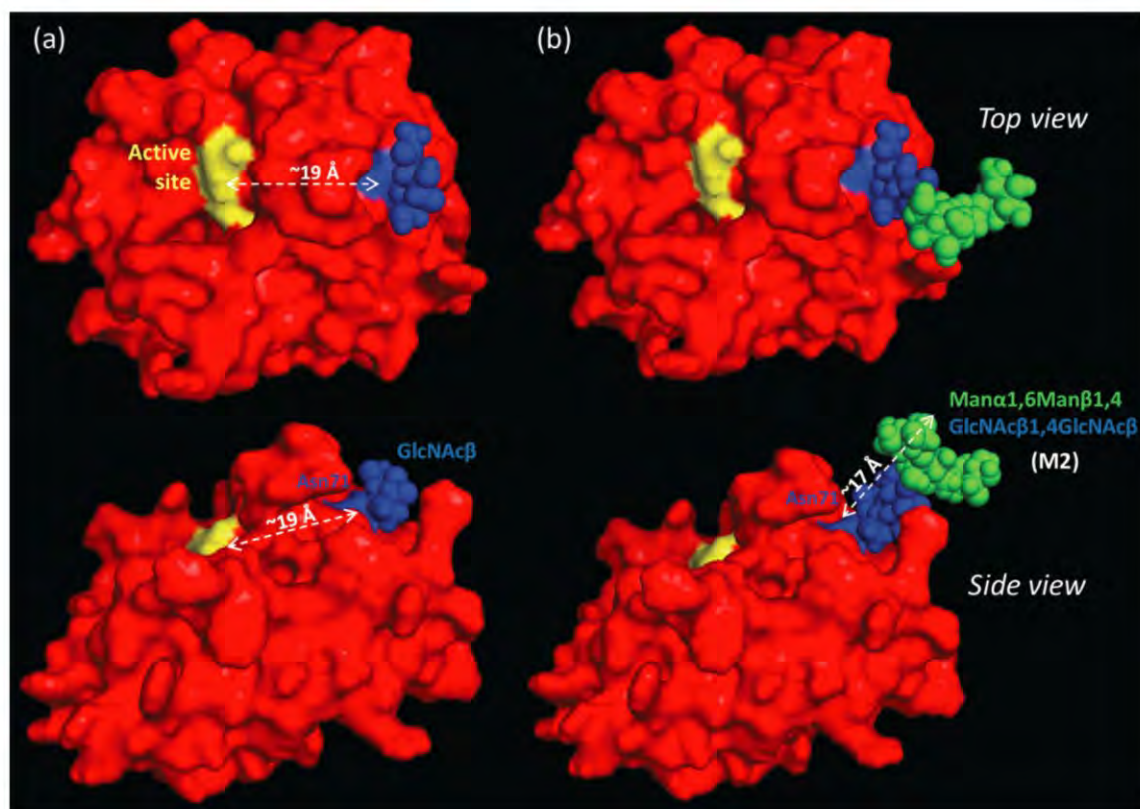


Figure 6. Top and side view of nCG illustrating the proximity (~ 19 Å) of the active site to the Asn71-glycosylation site conjugated with (a) GlcNAc β and (b) M2 (Man α 1,6Man β 1,4GlcNAc β 1,4GlcNAc β). Color scheme: yellow denotes His64, Asp108, and Ser201 forming the active site of nCG; blue denotes the Asn71-glycosylated residue and the conjugated GlcNAc residues; and green denotes mannose residues. The approximate height of the M2 N-glycan (~ 17 Å) is illustrated.

2.8. Spatial Considerations of nCG Structure Advance our Understanding of the Unconventional Asn71-Glycosylation

The Asn71-glycosylation site displayed medium-low solvent accessibility (NACCESS score: 44.1) upon assessment of the 3D structure of maturely folded nCG. We have previously demonstrated that the solvent accessibility of N-glycosylation sites of maturely folded glycoproteins correlates with the degree of N-glycan processing at that site and, thus, determines multiple glycan features including the glycan type, core fucosylation, and branching [57]. We have also demonstrated that subcellular-specific N-glycosylation appears to be related to differential solvent accessibilities of the N-glycosylation sites of proteins residing in different subcellular compartments [58]. Asn sites displaying paucimannosylation were shown to have higher solvent accessibility in comparison to the relatively inaccessible high mannose containing sites (NACCESS score typically 0–40), indicating that the truncated paucimannosidic proteins are generated by exposure to glycan processing by hydrolases (*i.e.*, hexosaminidases and mannosidases) [15]. No protein features other than this differential accessibility and the subcellular

localization have so far been correlated with the expression of these unusual paucimannosidic structures that are abundant in the azurophilic granules of neutrophils.

The medium-low solvent accessibility of Asn71 on nCG implies that the conjugated *N*-glycan intermediates were only partially available for processing during biosynthesis to the highly truncated GlcNAc β and Fuc α 1,6GlcNAc β glycoforms. In comparison, the Asn-sites of the M2F-carrying azurocidin and NE were found to be highly accessible (NACCESS score: 80.8–103.1). Hence, solvent accessibility alone does not explain the extreme Asn71-glycan truncation on nCG, but is congruent with the relatively low degree of core fucosylation (~30%) of nCG *N*-glycans. We are currently investigating the presence of other protein features required for the generation of paucimannose, chitobiose core, and GlcNAc β -Fuc α 1,6GlcNAc β -containing glycoproteins.

2.9. Subcellular-Specific *N*-Glycosylation of nCG in Human Neutrophils

Using site-specific profiling of enriched tryptic glycopeptides [15] and subcellular-specific libraries of neutrophil glycoproteins [16], we previously suggested that paucimannosidic and monoantennary complex (NeuAc $_1$ Gal $_1$ Man $_3$ GlcNAc $_3$ Fuc $_{0-1}$) *N*-glycans are carried by glycoproteins localizing to different subcellular compartments of the human neutrophil *i.e.*, azurophilic and the specific granules, respectively [15]. This was supported by the pronounced spatio-temporally regulated biosynthesis of glycoproteins in neutrophils generating compartment-specific *N*-glycosylation during the maturation of these immune cells in the bone marrow [15]. This process is referred to as “targeted-by-timing” and thought to be responsible for the compartment-specific *N*-glycosylation of neutrophils [15,59,60]. Thus, the observation of both paucimannosidic and monoantennary complex Asn71-glycans (as well as the further truncated chitobiose core structures) on nCG was, at first, rather surprising. However, nCG has in fact been found to reside in the azurophilic (~75%), in the specific granules (~15%), and in other compartments [16], thereby supporting the feature of subcellular-specific *N*-glycosylation on the same site of the same glycoprotein in different compartments within the human neutrophil. Isolation and structural analysis of nCG from the individual subcellular compartments of the human neutrophil are needed to confirm this proposed relationship. Although few other studies have reported the presence of truncated chitobiose glycoproteins from multiple cellular origins in mammals and invertebrates [45–49], indicating that the human neutrophil may be just one amongst many biological systems displaying these structures, their exact subcellular localization and potential functions remain to be investigated.

3. Experimental Section

3.1. Origin and Initial Handling of nCG

Purified human nCG (UniProt accession number: P08311) originating from resting neutrophils isolated from whole blood of a pool of healthy individuals was purchased from Lee BioSolutions, product number: 186-10 (St Louis, MO, USA). The purity was assessed by sodium dodecyl sulfate polyacrylamide gel electrophoresis (SDS-PAGE) (Bio-Rad, Sydney, Australia) upon arrival (see Figure S1), and the protein was aliquoted (20 μ g) and stored at -20 °C until use.

3.2. N-Glycan Release and Handling

Proteolytical inactivation of nCG was achieved using 1.5 mM PMSF for 90 min at 22 °C (see Figure S1). Subsequently, nCG was reduced using 10 mM dithiothreitol (final concentration) for 45 min at 56 °C and alkylated using 25 mM iodoacetic acid (final concentration) for 30 min in the dark at 22 °C. nCG was then analyzed by SDS-PAGE under reducing and denaturing conditions, using a 4–15% gradient gel at 120 V for 1 h at 22 °C. Subsequently, the protein was transferred to a primed 0.45- μ m PVDF membrane (Millipore, Bayswater, Australia) using a trans-blot turbo transfer system (BioRad) and stained with Direct Blue (Sigma-Aldrich, Castle Hill, Australia). The resulting 24–26 kDa gel band was excised and washed in separate wells in a flat bottom polypropylene 96-well plate (Corning Life Sciences, Corning, NY, USA). N-glycans were released and prepared from the membrane as previously described [20]. In brief, 3.5 U N-glycosidase F (*Flavobacterium meningosepticum*, Roche, Castle Hill, Australia) was used per 10 μ g protein in a 10 μ L water/well for 16 h at 37 °C. Released N-glycans were incubated with 100 mM ammonium acetate (pH 5) for 1 h at 22 °C. Glycan reduction was performed with 1 M sodium borohydride in 50 mM potassium hydroxide for 3 h at 50 °C, followed by glacial acetic acid quenching of the reaction. Dual desalting steps were performed in micro-SPE formats with strong cation exchange/C18 (where N-glycans are not retained) and PGC (where N-glycans are retained) stationary phases, respectively. Elution from the PGC-SPE columns was performed with 40% (v/v) acetonitrile (ACN) containing 0.1% (v/v) TFA and dried by vacuum centrifugation. Fractions were taken up in 10 μ L of water and analyzed using PGC-LC-MS/MS.

3.3. Exoglycosidase Treatment of Released N-Glycans

Aliquots of released and reduced N-glycans were digested for 16 h at 37 °C with multiple exoglycosidases in a final reaction volume of 10 μ L. Specifically, digestions were performed with α 2,3/6/8-unspecific sialidase (2 U) from *Arthrobacter ureafaciens* and the α 2,3-specific sialidase (2 U) from *Streptococcus pneumonia* in 50 mM sodium phosphate, pH 6 buffer. The α 1,2/3- > α 1,6-linkage-preferring Jack bean meal α -mannosidase (2 U) was performed in 20 mM sodium acetate, 2 mM zinc chloride, pH 5 buffer. All enzymes were purchased from Prozyme (Hayward, CA, USA). The exoglycosidases were removed by retention on the strong cation exchange/C18 and thus separated from the glycans in the sample preparation prior to PGC-LC-MS/MS.

3.4. PGC-LC-ESI-MS/MS-Based N-Glycome Profiling

N-glycans were analyzed by capillary LC-MS/MS (Agilent 1260 Infinity) using an ESI ion trap mass spectrometer (LC/MSD Trap XCT Plus Series 1100, Agilent Technologies, Melbourne, Australia). Samples were injected onto a PGC-LC capillary column (Hypercarb KAPPA, 5 μ m particle size, 200 Å pore size, 180 μ m inner diameter x 100 mm length, Thermo Scientific, Scoresby, Australia) and separation of N-glycans was carried out over a linear gradient of 0–45% (v/v) ACN/10 mM ammonium bicarbonate for 85 min at a constant flow rate of 2 μ L/min. The sample injection volume was 3 μ L. The acquisition range was m/z 200–2200. The acquisition was performed in negative ionization polarity in a data-dependent acquisition manner where the top two most abundant precursors in each full scan spectrum were selected for MS/MS using CID. The mass spectrometer was calibrated using a tune mix

(Agilent Technologies). Mass spectra were viewed and analyzed using DataAnalysis v4.0 (Bruker Daltonics, Melbourne, Australia). Glycoworkbench v1.2.4 assisted in the annotation and visualization of the *N*-glycan structures [61].

3.5. In-Solution Glycopeptide Generation, Enrichment, and Deglycosylation

nCG was proteolytically inactivated, reduced, and alkylated as described above. In-solution proteolytic digestion was carried out using bovine pancreas chymotrypsin (sequence grade, Roche) at 1:20 enzyme/substrate ratio (w/w) for 18 h at 25 °C in aqueous 50 mM ammonium bicarbonate, pH 8.4. The resulting chymotryptic peptide mixture was aliquoted, dried, and stored at −20 °C until use. Glycopeptide enrichment from the chymotryptic peptide mixture was performed by redissolving nCG in 10 µL of 80% (v/v) ACN in aqueous 1% (v/v) TFA using a custom-made ZIC-HILIC SPE equipped with a C18 disc (Millipore) to allow packing of the ZIC-HILIC material in the micro-column. The stationary phase consisted of ZIC-HILIC resin (10 µm particle size, 200 Å pore size, Sequant/Merck, Solna, Sweden). The columns were prepared as previously described [53]. In brief, the ZIC-HILIC resin was packed in the column (height: 5–10 mm, column volume: ~0.5–1 µL) and equilibrated in 50 µL mobile phase consisting of 80% (v/v) ACN/1% (v/v) TFA. Samples were loaded repeatedly onto the column in successive rounds before washing the column twice with 50 µL of the mobile phase. The enriched glycopeptides were then eluted using 2 × 50 µL 1% (v/v) TFA. An additional elution step with 50 µL of 80% (v/v) ACN/1% (v/v) TFA was carried out to ensure all glycopeptides were eluted from the C18 base of the column. Fractions were dried and taken up in 10 µL of 0.1% (v/v) formic acid (FA) for multiple LC-MS/MS injections. De-*N*-glycosylation was performed by redissolving aliquots of the chymotryptic peptide mixtures in 50 µL water and incubation with 10 U *N*-glycosidase F (Roche) for 16 h at 37 °C.

3.6. LC-MS/MS-Based *N*-Glycopeptide Analysis

nCG peptide mixtures were analyzed by ESI-MS/MS in positive polarity using an HCT 3D ion trap (Bruker Daltonics) coupled to an Ultimate 3000 LC (Dionex, Australia). The samples were loaded directly onto a C18 column (Proteocol HQ303, 300 µm inner diameter x 10 cm length, 3 µm particle size, 300 Å pore size, SGE, Australia). The column was equilibrated in 100% solvent A consisting of aqueous 0.1% (v/v) FA and a gradient up to 30% (0.5%/min slope) and a second gradient up to 60% (4.2%/min slope) of solvent B consisting of 0.1% (v/v) FA in ACN for 60 min and 7 min, respectively, before washing the column in 80% solvent B for 10 min and re-equilibration in the starting condition. A constant flow rate of 5 µL/min was used. The chymotryptic peptide mixture was analyzed with and without ZIC-HILIC-SPE-based glycopeptide enrichment in technical triplicates. Two injections (5 µL/injection) was performed in separate runs using the following setups: (1) LC-MS/MS analysis, where an MS full scan (m/z 300–2200; scan speed: 8100 $m/z/s$) was followed by a data-dependent fragmentation of the three most abundant signals using CID; and (2) LC-MS/MS analysis, where a MS full scan (m/z 400–1800) was followed by an ETD event of the two most abundant signals in the full scan. The ETD settings were as follows: ion count control reactant target ETD: 600,000, reactant accumulation time: 4–20 ms (\leq 200 ms), reaction time: 150 ms. Both CID- and ETD-LC-MS/MS were used for site-specific characterization of the nCG glycoforms. The mass accuracy of the mass spectrometer was

calibrated using a tune mix (Agilent Technologies) prior to acquisition. Mass spectra were viewed and analyzed using DataAnalysis v4.0 (Bruker Daltonics) and analysis was performed using GPMW v10.0 (Lighthouse, Odense, Denmark) [62] using the protein sequence of nCG (UniProt accession number: P08311), azurocidin (UniProt accession number: P20160) and NE (UniProt accession number: P08246).

3.7. Intact nCG Profiling

Intact nCG glycoprotein (1 µg) was analyzed by ESI-MS in positive ion polarity mode using a high-resolution/high mass accuracy QTOF 6538 mass spectrometer (Agilent Technologies) coupled to a capillary LC (Agilent 1260 Infinity). nCG was loaded directly onto a C4 column (Proteocol C4Q, 3 µm particle size, 300 Å pore size, 300 µm inner diameter x 10 cm length, SGE, Australia). The column was equilibrated in identical mobile phases as for the C18 column (described above) with a gradient up to 60% (v/v) (2%/min slope) of solvent B before washing the column in 99% (v/v) solvent B for 10 min and re-equilibration in the starting condition. A constant flow rate of 5 µL/min was used. One-microliter injections were used. Various fragmentor potentials (150–400 V) were tested in separate runs using the following MS settings in high-resolution (4 GHz) mode: MS full scan (m/z 400–2500), drying gas temperature 300 °C, drying gas flow rate 8 L/min, nebulizer pressure 10 psig, capillary potential 4300 V, skimmer potential 65 V. The mass accuracy of the mass spectrometer was calibrated using a tune mix (Agilent Technologies) prior to acquisition. An internal mass calibration sample was infused continuously during the LC-MS run to allow accurate and automated in-spectrum mass calibration. Generally, mass accuracies better than 2 ppm were achieved. Mass spectra were viewed and analyzed with MassHunter workstation vB.06 (Agilent Technologies).

3.8. Profiling nCG N-Glycans, N-Glycopeptides, and Intact Glycoprotein

The detailed nCG N-glycans structures were manually determined by their monoisotopic masses, CID-MS/MS fragmentation patterns, and their relative and absolute retention times based on the PGC-LC-MS/MS N-glycome data (see Figure S3 and Table S1 for data supporting the N-glycan characterization). The relative distribution of the individual N-glycans was estimated based on the relative peak area of the extracted ion chromatograms (EICs) of all observed charge states of each N-glycan against the total EIC peak area of all observed N-glycans.

The structure of the observed N-glycopeptides were manually determined by their monoisotopic masses, CID- and ETD-MS/MS fragmentation patterns and retention times based on the RP-LC-MS/MS analysis of chymotryptic N-glycopeptides (see Figure S4 and Table S2 for data supporting the N-glycopeptide characterization).

Chymotryptic Asn71-glycopeptides of nCG eluted around 39 ± 1 min (Figure S7). LC-MS/MS spectral data from both the non-enriched and ZIC-HILIC-SPE-enriched glycopeptide fractions were used for site-specific characterization of Asn71-glycosylation. Only the non-enriched peptide mixtures were used for quantitative glycoprofiling. Briefly, the distribution of the glycoforms and the site occupancy level were estimated from the relative EICs area of all observed charge states of Asn71-glycopeptides by assuming equal ionization efficiencies of these related molecular species [30,63].

Intact nCG was profiled by deconvoluting the obtained spectra using the default settings in the maximum entropy algorithm. The relative abundance of the observed glycoforms was determined

from their relative EICs area as calculated using BioConfirm in MassHunter workstation vB.06 (Agilent Technologies).

3.9. Glycoprotein Modeling

The 3D protein structure of nCG obtained by X-ray crystallography (PDB accession number: 1CGH) was used for modeling and solvent accessibility determination [8]. This particular 3D structure was chosen over other available structures due to its high sequence coverage of nCG, spatial resolution and the natural source of the protein, which was purified directly from human neutrophils. Visualization and distance measurements were performed using PyMOL Molecular Graphic System, v1.3 (Schrödinger, LLC) and RasMol v2.7.5, respectively. *N*-glycans were modeled on Asn71 of nCG *in silico* using the default torsion angles provided by Glyprot [64]. The solvent accessibilities of Asn71 and the individual methionine residues of nCG were determined using NACCESS, a solvent accessibility determination program [65]. The atomic accessible areas (van der Waal's interactions) were measured in absolute arbitrary units by rolling a 5 Å probe on the protein surface of nCG [66].

3.10. Statistics

Data points collected as technical triplicates were presented as mean \pm standard deviation (SD). Statistical regression analyses were carried out using Microsoft Excel.

4. Conclusions

Developments in LC-MS/MS-based glycoproteomics [67,68] and “top down” glycoprofiling of intact glycoproteins [33,69] are providing us with powerful tools that undoubtedly will advance our understanding of many structural aspects of glycobiology. However, it remains important to stress that these analytical tools are still relatively immature and, at present, incapable by themselves of providing information on all the levels of structural heterogeneity displayed by glycoproteins, even those with a single site of glycosylation, as clearly illustrated in this study. Therefore, it is still necessary to apply an array of technologies, in particular when mapping proteins displaying the described truncated *N*-glycosylation.

Herein, detailed site-specific Asn71-glycoprofiling using glycomics, glycopeptide, and intact glycoprotein MS analysis has documented that nCG carries unconventional *N*-glycosylation including a truncated chitobiose core (GlcNAc β and Fuc α 1,6GlcNAc β), as well as paucimannosidic (M1, M1F, M2, and M2F) and monoantennary sialo *N*-glycans. This structural library of the nCG molecular heterogeneity further confirms the unconventional and subcellular-specific *N*-glycosylation in the human neutrophil. The functional consequences of the unique glycosylation utilized by human neutrophils remain to be elucidated and we are currently investigating the functional role of the unconventional Asn71-glycosylation of nCG by building on the observations provided here.

Acknowledgments

This research was facilitated through access to the Australian Proteomics Analysis Facility (APAF). Ian Loke was supported by an international Macquarie University Research Scholarship (iMQRES) and an Australian Cystic Fibrosis postgraduate studentship. Morten Thaysen-Andersen was supported by an Early Career Fellowship from the Cancer Institute, NSW, Australia. Jodie Abrahams and Edward Moh are thanked for technical assistance.

Author Contributions

Ian Loke and Morten Thaysen-Andersen designed the study. Ian Loke performed the experiments. Ian Loke and Morten Thaysen-Andersen analyzed the data. Ian Loke, Nicolle H. Packer, and Morten Thaysen-Andersen derived the results and the conclusions. Ian Loke, Nicolle H. Packer, and Morten Thaysen-Andersen wrote the paper.

Conflicts of Interest

The authors declare no conflict of interest.

References

1. Garwicz, D.; Lennartsson, A.; Jacobsen, S.E.; Gullberg, U.; Lindmark, A. Biosynthetic profiles of neutrophil serine proteases in a human bone marrow-derived cellular myeloid differentiation model. *Haematologica* **2005**, *90*, 38–44.
2. Korkmaz, B.; Moreau, T.; Gauthier, F. Neutrophil elastase, proteinase 3 and cathepsin G: Physicochemical properties, activity and physiopathological functions. *Biochimie* **2008**, *90*, 227–242.
3. Pham, C.T. Neutrophil serine proteases: Specific regulators of inflammation. *Nat. Rev. Immunol.* **2006**, *6*, 541–550.
4. Sambrano, G.R.; Huang, W.; Faruqi, T.; Mahrus, S.; Craik, C.; Coughlin, S.R. Cathepsin G activates protease-activated receptor-4 in human platelets. *J. Biol. Chem.* **2000**, *275*, 6819–6823.
5. Guyot, N.; Wartelle, J.; Malleret, L.; Todorov, A.A.; Devouassoux, G.; Pacheco, Y.; Jenne, D.E.; Belaouaj, A. Unopposed cathepsin G, neutrophil elastase, and proteinase 3 cause severe lung damage and emphysema. *Am. J. Pathol.* **2014**, *184*, 2197–2210.
6. Garwicz, D.; Lindmark, A.; Persson, A.M.; Gullberg, U. On the role of the proform-conformation for processing and intracellular sorting of human cathepsin G. *Blood* **1998**, *92*, 1415–1422.
7. Salvesen, G.; Enghild, J.J. An unusual specificity in the activation of neutrophil serine proteinase zymogens. *Biochemistry* **1990**, *29*, 5304–5308.
8. Hof, P.; Mayr, I.; Huber, R.; Korzus, E.; Potempa, J.; Travis, J.; Powers, J.C.; Bode, W. The 1.8 Å crystal structure of human cathepsin G in complex with Suc-Val-Pro-PheP-(OPh)₂: A Janus-faced proteinase with two opposite specificities. *EMBO J.* **1996**, *15*, 5481–5491.
9. Korkmaz, B.; Horwitz, M.S.; Jenne, D.E.; Gauthier, F. Neutrophil elastase, proteinase 3, and cathepsin G as therapeutic targets in human diseases. *Pharmacol. Rev.* **2010**, *62*, 726–759.
10. Burster, T.; Macmillan, H.; Hou, T.; Boehm, B.O.; Mellins, E.D. Cathepsin G: Roles in antigen presentation and beyond. *Mol. Immunol.* **2010**, *47*, 658–665.

11. Salvesen, G.; Farley, D.; Shuman, J.; Przybyla, A.; Reilly, C.; Travis, J. Molecular cloning of human cathepsin G: Structural similarity to mast cell and cytotoxic T lymphocyte proteinases. *Biochemistry* **1987**, *26*, 2289–2293.
12. Watorek, W.; Halbeek, H.; Travis, J. The isoforms of human neutrophil elastase and cathepsin G differ in their carbohydrate side chain structures. *Biol. Chem. Hoppe-Seyler* **1993**, *374*, 385–393.
13. Garwicz, D.; Lindmark, A.; Gullberg, U. Human cathepsin G lacking functional glycosylation site is proteolytically processed and targeted for storage in granules after transfection to the rat basophilic/mast cell line RBL or the murine myeloid cell line 32D. *J. Biol. Chem.* **1995**, *270*, 28413–28418.
14. Venkatakrishnan, V.; Thaysen-Andersen, M.; Chen, S.C.; Nevalainen, H.; Packer, N.H. Cystic fibrosis and bacterial colonization define the sputum *N*-glycosylation phenotype. *Glycobiology* **2015**, *25*, 88–100.
15. Thaysen-Andersen, M.; Venkatakrishnan, V.; Loke, I.; Laurini, C.; Diestel, S.; Parker, B.L.; Packer, N.H. Human neutrophils secrete bioactive paucimannosidic proteins from azurophilic granules into pathogen-infected sputum. *J. Biol. Chem.* **2015**, *290*, 8789–8802.
16. Rorvig, S.; Ostergaard, O.; Heegaard, N.H.; Borregaard, N. Proteome profiling of human neutrophil granule subsets, secretory vesicles, and cell membrane: Correlation with transcriptome profiling of neutrophil precursors. *J. Leukocyte Biol.* **2013**, *94*, 711–721.
17. Ruhaak, L.R.; Stroble, C.; Underwood, M.A.; Lebrilla, C.B. Detection of milk oligosaccharides in plasma of infants. *Anal. Bioanal. Chem.* **2014**, *406*, 5775–5784.
18. Thomsson, K.A.; Karlsson, N.G.; Hansson, G.C. Liquid chromatography-electrospray mass spectrometry as a tool for the analysis of sulfated oligosaccharides from mucin glycoproteins. *J. Chromatogr. A* **1999**, *854*, 131–139.
19. Stavenhagen, K.; Kolarich, D.; Wührer, M. Clinical glycomics employing graphitized carbon liquid chromatography-mass spectrometry. *Chromatographia* **2015**, *78*, 307–320.
20. Jensen, P.H.; Karlsson, N.G.; Kolarich, D.; Packer, N.H. Structural analysis of *N*- and *O*-glycans released from glycoproteins. *Nat. Protoc.* **2012**, *7*, 1299–1310.
21. Pabst, M.; Bondili, J.S.; Stadlmann, J.; Mach, L.; Altmann, F. Mass + retention time = structure: A strategy for the analysis of *N*-glycans by carbon LC-ESI-MS and its application to fibrin *N*-glycans. *Anal. Chem.* **2007**, *79*, 5051–5057.
22. Lee, L.Y.; Thaysen-Andersen, M.; Baker, M.S.; Packer, N.H.; Hancock, W.S.; Fanayan, S. Comprehensive *N*-glycome profiling of cultured human epithelial breast cells identifies unique secretome *N*-glycosylation signatures enabling tumorigenic subtype classification. *J. Proteome Res.* **2014**, *13*, 4783–4795.
23. Palmisano, G.; Larsen, M.R.; Packer, N.H.; Thaysen-Andersen, M. Structural analysis of glycoprotein sialylation—Part II: LC-MS based detection. *RSC Adv.* **2013**, *3*, doi: 10.1039/c3ra42969e
24. Olczak, M.; Watorek, W. Structural analysis of *N*-glycans from human neutrophil azurocidin. *Biochem. Biophys. Res. Commun.* **2002**, *293*, 213–219.
25. Sumer-Bayraktar, Z.; Nguyen-Khuong, T.; Jayo, R.; Chen, D.D.; Ali, S.; Packer, N.H.; Thaysen-Andersen, M. Micro- and macroheterogeneity of *N*-glycosylation yields size and charge isoforms of human sex hormone binding globulin circulating in serum. *Proteomics* **2012**, *12*, 3315–3327.

26. Kolarich, D.; Jensen, P.H.; Altmann, F.; Packer, N.H. Determination of site-specific glycan heterogeneity on glycoproteins. *Nat. Protoc.* **2012**, *7*, 1285–1298.
27. Hogan, J.M.; Pitteri, S.J.; Chrisman, P.A.; McLuckey, S.A. Complementary structural information from a tryptic *N*-linked glycopeptide via electron transfer ion/ion reactions and collision-induced dissociation. *J. Proteome Res.* **2005**, *4*, 628–632.
28. Wührer, M.; Catalina, M.I.; Deelder, A.M.; Hokke, C.H. Glycoproteomics based on tandem mass spectrometry of glycopeptides. *J. Chromatogr. B Analyt. Technol. Biomed. Life Sci.* **2007**, *849*, 115–128.
29. Peterman, S.M.; Mulholland, J.J. A novel approach for identification and characterization of glycoproteins using a hybrid linear ion trap/FT-ICR mass spectrometer. *J. Am. Soc. Mass Spectrom.* **2006**, *17*, 168–179.
30. Stavenhagen, K.; Hinneburg, H.; Thaysen-Andersen, M.; Hartmann, L.; Silva, D.V.; Fuchser, J.; Kaspar, S.; Rapp, E.; Seeberger, P.H.; Kolarich, D. Quantitative mapping of glycoprotein micro-heterogeneity and macro-heterogeneity: An evaluation of mass spectrometry signal strengths using synthetic peptides and glycopeptides. *J. Mass Spectrom.* **2013**, *48*, 627–639.
31. Häggglund, P.; Bunkenborg, J.; Elortza, F.; Jensen, O.N.; Roepstorff, P. A new strategy for identification of *N*-glycosylated proteins and unambiguous assignment of their glycosylation sites using HILIC enrichment and partial deglycosylation. *J. Proteome Res.* **2004**, *3*, 556–566.
32. Stimson, E.; Hope, J.; Chong, A.; Burlingame, A.L. Site-specific characterization of the *N*-linked glycans of murine prion protein by high-performance liquid chromatography/electrospray mass spectrometry and exoglycosidase digestions. *Biochemistry* **1999**, *38*, 4885–4895.
33. Leymarie, N.; Griffin, P.J.; Jonscher, K.; Kolarich, D.; Orlando, R.; McComb, M.; Zaia, J.; Aguilan, J.; Alley, W.R.; Altmann, F.; *et al.* Interlaboratory study on differential analysis of protein glycosylation by mass spectrometry: The ABRF glycoprotein research multi-institutional study 2012. *Mol. Cell. Proteom.* **2013**, *12*, 2935–2951.
34. Domon, B.; Costello, C.E. A systematic nomenclature for carbohydrate fragmentations in FAB-MS/MS spectra of glycoconjugates. *Glycoconjugate J.* **1988**, *5*, 397–409.
35. Everest-Dass, A.V.; Abrahams, J.L.; Kolarich, D.; Packer, N.H.; Campbell, M.P. Structural features for distinguishing *N*- and *O*-linked glycan isomers by LC-ESI-IT MS/MS. *J. Am. Soc. Mass Spectrom.* **2013**, *24*, 895–906.
36. Harvey, D.J. Fragmentation of negative ions from carbohydrates: Part 3. Fragmentation of hybrid and complex *N*-linked glycans. *J. Am. Soc. Mass Spectrom.* **2005**, *16*, 647–659.
37. Winchester, B. Lysosomal metabolism of glycoproteins. *Glycobiology* **2005**, *15*, 1R–15R.
38. Balog, C.I.; Stavenhagen, K.; Fung, W.L.; Koeleman, C.A.; McDonnell, L.A.; Verhoeven, A.; Mesker, W.E.; Tollenaar, R.A.; Deelder, A.M.; Wührer, M. *N*-glycosylation of colorectal cancer tissues: A liquid chromatography and mass spectrometry-based investigation. *Mol. Cell. Proteomics* **2012**, *11*, 571–585.
39. Dahmen, A.C.; Fergen, M.T.; Laurini, C.; Schmitz, B.; Loke, I.; Thaysen-Andersen, M.; Diestel, S. Paucimannosidic glycoepitopes are functionally involved in proliferation of neural progenitor cells in the subventricular zone. *Glycobiology* **2015**, *25*, 869–880.

40. Hashii, N.; Kawasaki, N.; Itoh, S.; Nakajima, Y.; Kawanishi, T.; Yamaguchi, T. Alteration of *N*-glycosylation in the kidney in a mouse model of systemic lupus erythematosus: Relative quantification of *N*-glycans using an isotope-tagging method. *Immunology* **2009**, *126*, 336–345.
41. Ravnsborg, T.; Houen, G.; Hojrup, P. The glycosylation of myeloperoxidase. *Biochim. Biophys. Acta* **2010**, *1804*, 2046–2053.
42. Zoega, M.; Ravnsborg, T.; Hojrup, P.; Houen, G.; Schou, C. Proteinase 3 carries small unusual carbohydrates and associates with alpha-defensins. *J. Proteomics* **2012**, *75*, 1472–1485.
43. Babu, P.; North, S.J.; Jang-Lee, J.; Chalabi, S.; Mackerness, K.; Stowell, S.R.; Cummings, R.D.; Rankin, S.; Dell, A.; Haslam, S.M. Structural characterisation of neutrophil glycans by ultra sensitive mass spectrometric glycomics methodology. *Glycoconjugate J.* **2009**, *26*, 975–986.
44. Chu, F.K. Requirements of cleavage of high mannose oligosaccharides in glycoproteins by peptide *N*-glycosidase F. *J. Biol. Chem.* **1986**, *261*, 172–177.
45. Medzihradszky, K.F.; Kaasik, K.; Chalkley, R.J. Tissue-specific glycosylation at the glycopeptide level. *Mol. Cell. Proteomics* **2015**, *14*, 2103–2110.
46. Trinidad, J.C.; Schoepfer, R.; Burlingame, A.L.; Medzihradszky, K.F. *N*- and *O*-glycosylation in the murine synaptosome. *Mol. Cell. Proteomics* **2013**, *12*, 3474–3488.
47. Wang, Z.; Udeshi, N.D.; Slawson, C.; Compton, P.D.; Sakabe, K.; Cheung, W.D.; Shabanowitz, J.; Hunt, D.F.; Hart, G.W. Extensive crosstalk between *O*-GlcNAcylation and phosphorylation regulates cytokinesis. *Sci. Signal.* **2010**, doi:10.1126/scisignal.2000526.
48. Kim, Y.C.; Jahren, N.; Stone, M.D.; Udeshi, N.D.; Markowski, T.W.; Witthuhn, B.A.; Shabanowitz, J.; Hunt, D.F.; Olszewski, N.E. Identification and origin of *N*-linked β -D-N-acetylglucosamine monosaccharide modifications on arabidopsis proteins. *Plant Physiol.* **2013**, *161*, 455–464.
49. Klement, E.; Lipinski, Z.; Kupihar, Z.; Udvardy, A.; Medzihradszky, K.F. Enrichment of *O*-GlcNAc modified proteins by the periodate oxidation-hydrazide resin capture approach. *J. Proteome Res.* **2010**, *9*, 2200–2206.
50. Campanelli, D.; Detmers, P.A.; Nathan, C.F.; Gabay, J.E. Azurocidin and a homologous serine protease from neutrophils. Differential antimicrobial and proteolytic properties. *J. Clin. Invest.* **1990**, *85*, 904–915.
51. Lominadze, G.; Powell, D.W.; Luerman, G.C.; Link, A.J.; Ward, R.A.; McLeish, K.R. Proteomic analysis of human neutrophil granules. *Mol. Cell. Proteomics* **2005**, *4*, 1503–1521.
52. Thaysen-Andersen, M.; Mysling, S.; Hojrup, P. Site-specific glycoprofiling of *N*-linked glycopeptides using MALDI-TOF MS: Strong correlation between signal strength and glycoform quantities. *Anal. Chem.* **2009**, *81*, 3933–3943.
53. Mysling, S.; Palmisano, G.; Hojrup, P.; Thaysen-Andersen, M. Utilizing ion-pairing hydrophilic interaction chromatography solid phase extraction for efficient glycopeptide enrichment in glycoproteomics. *Anal. Chem.* **2010**, *82*, 5598–5609.
54. Lindmark, A.; Gullberg, U.; Lindgren, G.; Persson, A.M.; Nilsson, E.; Olsson, I. Carboxyl-terminal prodomain-deleted human leukocyte elastase and cathepsin G are efficiently targeted to granules and enzymatically activated in the rat basophilic/mast cell line RBL. *J. Biol. Chem.* **1995**, *270*, 12912–12918.

55. Shao, B.; Belaouaj, A.; Verlinde, C.L.; Fu, X.; Heinecke, J.W. Methionine sulfoxide and proteolytic cleavage contribute to the inactivation of cathepsin G by hypochlorous acid: An oxidative mechanism for regulation of serine proteinases by myeloperoxidase. *J. Biol. Chem.* **2005**, *280*, 29311–29321.
56. Li, X.; Cournoyer, J.J.; Lin, C.; O'Connor, P.B. Use of ¹⁸O labels to monitor deamidation during protein and peptide sample processing. *J. Am. Soc. Mass Spectrom.* **2008**, *19*, 855–864.
57. Thaysen-Andersen, M.; Packer, N.H. Site-specific glycoproteomics confirms that protein structure dictates formation of *N*-glycan type, core fucosylation and branching. *Glycobiology* **2012**, *22*, 1440–1452.
58. Lee, L.Y.; Lin, C.H.; Fanayan, S.; Packer, N.H.; Thaysen-Andersen, M. Differential site accessibility mechanistically explains subcellular-specific *N*-glycosylation determinants. *Front. Immunol.* **2014**, doi:10.3389/fimmu.2014.00404.
59. Borregaard, N.; Cowland, J.B. Granules of the human neutrophilic polymorphonuclear leukocyte. *Blood* **1997**, *89*, 3503–3521.
60. Borregaard, N.; Sorensen, O.E.; Theilgaard-Monch, K. Neutrophil granules: A library of innate immunity proteins. *Trends Immunol.* **2007**, *28*, 340–345.
61. Ceroni, A.; Maass, K.; Geyer, H.; Geyer, R.; Dell, A.; Haslam, S.M. Glycoworkbench: A tool for the computer-assisted annotation of mass spectra of glycans. *J. Proteome Res.* **2008**, *7*, 1650–1659.
62. Peri, S.; Steen, H.; Pandey, A. GPMW—A software tool for analyzing proteins and peptides. *Trends Biochem. Sci.* **2001**, *26*, 687–689.
63. Leymarie, N.; Zaia, J. Effective use of mass spectrometry for glycan and glycopeptide structural analysis. *Anal. Chem.* **2012**, *84*, 3040–3048.
64. Bohne-Lang, A.; von der Lieth, C.W. GlyProt: In silico glycosylation of proteins. *Nucleic Acids Res.* **2005**, *33*, W214–W219.
65. Hubber, S.J.; Thornton, J.M. *NACCESS Computer Program, Department of Biochemistry and Molecular Biology*; University College London: London, UK, 1993.
66. Lee, B.; Richards, F.M. The interpretation of protein structures: Estimation of static accessibility. *J. Mol. Biol.* **1971**, *55*, 379–400.
67. Thaysen-Andersen, M.; Packer, N.H. Advances in LC-MS/MS-based glycoproteomics: Getting closer to system-wide site-specific mapping of the *N*- and *O*-glycoproteome. *Biochim. Biophys. Acta* **2014**, *1844*, 1437–1452.
68. Kolli, V.; Schumacher, K.N.; Dodds, E.D. Engaging challenges in glycoproteomics: Recent advances in MS-based glycopeptide analysis. *Bioanalysis* **2015**, *7*, 113–131.
69. Rosati, S.; Yang, Y.; Barendregt, A.; Heck, A.J. Detailed mass analysis of structural heterogeneity in monoclonal antibodies using native mass spectrometry. *Nat. Protoc.* **2014**, *9*, 967–976.

© 2015 by the authors; licensee MDPI, Basel, Switzerland. This article is an open access article distributed under the terms and conditions of the Creative Commons Attribution license (<http://creativecommons.org/licenses/by/4.0/>).

4.3 Overview of main findings, conclusions and future directions

Main findings and conclusions

- The use of complementary LC-MS/MS approaches comprising of *N*-glycan, *N*-glycopeptide and intact glycoprotein analyses enabled detailed and accurate *N*-glycosylation profiling of nCG. In addition, the parallel use of these analytical strategies facilitated the discovery of two methionine oxidised C-terminal truncation variants of nCG.
- For the first time, the single Asn71-*N*-glycosylation site of nCG was shown to carry predominately ultra-truncated GlcNAc β - and Fuc α 1,6GlcNAc β - glycans. Paucimannosidic (M1, M1F, M2) and complex sialylated monoantennary *N*-glycans (FA1G1S1) were also present on nCG in lower abundance.
- The unconventional GlcNAc- and Fuc α 1,6GlcNAc-glycans lack PGC-LC retention and are *N*-glycosidase F insensitive. The qualitative and quantitative discrepancy between the *N*-glycan and *N*-glycopeptide data illustrated the importance of performing multiple levels of structural analysis to enable a detailed and accurate description of the *N*-glycosylation of neutrophil proteins carrying unusual *N*-glycans.
- The data indicated that a minimum degree of local hydrophilicity is required for efficient enrichment of *N*-glycopeptides using zwitterionic hydrophilic interaction liquid chromatography (ZIC-HILIC) SPE. The truncated chitobiose core and paucimannosidic structures of Asn71 of nCG produced insufficient hydrophilicity for reproducible HILIC retention whereas Asn71-glycopeptides carrying the longer sialo-glycans were efficiently enriched.
- The Asn71 glycosylation site has a relatively low solvent accessibility on the surface of maturely folded nCG, suggesting that the *N*-glycans on this site were only partially available for processing during biosynthesis. The presence of GlcNAc β - and Fuc α 1,6GlcNAc β - on this site suggest that, in addition to solvent accessibility, other protein structural features may also contribute to the generation of these unconventional structures on nCG.
- The distal position of Asn71 relative to the active site of nCG suggests that the short *N*-glycans on this site are unlikely to interfere with the proteolytic activity of this serine protease.

Future directions

- The biosynthesis of the truncated chitobiose structures on nCG remains to be resolved. As nCG is a central protease involved in innate immunity (Burster et al., 2010), it becomes not only important to determine how these structures arise during the maturation of *N*-glycoproteins but also their functional relevance in neutrophil immune defence.
- These truncated chitobiose structures could arise due to the action of endogenous endoglycosidases such as Endo- β -N-acetylglucosaminidase (ENGase). ENGases has been reported in human (Tadashi et al., 2002) but have yet to be shown to act on properly folded *N*-glycoproteins *in vivo* (Huang et al., 2015; Suzuki, 2016). ENGases might also be present in the azurophilic granules of neutrophils. The enzymatic action of this endoglycosidase on *N*-glycoproteins can be determined by mass spectrometry in future. In addition, their presence in the azurophilic granules of neutrophils can be investigated through the use of gene expression arrays and immunocytochemistry.
- The potential modulatory roles of *N*-glycosylation on the protease activity, structural conformation and interaction partners of nCG remain to be determined. As ENGases have also been identified in *Streptococcus pyogenes* and shown to hydrolyse the chitobiose core *N*-glycans of IgG (Collin and Olsen, 2001), the presence of the single β -linked GlcNAc residue on nCG might be a protective mechanism to preserve immunological functions in addition to the anti-microbial activity of nCG. This should be investigated in the future using bacterial co-cultures with paucimannosidic proteins present in the azurophilic granules to determine if these bacterial derived ENGases could hydrolyse the *N*-glycan structures present on these *N*-glycoproteins.
- The serine protease proteinase 3 has also been reported to carry these truncated structures similar to nCG (Zoega et al., 2012). In contrast, other serine proteases such as HNE and azurocidin carries mainly paucimannosidic *N*-glycans (**Chapter 5**) (Olczak and Watorek, 2002). This could be due to the localisation of HNE and azurocidin in the micro-environment within the azurophilic granules that differs from the localisation of PR3 and nCG. Therefore, PR3 and nCG might encounter ENGases within their micro-environment but are not seen by HNE and azurocidin. This could explain the ultra-truncated structures carried by PR3 and nCG but not on HNE and azurocidin. The presence of such micro-environment within the azurophilic granule compartment should be investigated in the future through live cell imaging with the use of highly specific and ultrasensitive two

photon fluorescence imaging or spinning disk confocal microscopy to enable higher visualisation of the micro-environment within the granule compartment (Babes and Kubes, 2016; Lim et al., 2015).

- The presence of truncated chitobiose structures have been reported to be present in the mouse brain and liver as well as in mammalian cell lines and invertebrates (Kim et al., 2013; Medzihradszky et al., 2015; Trinidad et al., 2013; Wang et al., 2010). At present, only a few studies have reported the presence of these truncated structures in human (Nagae et al., 2014; Zoega et al., 2012). A similar cell- and tissue-wide distribution of these structures in human tissues and cells remain to be explored. This can be studied using glycoproteomics to identify the site-specific attachments of these unconventional structures (Trinidad et al., 2013). In addition, the use of lectins such as the GlcNAc-specific succinylated wheat germ agglutinin (sWGA)(Monsigny et al., 1979) with immunoblotting may also help to establish their presence within the human glycoproteome.

Chapter 5: Paucimannosylation modulates the innate immune functions of human neutrophil elastase across the distinct granules of human neutrophils

5.1 Rationale

The critical role of HNE, as a serine protease glycoprotein residing predominantly in the azurophilic granule, has been well established in various studies of immune-related diseases including CF, neutropenia and chronic obstructive pulmonary disease (Horwitz et al., 2007; Le Gars et al., 2013; Tidwell et al., 2014). Given the importance of HNE in mediating an effective immune response, it is surprising that the structural aspects of HNE still remain unresolved, including details of its site-specific *N*-glycosylation. Early studies using nuclear magnetic resonance (Watorek et al., 1993) and X-ray crystallography (Hansen et al., 2011) revealed the presence of mannose-terminating *N*-glycans on HNE. These methods are used for elucidating the three dimensional structure of an intact protein, but they generally do not provide more than qualitative information about the structures and distribution of the conjugated glycans. Thus, the glycosylation site occupancies, the micro- and macro-heterogeneity of the conjugated *N*-glycans and the presence of other PTMs on HNE remain largely unreported. The knowledge of any potential involvement of HNE *N*-glycans on the rate of HNE proteolysis or their involvement in any protein-independent functions is similarly sparse.

Initial observations presented in **Chapter 2** and **4** suggested that three putative *N*-glycosylation sites of HNE (Asn88, Asn124, Asn173) displayed paucimannosylation, but the site-specific micro- and macro-heterogeneity of the *N*-glycosylation sites were not determined. As paucimannosylated HNE was identified in the bacterial colonised neutrophil-rich sputum of CF patients, it was speculated that paucimannosylated HNE may contribute towards pathogen defence by neutrophils. In addition, since HNE is a crucial protease that is known to be also involved in other non-pathogenic aspects of resolving inflammation (Renata et al., 2005), we hypothesised that the *N*-glycosylation of HNE may also modulate this potent serine protease in such non-sterile conditions. Before we can understand the influence of *N*-glycosylation on the function of HNE in innate immunity, the exact structures and the distribution of the *N*-glycans carried by HNE needs to be accurately mapped in a site-specific manner.

Using parallel glycoproteomic strategies by the application of the three complementary LC-MS/MS methodologies presented in **Chapter 4** (*N*-glycan, *N*-glycopeptide and intact glycoprotein analyses), a site-specific *N*-glycoproteomic profiling of HNE purified from healthy human neutrophils was performed here as presented in **Publication V**.

Having mapped the *N*-glycosylation of HNE, the functional involvement of the abundant paucimannosylation of HNE was also investigated (**Publication V**). Finally, to validate the observations of paucimannosylated HNE in neutrophil granules, I performed subcellular fractionation of resting human neutrophils to obtain protein extracts from the individual neutrophil granules (see **Chapter 5, section 5.3**). I performed these experiments with a particular focus on the paucimannose-rich azurophilic granules in my visit to the laboratories of the late Professor Niels Borregaard at the University of Copenhagen, Denmark. The *N*-glycosylation of the azurophilic granule proteins was investigated with an *N*-glycomics approach using PGC-LC-ESI-CID-MS/MS.

In summary, this chapter provides for the first time, the detailed *N*-glycosylation profile of HNE, data showing the contribution of *N*-glycosylation towards modulating the innate immune functions of HNE and the *N*-glycosylation profile of the azurophilic granule compartment of human neutrophils.

5.2 Publication V: Paucimannose rich *N*-glycosylation of human neutrophil elastase modulates its immune function

Publication: Loke, I., Østergaard, O., Heegaard N., Packer, N.H., Thaysen-Andersen, M. Paucimannose rich *N*-glycosylation of human neutrophil elastase modulates its immune function, Molecular Cellular Proteomics, 2017, doi: 10.1074/mcp.M116.066746mcp.M116.066746, in press.

This research was originally published in Molecular Cellular Proteomics. Loke, I., Østergaard, O., Heegaard N., Packer, N.H., Thaysen-Andersen, M. Paucimannose rich *N*-glycosylation of human neutrophil elastase modulates its immune function. *Molecular Cellular Proteomics*. 2017. © the American Society for Biochemistry and Molecular Biology.

Supplementary Materials are available in the enclosed DVD.

Author contributions: Conception of study and experimental design – IL and MTA, data collection and analysis – IL, OO and MTA, data interpretation and extraction of conclusions – IL and MTA, manuscript preparation – IL and MTA, editing and reviewing – MTA, OO, NP and NH.

For the subcellular *N*-glycosylation profile of the azurophilic granules, Dr. Morten Thaysen-Andersen, Professor Niels Borregaard and I were responsible for the study design. Ms Charlotte Horn and I were responsible for the data collection. I was responsible for the interpretation of the *N*-glycomics experiments of the subcellular fractionated granule proteins.

Paucimannose-Rich *N*-glycosylation of Spatiotemporally Regulated Human Neutrophil Elastase Modulates Its Immune Functions*[§]

✉ Ian Loke[‡], Ole Østergaard[§], Niels H. H. Heegaard[§], Nicolle H. Packer[‡],
and ✉ Morten Thaysen-Andersen^{‡¶}

Human neutrophil elastase (HNE) is an important *N*-glycosylated serine protease in the innate immune system, but the structure and immune-modulating functions of HNE *N*-glycosylation remain undescribed. Herein, LC-MS/MS-based glycan, glycopeptide and glycoprotein profiling were utilized to first determine the heterogeneous *N*-glycosylation of HNE purified from neutrophil lysates and then from isolated neutrophil granules of healthy individuals. The spatiotemporal expression of HNE during neutrophil activation and the biological importance of its *N*-glycosylation were also investigated using immunoblotting, cell surface capture, native MS, receptor interaction, protease inhibition, and bacteria growth assays. Site-specific HNE glycoproteomic analysis demonstrated that unusual paucimannosidic *N*-glycans, particularly Man α 1,6Man β 1,4GlcNAc β 1,4(Fuc α 1,6)GlcNAc β , predominantly occupied Asn124 and Asn173. The equally unusual core fucosylated monoantenna complex-type *N*-sialoglycans also decorated these two fully occupied sites. In contrast, the mostly unoccupied Asn88 carried nonfucosylated paucimannosidic *N*-glycans probably resulting from low glycosylation site solvent accessibility. Asn185 was not glycosylated. Subcellular- and site-specific glycoproteomic analysis showed highly uniform *N*-glycosylation of HNE residing in distinct neutrophil compartments. Stimulation-induced cell surface mobilization demonstrated a spatiotemporal regulation, but not cell surface-specific glycosylation signatures, of HNE in activated human neutrophils. The three glycosylation sites of HNE were located distal to the active site indicating glycan functions other than interference with HNE enzyme activity. Functionally, the paucimannosidic HNE glycoforms displayed preferential binding to human mannose binding lectin compared with the HNE sialoglycoforms, sug-

gesting a glycoform-dependent involvement of HNE in complement activation. The heavily *N*-glycosylated HNE protease inhibitor, α 1-antitrypsin, displayed concentration-dependent complex formation and preferred glycoform-glycoform interactions with HNE. Finally, both enzymatically active HNE and isolated HNE *N*-glycans demonstrated low micromolar concentration-dependent growth inhibition of clinically-relevant *Pseudomonas aeruginosa*, suggesting some bacteriostatic activity is conferred by the HNE *N*-glycans. Taken together, these observations support that the unusual HNE *N*-glycosylation, here reported for the first time, is involved in modulating multiple immune functions central to inflammation and infection. *Molecular & Cellular Proteomics* 16: 10.1074/mcp.M116.066746, 1–21, 2017.

Neutrophils, the most abundant immune cell population in blood, are integral to the human innate immune system by forming a first line of defense against invading pathogens and by assisting in resolving inflammation. Chemically distinct granule compartments, which are characterized by their unique proteome content including an arsenal of antimicrobial proteins and peptides, are found within neutrophils, most notably, the primary (azurophilic), secondary (specific) and tertiary (gelatinase) granules (1). Other neutrophilic compartments including the secretory vesicles and the ficolin granules have been reported (2).

The large family of serine proteases, which includes human neutrophil elastase (HNE)¹, proteinase 3, azurocidin, and neu-

From the [‡]Department of Chemistry and Biomolecular Sciences, Macquarie University, Sydney, NSW, 2109, Australia; [§]Department of Autoimmunology and Biomarkers, Statens Serum Institut, DK-2300 Copenhagen, Denmark

Received December 27, 2016, and in revised form, June 4, 2017

Published, MCP Papers in Press, June 19, 2017, DOI 10.1074/mcp.M116.066746

Author contributions: I.L. and M.T.-A. designed the research. I.L., N.H., N.P., and M.T.-A. supplied reagents and access to instrumentation. I.L., O.Ø. performed the experiments. I.L., O.Ø. and M.T.-A. analysed the data. I.L., O.Ø., N.H., N.P., and M.T.-A. wrote the paper.

¹ The abbreviations used are: HNE, human neutrophil elastase; A1AT, α 1-antitrypsin; ACN, acetonitrile; CBG, corticosteroid binding globulin; CF, cystic fibrosis; CMB, coomassie brilliant blue; dHex, deoxyhexose; DTT, dithiothreitol; ETD, electron transfer dissociation; FA, formic acid; fMLP, N-formylmethionine-leucyl-phenylalanine; Fuc, fucose; GlcNAc, *N*-acetylglucosamine; HBSS, Hank's Balanced Salt Solution; Hex, hexose; HexNAc, *N*-acetylhexosamine; HILIC, hydrophilic interaction liquid chromatography; LPS, lipopolysaccharide; Man, mannose; MBL, mannose binding lectin; MPO, myeloperoxidase; mRCL, mannose-recognising C-type lectin receptor; MWCO, molecular weight cut off; nCG, neutrophil cathepsin G; NET, neutrophil extracellular trap; NHS, N-hydroxysuccinimide ester; NeuAc, *N*-acetylneuraminic acid; OD, optical density; PDB, Protein Data Bank; PGC, porous graphitized carbon; PMA, phorbol myristate acetate;

Structure/Function of Neutrophil Elastase *N*-glycosylation

trophil cathepsin G (nCG), are preferentially stored in the azurophilic granules, but also reside in the specific and gelatinase granules (3) and on the cell surfaces of activated neutrophils albeit at lower levels (4). These potent serine proteases are serving crucial immune functions central to the diapedesis, chemotaxis, and bactericidal activities of neutrophils including phagocytosis and degranulation (5). Protective functions of serine proteases were demonstrated in mice by a higher frequency of *Mycobacterium tuberculosis* infection upon inhibition of the serine protease activity (6). This was supported by the observation that serine protease deficient human neutrophils lack bactericidal activity, leaving affected individuals severely immune compromised (7). Among the serine proteases, HNE is particularly important in chronic inflammatory lung diseases e.g. cystic fibrosis (CF) (8) and in hematological disorders e.g. cyclic and severe congenital neutropenia (9–11).

The *ELANE* gene encoding the monomeric and heavily glycosylated HNE is highly expressed in the promyelocytic stage of cells committed to undergo myeloid lineage differentiation into neutrophils within the bone marrow (12). The directly encoded gene product is an inactive preproprotein precursor that is converted to the mature serine protease upon extensive proteolytic processing and post-translational modification (13). The 27 amino acid-long signal peptide of HNE is quickly removed by signal peptidases, followed by the addition and processing of *N*-glycosylation and the removal of the N- and C-terminal propeptides by other peptidases (14). It has been proposed that adaptor protein 3 (15) and serglycin (16) direct HNE and other proteins expressed in promyelocytes to the azurophilic granules by timing rather than by specific protein signals/motifs (17). Mature HNE is predicted to consist of 218 amino acid residues, and harbors four disulfide bonds and four putative *N*-glycosylation sites (Asn88, Asn124, Asn173, Asn185, numbering based on the preproprotein sequence) (supplemental Fig. S1), leaving the mature protein product with an apparent molecular mass of 25–27 kDa (18). The catalytic activity of HNE relies on its His-Asp-Ser triad, a conserved structural feature mirrored in other serine proteases, in which Ser202 confers the proteolytic activity (19). The potent HNE can be inhibited at the site of inflammation by endogenous serine protease inhibitors (serpins) including α 1-antitrypsin (A1AT), an abundant plasma *N*-glycoprotein produced by hepatocytes (20).

HNE may be released from neutrophils upon stimuli-induced activation by lipopolysaccharide (LPS) or N-formylmethionine-leucyl-phenylalanine (fMLP) (21, 22). In the extracellular environment, HNE serves multiple protective and regulatory roles within the innate immune system. For example, HNE inhibits the growth of Gram-negative bacteria such

as *Pseudomonas aeruginosa* in the airways (23) and facilitates the release of anti-inflammatory cortisol from corticosteroid binding globulin (CBG) at inflammatory sites (24). However, because of its high enzymatic activity, excessive secretion of HNE can damage the connective tissues of the lungs by causing proteolytic degradation of elastin, fibronectin and collagen, as commonly observed in chronic obstructive pulmonary disease and in chronic inflammation (25). Imbalanced A1AT-based inhibition may contribute to this uncontrolled proteolysis by HNE in such conditions (26). HNE is also implicated in the formation of neutrophil extracellular traps (NETs) (27, 28), but the role(s) of NETs in innate immune defense are not fully elucidated (29).

Despite the established biological significance of HNE, the site-specific structure and function of the HNE *N*-glycosylation remains undocumented. To the best of our knowledge, only studies using nuclear magnetic resonance and X-ray crystallography have provided qualitative and still incomplete structural insights into the *N*-glycosylation of HNE. Short mannose-terminating *N*-glycans were primarily reported on Asn124 and Asn173, whereas Asn88 was generally reported as being unoccupied on HNE (30, 31). These otherwise powerful analytical techniques for structural elucidation are, however, typically not suitable for accurate profiling of *N*-glycoproteins. The distribution of HNE glycoforms, glycosylation site occupancy and the presence of other post-translational modifications on HNE were also not described in these past studies.

Functionally, genetic mutations were induced near, but not directly at, the putative *N*-glycosylation sites of HNE in a myeloid cell line to assess how the local structures around the *N*-glycosylation sites affect HNE folding, stability and activity (32). Mutations near Asn88 and Asn124 altered the *N*-glycan processing, secretion and the proteolytic activity of HNE, but the *N*-glycosylation structure and function relationship of HNE was not investigated. In fact, given the importance of HNE in mediating a functional host immune response (33, 34), and the increasing appreciation that protein *N*-glycosylation significantly modulates the function of proteins (35, 36), the structure/function relationship of the *N*-glycosylation of this vital serine protease remains understudied.

Herein, we present the first detailed site-specific structural and functional characterization of HNE *N*-glycosylation from resting and activated human neutrophils from healthy individuals. Structural analyses revealed unusual *N*-glycans occupying three utilized HNE *N*-glycosylation sites i.e. Asn88, Asn124, and Asn173. The putative Asn185 site was not glycosylated. It was found that the *N*-glycosylation of HNE is more likely to contribute to immunomodulatory functions during innate immune processes than interfering directly with the HNE enzymatic activity. These observations are important to increase our understanding of the structure, functional importance and spatiotemporal regulation of central neutrophil proteins carrying unusual *N*-glycosylation.

RP, reversed phase; SPE, solid phase extraction; TBST, tris buffered saline with Tween 20; TFA, trifluoroacetic acid; XIC, extracted ion chromatogram.

EXPERIMENTAL PROCEDURES

Isolation of Blood-derived Human Neutrophils—Human resting neutrophils were isolated from the peripheral blood of a single healthy male donor after informed consent was obtained. The collection, handling and biomolecular analysis of healthy human neutrophils were approved by the Human Research Ethics Committee at Macquarie University, Sydney, Australia (Reference no. 5201500409). Neutrophils were isolated over multiple separate experiments from 40 ml freshly drawn blood collected in EDTA tubes (BD Biosciences, Australia). The donor and the collection volume, time and day were kept constant to reduce unnecessary donor variation. The neutrophils were isolated with polymorphprep density centrifugation (Axis Shield, Norway) followed by hypotonic lysis of the remaining erythrocytes with cold filtered high purity (MilliQ) water. Cell counts ($>1 \times 10^7$ cells/ml) and viabilities ($>90\%$) of isolated neutrophils were determined using a Muse cell analyzer (Merck-Millipore, Australia). The purity of the neutrophil cell population ($>95\%$) was estimated based on Wright-Giemsa stained cells prepared using a cytospin centrifuge (Thermo Scientific, Australia). Low abundance ($\sim 2\text{--}3\%$) of other interfering cell types including erythrocytes, basophils and eosinophils were identified. The isolated neutrophils were used immediately for the structural and functional experiments.

Origin and Handling of Purified HNE—Enzymatically active human HNE (UniProtKB accession number: P08426) was purified from blood-isolated resting neutrophils from a pool of healthy individuals (Lee BioSolutions, MI, product number 342–40–1) using active site-based affinity and ion exchange liquid chromatography. Upon arrival, HNE was highly pure ($>95\%$) and displayed full structural and functional integrity (i.e. showed high enzyme activity on various substrates) as assessed by SDS-PAGE (Invitrogen, Australia) and immunoblotting with rabbit anti-HNE (1:500, kind gift from Prof Niels Borregaard, University of Copenhagen, Denmark) and by its ability to rapidly cleave CBG (24). HNE was stored in a soluble form at $1.9 \mu\text{g}/\mu\text{l}$ in 50 mM sodium acetate and 600 mM sodium chloride buffer, pH 5.5 at 4°C until use. Protein concentrations were determined at 280 nm absorbance with a percent extinction coefficient (ϵ 1%) of 10 using a Nanodrop spectrophotometer (Thermo Scientific).

N-glycan Release and Clean-up—HNE (20 μg) was proteolytically inactivated with 1.5 mM PMSF, 90 min, 22°C . Subsequently, the cysteine residues of HNE were reduced using 10 mM dithiothreitol (DTT) in 100 mM ammonium bicarbonate (pH 8.4), 45 min, 56°C and alkylated using 25 mM iodoacetamide in 100 mM ammonium bicarbonate (pH 8.4) (both final concentrations), 30 min in the dark, 22°C . The protein was then blotted on a primed 0.45 μm PVDF membrane (Merck-Millipore) and stained with Direct Blue (Sigma-Aldrich, Australia). The stained protein spots were excised, transferred to separate wells in a flat bottom polypropylene 96-well plate (Corning Life Sciences, Australia), blocked with 1% (w/v) polyvinylpyrrolidone in 50% (v/v) methanol and washed with MilliQ water. N-glycans were then released and handled as previously described (37). In brief, enzymatic release was performed using 3.5 U *Flavobacterium meningosepticum* N-glycosidase F (Roche, Australia) per 20 μg HNE in 10 μl water/well, 16 h, 37°C . The unstable amino groups ($-\text{NH}_2$) of the reducing end GlcNAc residues of N-glycosidase F-released N-glycans were allowed to spontaneously convert to hydroxyl groups ($-\text{OH}$) in weak acid using 100 mM ammonium acetate, pH 5, 1 h, 22°C to facilitate for subsequent quantitative reduction to glycan alditols. Reduction was carried out using 1 M sodium borohydride in 50 mM potassium hydroxide, 3 h, 50°C . The reaction was stopped by glacial acetic acid quenching. Dual desalting was then performed in micro-solid phase extraction (SPE) formats using strong cation exchange/C18 (where N-glycans are not retained) and porous graphitised carbon (PGC) (where N-glycans are retained) as stationary phases, respectively. The desalted N-glycans were eluted from the PGC-SPE columns

using 40% (v/v) ACN containing 0.1% (v/v) aqueous TFA, dried, and dissolved in 10 μl MilliQ water for N-glycan analysis. Bovine fetuin carrying sialo-N-glycans (Sigma-Aldrich) and the paucimannose-rich nCG (38) were included as control glycoproteins to ensure efficient N-glycan release, clean-up and analysis.

Glycan standards were used to determine some structural aspects of HNE N-glycans. M2 N-glycan isoforms were generated from chicken ovalbumin (Sigma-Aldrich) by sequential exoglycosidase digestion using 1 U *Streptococcus pneumoniae* β -N-acetylhexosaminidase and 1 U Jack bean α 1,3/6-linkage specific mannosidase (both from ProZyme, CA) using buffers and incubation times as recommended by the manufacturer. Synthetically generated and structurally validated M2 N-glycan (Product number MC0420) was obtained from Dextra Laboratories, Reading, UK. The N-glycan standards were reduced and desalted using PGC-SPE as described above prior to PGC-LC-MS/MS analysis.

N-glycan Analysis—Purified N-glycans were separated and detected by PGC-LC-MS/MS performed on an Agilent 1260 Infinity HPLC connected to an ESI ion trap mass spectrometer (LC/MSD Trap XCT Plus Series 1100, Agilent Technologies, Australia). The N-glycans (3 μl injection volume, ~ 200 pmol) were loaded on a PGC HPLC capillary column (Hypercarb KAPPA, 5 μm particle size, 200 \AA pore size, 180 μm inner diameter \times 100 mm length, Thermo Scientific) and separated using a linear gradient of 0–45% (v/v) ACN/10 mM ammonium bicarbonate over 85 min at a 2 $\mu\text{l}/\text{min}$ flow rate. The acquisition range was m/z 300–2200 and detection was performed in negative ionisation polarity mode with data-dependent acquisition. The top-three most abundant precursors in each full scan spectrum were selected for MS/MS using resonance activation (ion trap) CID performed with smart fragmentation (start/end amplitude 30–200%) at 1.0 V and an isolation window of 4 Th with a maximum accumulation time of 200 ms. Smart ion charge control was enabled with a smart parameter setting target of m/z 900. ESI was performed using a capillary voltage of +3.2 kV, a nitrogen drying gas flow of 6 liters/min at 325°C , and a nitrogen-based nebuliser pressure of 12 psi. Dynamic exclusion was inactivated over the entire LC-MS/MS acquisition period. The mass spectrometer was calibrated using a tune mix (Agilent Technologies). The mass accuracy of the precursor and product ions was typically better than 0.5 Da. The N-glycan mixtures were analyzed in technical triplicates ($n = 3$). Mass spectra were viewed and inspected using DataAnalysis v4.0 (Bruker Daltonics, Australia). GlycoMod (<http://web.expasy.org/glycomod/>) and GlycoWorkbench v2.1 assisted in the annotation and visualization of the N-glycans (39, 40).

N-glycopeptide Generation and Enrichment—Approximately 10 μg HNE was reduced and alkylated as described above, but without PMSF-based inactivation to allow HNE to partially “self-digest” to generate appropriate (glyco)peptides for downstream LC-MS/MS analysis. Alkylation was quenched with 30 mM DTT (final concentration) before in-solution proteolytic digestion was carried out using porcine trypsin (sequencing grade, Promega, Australia) at a 1:20 enzyme/substrate ratio (w/w) in 50 mM ammonium bicarbonate, pH 8.4, 18 h, 37°C . The majority ($\sim 70\%$) of the resulting peptide mixture was enriched for glycopeptides as described previously, but with a minor modification (41). After first drying and redissolving this fraction in 10 μl loading solvent consisting of 80% ACN:1% TFA:19% H_2O (v/v/v), the sample was then applied to custom-made hydrophilic interaction liquid chromatography (HILIC) SPE columns packed to an extended column height of 22 mm in GELoader tips (Eppendorf, Australia) with zwitterionic HILIC resin (ZIC-HILIC, 10 μm particle size, 200 \AA pore size, kindly donated by Merck KGaA, Darmstadt, Germany). The relative long high-capacity SPE columns were utilized because we have experience that peptides displaying shorter (truncated) N-glycans may not be well retained using ZIC-HILIC (38).

Structure/Function of Neutrophil Elastase N-glycosylation

Columns were packed on top of a C8 Empore SPE disc for resin retention (Sigma-Aldrich) (42). Columns were then equilibrated in 50 μ l loading solvent and the peptide samples were loaded and reloaded in successive rounds before the columns were washed twice with 50 μ l loading solvent. The enriched HNE glycopeptides were eluted with $2 \times 50 \mu$ l 1% (v/v) TFA and then with 50 μ l loading solvent to ensure complete glycopeptide elution. The remaining 30% of the peptide mixture was used directly for LC-MS/MS analysis after desalting on C18 micro-SPE stage tips (Merck-Millipore). The Asn88 N-glycan site occupancy of HNE (the only site displaying macro-heterogeneity) was determined after de-N-glycosylation, which was achieved by incubating the nonenriched peptide mixture with 10 U N-glycosidase F (Roche) in 100 mM ammonium bicarbonate (pH 8.4), 16 h, 37 °C. This is an accurate method for estimating N-glycosylation site occupancy (43). The resulting peptide mixture was desalted with C18 micro-SPE tips. All desalted peptide fractions were dried and taken up in 15 μ l 0.1% (v/v) formic acid (FA) before LC-MS/MS analysis.

N-glycopeptide Analysis—The HNE peptide mixtures were analyzed by ESI-LC-MS/MS in positive polarity mode using an HCT 3D ion trap (Bruker Daltonics) coupled to a Dionex Ultimate 3000 HPLC (Thermo Scientific). The samples were loaded directly onto a C18 column (Proteocol HQ303, 300 μ m inner diameter \times 10 cm length, 3 μ m particle size, 300 Å pore size, SGE Analytical Science, Australia), which was heated to 50 °C. The column was equilibrated in 100% solvent A consisting of 0.1% (v/v) FA. After 8 min isocratic flow in solvent A, multisegmented linear gradients of solvent B increasing up to 30% over 60 min and then up to 60% over 7 min were applied before the column was washed in either 80% or 100% solvent B for 10 min and re-equilibrated back to the starting condition. Solvent B consisted of 0.1% (v/v) FA in ACN. A constant flow rate of 5 μ l/min was used. Injections (5 μ l/injection) were performed using the following two LC-MS/MS strategies that shared the same ESI conditions *i.e.* a capillary voltage of -4 kV, a nitrogen drying gas flow of 5 liters/min at 300 °C and a nitrogen nebuliser pressure of 15 psi: (1) MS full scans (m/z 300–2,200, scan speed of 8100 $m/z/s$) were followed by data-dependent fragmentation of the three most abundant signals in each full scan using resonance activation (ion trap) CID performed at 35% normalized collision energy, maximum accumulation time of 200 ms with smart ion charge control and smart fragmentation enabled (start/end amplitude of 30–200%), and (2) MS full scans (m/z 200–1800, scan speed of 8100 $m/z/s$) were followed by electron transfer dissociation (ETD) of the three most abundant signals present in each full scan. The ETD used an ion count control reactant target of 600,000 ions of fluoranthene, the maximum reactant accumulation time was 200 ms (actual accumulation time was 4–20 ms), and the reaction time was 150 ms. The ETD reaction used ultra-high purity methane (99.999% purity, BOC, Australia) as a carrier gas at 35–37 psi. Precursor ions were dynamically excluded for 1.5 min after three MS/MS events in both LC-MS/MS acquisition strategies. The mass spectrometer was calibrated using a tune mix (Agilent Technologies) prior to acquisition and the mass accuracy of the precursor and product ions were generally better than 0.5 Da. To determine the percentage relative abundance of each glycopeptide, the peptide mixture was analyzed with and without glycopeptide enrichment in technical triplicates. Two independent digestion experiments were carried out (two sets of technical triplicates in each digestion experiment, in total $n = 6$). To estimate the Asn88 macro-heterogeneity, the N-glycosidase F treated nonenriched HNE peptide mixtures were analyzed in technical triplicates ($n = 3$). Mass spectra were viewed and manually annotated using Data Analysis v4.0 (Bruker Daltonics) and GPMW v10.0 (Lighthouse Data, Odense, Denmark) using the canonical protein sequence of HNE (UniProtKB, P08246).

Analysis of Intact HNE and HNE Protein Complexes—Intact HNE (~1 μ g) was analyzed by ESI-LC-MS in positive ion polarity mode

using a high resolution/high mass accuracy Q-TOF 6538 mass spectrometer (Agilent Technologies) coupled to a capillary HPLC (Agilent 1260 Infinity). Purified HNE was loaded directly onto a C4 column (Proteocol C4Q, 3 μ m particle size, 300 Å pore size, 300 μ m inner diameter \times 10 cm length, SGE Analytical Science) using 1 μ l injections. The column was equilibrated and operated in identical mobile phases as for the glycopeptide analysis on the C18 column (described above). From a starting condition of 100% solvent A, a linear gradient up to 60% (v/v) over 30 min (2%/min slope) of solvent B was applied before the column was washed in 99% (v/v) solvent B for 10 min and re-equilibrated back to the starting condition. The flow rate was kept constant at 5 μ l/min. A fragmentor potential of +200 V was used with the following MS settings in high resolution (4 GHz) mode: The MS full scan range was m/z 400–2500, the nitrogen drying gas flow rate was 8 liters/min at 300 °C, the nitrogen nebuliser pressure was 10 psi, the capillary potential was +4.3 kV, and the skimmer potential was +65 V. Beam-type CID-MS/MS fragmentation of the m/z 1146.3 signal, which was the most abundant ion of intact HNE, was performed at 55% normalized collision energy. HNE protein complexes (described below) were analyzed using the same conditions. Both intact (from here called “native”) HNE and HNE protein complexes were analyzed in technical triplicates ($n = 3$). The mass spectrometer was calibrated using a tune mix (Agilent Technologies) prior to acquisition and the mass accuracy of native HNE and the glycoprotein complexes were typically better than 20 ppm as assessed after spectral deconvolution. Mass spectra were viewed and analyzed with MassHunter work station vB.06 (Agilent Technologies).

Glycoproteomics of HNE N-glycans, N-glycopeptides and Intact Glycoprotein—HNE N-glycans were manually characterized in deep structural details using the PGC-LC-MS/MS data (44). In short, the characterization was based on accurate matches of the theoretical and experimental monoisotopic precursor masses, and substantial support of the candidate glycans by the observation of predicted glycan fragment ions in the corresponding CID-MS/MS spectra and predicted relative and absolute PGC-LC retention patterns that followed the retention rules for reduced but otherwise native N-glycans (38). The mass tolerance between the theoretical and experimental N-glycan masses was 1 Da to accommodate the limited mass accuracy/resolution of the ion trap. The structural details of the glycan species such as the α 1,3/6-mannose arm position of the single sialyl LacNAc or the β 1,2-linked GlcNAc residue in the nonreducing end of the glycan were verified by the observation of the particularly useful diagnostic ion (D ion) in the CID-MS/MS spectra (45, 46). Using this information, monosaccharide compositions, glycan sequences, topologies, and some N-glycan glycosidic linkages could be assigned. Other structural details of the glycan species *e.g.* the existence of a β -linked mannosidic chitobiose in the reducing end of the glycan were inferred based on established knowledge of human N-glycosylation and the biosynthetic relatedness between the observed structures (47, 48). N-glycans are depicted throughout according to the established symbol nomenclature (49).

HNE N-glycopeptides were manually characterized using the reversed phase (RP)-LC-MS/MS data (38). In short, candidate glycopeptides were identified based on 1) matches (better than 1 Da) of the theoretical and experimental monoisotopic precursor masses, 2) the presence of relevant oxonium ions (*e.g.* m/z 366.1, 528.1, 657.1) in the CID fragment spectra, and 3) the retention time of the glycopeptides eluting in clusters within 1–3 min (50). The theoretical N-glycopeptide masses were generated using GPMW v10.0 (Lighthouse Data), which assisted the glycopeptide identification. Verification of the identity of these glycopeptides was determined by the observation of the predicted peptide fragment ions *i.e.* b/y and c/z ion series and the glycan fragment ions *e.g.* the abundant peptide + GlcNAc (Y1

ion) with and without a dHex for core fucosylated glycopeptides in the corresponding CID- and ETD-MS/MS spectra.

Quantitative site-specific glycoproteomics of HNE was performed as follows: 1) To determine the percentage relative abundance of each glycopeptide form with a N-glycosylation site (micro-heterogeneity), the area-under-curve of extracted ion chromatograms (XICs) of the respective glycopeptides was quantified after a minimal degree of Gaussian smoothing of all observed charge states of the individual N-glycosylated peptides against all observed glycopeptides covering that particular N-glycosylation site within the nonenriched peptide mixture. In doing this, similar ionization efficiencies of these related molecular species were assumed (43, 51). 2) The Asn88 site occupancy (macro-heterogeneity) was estimated by comparing the XIC areas of N-glycosidase F-generated de-N-glycosylated peptides (observed as deamidated *i.e.* $\Delta m = +1$ Da) and nonglycosylated peptides. A minor degree of spontaneous nonenzymatic deamidation was observed in a deamidation control without N-glycosidase F treatment performed in parallel under identical incubation conditions. The spontaneous deamidation was considered when assessing the site occupancy. This approach has the advantage of limiting potential ionization differences between glycosylated and nonglycosylated peptides and simplifying the N-glycosylation site occupancy estimation (43). The Asn124 and Asn173 sites were fully occupied by N-glycosylation based on the lack of nonglycosylated and spontaneously deamidated peptides covering these two N-glycosylation sites in the unenriched HNE peptide mixture.

The glycoforms of native HNE were profiled by deconvoluting the multi-charged signals within the corresponding mass spectra using the maximum entropy algorithm in Bioconfirm within the MassHunter Work station vB.06 (Agilent Technologies). A mass range of 20–30 kDa, mass stepping of 1 and height filters set to a peak signal-to-noise ratio of 0.5 were used for spectral deconvolution. The HNE N-glycoforms were assigned based on accurate matches of the experimental average precursor masses (apex of deconvoluted signals) to the masses of theoretical glycoforms predicted to exist based on the prior site-specific N-glycopeptide and N-glycan profiling. The maximum mass difference allowed between the theoretical and experimental glycoprotein masses was 20 ppm. For comparative studies, the individual HNE glycoforms were quantitatively profiled using the relative height of the identified signals within the deconvoluted spectra.

Compartment-specific N-glycosylation Analysis of HNE from Human Neutrophil Granules—The distinct proteomes residing in the subcellular compartments of resting human neutrophils isolated from a healthy donor have been mapped (3). This proteomics data set was re-interrogated to perform compartment-specific HNE glycoproteomics. In short, resting human neutrophils were purified from freshly drawn peripheral blood using dextran sedimentation, followed by density centrifugation using Histopaque (GE Healthcare, Denmark). The remaining erythrocytes were lysed as described above (3). Proteins were extracted from the individual neutrophil granules isolated by Percoll density gradients after cellular cavitation using a Parr bomb pressurized with scientific grade nitrogen and then separated using SDS-PAGE. The purity of the isolated granules was validated using ELISA assays performed using antibodies with validated specificity toward granule-specific proteins. The granule-specific proteomics data was acquired from multiple SDS-PAGE gel fractions using high resolution/high mass accuracy LC-MS/MS on an LTQ Orbitrap XL mass spectrometer (Thermo Scientific) with linear ion trap CID fragmentation. The raw data is available at ProteomeXchange under the identifier PXD005559. Only the SDS-PAGE gel fractions containing HNE in the highest abundance (*i.e.* fraction 6) was used for the subcellular-specific glycoproteomics of HNE. The azurophilic, specific, gelatinase, and ficolin granules as well as the secretory vesicle and

the plasma membrane fractions were investigated. The raw LC-MS/MS data files originating from two technical replicate experiments were used directly without any further processing for “first-pass” N-glycopeptide identification using Byonic v2.6 (Protein Metrics Inc, CA). Searches were performed using the entire human proteome (*Homo sapiens*, 20,198 reviewed entries in UniProtKB, released September 2015) and the common mammalian N-glycome (309 monosaccharide compositions, default N-glycome database in Byonic). The raw data files were first analyzed by Preview (Protein Metrics Inc). The following search parameters as recommended by Preview were used: Carbamidomethylation was a fixed Cys modification, whereas Met oxidation and Asn/Gln deamidation were variable modifications. The mass tolerance was set to 20 ppm and 0.6 Da for precursor and product ions, respectively. Decoys were included and a maximum protein false discovery rate of 1% was allowed for the search. Trypsin cleavage with two missed cleavages and full protease specificity was utilized. Precursor isotope selection was performed at “narrow” with the maximum precursor mass of 10,000 Da. The precursor and charge assignments were computed from the MS1 spectra. The CID-MS/MS spectra of the identified HNE glycopeptides with a Byonic score above 100 (52) that matched previously observed HNE glycopeptides from whole neutrophil lysates or were biosynthetically-related, were manually annotated and validated with Xcalibur (Thermo Scientific) using the same criteria as for the glycopeptide characterization of HNE from neutrophil lysates (see above). The confirmed HNE glycopeptides were quantified based on their relative XIC peak areas as described above. Granule-specific heat maps and regression profiles were generated using Microsoft Excel based on the relative abundance of the observed Asn88 and Asn173 N-glycopeptides. Low abundance N-glycoforms (< 0.5%) were excluded in the heat maps. Asn124 N-glycopeptides were not observed in the dataset. Hierarchical clustering was performed using Euclidean distance with GenePatterns 2.0 (53).

Visualization and Solvent Accessibility of HNE—In total, nineteen three-dimensional (3D) protein structures of naturally occurring HNE obtained by X-ray crystallography were available from the protein data bank (PDB, <http://www.rcsb.org/pdb>). These structures were used to visualize and accurately determine the solvent accessibility of the HNE N-glycosylation sites. Visualization was performed using PyMOL Molecular Graphic System, v1.74 (Schrodinger, LLC, MA) using a representative high-resolution structure of HNE (PDB: 3Q77, 1.86 Å). The solvent accessibilities of the glycosylation sites of monomeric HNE were determined using NACCESS (54). Specifically, the atomic accessible areas (van der Waal's interactions) of the individual Asn residues forming the three occupied N-glycosylation sites were measured in arbitrary (unit-less) but comparable values by rolling a spherical probe with a radius of 5 Å on the protein surface of HNE. The most abundant N-glycans were modeled *in silico* on Asn124 and Asn173 of HNE (PDB: 3Q77) with the default torsion angles provided by the Glycoprotein builder functionality of GLYCAM web (<http://glycam.org>).

HNE Cell Surface Expression Assay—Human resting neutrophils isolated from blood were stimulated in three technical replicates ($n = 3$) using $\sim 1 \times 10^7$ neutrophils per replicate. As a vehicle control, 0.1% (v/v) DMSO in sterile filtered calcium containing Hanks' balanced salt solution (1.3 mM CaCl_2 , 5.4 mM KCl, 0.3 mM Na_2HPO_4 , 0.4 mM KH_2PO_4 , 4.2 mM NaHCO_3 , 137 mM NaCl, 5.6 mM D-(+)-glucose, pH 7.4) was used. The stimulation mixture consisted of 1 mM phorbol myristate acetate (PMA) in DMSO (Sigma-Aldrich), 5 $\mu\text{g}/\text{ml}$ *E. coli* 0127:E8 LPS and 5 $\mu\text{g}/\text{ml}$ *Salmonella enterica* serotype typhimurium LPS (Sigma-Aldrich), 1.25 mM latrunculin B in DMSO (Abcam, Australia), 2.5 μM ionomycin calcium salts in DMSO (Abcam) and 1 μM fMLP in DMSO (Sigma-Aldrich) (all final concentrations diluted in calcium containing HBSS). Cells were stimulated for 30 min at 37 °C under

Structure/Function of Neutrophil Elastase N-glycosylation

shaking condition. The activation of neutrophils was validated in technical (activation) triplicates ($n = 3$) using a myeloperoxidase (MPO) activity assay. Briefly, 100 μ l of secreted and cell lysate protein fractions (cells lysed with 0.1% Triton X-100), were obtained from the same number of stimulated and nonstimulated neutrophils. After the addition of 150 μ l 3,3',5,5'-tetramethylbenzidine (Sigma-Aldrich) reagent, all samples were incubated for 30 min, 22 °C. The reactions were stopped using 1 M sulfuric acid (Sigma-Aldrich) and the products of the reactions were measured as a proxy for MPO activity at an absorbance of 450 nm using a plate reader (BMD technologies, Australia). The cell viabilities were monitored using trypan blue exclusion. The degree of MPO release was calculated using the following formula: $(OD_{450\text{ nm, secreted protein fraction}})/(OD_{450\text{ nm, secreted protein fraction}} + OD_{450\text{ nm, cell lysate protein fraction}}) \times 100\%$.

Activated and resting neutrophils were washed with 1 \times phosphate buffered saline (PBS). Cell surface biotinylation was then carried out on pooled activated and resting neutrophils as previously described (55) using a trifunctional labeling agent provided in a cell surface capture kit (Pierce, Thermo Scientific). In short, cell surface proteins were labeled with N-hydroxysuccinimide ester (NHS)-biotinylation and captured on a Neutravidin stationary phase. The flow-through fraction was collected and these nonbiotinylated proteins were considered as intracellular proteins. The cell surface enriched (biotinylated) proteins were eluted with SDS-PAGE buffer containing 50 mM DTT and the proteins were precipitated overnight in cold acetone (−20 °C), resuspended in 2% (w/v) SDS in 25 mM ammonium bicarbonate and separated and visualized on a Coomassie Brilliant Blue (CMB)-stained 4–12% SDS-PAGE (Invitrogen) under reducing conditions. The gel separated proteins were transferred to nitrocellulose or PVDF membranes (Bio-Rad, Australia) for immunoblotting with Trans-Blot Turbo (Bio-Rad), blocked with 3% (w/v) bovine serum albumin in Tris buffered saline with 0.1% (v/v) Tween 20 (TBST) for 1 h at room temperature. The membranes were incubated with different primary antibodies in TBS overnight, washed in TBST and then incubated with matching secondary antibodies. Specifically, HNE was detected using rabbit anti-HNE (1:500, overnight, 4 °C) followed by an IRDye® fluorophore-conjugated goat anti-rabbit IgG (1:13,000, 30 min, 22 °C) (Licor Biosciences, NE). Paucimannosidic epitopes were determined using paucimannose-recognizing mouse IgM (called Mannitou, undiluted concentration, overnight, 4 °C, kind gift from Dr Simone Diestel, University of Bonn, Germany) and HRP-conjugated anti-mouse IgM (1:3000, 1 h, 22 °C) (Life Technologies, Australia). Mannitou has been previously validated to recognize paucimannosidic N-glycans (56). Blots were visualized on the Odyssey imager (Licor Biosciences) using the green fluorescence channel and the chemiluminescence channel on the ChemiDoc MP system (Bio-Rad) upon application of the HRP chemiluminescent substrates (Bio-Rad). Band intensities were quantified using Image studio (Licor Biosciences) and Image J (NIH) after normalization for cells and protein loading using the total protein intensity per lane as measured on matching CMB stained gels analyzed in parallel. This method yields a reasonable accurate quantitative estimate of the relative protein abundance (57). The sample preparation, LC-MS/MS-acquisition and annotation of peptides and glycopeptides from cell-surface expressed HNE were performed as described above.

Human MBL Binding Assay—Binding of HNE to human mannose binding lectin (MBL) was assessed by firstly diluting 100 μ g HNE in 2 ml binding buffer (20 mM CaCl_2 , 1.25 M NaCl, 10 mM Tris-HCl, pH 7.4) and then applying this solution to 2 ml MBL-agarose slurry (product number 22212, Thermo Scientific) packed in a polystyrene tube (product number 29922, Thermo Scientific) to a final column volume of 1 ml. The column was washed with 6 ml binding buffer at 4 °C prior to sample loading. HNE was loaded onto the column using gravity and the flow-through was re-loaded back onto the same column.

While the sample was applied the second time, the column exit was capped and the column was incubated overnight at 4 °C. The column was then washed with binding buffer at 4 °C until all non-specifically bound proteins were depleted from the column as measured by 280 nm absorbance using a biospectrometer (Eppendorf). This unbound protein fraction was collected for parallel analysis. The column and the elution buffer consisting of 10 mM EDTA, 1.25 M NaCl, 10 mM Tris-HCl, pH 7.4 were then equilibrated at room temperature for at least 1 h. Elution was carried out at room temperature by applying 1.2 ml elution buffer to the column using a gravity-based flow. The eluent was collected and re-loaded back to the column, which was then incubated with a capped column exit at room temperature for at least 1 h. The eluate was hereafter collected, which was pooled with additional eluting fractions using the same elution buffer. Complete elution of bound protein was ensured by measuring the protein absorbance of the eluting fractions at 280 nm. The eluates were concentrated, desalted and buffer exchanged into 0.1% (v/v) FA using 10 kDa molecular weight cut off (MWCO) filters (Merck-Millipore) prior to LC-MS analysis. HNE, which was not incubated with MBL, but otherwise treated like the rest of the samples (here called “native HNE”), and the MBL-unbound and MBL-bound HNE were analyzed in their intact form using high resolution LC-Q-TOF-MS. HNE glycoforms were quantitatively profiled using the relative height of the relevant signals within the deconvoluted spectra. Technical triplicate ($n = 3$) analyses of the binding experiments were carried out.

A1AT-based Inhibition Assay—The A1AT-based inhibition of HNE was assessed by incubating human A1AT purified from pooled plasma of healthy individuals (Sigma-Aldrich, A9024) with HNE in a 1:1 (19.6 μ M:19.6 μ M) and in a 3:1 molar ratio (58.8 μ M:19.6 μ M) in a physiological buffer consisting of 100 mM Tris-HCl, pH 7.6 for 30 min at room temperature without mixing. Technical (inhibition) triplicates ($n = 3$) were carried out at both ratios. Reactions were quenched by the addition of 1.5 mM PMSF (final concentration) after incubation. A fraction of the incubated samples containing covalently bound A1AT/HNE complexes and uncomplexed A1AT and HNE were separated and visualized on a CMB stained 4–12% SDS-PAGE gel (Invitrogen) under nonreducing conditions. Matching gels were used for immunoblotting by utilizing rabbit anti-human HNE (1:500) after transferring the proteins to a nitrocellulose membrane (Bio-Rad) exactly as described above. Visualization was performed with an IRDye® fluorophore-conjugated goat anti-rabbit IgG (1:13,000, Licor Biosciences) using the Odyssey imager (Licor Biosciences) with the green fluorescence channel. The remainder of the protein mixtures was concentrated, desalted and buffer exchanged into 0.1% (v/v) FA using 10 kDa MWCO filters (Merck-Millipore) prior to native LC-MS analysis (see above). Uncomplexed HNE, which eluted separately in the LC-MS analysis, was identified and quantified after deconvolution using the relative height of the apex of the relevant MS signals while the glycoforms of coeluting uncomplexed A1AT and the HNE:A1AT complexes were identified and quantified with the assistance of existing N-glycoproteins of human A1AT (58, 59) after spectral deconvolution using a mass stepping of 1 and height filters set to a peak signal-to-noise ratio of 0.5.

Bacteriostatic Assay—The clinically relevant *Pseudomonas aeruginosa* PASS1 strain was isolated and cultured to mid-log growth phase as previously described (60, 61). PASS1 was then washed twice in 1 \times PBS and diluted to an $OD_{600\text{ nm}}$ of 0.1 in Luria Beria broth before use. N-glycans were released from HNE by N-glycosidase F and desalted using PGC-SPE as described above, but the N-glycans were used in their free nonreduced form in the bacteriostatic assay. Enzymatically active HNE (1.8 μ M and 3.6 μ M), the released N-glycans from the same concentrations of HNE and appropriate controls (containing media only) were separately added to PASS1 cultures in total volumes of 100 μ l Luria Beria broth per well in a 96-well flat bottom microtiter

plate kept at 37 °C. The growth of PASS1 was then monitored over a period of 12 h using absorbance ($OD_{600\text{ nm}}$), which was measured automatically with 30 min intervals using a microplate reader (BMG technologies). Technical (growth inhibition) triplicates ($n = 3$) of all culture experiments were carried out.

Statistics—Data points and error are presented as mean \pm standard deviation (S.D.) or standard error of mean (S.E.) as indicated for the individual experiments. Statistical regression analyses and significance testing were carried out using Microsoft Excel. The significance of the individual experiments was assessed by paired and unpaired two-tailed type 2 Student's *t*-tests as indicated where $p < 0.05$ was chosen as the minimum acceptable level of confidence to support a rejection of the proposed null hypothesis, e.g. difference of two means. The nature of the replicates (biological or technical) and the sample numbers (n) used for the individual experiments are described above.

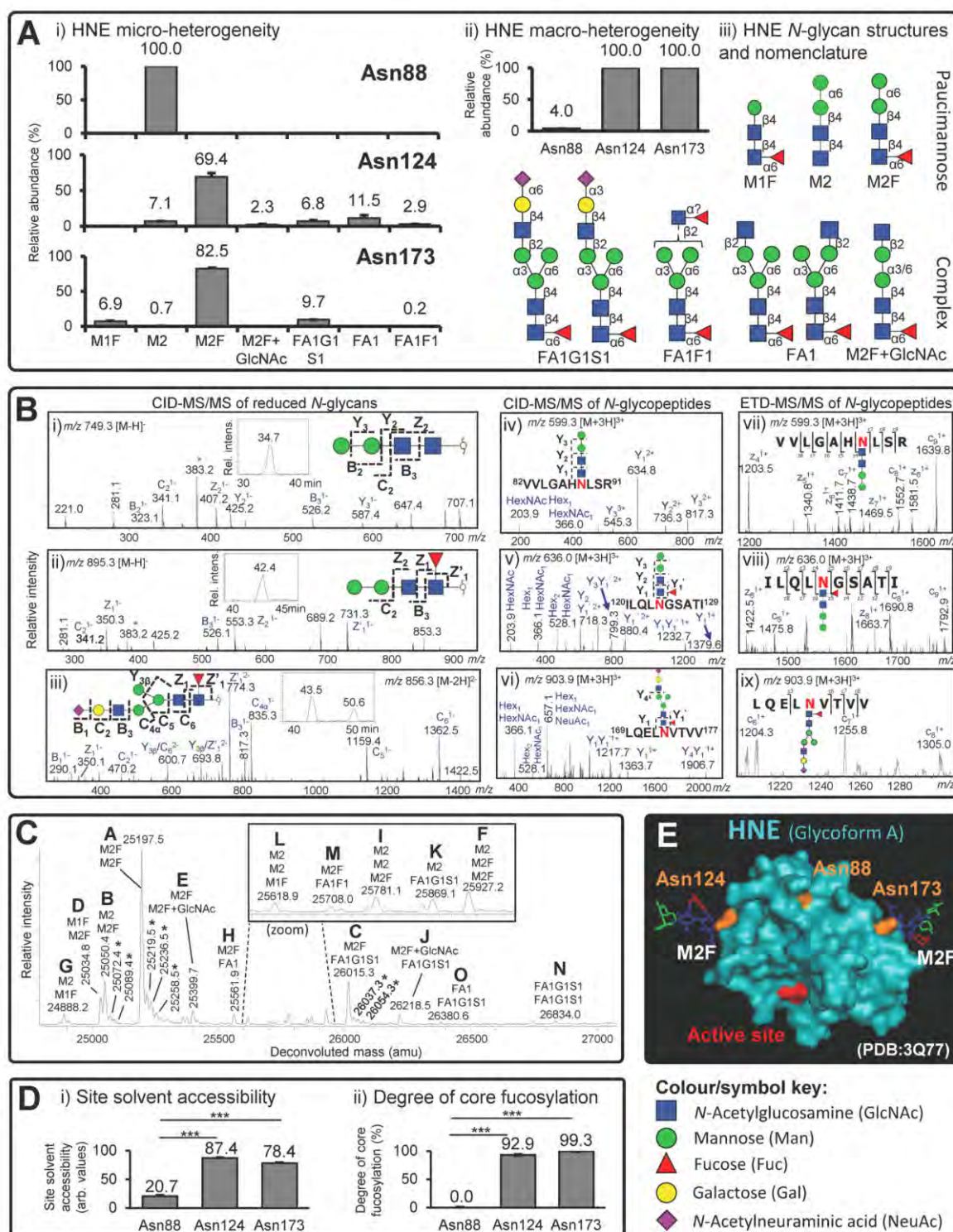
Experimental Design and Statistical Rationale—The experimental design, number of replicates and statistical rationale have been described above for the individual experiments performed in this study.

RESULTS AND DISCUSSION

Site-specific N-glycoproteomics Reveals Unusual Glycosylation Signatures of HNE—N-glycopeptide, N-glycan, and intact N-glycoprotein analyses were used for the site-specific characterization of the N-glycosylation of naturally occurring and enzymatically active HNE derived from resting neutrophils isolated from healthy individuals. LC-MS/MS-based site-specific glycoproteomics of the enriched and nonenriched intact N-glycopeptides facilitated complete coverage of all four putative N-glycosylation sites of HNE i.e. Asn88, Asn124, Asn173, and Asn185 (supplemental Fig. S2, supplemental Fig. S4B, and supplemental Table S1). Asn185 was not utilized as a glycosylation site. The three occupied N-glycosylation sites (Asn88, Asn124, and Asn173) displayed relatively limited micro-heterogeneity (Fig. 1A i), and showed site-specific differences in their occupancy (macro-heterogeneity) (Fig. 1A ii). Asn124 and Asn173 were both fully occupied (100% site occupancy, $n = 3$) by five or six monosaccharide compositions at each site based on the lack of both nonglycosylated and spontaneously deamidated peptides covering these two N-glycosylation sites in the unenriched HNE (glyco)peptide mixture. In contrast, a single monosaccharide composition only infrequently occupied the Asn88 site ($4.0\% \pm 1.1\%$ site occupancy, $n = 3$). The observed monosaccharide compositions corresponded to unconventional paucimannosidic and complex-type N-glycans. PGC-LC-MS/MS of reduced, but otherwise native, HNE N-glycans revealed their exact structures including their topology (sequence and branching patterns) and glycosidic linkages (supplemental Fig. S3A). In total, only nine N-glycan isomers were observed at both the N-glycan and N-glycopeptide level (Fig. 1A iii and supplemental Table S2). All reported structures were validated using CID-MS/MS for the HNE N-glycans (Fig. 1B i–iii and supplemental Fig. S3B) whereas complementary CID- and ETD-MS/MS dissociation methods were applied to the HNE N-glycopeptides (Fig. 1B iv–ix and supplemental Fig. S4A). These analyses demonstrated that the single Asn88-glycan

was $\text{Man}\alpha 1,6\text{Man}\beta 1,4\text{GlcNAc}\beta 1,4\text{GlcNAc}\beta$ (hereafter called M2). Because of their biosynthetic relatedness, the abundant N-glycan of Asn124 and Asn173 was suggested to be the matching core fucosylated species also only observed as a single isomer i.e. $\text{Man}\alpha 1,6\text{Man}\beta 1,4\text{GlcNAc}\beta 1,4(\text{Fuc}\alpha 1,6)\text{GlcNAc}\beta$ (hereafter called M2F) (relative abundance: Asn124: $69.4\% \pm 5.2\%$ and Asn173: $82.5\% \pm 0.8\%$). Interestingly, both bimannosylchitobiose structures appeared only as the $\alpha 1,6$ -Man-terminating isomer (see inserts in Fig. 1B i–ii showing single eluting isomers), in agreement with past observations reported in other neutrophil N-glycome studies (38, 60, 62, 63). The presence of the $\alpha 1,6$ -Man-terminating isomer was supported by its PGC-LC retention time that agreed with the PGC retention time of a synthetic $\alpha 1,6$ -Man-terminating M2 reference compound and the $\alpha 1,6$ -Man-terminating isomer of artificial M2 generated from chicken ovalbumin (see insert in supplemental Fig. S3B, Glycan #2). The $\alpha 1,3$ -linked Man isomer was absent for both M2 and M2F. This suggests that the $\alpha 1,3$ -linked Man of the conserved trimannosyl-chitobiose core and any monosaccharide residues decorating the N-glycan core including $\beta 1,2$ -GlcNAc residues, are efficiently and selectively removed by glycosidases during or after HNE biosynthesis. Given that other neutrophil proteins including nCG, azurocidin and proteinase 3 have been reported to be highly paucimannosylated (38, 60, 63, 64), it indicates that paucimannosylation is a commonly utilized N-glycoprotein feature of human neutrophils. The complex N-glycans decorating Asn124 and Asn173 appeared as two highly unusual isobaric sialyl-linkage isomers (see insert in Fig. 1B iii for the PGC-LC separated isomers) i.e. $\text{NeuAc}2,3/6\text{Gal}\beta 1,4\text{GlcNAc}\beta 1,2\text{Man}\alpha 1,6(\text{Man}\alpha 1,3)\text{Man}\beta 1,4\text{GlcNAc}\beta 1,4(\text{Fuc}\alpha 1,6)\text{GlcNAc}\beta$ (hereafter collectively called FA1G1S1) (relative abundance: Asn124: $6.8\% \pm 1.8\%$ and Asn173: $9.7\% \pm 0.4\%$) (Fig. 1A i). Interestingly, the fully processed and mature monoantenna of these two isomeric sialylated structures was exclusively positioned on the 3'-Man arm based on the absence of D ions in the MS/MS spectra, thereby yielding protection from degrading $\alpha 1,3$ -mannosidases that appear active in neutrophils as judged by the prevalent M2 and M2F. Other unconventional biosynthetically-related N-glycans of the monoantennary complex type (FA1F1 and FA1) and the paucimannosidic type (M1F) were also observed to be conjugated to Asn124 and Asn173 (Fig. 1A i). Although rarely reported, we have recently characterized similar monoantennary sialoglycans on nCG (38) and these structures were also seen in relative high abundance in pathogen-infected sputum and in isolated resting neutrophils (60). Interestingly, these structures have been reported as free N-glycans in stomach cancer-derived cell lines (65) and mouse embryonic fibroblasts (66), where the monoantenna was also proposed to be positioned on the 3'-Man arm. In contrast to nCG, HNE did not display the highly truncated chitobiose type N-glycans i.e. $(\pm\text{GlcNAc}\beta 1,4)(\pm\text{Fuc}\alpha 1,6)\text{GlcNAc}\beta$ (38). Taken together, these observations support that human neutrophils can

Structure/Function of Neutrophil Elastase N-glycosylation



generate highly unusual N-glycosylation including paucimannosylation and monoantennary sialylation in a site-specific manner on HNE.

Supported by an extensive sequence coverage (>75%) (supplemental Fig. S4B), the HNE peptide mapping showed no evidence of other PTMs. The peptide analysis also indicated that Ile30 forms the N-terminal of the mature, fully processed, HNE polypeptide chain in accordance with the predicted amino acid sequence of HNE based on previous cDNA sequencing (14) (supplemental Fig. S1). In contrast to the reported Gln247 (67), we observed that Arg248 instead forms the C-terminal of mature HNE similarly to an Arg-terminating proteoform of nCG (38). No polypeptide sequence heterogeneity of HNE with respect to C- and N-terminal truncation forms was observed in our peptide analysis. The C-terminal arginine residues of HNE and nCG may provide these already highly cationic serine proteases with even higher isoelectric points, but the biological importance of their basic nature remains insufficiently understood (16).

Reflecting the limited micro- and macro-heterogeneity observed here and elsewhere (68), high mass accuracy LC-Q-TOF-MS detected only fifteen compositional glycoforms of intact HNE, which all agreed very well with the prior HNE N-glycopeptide and N-glycan analyses (Fig. 1C and supplemental Fig. S5A). Beam-type CID-MS/MS fragmentation of intact HNE was used to confirm that Arg248 forms the true C-terminal of the glycoprotein (supplemental Fig. S5B). Glycoform A (molecular mass, $M = 25197.5$ Da) was the most abundant species, most likely corresponding to a monomeric HNE glycoform displaying unoccupied Asn88 and M2F conjugated to both Asn124 and Asn173. Also in agreement with the site-specific glycoprofiles, glycoform B ($M = 25050.4$ Da) carrying most likely M2 and M2F on Asn124 and Asn173 and

displaying an unoccupied Asn88 was also abundant, as was glycoform C ($M = 26015.3$ Da) carrying monosaccharide compositions potentially corresponding to M2F and FA1G1S1 moieties. Several HNE glycoforms of lower abundance were detected to be carrying M2 as a third N-glycan presumably on Asn88 (glycoform F, I, and L). Although the HNE glycoforms are strongly supported by the glycopeptide data, top down electron transfer/capture dissociation experiments are required to confirm the site-specific distribution of these multi-glycosylated forms of HNE (69). Taken together, the accurate mass analysis of native HNE confirmed the site-specific glycopeptide profiles, validated the N- (Ile30) and C- (Arg248) termini of mature HNE and simultaneously demonstrated that unusual paucimannosidic N-glycans were carried by enzymatically active intact HNE, proved the absence of other PTMs, and confirmed that the molecular mass of the mature HNE proteoforms is 25–27 kDa in agreement with previous, less accurate, estimates based on gel electrophoresis (30, 70).

Solvent Accessibility and Spatial Positioning of N-glycosylation Sites on mature HNE—Asn88 has a unique glycosylation signatures (low site occupancy and lacking both core fucosylation and complex-type structures) relative to the two more processed glycosylated sites, Asn124 and Asn173. The possible protein structural differences around the glycosylation sites causing these site-specific glycosylation differences were investigated using nineteen 3D structures of neutrophil-derived HNE solved using X-ray crystallography available from the Protein Data Bank (supplemental Table S3). Significantly lower solvent accessibility of Asn88 was observed (NACCESS score: 20.7 ± 1.4) compared with the accessibilities of Asn124 (87.4 ± 0.7 , $p < 0.001$) and Asn173 (78.4 ± 1.0 , $p < 0.001$, paired two-tailed type 2 Student's *t*-tests) (all

FIG. 1. Site-specific characterization of HNE N-glycosylation. A, i) Limited structural micro-heterogeneity (relative glycan distribution, %, mean \pm S.E., $n = 6$). ii) Differential macro-heterogeneity (site occupancy, %, mean \pm S.E., $n = 3$) across the three utilized HNE N-sites *i.e.* Asn88, Asn124 and Asn173. iii) Overview of the characterized HNE N-glycan structures and their short-hand nomenclature (see bottom for key and symbol nomenclature) (49). B, Comprehensive glycan and glycopeptide MS/MS spectral data supporting the structural characterization. The spectra were annotated and the corresponding structures were assigned based on the identified glycan and peptide fragments (as well as molecular mass and retention time) following the established fragmentation rules and nomenclature. Resulting fragments have only been partially annotated for the sake of clarity; See supplemental Fig. S3B and supplemental Fig. S4A for all supporting fully annotated spectra. * denotes cross-ring fragment ion. Left: Annotated ion trap CID-MS/MS spectra of reduced N-glycans as exemplified by the three main HNE N-glycans *i.e.* i) M2, ii) M2F and iii) FA1G1S1 ($\alpha 2,6$ sialyl-linkage), see inserts for XIC-based PGC-LC elution pattern. Middle/Right: Annotated ion trap CID- and ETD-MS/MS spectra, respectively, of the major HNE N-glycopeptides, iv and vii) Asn88-M2, v and viii) Asn124-M2F, and vi and ix) Asn173-FA1G1S1, respectively. C, Glycoprofiling of intact HNE. The deconvoluted spectrum shows the fifteen identified HNE glycoforms (labeled A-O, in the order of high to low relative abundance) identified by high resolution LC-ESI-Q-TOF mass spectrometry. The proposed glycans conjugated to the intact mature HNE polypeptide chain (Ile30-Arg248) are indicated in a site-unspecific manner with the short-hand nomenclature by considering the previously determined site-specific glycopeptide and glycan data. * denotes adduct formation of HNE, see supplemental Fig. S5A for more. D, Relationship between the N-glycosylation and tertiary structure around the N-glycosylation sites of HNE as shown by the clear correlation between i) the solvent accessibility of the three HNE N-glycosylation sites assessed using nineteen PDB structures of neutrophil-derived HNE (mean \pm S.E. of arbitrary (unit-less) but comparable values, $n = 19$ 3D structures, *** denotes $p < 0.001$ using paired two-tailed type 2 Student's *t*-tests), see supplemental Table S3 for more details and ii) the degree of N-glycan core fucosylation (in %) of the individual HNE N-glycosylation sites based on N-glycopeptide analysis (mean \pm S.E., $n = 6$ technical replicates; *** denotes $p < 0.001$ using unpaired two-tailed type 2 Student's *t*-tests). E, Spatial location of the active site relative to the three utilized N-glycosylation sites on a representative 3D structure (PDB: 3Q77) of human neutrophil-derived monomeric HNE. M2F was modeled *in silico* on Asn124 and Asn173 by utilizing their default torsion angles provided by GLYCAM whereas Asn88 was left unoccupied (*i.e.* Glycoform A was visualized). Protein color scheme: The active site (His39, Asp117, Ser217 based on preproprotein amino acid sequence) is in red and the three N-glycosylation sites are in orange. The monosaccharide colors follow the symbol nomenclature used throughout (see key below) (49).

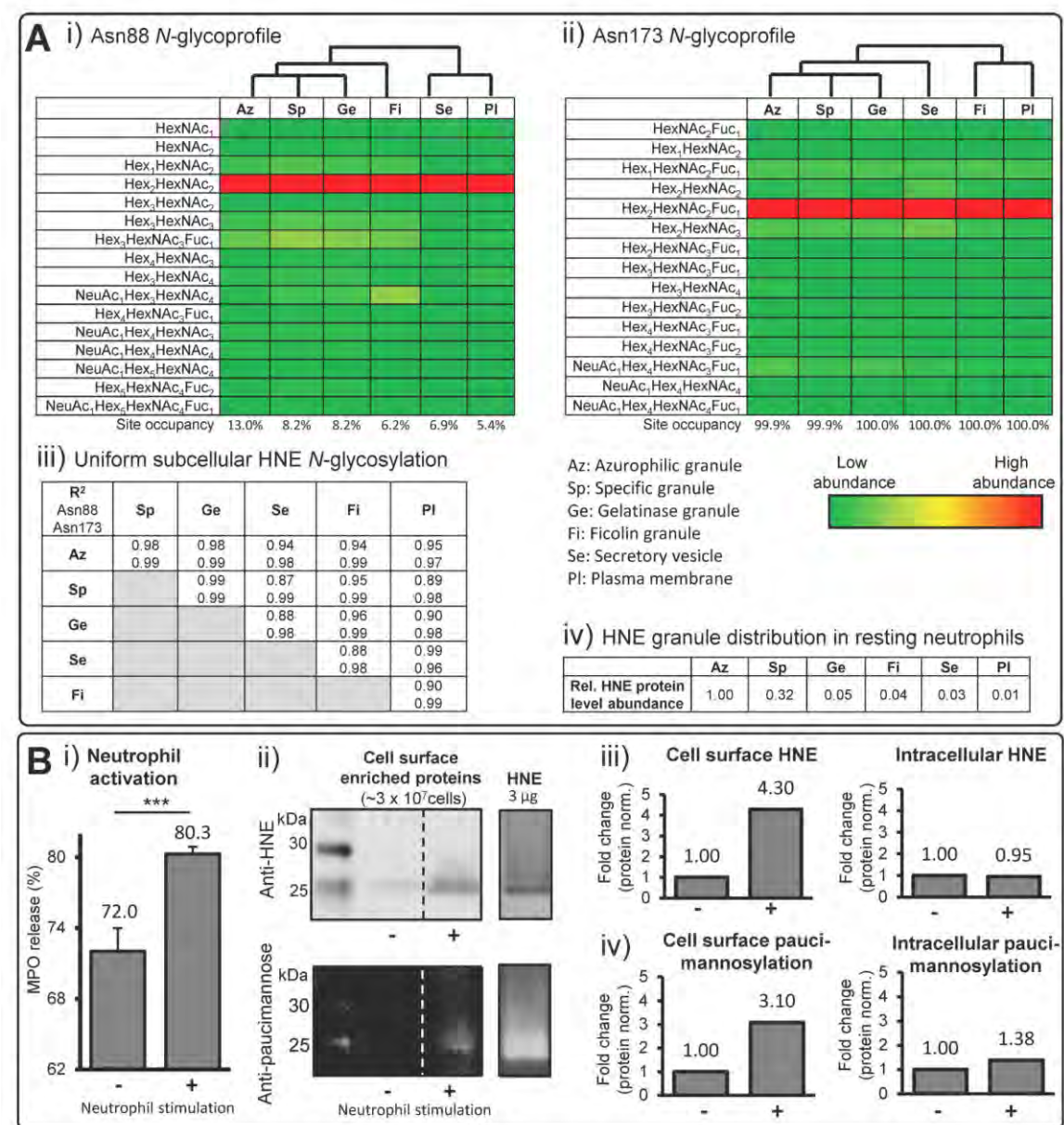
Structure/Function of Neutrophil Elastase N-glycosylation

as mean \pm S.E., $n = 19$) (Fig. 1D i). The differential site accessibilities agreed well with the observation that the relatively hidden Asn88 only carried N-glycans completely lacking core fucosylation, whereas the surface exposed Asn124 and Asn173 sites were highly core fucosylated ($92.9\% \pm 0.3\%$ and $99.3\% \pm 0.1\%$, respectively, both $p < 0.001$) (mean \pm S.E., $n = 6$) (Fig. 1D ii). We previously showed that the extent of core fucosylation is heavily influenced by the local structure and the solvent accessibility of the N-glycosylation site being modified (71). The Asn124- and Asn173-glycans also displayed other features associated with a high degree of glycan processing including antenna extension and NeuAc capping; however, it remains unclear if such glycan structural elements further away from the protein surface are similarly affected by solvent exposure. The influence of the solvent accessibility on any glycan truncation by hydrolases (e.g. β -hexosaminidase and α - β -mannosidases) after protein folding also remains unclear. Dissecting out such structural-biosynthetic mechanistic relationship(s) would advance our understanding of the biosynthetic generation of paucimannosidic proteins and the even shorter chitobiose type structures.

The transfer of the initial N-glycan precursor, which effectively determines the degree of site occupancy, takes place on unfolded or only partially folded glycoproteins early in the endoplasmic reticulum (48). Hence, the 3D structures of maturely folded HNE are not suitable to probe the mechanisms driving the site-specific occupancy differences. Although the Asn88 sequon (NLS) is followed immediately by an arginine residue (Arg91), which reportedly favors the N-glycan transfer rate because of its beneficial positive charge (72), Asn88 still displayed very low glycan site occupancy. Thus, it is likely that other yet-to-be-determined primary and secondary structural features around the glycosylation sites are responsible for generating these site occupancy differences. Finally, as demonstrated on a representative 3D structure of neutrophil-derived HNE (PDB: 3Q77), it is interesting to note that the three utilized N-glycosylation sites of HNE are positioned distal to the active site of the protease (Fig. 1E). This implies that the relative simple HNE N-glycans of short length and limited volume are more likely involved in other functions than in direct modulation of HNE proteolytic activity.

Uniform N-glycosylation of HNE Residing in Various Neutrophil Compartments—We have recently used subcellular proteomics to show that the individual granule compartments of human neutrophils harbor distinct subproteomes (3). This LC-MS/MS dataset was here manually reinterrogated with the purpose of performing a detailed subcellular- and site-specific N-glycoproteomic of HNE. Glycosylated and nonglycosylated tryptic peptides covering Asn88 and Asn173 (but not Asn124 because of tryptic peptides that were too large for efficient MS detection) were confidently identified (supplemental Table S4), facilitating a granule-specific assessment of both the micro- and macro-heterogeneity of these two HNE glycosylation sites. This highly sensitive, compartment-spe-

cific data provided identification of many relatively low-abundant monosaccharide compositions at each site, but importantly, the resulting glycoproteomic profiles matched reasonably well our site-specific glycoproteomic profiles of HNE extracted from whole resting neutrophils (see Fig. 1A i). Across all compartment lysates of Asn88 was largely unoccupied (~ 87 – 95%), but harbored a significant proportion of M2 (~ 3 – 7%), whereas Asn173 was almost fully occupied by M2F (~ 55 – 75%) and complex-type ($\sim 30\%$) sialylated and neutral N-glycans. Interestingly, these studies showed surprisingly little variation in the N-glycosylation of HNE residing in the various neutrophil compartments as illustrated by highly similar heat maps representing their site-specific glycan (i.e. monosaccharide composition) distribution (Fig. 2A i–ii). With unsupervised hierarchical clustering, the Asn88- and Asn173-glycosylation of HNE residing in the three major granules i.e. azurophilic, specific and gelatinase granules proved to be slightly more similar than the glycosylation signatures of HNE residing in other compartments and on the plasma membrane. Minor granule-specific differences were also observed with respect to the glycan occupancies of Asn88 and Asn173. However, irrespective of compartment origin, the site-specific N-glycosylation was surprisingly uniform across the granule compartments as demonstrated by very high correlation coefficients of both N-sites ($R^2 = 0.87$ – 0.99) (Fig. 2A iii). The strong HNE glycoform similarities across the neutrophil granules are somewhat unexpected for a number of reasons i.e. 1) subcellular-specific N-glycosylation is a feature of several human cell types (73), 2) we have previously suggested that paucimannosylation is an N-glycan feature that appears to be preferentially displayed by proteins residing in the azurophilic compartment in human neutrophils (60), 3) the various neutrophil compartments, where the final glycoprotein processing presumably takes place, are thought to be formed at different times during myelopoiesis (17) and, as a result of temporal hydrolase expression during myelopoiesis, harbor different granular levels of various glycan processing enzymes (60) and, finally, 4) limited protein exchange reportedly occur between the neutrophil granules after their formation (3, 74). The compartment-specific proteome data also showed that HNE, under resting conditions, primarily resides in the azurophilic (relative level set to 100%) and specific (32%) granules, whereas less HNE protein is found in the gelatinase (5%) and ficolin (4%) granules or in the secretory vesicles (3%) and on the plasma membrane (1%) (Fig. 2A iv). Thus, it appears that human neutrophils can synthesize the same set of biosynthetically related HNE glycoforms and in similar ratios during the maturation stages, but that HNEs end up being unevenly distributed across the various intracellular compartments and on the cell surface of neutrophils. The latter observation is supported by the “targeting by timing” hypothesis proposed by Borregaard and coworkers suggesting that the various neutrophil granules are filled with different proteins reflecting the different protein expression profiles during time-separated granule formation in developing myelo-



Structure/Function of Neutrophil Elastase N-glycosylation

cytes. Hence, neutrophil proteins that are synthesized simultaneously in maturing neutrophils will end up in the same granule compartment (75).

Interestingly, the peculiar FA1F1 structure carried by HNE on Asn124 and Asn173 was found across all granules, but present at too low relative abundance (< 3%) to assess whether significant differences in its granule distribution occurred. The unusual GlcNAc-Fuc epitope at the nonreducing end of this structure does not conform to the established N-glycan biosynthetic pathway, but indicates that this structural feature arises from the trimming of a more elongated antenna by the action of β -galactosidases (and possible also α -sialidases) present in the neutrophil granules (3, 76). The exact enzymatic pathway that allows the biosynthesis of this structure as well as many other spatial and temporal aspects of the glycosylation machinery of developing neutrophils remain to be determined.

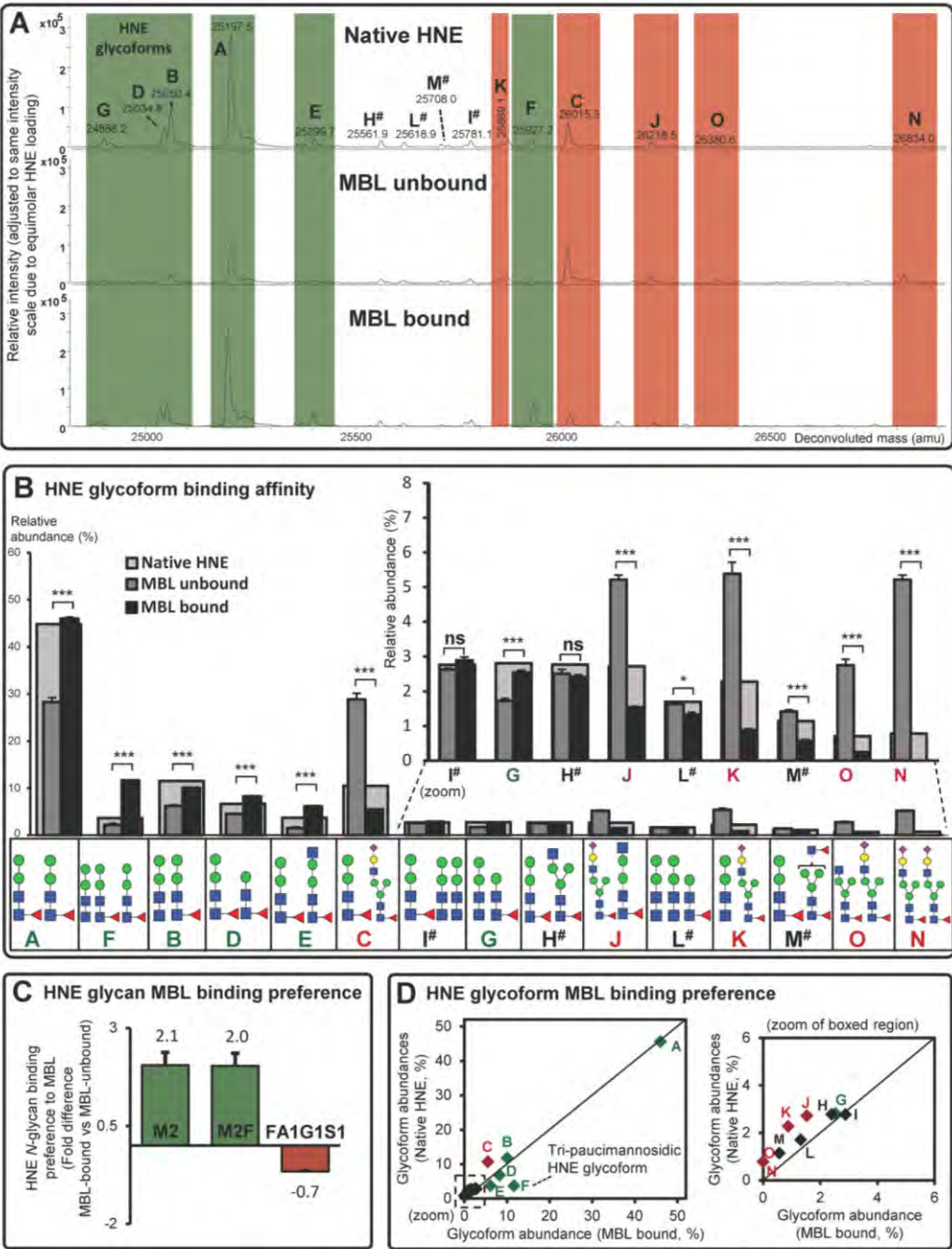
Stimuli-induced Expression of Paucimannosidic-rich HNE on the Neutrophil Cell Surface—Antimicrobial glycoproteins and peptides secreted from neutrophil compartments via degranulation mechanisms are critical in the pathogen defense system and in other immune functions of the host (1). Although HNE has been reported to associate with the neutrophil cell surface upon activation (77, 78), the molecular details underpinning the mobilization and the retention of soluble HNE at the plasma membrane as well as the N-glycosylation of cell surface HNE of activated human neutrophils are yet to be explored. These research questions are particularly interesting considering that neutrophils are known to express an A1AT-resistant form of HNE on their cell surfaces (4, 22) and the fact that paucimannosidic N-glycoproteins are increasingly being associated with important extracellular functions in inflammation and infection (79, 80).

In agreement with literature (81), human resting neutrophils were activated *ex vivo* upon chemical stimulation with a mixture of PMA, LPS, and chemo-attractant peptides as evaluated by the increased secretion of MPO (Fig. 2B i), which is a well-established marker of neutrophil activation. Importantly, the resting and activated neutrophils maintained similar viabilities (~55–70%) as assessed by trypan blue exclusion over

the 30 min stimulation experiment, ruling out significantly higher contributions of intracellular glycoproteins from potential cell death and leakage because of plasma membrane deterioration in activated neutrophils. By utilizing a cell surface protein capture approach, immunoblotting and mass spectrometry (Fig. 2B ii–iii and supplemental Fig. S6), we showed that activation enhanced HNE expression on the neutrophil cell surface relative to its constitutive expression on resting neutrophils and only caused a negligible reduction in the amount of intracellular HNE as evaluated by reactivity to anti-HNE antibodies. Complementary (opposite) changes of the intra- and extracellular levels of HNE upon neutrophil stimulation were expected because the *de novo* protein synthesis and degradation were considered to be negligible over the 30 min stimulation experiment. However, the negligible reduction in the intracellular levels of HNE upon neutrophil stimulation may be explained by the relatively weak HNE cell surface expression (1%) (see Fig. 2A iv). LC-MS/MS based peptide identification confirmed that the 25–27 kDa gel region contained HNE (supplemental Fig. S7). Thus, the experiments showed that the majority of HNE remained in an intracellular location upon stimulation in agreement with the observations that granular HNE can undergo both intra- and extracellular degranulation by granule fusion with intracellular phagolysosomes (82) and the plasma membrane (83), respectively. The lower propensity of the HNE-rich azurophilic granules to fuse with the plasma membrane compared with the specific and gelatinase granules upon stimulation and their ability to translocate to the nucleus of neutrophils support these observations (2, 28, 84).

To probe the N-glycosylation of cell surface-bound HNE of neutrophils undergoing activation, immunoblotting with a paucimannose-reactive antibody, Mannitou (56), was performed and the signals in the 25–27 kDa gel region were assessed. Stimulated neutrophils showed an increased level of cell surface paucimannosylation relative to the constitutive level under resting condition (Fig. 2B ii, iv and supplemental Fig. S6). This increase was comparable to the activation-induced increase in cell surface HNE (Fig. 2B iii). Mass spectrometry confirmed the presence of HNE paucimannosylation

activation marker, MPO, was increased in secretions from human resting neutrophils as assessed by reinterrogation of the granule-specific stimulated (+) relative to resting (–) neutrophils while the cell viabilities remained unchanged, indicating active degranulation (mean \pm S.D., $n = 3$ technical replicates, *** denotes $p < 0.001$ using unpaired two-tailed type 2 Student's *t*-tests). ii) HNE- (top gel) and paucimannose-specific (bottom gel) immunoblotting of stimulated (+) and resting (–) human neutrophils showed spatiotemporal regulation of paucimannosylated HNE on the cell surface of activated neutrophils. Cell surface proteins were extracted by NHS-biotinylation and captured on a Neutravidin stationary phase from $\sim 3 \times 10^7$ cells in both conditions ($n = 3$ technical replicates). Broken lines denote nonneighboring lanes from immuno blots on the same gel (same exposure and contrast). Purified HNE (3 μ g) is shown in a separate lane to illustrate the reactivity to anti-HNE and anti-paucimannosidic antibodies and visualize the molecular mass of HNE, see Fig. S6 for more. iii) Quantitation of cell surface (left) and intracellular (right) HNE in the immunoblotted HNE gel region (~25–27 kDa) of stimulated relative to resting human neutrophils. Signal intensities were quantified using densitometry after normalization for total protein loading and presented as fold difference of stimulated *versus* resting neutrophils, $n = 3$ pooled technical replicates. iv) Quantitation of the degree of cell surface (left) and intracellular (right) paucimannosylation in the immunoblotted HNE gel region (~25–27 kDa) of stimulated relative to resting human neutrophils. Signal intensities were quantified using densitometry after normalization for total protein loading and presented as fold difference of stimulated *versus* resting neutrophils, $n = 3$ pooled technical replicates.



Structure/Function of Neutrophil Elastase N-glycosylation

on the surface of activated neutrophils by the identification of Asn88-M2 and Asn124-M2F glycopeptides derived from cell surface captured HNE (supplemental Fig. S8), but the signal strength proved too weak to perform an accurate qualitative and quantitative site-specific analysis using LC-MS/MS as performed for plasma membrane HNE of resting neutrophils (Fig. 2A). The level of intracellular paucimannosylation remained relatively constant upon stimulation, further supporting that the bulk of paucimannosylated proteins including HNE reside in nonmobile granules or within granules that undergo intracellular fusion during neutrophil activation (28). Taken together, our analyses indicate that paucimannosidic-rich HNE glycoforms are expressed on the surface of neutrophils during resting conditions and that similarly paucimannosylated intracellular HNE can be mobilized to the cell surface upon neutrophil activation.

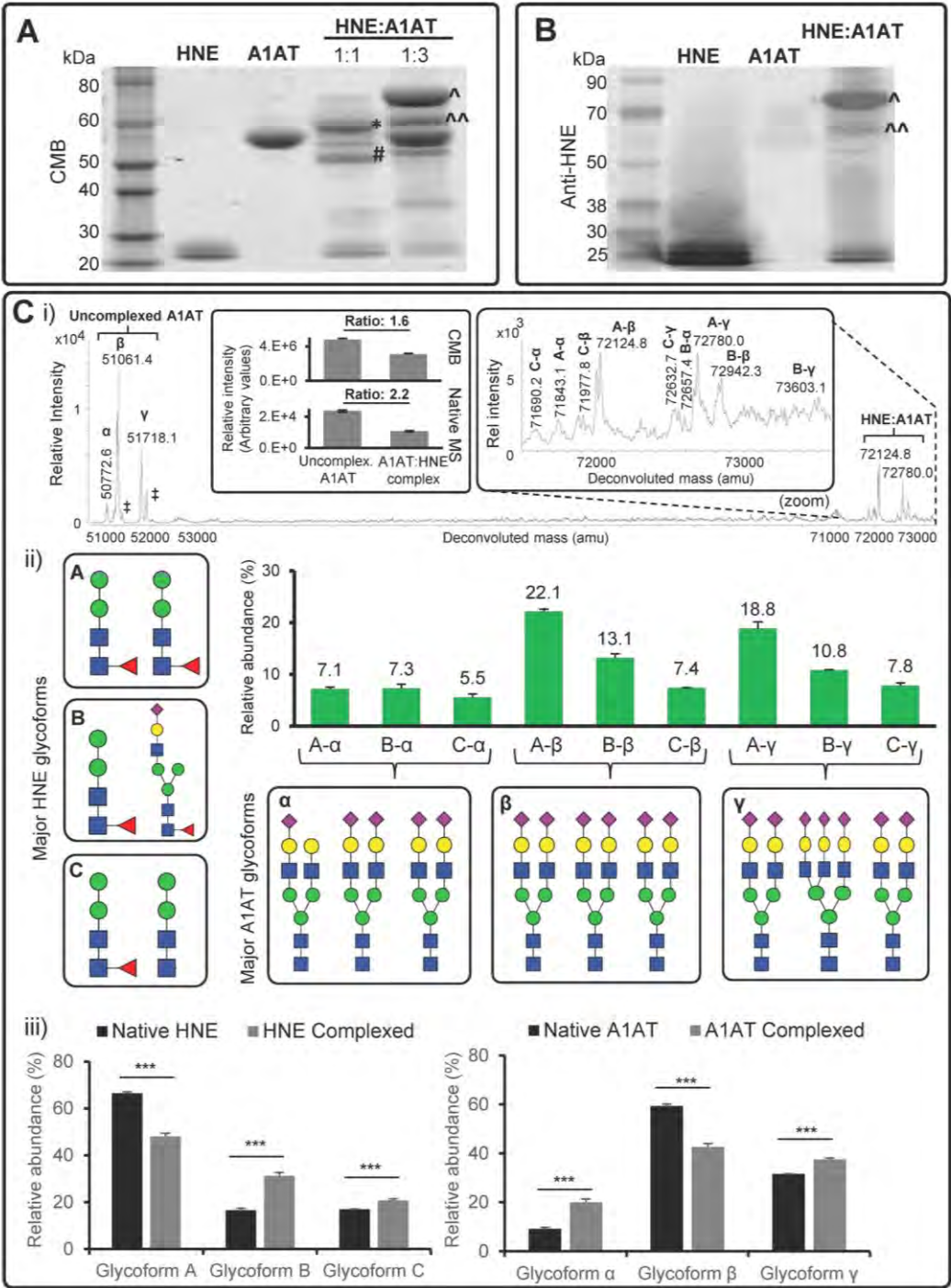
Although the exact molecular details of the mechanism(s) facilitating plasma membrane association remain unknown, the positively charged arginine-rich HNE was suggested to be retained on the surface of activated neutrophils by forming electrostatic interactions with membrane-tethered/associated chondroitin sulfate- and heparin sulfate-containing proteoglycans (77). Given the highly hydrophilic and flexible nature of *N*-glycans (85), the partially charged *N*-glycans on HNE may directly modulate such interactions and/or more indirectly mask protein surface charges as mechanistically shown for sialoglycans of other *N*-glycoproteins (24). Computational analysis suggests that the three occupied glycosylation sites of membrane-retained HNE display *N*-glycans that face and extend into the extracellular milieu (86). Thus, the paucimannose-rich *N*-glycosylation of HNE may likely mediate cell-cell communication with immune cells including dendritic cells and macrophages that are known to express mannose recognizing C-type lectin receptors (mrCLRs) with affinity to mannosylated glycoepitopes (87, 88). The interplay between neutrophils and other immune cells at inflammatory sites has received considerable attention recently; not least in cancer where tumor associated neutrophils have been reported (89, 90). In addition, the unusual HNE sialoglycans may also contribute to the extravasation process by interacting with

selectins expressed by the endothelium (91), if these sialoglycoforms of HNE are presented and correctly oriented on the neutrophil surface at the appropriate time. The potential of paucimannosylated HNE to interact with mrCLRs from the cell surface of activated neutrophils was investigated to provide further insights into neutrophil-mediated immune communication.

Glycoform-dependent Binding of Mannosylated HNE to Human MBL—Given the highly unusual and mannose-rich *N*-glycosylation of the spatiotemporally-regulated HNE, we probed the binding potential and affinity preferences of glycosylated HNE to a central mrCLR in inflammation. This is pertinent because of (1) the accessible nature of the HNE *N*-glycans localized distal to the active site (see above), (2) the fact that HNE is an important glycoprotein involved in many innate immunological processes (92), and (3) the family of mrCLRs including the soluble MBL (93) and the mannosidic glycoprotein ligands are increasingly recognized as key players in innate immunity (79, 94). In fact, MBL is, similarly to HNE, enriched in inflamed/infected airways (95) where it was found to be resistant to HNE degradation (96). We therefore investigated if HNE and human MBL are interaction partners and, if so, whether paucimannosylated forms of HNE show binding preference to MBL over other HNE glycoforms.

Immobilized human MBL affinity chromatography with LC-MS-based analysis of the native and MBL-bound/unbound glycoforms of HNE revealed that some paucimannosidic *N*-glycoforms carrying M2F and M2 (e.g. glycoforms A, B, D, E, F, and G) appeared to be overrepresented in the MBL-bound relative to the MBL-unbound fractions (Fig. 3A, green shading). In total, the binding preference of six HNE glycoforms to human MBL was confirmed by quantitatively comparing the relative distribution of the MBL-bound and unbound HNE glycoforms based on the relative height of their respective deconvoluted signals ($0.0001 < p < 0.001$ for all six glycoforms) (Fig. 3B and supplemental Table S5). Further assessment of the individual *N*-glycans validated that both the mannosylated M2 and M2F clearly displayed preferential affinity to human MBL (2.1 ± 0.3 and 2.0 ± 0.3 -fold binding preference, respectively) (all as mean \pm S.E., $n = 3$) (Fig. 3C). In contrast,

FIG. 3. Glycoform-dependent binding of HNE to human MBL. A, Representative deconvoluted mass spectra of native (top), MBL-unbound (middle) and MBL-bound (bottom) intact HNE. Examples of over- (i.e. M2- and M2F-containing HNE) and under-represented (i.e. FA1G1S1-containing HNE) glycoforms in the MBL-bound relative to the MBL-unbound HNE spectra are highlighted in green and red, respectively. * denotes HNE glycoforms containing paucimannosidic structures that do not demonstrate enhanced/reduced MBL binding. B, The MBL binding affinity was quantified for the fifteen glycoforms of MBL-unbound HNE (dark gray bars) and MBL-bound HNE (black bars) (mean \pm S.E., $n = 3$ technical replicates; ns, not significant ($p \geq 0.05$); *, $p < 0.05$ and ***, $p < 0.001$ using unpaired two-tailed type 2 Student's *t*-tests). The glycoform distribution of native HNE is indicated for reference (overlaid, larger light gray bars) and the glycoform structure, nomenclature and any binding preference or discrimination are indicated in green and red, respectively. * denotes HNE glycoforms containing paucimannosidic structures that do not demonstrate enhanced/reduced MBL binding. C, The MBL binding preferences of the individual M2, M2F and FA1G1S1 HNE *N*-glycans were determined (presented as fold difference of MBL-bound versus MBL-unbound HNE, mean \pm S.E., $n = 3$ technical replicates). D, Comparison of the distribution of native HNE and MBL-bound HNE *N*-glycoforms. Significantly over- and under-represented HNE glycoforms relative to a perfect regression line (identity line) forced between (0, 0) and (1, 1) are in green diamonds and red diamonds, respectively. The HNE glycoform F carrying tri-paucimannosidic structures demonstrated preferential binding to MBL whereas the sialoglycoforms (Glycoform C, J, K, N, and O) bound to a lesser degree. Paucimannosidic HNE glycoforms that did not demonstrate enhanced/reduced MBL binding are shown as black diamonds.



Structure/Function of Neutrophil Elastase N-glycosylation

clear binding discrimination was shown against the FA1G1S1 sialoglycans (0.7 ± 0.01 -fold discrimination), which could be appreciated by relative signal suppression of all five HNE sialoglycoforms (glycoforms C, J, K, N, and O in Fig. 3A–3B, red shading). By comparing the distribution of MBL-bound HNE glycoforms to the native HNE glycoform distribution, it became clear that the HNE glycoform F carrying three paucimannosidic *N*-glycans (two M2F *N*-glycans and a single M2 *N*-glycan), was a highly preferred binding partner compared with the other HNE glycoforms as shown by its deviation from the perfect regression line (identity line) in the scatter plot (Fig. 3D). This preferential binding to MBL could relate to the higher valency of the *N*-linked mannoglycans forming the glycoform F relative to glycoform A (87). Despite also carrying three paucimannosidic *N*-glycans, HNE glycoform I and L surprisingly did not display enhanced MBL binding. M2F and GlcNAc (\pm Fuc)-capped trimannosyl-chitobiose structures carried by the HNE glycoforms H and M also did not display enhanced MBL binding. The lack of MBL binding preference of these glycoforms may relate to their decoration by only a single high-affinity M2F and/or be because of a spatial interplay between the three HNE *N*-glycans facilitating a global protein structure that disfavored MBL binding (97). Taken together, this indicates that paucimannosidic ligands, in particular multivalent core fucosylated dimannosylchitobiose structures, are important to facilitate efficient MBL binding. In analogy, high mannosidic protein ligands have been shown to display high avidity binding to various mrCLRs by means of multivalent interactions either facilitated by their multimannosylated antennas or through the assembly in micro-domains (mannose patches) on protein surfaces (98).

In conclusion, our data show that HNE interacts with human MBL *in vitro* and that the *N*-glycosylation of HNE facilitates binding through paucimannosidic ligand/receptor mechanisms like previously reported interactions of highly mannosylated glycoproteins to MBL (99, 100). It is tempting to speculate that neutrophils synthesize a spectrum of related glycoforms of HNE spanning high-affinity (containing up to three paucimannosidic moieties, two being M2F) to low-affinity (up to two sialoglycans) variants to fine-tune the amount of

binding to MBL and possibly to other mrCLRs e.g. SP-A and SP-D present in inflamed airways.

Proteolytic Inhibition of HNE Through Glycoform-dependent Interactions with A1AT—Human A1AT, an abundant 52 kDa sialoglycoprotein in blood, contains three occupied *N*-glycosylation sites (Asn70, Asn107, Asn271) and is the main physiological inhibitor of HNE (20). The ability of neutrophils to express an enzymatically active cell surface A1AT-resistant form of HNE, represents a nonoxidative mechanism to preserve the potent proteolytic activity of HNE in the presence of equally potent inhibitors such as A1AT in the extracellular milieu (4). As the inhibitory action of A1AT is important to mitigate lung airway damage caused by excessive HNE proteolysis (101, 102), we investigated if the unusual HNE *N*-glycosylation is involved in regulating the A1AT-based inhibition by interfering with the covalent HNE/A1AT complex formation.

As indicated by the protein staining and anti-HNE-based immunoblotting of the gel-separated proteins, an enzyme-to-inhibitor molar ratio of 1:3 resulted in an intact HNE/A1AT complex (~73 kDa), a less intense truncated HNE/A1AT complex (~60 kDa) and an excess of A1AT inhibitor at ~52 kDa (Fig. 4A–4B). Truncation of the 60 kDa HNE:A1AT complex was assessed based on the shift in its molecular weight relative to the intact 73 kDa HNE/A1AT complex as previously reported (103). In contrast, equimolar (1:1) A1AT-based inhibition of HNE formed less HNE:A1AT complex and this complex was predominantly truncated (~60 kDa). In order to study the interaction between HNE and A1AT, an enzyme-to-inhibitor molar ratio of 1:3 was utilized and subjected to native LC-Q-TOF-MS as sufficient amount of the intact 73 kDa HNE:A1AT complex was formed.

Native high-resolution LC-Q-TOF-MS indicated that uncomplexed A1AT (as well as the native form) carried three major glycoforms (here called glycoform α , β and γ) (Fig. 4C i and supplemental Fig. S9). These three glycoforms comprised biantennary mono- and disialylated *N*-glycans and bi- and triantennary fully sialylated *N*-glycans in agreement with previously reported site-specific *N*-glycoproteomes of plasma-derived human A1AT (58, 104). The accurate intact protein mass analysis indicated that all A1AT glycoforms were cysteiny-

FIG. 4. **Glycoform-glycoform enzyme-inhibitor complex formation of HNE and blood plasma-derived human A1AT.** A, CMB staining of isolated HNE, isolated human A1AT and HNE:A1AT complexes and uncomplexed proteins after mixing the two glycoprotein binding partners in a 1:1 and 1:3 ratio. *,[#] denote a truncated HNE:A1AT complex (~60 kDa) and a truncated uncomplexed (native) A1AT (~52 kDa), respectively. ^,^^ denote the intact (~73 kDa) and the truncated form (~60 kDa) of the HNE:A1AT complex, respectively. B, Immunoblot of HNE:A1AT complexes (1:3 ratio) using anti-HNE antibodies. ^, ^^ as denoted in A. Purified HNE (positive control) and A1AT (negative control) were included. C, i) The deconvoluted ESI mass spectrum shows signals corresponding to various major glycoform-glycoform complexes of HNE (A-C):A1AT(α - γ) at 1:3 ratio (see zoom for magnification) and the coeluting uncomplexed A1AT as analyzed by high resolution native LC-Q-TOF-MS. For example, the signal at 72124.8 Da, labeled as A- β , corresponds to HNE glycoform A (two M2F *N*-glycans conjugated to HNE) complexed with the biantennary disialylated A1AT glycoform β . The degree of complex formation was assessed using signal intensities from the CMB gels (upper panel) and native MS (lower panel) as shown in the insert. [†] denotes low abundance A1AT glycoforms carrying fucosylated *N*-glycans. ii) Glycoform distribution of the observed HNE:A1AT complexes, see inserted boxes for structures and nomenclature of major glycoforms of HNE and A1AT. Mean \pm S.E., $n = 3$ technical replicates. See supplemental Fig. S9 for the complete list of identified HNE:A1AT glycoforms. iii) The glycoforms of the HNE:A1AT complex were compared with the glycoform distribution of native HNE and native A1AT to determine any glycoform-glycoform preferences in the enzyme:inhibitor complex formation (Mean \pm S.E., $n = 3$ technical replicates; ***, $p < 0.001$ using unpaired two-tailed type 2 Student's *t*-tests).

lated ($\Delta m = +119.0$ Da) as previously reported (58), but otherwise not modified beyond the expected polypeptide chain trimming and the N-glycosylation. Few A1AT glycoforms carrying fucosylated N-glycans (labeled as ‡ in Fig. 4C i) were also observed as previously described (105). However, these structures were not considered further in this glycoanalysis because of their low abundance. Micro-heterogeneous features of the HNE:A1AT complex were observed (Fig. 4C i, insert). The agreement of CMB (Fig. 4A) and native MS-based quantitation of the uncomplexed-to-complexed A1AT ratio (both close to 2 as expected) indicated little, if any, MS-induced gas-phase dissociation of the formed HNE:A1AT complex. In total, nine major HNE:A1AT complex glycoforms were identified and quantified from combinations of already observed glycoforms of native A1AT (α , β , and γ) and HNE (A, B, and C) (Fig. 4C ii). By comparing the HNE:A1AT complex glycoform distribution to the N-glycosylation of native HNE and native A1AT (Fig. 4C iii and supplemental Table S6), it was observed that glycoform B of HNE (sialoglycoform *i.e.* FA1G1S1) and glycoform α of A1AT (*i.e.* undersialylated glycoform) were overrepresented in the HNE:A1AT complex ($n = 3$ technical replicates, $p < 0.001$). This indicates that sialylated HNE has a higher propensity for engaging in an inhibitor complex with an undersialylated form of A1AT. Although the molecular mechanisms underpinning these HNE:A1AT complex preferences remain unclear, it could be speculated that the negatively charged sialoform of HNE interact strongly with its own highly cationic protein surface and thereby causes less sterical hindrance upon A1AT interaction. Conversely, less sialylated A1AT may more readily bind to HNE because it is sterically less likely to cause interference, while being sufficiently anionic via its sialoglycans and the negatively charged protein surface interface at the exosite of A1AT to interact strongly with HNE. These anionic residues at the A1AT exosite have been shown previously to be important for protease binding (106). This potential glycoform-glycoform preference for protein complex formation is, to the best of our knowledge, the first example indicating that N-glycosylation of both protein partners influences their propensity to engage in a complex.

HNE-based cleavage of the A1AT loop is the initial step in the irreversible covalent binding and inhibition of the HNE activity by distorting its active site (107, 108). Oxidation of Met351 or Met358 on the reactive center loop of A1AT has been shown to be an alternative mechanism to reduce the ability of A1AT to inhibit HNE (109). A1AT was not oxidized in our experiments, but the highly oxidative environment at inflammatory sites, which contains large amount of reactive oxygen species secreted during the respiratory burst from activated neutrophils, may efficiently inactivate A1AT to preserve the HNE activity when it is degranulated (110). Restoration of the anti-protease activity to limit the local tissue damage by HNE after A1AT oxidative inactivation has also been reported (111), demonstrating a delicate homeostatic balance involving the

inactivation and activation of anti-protease activity during inflammation, which can be easily deregulated in lung diseases such as CF (112). The glycosylation of A1AT was previously suggested to confer resistance toward degradation and extending its half-life in circulation (113). Our observations suggest that protein N-glycosylation in addition serves to modulate the A1AT-based inhibition of the proteolytic efficiency of HNE in intricate ways during innate immune processes.

HNE and Its N-glycans are Bacteriostatic Toward P. aeruginosa—HNE mediates protection against pathogens such as *P. aeruginosa* by degrading proteins of the outer bacterial membrane (23, 114). However, other potential protective functions mediated by HNE and the importance of HNE N-glycosylation have not been studied in the context of pathogen killing, in part, because of the lack of structural information of the exact N-glycosylation of HNE. We here also investigated whether the unusual N-glycans of HNE influence the growth of a common type of pathogenic bacteria found in inflamed airways.

The clinical *P. aeruginosa* strain (PASS1) isolated from a CF patient (61) was cultured with physiological relevant concentrations (low micromolar *i.e.* 1.8 μM and 3.6 μM) of enzymatically active HNE as well as with isolated HNE N-glycans. The enzyme activity of HNE was confirmed by rapid CBG cleavage using gel electrophoresis as shown previously (24). The bacterial growth profile was monitored over 12 h at 37 °C. As expected, enzymatically active HNE significantly inhibited the growth of PASS1 relative to the growth profile of PASS1 without HNE in a concentration-dependent manner ($n = 3$ technical replicates, $p < 0.05$) (supplemental Fig. S10A). Interestingly, free HNE N-glycans (3.6 μM) inhibited the bacterial growth comparable with the enzymatically active HNE (1.8 μM). We also observed that the paucimannose-rich nCG, another potent serine protease produced and used by human neutrophils for bacterial defense, and its released N-glycans displayed similar bacteriostatic effects on PASS1 within the same concentration range (supplemental Fig. S10B). Although the underlying mechanisms remain unknown, the apparent bacteriostatic effects at low concentrations of paucimannosidic and monosialylated free N-glycans is intriguing and has to the best of our knowledge not been reported previously. Further work is needed to pin-point which HNE N-glycan or N-glycan subsets display growth inhibitory effects toward *P. aeruginosa*.

CONCLUSIONS

This is the first report on the detailed structure and function of the N-glycosylation of HNE, a key serine protease in inflammation and bacterial infection. The deep site- and sub-cellular-specific glycoprofiling of HNE from resting neutrophils showed that HNE carries uniform but highly unusual site-specific N-glycosylation across multiple granular compartments and is undergoing spatiotemporal regulation upon neutrophil activation. The nonconventional paucimannosidic and monosialylated N-glycans abundantly decorating HNE

Structure/Function of Neutrophil Elastase N-glycosylation

showed intriguing immune-related functions by facilitating and/or modulating the binding of HNE to an immunological relevant mannose receptor, MBL, and to a key inhibitory anti-protease, A1AT, present within inflamed airways. These intriguing observations generate novel insights into the structure and functional relationship of a central player in innate immunity and advance our understanding of the refined molecular and cellular mechanisms and the importance of protein N-glycosylation in the inflamed microenvironment relevant for multiple immune diseases.

Acknowledgments—We thank Ms Charlotte Horne, Dr Simone Diestel, Dr Liisa Kautto, Dr Jodie Abrahams, Dr Zeynep Sumer-Bayraktar, and Mr Christopher Ashwood for providing valuable chemicals and reagents, and for expert technical assistance. Ms Serene Gwee is thanked for proof reading and fruitful discussions. Finally, we would like to sincerely thank Prof Niels Borregaard, University of Copenhagen, Denmark for providing outstanding scientific inspiration in neutrophil biology.

DATA AVAILABILITY

The LC-MS/MS data supporting the reported HNE N-glycopeptides and N-glycans including the observed precursor masses (*m/z* and charge states), annotated MS/MS spectra and LC retention times are available in the supplementary files. The LC-MS data supporting the native glycoprotein analyses and the HNE:MBL and HNE:A1AT binding assays, including the observed deconvoluted masses and their relative abundance are also available in the supplementary files. The LC-MS/MS proteomics data supporting the subcellular- and site-specific N-glycosylation analysis of HNE present across the neutrophil granule compartments have been deposited to the ProteomeXchange Consortium (<http://proteomecentral.proteomexchange.org>) via the PRIDE partner repository with the data set identifier PXD005559.

* I.L. was supported by an international Macquarie University Research Scholarship (iMQRES) and an Australian Cystic Fibrosis postgraduate studentship. M.T.-A. was supported by a fellowship from the Cancer Institute NSW, Australia, and a Macquarie University Research Development Grant (MQRDG).

§ This article contains supplemental material.

The authors declare no conflict of interest.

¶ To whom correspondence should be addressed: Biomolecular Discovery and Design Research Centre, Department of Chemistry and Biomolecular Sciences, Macquarie University, Sydney, NSW 2109, Australia. Tel.: +61-2-9850-7487; Fax: +61-2-9850-6192; E-mail: morten.andersen@mq.edu.au.

REFERENCES

- Borregaard, N., Sorensen, O. E., and Theilgaard-Monch, K. (2007) Neutrophil granules: a library of innate immunity proteins. *Trends Immunol.* **28**, 340–345.
- Rorvig, S., Honore, C., Larsson, L. I., Ohlsson, S., Pedersen, C. C., Jacobsen, L. C., Cowland, J. B., Garred, P., and Borregaard, N. (2009) Ficolin-1 is present in a highly mobilizable subset of human neutrophil granules and associates with the cell surface after stimulation with fMLP. *J. Leukoc. Biol.* **86**, 1439–1449.
- Rorvig, S., Ostergaard, O., Heegaard, N. H., and Borregaard, N. (2013) Proteome profiling of human neutrophil granule subsets, secretory vesicles, and cell membrane: correlation with transcriptome profiling of neutrophil precursors. *J. Leukoc. Biol.* **94**, 711–721.
- Owen, C. A., Campbell, M. A., Sannes, P. L., Boukedes, S. S., and Campbell, E. J. (1995) Cell surface-bound elastase and cathepsin G on human neutrophils: a novel, non-oxidative mechanism by which neutrophils focus and preserve catalytic activity of serine proteinases. *J. Cell Biol.* **131**, 775–789.
- Nauseef, W. M., and Borregaard, N. (2014) Neutrophils at work. *Nat. Immunol.* **15**, 602–611.
- Reece, S. T., Loddenkemper, C., Askew, D. J., Zedler, U., Schommer-Leitner, S., Stein, M., Mir, F. A., Dorhoi, A., Mollenkopf, H. J., Silverman, G. A., and Kaufmann, S. H. (2010) Serine protease activity contributes to control of *Mycobacterium tuberculosis* in hypoxic lung granulomas in mice. *J. Clin. Invest.* **120**, 3365–3376.
- Gombart, A. F., and Koeffler, H. P. (2002) Neutrophil specific granule deficiency and mutations in the gene encoding transcription factor C/EBP(epsilon). *Curr. Opin. Hematol.* **9**, 36–42.
- Le Gars, M., Descamps, D., Roussel, D., Sausseureau, E., Guillot, L., Ruffin, M., Tabary, O., Hong, S. S., Boulanger, P., Paulais, M., Malleret, L., Belaouaj, A., Edelman, A., Huerre, M., Chignard, M., and Sallenave, J. M. (2013) Neutrophil elastase degrades cystic fibrosis transmembrane conductance regulator via calpains and disables channel function in vitro and in vivo. *Am. J. Respir. Crit. Care Med.* **187**, 170–179.
- Tidwell, T., Wechsler, J., Nayak, R. C., Trump, L., Salipante, S. J., Cheng, J. C., Donadieu, J., Glaubach, T., Corey, S. J., Grimes, H. L., Lutzko, C., Cancelas, J. A., and Horwitz, M. S. (2014) Neutropenia-associated ELANE mutations disrupting translation initiation produce novel neutrophil elastase isoforms. *Blood* **123**, 562–569.
- Horwitz, M. S., Duan, Z., Korkmaz, B., Lee, H. H., Mealiffe, M. E., and Salipante, S. J. (2007) Neutrophil elastase in cyclic and severe congenital neutropenia. *Blood* **109**, 1817–1824.
- Nayak, R. C., Trump, L. R., Aronow, B. J., Myers, K., Mehta, P., Kalfa, T., Wellendorf, A. M., Valencia, C. A., Paddison, P. J., Horwitz, M. S., Grimes, H. L., Lutzko, C., and Cancelas, J. A. (2015) Pathogenesis of ELANE-mutant severe neutropenia revealed by induced pluripotent stem cells. *J. Clin. Invest.* **125**, 3103–3116.
- Kettritz, R. (2016) Neutral serine proteases of neutrophils. *Immunol. Rev.* **273**, 232–248.
- Lindmark, A., Persson, A. M., and Olsson, I. (1990) Biosynthesis and processing of cathepsin G and neutrophil elastase in the leukemic myeloid cell line U-937. *Blood* **76**, 2374–2380.
- Gullberg, U., Lindmark, A., Lindgren, G., Persson, A. M., Nilsson, E., and Olsson, I. (1995) Carboxyl-terminal prodomain-deleted human leukocyte elastase and cathepsin G are efficiently targeted to granules and enzymatically activated in the rat basophilic/mast cell line RBL. *J. Biol. Chem.* **270**, 12912–12918.
- Benson, K. F., Li, F. Q., Person, R. E., Albani, D., Duan, Z., Wechsler, J., Meade-White, K., Williams, K., Acland, G. M., Niemeyer, G., Lathrop, C. D., and Horwitz, M. (2003) Mutations associated with neutropenia in dogs and humans disrupt intracellular transport of neutrophil elastase. *Nat. Genet.* **35**, 90–96.
- Niemann, C. U., Abrink, M., Pejler, G., Fischer, R. L., Christensen, E. I., Knight, S. D., and Borregaard, N. (2007) Neutrophil elastase depends on serylarginine proteoglycan for localization in granules. *Blood* **109**, 4478–4486.
- Cowland, J. B., and Borregaard, N. (2016) Granulopoiesis and granules of human neutrophils. *Immunol. Rev.* **273**, 11–28.
- Sinha, S., Watorek, W., Karr, S., Giles, J., Bode, W., and Travis, J. (1987) Primary structure of human neutrophil elastase. *Proc. Natl. Acad. Sci. U.S.A.* **84**, 2228–2232.
- Korkmaz, B., Horwitz, M. S., Jenne, D. E., and Gauthier, F. (2010) Neutrophil elastase, proteinase 3, and cathepsin G as therapeutic targets in human diseases. *Pharmacol. Rev.* **62**, 726–759.
- Lussier, B., and Wilson, A. A. (2016) Alpha-1 Antitrypsin: The Protein. pp. 17–30, Humana Press, New York.
- Grigorieva, D. V., Gorudko, I. V., Sokolov, A. V., Kostevich, V. A., Vasilyev, V. B., Cherenkevich, S. N., and Panasenko, O. M. (2016) Myeloperoxidase Stimulates Neutrophil Degranulation. *Bull. Exp. Biol. Med.* **161**, 495–500.
- Clemmensen, S. N., Jacobsen, L. C., Rorvig, S., Askaa, B., Christensen, K., Iversen, M., Jorgensen, M. H., Larsen, M. T., van Deurs, B., Ostergaard,

- O., Heegaard, N. H., Cowland, J. B., and Borregaard, N. (2011) Alpha-1-antitrypsin is produced by human neutrophil granulocytes and their precursors and liberated during granule exocytosis. *Eur. J. Haematol.* **86**, 517–530
23. Hirche, T. O., Benabid, R., Deslee, G., Gangloff, S., Achilefu, S., Gueunou, M., Lebargy, F., Hancock, R. E., and Belaouaj, A. (2008) Neutrophil elastase mediates innate host protection against *Pseudomonas aeruginosa*. *J. Immunol.* **181**, 4945–4954
24. Sumer-Bayraktar, Z., Grant, O. C., Venkatakrishnan, V., Woods, R. J., Packer, N. H., and Thaysen-Andersen, M. (2016) Asn347 glycosylation of corticosteroid-binding globulin fine-tunes the host immune response by modulating proteolysis by *Pseudomonas aeruginosa* and neutrophil elastase. *J. Biol. Chem.* **291**, 17727–17742
25. Sinden, N. J., Baker, M. J., Smith, D. J., Kreft, J. U., Dafforn, T. R., and Stockley, R. A. (2015) alpha-1-antitrypsin variants and the proteinase/antiproteinase imbalance in chronic obstructive pulmonary disease. *Am. J. Physiol. Lung Cell Mol. Physiol.* **308**, L179–190
26. Hoenderdos, K., and Condiliffe, A. (2013) The neutrophil in chronic obstructive pulmonary disease. *Am. J. Respir. Cell Mol. Biol.* **48**, 531–539
27. Papayannopoulos, V., Metzler, K. D., Hakkim, A., and Zychlinsky, A. (2010) Neutrophil elastase and myeloperoxidase regulate the formation of neutrophil extracellular traps. *J. Cell Biol.* **191**, 677–691
28. Metzler, K. D., Goosmann, C., Lubojemska, A., Zychlinsky, A., and Papayannopoulos, V. (2014) A myeloperoxidase-containing complex regulates neutrophil elastase release and actin dynamics during NETosis. *Cell Reports* **8**, 883–896
29. Sorensen, O. E., and Borregaard, N. (2016) Neutrophil extracellular traps - the dark side of neutrophils. *J. Clin. Invest.* **126**, 1612–1620
30. Watorek, W., Halbeek, H., and Travis, J. (1993) The isoforms of human neutrophil elastase and cathepsin G differ in their carbohydrate side chain structures. *Biochem. Biophys. Res. Commun.* **194**, 385–393
31. Hansen, G., Gielen-Haertwig, H., Reinemer, P., Schomburg, D., Harrenga, A., and Niefind, K. (2011) Unexpected active-site flexibility in the structure of human neutrophil elastase in complex with a new dihydropyrimidine inhibitor. *J. Mol. Biol.* **409**, 681–691
32. Kolner, I., Sodeik, B., Schreck, S., Heyn, H., von Neuhoff, N., Gernshausen, M., Zeidler, C., Kruger, M., Schlegelberger, B., Welte, K., and Beger, C. (2006) Mutations in neutrophil elastase causing congenital neutropenia lead to cytoplasmic protein accumulation and induction of the unfolded protein response. *Blood* **108**, 493–500
33. Kawata, J., Yamaguchi, R., Yamamoto, T., Ishimaru, Y., Sakamoto, A., Aoki, M., Kitano, M., Umehashi, M., Hirose, E., and Yamaguchi, Y. (2016) Human neutrophil elastase induce interleukin-10 expression in peripheral blood mononuclear cells through protein kinase C θ and δ and phospholipase pathways. *Cell J.* **17**, 692–700
34. Chawla, A., Alatrash, G., Phillips, A. V., Qiao, N., Sukhumalchandra, P., Kerros, C., Diaconu, I., Gall, V., Neal, S., Peters, H. L., Clise-Dwyer, K., Moldrem, J. J., and Mittendorf, E. A. (2016) Neutrophil elastase enhances antigen presentation by upregulating human leukocyte antigen class I expression on tumor cells. *Cancer Immunol. Immunother.* **65**, 741–751
35. Salazar, V. A., Rubin, J., Moussaoui, M., Pulido, D., Nogueira, M. V., Venge, P., and Boix, E. (2014) Protein post-translational modification in host defense: the antimicrobial mechanism of action of human eosinophil cationic protein native forms. *FEBS J.* **281**, 5432–5446
36. Hulsmeier, A. J., Tobler, M., Burda, P., and Hennet, T. (2016) Glycosylation site occupancy in health, congenital disorder of glycosylation and fatty liver disease. *Sci. Rep.* **6**, 33927
37. Jensen, P. H., Karlsson, N. G., Kolarich, D., and Packer, N. H. (2012) Structural analysis of N- and O-glycans released from glycoproteins. *Nat. Protoc.* **7**, 1299–1310
38. Loke, I., Packer, N. H., and Thaysen-Andersen, M. (2015) Complementary LC-MS/MS-based N-Glycan, N-Glycopeptide, and intact N-glycoprotein profiling reveals unconventional Asn71-glycosylation of human neutrophil cathepsin G. *Biomolecules* **5**, 1832–1854
39. Ceroni, A., Maass, K., Geyer, H., Geyer, R., Dell, A., and Haslam, S. M. (2008) GlycoWorkbench: a tool for the computer-assisted annotation of mass spectra of glycans. *J. Proteome Res.* **7**, 1650–1659
40. Cooper, C. A., Gasteiger, E., and Packer, N. H. (2001) GlycoMod—a software tool for determining glycosylation compositions from mass spectrometric data. *Proteomics* **1**, 340–349
41. Mysling, S., Palmisano, G., Hojrup, P., and Thaysen-Andersen, M. (2010) Utilizing ion-pairing hydrophilic interaction chromatography solid phase extraction for efficient glycopeptide enrichment in glycoproteomics. *Anal. Chem.* **82**, 5598–5609
42. Parker, B. L., Thaysen-Andersen, M., Fazakerley, D. J., Holliday, M., Packer, N. H., and James, D. E. (2016) Terminal galactosylation and sialylation switching on membrane glycoproteins upon TNF-alpha-induced insulin resistance in adipocytes. *Mol. Cell. Proteomics* **15**, 141–153
43. Stavenhagen, K., Hinneburg, H., Thaysen-Andersen, M., Hartmann, L., Varon Silva, D., Fuchser, J., Kaspar, S., Rapp, E., Seeberger, P. H., and Kolarich, D. (2013) Quantitative mapping of glycoprotein micro-heterogeneity and macro-heterogeneity: an evaluation of mass spectrometry signal strengths using synthetic peptides and glycopeptides. *J. Mass Spectrom.* **48**, 627–639
44. Sethi, M. K., Kim, H., Park, C. K., Baker, M. S., Paik, Y. K., Packer, N. H., Hancock, W. S., Fanayan, S., and Thaysen-Andersen, M. (2015) In-depth N-glycome profiling of paired colorectal cancer and non-tumorigenic tissues reveals cancer-, stage- and EGFR-specific protein N-glycosylation. *Glycobiology* **25**, 1064–1078
45. Everest-Dass, A. V., Abrahams, J. L., Kolarich, D., Packer, N. H., and Campbell, M. P. (2013) Structural feature ions for distinguishing N- and O-linked glycan isomers by LC-ESI-IT MS/MS. *J. Am. Soc. Mass Spectrom.* **24**, 895–906
46. Stadlmann, J., Pabst, M., Kolarich, D., Kunert, R., and Altmann, F. (2008) Analysis of immunoglobulin glycosylation by LC-ESI-MS of glycopeptides and oligosaccharides. *Proteomics* **8**, 2858–2871
47. Winchester, B. (2005) Lysosomal metabolism of glycoproteins. *Glycobiology* **15**:1R–15R
48. Aebi, M. (2013) N-linked protein glycosylation in the ER. *Biochim. Biophys. Acta* **1833**, 2430–2437
49. Varki, A., Cummings, R. D., Aebi, M., Packer, N. H., Seeberger, P. H., Esko, J. D., Stanley, P., Hart, G., Darvill, A., Kinoshita, T., Prestegard, J. J., Schnaar, R. L., Freeze, H. H., Marth, J. D., Bertozzi, C. R., Etzler, M. E., Frank, M., Vilegenthart, J. F., Lütteke, T., Perez, S., Bolton, E., Rudd, P., Paulson, J., Kanehisa, M., Toukach, P., Aoki-Kinoshita, K. F., Dell, A., Narimatsu, H., York, W., Taniguchi, N., and Kornfeld, S. (2015) Symbol nomenclature for graphical representations of glycans. *Glycobiology* **25**, 1323–1324
50. Dalpathado, D. S., and Desaire, H. (2008) Glycopeptide analysis by mass spectrometry. *Analyst* **133**, 731–738
51. Leymarie, N., and Zala, J. (2012) Effective use of mass spectrometry for glycan and glycopeptide structural analysis. *Anal. Chem.* **84**, 3040–3048
52. Lee, L. Y., Moh, E. S., Parker, B. L., Bern, M., Packer, N. H., and Thaysen-Andersen, M. (2016) Toward automated N-glycopeptide identification in glycoproteomics. *J. Proteome Res.* **15**, 3904–3915
53. Reich, M., Liefeld, T., Gould, J., Lerner, J., Tamayo, P., and Mesirov, J. P. (2006) GenePattern 2.0. *Nat. Genet.* **38**, 500–501
54. Hubber, S. J., and Thornton, J. M. (1993) NACCESS computer program. Department of Biochemistry and Molecular Biology, University College, London
55. Hormann, K., Stukalov, A., Muller, A. C., Heinz, L. X., Superti-Furga, G., Colinge, J., and Bennett, K. L. (2016) A surface biotinylation strategy for reproducible plasma membrane protein purification and tracking of genetic and drug-induced alterations. *J. Proteome Res.* **15**, 647–658
56. Zipser, B., Bello-DeOcampo, D., Diestel, S., Tai, M. H., and Schmitz, B. (2012) Mannitox monoclonal antibody uniquely recognizes paucimannose, a marker for human cancer, stemness, and inflammation. *J. Carbohydr. Chem.* **31**, 504–518
57. Eaton, S. L., Roche, S. L., Liavero Hurtado, M., Oldknow, K. J., Farquharson, C., Gillingwater, T. H., and Wishart, T. M. (2013) Total protein analysis as a reliable loading control for quantitative fluorescent Western blotting. *PLoS ONE* **8**, e72457
58. Kolarich, D., Weber, A., Turecek, P. L., Schwarz, H. P., and Altmann, F. (2006) Comprehensive glyco-proteomic analysis of human alpha1-antitrypsin and its charge isoforms. *Proteomics* **6**, 3369–3380
59. Kolarich, D., Turecek, P. L., Weber, A., Mitterer, A., Graninger, M., Mattheissen, P., Nicolaes, G. A., Altmann, F., and Schwarz, H. P. (2006) Biochemical, molecular characterization, and glycoproteomic analyses

Structure/Function of Neutrophil Elastase N-glycosylation

- of alpha(1)-proteinase inhibitor products used for replacement therapy. *Transfusion* **46**, 1959–1977
60. Thaysen-Andersen, M., Venkatakrishnan, V., Loke, I., Laurini, C., Diestel, S., Parker, B. L., and Packer, N. H. (2015) Human neutrophils secrete bioactive paucimannosidic proteins from azurophilic granules into pathogen-infected sputum. *J. Biol. Chem.* **290**, 8789–8802
 61. Penesyan, A., Kumar, S. S., Kamath, K., Shathili, A. M., Venkatakrishnan, V., Krisp, C., Packer, N. H., Molloy, M. P., and Paulsen, I. T. (2015) Genetically and phenotypically distinct *Pseudomonas aeruginosa* cystic fibrosis isolates share a core proteomic signature. *PLoS ONE* **10**, e0138527
 62. Venkatakrishnan, V., Thaysen-Andersen, M., Chen, S. C., Nevalainen, H., and Packer, N. H. (2015) Cystic fibrosis and bacterial colonization define the sputum N-glycosylation phenotype. *Glycobiology* **25**, 88–100
 63. Olczak, M., and Watorek, W. (2002) Structural analysis of N-glycans from human neutrophil azurocidin. *Biochem. Biophys. Res. Commun.* **293**, 213–219
 64. Zoega, M., Ravnsborg, T., Hojrup, P., Houen, G., and Schou, C. (2012) Proteinase 3 carries small unusual carbohydrates and associates with alpha-defensins. *J. Proteomics* **75**, 1472–1485
 65. Ishizuka, A., Hashimoto, Y., Naka, R., Kinoshita, M., Kakehi, K., Seino, J., Funakoshi, Y., Suzuki, T., Kameyama, A., and Narimatsu, H. (2008) Accumulation of free complex-type N-glycans in MKN7 and MKN45 stomach cancer cells. *Biochem. J.* **413**, 227–237
 66. Seino, J., Wang, L., Harada, Y., Huang, C., Ishii, K., Mizushima, N., and Suzuki, T. (2013) Basal autophagy is required for the efficient catabolism of sialyloligosaccharides. *J. Biol. Chem.* **288**, 26898–26907
 67. Korkmaz, B., Moreau, T., and Gauthier, F. (2008) Neutrophil elastase, proteinase 3 and cathepsin G: physicochemical properties, activity and physiopathological functions. *Biochimie* **90**, 227–242
 68. Huang, W., Yamamoto, Y., Li, Y., Dou, D., Alliston, K. R., Hanzlik, R. P., Williams, T. D., and Groutas, W. C. (2008) X-ray snapshot of the mechanism of inactivation of human neutrophil elastase by 1,2,5-thiadiazolidin-3-one 1,1-dioxide derivatives. *J. Med. Chem.* **51**, 2003–2008
 69. Bourgoignie-Voillard, S., Leymarie, N., and Costello, C. E. (2014) Top-down tandem mass spectrometry on RNase A and B using a Qh/FT-ICR hybrid mass spectrometer. *Proteomics* **14**, 1174–1184
 70. Twumasi, D. Y., and Liener, I. E. (1977) Proteinases from purulent sputum. Purification and properties of the elastase and chymotrypsin-like enzymes. *J. Biol. Chem.* **252**, 1917–1926
 71. Thaysen-Andersen, M., and Packer, N. H. (2012) Site-specific glycoproteomics confirms that protein structure dictates formation of N-glycan type, core fucosylation and branching. *Glycobiology* **22**, 1440–1452
 72. Mellquist, J. L., Kasturi, L., Spitalnik, S. L., and Shakin-Eshleman, S. H. (1998) The amino acid following an asn-X-Ser/Thr sequon is an important determinant of N-linked core glycosylation efficiency. *Biochemistry* **37**, 6833–6837
 73. Lee, L. Y., Lin, C. H., Fanayan, S., Packer, N. H., and Thaysen-Andersen, M. (2014) Differential site accessibility mechanistically explains subcellular-specific N-glycosylation determinants. *Front. Immunol.* **5**, 404
 74. Borregaard, N., and Cowland, J. B. (1997) Granules of the human neutrophilic polymorphonuclear leukocyte. *Blood* **89**, 3503–3521
 75. Le Cabec, V., Cowland, J. B., Calafat, J., and Borregaard, N. (1996) Targeting of proteins to granule subsets is determined by timing and not by sorting: The specific granule protein NGAL is localized to azurophilic granules when expressed in HL-60 cells. *Proc. Natl. Acad. Sci. U.S.A.* **93**, 6454–6457
 76. Lominadze, G., Powell, D. W., Luerman, G. C., Link, A. J., Ward, R. A., and McLeish, K. R. (2005) Proteomic analysis of human neutrophil granules. *Mol. Cell. Proteomics* **4**, 1503–1521
 77. Campbell, E. J., and Owen, C. A. (2007) The sulfate groups of chondroitin sulfate- and heparan sulfate-containing proteoglycans in neutrophil plasma membranes are novel binding sites for human leukocyte elastase and cathepsin G. *J. Biol. Chem.* **282**, 14645–14654
 78. Korkmaz, B., Attucci, S., Juliano, M. A., Kalupov, T., Jourdan, M. L., Juliano, L., and Gauthier, F. (2008) Measuring elastase, proteinase 3 and cathepsin G activities at the surface of human neutrophils with fluorescence resonance energy transfer substrates. *Nat. Protoc.* **3**, 991–1000
 79. Loke, I., Kolarich, D., Packer, N. H., and Thaysen-Andersen, M. (2016) Emerging roles of protein mannosylation in inflammation and infection. *Mol. Aspects Med.* **51**, 31–55
 80. Robajac, D., Vanhooren, V., Masnikosa, R., Mikovic, Z., Mandic, V., Libert, C., and Nedic, O. (2016) Preeclampsia transforms membrane N-glycome in human placenta. *Exp. Mol. Pathol.* **100**, 26–30
 81. Lollike, K., Lindau, M., Calafat, J., and Borregaard, N. (2002) Compound exocytosis of granules in human neutrophils. *J. Leukoc. Biol.* **71**, 973–980
 82. Reeves, E. P., Lu, H., Jacobs, H. L., Messina, C. G., Bolsover, S., Gabella, G., Potma, E. O., Warley, A., Roes, J., and Segal, A. W. (2002) Killing activity of neutrophils is mediated through activation of proteases by K⁺ flux. *Nature* **416**, 291–297
 83. Potera, R. M., Jensen, M. J., Hilkin, B. M., South, G. K., Hook, J. S., Gross, E. A., and Moreland, J. G. (2016) Neutrophil azurophilic granule exocytosis is primed by TNF-alpha and partially regulated by NADPH oxidase. *Innate Immun.* **8**, 635–646
 84. Sengelov, H., Follin, P., Kjeldsen, L., Lollike, K., Dahlgren, C., and Borregaard, N. (1995) Mobilization of granules and secretory vesicles during in vivo exudation of human neutrophils. *J. Immunol.* **154**, 4157–4165
 85. Petrescu, A. J., Petrescu, S. M., Dwek, R. A., and Wormald, M. R. (1999) A statistical analysis of N- and O-glycan linkage conformations from crystallographic data. *Glycobiology* **9**, 343–352
 86. Hajjar, E., Mihajlovic, M., Witko-Sarsat, V., Lazaridis, T., and Reuter, N. (2008) Computational prediction of the binding site of proteinase 3 to the plasma membrane. *Proteins* **71**, 1655–1669
 87. van Liempt, E., Bank, C. M., Mehta, P., Garcia-Vallejo, J. J., Kawan, Z. S., Geyer, R., Alvarez, R. A., Cummings, R. D., Kooyk, Y., and van Die, I. (2006) Specificity of DC-SIGN for mannose- and fucose-containing glycans. *FEBS Lett.* **580**, 6123–6131
 88. Lai, J., Bernhard, O. K., Turville, S. G., Harman, A. N., Wilkinson, J., and Cunningham, A. L. (2009) Oligomerization of the macrophage mannose receptor enhances gp120-mediated binding of HIV-1. *J. Biol. Chem.* **284**, 11027–11038
 89. Coffelt, S. B., Wellenstein, M. D., and de Visser, K. E. (2016) Neutrophils in cancer: neutral no more. *Nat. Rev. Cancer* **16**, 431–446
 90. Singel, K. L., and Segal, B. H. (2016) Neutrophils in the tumor microenvironment: trying to heal the wound that cannot heal. *Immunol. Rev.* **273**, 329–343
 91. Moore, K. L., Patel, K. D., Bruehl, R. E., Li, F., Johnson, D. A., Lichenstein, H. S., Cummings, R. D., Bainton, D. F., and McEver, R. P. (1995) P-selectin glycoprotein ligand-1 mediates rolling of human neutrophils on P-selectin. *J. Cell Biol.* **128**, 661–671
 92. Pham, C. T. (2006) Neutrophil serine proteases: specific regulators of inflammation. *Nat. Rev. Immunol.* **6**, 541–550
 93. Ip, W. K., Takahashi, K., Ezekowitz, R. A., and Stuart, L. M. (2009) Mannose-binding lectin and innate immunity. *Immunol. Rev.* **230**, 9–21
 94. Arnold, J. N., Wormald, M. R., Suter, D. M., Radcliffe, C. M., Harvey, D. J., Dwek, R. A., Rudd, P. M., and Sim, R. B. (2005) Human serum IgM glycosylation: identification of glycoforms that can bind to mannann-binding lectin. *J. Biol. Chem.* **280**, 29080–29087
 95. Fidler, K. J., Hilliard, T. N., Bush, A., Johnson, M., Geddes, D. M., Turner, M. W., Alton, E. W., Klein, N. J., and Davies, J. C. (2009) Mannose-binding lectin is present in the infected airway: a possible pulmonary defence mechanism. *Thorax* **64**, 150–155
 96. Butler, G. S., Sim, D., Tam, E., Devine, D., and Overall, C. M. (2002) Mannose-binding lectin (MBL) mutants are susceptible to matrix metalloproteinase proteolysis: potential role in human MBL deficiency. *J. Biol. Chem.* **277**, 17511–17519
 97. Gabius, H.-J., Kaltner, H., Kopitz, J., and André, S. (2015) The glyco-biology of the CD system: a dictionary for translating marker designations into glycan/lectin structure and function. *Trends Biochem. Sci.* **40**, 360–376
 98. Cohen, M. (2015) Notable aspects of glycan-protein interactions. *Biomolecules* **5**, 2056–2072
 99. Mazumder, P., and Mukhopadhyay, C. (2012) Conformations, dynamics and interactions of di-, tri- and pentamannoside with mannose binding lectin: a molecular dynamics study. *Carbohydr. Res.* **349**, 59–72
 100. Weis, W. I., Drickamer, K., and Hendrickson, W. A. (1992) Structure of a c-type mannose-binding protein complexed with an oligosaccharide. *Nature* **360**, 127–134
 101. Garratt, L. W., Sutanto, E. N., Ling, K. M., Looi, K., Iosifidis, T., Martynovich, K. M., Shaw, N. C., Buckley, A. G., Kicic-Starcevic, E.,

- Lannigan, F. J., Knight, D. A., Stick, S. M., and Kicic, A. (2016) Alpha-1 antitrypsin mitigates the inhibition of airway epithelial cell repair by neutrophil elastase. *Am. J. Respir. Cell Mol. Biol.* **54**, 341–349
102. Janciauskiene, S., and Welte, T. (2016) Well-known and less well-known functions of alpha-1 antitrypsin. Its role in chronic obstructive pulmonary disease and other disease developments. *Ann Am Thorac Soc* **13**, S280–288
 103. Ogushi, F., Fells, G. A., Hubbard, R. C., Straus, S. D., and Crystal, R. G. (1987) Z-type alpha 1-antitrypsin is less competent than M1-type alpha 1-antitrypsin as an inhibitor of neutrophil elastase. *J. Clin. Invest.* **80**, 1366–1374
 104. McCarthy, C., Saldova, R., Wormald, M. R., Rudd, P. M., McElvaney, N. G., and Reeves, E. P. (2014) The role and importance of glycosylation of acute phase proteins with focus on alpha-1 antitrypsin in acute and chronic inflammatory conditions. *J. Proteome Res.* **13**, 3131–3143
 105. McCarthy, C., Saldova, R., O'Brien, M. E., Bergin, D. A., Carroll, T. P., Keenan, J., Meleady, P., Henry, M., Clynes, M., Rudd, P. M., Reeves, E. P., and McElvaney, N. G. (2014) Increased outer arm and core fucose residues on the N-glycans of mutated alpha-1 antitrypsin protein from alpha-1 antitrypsin deficient individuals. *J. Proteome Res.* **13**, 596–605
 106. Rashid, Q., Kapil, C., Singh, P., Kumari, V., and Jaisraipuri, M. A. (2015) Understanding the specificity of serpin-protease complexes through interface analysis. *J. Biomol. Struct. Dyn.* **33**, 1352–1362
 107. Elliott, P. R., Lomas, D. A., Carrell, R. W., and Abrahams, J. P. (1996) Inhibitory conformation of the reactive loop of alpha 1-antitrypsin. *Nat. Struct. Biol.* **3**, 676–681
 108. Dementiev, A., Dobo, J., and Gettins, P. G. (2006) Active site distortion is sufficient for proteinase inhibition by serpins: structure of the covalent complex of alpha1-proteinase inhibitor with porcine pancreatic elastase. *J. Biol. Chem.* **281**, 3452–3457
 109. Taggart, C., Cervantes-Laurean, D., Kim, G., McElvaney, N. G., Wehr, N., Moss, J., and Levine, R. L. (2000) Oxidation of either methionine 351 or methionine 358 in alpha 1-antitrypsin causes loss of anti-neutrophil elastase activity. *J. Biol. Chem.* **275**, 27258–27265
 110. Luisetti, M., and Travis, J. (1996) Bioengineering: α 1-proteinase inhibitor site-specific mutagenesis. *Chest* **110**, 278S–283S
 111. Carp, H., Janoff, A., Abrams, W., Weinbaum, G., Drew, R. T., Weissbach, H., and Brot, N. (1983) Human methionine sulfoxide-peptide reductase, an enzyme capable of reactivating oxidized alpha-1-proteinase inhibitor in vitro. *Am. Rev. Respir. Dis.* **127**, 301–305
 112. Laval, J., Ralhan, A., and Hartl, D. (2016) Neutrophils in cystic fibrosis. *Biol. Chem.* **397**, 485–496
 113. Sarkar, A., and Wintrobe, P. L. (2011) Effects of glycosylation on the stability and flexibility of a metastable protein: the human serpin alpha(1)-antitrypsin. *Int J Mass Spectrom* **302**, 69–75
 114. Wasiluk, K. R., Skubitz, K. M., and Gray, B. H. (1991) Comparison of granule proteins from human polymorphonuclear leukocytes which are bactericidal toward *Pseudomonas aeruginosa*. *Infect. Immun.* **59**, 4193–4200

5.3 The *N*-glycome of purified neutrophil granule proteins using subcellular fractionation

In **Publication V**, paucimannosylated HNE was observed to be present in all neutrophil granules but was particularly abundant in the azurophilic granules. In order to determine if paucimannosylation is an enriched feature specifically in the azurophilic granules of neutrophils, it is required to determine the *N*-glycome of all neutrophil granule compartments including the azurophilic-, specific-, gelatinase-granules, the secretory vesicles and the plasma membrane of neutrophils.

In order to isolate the respective neutrophil granules, subcellular fractionation was performed by gently disrupting the cell membrane of blood-derived neutrophils using nitrogen cavitation, followed by a Percoll density gradient separation as previously described (Clemmensen et al., 2014). In short, the principle of nitrogen cavitation is to pressurise neutrophils in a Parr nitrogen bomb in a disruption buffer that mimics the intracellular environment within the neutrophils (**Figure 1**). This pressurisation allows nitrogen to dissolve in the lipid membrane of the cells to aid in the disruption of the cell membrane that occurs by shear stress when the cells are forced through the valve located at the outlet nozzle of the bomb. This permits the granules and other organelles (also known as the cavitate) to be collected. As this is a gentle method that breaks the surface cell membrane, compared to other methods such as the use of Teflon or mortar and pestle homogenisation that are known to break open intracellular organelles (Hunter and Commerford, 1961), the granule membranes are left intact using nitrogen cavitation.

Percoll density gradient separation relies on differential densities of the organelles to ensure a successful separation of the neutrophil granules. Percoll was chosen as the separation medium as it is non-viscous and its osmolarity can be easily determined by the medium in which the Percoll is diluted in. These properties of Percoll allow the subcellular granules to reach their respective isopycnic densities during high speed centrifugation (Kjeldsen et al., 1999). Simultaneously, a self-generated density gradient that decreases towards the top of the separation tube is established. As azurophilic granules display the highest density, they will sediment at the bottom of the tube. Specific- and gelatinase-granules and secretory vesicles are comparably much lighter in density and are localised towards the top after centrifugation. As a result, this will form a three layer gradient. In order to separate the plasma membrane from the intracellular granules, a fourth layer utilises the flotation gradient to discriminate between them. A flotation gradient occurs since the density of the plasma membrane is much

lesser than the Percoll solution in which they are layered. Therefore, this four layer Percoll gradient allows the physical separation of the neutrophil granules. At the same time, this gradient also separates the granules from the plasma membrane.

After separation and collection of the granule fractions, sandwich enzyme-linked immunosorbent assays (ELISA) were used to determine the purity of the isolated granule proteins. *N*-glycans were then released from pooled fractions containing these proteins by enzymatic treatment using *N*-glycosidase F and the *N*-glycome analysed using PGC-LC-MS/MS.

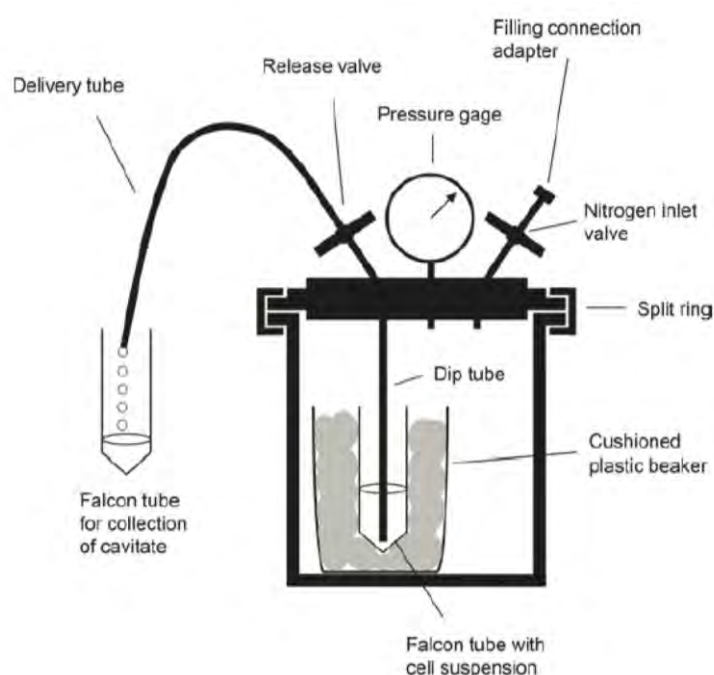


Figure 1. Schematic illustration of the Parr nitrogen bomb during nitrogen cavitation of human neutrophils in suspension. The cells are placed inside the Parr bomb, pressurised with nitrogen and after 5 to 10 min, the cavitate containing the individual intracellular granules are obtained through the gentle disruption of the cell membrane and is collected in a falcon tube for further granule purification. Image reproduced from *Methods in Molecular Biology, Subcellular Fractionation of Human Neutrophils and Analysis of Subcellular Markers*, 1124, 2014, 53-76, Clemmensen et al., with permission from Springer. (Clemmensen et al., 2014).

5.4 Materials and Methods

5.4.1 Isolation of blood-derived human neutrophils for subcellular fractionation

Human resting neutrophils were isolated from the peripheral blood of healthy donors (n= 3) after informed consent were obtained with ethics approval (Reference no. 5201500409,

HREC/08/RPAH/431 and X14-0074). Neutrophils were isolated from 200 ml of freshly drawn blood collected in acid citrate dextrose (ACD) anti-coagulant in a 4:1 (v:v) ratio. Collected blood was mixed 1:1 with 2% (v/v) dextran in sterile 0.9% (v/v) saline (GE Healthcare) by inversion and left to sit upright on the bench for 30 min at room temperature to allow the sedimentation of erythrocytes. The leukocyte-rich, erythrocyte-poor upper layer was aspirated and placed in 50 ml Falcon tubes. Cells were pelleted using centrifugation at 200g for 10 min at 4°C and the supernatant was discarded. Cell pellets were resuspended with 30 ml sterile 0.9% (v/v) saline and was layered over 16 ml of Lymphoprep medium at a density of 1.077 g/ml (GE Healthcare). After centrifugation at 400g for 30 min at 4°C, the buffy coat consisting of lymphocytes, monocytes and platelets was removed and the neutrophil-eosinophil rich pellet was resuspended in 10 ml cold sterile MilliQ water with vortexing to remove residual red cells. Isotonicity was restored with equal volume of sterile 1.8% (v/v) saline. Cells were then pelleted at 200g for 6 min at 4°C. Purified neutrophils were resuspended in 0.9% (v/v) saline and manually counted using a hemocytometer (Thermo Scientific). The purity of the isolation was confirmed to be >98% by examining a Cytospin prepared slide (Thermo Scientific) using a bright-field light microscopy.

5.4.2 Disruption of neutrophils by nitrogen cavitation

A final concentration of 5 mM diisopropyl fluorophosphate serine protease inhibitor was added to 3×10^8 purified neutrophils and left on ice for 5 min. Cells were centrifuged at 200g for 6 min and the supernatant was removed. 7 ml of 1x disruption buffer (100 mM KCl, 3 mM NaCl, 3.5 mM MgCl₂, 1.5 mM ethylene glycol-bis(β-aminoethyl ether)-N,N,N',N'-tetraacetic acid (EGTA), 10 mM piperazine-N,N'-bis[2-ethanesulfonic acid], pH 6.8) supplemented with 0.1 μM ATP(Na)₂ and 0.5 μM phenylmethylsulfonyl fluoride (PMSF) (all final concentrations) was used to resuspend the cells by vortexing in a 50 ml Falcon tube. The cell suspension was placed in a precooled nitrogen gas-pressurised Parr cavitation bomb (Parr instruments, USA) and left in the cold for 5 min. With a 50 ml collection Falcon tube, the cavitate was collected in the presence of 100 mM EGTA in a fresh 50 ml tube in a dropwise manner and centrifuged at 400 g for 15 min. The resulting post-nuclear supernatant containing the intracellular organelles and granule proteins and membrane was collected for subsequent density gradient centrifugation.

5.4.3 Four-layer Percoll density gradient separation

Percoll was used for the density gradient separation of neutrophil granules. Stock Percoll solution at a density of 1.130 g/ml (GE Healthcare, Denmark) was mixed with 10x disruption

buffer to prepare various densities of Percoll solutions. The placement orders of the final density of the Percoll solutions, from the bottom of a polycarbonate centrifuge tube are shown in **Table 1**. Percoll solutions were dispensed carefully into the tube using a 14G x 3^{1/4} inch needle.

| Placement order (from bottom to top of polycarbonate tube) | Percoll solution final density (g/ml)* | Volume of solution (ml) | Notes |
|--|---|-------------------------------|--|
| 1 st | 1.03 | 9 | |
| 2 nd | 1.06 | 9 | 1:1 (v:v) ratio mix of post-nuclear supernatant and Percoll solution (initial density of 1.11 g/ml) |
| 3 rd | 1.09 | 9 | A sharp demarcation should be observed between these two layers |
| 4 th | 1.12 | 9 | |

Table 1: Placement layers of Percoll solutions for density gradient separation of neutrophil granules.

*Prepared from a Percoll stock density of 1.130 g/ml with 10x disruption buffer.

The gradient tube was centrifuged at 37,000g for 30 min in a fixed angle rotor centrifuge (Sorvall RC-5B, Thermo Scientific), resulting in four band layers in the Percoll gradient (**Figure 2A**). A peristaltic pump (Amersham) and an automated fraction collector (FRAC-200, Amersham) were used to collect 1 ml fractions from the four band layers in the Percoll gradient tube into transparent plastic tubes. A total of 36 fractions were collected.

5.4.4 Measurement of subcellular protein markers using immunoassays

The specific fractions analysed, and the antibodies and their dilutions used to detect specific granule protein markers using sandwich ELISA are shown in **Table 2**. Fractions containing granule proteins and standards were pre-diluted with dilution buffer consisting of 0.5 M NaCl, 3 mM KCl, 8 mM Na₂HPO₄/KH₂PO₄, 1% (w/v) BSA, 1% (v/v) Triton X-100, pH 7.2 before ELISA was carried out. Capture antibodies diluted in carbonate buffer (50 mM Na₂CO₃/NaHCO₃, pH 9.6) were first coated on high binding ELISA plates (Thermo Scientific, Denmark) at 100 µl per well overnight at room temperature. The next day, the plates were washed in wash buffers consisting of 0.5 M NaCl, 3 mM KCl, 8 mM Na₂HPO₄/KH₂PO₄, 1% (v/v) Triton X-100, pH 7.2, then quenched with 200 µl of dilution buffer and incubated for 1 h. The ELISA plates were washed again with wash buffer and the samples and standards were applied at 100 µl per well in duplicates. Plates were incubated for 1 h and washed again in wash buffer before applying detection antibodies at 100 µl per well. Incubation was allowed

for 1 h at room temperature. Plates were then washed again and HRP-conjugated reagents were added at 100 μ l per well and incubated for 1 h. An ortho-phenylenediamine colour solution buffer was poured over the plates for equilibration and left to incubate for 5 min before the ELISA plates were emptied by inversion. Subsequently, 30% (v/v) hydrogen peroxide (Merck Millipore) was added to the colour solution buffer before use and 100 μ l of this solution was added to the individual wells on the ELISA plate and incubated in the dark for 10-30 min for colour development. Reactions were terminated by the addition of 100 μ l 2N sulphuric acid to each well and the plate was read at 492 nm using a plate reader. Granule fractions displaying similar granule protein marker features were pooled together.

5.4.5 Percoll removal using ultra-centrifugation

Pooled granule fractions were ultracentrifuged at 100,000g for 90 min, resulting in the formation of a hard pellet. Precipitated proteins will form a disc or a lump above the Percoll, which was collected using a glass Pasteur pipette and transferred into cryo-vials (Thermo Scientific). The respective granule protein extract fractions, now essentially free of any contaminating Percoll, were dried using a vacuum centrifuge for long term storage at -80°C before these samples were used for structural characterisation

Table 2. Granule fractions, antibodies and dilutions used for ELISA marker assays to validate the fractionated purified granule proteins of neutrophils. *In house antibodies were available from Professor Niels Borregaard, University of Copenhagen, Denmark.

| Granule marker protein used for ELISA (neutrophil compartment) | Dilution ratios of fraction (v:v) | Capture antibodies and their dilution ratio (Supplier, product, dilution, vv) | Detection antibodies and their dilution ratio (Supplier, product, dilution, v:v) | HRP-conjugated reagent and dilution ratio (Supplier, product, dilution, v:v) | Standards (dilutions performed) |
|--|---|---|---|--|---|
| Myeloperoxidase (MPO) (Azurophilic granule) | 1:2,000 and 1:5,000 | Rabbit anti-MPO (Dako, A03998, 1: 20,000) | Biotinylated rabbit anti-MPO (Dako, A03998, 1:250) | HRP-Avidin (eBioscience 18-4100, 1:3,000) | MPO purified from neutrophils (0-100 ng/ml) |
| Neutrophil gelatinase associated lipocalin (NGAL) (Specific granules) | 1:2,000 and 1:5,000 | Rabbit anti-NGAL (In house*, 1:1,000) | Biotinylated rabbit anti-NGAL (In house*, 1:10,000) | HRP-Avidin (eBioscience 18-4100, 1:3,000) | NGAL purified from neutrophils (0-2 ng/ml) |
| Gelatinase (Gelatinase granules) | 1:2,000 and 1:5,000 | Rabbit anti-gelatinase (In house*, 1:2,000) | Biotinylated rabbit anti-gelatinase (In house*, 1:1,000) | HRP-Avidin (eBioscience 18-4100, 1:3,000) | Gelatinase purified from neutrophils (0-5 ng/ml) |
| Human serum albumin (HSA) (Secretory vesicles) | 1:15 | Rabbit anti-albumin (Dako, A0001, 1:5,000) | Biotinylated rabbit anti-HSA (Dako, A03998, 1:7,000) | HRP-Avidin (eBioscience 18-4100, 1:3,000) | HSA purified from neutrophils (0-250 ng/ml) |
| HLA class I (Plasma membrane) | 1:15 | Rabbit anti- β 2-microglobulin (Dako, A0072, 1:1,000) | Mouse anti-HLA-ABC (Dako, M0736, 1:750) | HRP-rabbit-anti-mouse Ig (Dako, P0260, 1:1,500) | Dilution buffer for subtraction of background |

5.4.6 Deglycosylation and N-glycome analysis of azurophilic granule proteins

The isolated azurophilic granule proteins (~20 µg) were resuspended in 8 M urea and handled and analysed exactly as described in **Chapter 3**, Materials and Methods, Section 3.3.3.

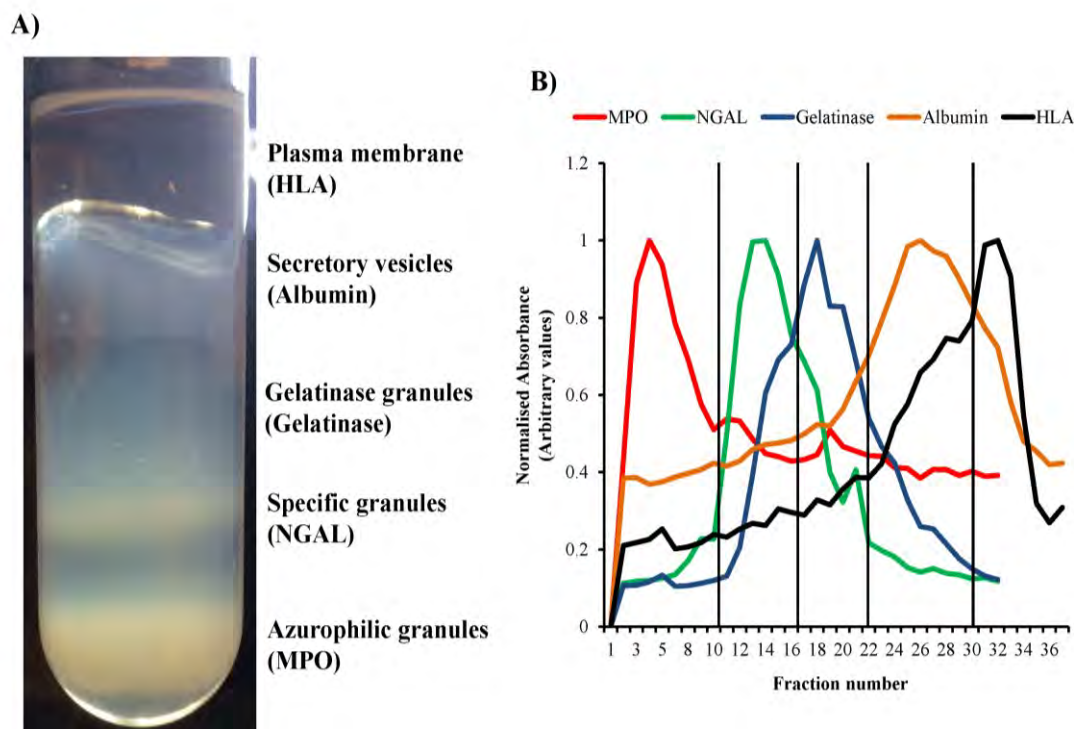


Figure 2. A four-layer Percoll density gradient for the subcellular fractionation of the individual granules in human neutrophils **(A)** A representative photograph of the four-layer Percoll density gradient after centrifugation. **(B)** Distribution profile of marker proteins for the granule compartments and the plasma membrane of human neutrophils as determined by ELISA of the individual fractions collected and numbered from the bottom of the tube shown in panel A. Subcellular marker proteins: MPO for azurophilic granules (red), neutrophil gelatinase associated lipocalin (NGAL) for specific granules (green), gelatinase for gelatinase granules (blue), albumin for secretory vesicles (orange) and human leucocyte antigen (HLA) for plasma membrane (black). The solid vertical lines denote the fractions that were pooled for the individual compartments.

5.5 Results

5.5.1 Determining the purity of the isolated neutrophil granule proteins

In order to evaluate the purity of the fractionated granule proteins obtained from resting neutrophils, ELISA was used to profile granule marker proteins throughout the subcellular compartments separated in the four layer Percoll gradient after centrifugation, **Figure 2A-B**.

For example, the distribution of MPO was observed to be present in fraction 1 to 32, with its peak abundance at around fraction 5. It was also observed that NGAL was predominantly found in fraction 10 to 16 (peak abundance in fraction 14). Gelatinase was highly present in fraction 17 to 22 and albumin and HLA were found to be abundant in fraction 23 to 30 and 31 to 36, respectively. These indicated fractions containing their specific marker proteins were pooled to form the isolated granule protein subsets.

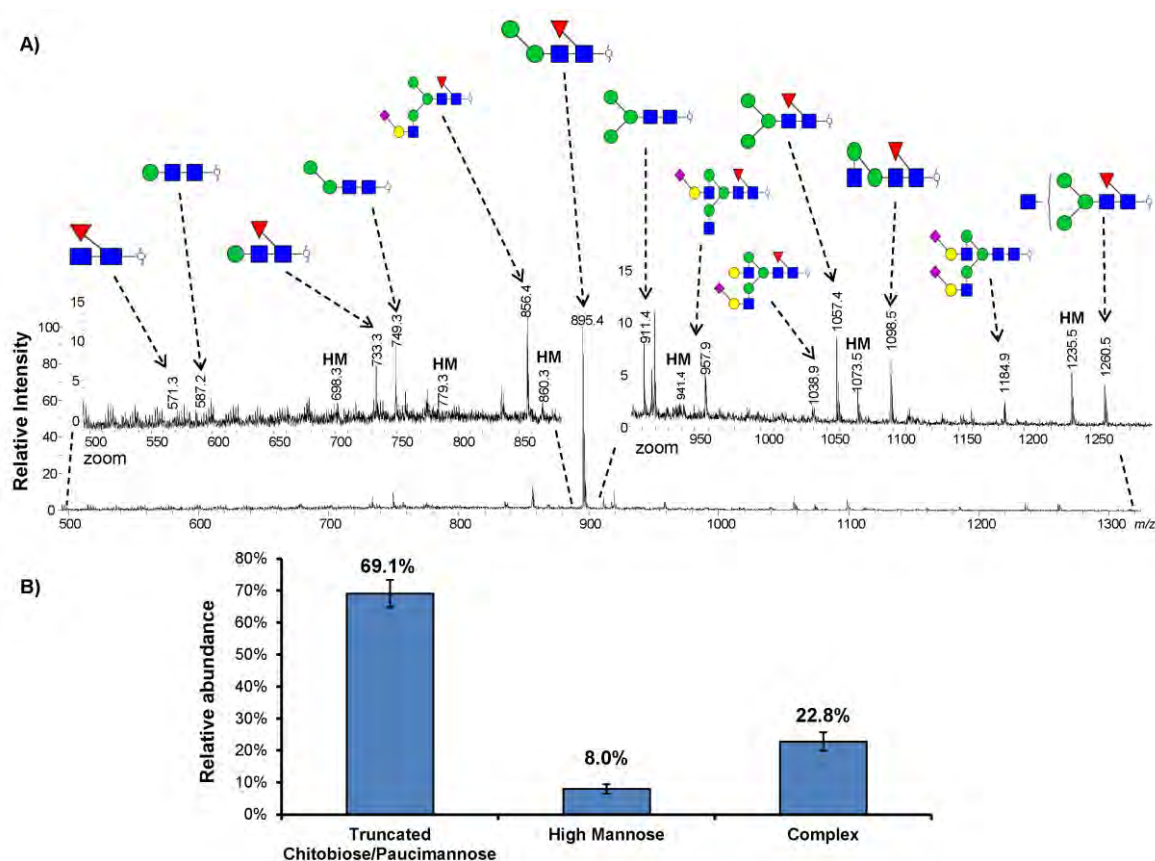


Figure 3. (A) Representative summed mass spectrum of the PGC-LC-MS/MS analysis providing an overview of the N -glycans observed from proteins isolated from the azurophilic granule. The major paucimannosidic and complex structures are annotated in the spectrum (see inserts for zoomed regions of the m/z region). HM denotes high mannose structures (including M4, which does not fall into our classification of paucimannosidic glycans). Structures shown are deduced from interpretation of data of precursor ion masses, LC isomer separation, and MS/MS diagnostic and fragment ions. (B) Relative percentage abundance of the three observed classes of N -glycans derived from the proteins residing in the azurophilic granule compartment of healthy resting neutrophils ($n = 3$ biological replicates, mean \pm S.E.M). The structures and the relative abundances of the observed N -glycans are summarised in Table 3.

Table 3. Structural assignments and relative abundances of the observed *N*-glycans released from isolated proteins residing in the azurophilic granule of resting human neutrophils.

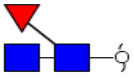

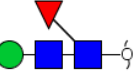
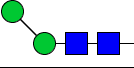
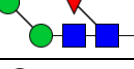
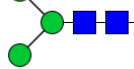
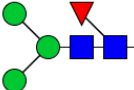
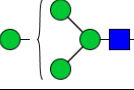
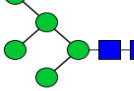
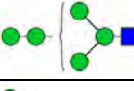
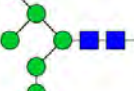
| Glycan type, short-hand nomenclature and proposed structures of observed <i>N</i> -glycans | | Observed mass (<i>m/z</i>) | | Relative abundance (%) |
|--|--|------------------------------|----------------------|---|
| | | [M-H] ¹⁻ | [M-2H] ²⁻ | (n = 3 biological replicates, mean ± S.E.M) |
| Truncated chitobiose core / Paucimannose | M0F  | 571.3 | | 0.3 ± 0.2 |
| | M1  | 587.3 | | 1.5 ± 1.4 |
| | M1F  | 733.3 | | 4.2 ± 0.2 |
| | M2  | 749.3 | | 4.5 ± 0.2 |
| | M2F  | 895.5 | | 50.9 ± 5.5 |
| | M3  | 911.4 | | 3.3 ± 0.4 |
| | M3F  | 1057.3 | | 4.5 ± 0.2 |
| High Mannose | M4  | 1073.4 | | 1.4 ± 0.1 |
| | M5  | 1235.6 | | 3.0 ± 0.4 |
| | M5  | | | 0.7 ± 0.1 |
| | M6  | | 698.3 | 1.2 ± 0.5 |

Table 3. (Continued) Structural assignments and relative abundances of the observed *N*-glycans released from isolated proteins residing in the azurophilic granule of resting human neutrophils.

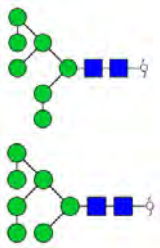
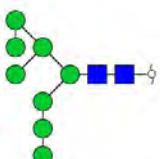
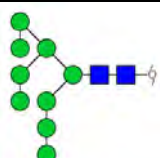
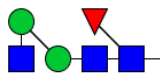
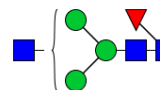
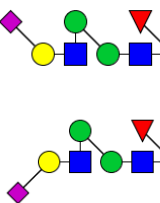
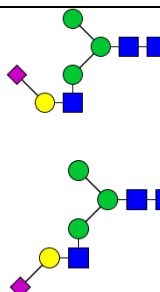
| Glycan type, short-hand nomenclature and proposed structures of observed <i>N</i> -glycans | | Observed mass (<i>m/z</i>) | | Relative abundance (%) |
|--|---|------------------------------|----------------------|---|
| | | [M-H] ¹⁻ | [M-2H] ²⁻ | (n = 3 biological replicates, mean ± S.E.M) |
| High Mannose | M7  | | 779.4 | 0.5 ± 0.2 0.5 ± 0.1 |
| | M8  | | 860.4 | 0.2 ± 0.1 |
| | M9  | | 941.2 | 0.6 ± 0.1 |
| Complex | M2F + (GlcNAc)  | 1098.5 | | 1.6 ± 1.1 |
| | M3F + (GlcNAc)  | 1260.5 | | 1.7 ± 0.3 |
| | Bimannosyl-chitobiose core monoantennary core fucosylated monosialylated  | | 775.3 | 1.0 ± 0.2 0.1 ± 0.1 |
| | A1G1S1  | | 783.3 | 0.6 ± 0.1 0.1 ± 0.0 |

Table 3 (Continued). Structural assignments and relative abundances of the observed *N*-glycans released from isolated proteins residing in the azurophilic granule of resting human neutrophils.

| Glycan type, short-hand nomenclature and proposed structures of observed <i>N</i> -glycans | | Observed mass (<i>m/z</i>) | | Relative abundance (%) (n = 3 biological replicates, Mean ± S.E.M) |
|--|-------------|------------------------------|----------------------|--|
| | | [M-H] ¹⁻ | [M-2H] ²⁻ | |
| Complex | FA1G1S1 | | | 12.1 ± 0.8 |
| | | | 856.3 | 1.1 ± 0.2 |
| | | | | 0.6 ± 0.1 |
| | FA2G1S1 | | | 2.6 ± 0.5 |
| | | | 957.9 | 0.2 ± 0.1 |
| | FA2G2S1 | | 1038.9 | 0.7 ± 0.2 |
| | FA2G2S2 | | | 0.6 ± 0.1 |
| | | | 1184.5 | 0.6 ± 0.2 |

5.5.2 Characterisation of *N*-glycans of isolated proteins in the azurophilic granules

The *N*-glycome of the azurophilic granule residing proteins of resting neutrophils from three healthy individuals were characterised using capillary PGC-LC-MS/MS (**Figure 3A**). The *N*-glycans were released as described in the materials and methods in section 5.4.6. The glycans were structurally assigned based on their molecular mass and manual interpretation of their resulting MS/MS fragment spectra and the presence or absence of diagnostic fragmentation ions and their retention time (Everest-Dass et al., 2013a; Harvey, 2005c). In addition, the established knowledge of the *N*-glycan biosynthesis pathway in mammals was taken into account as summarised in **Chapter 3**. A total of 31 *N*-glycans covering 21 monosaccharide compositions were identified to be carried by the azurophilic granule-resident proteins including the dominating class of truncated chitobiose/paucimannosidic structures (which were grouped together due to their common truncated nature) at ~69%, the less abundant complex type structures (~23%) and the high mannose type structures (~8%) (**Figure 3B**, **Table 3**).

5.5.3 Structural determination of paucimannosidic *N*-glycans of azurophilic granule origin

As paucimannosidic *N*-glycans were carried in abundance by the azurophilic granule proteins (~69%), their exact structures were investigated in the context of their monosaccharide composition, topology and glycosidic linkages. Particularly the abundant M2 (m/z 749.3, $[M-H]^{-1}$) and M2F structures (m/z 895.4, $[M-H]^{-1}$) were investigated. In addition to ensuring that the correct molecular masses were observed, the structural assessment was initially performed by comparing the PGC-LC retention time of the M2 and M2F *N*-glycans to the already established retention times of identical structures carried by the azurophilic granule resident nCG (**Publication IV**) and HNE (**Publication V**). The retention time of azurophilic granule M2 aligned well with the retention time of M2 carried by nCG and HNE, **Figure 4A**. The PGC-LC retention time of the related core fucosylated structure M2F, was also observed to be similar across the three samples, **Figure 4B**. We have previously shown that M2 carried by nCG and HNE terminates in an α 1,6-linked mannosyl residue at the non-reducing end as shown using exoglycosidase digestion with α 1,2/3 > α 1,6 mannosidase and by spectral and retention time matching to known M2 standards in **Publication IV**. The associated CID-MS/MS spectra were also compared between the pool of azurophilic granule proteins and the two purified azurophilic granule-resident glycoproteins, which showed a high degree of match between the fragment profiles (see **Supplementary Material, Figure S1 in the enclosed DVD**). In addition, the α 1,3-linked mannose capped form of M2 generated artificially from chicken ovalbumin using glycosidases, showed very different elution on PGC-LC (see **Supplementary Material, Figure S2 in the enclosed DVD**). Taken together, this showed that the α 1,6 mannosyl-capped forms are the only isomers of the highly abundant M2 and M2F structures in neutrophil azurophilic granules. These observations further validate the existence of these paucimannosylated species on nCG and HNE from healthy neutrophils.

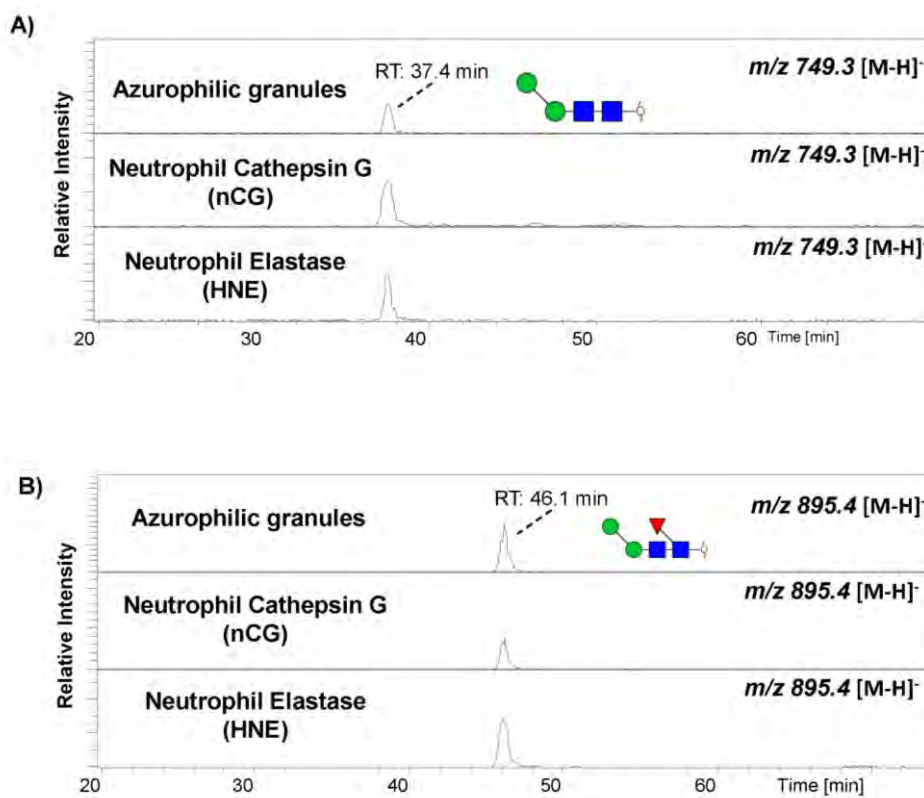


Figure 4. Selected EICs from the PGC-LC-MS/MS-based *N*-glycome analyses in negative polarity mode showing the retention time (RT) of paucimannosidic (A) M2 (m/z 749.3) and (B) M2F (m/z 895.4) *N*-glycans released from the isolated pool of azurophilic granule proteins (top EIC), purified nCG (middle EIC) and HNE (bottom EIC).

5.5.4 Structural determination of the complex *N*-sialo-glycans of azurophilic granule origin

Approximately 23% of the azurophilic granule *N*-glycome was shown to consist of complex type *N*-glycans. An unusual complex monoantennary trimannosyl-core fucosylated sialoglycan, hereafter called FA1G1S1, was observed to be particularly abundant (~13%) in the azurophilic granules. FA1G1S1 was previously observed to be carried by human nCG and HNE as two isomeric species. These two isomers comprising of the α 2,6- and α 2,3-linked sialylated form as confirmed by the use of α 2,3/6/8-sialyl-linkage unspecific and α 2,3-sialyl linkage specific sialidases (**Publication IV** and **Publication V**). By comparing the PGC-LC retention time of the observed FA1G1S1 structures to the similar structures released from nCG and HNE and by looking at diagnostic ions (i.e. D ions) in the MS/MS spectra, it was confirmed that FA1G1S1 was present as two main isomers in the azurophilic granules (i.e. α 2,6- and α 2,3-linked sialylation of the 3' Man arm and that a third isomer of very low abundance was also present, **Figure 5A**. The α 2,6-sialylated isomer was the most abundant

isomer for all three samples. Based on the retention time (~62 min) and the MS/MS fragmentation profile, this third isomer in the azurophilic granule appeared to be the α 2,3 sialylated on the 6'-mannose arm. This was confirmed by the presence of the diagnostic D-ion (m/z 979.3) that is particularly useful for locating the antenna of *N*-glycans carrying sialylated lactosamine, **Figure 5B** (Everest-Dass et al., 2013a; Harvey, 2005b).

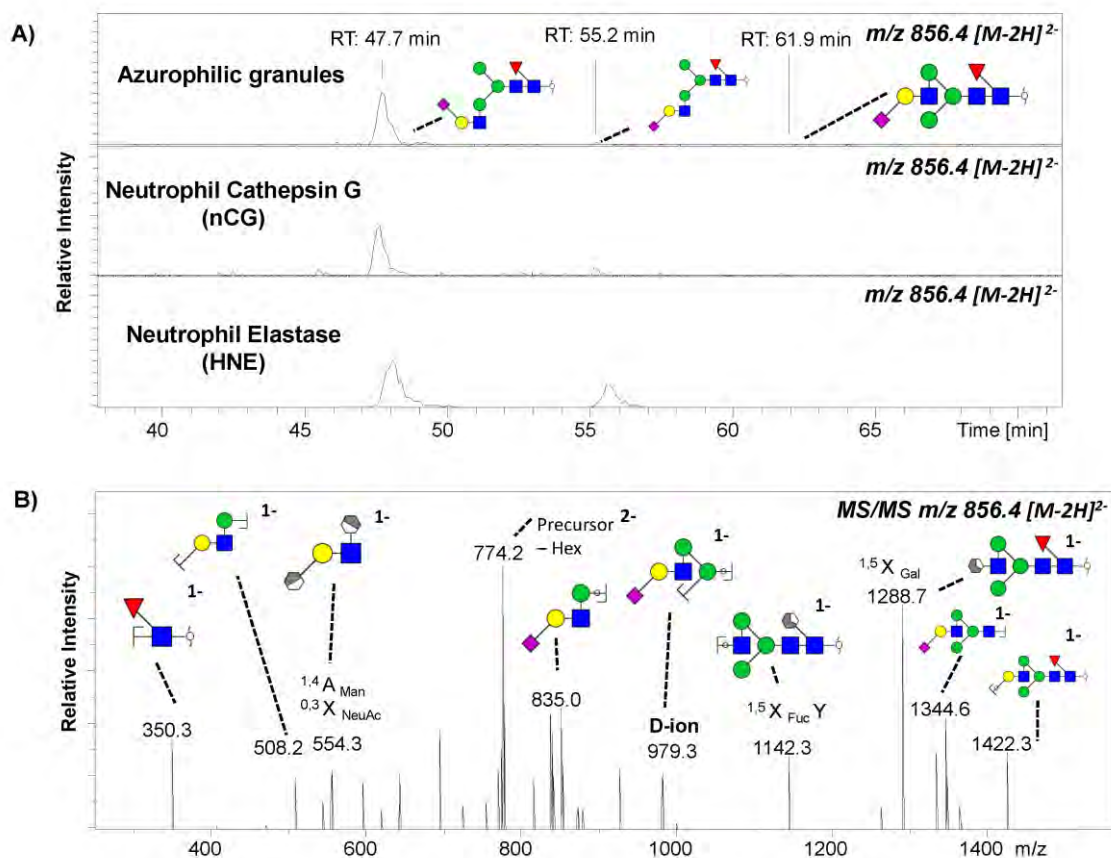


Figure 5. (A) Selected EICs from the PGC-LC-ESI-CID-MS/MS-based *N*-glycome analyses showing the efficient separation of the isomers of the unusual monoantennary trimannosyl-core fucosylation sialo-glycan FA1G1S1 sialo-isomers (m/z 856.4) released from azurophilic granule proteins (top EIC), nCG (middle EIC) and HNE (bottom EIC). Retention times (RT) are indicated. (B) CID-MS/MS fragmentation spectra of the low abundant form FA1G1S1 eluting at 61.9 min. The other more abundant forms of FA1G1S1 have been presented in Chapter 4/Publication IV. The presence of the D-ion indicates that the extended sialylation is located on the 6' mannose arm of FA1G1S1.

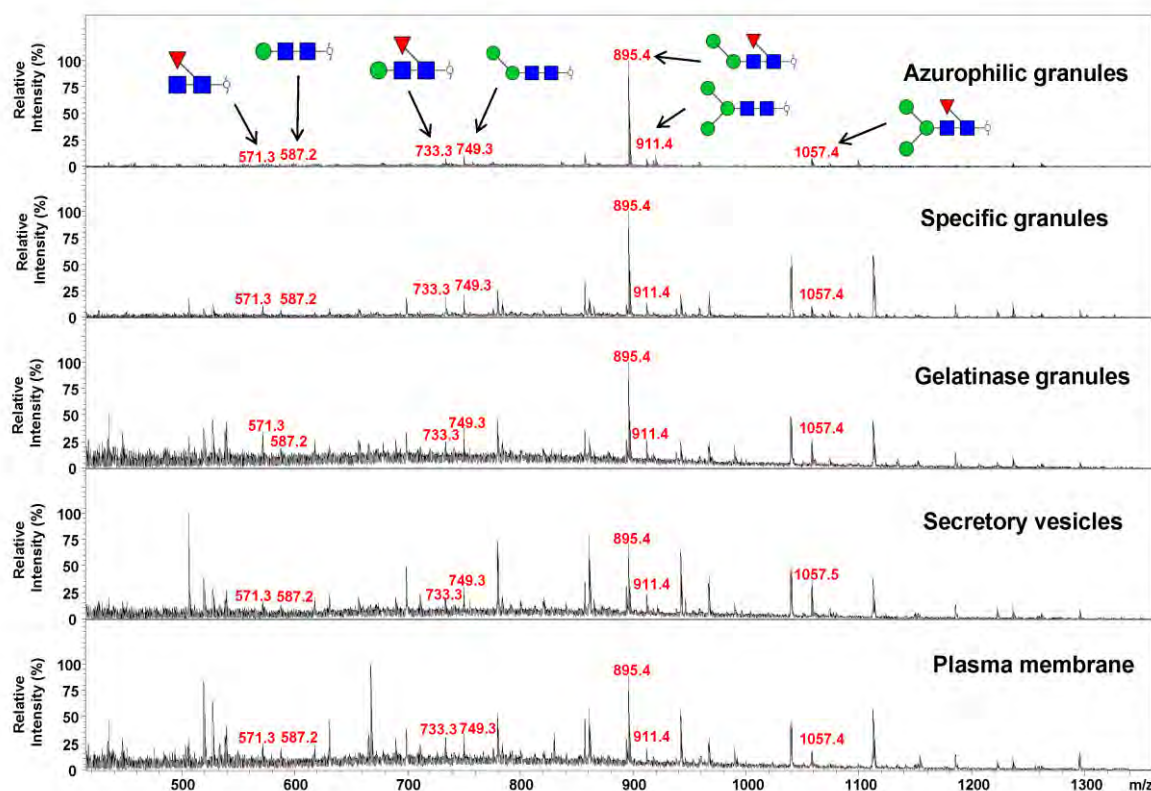


Figure 6. Representative summed mass spectra of the PGC-LC-MS/MS analyses providing an overview of the *N*-glycome profiles observed from the proteins isolated from the neutrophil granules ie. azurophilic-, specific-, and gelatinase granules, the secretory vesicles and the plasma membrane. Masses highlighted in red denote the paucimannosidic structures identified based on their molecular mass, LC isomer retention and MS/MS fragmentation profiles.

5.5.5 Protein paucimannosylation is not confined to the azurophilic granules

We have previously suggested that protein paucimannosylation is enriched in the azurophilic granule (**Publication II**). In order to confirm that paucimannosylation is an enriched glyco-signature in the azurophilic granules of neutrophils, the *N*-glycome of the azurophilic, specific, and gelatinase granules, as well as the secretory vesicles and the plasma membrane were compared. The comparisons showed that paucimannosidic *N*-glycans, in particular M2F, were also present in other neutrophil granules, **Figure 6**. However, a quantitative evaluation demonstrated that the paucimannosidic glycans were significantly enriched in the azurophilic granule (~70%) relative to the other granule compartments (~20-35%), **Figure 7**. The relative abundance of high mannose and complex type structures also appeared to be very different throughout the granule compartments, with the lowest abundance in the azurophilic granules.

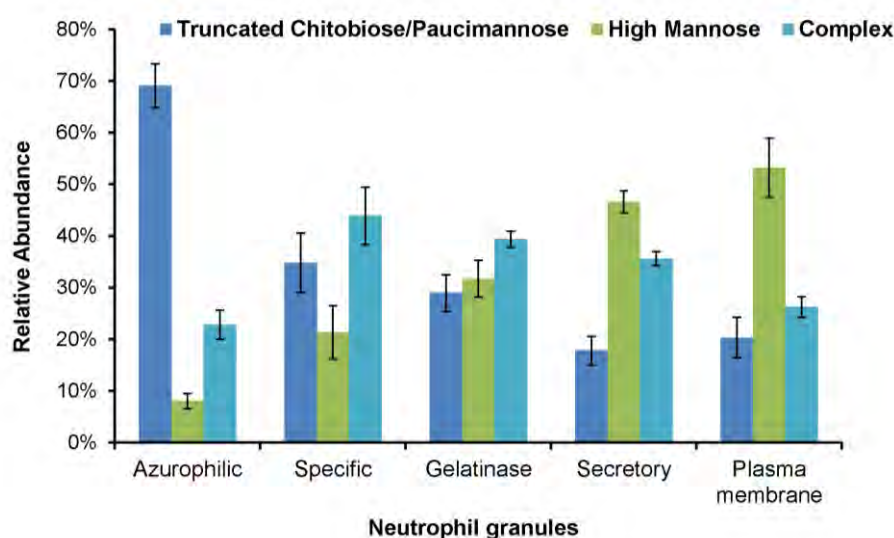


Figure 7. Comparison of the distribution of the three observed classes of *N*-glycans in the isolated granule compartments of healthy resting neutrophils ($n = 3$ biological replicates, mean \pm S.E.M). Protein paucimannosylation was found to be highly enriched in the azurophilic granules.

5.6 Discussion

Previous studies documented that the proteomes of the individual granule compartments of human neutrophils are highly distinct (Lominadze et al., 2005; Rorvig et al., 2013), suggesting that these organelles are underpinned by different biochemistry and protein function. In this chapter, I have presented the first report describing the *N*-glycome of isolated azurophilic granules from resting human neutrophils, a compartment used by neutrophils to mediate immunological responses. I have also characterised the *N*-glycosylation of the other granules found in resting healthy neutrophils. These observations agree well with earlier studies that have reported the *N*-glycosylation of various azurophilic granule proteins including azurocidin and PR3 (Olczak and Watorek, 2002; Zoega et al., 2012) and my own discoveries relating to the *N*-glycosylation of nCG and HNE (described in **Chapter 4**, **Publication IV** and **Publication V**). The observations presented here are also largely in agreement to an earlier report on the *N*-glycosylation of human neutrophil lysates (Babu et al., 2009).

PGC-LC-MS/MS-based glycomics of isolated neutrophil granules demonstrated an abundance of paucimannosidic *N*-glycans, in particular the α 1,6-mannose-terminating M2F, in the azurophilic granule. M2F was also similarly observed in high abundance in several key azurophilic granule proteins such as nCG (**Publication IV**), HNE (**Publication V**) and azurocidin (Olczak and Watorek, 2002). As subcellular fractionation using nitrogen cavitation

does not disrupt the granule membrane (Clemmensen et al., 2014), it remains one of the only efficient means to generate insight into the biochemistry underpinning the individual neutrophil granules compared to the use of the crude neutrophil whole cell lysates generated from cellular homogenisation.

Using existing proteome datasets as shown in **Publication V**, the M2 and M2F carrying HNE was surprisingly uniformly *N*-glycosylated across the azurophilic-, specific-, gelatinase-granules, in the secretory vesicles and in the plasma membrane isolated from healthy neutrophils. Although this proteomics data only allowed a subcellular- and site-specific evaluation of the monosaccharide composition of the two sites of HNE, these observations suggested that M2 and M2F are abundantly and consistently carried by HNE, regardless of its granule origin. By inference, this uniformity also suggests that M2(F) displays α 1,6-mannosyl terminating epitopes that may be generated by the action of a human α -mannosidase in the preferential hydrolysis of the α 1,3-mannose residues of M3(F) precursors in the biosynthetic pathway or in the respective granules compartments where the glycoproteins are eventually stored (Winchester, 2005).

The presence of M2F with terminal GlcNAc capping in the azurophilic granules also suggests that the *N*-glycans are processed by these mannosidases within the granule compartment, possibly after or in the process of trimming of their β -linked terminal GlcNAc moieties by the action of hexosaminidases such as Hex A and/or Hex B. The gene expression of Hex A, Hex B and α -mannosidases are known to be highly active during the promyelocytic stage of neutrophils in the bone marrow as discussed in **Chapter 3**.

A truncated chitobiose core M0F was also observed in the *N*-glycome of proteins residing in the azurophilic granules. The generation of M0F may be due to the activity of human β -mannosidases where a high gene expression of β -mannosidases was also observed during the bone marrow development of maturing neutrophils (Theilgaard-Monch et al., 2005).

In comparison to the azurophilic granules, paucimannosylation appears to be also present in other neutrophil granules based on the summed MS spectra as shown in **Figure 6** and their relative abundance shown in **Figure 7**. This observation aligns well with the “targeting by timing” hypothesis proposed by Borregaard and co-workers that those neutrophil granule proteins are packaged in the storage granules at the time that they are synthesised and not through the use of any sorting recognition motifs (Borregaard and Cowland, 1997; Le Cabec et al., 1997). This hypothesis also explains the heterogeneity of the proteome in the individual

granules shown in previous studies (Lominadze et al., 2005; Rorvig et al., 2013). However, this hypothesis does not explain how neutrophil glycoproteins are *N*-glycosylated after protein translation.

Furthermore, the finding of ultra-truncated *N*-glycans carried by azurophilic granule-specific serine proteases such as nCG in **Chapter 4** and PR3 (Zoega et al., 2012), suggest that these structures will not be detected solely with the analysis of released *N*-glycans as performed in this chapter and, thus, would be overlooked given their resistance towards *N*-glycosidase F and in addition to their lack of retention on PGC-LC-MS. It may also be difficult to discriminate these structures from interfering salts and contaminant ions during PGC-LC-MS due to their low molecular masses. Although nCG and PR3 are known to be highly abundant in the azurophilic granules (Borregaard and Cowland, 1997), proteome analysis of other neutrophil granules (i.e. specific- and gelatinase-granules and secretory vesicles) suggests that nCG and PR3 are also present albeit at a lower abundance in these compartments (Rorvig et al., 2013). Therefore, it is likely that these ultra-truncated structures could also be present and may even prove to be prevalent modifications in other neutrophil granules from the azurophilic granules. This further exemplifies the need to apply multiple complementary LC-MS methodologies to achieve comprehensive and accurate *N*-glycoprofiling of these unusual structures decorating the neutrophil granule proteins.

The involvement of the mannose-6-phosphate receptor (M6P) trafficking pathway for the targeting of MPO to the various granules in HL-60 cells (Nauseef et al., 1992) and recently in some transfected breast cancer cell lines (Laura et al., 2016), have been studied. The authors concluded that the M6P pathway is unlikely to be involved in the granule trafficking of MPO. Paradoxically, the azurophilic granules have been shown previously to express M6P receptors (Cieutat et al., 1998). In addition, the corresponding decrease in the abundance of paucimannosidic structures from the azurophilic granules to the plasma membrane accurately reflects the decreasing gene transcription of paucimannosidic glycoproteins as has been documented previously (Theilgaard-Monch et al., 2005).

The enrichment of protein paucimannosylation in the azurophilic granules relative to the rest of the neutrophil granules, suggests that a majority of the paucimannosidic azurophilic proteins, after exiting from the ER, were directed to the azurophilic granules, deviating away from the main *N*-glycosylation biosynthesis pathway in the Golgi apparatus that is well established for the *N*-glycosylation of glycoproteins with resulting highly branched structures

(Aebi, 2013). This hypothesis was further supported by the low abundance of high mannose and complex structures carried by azurophilic granule-specific glycoproteins. Based on these observations, it is likely that an alternative sorting pathway exists that is independent from the M6P targeting pathway.

In addition, given that paucimannosidic structures were also present in other neutrophil granules apart from the azurophilic granules, it suggests that an alternative sorting pathway may co-exist with the main *N*-glycosylation machinery for the generation of highly branched structures. This was reflected by the higher abundance of glycoproteins carrying complex structures in the specific-, gelatinase- granules, secretory vesicles and the plasma membrane. Therefore, the question of how paucimannosylated proteins are trafficked to the respective neutrophil granules needs to be further investigated.

Interestingly, an unusual monoantennary sialo-glycan FA1G1S1 was observed in abundance in the azurophilic granules but its abundance decreases from the specific granules to the plasma membrane (~13% to 6%). These structures have been reported previously as free *N*-glycans in the cell cytoplasm and in other mammalian cells (Huang et al., 2015; Tadashi et al., 2002). The functional relevance of these *N*-glycans remains unknown but it is likely that these sialic acid terminating structures may play important roles in the activation of neutrophils during inflammatory conditions by binding to selectins; lectins that recognise sialic acid residues. More importantly, these structures could also act as a means of communication with other immune cells or other non-immune cell types when these granule proteins are degranulated into the extracellular environment or when they are expressed on the cell surface of activated neutrophils.

Finally, the observation of the highly enriched paucimannosylation in azurophilic granules of neutrophils serves as a validation for the initial observations of paucimannosidic proteins originating from the azurophilic granules of activated neutrophil in the inflamed and bacterial colonised sputum of CF patients (**Publication II**). The study of a larger patient cohort and from related inflamed pathologies is required to better understand the presence and importance of the *N*-glycosylation of these granules in human neutrophils.

5.7 Overview of main findings, conclusions and future directions

Main findings and conclusions

- HNE displayed predominantly paucimannosidic M2F *N*-glycans at the two exposed *N*-glycosylation sites (Asn124 and Asn173), whereas Asn88 carried some M2 but was predominately unoccupied. Asn185 (NVC glycosite) was not observed to be glycosylated. Knowledge of the site-specific glycosylation profile of HNE is important, not only to understand how *N*-glycosylation influences HNE protease activity, but also to aid in the design of specific inhibitors to augment their activities during inflammation and infections.
- Low glycosylation site solvent accessibility may explain the limited processing of the Asn88 *N*-glycan (lack of core fucosylation). This observation suggests that the protein structure and the associated glycosylation site solvent accessibility dictate the formation of the type of *N*-glycans and core fucosylation.
- The site-specific *N*-glycosylation, but not the protein level, of HNE was found to be surprisingly uniform across the various neutrophil granules. This finding has not been documented previously and this knowledge will contribute to our understanding on how neutrophil granule proteins are trafficked across the various granules upon biosynthesis.
- Activated neutrophils displayed increased levels of paucimannosidic HNE on their cell surface relative to its constitutive expression under resting conditions, but did not show a cell surface-specific glycosylation signature. This observation is important as the display of protein paucimannosylation on the cell surface could reveal insights into how neutrophils utilise this unique glyco-signature in mediating immunological responses.
- Paucimannosidic-rich HNE glycoforms displayed preferential binding, over complex sialoglycoforms, towards human MBL. This further validates previous observations that mannosylated glycoforms are important in mediating immunological processes during inflammation and infections.
- HNE displayed concentration-dependent complex formation and thereby protease inhibition with its main physiological inhibitor, human α 1-antitrypsin (A1AT). Previously unreported preferential glycoform-glycoform interactions were demonstrated. An understanding of this interaction is critical to design future recombinant A1AT inhibitors to mitigate HNE protease activities in inflamed lung airways.

- Enzymatically active HNE and the complement of its released *N*-glycans showed concentration-dependent growth inhibition of a clinical strain of *P. aeruginosa* at physiological levels, thereby suggesting weak bacteriostatic activity of paucimannosylation. This observation is important to understand the contribution of protein paucimannosylation towards HNE bacteriostatic activities.
- Protein paucimannosylation, in particular M2F carrying glycoproteins, is heavily enriched in azurophilic granules, but is still observed at lower levels in other granules in resting human neutrophils. An understanding of their abundance in the various neutrophil granules could provide insights on the functional relevance of these M2F structures in neutrophil biology.
- Isomers of the unusual monoantennary sialo-glycan, FA1G1S1, were intriguingly abundant in the azurophilic granules while high mannose type structures were in relatively lower abundance in this compartment. In contrast, high mannose and complex structures dominated the specific and gelatinase granules, as well as the secretory vesicles and the plasma membrane of neutrophils. These observations have not been previously reported and could reveal important contributions of *N*-glycosylation towards the structure and functions of neutrophil glycoproteins utilised during neutrophil immunological activities.

Future questions

- How is the soluble HNE retained on the cell surface of neutrophils and what is the functional relevance of the *N*-glycosylation of cell surface HNE on activated neutrophils? It is important to address this in the future to better understand how protein paucimannosylation on cell surface expressed HNE assists in mediating immunological responses or communication between activated neutrophils and other immune cells.
- Do the MBL binding of paucimannosidic HNE trigger complement activation or cell activation and does paucimannosylation of HNE have other immunity-dependent or independent functions? Understanding of this aspect will help to reveal additional immunological contribution of protein paucimannosylation towards complement or cell activation.
- What are the molecular interactions between HNE and A1AT and how do the specific glycoforms serve to manipulate (enhance/reduce) the enzyme/inhibitor binding? It will be of great interest to determine this in the future as it will aid in the design of recombinant A1AT that are used currently for therapeutic purposes to mitigate HNE deleterious activities in the lung airways.

- Is protein paucimannosylation demonstrating *bona fide* bacteriostatic activity and, if so, what are the molecular mechanism(s) facilitating the growth inhibition of *Pseudomonas aeruginosa*? An understanding of this aspect will contribute to the current knowledge in the generation and engineering of glycoproteins displaying structures that can provide bacteriostatic activity towards *Pseudomonas aeruginosa*.
- What is the trafficking pathway that predominantly directs paucimannosylated proteins to the azurophilic granules and is this mechanism also responsible for the *N*-glycan truncation? Insights into this trafficking pathway can help us to understand how neutrophil glycoproteins are shuttled and stored in the granules. How this pathway operates is currently unknown.
- Are altered physiologies and/or pathological conditions sufficient to alter the glycosylation of the azurophilic granule and the other compartments of human neutrophils? If so, are any such changes involved in driving or contributing to an immune-compromised state of such individuals. These aspects need to be addressed in the future as the alteration of the *N*-glycosylation profiles of the various neutrophil granule glycoproteins could influence the immunological functions of neutrophils during inflammation and infections.
- Is paucimannosylation a feature in other human immune cells and other cell types apart from neutrophils? This will be addressed in the next chapter.

Chapter 6: *N*-glycomics indicates that protein paucimannosylation is a multi-cellular *N*-glycan feature in inflammation, stemness and cancer

6.1 Rationale

Previous chapters have focused on describing protein paucimannosylation as a significant glyco-signature in human neutrophils. However, the presence of protein paucimannosylation in other human immune and non-immune cells remains under-investigated. The Consortium of Functional Glycomics (CFG) initiated a project in 2001 that focused on characterising the cellular *N*-glycome of important immune cell populations using matrix-assisted laser desorption/ionisation-time of flight-mass spectrometry (MALDI-TOF-MS) profiling of permethylated *N*-glycans as a higher-throughout semi-automated analytical platform. The low mass paucimannosidic structures were not the focus of these studies and were, as a consequence of low *m/z* mass spectral cut offs, not reported. However, the deposited mass spectral data available in the public CFG database allowed a retrospective analysis of the *N*-glycome data where the overlooked paucimannosylation from various immune cell types could be investigated. The initial assessment of this data indicated that protein paucimannosylation is not solely confined to neutrophils, but was also observed in other myeloid and lymphoid cells (Dr Morten Thaysen-Andersen, unpublished observation). However, *N*-glycome data from platelets and a range of other cell types were not available in the CFG initiative. In addition, for the purpose of this study, the available CFG *N*-glycome data lacked some experimental consistency to allow for a proper *N*-glycome comparison between the cell types of interest in order to confidently determine which cells have the capacity to synthesise paucimannosylated proteins.

Motivated by this rationale and these initial findings, I set out to investigate the expression of protein paucimannosylation in a range of white blood cells including neutrophils, lymphocytes and platelets isolated from the peripheral blood of a healthy donor based on PGC-LC-ESI-MS/MS profiling of reduced, but otherwise native, *N*-glycans, to obtain quantitative in-depth glycan structural information. In addition, the *N*-glycome of a differentiated monocytic human cell line (THP-1) resembling human macrophages (see **Publication VI in enclosed DVD**) and a glioblastoma human cell line (A172) (see **Publication VII in enclosed DVD**), were also profiled to determine the degree of protein paucimannosylation in these cell types in different physiological and pathological conditions. Taken together, this chapter compares and describes, for the first time, the expression of protein paucimannosylation across a selection of immune and non-immune cells in normal cellular homeostasis and during altered physiology including cellular differentiation, proliferation and bacterial infection.

6.2 Introduction

Protein paucimannosylation is a well-known *N*-glycosylation signature of invertebrates and in other lower organisms (Shin et al., 2016). **Chapters 1-5** have focused on expanding this knowledge by, for the first time, describing this *N*-glycosylation feature in pathogen-positive sputum proteins from inflamed lungs where the cellular origin was identified to be from human neutrophils and its intracellular granules. Neutrophils are front line myeloid immune cells critical in the innate immune defence against foreign pathogens (Borregaard, 2015). In addition to neutrophils, other myeloid cells such as eosinophils and basophils, platelets, monocytes and macrophages also play important immunological roles, for example, during allergy (Wen and Rothenberg, 2016), blood coagulation (Bye et al., 2016) and pathogen infections (Sica and Mantovani, 2012), respectively. As depicted by the classical haematopoiesis diagram shown in **Chapter 1, Figure 2**, the myeloid cells are known to arise from myeloid committed progenitor stem cells. In contrast, lymphoid immune cells such as the lymphocytes and NK cells arise from lymphoid committed progenitor stem cells and are commonly classified as adaptive immune cells (Tay et al., 2016). Importantly, both the innate and adaptive arm of the human immune system arises from the same pluripotent HSCs.

Earlier studies have reported on the total cellular *N*-glycome of neutrophils, eosinophils and basophils using established MALDI-TOF-MS profiling technologies (Babu et al., 2009; North et al., 2012). The datasets supporting these publications were deposited in the highly useful CFG database (<http://www.functionalglycomics.org/glycomics/publicdata/glycoprofiling-new.jsp>) for public access. In addition to the availability of the *N*-glycome data of these granulocytic cells, the CFG database also contains publicly available *N*-glycome datasets of other immune cell populations including monocytes, macrophages, lymphocytes and NK cells. However, platelets and several other haematopoietic immune cells in humans were not studied or were not made available in the CFG database. To initially assess the cellular distribution of paucimannosidic *N*-glycans in the immune system, retrospective analysis of the CFG glycome datasets derived from the various immune cell populations was performed. The results indicated that protein paucimannosylation is not confined to neutrophils, but is also present in other immune cells (**Figure 1**) (Dr Morten Thaysen-Andersen, unpublished observation). These paucimannosidic *N*-glycans were not reported as they were mostly found in the lower *m/z* region below *m/z* 1,000 and that the spectra peaks recorded in the CFG datasets only annotated *N*-glycan structures above *m/z* 1,500. Therefore, these paucimannosidic *N*-glycans were overlooked.

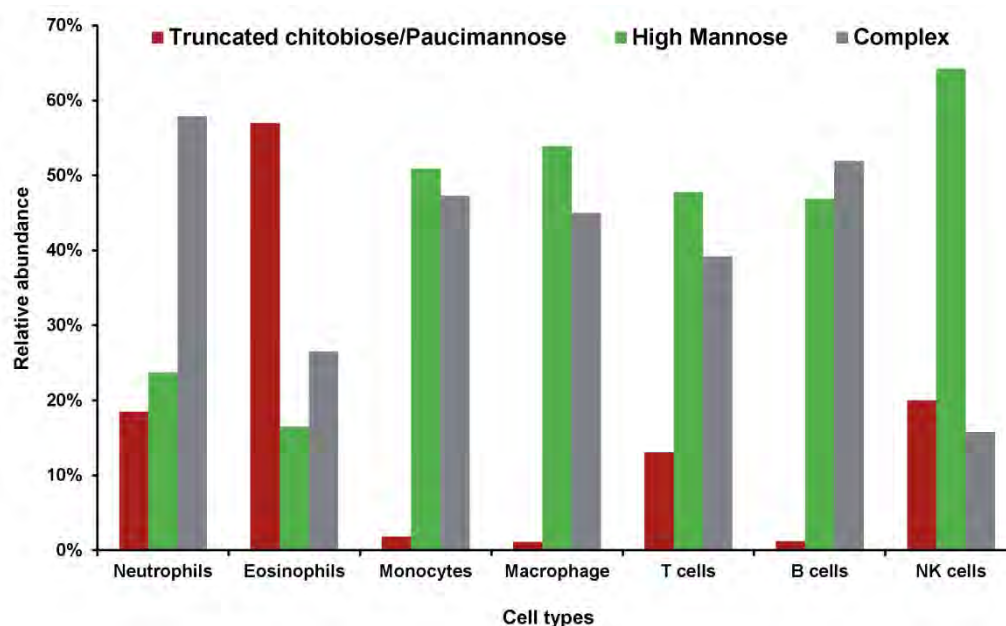


Figure 1. Distribution of the three main *N*-glycan types in various human immune cell populations as obtained by the retrospective analysis of the various cell *N*-glycome datasets available in the CFG database (<http://www.functionalglycomics.org/glycomics/publicdata/glycoprofiling-new.jsp>). Protein paucimannosylation (red) is not only present in neutrophils and in other granulocytes (i.e. eosinophils), but may also be synthesised by other immune cells. Green and grey bars denote high mannose and complex type structure. Data adopted from initial data interrogation performed by Dr Morten Thaysen-Andersen (unpublished observation). CFG *N*-glycome datasets analysed are listed in Supplementary Materials, Table S2 enclosed in the DVD.

In addition, several studies, from my own and other research laboratories, have recently indicated the presence of human paucimannosylated glycoproteins in a range of inflammatory and infectious conditions. For example, during CF, colorectal cancer and prostate cancer (Balog et al., 2012; Sethi et al., 2014; Shah et al., 2015; Venkatakrishnan et al., 2015). Together, these intriguing early observations suggest that protein paucimannosylation may also arise from other cellular sources than solely from a neutrophil origin. The immunological processes associated with these reports are known to involve *N*-glycoproteins that are produced and secreted from a variety of myeloid and lymphoid immune cells (Coelho et al., 2010; Salazar et al., 2014). Interestingly, other lines of evidence also indicate that immune cells are not the only cell types that are capable of presenting paucimannosylated glycoproteins. For example, glycoproteins derived from cells that are intricately involved in cellular development such as buccal epithelial cells (Everest-Dass et al., 2012) and neuronal synaptosomes (Trinidad et al., 2013) were shown to carry paucimannosylation.

To increase the understanding of the biological roles of protein paucimannosylation, it is important to describe the exact cellular origin of paucimannosidic glycoproteins from the various immune cell and non-immune cell populations during normal cellular homeostasis and in altered physiological conditions. This knowledge will contribute to building up a more complete picture of the capacity of human cells in producing produce paucimannosidic proteins, and provide insights to dissect further the functional importance of paucimannosidic glycoepitopes in the many complex processes related to cellular homeostasis, inflammation and infections.

In order to validate the hypothesis of a cell-wide expression of paucimannosylation as supported by the CFG glycome data and also to better understand the role of these paucimannosidic structures in innate and adaptive immunity, mapping the exact structure and localisation of these unconventional glycoepitopes is required. In this chapter, neutrophils, lymphocytes and platelets were purified from blood of the same donor to facilitate an accurate comparative *N*-glycome analysis using PGC-LC-MS/MS profiling. In addition, the *N*-glycome of a macrophage-like cell line (differentiated THP-1 cells) was studied as well as an immortal (cancerous) human glioblastoma cell line (A172). This is to assess the wider expression of human protein paucimannosylation across the three cellular pillars supporting immunity, “stemness” and cancer. These three physiological conditions have previously been suggested to be the biological systems where paucimannosylation may be present and functionally important (Zipser et al., 2012).

6.2 Materials and Methods

6.2.1 Blood collection and isolation of blood-derived human white blood cells

Human white blood cells were isolated from peripheral blood of a single healthy male donor after informed consent was obtained. The collection, handling and biomolecular analysis of healthy human neutrophils were approved by the Human Research Ethics Committee at Macquarie University, Sydney, Australia (Reference no. 5201500409). In order to obtain the buffy coat layer, which contains the mononuclear cells (e.g. lymphocytes, monocytes and platelets), 60 ml freshly drawn blood were collected in EDTA anti-coagulant tubes (BD Bioscience, Australia), diluted 1:1 (v/v) with HBSS without calcium and mixed well. Diluted blood was layered carefully in a 1:1 (v/v) ratio over Histopaque (density: 1.077 g/ml, Sigma-Aldrich) in 50 ml Falcon tubes. Tubes were centrifuged at 400g for 45 min at 25°C using a swing bucket centrifuge with no brakes. After centrifugation, three layers were observed: 1)

the plasma layer, which was discarded 2) the buffy coat layer, which was aliquoted into a fresh 50 ml Falcon tube 3) the neutrophil and red (erythrocyte) cell layer, which was aliquoted into a fresh 15 ml Falcon tube.

6.2.2 Isolation of platelets from buffy coats

To obtain purified platelets, 25 ml HBSS without calcium was added to the buffy coat in a 50 ml Falcon tube and centrifuged for 10 min at 100g at 20°C. The resulting supernatant (1st wash) was saved and another 10 ml HBSS without calcium was added to resuspend the cells. Cells were centrifuged again at 100g for 10 min at 20°C. The supernatant (2nd wash) was pooled together with the 1st wash in a 50 ml Falcon tube and subjected to a harder centrifugation step at 1,700g for 10 min at 20°C to pellet the cells. The remaining cell pellet obtained after these washes, which contained the lymphocyte and monocyte populations, was used subsequently as described in the following section.

6.2.3 Isolation of total lymphocytes

In order to isolate the total lymphocytes consisting of both B and T lymphocytes, the cell pellet obtained above from buffy coats (containing lymphocytes and monocytes) was resuspended in 10 ml of Dulbecco's Modified Eagle Medium (DMEM) without serum (Life Technologies) and aliquoted into a T75 cell culture flask (Corning). Isolation of lymphocytes was performed as described previously (Bennett and Breit, 1994) with minor modifications. Resuspended cells were aliquoted aseptically into a T75 cell culture flask and incubated upright in a 37°C humidified cell culture incubator equilibrated in 5% (v/v) CO₂ for at least 3 h to allow monocytes to adhere to the plastic surface of the flask. The supernatant layer containing the lymphocytes was then carefully removed and placed in a fresh 15 ml tube. The collected cells were washed in HBSS without calcium, followed by centrifugation at 400g for 10 min at 20°C before use. Monocytes were not harvested as their adherence to plastic surfaces has been reported to induce cell activation (Zhou et al., 2012), which, in turn, may influence their *N*-glycome expression profiles.

6.2.4 Isolation of neutrophils

To obtain purified neutrophils, the neutrophil and red cell layer (see Section 6.2.1) was mixed by inversion with 2 ml 3% (v/v) dextran (Sigma Aldrich) in 0.15 M sodium chloride. Cells were incubated for 20 min in a 37°C humidified cell culture incubator equilibrated in 5% (v/v) CO₂ to allow the red cells to sediment, leaving a whitish “neutrophil-rich” layer at the top. This layer was aliquoted into a fresh 15 ml tube and 1.8% (v/v) sodium chloride was

added to restore the physiological osmolarity of the solution. Cells were centrifuged at 270g for 10 min and the supernatant was removed. Red cell lysis was performed using cold sterile filtered MilliQ water by vortexing for 30 s before physiological tonicity was restored with 1.8% (v/v) sodium chloride. Cells were pelleted by centrifugation at 480g for 10 min before use.

6.2.5 Determination of the purity, viability and morphology of the isolated cell populations

The purity and morphology of the isolated white blood cell populations were determined by microscopy. Cells were prepared on glass slides using a cyto-centrifuge (Thermo Scientific) and stained using the Wright-Giemsa staining method (Sigma-Aldrich) for 10 min (Hoffman, 2013). After cytopinning and staining the cell on the glass slides, the residual dye was washed off using tap water and the slides were allowed to dry before the slides were mounted in DPX mounting media (Thermo Scientific). Slides were inspected using a bright field microscope (Olympus, Australia). Cell purity was determined by counting a total of at least 100 cells from each microscopic field to quantitatively assess the isolated cell populations. Cell viability was measured using trypan blue exclusion.

6.2.6 Cell lysis

To obtain total cell lysate proteins, the respective white blood cell populations were lysed using probe sonication in a RIPA buffer (1 M Tris-HCl, pH 8.0, 5 M NaCl, 0.01% (v/v) Triton X-100, 0.01% (w/v) sodium deoxycholate, 10% (v/v) SDS) supplemented with protease inhibitor (Roche). In total, 200 µl RIPA buffer with protease inhibitors was used to resuspend the cell pellets and the suspension was placed on ice for 20 min. Cells were lysed using probe sonication (Sonar, Australia) at 1 s interval bursts for three times at 20% power output before centrifugation at 10,000g for 10 min at 4°C. The resulting supernatant containing the total cell lysate proteins were aliquoted and stored at -80°C before use.

6.2.7 N-glycan release, N-glycome profiling and N-glycan data analysis

The total protein concentration from the cell lysates of the respective white cell populations was determined using the Direct Detect method (Merck-Millipore) to allow for protein normalisation prior to the de-*N*-glycosylation experiments. Proteins were reduced and alkylated, de-glycosylated and the *N*-glycans were analysed in their reduced, but otherwise native form, exactly as described in **Chapter 3**, Materials and Methods, Section 3.3.3.

6.2.8 Other methods used for published data presented in this chapter

To determine the total hexosaminidase and Hex A activity present in the culture media supernatant of uninfected and *M.tb* infected macrophages, a hexosaminidase activity assay was performed. The *N*-glycome of the whole cell lysates in uninfected and infected macrophages was also analysed. The experimental details for the hexosaminidase activity assay and the *N*-glycome analysis are described on page 252 and page 249 respectively in **Publication VI** presented in the supplementary materials of this chapter enclosed in the DVD. For the release and the analysis of *N*-glycans from the cell lysates and microsomal membrane proteins of A172 cells, the experimental details are described on page 878 in **Publication VII** presented in the supplementary materials of this chapter enclosed in the DVD.

6.3 Results

6.3.1 Cell purity and morphology of isolated immune cells

To determine the purity and the morphology of the isolated cells, visual inspection of the Giemsa-Wright stained cells was performed using microscopy. More quantitative measurements of the cell purity were then performed by counting of at least 100 cells from each microscopic field. **Table 1** shows the isolated cell population, their purity and representative morphologies and sizes of the Giemsa-Wright stained cells. In general, all cells were isolated to high purity (94.3%-100%). Importantly, the Giemsa-Wright stained cells were observed to be intact and of full integrity, and were not activated (i.e. were “resting”) as evaluated based on their cell morphology. Cell viability measured by trypan blue exclusion was between 70%-80%. Having confirmed high purity and integrity of the desired cell populations, the cells were lysed and the total protein extracts were subjected to de-*N*-deglycosylation for *N*-glycome analysis.


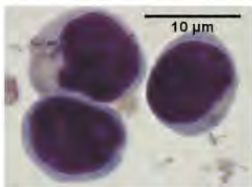
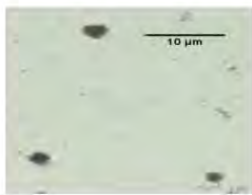
| Cell population isolated | Purity % (mean \pm S.D) | Giemsa-Wright stained cells |
|--------------------------|------------------------------|--|
| Neutrophils | 94.3 \pm 2.1 |  |
| Lymphocytes | 96.3 \pm 1.5 |  |
| Platelets | 100 |  |

Table 1. Purity, morphology and size of the isolated cell populations (i.e. neutrophils, lymphocytes, platelets) as determined by microscopy-based inspection and cell counting after Giemsa-Wright staining (mean \pm S.D, n = 3 technical replicates, >100 cells were counted from each microscopic field in each experiment).

6.3.2 Whole cell *N*-glycome profiling of neutrophils, lymphocytes and platelets

All *N*-glycans released from the total protein extracts of neutrophils, lymphocytes and platelet lysates were analysed using PGC-LC-ESI-CID-MS/MS as described in previous chapters. The monosaccharide compositions, the glycosidic linkages, branching and other structural features of the observed glycans were assigned based on manual interpretation of the PGC-LC retention, MS/MS fragmentation data and the observation of diagnostic fragmentation ions (Everest-Dass et al., 2013a; Harvey, 2005c). Some structural aspects were inferred based on the established knowledge of human *N*-glycosylation and the biosynthetic relatedness between the observed glycoforms (Aebi, 2013; Winchester, 2005) as well as from observations made from the previous glycome profiling of purified neutrophils and pathogen-positive sputum from inflamed lungs (**Chapter 2**). The *N*-glycan distribution was estimated based on the relative EIC peak areas from a triplicate *N*-glycan release and analysis (n = 3) from the respective isolated cell populations.

The observed *N*-glycans were classified into their main *N*-glycan types for initial comparison between the cells, **Figure 2**. The truncated chitobiose core/paucimannosidic types (which were grouped together due to their common truncated nature) as well as high mannose and complex type *N*-glycans were observed in neutrophils spanning 20 monosaccharide compositions and a total of 21 *N*-glycan isomers. In comparison, 14 monosaccharide compositions spanning a total of 16 and 21 *N*-glycan structures were observed from the lymphocyte and platelet cell populations, respectively (see **Supplementary Material, Table S1 enclosed in the DVD**). The truncated chitobiose/paucimannosidic *N*-glycans were clearly the most abundant structures in neutrophils (73.9%) relative to the high mannose and complex type structures (12-14%)

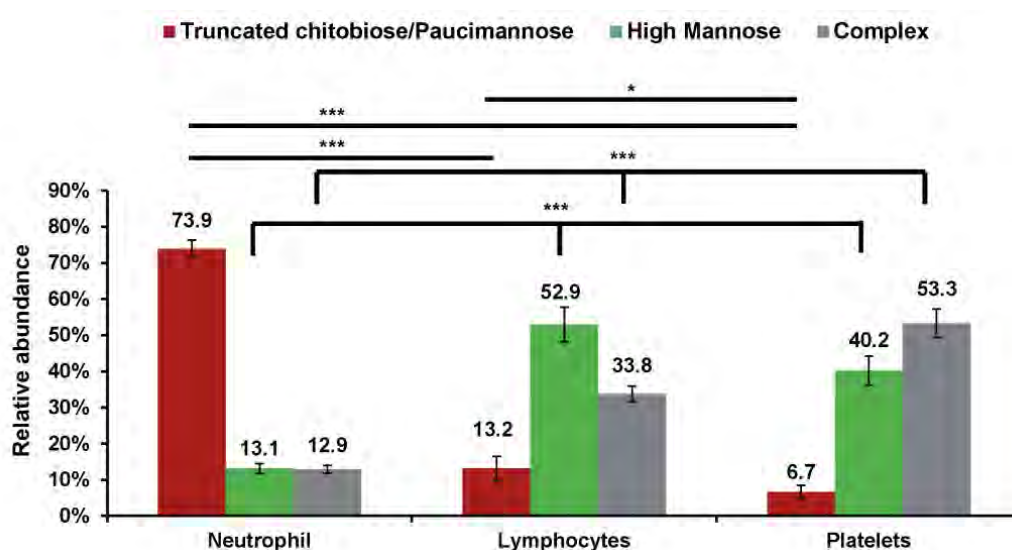


Figure 2. Distribution and comparison of the three main *N*-glycan types of the total protein extracts of neutrophils, lymphocytes and platelets (mean \pm S.D, $n = 3$ technical replicates) isolated from the same donor. * denotes $P < 0.05$, *** denotes $P < 0.001$ using two-tailed paired student's T tests.

Lymphocytes, in contrast, carried a larger proportion of high mannose structures (53%) and complex type structures (34%) and relatively less paucimannosidic *N*-glycans (13%) in their total *N*-glycome. In platelets, the complex type structures were the most abundant structures (53%), followed by the high mannose structures (40%). The relative abundance of paucimannosidic *N*-glycans in platelets (6.7%) were significantly lower compared to the lymphocytes ($P < 0.05$) and neutrophils ($P < 0.001$). The high mannose and complex type structures in lymphocytes and platelets appeared in higher abundance compared to the neutrophils ($P < 0.001$).

The M2F, which was identified as a single α 1,6-linked mannose terminating isomer from the PGC-LC-MS/MS data, is a high-abundance *N*-glycan in neutrophils (see Chapters 1, 4 and 5 for more). These structures were also identified in lymphocytes and platelets (**Table S1**). To ascertain if the M2F *N*-glycans present in lymphocytes and platelets were also of the α 1,6-linked mannose terminating isomer, a comparison was made with between the PGC-LC elution peaks of M2F in neutrophils, lymphocytes and platelets. The M2F elution peak of HNE, which is known to carry the α 1,6-linked mannose terminating isomer (**Chapter 4-5**) was also included as a well-characterised reference. As shown in **Figure 3**, the single α 1,6-mannosyl isomer of M2F *N*-glycan was found to elute at ~38 min in all cell types (i.e. neutrophils, lymphocytes and platelets), matching the elution time of M2F carried by HNE. The corresponding CID-MS/MS fragment spectra of these species were also highly similar, supporting that all the investigated cell types carried the same M2F *N*-glycan (**Supplementary Material, Figure S1 enclosed in the DVD**).

In order to assess the relatedness between the *N*-glycome profiles of the three types of immune cells, a cluster analysis was performed using the distribution (percentage relative abundances) of the observed *N*-glycans. As illustrated in **Figure 4**, the *N*-glycome of the lymphocyte and platelet populations clustered strongly together whereas the *N*-glycome of neutrophils appeared to be, in a relative sense, more unique. This was not surprising as the degree of paucimannosylation and chitobiose-core structures was more abundant in neutrophils compared to the lymphocytes and platelet populations. In addition, M2F paucimannosidic *N*-glycan were also less abundant in lymphocytes ($7.1\% \pm 1.9\%$) and platelets ($2.7\% \pm 1.1\%$) compared to neutrophils (47.2 ± 4.0) (All as mean \pm S.D). It should also be noted that M0F, M1F, M2 and M2F paucimannosidic *N*-glycans were not observed in lymphocytes and platelets but were only exclusively observed in neutrophils.

Comparing the above results to the *N*-glycome of neutrophils and T lymphocytes analysed retrospectively from the CFG glycome data (**Figure 1**), the percentage relative abundance of the truncated chitobiose-core/paucimannosidic structures from the CFG glycome data were much lower. In addition, high mannose and complex structures were reported at higher relative abundance compared to the results obtained in this study. In contrast, the T lymphocyte populations were observed to contain similar relative abundance of truncated chitobiose-core/paucimannosidic, high mannose and complex structures when compared to the results obtained in this study.

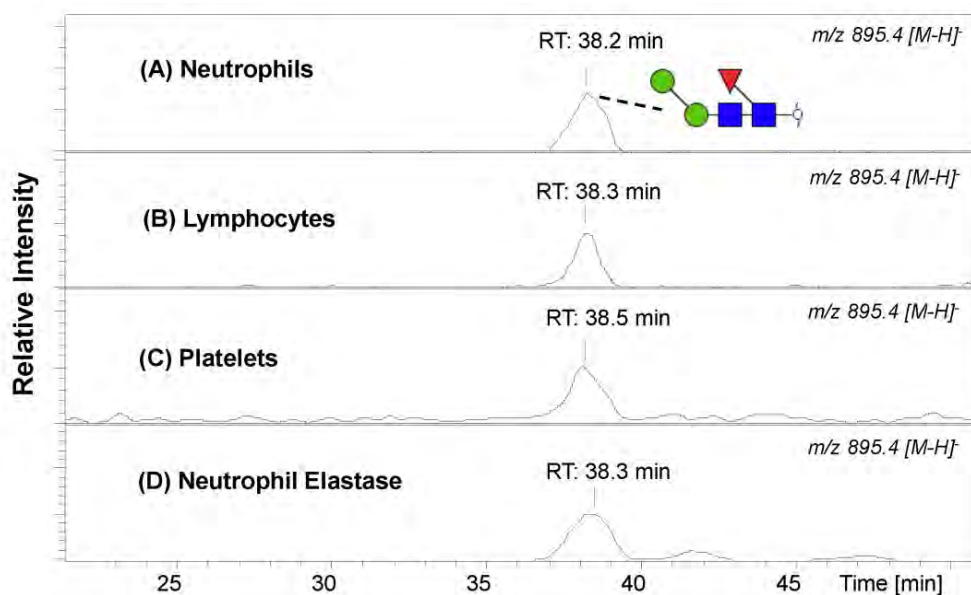


Figure 3. Representative EICs of the M2F paucimannosidic *N*-glycan released from total protein extracts of human neutrophils (A), lymphocytes (B) and platelets (C) demonstrating that paucimannosidic *N*-glycans are not uniquely expressed in human neutrophils. The elution profile of M2F released from HNE (D) was also included here as a well characterised reference (see Chapter 5, Publication V for more). The retention time (RT) of the eluting M2F structures is indicated.

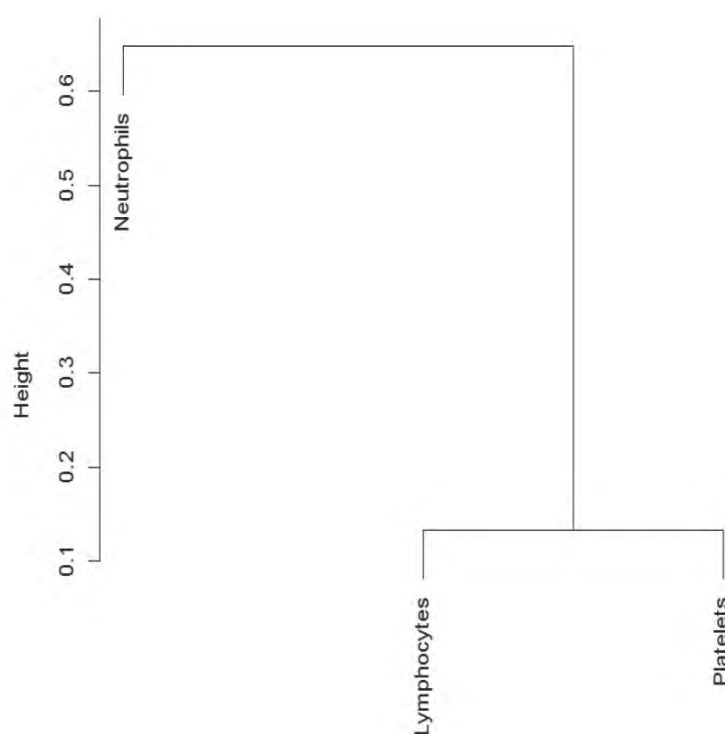


Figure 4. Cluster dendrogram based on the *N*-glycome of neutrophils, lymphocytes and platelets measured using the distribution (% relative abundance) of the observed *N*-glycans as shown in Table S1. The *N*-glycome of lymphocytes and platelets clustered more strongly together than neutrophils, suggesting that the *N*-glycome of neutrophils is relatively more distinct compared to the *N*-glycome of lymphocytes and platelets. Hierarchical clustering was performed using Euclidean distance.

6.3.3 Expression of paucimannosylation in macrophages and alterations upon tuberculosis infection

Although the *N*-glycome profiles of human monocytes including macrophages and DCs from the myeloid lineage were not isolated and analysed from healthy donor blood, an immortalised (cancerous) human monocytic cell line THP-1 was, as a part of a larger collaborative effort, investigated with the primary purpose of studying the manipulation of the glycoproteome or proteome of macrophages during tuberculosis (TB) infection (**Publication VI**). To fulfil one of the aims of this thesis to explore the expression of protein paucimannosylation in other immune cells apart from neutrophils, the secondary purpose was to determine the capacity of naïve and *M.tb* infected macrophages to generate paucimannosylation. The results are extracted from **Publication VI** as attached in the supplementary materials and are shown below.

Upon *in vitro* differentiation with PMA, functional macrophage-like cells were obtained and the cells were lysed and analysed using PGC-LC-ESI-CID-MS/MS (**Figure 5A**). The results demonstrated an abundance of paucimannosidic structures making up approximately half of the total *N*-glycome. Interestingly, the relative abundance of the intracellular (whole cell lysate) paucimannosylation in infected macrophages quickly decreased during the event of an *M. tb* infection. This suggests that paucimannosylated proteins are most likely secreted from a yet unknown paucimannosidic-compartment of macrophages upon the onset of *M. tb* infection. This may suggest that these glycoproteins are involved in providing immune functions associated with protection against this deleterious infection. In support of this infection-driven secretion of paucimannosylated protein hypothesis, a hexosaminidase activity assay was performed to measure the total hexosaminidase (Hex A and B) and Hex A activities present in the secreted protein environment. As shown in **Figure 5B**, *M. tb* infection induced the gradual release of Hex A significantly as the infection period increases. Although the total hexosaminidase activity was also altered post-infection, it did not display significance differences when compared to the uninfected macrophages.

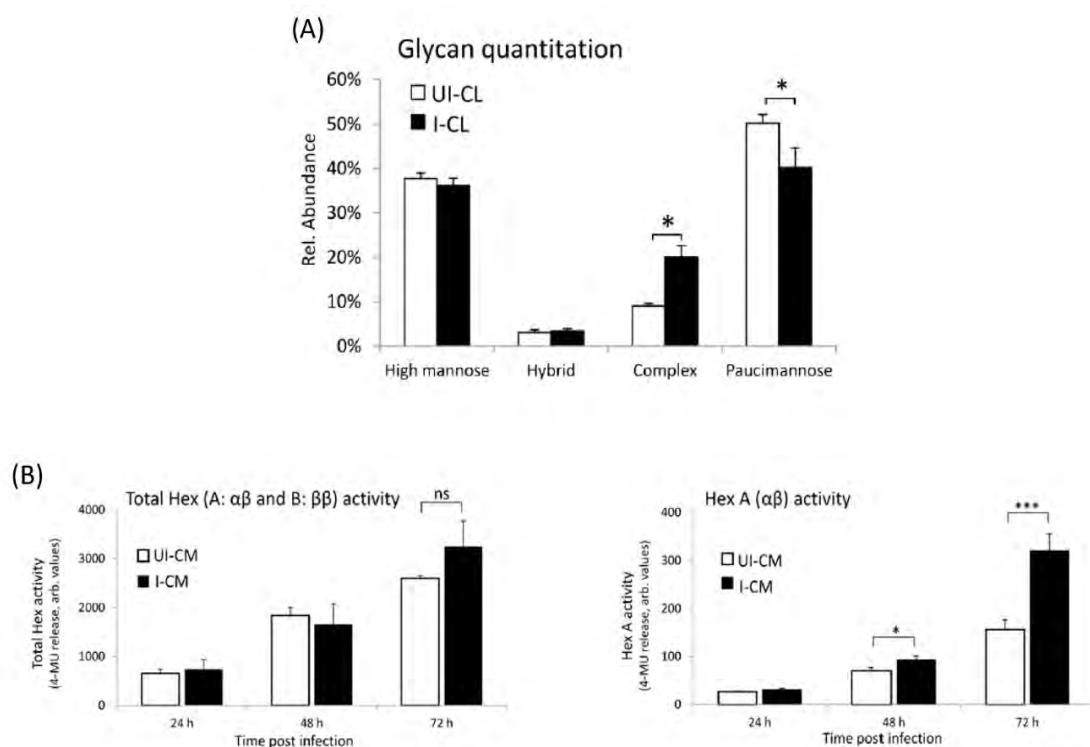


Figure 5. (A) Relative abundance of *N*-glycan types in the cell lysates (CL) of uninfected (UI, white bars) and *M. tb* infected (I, black bars) of macrophages assessed using PGC-LC-ESI-CID-MS/MS. Data points presented as mean \pm S.D, $n = 3$ biological replicates. **(B)** Total hexosaminidase (Hex A and B) and Hex A activities as measured in the culture media (CM) of uninfected (UI, white bars) and *M. tb* infected (I, black bars) macrophages respectively at 24 h, 48 h and 72 h post infection. Data points presented as mean \pm S.E.M, $n = 3$ biological replicates. Reprinted (adapted) with permission from Hare, N.J., Lee, L.Y., Loke, I., Britton, W.J., Saunders, B.M., Thaysen-Andersen, M., 2017. *Mycobacterium tuberculosis* Infection Manipulates the Glycosylation Machinery and the *N*-Glycoproteome of Human Macrophages and Their Microparticles. *Journal of Proteome Research* 16 (1), 247-263. © 2017 American Chemical Society.

6.3.4 Expression and importance of paucimannosylation in A172 cells

In addition to haematopoietic immune cells, immortal human glioblastoma A172 cells, a cell line derived from astrocytes in the nervous system were also investigated (**Publication VII**). The results were extracted from **Publication VII** as attached in the supplementary materials and are shown below. Proliferating resting A172 cells have been previously identified to express paucimannosylation using an immunocytochemistry approach (Zipser et al., 2012). In order to determine if paucimannosylation are involved in cellular proliferation and differentiation, A172 cells were treated with cytosine β -D-arabinofuranoside (AraC), an inhibitor of DNA synthesis to arrest cell proliferation and differentiation. These treated cells were found to express an increased abundance of paucimannosylation using an

immunocytochemistry approach. To confirm these findings, an *N*-glycome profiling using PGC-LC-MS/MS of the whole cell lysates and the microsomal fractions of these AraC treated A172 cells was performed.

As shown in **Figure 6**, several paucimannosidic structures were identified in the cell lysate and in the microsomal fraction, including the M2, M2F, M3 and M3F *N*-glycans. This not only demonstrates the presence of these paucimannosidic *N*-glycans in these cells, but also shows that these paucimannosidic glycoepitopes may be involved in the regulation of cell proliferation, differentiation of these neuronal cells and more importantly, involved in mediating immune response and cellular development in the brain.

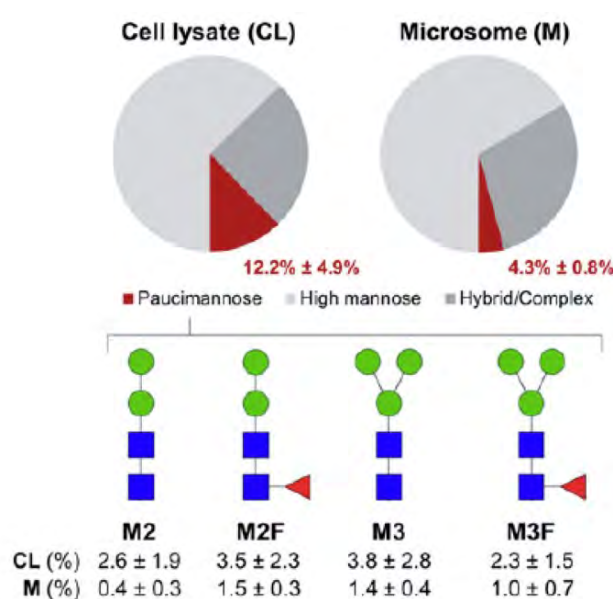


Figure 6. Distribution of *N*-glycan types present in the cell lysate (CL) and microsomal (M) fractions of AraC treated A172 cells. Top: The proportions of paucimannosidic *N*-glycans are highlighted together with their percentage relative abundance out of the total *N*-glycome are shown in red. Bottom: The percentage relative abundance of the individual paucimannosidic *N*-glycan species identified out of the total *N*-glycome. Reprinted (adapted) from Dahmen, A.C., Fergen, M.T., Laurini, C., Schmitz, B., Loke, I., Thaysen-Andersen, M., Diestel, S., 2015. Paucimannosidic glycoepitopes are functionally involved in proliferation of neural progenitor cells in the subventricular zone. *Glycobiology* 25 (8), 869-880, by permission of Oxford University Press.

6.4 Discussion

In 2001, the steering committee of CFG initiated an important *N*-glycan mapping exercise of various immune cells including neutrophils and lymphocytes (Babu et al., 2009; North et al., 2012). These profiling studies were performed on permethylated *N*-glycans using the

established MALDI-TOF-MS profiling technology. However, paucimannosidic *N*-glycans were not annotated in the low mass region of these spectra data deposited in the CFG database. In addition, the *N*-glycome of platelets was not studied in the CFG initiative. This is coupled with potential variability of the analysed samples arising from different donor origins, sample preparation, MS analysis and a low number of replicates. Therefore, this may not be sufficient to allow for a proper *N*-glycome comparison across the immune cells of interest.

As shown in **Chapters 2, 4 and 5**, protein paucimannosylation is a significant glyco-signature of neutrophils. The results presented in this chapter clearly support this observation. In addition, the data confirmed that protein paucimannosylation was also present in lymphocytes and platelets, albeit as a much less prominent glyco-feature. This was statistically supported and reflected in the cluster dendrogram based on the quantitative *N*-glycome landscape observed in these immune cells (**Figure 4**). The level of paucimannosylation (13%) in the preparation of total lymphocytes capturing all lymphocytes including both T- and B-lymphocytes agreed well with the retrospective interrogation of the CFG glycome data that showed a paucimannosylation level of 12.6% in T lymphocytes (**Figure 1**). The distribution of high mannose and complex structures in lymphocytes isolated in this study were also largely in qualitative and quantitative agreement with the CFG glycome data. Despite the fact that different lymphocyte isolation methods were used in these two studies, the resulting glycomes were comparable in that T lymphocytic cells are known to account for ~80% of all circulating lymphocytes (Coico and Sunshine, 2009). The agreement of the glycome data from these studies validates the two different *N*-glycan mapping strategies and indicates a high sample (cellular) purity of the lymphocyte preparation present in this chapter. Importantly, these data confirm that lymphoid cells also have the capacity to produce protein paucimannosylation but as a less prominent signature within their *N*-glycan repertoire.

This data presented here also provides the first detailed description of the whole cell *N*-glycome of blood-derived non-activated platelets and, importantly, generates the first evidence to suggest that platelets are also capable of producing paucimannosylated proteins. Platelets are important for normal blood clotting and haemostasis (Clemetson, 2012). The von Willibrand factor (vWF), a multimeric glycoprotein localised in the α -granules of platelets, is a key component to facilitate platelet adhesion to damaged endothelium (Sadler, 1998). Recently, the *N*-glycome of isolated human vWF was characterised using MALDI-TOF-MS. High mannose and mono- and di-sialylated complex type structures were reported as being the abundant *N*-glycans conjugated to vWF (Canis et al., 2012). However, paucimannosidic

N-glycans were not observed on vWF. Furthermore, a disintegrin and metalloproteinase 10 (ADAM10) purified from human platelets (Schuck et al., 2016) were also shown to carry mainly high mannose and complex type structures (Escrevente et al., 2008). These observations quantitatively align with the glycomics-based observations presented in this study, suggesting that paucimannosidic structures are minor components of the *N*-glycome in platelets. However, this provides little actual evidence that platelets are capable of producing paucimannosylation of proteins with full structural integrity and bioactivity.

It should be noted that these reported studies were also performed using the established MALDI-TOF-MS platform and due to the fact that these paucimannosidic structures are low in masses, they may be overlooked and thus not reported. Nevertheless, future studies involving the use of glycoproteomics and intact glycoprotein analysis for an in-depth characterisation of platelet-derived proteins are required to validate the presence of these paucimannosidic structures. This is important to confirm that the paucimannosidic *N*-glycan remains conjugated to protein carriers and to assess their potential functions.

Interestingly, the abundant M2F *N*-glycan appears as a single α 1,6-linked mannose terminating isomer across the investigated cell types i.e. neutrophils, lymphocytes and platelets (**Figure 3**). This suggests a somewhat conserved mechanism pertaining to the biosynthesis of the paucimannose-containing glycoproteins in these immune cell populations. Specifically, it suggests that the α 1,3-linked mannose of the conserved trimannosyl-chitobiose core and the monosaccharide residues usually decorating the *N*-glycan core, including the β 1,2-GlcNAc residues present in many glycan intermediates, are efficiently and selectively removed by linkage-specific glycosidases during or after the biosynthesis of these glycoproteins. The preference of the lysosomal mannosidase to cleave α 1,3-linked mannosyl residues and leave the α 1,6-linked mannose arm intact has been described previously, suggesting that this exoglycosidase may be, in part, involved in the generation of paucimannosylation across multiple cell types (Winchester, 2005). In summary, it is clear that multiple aspects of the biosynthetic route(s) underpinning protein paucimannosylation across the immune cells remain unknown following this initial discovery of paucimannosylation in multiple immune cell types. Ultimately, these observations are important to spur future research into this exciting area.

In addition to the immune cells discussed above, the *N*-glycome of macrophages was also investigated to determine their capabilities to express paucimannosylated proteins under pathological conditions. In this case, macrophages were infected with *M. tb*. In the literature,

M. tb is known to modulate the human immune response during an infection process, in particular, by targeting the macrophages as a cellular niche for their survival in the host has been well established (Awuh and Flo, 2016; Kang et al., 2005). However, the *M. tb* and/or host-driven manipulation of the macrophage glycome or glycoproteome upon infection, if any, remain unexplored. In addition, prior to our own investigation presented in the **Publication VI**, little was known of the ability of human macrophages to produce paucimannosylation. In summary, the data presented confirmed that macrophages, in this case, macrophage-like cells, are capable of abundantly producing and presenting paucimannosidic features. Interestingly, macrophages have also been documented to uptake apoptotic neutrophils and acquire neutrophil granules to limit *M. tb* infections (Tan et al., 2006). In addition, these paucimannosylated proteins might also originate from the intracellular lysosomes of the macrophages. Furthermore, it is currently unknown how these intracellular paucimannosylated proteins were reduced during infection, but this might be attributed to an increased in secretion of these paucimannosylated proteins during an *M. tb* infection. The reduction in protein paucimannosylation upon *M. tb* infection clearly warrants further investigation.

In addition, it can also be envisaged that the hexosaminidases (Hex A and B) by themselves, confer some immune function including protection against *Mycobacterium*. Although less likely considering the short infection period used in the conducted experiments (24-72 h), the observed decrease in intracellular paucimannosylation upon *M. tb* infection could also indicate that *Mycobacteria* (or alternatively the host macrophages), are capable of quickly manipulating the *N*-glycosylation machinery. This could therefore alter the glycoproteome of the macrophages by reducing the enzymatic activity of hexosaminidases and mannosidases that are, in part, involved in the biosynthesis of paucimannosylated proteins as discussed in **Chapter 3**.

Apart from these haematopoietic immune cells, we also found that paucimannosidic *N*-glycans were produced by, and are functionally important glycoepitopes in an astrocyte derived cell line A172 glioblastoma cells in the regulation of their cell proliferation and differentiation. In addition, developing neural progenitor stem cells present in the subventricular zone of the hippocampus found in early mouse brains also express paucimannosidic *N*-glycans as determined using immunocytochemistry (**Publication VII**). All these observations were in agreement with previously reported roles of paucimannosidic glycoproteins in the maintenance and differentiation of neural stem cells (Yagi et al., 2012).

These observations also demonstrate that in addition to their involvement in immunity and inflammation, paucimannosylation is also present and vitally important in physiologies centred around cancer progression and “stemness” including neural development as previously suggested (Zipser et al., 2012).

6.5 Overview of main findings, conclusions and future directions

Main findings and conclusions

- Cell-specific *N*-glycome analysis confirmed that protein paucimannosylation is a prominent glycosylation signature of human neutrophils and also highlighted that paucimannosidic features are present in other immune cell types i.e. lymphocytes and platelets, albeit in lower amounts, as indicated in the initial analysis of the CFG glycome data that were not annotated previously.
- The prominent paucimannosidic M2F *N*-glycan appeared consistently as a single α 1,6-mannosyl terminating isomer across the investigated immune cells, indicating a conserved biosynthetic apparatus responsible for paucimannosidic glycoprotein production.
- Human macrophage-like cells (THP-1) were demonstrated to have the capacity to produce paucimannosidic *N*-glycosylation as a significant glyco-feature. The degree of paucimannosylation in these macrophages was reduced compared to neutrophils, possibly by means of secretion upon infection with *Mycobacteria*, suggesting an extracellular immune function of the paucimannosidic proteins in TB.
- Paucimannosidic *N*-glycosylation is not restricted to haematopoietic immune cells, but was also shown to be present in oncogenic glioblastoma A172 astrocyte derived glioblastoma cells and in developing neural progenitor stem cells in postnatal mouse brains, where these glyco-features were shown to be important and for the maintenance and differentiation of neural stem cells.
- In summary, it appears that paucimannosylation is not restricted to neutrophils and that many cells, in particular the ones centric to inflammation, “stemness” and cancer, have an ability to produce protein paucimannosylation as a significant glycosylation feature. This thereby expands our view of the mammalian *N*-glycan repertoire.

Future directions

- The capacity of all blood-derived immune cells within the human hematopoietic network of cells including monocytes, eosinophils, basophils and NK cells should systematically be investigated for their capacity to generate paucimannosylation using glycomics-based

approaches. This is to confirm the initial findings from the CFG glycome data and to complete the picture of immune cell-specific paucimannose production.

- It would be of interest to include a much larger donor cohort in the above-mentioned “donor-paired” cell-specific assessment study in order to assess individual-specific variations in their capacity to produce paucimannosylated proteins. These studies could include immune cells isolated from a variety of healthy donors and individuals with relevant genotypes (e.g. hexosaminidase-deficient TSD/SD patients) and altered physiological or pathological conditions (e.g. bacteria-infected individuals) to better correlate the degree of paucimannosylation with the genotype/phenotype of specific cell types.
- The expression of protein paucimannosylation in other non-immune human cell types such as epithelial- stem- and cancer- cells, should also be investigated in a more systematic fashion using immunocytochemistry and gene expression arrays to ascertain their spatiotemporal expression in a higher-throughput manner under normal or altered homeostatic conditions. These findings could be confirmed using glycomics based approaches.
- For all of the paucimannose-positive cells identified, molecular and cellular aspects associated with the structure, function and biosynthesis of these unconventional glyco-features should eventually be investigated in these other human immune cells, similar to the on-going efforts presented in this thesis to dissect the structure, function and biosynthesis of paucimannosylation in human neutrophils. The inclusion of glycoproteomics and intact glycoprotein analysis in these studies is important to analyse the paucimannosidic glycans conjugated to the protein carriers that may play a role in modulating the protein function or facilitating a function independently of the protein carrier.

Chapter 7: Summary and Conclusion

7.1 Main summary

The motivation and the specific research aims of this thesis were conceived based on an extensive literature review (**Publication I**). The review clearly illustrates that there is increasing evidence supporting protein mannosylation, including both high mannosylation and paucimannosylation, is deeply involved in various inflammatory and infectious conditions. For example, the literature documented that mannosidic glycoepitopes are systemically over-expressed and highly abundant in micro-environment centric to cancer and pathogenic infections (Balog et al., 2012; Lee et al., 2014a). Importantly, these mannosidic glycoepitopes were shown to be recognised by specialised mannose-recognising receptors that are widely expressed on various immune cell types and as soluble forms in extracellular fluids, thereby further supporting their involvement in innate immunity. Compared to the more widely studied high mannose glycans, paucimannosidic glycoepitopes have historically received much less attention since they, until the discoveries described in this thesis, have been largely neglected due to the perception that these glycans are cellular degradation products. However, as also summarised in the literature review, scattered yet convincing studies have recently presented solid evidence proving that paucimannosidic *N*-glycans and/or paucimannosylated proteins are also highly abundant during inflammatory and infectious conditions and that they are equally capable of being recognised by mrCLRs.

The initial work presented in **Publication II** showed that the less-reported paucimannosidic *N*-glycans were found to be carried by proteins residing in the azurophilic granules of human neutrophils. This unconventional (fourth) class of *N*-glycoproteins was readily degranulated from resting neutrophils upon virulent bacterial stimulation, suggesting potential contributions of these paucimannosylated proteins and their mannosylated glycoepitopes towards the immunological functions of neutrophils.

From these initial observations, this thesis extends these findings through a three-pronged approach. First, the biosynthetic machinery of protein paucimannosylation in human neutrophils was assessed by studying β -hexosaminidase deficient SD neutrophils relative to healthy neutrophils. Results demonstrated a reduction in protein paucimannosylation in the *N*-glycome of SD neutrophils as confirmed by PGC-LC-ESI-CID-MS/MS and immunoblotting. This, for the first time, shows that human β -hexosaminidases are involved in the generation of protein paucimannosylation in human neutrophils. Interestingly, the reduction in protein paucimannosylation was also observed in hexosaminidase-knockout mutants of the legume

Lotus japonicus (**Publication III**). Given the short lifespan of blood isolated human neutrophils *ex vivo*, an *in vitro* proof-of-concept experiment utilising siRNA silenced hexosaminidase in HL-60 neutrophil-like cells was also presented in this thesis. The ability to genetically manipulate the hexosaminidase activities in these cells will be a useful tool not only provide a deeper understanding into the generation of protein paucimannosylation in human neutrophils and their potential influence on neutrophil-mediated immune functions, but also serves to complement the knowledge gained from the hexosaminidase deficient SD neutrophils.

To understand the functions of a protein *N*-glycosylation, it is important to first understand the site-specific *N*-glycosylation profile of a glycoprotein. The second approach presented in this thesis was to investigate the site-specific protein *N*-glycosylation profile of two important serine proteases that are heavily utilised during neutrophil-mediated immune functions. Briefly, the *N*-glycome of nCG and HNE was characterised using PGC-LC-ESI-CID-MS/MS. Site-specific *N*-glycoproteotyping of nCG and HNE was then performed using a “bottom-up” *N*-glycopeptide based approach by C18 RP-LC-ESI-CID/ETD-MS/MS. “Top-down” intact glycoprotein *N*-glycoproteotyping was also performed using RP-LC-ESI-QTOF-MS. The use of these complementary LC-MS/MS approaches was crucial in this thesis to provide a holistic overview of the *N*-glycosylation of nCG and HNE, which was unknown when I started my PhD (**Publication IV and Publication V**). This lack of structural detail was surprising, considering the fact that nCG and HNE play pivotal roles in mediating the immune functions of neutrophils and in numerous inflammatory and infectious diseases.

Serendipitously, ultra-truncated *N*-glycans were found to be carried by nCG, a feature that has not been identified previously on nCG. In contrast, HNE was shown to carry predominately M2F *N*-glycan structures but ultra-truncated *N*-glycans were not observed. These observations may suggest that these proteins might reside in different micro-environments within the neutrophil granules, thereby differing in their encounters with various (de)glycosylation enzymes. These findings not only provide further insights into the biosynthetic machinery of neutrophil granule glycoproteins, but also serve to question the existing “targeting by timing” hypothesis.

With the *N*-glycosylation profiles of these paucimannosylated glycoproteins, the functional aspects of protein paucimannosylation in neutrophil-mediated immune response were investigated as a third approach. Paucimannose-rich HNE was shown to be expressed on the

cell surface of activated neutrophils, binds preferentially to human MBL and displayed preferential complex formation with A1AT. Interestingly, the released *N*-glycans of HNE demonstrated weak bacteriostatic activity against a clinical isolate of *Pseudomonas aeruginosa*. The multiple lines of evidences presented in this thesis unequivocally showed that protein paucimannosylation plays important immuno-modulatory roles of HNE in the context of innate immunity and pathogen infections.

In addition, the subcellular *N*-glycome profile of purified neutrophil granules using subcellular fractionation was also investigated for the first time using PGC-LC-ESI-CID-MS/MS (**Chapter 5.3**). Results demonstrated a high abundance of paucimannosylated proteins in the azurophilic granules of neutrophils, confirming the initial observations presented in **Publication II**. However, paucimannosylated proteins were also found in other neutrophil granules but were significantly lower in abundance compared to the azurophilic granules. Therefore, these observations demonstrate the power of glycomics and glycoproteomics in elucidating the structural features of this class of unconventional *N*-glycans in the subcellular granules present in human neutrophils.

Furthermore, the presence of paucimannosylation is not unique to human neutrophils but can also be found in other human immune and non-immune cell types including macrophages, platelets, lymphocytes and neuronal stem cells under normal and altered physiological conditions (**Chapter 6, Publication VI, VII**). It is clear that protein paucimannosylation is not a *N*-glycosylation feature that is strictly confined to human neutrophils, but is more a general glycoepitope that is expressed in varying amounts in a spatial-temporal manner across specific immune, cancer and neuronal cells in the human organism.

Ultimately, the biosynthesis, structure and functions of paucimannosylated *N*-glycoproteins in human neutrophils and other cell types were investigated in this thesis. This involves using a combination of state-of-the-art mass spectrometry based technologies for structural elucidation with *N*-glycomics and *N*-glycoproteomics, together with a variety of tools used widely in cellular and molecular biology. In addition, the functional importance of these unconventional glycoepitopes in processes related to inflammation and infection were studied using a variety of functional assays and biological samples in conjunction with the obtained structural data. In short, this thesis provides unequivocal evidence for the capacity of human cells to produce, store and secrete paucimannosylation on intact and bioactive proteins, building support for immune-centric roles of this unconventional glycan modification and

opening up many unexplored avenues to spur future new and exciting research into this area. An overview showing selected new discoveries and observations, classified into the three main pillars of protein paucimannosylation based on the work presented in this thesis is shown in **Figure 1**.

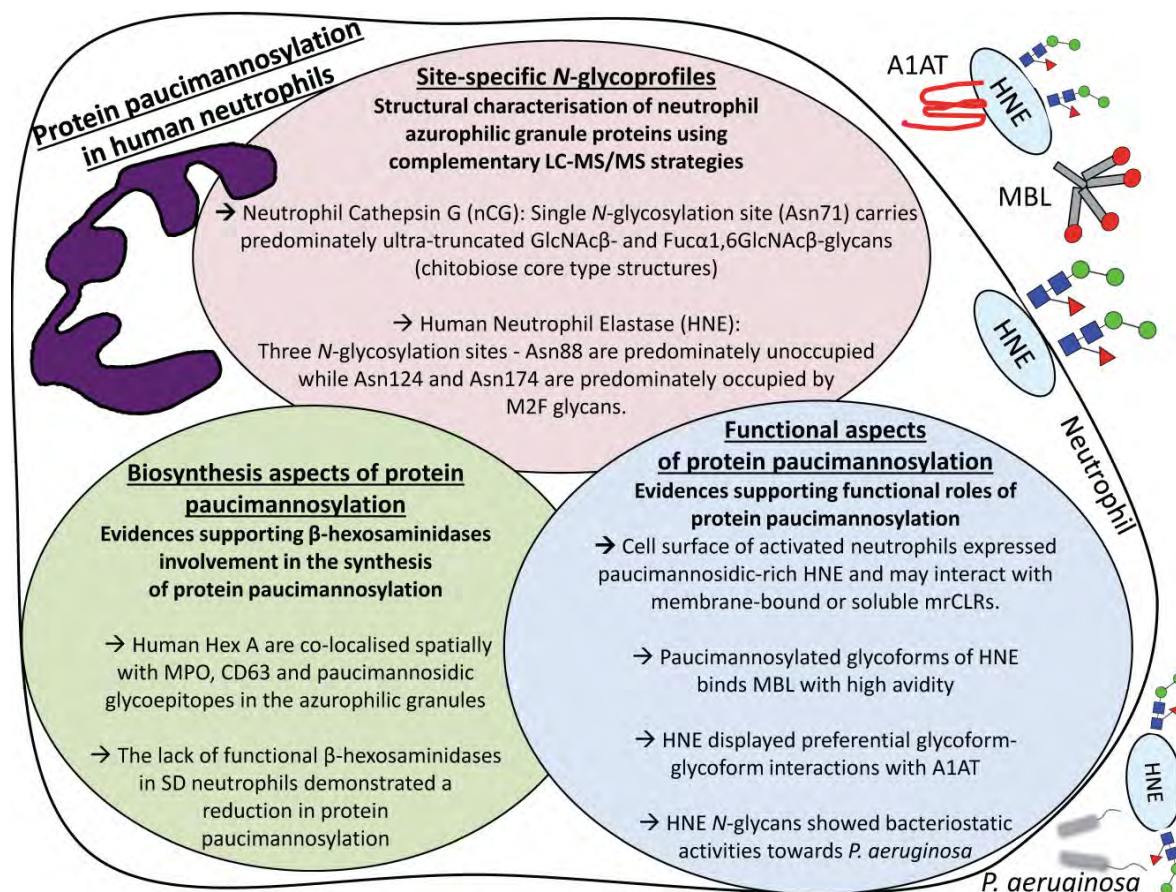


Figure 1. An overview showing selected new discoveries and observations classified into the three main pillars consisting of the biosynthesis, structural and functional aspects of protein paucimannosylation based on the work presented in this thesis.

The following sections in this chapter serve the purpose of highlighting rather than explicitly scrutinising the main findings disseminated in the individual chapters of this thesis. It also aims to relate the relevance of these discoveries, here classified into three main pillars consisting of the biosynthesis, structure and function of paucimannosylation, in light of the existing knowledge and to highlight possible future avenues for research.

7.2 The biosynthesis of paucimannosylated *N*-glycoproteins in human neutrophils

Protein paucimannosylation has been considered a glycosylation signature of the invertebrates and in other lower organisms and have been repeatedly reported to be absent in humans and other mammals (Schachter, 2009; Schachter and Boulianne, 2011; Shihao et al., 2002). In addition to establishing support for the presence and functional involvement of mammalian paucimannosylation in the literature (**Chapter 1, Publication I**), the initial discovery of paucimannosidic *N*-glycoproteins in neutrophil-rich sputum of CF patients infected with *Pseudomonas aeruginosa* (**Chapter 2, Publication II**) encouraged me to explore the structure, biosynthesis and function of human paucimannosylation in greater details as presented in this thesis. Glycomics and glycoproteomics were integral to facilitate in-depth structural insights in these early observations, thereby illustrating the power and importance of the 'omics technologies to explore and uncover new structural features of the glycoproteome. These unconventional *N*-glycans were found to be of predominantly neutrophil origin and are carried by azurophilic granule-resident proteins. Mechanistically, the paucimannosylated proteins were also found to be degranulated from resting human neutrophils upon virulent stimulation. In addition, human β -hexosaminidases were hypothesised to be involved in the biosynthesis of paucimannosylation in human neutrophils, a hypothesis I was later able to confirm.

Building on these initial observations, immunocytochemistry of human resting neutrophils (purified from whole blood) and neutrophil-like cells (HL-60, grown and differentiated in *in vitro* cell cultures) using β -hexosaminidase-reactive antibodies, showed that these enzymes were localised and enriched within the azurophilic granules of neutrophils. The contribution of the β -hexosaminidases in the generation of paucimannosylated *N*-glycoproteins was also investigated (**Chapter 3**). Specifically, the subcellular localisation of the Hex A heterodimeric variant ($\alpha\beta$) in human neutrophils was determined using immunocytochemistry and found to co-localise with the well characterised azurophilic granule-resident MPO and CD63, together with the paucimannosidic glycoepitopes. These sets of experiments were facilitated by the access to one of just two known antibodies with a defined reactivity toward paucimannosidic glycoepitopes (Zipser et al., 2012). This demonstrates the need for continued requirement for specific and well characterised antibodies in biochemistry-based and glycobiological research to identify these glycoepitopes. The other antibodies (mAB 100-4G11) were generated from

Schistosoma-infected or immunized mice and were also found to be reactive towards paucimannosidic glycoepitopes in the whole cell lysates of haematopoietic immune cells (van Remoortere et al., 2003).

Next, the *N*-glycomes of whole cell lysates of neutrophils isolated from the whole blood of a *HEXB*^{-/-} SD patient and an age-paired healthy individual were then mapped and compared using PGC-LC-ESI-CID-MS/MS. The SD phenotype, as opposed to TSD, is particularly valuable to study in the first instance, since the lack of a functional β subunit renders both the $\alpha\beta$ (Hex A) and $\beta\beta$ (Hex B) isoenzymes impaired in their activities and thereby, in theory, would be ideal to study their contribution toward the synthesis of protein paucimannosylation. The structural glycan features of these two samples were further validated through immunoblotting. These experiments demonstrated that SD neutrophils had a reduced degree of protein paucimannosylation, with a concomitant increase in high mannose and complex type structures relative to the healthy neutrophils. The altered neutrophil glycosylation was attributed to the absence of functional hexosaminidases in SD neutrophils, which was confirmed in the clinic using an accurate enzyme activity assay (Hex B activity in SD: 40 nmol/h/mg vs normal: 1223 nmol/h/mg). These provided strong support for the glyco-enzyme:product relationship of the human β -hexosaminidase and paucimannosylation. Further support for this association was also obtained from the glycomics based observations made in a series of hexosaminidase-knockout mutants (i.e. *HEXO1* and *HEXO2*) generated by a collaborator in the legume *Lotus japonicus* (**Chapter 3, Publication III**) and observations made by others in the plant *Nicotiana benthamiana* (Shin et al., 2016). Earlier studies have focused almost exclusively on studying the link between the β -hexosaminidases and the catabolism of the glycosaminoglycans and glycosphingolipids (GM2 \rightarrow GM3). These studies were establishing the physiological consequences of a reduced degradation of these products, as opposed to the lack of the generation of paucimannosidic *N*-glycoproteins, in β -hexosaminidase-deficient individuals such as SD and TSD patients (Hou et al., 1998; Tropak et al., 2004).

In light of the results described in **Chapter 3**, this represent the first report of reduced protein paucimannosylation in the neutrophils of SD patients and the molecular association between the β subunit of the human hexosaminidase and protein paucimannosylation. However, the residual degree of paucimannosylation in the SD neutrophils indicated that an alternative enzyme or biosynthesis pathways could exist. For example, the higher-than-expected use of the Hex S ($\alpha\alpha$) variant or an unexpected utilisation of the cytoplasmic Hex D enzyme

(encoded by *HEXDC*) are still to be discovered. Nevertheless, these data have now provided evidence on the contribution of hexosaminidases towards the biosynthesis of paucimannosylated proteins in neutrophils. However, it remains to be determined if and how the deficient β -hexosaminidase affects the immunological response of neutrophils; these could be critical question to address in order to further determine the exact pathogenesis of SD and TSD. Although the pathologies of these two LSD have been traditionally associated with the build-up of gangliosides in the brain causing mental retardation (Hall et al., 2014), it may be speculated that a secondary contributing disease-mechanism is a compromised immune response caused by, for example, altered neutrophils showing a poor paucimannosidic *N*-glycome phenotype.

In order to study the functional consequence of hexosaminidase-deficiency in neutrophils in greater details and in a more controlled manner, a set of initial proof-of-concept siRNA-based *HEXA* and *HEXB* silencing experiments on HL-60 neutrophil-like cells was performed. The first aim was to assess the susceptibility of these cells to undergo manipulation of the hexosaminidase gene expression and to determine the optimal experimental conditions for such alterations. Results demonstrated that pre-plated cells with siPORT transfection reagent at 150 pmol siRNA were useful, if not ideal, for efficient transfection. In addition to the chosen siRNA approach, the use of shRNA and CRISPR/Cas9 could also be explored in the future to provide more stable gene knockouts. Irrespective of the gene modulation strategy, these mutant neutrophil-like cells, together with blood isolated neutrophils from SD/TSD patients are valuable samples that are needed to understand the exact function of paucimannosylation and the role of β -hexosaminidases in neutrophils in the context of innate immunity and pathogen infections.

7.3 Structural characterisation of paucimannosylated azurophilic granule *N*-glycoproteins in neutrophils

The site-specific *N*-glycosylation profile of nCG was determined by using complementary LC-MS/MS analytical platforms (**Chapter 4, Publication IV**). The results revealed that nCG predominantly carries ultra-truncated GlcNAc β - and Fuc α 1,6GlcNAc β -glycans, the so-called and less reported chitobiose core type structures at its single *N*-glycosylation site (Asn71). The paucimannosidic (M1, M1F, M2) and complex sialylated monoantennary *N*-glycans (FA1G1S1) were also present in lower abundance.

As a side note, the discovery of these unusually truncated *N*-glycans on biological important proteins critically affects how we should choose the optimal strategy for accurate *N*-glycan profiling in the future. Although PGC-LC-MS/MS has been applied in many characterisation studies of *N*-glycans on a single glycoprotein level (Parker et al., 2013; Sumer-Bayraktar et al., 2012), complex protein mixtures obtained from whole cells and tissues such as salivary and buccal cells and ovarian cancer tissues (Anugraham et al., 2014; Everest-Dass et al., 2016; Stadlmann et al., 2008), has been found to be accurate when benchmarked to other techniques (Leymarie et al., 2013). In this thesis, I have demonstrated that this technique may not be ideal to accurately profile these unconventional structures, due to their lack of retention on PGC and the observation that they may be, at least in part, *N*-glycosidase F insensitive as previously reported (Chu, 1986). Similarly, MALDI-TOF-MS profiling is also likely to be sub-optimal to profile truncated chitobiose core/paucimannose-positive glycan mixtures due to the potential *m/z* interference of the low mass glycans and the matrix ions, which are typically abundant below 1,000 *m/z*.

In addition, the current lack of MS/MS spectral data and assignments of the paucimannosidic and chitobiose type structures in the existing glycan databases such as UniCarb-DB (Hayes et al., 2011) and UniCarb-KB (Campbell et al., 2014a) at present, impede the investigation of these structures by the glycomics community. Hence, it should now be a priority to deposit representative tandem mass spectra of the individual *N*-glycans in order to support future discoveries in this space.

Other observations further highlighted the need for special considerations or the development of a new “paucimannose-specific analytical tool box” to accurately map these unusual structures using the large scale ‘omics technologies. As an example, when studying the *N*-glycosylation of nCG and other isolated neutrophil glycoproteins, a minimum degree of hydrophilicity was found to be required for reproducible and efficient *N*-glycopeptide enrichment using ZIC-HILIC SPE prior to downstream RP-LC-ESI-MS/MS analysis of the intact glycopeptides. Peptides conjugated with truncated chitobiose core and paucimannosidic structures did not always provide sufficient localised hydrophilicity for full HILIC retention, creating a clear bias in the resulting MS profiles for these glycopeptides. In those cases, the peptide portion of the glycopeptide appears to be an important determinant in deciding the degree of HILIC retention.

Importantly, this study also demonstrated another benefit of using multiple analytical platforms for the characterisation of *N*-glycoproteins. The qualitative and quantitative discrepancy between the *N*-glycan and *N*-glycopeptide data of nCG was resolved with the use of intact glycoprotein profiling. Intact glycoprotein profiling, also known as top-down profiling is, when available and applicable to the glycoprotein of interest, superior to the more bottom-up approaches due to the holistic structural insight it provides. However, it should be mentioned that intact glycoprotein analysis is still in its infancy and is, at present, only amenable to relatively small and less heterogeneous glycoproteins. Taken together, these structural glycoprotein studies emphasise the value and importance of performing multiple levels of structural analysis to obtain a detailed and accurate *N*-glycosylation profile of the analyte of interest.

The parallel application of these three complementary LC-MS/MS technologies also facilitated a deep site-specific *N*-glycoprofile of HNE purified from healthy human neutrophils (**Chapter 5, Publication V**). Paucimannosidic *N*-glycans, in particular the M2F structures, predominately occupied the Asn124 and Asn173 glycosylation sites of HNE. The complex monoantennary sialo-glycan FA1G1S1, was also identified from these glycosylation sites, which agreed very well with the solvent exposure/high accessibility of these two glycosylation sites on the surface of HNE relative to the inaccessible third site (Asn88). The Asn88 glycosylation site was largely observed to be unoccupied, but was also found to be displaying some afucosylated M2 glycosylation. The lack of core fucosylation also agrees very well with the low solvent accessibility at this glycosylation site, a relationship that has been unravelled and appreciated previously (Thaysen-Andersen and Packer, 2012).

Surprisingly, subcellular-specific glycopeptide analysis demonstrated that HNE was uniformly *N*-glycosylated across the different neutrophil granules including the azurophilic-, specific-, and gelatinase granules, as well as in the secretory vesicles and on the plasma membrane of resting neutrophils. The data also indicated that HNE was preferentially localised in the azurophilic granules when measured by protein abundance level. These observations of uniform *N*-glycosylation across granules were rather unexpected, considering past literature reporting subcellular-specific *N*-glycosylation (Lee et al., 2014a) and that the data presented in **Chapter 2, Publication II** indicated that paucimannose is an enriched glycosylation feature of the azurophilic granules in human neutrophils. This intriguing discrepancy, which also questions the more established “targeted by timing” hypothesis (Borregaard and Cowland, 1997), prompted a new set of experiments where the *N*-glycome of

the individual purified neutrophil granules were mapped using PGC-LC-MS/MS. Subcellular fractionation of neutrophil granules using nitrogen cavitation is a gentle method of disrupting the cell membrane (Clemmensen et al., 2014) and was thus, the chosen method to obtain purified neutrophil granules prior to *N*-glycome analysis. Results obtained from these experiments showed that paucimannosylation was observed to be highly enriched in the azurophilic granules relative to the other neutrophil granules. This validates the initial observation on the enrichment of protein paucimannosylation in these azurophilic granules of the human neutrophils as described in **Chapter 2, Publication II**. However, it simultaneously leaves open mechanistic questions as to how certain azurophilic proteins including HNE can receive highly uniform *N*-glycosylation when appearing in multiple intracellular neutrophil granules.

On a more protein-centric context, the detailed and accurate site-specific *N*-glycoprofile of nCG and HNE, and the site-unspecific *N*-glycome of the neutrophil granules described in this thesis, now contributes to an essential resource that was not available previously for biochemists, immunologists and glycobiologists. This will help to facilitate future research aiming to understand the exact structure and function of nCG and HNE, together with the importance of *N*-glycosylation, specifically the role of paucimannosidic *N*-glycans carried by these essential serine proteases.

7.4 Functional aspects of paucimannosylation on HNE

As discussed in the introduction and in the earlier chapters of this thesis, it is clear that protein glycosylation is involved in numerous important cellular processes such as cell-cell interactions, cell-cell communication and signalling (Varki, 2017). On the protein level, glycosylation is also known to be involved in essential processes such as ensuring the correct protein folding, conformation, stability, solubility, protein-protein interactions and protein trafficking (Hartholt et al., 2016; Scott et al., 2013; Sumer-Bayraktar et al., 2011). Hence, the glycosylation of a protein have the ability of modulating or directly changing its function and thereby, in turn, influence the more overarching cellular processes.

As the heavily paucimannosylated HNE is a central protease involved in the immunological response of neutrophils and in the pathogenesis of various diseases such as CF, one of the aims of this thesis was to investigate the role(s) of paucimannosylation on HNE (**Chapter 5, Publication V**). Despite the biological significance of HNE in immunity, it was surprising to find that no studies have assessed how *N*-glycosylation affects the protease activity of HNE or

its effects in the multiple immune functions of this protease that is highly active during normal host immune response. This gap in knowledge may, in part, be due to the lack of a detailed site-specific *N*-glycosylation profile of HNE that was not available until recently as described in **Chapter 5, Publication V**. This underscores the importance of performing a deep site-specific *N*-glycoprofiling of glycosylated proteins to facilitate important investigations of how *N*-glycans can modulate the functions of *N*-glycoproteins.

Despite being a soluble glycoprotein without membrane domains, HNE has been reported to be associated with the cell surface of activated neutrophils (Owen et al., 1995). This may allow the neutrophil to control the distribution and direct the activity of the highly potent HNE protease. Through this process, it may also help to limit potential damage from excessive proteolytic degradation by HNE at unwanted locations. It was also suggested that the cell surface variant of HNE is not susceptible to protease inhibition by A1AT to the same degree as the secreted HNE variant (Owen et al., 1995). The exact mechanism of the cell surface retention of HNE is still not understood, but is thought to be facilitated by the sulfate groups of chondroitin sulfate and heparin sulfate containing proteoglycans at the plasma membrane of neutrophils, serving as binding sites to the highly positively charged HNE protein surface (Campbell and Owen, 2007). The site-specific *N*-glycosylation of HNE on the cell surface of resting and activated neutrophils remained, similar to the *N*-glycoprofile of HNE stored intracellularly within the cytoplasmic granules, undescribed until the efforts as presented in this thesis. Intracellular paucimannosidic-rich HNE was shown to be actively mobilised to the cell surface of human neutrophils upon stimulation (activation) (**Chapter 5, Publication V**). The discovery of paucimannosidic-rich HNE on the cell surface of activated neutrophils suggested a plausible role of protein paucimannosylation in the modulation of an HNE-mediated immune response conferred by activated neutrophils. This was supported by computational analysis of the HNE protein structure suggesting that the *N*-glycosylation sites of membrane-retained HNE carry *N*-glycans that face and extend into the extracellular milieu (Hajjar et al., 2008). The detailed site-specific *N*-glycoprofile of HNE established that Asn124 and Asn173 carry predominantly M2F structures. Therefore, it seems reasonable to suggest that cell surface paucimannosylated glycoforms of HNE may mediate cell-cell communication or interactions with mrCLRs such as MBL (see below) or trigger other still unknown immune responses. Although these glycan-mediated processes in the immune system needs to be validated in the future and mechanistically investigated, these observations

indicate that neutrophils may utilise protein paucimannosylation as a molecular approach in modulating multiple immune processes within the host immune system.

In support of the above speculations, specific HNE glycoforms containing M2F structures were found to bind preferentially to MBL, a soluble mrCLR found in inflamed lungs (**Chapter 5, Publication V**). HNE is also found in the inflamed lung airway environment where neutrophils are being recruited to the site of inflammation and undergo degranulation upon activation. Furthermore, a tri-paucimannosidic HNE glycoform was shown to be a highly preferred binding partner of MBL, in agreement with previous reports demonstrating high avidity binding of multi-mannosylated structures to mannose recognising receptors (Feinberg et al., 2001). In summary, these findings have now established that biological important paucimannosidic *N*-glycoprotein are capable of binding to mrCLRs. It still remains for future research to unravel whether the binding of paucimannosidic proteins to mrCLRs is facilitating the transmission of specific signals. For example, to activate the lectin complement pathway for MBL or using immunoreceptor tyrosine-based activation/inhibition motif (ITAM/ITIM) signalling motifs with respect to other membrane bound mrCLRs such as mannose receptors or if the binding is more relevant in the context of cell-cell interactions potentially acting as molecular decoys or mimicry.

Furthermore, there has been a continuous push in the development of small molecule therapeutics that are able to inhibit the deleterious elastin degrading activity of HNE in a controlled manner, particularly in pulmonary diseases where excessive HNE-based degradation occur (Groutas et al., 2011; Tsai and Hwang, 2015). It is also known that the main physiological inhibitor of HNE, A1AT, regulates the proteolysis activities of HNE. Imbalanced levels of A1AT and HNE via this mechanism can be a contributor of pulmonary damage and disease (Guyot et al., 2014). The A1AT-based inhibition of the human serine proteases has been well studied using X-ray crystallography (Elliott et al., 1996; Huntington et al., 2000). However, these studies were not assessed using HNE, but instead using the unglycosylated trypsin as a model serine protease. Only a single study has investigated the involvement of *N*-glycosylation in the anti-protease activity of A1AT, which was performed using hydrogen/deuterium exchange and mass spectrometry (Sarkar and Wintrode, 2011). The authors concluded that the glycosylation of A1AT are not likely to interfere with its anti-protease activity but may confer resistance towards its degradation by proteases and therefore extending its half-life in circulation. Hence, there is a gap in knowledge that prevents addressing the importance of *N*-glycosylation on the interactions between A1AT and HNE or

A1AT-HNE complexes since these aspects have not been previously considered in the earlier studies mentioned above.

As presented in **Chapter 5, Publication V**, HNE and A1AT were, for the first time, shown to display preferential glycoform-glycoform interactions. The sialylated HNE was found to exhibit a higher propensity for engaging in an inhibitor complex with an undersialylated form of A1AT. Although speculative in nature, this phenomenon may be due to the fact that less sialylated A1AT may bind to HNE more readily as it is less likely to cause steric hindrance. The abundant sialylation of A1AT and the negatively charged amino acid residues found at the exosite of A1AT may, in contrast, play stimulating roles in the binding to HNE via electrostatic mechanisms, which has a highly basic protein surface with a net charge of +10 at neutral pH (Rashid et al., 2015). However, future structural biological research and investigations through the use of molecular dynamic simulations may be required to obtain more insights into their exact interactions (Andersen et al., 2016). To the best of my knowledge, this is the first study that has assessed and determined the influence of *N*-glycosylation on both protein partners with respect to the propensity of their respective glycoforms to engage in a common enzyme: inhibitor complex. The findings presented here, and the future research it encourages, may have an impact on the rational design and development of recombinant forms of human A1AT for therapeutic usage (McElvaney, 2016; Pirooznia et al., 2013).

Chapter 5, Publication V also presented a highly exciting yet still not fully resolved observation, demonstrating that HNE and the released *N*-glycans from HNE display weak bacteriostatic activity towards a clinically isolated strain of *Pseudomonas aeruginosa*. Although HNE is known for its bacteriostatic activity through its potent proteolytic activity (Belaouaj et al., 1998; Hirche et al., 2008), this is the first time that bacteriostatic activity has been reported, solely facilitated by the released *N*-glycans of HNE. The mechanism of the bacteriostatic activity of the released *N*-glycans might be attributed to the binding of these *N*-glycans to the lectins or so-called adhesins such as PA-IIL that are expressed by *Pseudomonas aeruginosa*. These adhesins have been known to bind to mannosidic glycoepitopes, but with much lower affinities compared to fucosylated glycoepitopes (Mitchell et al., 2005). Nevertheless, how this binding confers bacteriostatic activity is still currently unknown. It is also plausible, at this stage that the current interpretation of “bacterial growth inhibition” over the 12 h time course period in the bacteriostatic activity assay, may be caused by a metabolic switch of *Pseudomonas aeruginosa* due to the presence of a new carbon-rich environment

when *N*-glycans are added. Following this line of thought, the HNE *N*-glycans might be sensed by the bacteria as a carbohydrate-rich environment and a potential carbon source which may, in turn, be conducive for biofilm formation through its quorum sensors (De Kievit et al., 2001). Thus, this could temporally reduce the metabolism and growth rate of the bacteria. However, this alternative mechanism as opposed to the original and more exciting interpretation of a true bacteriostatic activity of the *N*-glycans needs to be fully explored in the future.

In conclusion, the above findings have provided multiple lines of evidence of different nature to support the role of paucimannosylation of HNE in modulating its immune function and the host immune system. It is highly likely that these protein-specific functions of paucimannosylation, which needs to be validated further through orthogonal methods, are facilitated through various different molecular mechanisms. These findings will be useful to better understand the function and implication of protein paucimannosylation in neutrophil biology, and may serve as a source of fundamental knowledge to stimulate the design of therapeutic targets and candidates in the future to resolve inflammatory conditions or the prevention of bacterial infections.

7.5 Protein paucimannosylation in other human cell types

Apart from human neutrophils, this thesis has also uncovered that protein paucimannosylation is also a feature of other human cell types. Initially, the capacity of a range of immune cell populations to produce protein paucimannosylation was explored from publicly available CFG glycome datasets. These preliminary observations indicated that protein paucimannosylation was found in both myeloid and lymphoid cells (Dr Morten Thaysen-Andersen, unpublished observations). However, the *N*-glycome of platelets and other immune and non-immune cells could not be studied using this retrospective data analysis approach. Thus, the initial CFG-based studies were expanded (as presented in **Chapter 6**) by isolating immune cells from a single donor and performing *N*-glycan profiling using PGC-LC-MS/MS. These efforts illustrated that lymphocytes and platelets do have the capacity to produce paucimannosidic *N*-glycans, albeit as a less significant glycosylation signature compared to neutrophils, where paucimannosylation appeared as a dominating feature. In addition in establishing that human neutrophils are not unique in their capacity to generate paucimannosylation, this is also the first report detailing the *N*-glycome of whole resting platelets, which consist mostly of high mannose and complex type *N*-glycans. These studies

also served the purpose of validating and adding further structural depth to the *N*-glycome of lymphocytes and neutrophils that were previously documented in the CFG glycome database by the less informative MALDI-TOF-MS profiling technology.

In addition, the regulation of the *N*-glycoproteome and proteome, in particular changes in the paucimannosidic species of macrophage-like cells differentiated from the myelocytic cell line THP-1, were studied in **Chapter 6, Publication VI** over a 72 h time course during *M. tb* infection to stimulate early TB infection. It was noted that the intracellular level of protein paucimannosylation in infected cells decreased significantly upon *M. tb* infection. The ability of *M. tb* to modulate the immune response of infected macrophages for its survival by mechanisms of limiting lysosome-phagosome fusion and reducing organelle acidification has been shown previously (Awuh and Flo, 2016; Kang et al., 2005). The reduction in the intracellular paucimannosylated proteins might be attributed to an increase in secretion of these proteins into the extracellular matrix, where they could have further potential functions in mediating the immune response by the host. Alternatively it could also be pathogen driven by *M. tb*. In addition, the reduction in Hex A activity suggests that these hexosaminidases might confer some host immune protection against *Mycobacterium*.

The finding of paucimannosylation in other immune white blood cells suggests that protein paucimannosylation could serve wider, perhaps less specialised, functional roles in lymphocytes, platelets, macrophages and potentially other myeloid cells such as eosinophils, basophils and monocytes, together with lymphoid cells such as NK cells. The latter were not studied in this thesis and their *N*-glycomes remain to be mapped in order to determine their paucimannose generating capacity.

Nevertheless, it is important to stress that *N*-glycome analyses of the whole cell lysates of these immune cells are not sufficient in itself to establish that protein paucimannosylation is an important structural and functional feature in these immune cells. System-wide glycoproteomics analysis in the individual immune cell populations and even on the subcellular level, will ensure that these truncated structures are carried by proteins rather than being degradation products. This could provide more insights into the nature of the protein carriers and in turn, may provide some early clues as to the function of these paucimannosylated *N*-glycoproteins in the various cell types.

In addition to haematopoietic immune cells, protein paucimannosylation was also identified in neural progenitor stem cells localised in the subventricular zone of the hippocampus in the

mouse brain (**Publication VII**). Glioblastoma cells A172 cells treated with AraC, displayed an increase in paucimannosidic glycoepitopes with arrested cell proliferation compared to normal proliferating cells. This demonstrates that paucimannosylated proteins in these cells may be involved in the regulation of cell proliferation and differentiation. Recently, human induced pluripotent stem cells and embryonic stem cells have also been documented to carry paucimannosylated proteins (Furukawa et al., 2016; Satomaa et al., 2009). All these observations suggest that paucimannosylation might be important in the maintenance of “stemness” in early progenitor stem cells and during neuronal development in the brain.

At this stage, it is not known if protein paucimannosylation is present in other human cell types apart from those that were studied within the scope of this thesis. As such, *N*-glycome profiling of other human cell types including hepatocytes that are known to be rich in β -hexosaminidases (Hechtman and Kachra, 1980) and the specialised mast cells and DCs would be highly interesting. The presence of protein paucimannosylation in human neutrophils, lymphocytes, platelets, macrophages and in neural stem cells points to a wider presence of paucimannose in other cell types that are yet-to-be investigated. This has been generally supported by the retrospective curation of the limited literature and available raw empirical data in this field. Taken together, multiple lines of evidence demonstrate that paucimannosylation, apart from its function in immunity, may play wider roles during cellular development and differentiation. These cellular processes can generally be classified into physiological and pathological conditions that are centric to immunity, inflammation, stemness and cancer (Zipser et al., 2012).

7.6 Concluding remarks

The main aim of this thesis was to increase our understanding of the newly discovered glycan modification; protein paucimannosylation in human neutrophils in the context of their biosynthesis, structure and function. These aspects were investigated at multiple cellular levels including the whole cell level, for example, the whole neutrophil lysates and the subcellular level involving the analysis of neutrophil granules and the plasma membrane. In both of these domains, the biomolecular focus was either system-wide, for example, the detection of the entire *N*-glycome or *N*-glycoproteome or targeted to specific analytes at a single glycoprotein level. The combined use of glycomics, glycoproteomics and intact glycoprotein analysis techniques has enabled 1) deep glycan characterisation, 2) the determination of their relative abundances and 3) the site-specific glycan occupancies of

several important azurophilic granule glycoproteins. In addition, these techniques were also essential for mapping the system-wide *N*-glycosylation features of neutrophils.

Importantly, the observation of ultra-truncated chitobiose core structures on nCG clearly deserves further investigation to elucidate their functional roles in the host immune system or in the folding of the protein during synthesis. The capacity of the paucimannose-rich HNE to modulate its immune functions through interactions with mCLRs and the inhibitory interplay with A1AT, indicate that paucimannosylation is essential to mediate immunological functions of neutrophils. This was further supported by the discovery of paucimannosylated HNE on the cell surface of activated neutrophils. In addition, the contribution of β -hexosaminidases in the generation of paucimannosylated proteins, as well as the presence of paucimannosylated protein in other immune cell populations and neural stem cells, further strengthens the wider functional roles that paucimannosylated proteins play in the host immune system and in maintaining normal cellular homeostasis. These results strongly support the importance of protein paucimannosylation in neutrophil biology.

In conclusion, the work described in this thesis provides substantial support for the notion that protein paucimannosylation is a significant glycosylation signature in human neutrophils and in other immune and non-immune cells. These unconventional *N*-glycosylation features are involved in a variety of immunological functions that, individually or as a whole, can serve to modulate or directly change the host immune response in a spatial-temporal fashion. The findings disseminated in this work are mostly open ended in nature and more questions than answers have been presented. Nonetheless, future research initiatives building on these findings presented in thesis will bring us one step closer to a more complete understanding of these unconventional and unusual glycoepitopes and their involvement in innate immunity. Together, all these points to the need of continuing and intensifying our research efforts into these intriguing glycoconjugates. This is to achieve a greater understanding of their functional roles under physiological and pathological conditions in order to answer further and more targeted biological questions.

References

- Abès, R., Teillaud, J.-L., 2010. Impact of Glycosylation on Effector Functions of Therapeutic IgG. *Pharmaceuticals* 3 (1), 146-157. doi:10.3390/ph3010146
- Abkowitz, J.L., Catlin, S.N., Gutter, P., 1996. Evidence that hematopoiesis may be a stochastic process in vivo. *Nature Medicine* 2 (2), 190-197.
- Aebi, M., 2013. N-linked protein glycosylation in the ER. *Biochimica et Biophysica Acta* 1833 (11), 2430-2437. doi:10.1016/j.bbamcr.2013.04.001
- Aebi, M., Bernasconi, R., Clerc, S., Molinari, M., 2010. N-glycan structures: recognition and processing in the ER. *Trends in Biochemical Sciences* 35 (2), 74-82. doi:10.1016/j.tibs.2009.10.001
- Akashi, K., Traver, D., Miyamoto, T., Weissman, I.L., 2000. A clonogenic common myeloid progenitor that gives rise to all myeloid lineages. *Nature* 404 (6774), 193-197. doi:10.1038/35004599
- Alberts, B., 2002. *Molecular biology of the cell*, 4th ed. Garland Science, New York.
- Alley, W.R., Jr., Mechref, Y., Novotny, M.V., 2009. Characterization of glycopeptides by combining collision-induced dissociation and electron-transfer dissociation mass spectrometry data. *Rapid Communications in Mass Spectrometry* 23 (1), 161-170. doi:10.1002/rcm.3850
- Altmann, F., Schwihla, H., Staudacher, E., Glossl, J., Marz, L., 1995. Insect cells contain an unusual, membrane-bound beta-N-acetylglucosaminidase probably involved in the processing of protein N-glycans. *Journal of Biological Chemistry* 270 (29), 17344-17349.
- Andersen, O.J., Risor, M.W., Poulsen, E.C., Nielsen, N.C., Miao, Y., Enghild, J.J., Schiott, B., 2016. The reactive center loop insertion in alpha-1-antitrypsin captured by accelerated molecular dynamics simulation. *Biochemistry*. doi:10.1021/acs.biochem.6b00839

- Anugraham, M., Jacob, F., Nixdorf, S., Everest-Dass, A.V., Heinzelmann-Schwarz, V., Packer, N.H., 2014. Specific glycosylation of membrane proteins in epithelial ovarian cancer cell lines: glycan structures reflect gene expression and DNA methylation status. *Molecular & Cellular Proteomics* 13 (9), 2213-2232. doi:10.1074/mcp.M113.037085
- Apweiler, R., Hermjakob, H., Sharon, N., 1999. On the frequency of protein glycosylation, as deduced from analysis of the SWISS-PROT database. *Biochimica et Biophysica Acta* 1473 (1), 4-8.
- Arthur, C.M., Cummings, R.D., Stowell, S.R., 2014. Using glycan microarrays to understand immunity. *Current Opinion in Chemical Biology* 18, 55-61. doi:10.1016/j.cbpa.2013.12.017
- Avinash, S., Nutan, S., Troy, M., Paige, L., Gary, E., 2014. Granule Protein Processing and Regulated Secretion in Neutrophils. *Frontiers in Immunology* 5. doi:10.3389/fimmu.2014.00448
- Awuh, J.A., Flo, T.H., 2016. Molecular basis of mycobacterial survival in macrophages. *Cellular and Molecular Life Sciences*. doi:10.1007/s00018-016-2422-8
- Babes, L., Kubes, P., 2016. Visualizing the Tumor Microenvironment of Liver Metastasis by Spinning Disk Confocal Microscopy. *Methods in Molecular Biology* 1458, 203-215. doi:10.1007/978-1-4939-3801-8_15
- Babu, P., North, S.J., Jang-Lee, J., Chalabi, S., Mackerness, K., Stowell, S.R., Cummings, R.D., Rankin, S., Dell, A., Haslam, S.M., 2009. Structural characterisation of neutrophil glycans by ultra sensitive mass spectrometric glycomics methodology. *Glycoconjugate Journal* 26 (8), 975-986. doi:10.1007/s10719-008-9146-4
- Bainton, D.F., Farquhar, M.G., 1966. Origin of granules in polymorphonuclear leukocytes. Two types derived from opposite faces of the Golgi complex in developing granulocytes. *Journal of Cell Biology* 28 (2), 277-301. PMC2106917
- Bakowski, B., Tschesche, H., 1992. Migration of polymorphonuclear leukocytes through human amnion membrane--a scanning electron microscopic study. *Biological Chemistry Hoppe-Seyler* 373 (7), 529-546.

References

- Balog, C.I., Stavenhagen, K., Fung, W.L., Koeleman, C.A., McDonnell, L.A., Verhoeven, A., Mesker, W.E., Tollenaar, R.A., Deelder, A.M., Wuhrer, M., 2012. N-glycosylation of colorectal cancer tissues: a liquid chromatography and mass spectrometry-based investigation. *Molecular & Cellular Proteomics* 11 (9), 571-585. doi:10.1074/mcp.M111.011601
- Barone, R., Sturiale, L., Fiumara, A., Palmigiano, A., Bua, R.O., Rizzo, R., Zappia, M., Garozzo, D., 2016. CSF N-glycan profile reveals sialylation deficiency in a patient with GM2 gangliosidosis presenting as childhood disintegrative disorder. *Autism Research* 9 (4), 423-428. doi:10.1002/aur.1541
- Bartlett, D.W., Davis, M.E., 2006. Insights into the kinetics of siRNA-mediated gene silencing from live-cell and live-animal bioluminescent imaging. *Nucleic Acids Research* 34 (1), 322-333. doi:10.1093/nar/gkj439
- Bedoui, S., Gebhardt, T., Gasteiger, G., Kastenmuller, W., 2016. Parallels and differences between innate and adaptive lymphocytes. *Nature Immunology* 17 (5), 490-494. doi:10.1038/ni.3432
- Belaouaj, A., McCarthy, R., Baumann, M., Gao, Z., Ley, T.J., Abraham, S.N., Shapiro, S.D., 1998. Mice lacking neutrophil elastase reveal impaired host defense against gram negative bacterial sepsis. *Nature Medicine* 4 (5), 615-618.
- Bennett, S., Breit, S.N., 1994. Variables in the isolation and culture of human monocytes that are of particular relevance to studies of HIV. *Journal of Leukocyte Biology* 56 (3), 236-240.
- Bennun, S.V., Hizal, D.B., Heffner, K., Can, O., Zhang, H., Betenbaugh, M.J., 2016. Systems Glycobiology: Integrating Glycogenomics, Glycoproteomics, Glycomics, and Other 'Omics Data Sets to Characterize Cellular Glycosylation Processes. *Journal of Molecular Biology*. doi:10.1016/j.jmb.2016.07.005
- Bern, M., Kil, Y.J., Becker, C., 2012. Byonic: advanced peptide and protein identification software. *Curr Protoc Bioinformatics* Chapter 13, 20. doi:10.1002/0471250953.bi1320s40

- Bhide, G.P., Colley, K.J., 2016. Sialylation of N-glycans: mechanism, cellular compartmentalization and function. *Histochemistry and Cell Biology*. doi:10.1007/s00418-016-1520-x
- Binker, M.G., Cosen-Binker, L.I., Terebiznik, M.R., Mallo, G.V., McCaw, S.E., Eskelinen, E.L., Willenborg, M., Brumell, J.H., Saftig, P., Grinstein, S., Gray-Owen, S.D., 2007. Arrested maturation of Neisseria-containing phagosomes in the absence of the lysosome-associated membrane proteins, LAMP-1 and LAMP-2. *Cellular Microbiology* 9 (9), 2153-2166. doi:10.1111/j.1462-5822.2007.00946.x
- Birnie, G.D., 1988. The HL60 cell line: a model system for studying human myeloid cell differentiation. *British Journal of Cancer. Supplement* 9, 41-45. PMC2149104
- Bjerregaard, M.D., Jurlander, J., Klausen, P., Borregaard, N., Cowland, J.B., 2003. The in vivo profile of transcription factors during neutrophil differentiation in human bone marrow. *Blood* 101 (11), 4322-4332. doi:10.1182/blood-2002-03-0835
- Björnsdóttir, H., Welin, A., Michaëlsson, E., Osla, V., Berg, S., Christenson, K., Sundqvist, M., Dahlgren, C., Karlsson, A., Bylund, J., 2015. Neutrophil NET formation Is regulated from the inside by myeloperoxidase-processed reactive oxygen species. *Free Radical Biology and Medicine*. doi:10.1016/j.freeradbiomed.2015.10.398
- Borregaard, N., 1997. Development of neutrophil granule diversity. *Annals of the New York Academy of Sciences* 832 (1 Phagocytes), 62-68. doi:10.1111/j.1749-6632.1997.tb46237.x
- Borregaard, N., 2015. Neutrophils. *eLS*, 1-11. doi:10.1002/9780470015902.a0001219.pub2
- Borregaard, N., Cowland, J.B., 1997. Granules of the human neutrophilic polymorphonuclear leukocyte. *Blood* 89 (10), 3503-3521.
- Borregaard, N., Kjeldsen, L., Rygaard, K., Bastholm, L., Nielsen, M.H., Sengelov, H., Bjerrum, O.W., Johnsen, A.H., 1992. Stimulus-dependent secretion of plasma proteins from human neutrophils. *Journal of Clinical Investigation* 90 (1), 86-96. doi:10.1172/jci115860

References

Borregaard, N., Sehested, M., Nielsen, B.S., Sengelov, H., Kjeldsen, L., 1995. Biosynthesis of granule proteins in normal human bone marrow cells. Gelatinase is a marker of terminal neutrophil differentiation. *Blood* 85 (3), 812-817.

Borregaard, N., Sorensen, O.E., Theilgaard-Monch, K., 2007. Neutrophil granules: a library of innate immunity proteins. *Trends in Immunology* 28 (8), 340-345. doi:10.1016/j.it.2007.06.002

Borregaard, N., Theilgaard-Monch, K., Sorensen, O.E., Cowland, J.B., 2001. Regulation of human neutrophil granule protein expression. *Current Opinion in Hematology* 8 (1), 23-27.

Bourgoin-Voillard, S., Leymarie, N., Costello, C.E., 2014. Top-down tandem mass spectrometry on RNase A and B using a Qh/FT-ICR hybrid mass spectrometer. *Proteomics* 14 (10), 1174-1184. doi:10.1002/pmic.201300433

Bousfield, G.R., Butnev, V.Y., White, W.K., Hall, A.S., Harvey, D.J., 2015. Comparison of Follicle-Stimulating Hormone Glycosylation Microheterogeneity by Quantitative Negative Mode Nano-Electrospray Mass Spectrometry of Peptide-N Glycanase-Released Oligosaccharides. *J Glycomics Lipidomics* 5 (1). doi:10.4172/2153-0637.1000129

Boussif, A., Rolas, L., Weiss, E., Bouriche, H., Moreau, R., Perianin, A., 2016. Impaired intracellular signaling, myeloperoxidase release and bactericidal activity of neutrophils from patients with alcoholic cirrhosis. *Journal of Hepatology* 64 (5), 1041-1048. doi:10.1016/j.jhep.2015.12.005

Breitling, J., Aeby, M., 2013. N-linked protein glycosylation in the endoplasmic reticulum. *Cold Spring Harbor Perspectives in Biology* 5 (8), a013359. doi:10.1101/cshperspect.a013359

Brummelkamp, T.R., Bernards, R., Agami, R., 2002. A system for stable expression of short interfering RNAs in mammalian cells. *Science* 296 (5567), 550-553. doi:10.1126/science.1068999

Burster, T., Macmillan, H., Hou, T., Boehm, B.O., Mellins, E.D., 2010. Cathepsin G: roles in antigen presentation and beyond. *Molecular Immunology* 47 (4), 658-665. doi:10.1016/j.molimm.2009.10.003

- Buszewski, B., Noga, S., 2012. Hydrophilic interaction liquid chromatography (HILIC)--a powerful separation technique. *Analytical and Bioanalytical Chemistry* 402 (1), 231-247. doi:10.1007/s00216-011-5308-5
- Bye, A.P., Unsworth, A.J., Gibbins, J.M., 2016. Platelet signaling: a complex interplay between inhibitory and activatory networks. *Journal of Thrombosis and Haemostasis* 14 (5), 918-930. doi:10.1111/jth.13302
- Calafat, J., Janssen, H., Knol, E.F., Malm, J., Egesten, A., 2000. The bactericidal/permeability-increasing protein (BPI) is membrane-associated in azurophil granules of human neutrophils, and relocation occurs upon cellular activation. *APMIS* 108 (3), 201-208.
- Calafat, J., Kuijpers, T.W., Janssen, H., Borregaard, N., Verhoeven, A.J., Roos, D., 1993. Evidence for small intracellular vesicles in human blood phagocytes containing cytochrome b558 and the adhesion molecule CD11b/CD18. *Blood* 81 (11), 3122-3129.
- Campbell, E.J., Owen, C.A., 2007. The sulfate groups of chondroitin sulfate- and heparan sulfate-containing proteoglycans in neutrophil plasma membranes are novel binding sites for human leukocyte elastase and cathepsin G. *Journal of Biological Chemistry* 282 (19), 14645-14654. doi:10.1074/jbc.M608346200
- Campbell, M.P., Nguyen-Khuong, T., Hayes, C.A., Flowers, S.A., Alagesan, K., Kolarich, D., Packer, N.H., Karlsson, N.G., 2014a. Validation of the curation pipeline of UniCarb-DB: building a global glycan reference MS/MS repository. *Biochimica et Biophysica Acta* 1844 (1 Pt A), 108-116. doi:10.1016/j.bbapap.2013.04.018
- Campbell, M.P., Peterson, R., Mariethoz, J., Gasteiger, E., Akune, Y., Aoki-Kinoshita, K.F., Lisacek, F., Packer, N.H., 2014b. UniCarbKB: building a knowledge platform for glycoproteomics. *Nucleic Acids Research* 42, D215-221. doi:10.1093/nar/gkt1128
- Canis, K., McKinnon, T.A., Nowak, A., Haslam, S.M., Panico, M., Morris, H.R., Laffan, M.A., Dell, A., 2012. Mapping the N-glycome of human von Willebrand factor. *Biochemical Journal* 447 (2), 217-228. doi:10.1042/BJ20120810

References

- Carestia, A., Kaufman, T., Schattner, M., 2016. Platelets: New Bricks in the Building of Neutrophil Extracellular Traps. *Frontiers in Immunology* 7. doi:10.3389/fimmu.2016.00271
- Caron, E., Hall, A., 1998. Identification of two distinct mechanisms of phagocytosis controlled by different Rho GTPases. *Science* 282 (5394), 1717-1721.
- Casal, J.A., Cano, E., Tutor, J.C., 2005. Beta-hexosaminidase isoenzyme profiles in serum, plasma, platelets and mononuclear, polymorphonuclear and unfractionated total leukocytes. *Clinical Biochemistry* 38 (10), 938-942. doi:10.1016/j.clinbiochem.2005.05.016
- Casal, J.A., Chabás, A., Tutor, J.C., 2003. Thermodynamic determination of beta-hexosaminidase isoenzymes in mononuclear and polymorphonuclear leukocyte populations. *American Journal of Medical Genetics. Part A* 116A (3), 229-233. doi:10.1002/ajmg.a.10891
- Catherman, A.D., Skinner, O.S., Kelleher, N.L., 2014. Top Down proteomics: facts and perspectives. *Biochemical and Biophysical Research Communications* 445 (4), 683-693. doi:10.1016/j.bbrc.2014.02.041
- Ceroni, A., Maass, K., Geyer, H., Geyer, R., Dell, A., Haslam, S.M., 2008. GlycoWorkbench: a tool for the computer-assisted annotation of mass spectra of glycans. *Journal of Proteome Research* 7 (4), 1650-1659. doi:10.1021/pr7008252
- Cham, B.P., Gerrard, J.M., Bainton, D.F., 1994. Granulophysin is located in the membrane of azurophilic granules in human neutrophils and mobilizes to the plasma membrane following cell stimulation. *The American Journal of Pathology* 144 (6), 1369-1380.
- Chandler, K.B., Costello, C.E., 2016. Glycomics and glycoproteomics of membrane proteins and cell-surface receptors: Present trends and future opportunities. *Electrophoresis* 37 (11), 1407-1419. doi:10.1002/elps.201500552
- Chang, H.H., Hemberg, M., Barahona, M., Ingber, D.E., Huang, S., 2008. Transcriptome-wide noise controls lineage choice in mammalian progenitor cells. *Nature* 453 (7194), 544-547. doi:10.1038/nature06965

- Cheng, A., Magdaleno, S., Vlassov, A.V., 2011. Optimization of transfection conditions and analysis of siRNA potency using real-time PCR. *Methods in Molecular Biology* 764, 199-213. doi:10.1007/978-1-61779-188-8_13
- Chu, F.K., 1986. Requirements of cleavage of high mannose oligosaccharides in glycoproteins by peptide N-glycosidase F. *Journal of Biological Chemistry* 261 (1), 172-177.
- Cieutat, A.M., Lobel, P., August, J.T., Kjeldsen, L., Sengelov, H., Borregaard, N., Bainton, D.F., 1998. Azurophilic granules of human neutrophilic leukocytes are deficient in lysosome-associated membrane proteins but retain the mannose 6-phosphate recognition marker. *Blood* 91 (3), 1044-1058.
- Clemetson, K.J., 2012. Platelets and primary haemostasis. *Thrombosis Research* 129 (3), 220-224. doi:10.1016/j.thromres.2011.11.036
- Clemmensen, S.N., Udby, L., Borregaard, N., 2014. Subcellular fractionation of human neutrophils and analysis of subcellular markers. *Methods in Molecular Biology* 1124, 53-76. doi:10.1007/978-1-62703-845-4_5
- Cobaleda, C., Jochum, W., Busslinger, M., 2007. Conversion of mature B cells into T cells by dedifferentiation to uncommitted progenitors. *Nature* 449 (7161), 473-477. doi:10.1038/nature06159
- Coelho, V., Krysov, S., Ghaemmighami, A.M., Emara, M., Potter, K.N., Johnson, P., Packham, G., Martinez-Pomares, L., Stevenson, F.K., 2010. Glycosylation of surface Ig creates a functional bridge between human follicular lymphoma and microenvironmental lectins. *Proceedings of the National Academy of Sciences of the United States of America* 107 (43), 18587-18592. doi:10.1073/pnas.1009388107
- Coico, R., Sunshine, G., 2009. *Immunology : a short course*, 6th ed. John Wiley, New Jersey
- Colli, W., 1993. Trans-sialidase: a unique enzyme activity discovered in the protozoan *Trypanosoma cruzi*. *FASEB Journal* 7 (13), 1257-1264.

References

Collin, M., Bigley, V., 2016. Monocyte, Macrophage, and Dendritic Cell Development: the Human Perspective. *Microbiol Spectr* 4 (5). doi:10.1128/microbiolspec.MCHD-0015-2015

Collin, M., Olsen, A., 2001. EndoS, a novel secreted protein from *Streptococcus pyogenes* with endoglycosidase activity on human IgG. *EMBO Journal* 20 (12), 3046-3055. doi:10.1093/emboj/20.12.3046

Collins, S.J., Ruscetti, F.W., Gallagher, R.E., Gallo, R.C., 1978. Terminal differentiation of human promyelocytic leukemia cells induced by dimethyl sulfoxide and other polar compounds. *Proceedings of the National Academy of Sciences of the United States of America* 75 (5), 2458-2462. doi:10.1073/pnas.75.5.2458

Conboy, J.J., Henion, J.D., 1992. The determination of glycopeptides by liquid chromatography/mass spectrometry with collision-induced dissociation. *Journal of the American Society for Mass Spectrometry* 3 (8), 804-814. doi:10.1016/1044-0305(92)80003-4

Cooper, C.A., Gasteiger, E., Packer, N.H., 2001. GlycoMod--a software tool for determining glycosylation compositions from mass spectrometric data. *Proteomics* 1 (2), 340-349. doi:10.1002/1615-9861(200102)1:2<340::AID-PROT340>3.0.CO;2-B

Cowland, J.B., Borregaard, N., 1999. The individual regulation of granule protein mRNA levels during neutrophil maturation explains the heterogeneity of neutrophil granules. *Journal of Leukocyte Biology* 66 (6), 989-995.

Cowland, J.B., Borregaard, N., 2016. Granulopoiesis and granules of human neutrophils. *Immunological Reviews* 273 (1), 11-28. doi:10.1111/imr.12440

Dahmen, A.C., Fergen, M.T., Laurini, C., Schmitz, B., Loke, I., Thaysen-Andersen, M., Diestel, S., 2015. Paucimannosidic glycoepitopes are functionally involved in proliferation of neural progenitor cells in the subventricular zone. *Glycobiology* 25 (8), 869-880. doi:10.1093/glycob/cwv027

Dalby, B., Cates, S., Harris, A., Ohki, E.C., Tilkins, M.L., Price, P.J., Ciccarone, V.C., 2004. Advanced transfection with Lipofectamine 2000 reagent: primary neurons, siRNA, and high-throughput applications. *Methods* 33 (2), 95-103. doi:10.1016/j.ymeth.2003.11.023

- Dalpathado, D.S., Desaire, H., 2008. Glycopeptide analysis by mass spectrometry. *Analyst* 133 (6), 731-738. doi:10.1039/b713816d
- Dam, S., Thaysen-Andersen, M., Stenkjaer, E., Lorentzen, A., Roepstorff, P., Packer, N.H., Stougaard, J., 2013. Combined n-glycome and n-glycoproteome analysis of the lotus japonicus seed globulin fraction shows conservation of protein structure and glycosylation in legumes. *Journal of Proteome Research* 12 (7), 3383-3392. doi:10.1021/pr400224s
- Dancey, J.T., Deubelbeiss, K.A., Harker, L.A., Finch, C.A., 1976. Neutrophil kinetics in man. *Journal of Clinical Investigation* 58 (3), 705-715. doi:10.1172/jci108517
- De Kievit, T.R., Gillis, R., Marx, S., Brown, C., Iglewski, B.H., 2001. Quorum-sensing genes in *Pseudomonas aeruginosa* biofilms: their role and expression patterns. *Applied and Environmental Microbiology* 67 (4), 1865-1873. doi:10.1128/aem.67.4.1865-1873.2001
- Delclaux, C., Delacourt, C., D'Ortho, M.P., Boyer, V., Lafuma, C., Harf, A., 1996. Role of gelatinase B and elastase in human polymorphonuclear neutrophil migration across basement membrane. *American Journal of Respiratory Cell and Molecular Biology* 14 (3), 288-295. doi:10.1165/ajrcmb.14.3.8845180
- Deshpande, N., Jensen, P.H., Packer, N.H., Kolarich, D., 2010. GlycoSpectrumScan: fishing glycopeptides from MS spectra of protease digests of human colostrum sIgA. *Journal of Proteome Research* 9 (2), 1063-1075. doi:10.1021/pr900956x
- Devi, S., Wang, Y., Chew, W.K., Lima, R., N, A.G., Mattar, C.N., Chong, S.Z., Schlitzer, A., Bakocevic, N., Chew, S., Keeble, J.L., Goh, C.C., Li, J.L., Evrard, M., Malleret, B., Larbi, A., Renia, L., Haniffa, M., Tan, S.M., Chan, J.K., Balabanian, K., Nagasawa, T., Bachelier, F., Hidalgo, A., Ginhoux, F., Kubes, P., Ng, L.G., 2013. Neutrophil mobilization via plerixafor-mediated CXCR4 inhibition arises from lung demargination and blockade of neutrophil homing to the bone marrow. *Journal of Experimental Medicine* 210 (11), 2321-2336. doi:10.1084/jem.20130056
- Di Palma, S., Boersema, P.J., Heck, A.J., Mohammed, S., 2011. Zwitterionic hydrophilic interaction liquid chromatography (ZIC-HILIC and ZIC-cHILIC) provide high resolution

References

separation and increase sensitivity in proteome analysis. *Analytical Chemistry* 83 (9), 3440-3447. doi:10.1021/ac103312e

Ding, L., Saunders, T.L., Enikolopov, G., Morrison, S.J., 2012. Endothelial and perivascular cells maintain haematopoietic stem cells. *Nature* 481 (7382), 457-462. doi:10.1038/nature10783

Domon, B., Costello, C.E., 1988. A systematic nomenclature for carbohydrate fragmentations in FAB-MS/MS spectra of glycoconjugates. *Glycoconjugate Journal* 5 (4), 397-409. doi:10.1007/bf01049915

Dudzik, D., Knas, M., Gocal, M., Borzym-Kluczyk, M., Szajda, S.D., Knas-Karaszevska, K., Tomaszewski, J., Zwierz, K., 2008. Activity of N-acetyl-beta-D-hexosaminidase (HEX) and its isoenzymes A and B in human milk during the first 3 months of breastfeeding. *Advances in Medical Sciences* 53 (2), 300-304. doi:10.2478/v10039-008-0036-6

Dunn, K.W., Kamocka, M.M., McDonald, J.H., 2011. A practical guide to evaluating colocalization in biological microscopy. *American Journal of Physiology: Cell Physiology* 300 (4), C723-742. doi:10.1152/ajpcell.00462.2010

Dyachenko, A., Wang, G., Belov, M., Makarov, A., de Jong, R.N., van den Bremer, E.T., Parren, P.W., Heck, A.J., 2015. Tandem Native Mass-Spectrometry on Antibody-Drug Conjugates and Submillion Da Antibody-Antigen Protein Assemblies on an Orbitrap EMR Equipped with a High-Mass Quadrupole Mass Selector. *Analytical Chemistry* 87 (12), 6095-6102. doi:10.1021/acs.analchem.5b00788

Eash, K.J., Greenbaum, A.M., Gopalan, P.K., Link, D.C., 2010. CXCR2 and CXCR4 antagonistically regulate neutrophil trafficking from murine bone marrow. *Journal of Clinical Investigation* 120 (7), 2423-2431. doi:10.1172/jci41649

Elliott, P.R., Lomas, D.A., Carrell, R.W., Abrahams, J.P., 1996. Inhibitory conformation of the reactive loop of alpha 1-antitrypsin. *Nature Structural Biology* 3 (8), 676-681.

Elzbieta, K., Paul, K., 2013. Neutrophil recruitment and function in health and inflammation. *Nature reviews. Immunology* 13 (3), 159-175. doi:10.1038/nri3399

- Emiliani, C., Beccari, T., Tabilio, A., Orlacchio, A., Hosseini, R., Stirling, J.L., 1990a. An enzyme with properties similar to those of beta-N-acetylhexosaminidase S is expressed in the promyelocytic cell line HL-60. *The Biochemical Journal* 267 (1), 111-117.
- Emiliani, C., Falzetti, F., Orlacchio, A., Stirling, J.L., 1990b. Treatment of HL-60 cells with dimethyl sulphoxide inhibits the formation of beta-N-acetylhexosaminidase S. *The Biochemical Journal* 272 (1), 211-215.
- Emiliani, C., Falzetti, F., Orlacchio, A., Stirling, J.L., 1990c. Treatment of HL-60 cells with dimethyl sulphoxide inhibits the formation of beta-N-acetylhexosaminidase S. *Biochemical Journal* 272 (1), 211-215. PMC1149678
- Ericksen, B., Wu, Z., Lu, W., Lehrer, R.I., 2005. Antibacterial activity and specificity of the six human $\{\alpha\}$ -defensins. *Antimicrobial Agents and Chemotherapy* 49 (1), 269-275. doi:10.1128/aac.49.1.269-275.2005
- Escrevente, C., Morais, V.A., Keller, S., Soares, C.M., Altevogt, P., Costa, J., 2008. Functional role of N-glycosylation from ADAM10 in processing, localization and activity of the enzyme. *Biochimica et Biophysica Acta* 1780 (6), 905-913. doi:10.1016/j.bbagen.2008.03.004
- Everest-Dass, A.V., Abrahams, J.L., Kolarich, D., Packer, N.H., Campbell, M.P., 2013a. Structural feature ions for distinguishing N- and O-linked glycan isomers by LC-ESI-IT MS/MS. *Journal of the American Society for Mass Spectrometry* 24 (6), 895-906. doi:10.1007/s13361-013-0610-4
- Everest-Dass, A.V., Jin, D., Thaysen-Andersen, M., Nevalainen, H., Kolarich, D., Packer, N.H., 2012. Comparative structural analysis of the glycosylation of salivary and buccal cell proteins: innate protection against infection by *Candida albicans*. *Glycobiology* 22 (11), 1465-1479. doi:10.1093/glycob/cws112
- Everest-Dass, A.V., Kolarich, D., Campbell, M.P., Packer, N.H., 2013b. Tandem mass spectra of glycan substructures enable the multistage mass spectrometric identification of determinants on oligosaccharides. *Rapid Communications in Mass Spectrometry* 27 (9), 931-939. doi:10.1002/rcm.6527

References

- Everest-Dass, A.V., Kolarich, D., Pascovici, D., Packer, N.H., 2016. Blood group antigen expression is involved in *C. albicans* interaction with buccal epithelial cells. *Glycoconjugate Journal*. doi:10.1007/s10719-016-9726-7
- Faurschou, M., Borregaard, N., 2003. Neutrophil granules and secretory vesicles in inflammation. *Microbes and Infection* 5 (14), 1317-1327. doi:10.1016/j.micinf.2003.09.008
- Faurschou, M., Kamp, S., Cowland, J.B., Udby, L., Johnsen, A.H., Calafat, J., Winther, H., Borregaard, N., 2005. Prodefensins are matrix proteins of specific granules in human neutrophils. *Journal of Leukocyte Biology* 78 (3), 785-793. doi:10.1189/jlb.1104688
- Feinberg, H., Mitchell, D.A., Drickamer, K., Weis, W.I., 2001. Structural basis for selective recognition of oligosaccharides by DC-SIGN and DC-SIGNR. *Science* 294 (5549), 2163-2166. doi:10.1126/science.1066371
- Fletcher, M.P., Seligmann, B.E., 1985. Monitoring human neutrophil granule secretion by flow cytometry: secretion and membrane potential changes assessed by light scatter and a fluorescent probe of membrane potential. *Journal of Leukocyte Biology* 37 (4), 431-447.
- Franc, V., Yang, Y., Heck, A.J., 2017. Proteoform profile mapping of the human serum Complement component C9 reveals unexpected new features of N-, O- and C-glycosylation. *Analytical Chemistry*. doi:10.1021/acs.analchem.6b04527
- Friedman, A.D., 2002. Transcriptional regulation of granulocyte and monocyte development. *Oncogene* 21 (21), 3377-3390. doi:10.1038/sj.onc.1205324
- Furukawa, J., Okada, K., Shinohara, Y., 2016. Glycomics of human embryonic stem cells and human induced pluripotent stem cells. *Glycoconjugate Journal* 33 (5), 707-715. doi:10.1007/s10719-016-9701-3
- Gadgil, H.S., Bondarenko, P.V., Pipes, G.D., Dillon, T.M., Banks, D., Abel, J., Kleemann, G.R., Treuheit, M.J., 2006. Identification of cysteinylated free cysteine in the Fab region of a recombinant monoclonal IgG1 antibody using Lys-C limited proteolysis coupled with LC/MS analysis. *Analytical Biochemistry* 355 (2), 165-174. doi:10.1016/j.ab.2006.05.037

- Gallagher, R., Collins, S., Trujillo, J., McCredie, K., Ahearn, M., Tsai, S., Metzgar, R., Aulakh, G., Ting, R., Ruscetti, F., Gallo, R., 1979. Characterization of the continuous, differentiating myeloid cell line (HL-60) from a patient with acute promyelocytic leukemia. *Blood* 54 (3), 713-733.
- Gama, M.R., da Silva, C.R.G., Collins, C.H., 2012. Hydrophilic interaction chromatography. *Trends in Analytical Chemistry* 37, 48-60.
- Gao, Y., Wells, L., Comer, F.I., Parker, G.J., Hart, G.W., 2001. Dynamic O-glycosylation of nuclear and cytosolic proteins: cloning and characterization of a neutral, cytosolic beta-N-acetylglucosaminidase from human brain. *Journal of Biological Chemistry* 276 (13), 9838-9845. doi:10.1074/jbc.M010420200
- Gasteiger, G., D'Osualdo, A., Schubert, D.A., Weber, A., Bruscia, E.M., Hartl, D., 2016. Cellular Innate Immunity: An Old Game with New Players. *Journal of Innate Immunity*. doi:10.1159/000453397
- Gault, J., Ferber, M., Machata, S., Imhaus, A.F., Malosse, C., Charles-Orszag, A., Millien, C., Bouvier, G., Bardiaux, B., Pehau-Arnaudet, G., Klinge, K., Podglajen, I., Ploy, M.C., Seifert, H.S., Nilges, M., Chamot-Rooke, J., Dumenil, G., 2015. *Neisseria meningitidis* Type IV Pili Composed of Sequence Invariable Pilins Are Masked by Multisite Glycosylation. *PLoS Pathogens* 11 (9), e1005162. doi:10.1371/journal.ppat.1005162
- Geissmann, F., Manz, M.G., Jung, S., Sieweke, M.H., Merad, M., Ley, K., 2010. Development of monocytes, macrophages, and dendritic cells. *Science* 327 (5966), 656-661. doi:10.1126/science.1178331
- Gentner, B., Visigalli, I., Hiramatsu, H., Lechman, E., Ungari, S., Giustacchini, A., Schira, G., Amendola, M., Quattrini, A., Martino, S., Orlacchio, A., Dick, J.E., Biffi, A., Naldini, L., 2010. Identification of hematopoietic stem cell-specific miRNAs enables gene therapy of globoid cell leukodystrophy. *Science Translational Medicine* 2 (58), 58ra84. doi:10.1126/scitranslmed.3001522
- Giebel, B., Punzel, M., 2008. Lineage development of hematopoietic stem and progenitor cells. *Biological Chemistry* 389 (7), 813-824. doi:10.1515/bc.2008.092

References

- Gil, G.C., Velandar, W.H., Van Cott, K.E., 2009. N-glycosylation microheterogeneity and site occupancy of an Asn-X-Cys sequon in plasma-derived and recombinant protein C. *Proteomics* 9 (9), 2555-2567. doi:10.1002/pmic.200800775
- Giuseppe, P., Martin, R.L., Nicolle, H.P., Morten, T.-A., 2013. Structural analysis of glycoprotein sialylation – part II: LC-MS based detection. *RSC Advances* 3 (45), 22706-22726. doi:10.1039/C3RA42969E
- Goetz, J.A., Mechref, Y., Kang, P., Jeng, M.H., Novotny, M.V., 2009. Glycomic profiling of invasive and non-invasive breast cancer cells. *Glycoconjugate Journal* 26 (2), 117-131. doi:10.1007/s10719-008-9170-4
- Goldmann, O., Medina, E., 2012. The expanding world of extracellular traps: not only neutrophils but much more. *Frontiers in Immunology* 3, 420. doi:10.3389/fimmu.2012.00420
- Gong, L., 2015. Comparing ion-pairing reagents and counter anions for ion-pair reversed-phase liquid chromatography/electrospray ionization mass spectrometry analysis of synthetic oligonucleotides. *Rapid Communications in Mass Spectrometry* 29 (24), 2402-2410. doi:10.1002/rcm.7409
- Gordon, S., 2016. Phagocytosis: An Immunobiologic Process. *Immunity* 44 (3), 463-475. doi:10.1016/j.immuni.2016.02.026
- Grayson, P.C., Kaplan, M.J., 2016. At the Bench: Neutrophil extracellular traps (NETs) highlight novel aspects of innate immune system involvement in autoimmune diseases. *Journal of Leukocyte Biology* 99 (2), 253-264. doi:10.1189/jlb.5BT0615-247R
- Greenberg, S., Grinstein, S., 2002. Phagocytosis and innate immunity. *Current Opinion in Immunology* 14 (1), 136-145.
- Groutas, W.C., Dou, D., Alliston, K.R., 2011. Neutrophil elastase inhibitors. *Expert Opinion on Therapeutic Patents* 21 (3), 339-354. doi:10.1517/13543776.2011.551115
- Guignard, C., Jouve, L., Bogeat-Triboulot, M.B., Dreyer, E., Hausman, J.F., Hoffmann, L., 2005. Analysis of carbohydrates in plants by high-performance anion-exchange

chromatography coupled with electrospray mass spectrometry. *Journal of Chromatography A* 1085 (1), 137-142.

Gutternigg, M., Kretschmer-Lubich, D., Paschinger, K., Rendic, D., Hader, J., Geier, P., Ranftl, R., Jantsch, V., Lochnit, G., Wilson, I.B., 2007. Biosynthesis of truncated N-linked oligosaccharides results from non-orthologous hexosaminidase-mediated mechanisms in nematodes, plants, and insects. *Journal of Biological Chemistry* 282 (38), 27825-27840. doi:10.1074/jbc.M704235200

Gutternigg, M., Rendic, D., Voglauer, R., Iskratsch, T., Wilson, I.B., 2009. Mammalian cells contain a second nucleocytoplasmic hexosaminidase. *Biochemical Journal* 419 (1), 83-90. doi:10.1042/BJ20081630

Guyot, N., Wartelle, J., Malleret, L., Todorov, A.A., Devouassoux, G., Pacheco, Y., Jenne, D.E., Belaaouaj, A., 2014. Unopposed cathepsin G, neutrophil elastase, and proteinase 3 cause severe lung damage and emphysema. *American Journal of Pathology* 184 (8), 2197-2210. doi:10.1016/j.ajpath.2014.04.015

Hajjar, E., Mihajlovic, M., Witko-Sarsat, V., Lazaridis, T., Reuter, N., 2008. Computational prediction of the binding site of proteinase 3 to the plasma membrane. *Proteins* 71 (4), 1655-1669. doi:10.1002/prot.21853

Hall, P., Minnich, S., Teigen, C., Raymond, K., 2014. Diagnosing Lysosomal Storage Disorders: The GM2 Gangliosidoses. *Curr Protoc Hum Genet* 83, 17 16 11-18. doi:10.1002/0471142905.hg1716s83

Hammond, C., Braakman, I., Helenius, A., 1994. Role of N-linked oligosaccharide recognition, glucose trimming, and calnexin in glycoprotein folding and quality control. *Proceedings of the National Academy of Sciences of the United States of America* 91 (3), 913-917. PMC521423

Hampton, M.B., Kettle, A.J., Winterbourn, C.C., 1998. Inside the neutrophil phagosome: oxidants, myeloperoxidase, and bacterial killing. *Blood* 92 (9), 3007-3017.

References

- Hang, I., Lin, C.W., Grant, O.C., Fleurkens, S., Villiger, T.K., Soos, M., Morbidelli, M., Woods, R.J., Gauss, R., Aepli, M., 2015. Analysis of site-specific N-glycan remodeling in the endoplasmic reticulum and the Golgi. *Glycobiology* 25 (12), 1335-1349. doi:10.1093/glycob/cwv058
- Hansen, G., Gielen-Haertwig, H., Reinemer, P., Schomburg, D., Harrenga, A., Niefind, K., 2011. Unexpected active-site flexibility in the structure of human neutrophil elastase in complex with a new dihydropyrimidone inhibitor. *Journal of Molecular Biology* 409 (5), 681-691. doi:10.1016/j.jmb.2011.04.047
- Hartholt, R.B., Wroblewska, A., Herczenik, E., Peyron, I., Ten Brinke, A., Rispens, T., Nolte, M.A., Slot, E., Claassens, J.W., Nimmerjahn, F., Verbeek, J.S., Voorberg, J., 2016. Enhanced uptake of blood coagulation factor VIII containing immune complexes by antigen presenting cells. *Journal of Thrombosis and Haemostasis*. doi:10.1111/jth.13570
- Harvey, D.J., 2005a. Fragmentation of negative ions from carbohydrates: part 2. Fragmentation of high-mannose N-linked glycans. *Journal of the American Society for Mass Spectrometry* 16 (5), 631-646. doi:10.1016/j.jasms.2005.01.005
- Harvey, D.J., 2005b. Fragmentation of negative ions from carbohydrates: part 3. Fragmentation of hybrid and complex N-linked glycans. *Journal of the American Society for Mass Spectrometry* 16 (5), 647-659. doi:10.1016/j.jasms.2005.01.006
- Harvey, D.J., 2005c. Structural determination of N-linked glycans by matrix-assisted laser desorption/ionization and electrospray ionization mass spectrometry. *Proteomics* 5 (7), 1774-1786. doi:10.1002/pmic.200401248
- Harvey, D.J., Royle, L., Radcliffe, C.M., Rudd, P.M., Dwek, R.A., 2008. Structural and quantitative analysis of N-linked glycans by matrix-assisted laser desorption ionization and negative ion nanospray mass spectrometry. *Analytical Biochemistry* 376 (1), 44-60. doi:10.1016/j.ab.2008.01.025
- Hashii, N., Kawasaki, N., Itoh, S., Nakajima, Y., Kawanishi, T., Yamaguchi, T., 2009. Alteration of N-glycosylation in the kidney in a mouse model of systemic lupus

- erythematosus: relative quantification of N-glycans using an isotope-tagging method. *Immunology* 126 (3), 336-345. doi:10.1111/j.1365-2567.2008.02898.x
- Hayes, C.A., Karlsson, N.G., Struwe, W.B., Lisacek, F., Rudd, P.M., Packer, N.H., Campbell, M.P., 2011. UniCarb-DB: a database resource for glycomic discovery. *Bioinformatics (Oxford, England)* 27 (9), 1343-1344. doi:10.1093/bioinformatics/btr137
- Headland, S.E., Norling, L.V., 2015. The resolution of inflammation: Principles and challenges. *Seminars in Immunology* 27 (3), 149-160. doi:10.1016/j.smim.2015.03.014
- Hechtman, P., Kachra, Z., 1980. Interaction of activating protein and surfactants with human liver hexosaminidase A and G(M2) ganglioside. *Biochemical Journal* 185 (3), 583-591.
- Heck, A.J., 2008. Native mass spectrometry: a bridge between interactomics and structural biology. *Nat Methods* 5 (11), 927-933. doi:10.1038/nmeth.1265
- Heck, A.J., Van Den Heuvel, R.H., 2004. Investigation of intact protein complexes by mass spectrometry. *Mass Spectrometry Reviews* 23 (5), 368-389. doi:10.1002/mas.10081
- Heit, B., Liu, L., Colarusso, P., Puri, K.D., Kubes, P., 2008. PI3K accelerates, but is not required for, neutrophil chemotaxis to fMLP. *Journal of Cell Science* 121 (Pt 2), 205-214. doi:10.1242/jcs.020412
- Hepbaldikler, S.T., Sandhoff, R., Kolzer, M., Proia, R.L., Sandhoff, K., 2002. Physiological substrates for human lysosomal beta -hexosaminidase S. *Journal of Biological Chemistry* 277 (4), 2562-2572. doi:10.1074/jbc.M105457200
- Hirche, T.O., Benabid, R., Deslee, G., Gangloff, S., Achilefu, S., Guenounou, M., Lebargy, F., Hancock, R.E., Belaaouaj, A., 2008. Neutrophil elastase mediates innate host protection against *Pseudomonas aeruginosa*. *Journal of Immunology* 181 (7), 4945-4954. doi:10.4049/jimmunol.181.7.4945
- Hitchen, P.G., Dell, A., 2006. Bacterial glycoproteomics. *Microbiology* 152 (Pt 6), 1575-1580. doi:10.1099/mic.0.28859-0

References

- Ho, C.S., Lam, C.W.K., Chan, M.H.M., Cheung, R.C.K., Law, L.K., Lit, L.C.W., Ng, K.F., Suen, M.W.M., Tai, H.L., 2003. Electrospray Ionisation Mass Spectrometry: Principles and Clinical Applications. *The Clinical Biochemist Reviews* 24 (1), 3-12.
- Hoffman, R., 2013. Hematology : basic principles and practice, 6th ed. Saunders/Elsevier, Philadelphia, PA.
- Hoffmann, E.d., Stroobant, V., 2007. Mass spectrometry : principles and applications, 3rd ed. J. Wiley, Chichester, England ; Hoboken, NJ.
- Hogan, J.M., Pitteri, S.J., Chrisman, P.A., McLuckey, S.A., 2005. Complementary structural information from a tryptic N-linked glycopeptide via electron transfer ion/ion reactions and collision-induced dissociation. *Journal of Proteome Research* 4 (2), 628-632. doi:10.1021/pr049770q
- Horwitz, M.S., Duan, Z., Korkmaz, B., Lee, H.H., Mealiffe, M.E., Salipante, S.J., 2007. Neutrophil elastase in cyclic and severe congenital neutropenia. *Blood* 109 (5), 1817-1824. doi:10.1182/blood-2006-08-019166
- Hou, Y., McInnes, B., Hinek, A., Karpati, G., Mahuran, D., 1998. A Pro504 --> Ser substitution in the beta-subunit of beta-hexosaminidase A inhibits alpha-subunit hydrolysis of GM2 ganglioside, resulting in chronic Sandhoff disease. *Journal of Biological Chemistry* 273 (33), 21386-21392.
- Huang, C., Harada, Y., Hosomi, A., Masahara-Negishi, Y., Seino, J., Fujihira, H., Funakoshi, Y., Suzuki, T., Dohmae, N., Suzuki, T., 2015. Endo- β -N-acetylglucosaminidase forms N-GlcNAc protein aggregates during ER-associated degradation in Ngly1-defective cells. *Proceedings of the National Academy of Sciences* 112 (5), 1398-1403. doi:10.1073/pnas.1414593112
- Huang, Y., Nie, Y., Boyes, B., Orlando, R., 2016. Resolving Isomeric Glycopeptide Glycoforms with Hydrophilic Interaction Chromatography (HILIC). *J Biomol Tech* 27 (3), 98-104. doi:10.7171/jbt.16-2703-003

- Huddleston, M.J., Bean, M.F., Carr, S.A., 1993. Collisional fragmentation of glycopeptides by electrospray ionization LC/MS and LC/MS/MS: methods for selective detection of glycopeptides in protein digests. *Analytical Chemistry* 65 (7), 877-884. doi:10.1021/ac00055a009
- Hulsmeier, A.J., Tobler, M., Burda, P., Hennet, T., 2016. Glycosylation site occupancy in health, congenital disorder of glycosylation and fatty liver disease. *Scientific Reports* 6, 33927. doi:10.1038/srep33927
- Hunter, M.J., Commerford, S.L., 1961. Pressure homogenization of mammalian tissues. *Biochimica et Biophysica Acta* 47, 580-586.
- Huntington, J.A., Read, R.J., Carrell, R.W., 2000. Structure of a serpin-protease complex shows inhibition by deformation. *Nature* 407 (6806), 923-926. doi:10.1038/35038119
- Ihara, H., Ikeda, Y., Taniguchi, N., 2006. Reaction mechanism and substrate specificity for nucleotide sugar of mammalian alpha1,6-fucosyltransferase--a large-scale preparation and characterization of recombinant human FUT8. *Glycobiology* 16 (4), 333-342. doi:10.1093/glycob/cwj068
- Ines, H., Anna, K., Ann-Kathrin, J., Kathrin, S., Nadine, D., Jennifer, B., Christina, B., Hélène, S., Francis, G., James, C.P., Tobias, W., Ulrich, A.M., 2011. Cathepsin G and Neutrophil Elastase Play Critical and Nonredundant Roles in Lung-Protective Immunity against *Streptococcus pneumoniae* in Mice. *Infection and Immunity* 79 (12), 4893-4901. doi:10.1128/IAI.05593-11
- Ingrid, K., Yamini, M.O., Ping, W., Hiroshi, J.M., Jeffery, S.C., Eric, J.B., 2008. Role for lysosomal enzyme β -hexosaminidase in the control of mycobacteria infection. *Proceedings of the National Academy of Sciences* 105 (2), 710-715. doi:10.1073/pnas.0708110105
- Jaeken, J., 2010. Congenital disorders of glycosylation. *Annals of the New York Academy of Sciences* 1214, 190-198. doi:10.1111/j.1749-6632.2010.05840.x

References

- Jensen, P.H., Karlsson, N.G., Kolarich, D., Packer, N.H., 2012. Structural analysis of N- and O-glycans released from glycoproteins. *Nature Protocols* 7 (7), 1299-1310. doi:10.1038/nprot.2012.063
- Joanne, E.N., Robin, A., Aricescu, A.R., Edward, J.E., Simon, J.D., Max, C., Raymond, J.O., 2007. Analysis of variable N-glycosylation site occupancy in glycoproteins by liquid chromatography electrospray ionization mass spectrometry. *Analytical Biochemistry* 361 (1), 149151. doi:10.1016/j.ab.2006.11.005
- Kang, P.B., Azad, A.K., Torrelles, J.B., Kaufman, T.M., Beharka, A., Tibesar, E., DesJardin, L.E., Schlesinger, L.S., 2005. The human macrophage mannose receptor directs mycobacterium tuberculosis lipoarabinomannan-mediated phagosome biogenesis. *Journal of Experimental Medicine* 202 (7), 987-999. doi:10.1084/jem.20051239
- Kaprio, T., Satomaa, T., Heiskanen, A., Hokke, C.H., Deelder, A.M., Mustonen, H., Hagstrom, J., Carpen, O., Saarinen, J., Haglund, C., 2015. N-glycomic profiling as a tool to separate rectal adenomas from carcinomas. *Molecular & Cellular Proteomics* 14 (2), 277-288. doi:10.1074/mcp.M114.041632
- Kawai, T., Akira, S., 2011. Toll-like receptors and their crosstalk with other innate receptors in infection and immunity. *Immunity* 34 (5), 637-650. doi:10.1016/j.immuni.2011.05.006
- Kelleher, D.J., Gilmore, R., 2006. An evolving view of the eukaryotic oligosaccharyltransferase. *Glycobiology* 16 (4), 47r-62r. doi:10.1093/glycob/cwj066
- Kerrigan, A.M., Brown, G.D., 2009. C-type lectins and phagocytosis. *Immunobiology* 214 (7), 562-575. doi:10.1016/j.imbio.2008.11.003
- Kessenbrock, K., Krumbholz, M., Schonermarck, U., Back, W., Gross, W.L., Werb, Z., Grone, H.J., Brinkmann, V., Jenne, D.E., 2009. Netting neutrophils in autoimmune small-vessel vasculitis. *Nature Medicine* 15 (6), 623-625. doi:10.1038/nm.1959
- Khoo, K.H., 2014. From mass spectrometry-based glycosylation analysis to glycomics and glycoproteomics. *Adv Neurobiol* 9, 129-164. doi:10.1007/978-1-4939-1154-7_7

- Kim, Y.C., Jahren, N., Stone, M.D., Udeshi, N.D., Markowski, T.W., Witthuhn, B.A., Shabanowitz, J., Hunt, D.F., Olszewski, N.E., 2013. Identification and origin of N-linked beta-D-N-acetylglucosamine monosaccharide modifications on Arabidopsis proteins. *Plant Physiology* 161 (1), 455-464. doi:10.1104/pp.112.208900
- Kimmel, M., 2014. Stochasticity and determinism in models of hematopoiesis. *Advances in Experimental Medicine and Biology* 844, 119-152. doi:10.1007/978-1-4939-2095-2_7
- Kizuka, Y., Taniguchi, N., 2016. Enzymes for N-Glycan Branching and Their Genetic and Nongenetic Regulation in Cancer. *Biomolecules* 6 (2). doi:10.3390/biom6020025
- Kjeldsen, L., Bainton, D.F., Sengelov, H., Borregaard, N., 1994. Identification of neutrophil gelatinase-associated lipocalin as a novel matrix protein of specific granules in human neutrophils. *Blood* 83 (3), 799-807.
- Kjeldsen, L., Bjerrum, O.W., Askaa, J., Borregaard, N., 1992. Subcellular localization and release of human neutrophil gelatinase, confirming the existence of separate gelatinase-containing granules. *Biochemical Journal* 287 (Pt 2), 603-610. PMC1133208
- Kjeldsen, L., Sengeløv, H., Borregaard, N., 1999. Subcellular fractionation of human neutrophils on Percoll density gradients. *Journal of Immunological Methods* 232 (1), 131-143.
- Klausen, P., Bjerregaard, M.D., Borregaard, N., Cowland, J.B., 2004. End-stage differentiation of neutrophil granulocytes in vivo is accompanied by up-regulation of p27kip1 and down-regulation of CDK2, CDK4, and CDK6. *Journal of Leukocyte Biology* 75 (3), 569-578. doi:10.1189/jlb.1003474
- Klebanoff, S.J., 2005. Myeloperoxidase: friend and foe. *Journal of Leukocyte Biology* 77 (5), 598-625. doi:10.1189/jlb.1204697
- Klebanoff, S.J., Rosen, H., 1978. The role of myeloperoxidase in the microbicidal activity of polymorphonuclear leukocytes. *Ciba Foundation Symposium* (65), 263-284.

References

- Kobayashi, T., Goto, I., Okada, S., Orii, T., Ohno, K., Nakano, T., 1992. Accumulation of lysosphingolipids in tissues from patients with GM1 and GM2 gangliosidoses. *Journal of Neurochemistry* 59 (4), 1452-1458.
- Kolarich, D., Jensen, P.H., Altmann, F., Packer, N.H., 2012. Determination of site-specific glycan heterogeneity on glycoproteins. *Nature Protocols* 7 (7), 1285-1298. doi:10.1038/nprot.2012.062
- Kolarich, D., Windwarder, M., Alagesan, K., Altmann, F., 2015. Isomer-Specific Analysis of Released N-Glycans by LC-ESI MS/MS with Porous Graphitized Carbon. *Methods in Molecular Biology* 1321, 427-435. doi:10.1007/978-1-4939-2760-9_29
- Kondo, M., Weissman, I.L., Akashi, K., 1997. Identification of clonogenic common lymphoid progenitors in mouse bone marrow. *Cell* 91 (5), 661-672.
- Korkmaz, B., Moreau, T., Gauthier, F., 2008. Neutrophil elastase, proteinase 3 and cathepsin G: physicochemical properties, activity and physiopathological functions. *Biochimie* 90 (2), 227-242. doi:10.1016/j.biochi.2007.10.009
- Korneluk, R.G., Mahuran, D.J., Neote, K., Klavins, M.H., O'Dowd, B.F., Tropak, M., Willard, H.F., Anderson, M.J., Lowden, J.A., Gravel, R.A., 1986. Isolation of cDNA clones coding for the alpha-subunit of human beta-hexosaminidase. Extensive homology between the alpha- and beta-subunits and studies on Tay-Sachs disease. *Journal of Biological Chemistry* 261 (18), 8407-8413.
- Kruger, P., Saffarzadeh, M., Weber, A.N., Rieber, N., Radsak, M., von Bernuth, H., Benarafa, C., Roos, D., Skokowa, J., Hartl, D., 2015. Neutrophils: Between host defence, immune modulation, and tissue injury. *PLoS Pathogens* 11 (3), e1004651. doi:10.1371/journal.ppat.1004651
- Kuijpers, T.W., Tool, A.T., van der Schoot, C.E., Ginsel, L.A., Onderwater, J.J., Roos, D., Verhoeven, A.J., 1991. Membrane surface antigen expression on neutrophils: a reappraisal of the use of surface markers for neutrophil activation. *Blood* 78 (4), 1105-1111.

- Lacy, P., Eitzen, G., 2008. Control of granule exocytosis in neutrophils. *Frontiers in Bioscience* 13, 5559-5570.
- Lamari, F.N., Kuhn, R., Karamanos, N.K., 2003. Derivatization of carbohydrates for chromatographic, electrophoretic and mass spectrometric structure analysis. *Journal of Chromatography. B: Analytical Technologies in the Biomedical and Life Sciences* 793 (1), 15-36.
- Larsen, M.R., Trelle, M.B., Thingholm, T.E., Jensen, O.N., 2006. Analysis of posttranslational modifications of proteins by tandem mass spectrometry. *Biotechniques* 40 (6), 790-798.
- Larsen, M.T., Hother, C., Hager, M., Pedersen, C.C., Theilgaard-Monch, K., Borregaard, N., Cowland, J.B., 2013. MicroRNA profiling in human neutrophils during bone marrow granulopoiesis and in vivo exudation. *PloS One* 8 (3), e58454. doi:10.1371/journal.pone.0058454
- Laura, R.P., Dong, D., Reynolds, W.F., Maki, R.A., 2016. T47D Cells Expressing Myeloperoxidase Are Able to Process, Traffic and Store the Mature Protein in Lysosomes: Studies in T47D Cells Reveal a Role for Cys319 in MPO Biosynthesis that Precedes Its Known Role in Inter-Molecular Disulfide Bond Formation. *PloS One* 11 (2), e0149391. doi:10.1371/journal.pone.0149391
- Le Cabec, V., Calafat, J., Borregaard, N., 1997. Sorting of the specific granule protein, NGAL, during granulocytic maturation of HL-60 cells. *Blood* 89 (6), 2113-2121.
- Le Cabec, V., Cowland, J.B., Calafat, J., Borregaard, N., 1996. Targeting of proteins to granule subsets is determined by timing and not by sorting: The specific granule protein NGAL is localized to azurophil granules when expressed in HL-60 cells. *Proceedings of the National Academy of Sciences of the United States of America* 93 (13), 6454-6457. doi:10.1073/pnas.93.13.6454
- Le Gars, M., Descamps, D., Roussel, D., Sausseureau, E., Guillot, L., Ruffin, M., Tabary, O., Hong, S.S., Boulanger, P., Paulais, M., Malleret, L., Belaaouaj, A., Edelman, A., Huerre, M., Chignard, M., Sallenave, J.M., 2013. Neutrophil elastase degrades cystic fibrosis transmembrane conductance regulator via calpains and disables channel function in vitro and

References

in vivo. *American Journal of Respiratory and Critical Care Medicine* 187 (2), 170-179. doi:10.1164/rccm.201205-0875OC

Lee, C.Y., Herant, M., Heinrich, V., 2011. Target-specific mechanics of phagocytosis: protrusive neutrophil response to zymosan differs from the uptake of antibody-tagged pathogens. *Journal of Cell Science* 124 (Pt 7), 1106-1114. doi:10.1242/jcs.078592

Lee, L.Y., Lin, C.H., Fanayan, S., Packer, N.H., Thaysen-Andersen, M., 2014a. Differential site accessibility mechanistically explains subcellular-specific N-glycosylation determinants. *Frontiers in Immunology* 5, 404. doi:10.3389/fimmu.2014.00404

Lee, L.Y., Thaysen-Andersen, M., Baker, M.S., Packer, N.H., Hancock, W.S., Fanayan, S., 2014b. Comprehensive N-glycome profiling of cultured human epithelial breast cells identifies unique secretome N-glycosylation signatures enabling tumorigenic subtype classification. *Journal of Proteome Research* 13 (11), 4783-4795. doi:10.1021/pr500331m

Lemieux, M.J., Mark, B.L., Cherney, M.M., Withers, S.G., Mahuran, D.J., James, M.N., 2006. Crystallographic structure of human beta-hexosaminidase A: interpretation of Tay-Sachs mutations and loss of GM2 ganglioside hydrolysis. *Journal of Molecular Biology* 359 (4), 913-929. doi:10.1016/j.jmb.2006.04.004

Leney, A.C., Heck, A.J., 2017. Native Mass Spectrometry: What is in the Name? *Journal of the American Society for Mass Spectrometry* 28 (1), 5-13. doi:10.1007/s13361-016-1545-3

Lewis, S.M., Bain, B.J., Bates, I., Dacie, J.V., Dacie, J.V., 2006. *Dacie and Lewis practical haematology*, 10th ed. Churchill Livingstone/Elsevier, Philadelphia.

Leymarie, N., Griffin, P.J., Jonscher, K., Kolarich, D., Orlando, R., McComb, M., Zaia, J., Aguilan, J., Alley, W.R., Altmann, F., Ball, L.E., Basumallick, L., Bazemore-Walker, C.R., Behnken, H., Blank, M.A., Brown, K.J., Bunz, S.C., Cairo, C.W., Cipollo, J.F., Daneshfar, R., Desaire, H., Drake, R.R., Go, E.P., Goldman, R., Gruber, C., Halim, A., Hathout, Y., Hensbergen, P.J., Horn, D.M., Hurum, D., Jabs, W., Larson, G., Ly, M., Mann, B.F., Marx, K., Mechref, Y., Meyer, B., Moginger, U., Neusubeta, C., Nilsson, J., Novotny, M.V., Nyalwidhe, J.O., Packer, N.H., Pompach, P., Reiz, B., Resemann, A., Rohrer, J.S., Ruthenbeck, A., Sanda, M., Schulz, J.M., Schweiger-Hufnagel, U., Sihlbom, C., Song, E., Staples, G.O., Suckau, D.,

- Tang, H., Thaysen-Andersen, M., Viner, R.I., An, Y., Valmu, L., Wada, Y., Watson, M., Windwarder, M., Whittal, R., Wuhler, M., Zhu, Y., Zou, C., 2013. Interlaboratory study on differential analysis of protein glycosylation by mass spectrometry: the ABRF glycoprotein research multi-institutional study 2012. *Molecular & Cellular Proteomics* 12 (10), 2935-2951. doi:10.1074/mcp.M113.030643
- Lim, C.S., Hong, S.T., Ryu, S.S., Kang, D.E., Cho, B.R., 2015. Two-Photon Probes for Lysosomes and Mitochondria: Simultaneous Detection of Lysosomes and Mitochondria in Live Tissues by Dual-Color Two-Photon Microscopy Imaging. *Chemistry, an Asian Journal* 10 (10), 2240-2249. doi:10.1002/asia.201500314
- Liu, H., Zhang, N., Wan, D., Cui, M., Liu, Z., Liu, S., 2014. Mass spectrometry-based analysis of glycoproteins and its clinical applications in cancer biomarker discovery. *Clinical Proteomics* 11 (1), 14-14. doi:10.1186/1559-0275-11-14
- Liu, X., Inbar, Y., Dorrestein, P.C., Wynne, C., Edwards, N., Souda, P., Whitelegge, J.P., Bafna, V., Pevzner, P.A., 2010. Deconvolution and Database Search of Complex Tandem Mass Spectra of Intact Proteins: A COMBINATORIAL APPROACH. *Molecular & Cellular Proteomics : MCP* 9 (12), 2772-2782. doi:10.1074/mcp.M110.002766
- Lollike, K., Dahlgren, C., Borregaard, N., 1995. Mobilization of granules and secretory vesicles during in vivo exudation of human neutrophils. *The Journal of Immunology* 154 (8), 4157-4165.
- Lominadze, G., Powell, D.W., Luerman, G.C., Link, A.J., Ward, R.A., McLeish, K.R., 2005. Proteomic analysis of human neutrophil granules. *Molecular & Cellular Proteomics* 4 (10), 1503-1521. doi:10.1074/mcp.M500143-MCP200
- Loziuk, P.L., Hecht, E.S., Muddiman, D.C., 2017. N-linked glycosite profiling and use of Skyline as a platform for characterization and relative quantification of glycans in differentiating xylem of *Populus trichocarpa*. *Analytical and Bioanalytical Chemistry* 409 (2), 487-497. doi:10.1007/s00216-016-9776-5

References

- Lu, J., Teh, C., Kishore, U., Reid, K.B., 2002. Collectins and ficolins: sugar pattern recognition molecules of the mammalian innate immune system. *Biochimica et Biophysica Acta* 1572 (2-3), 387-400. doi:10.1016/S0304-4165(02)00320-3
- Ma, C., Qu, J., Li, X., Zhao, X., Li, L., Xiao, C., Edmunds, G., Gashash, E., Song, J., Wang, P.G., 2016. Improvement of core-fucosylated glycoproteome coverage via alternating HCD and ETD fragmentation. *Journal of Proteomics* 146, 90-98. doi:10.1016/j.jprot.2016.06.003
- Mahla, R.S., Reddy, M.C., Prasad, D.V., Kumar, H., 2013. Sweeten PAMPs: Role of Sugar Complexed PAMPs in Innate Immunity and Vaccine Biology. *Frontiers in Immunology* 4, 248. doi:10.3389/fimmu.2013.00248
- Mahuran, D.J., 1999. Biochemical consequences of mutations causing the GM2 gangliosidosis. *Biochimica et Biophysica Acta* 1455 (2-3), 105-138.
- Mantovani, A., Cassatella, M.A., Costantini, C., Jaillon, S., 2011. Neutrophils in the activation and regulation of innate and adaptive immunity. *Nature Reviews: Immunology* 11 (8), 519-531. doi:10.1038/nri3024
- Manz, M.G., Boettcher, S., 2014. Emergency granulopoiesis. *Nature Reviews: Immunology* 14 (5), 302-314. doi:10.1038/nri3660
- Martinez-Lostao, L., Anel, A., Pardo, J., 2015. How Do Cytotoxic Lymphocytes Kill Cancer Cells? *Clinical Cancer Research* 21 (22), 5047-5056. doi:10.1158/1078-0432.CCR-15-0685
- Matsuoka, K., Tamura, T., Tsuji, D., Dohzono, Y., Kitakaze, K., Ohno, K., Saito, S., Sakuraba, H., Itoh, K., 2011. Therapeutic potential of intracerebroventricular replacement of modified human beta-hexosaminidase B for GM2 gangliosidosis. *Molecular Therapy* 19 (6), 1017-1024. doi:10.1038/mt.2011.27
- McDonald, B., Pittman, K., Menezes, G.B., Hirota, S.A., Slaba, I., Waterhouse, C.C., Beck, P.L., Muruve, D.A., Kubes, P., 2010. Intravascular danger signals guide neutrophils to sites of sterile inflammation. *Science* 330 (6002), 362-366. doi:10.1126/science.1195491

- McElvaney, N.G., 2016. Alpha-1 Antitrypsin Therapy in Cystic Fibrosis and the Lung Disease Associated with Alpha-1 Antitrypsin Deficiency. *Annals of the American Thoracic Society* 13 Suppl 2, S191-196. doi:10.1513/AnnalsATS.201504-245KV
- McEver, R.P., Moore, K.L., Cummings, R.D., 1995. Leukocyte trafficking mediated by selectin-carbohydrate interactions. *Journal of Biological Chemistry* 270 (19), 11025-11028.
- Medzihradszky, K.F., Kaasik, K., Chalkley, R.J., 2015. Tissue-Specific Glycosylation at the Glycopeptide Level. *Molecular & Cellular Proteomics* 14 (8), 2103-2110. doi:10.1074/mcp.M115.050393
- Meier, E.M., Schwarzmann, G., Furst, W., Sandhoff, K., 1991. The human GM2 activator protein. A substrate specific cofactor of beta-hexosaminidase A. *Journal of Biological Chemistry* 266 (3), 1879-1887.
- Metzler, K.D., Goosmann, C., Lubojemska, A., Zychlinsky, A., Papayannopoulos, V., 2014. A myeloperoxidase-containing complex regulates neutrophil elastase release and actin dynamics during NETosis. *Cell Rep* 8 (3), 883-896. doi:10.1016/j.celrep.2014.06.044
- Mitchell, E.P., Sabin, C., Snajdrova, L., Pokorna, M., Perret, S., Gautier, C., Hofr, C., Gilboa-Garber, N., Koca, J., Wimmerova, M., Imberty, A., 2005. High affinity fucose binding of *Pseudomonas aeruginosa* lectin PA-IIL: 1.0 Å resolution crystal structure of the complex combined with thermodynamics and computational chemistry approaches. *Proteins* 58 (3), 735-746. doi:10.1002/prot.20330
- Mitchell, T., Lo, A., Logan, M.R., Lacy, P., Eitzen, G., 2008. Primary granule exocytosis in human neutrophils is regulated by Rac-dependent actin remodeling. *American journal of physiology. Cell physiology* 295 (5), 65. doi:10.1152/ajpcell.00239.2008
- Miyasaki, K.T., Bodeau, A.L., 1992. Human neutrophil azurocidin synergizes with leukocyte elastase and cathepsin G in the killing of *Capnocytophaga sputigena*. *Infection and Immunity* 60 (11), 4973-4975.

References

- Mollinedo, F., Calafat, J., Janssen, H., Martin-Martin, B., Canchado, J., Nabokina, S.M., Gajate, C., 2006. Combinatorial SNARE complexes modulate the secretion of cytoplasmic granules in human neutrophils. *Journal of Immunology* 177 (5), 2831-2841.
- Monsigny, M., Roche, A.C., Sene, C., Maget-Dana, R., Delmotte, F., 1980. Sugar-lectin interactions: how does wheat-germ agglutinin bind sialoglycoconjugates? *European Journal of Biochemistry* 104 (1), 147-153.
- Monsigny, M., Sene, C., Obrenovitch, A., Roche, A.C., Delmotte, F., Boschetti, E., 1979. Properties of succinylated wheat-germ agglutinin. *European Journal of Biochemistry* 98 (1), 39-45.
- Moore, K.L., Patel, K.D., Bruehl, R.E., Li, F., Johnson, D.A., Lichenstein, H.S., Cummings, R.D., Bainton, D.F., McEver, R.P., 1995. P-selectin glycoprotein ligand-1 mediates rolling of human neutrophils on P-selectin. *Journal of Cell Biology* 128 (4), 661-671. PMC2199883
- Mora-Jensen, H., Jendholm, J., Fossum, A., Porse, B., Borregaard, N., Borregaard, N., Theilgaard-Mönch, K., 2011. Technical advance: immunophenotypical characterization of human neutrophil differentiation. *Journal of Leukocyte Biology* 90 (3), 629-634. doi:10.1189/jlb.0311123
- Moremen, K.W., Tiemeyer, M., Nairn, A.V., 2012. Vertebrate protein glycosylation: diversity, synthesis and function. *Nature Reviews: Molecular Cell Biology* 13 (7), 448-462.
- Nagae, M., Morita-Matsumoto, K., Arai, S., Wada, I., Matsumoto, Y., Saito, K., Hashimoto, Y., Yamaguchi, Y., 2014. Structural change of N-glycan exposes hydrophobic surface of human transferrin. *Glycobiology* 24 (8), 693-702. doi:10.1093/glycob/cwu033
- Nardy, A.F.F.R., Freire-de-Lima, C.G., Pérez, A.R., Morrot, A., 2016. Role of *Trypanosoma cruzi* Trans-sialidase on the Escape from Host Immune Surveillance. *Frontiers in Microbiology* 7, 348. doi:10.3389/fmicb.2016.00348
- Nauseef, W.M., McCormick, S., Yi, H., 1992. Roles of heme insertion and the mannose-6-phosphate receptor in processing of the human myeloid lysosomal enzyme, myeloperoxidase. *Blood* 80 (10), 2622-2633.

- Neelakshi, R.J., Madhavi, J.R., George, L., Gregory, C.L., Richard, A.W., Kenneth, R.M., 2007. The actin cytoskeleton regulates exocytosis of all neutrophil granule subsets. *American Journal of Physiology - Cell Physiology*. doi:10.1152/ajpcell.00384.2006
- Newburger, P.E., Chovaniec, M.E., Greenberger, J.S., Cohen, H.J., 1979. Functional changes in human leukemic cell line HL-60. A model for myeloid differentiation. *Journal of Cell Biology* 82 (2), 315-322. PMC2110469
- Nicolas-Avila, J.A., Adrover, J.M., Hidalgo, A., 2017. Neutrophils in Homeostasis, Immunity, and Cancer. *Immunity* 46 (1), 15-28. doi:10.1016/j.immuni.2016.12.012
- Nordenfelt, P., Tapper, H., 2011. Phagosome dynamics during phagocytosis by neutrophils. *Journal of Leukocyte Biology* 90 (2), 271-284. doi:10.1189/jlb.0810457
- North, S.J., von Gunten, S., Antonopoulos, A., Trollope, A., MacGlashan, D.W., Jr., Jang-Lee, J., Dell, A., Metcalfe, D.D., Kirshenbaum, A.S., Bochner, B.S., Haslam, S.M., 2012. Glycomic analysis of human mast cells, eosinophils and basophils. *Glycobiology* 22 (1), 12-22. doi:10.1093/glycob/cwr089
- O'Brien, P., Morin, P., Jr., Ouellette, R.J., Robichaud, G.A., 2011. The Pax-5 gene: a pluripotent regulator of B-cell differentiation and cancer disease. *Cancer Research* 71 (24), 7345-7350. doi:10.1158/0008-5472.can-11-1874
- Oheim, M., Li, D., 2007. Quantitative Colocalisation Imaging: Concepts, Measurements, and Pitfalls. *Imaging cellular and molecular biological functions*, 117-155. doi:10.1007/978-3-540-71331-9_5
- Okada, S.S., de Oliveira, E.M., de Araujo, T.H., Rodrigues, M.R., Albuquerque, R.C., Mortara, R.A., Taniwaki, N.N., Nakaya, H.I., Campa, A., Moreno, A.C., 2015. Myeloperoxidase in human peripheral blood lymphocytes: Production and subcellular localization. *Cellular Immunology*. doi:10.1016/j.cellimm.2015.11.003
- Olczak, M., Watorek, W., 2002. Structural analysis of N-glycans from human neutrophil azurocidin. *Biochemical and Biophysical Research Communications* 293 (1), 213-219. doi:10.1016/S0006-291X(02)00201-2

References

- Opdenakker, G., Rudd, P.M., Ponting, C.P., Dwek, R.A., 1993. Concepts and principles of glycobiology. *FASEB Journal* 7 (14), 1330-1337.
- Opdenakker, G., Van den Steen, P.E., Dubois, B., Nelissen, I., Van Coillie, E., Masure, S., Proost, P., Van Damme, J., 2001. Gelatinase B functions as regulator and effector in leukocyte biology. *Journal of Leukocyte Biology* 69 (6), 851-859.
- Orlacchio, A., Emiliani, C., Rambotti, P., Pioda, G.B., Davis, S., 1986. Alteration of beta-hexosaminidase activity and isoenzymes in human leukemic cells. *Biochemical Medicine and Metabolic Biology* 36 (3), 283-292.
- Owen, C.A., Campbell, M.A., Sannes, P.L., Boukedes, S.S., Campbell, E.J., 1995. Cell surface-bound elastase and cathepsin G on human neutrophils: a novel, non-oxidative mechanism by which neutrophils focus and preserve catalytic activity of serine proteinases. *Journal of Cell Biology* 131 (3), 775-789.
- Pabst, M., Altmann, F., 2008. Influence of electrosorption, solvent, temperature, and ion polarity on the performance of LC-ESI-MS using graphitic carbon for acidic oligosaccharides. *Analytical Chemistry* 80 (19), 7534-7542. doi:10.1021/ac801024r
- Pabst, M., Bondili, J.S., Stadlmann, J., Mach, L., Altmann, F., 2007. Mass + retention time = structure: a strategy for the analysis of N-glycans by carbon LC-ESI-MS and its application to fibrin N-glycans. *Analytical Chemistry* 79 (13), 5051-5057. doi:10.1021/ac070363i
- Pabst, M., Grass, J., Toegel, S., Liebming, E., Strasser, R., Altmann, F., 2012. Isomeric analysis of oligomannosidic N-glycans and their dolichol-linked precursors. *Glycobiology* 22 (3), 389-399. doi:10.1093/glycob/cwr138
- Panico, M., Bouche, L., Binet, D., O'Connor, M.J., Rahman, D., Pang, P.C., Canis, K., North, S.J., Desrosiers, R.C., Chertova, E., Keele, B.F., Bess, J.W., Jr., Lifson, J.D., Haslam, S.M., Dell, A., Morris, H.R., 2016. Mapping the complete glycoproteome of virion-derived HIV-1 gp120 provides insights into broadly neutralizing antibody binding. *Scientific Reports* 6, 32956. doi:10.1038/srep32956

- Parker, B.L., Thaysen-Andersen, M., Fazakerley, D.J., Holliday, M., Packer, N.H., James, D.E., 2016. Terminal galactosylation and sialylation switching on membrane glycoproteins upon TNF-alpha-induced insulin resistance in adipocytes. *Molecular & Cellular Proteomics* 15 (1), 141-153. doi:10.1074/mcp.M115.054221
- Parker, B.L., Thaysen-Andersen, M., Solis, N., Scott, N.E., Larsen, M.R., Graham, M.E., Packer, N.H., Cordwell, S.J., 2013. Site-specific glycan-peptide analysis for determination of n-glycoproteome heterogeneity. *Journal of Proteome Research* 12 (12), 5791-5800. doi:10.1021/pr400783j
- Patrie, S.M., Roth, M.J., Kohler, J.J., 2013. Introduction to glycosylation and mass spectrometry. *Methods in Molecular Biology* 951, 1-17. doi:10.1007/978-1-62703-146-2_1
- Pegg, C.L., Hoogland, C., Gorman, J.J., 2016. Site-specific glycosylation of the Newcastle disease virus haemagglutinin-neuraminidase. *Glycoconjugate Journal*. doi:10.1007/s10719-016-9750-7
- Perera, N.C., Wiesmüller, K.-H.H., Larsen, M.T., Schacher, B., Eickholz, P., Borregaard, N., Jenne, D.E., 2013. NSP4 is stored in azurophil granules and released by activated neutrophils as active endoprotease with restricted specificity. *Journal of immunology (Baltimore, Md. : 1950)* 191 (5), 2700-2707. doi:10.4049/jimmunol.1301293
- Pillay, J., den Braber, I., Vrisekoop, N., Kwast, L.M., de Boer, R.J., Borghans, J.A., Tesselaar, K., Koenderman, L., 2010. In vivo labeling with 2H2O reveals a human neutrophil lifespan of 5.4 days. *Blood* 116 (4), 625-627. doi:10.1182/blood-2010-01-259028
- Pirooznia, N., Hasannia, S., Arab, S.S., Lotfi, A.S., Ghanei, M., Shali, A., 2013. The design of a new truncated and engineered alpha1-antitrypsin based on theoretical studies: an antiprotease therapeutics for pulmonary diseases. *Theoretical Biology & Medical Modelling* 10, 36. doi:10.1186/1742-4682-10-36
- Poulos, M.G., Guo, P., Kofler, N.M., Pinho, S., Gutkin, M.C., Tikhonova, A., Aifantis, I., Frenette, P.S., Kitajewski, J., Rafii, S., Butler, J.M., 2013. Endothelial Jagged-1 is necessary for homeostatic and regenerative hematopoiesis. *Cell Rep* 4 (5), 1022-1034. doi:10.1016/j.celrep.2013.07.048

References

- Rashid, Q., Kapil, C., Singh, P., Kumari, V., Jairajpuri, M.A., 2015. Understanding the specificity of serpin-protease complexes through interface analysis. *Journal of Biomolecular Structure and Dynamics* 33 (6), 1352-1362. doi:10.1080/07391102.2014.947525
- Reinhold, B.B., Reinhold, V.N., 1992. Electrospray ionization mass spectrometry: Deconvolution by an Entropy-Based algorithm. *Journal of the American Society for Mass Spectrometry* 3 (3), 207-215. doi:10.1016/1044-0305(92)87004-i
- Renata, M.-K., Małgorzata, B., Monika, B., Barbara, M., Paweł, M., Jan, P., Joanna, B., 2005. Effects of elastase and cathepsin G on the levels of membrane and soluble TNF α . *Biological Chemistry* 386 (8), 801-811. doi:10.1515/BC.2005.094
- Reusch, D., Habegger, M., Selman, M.H., Bulau, P., Deelder, A.M., Wührer, M., Engler, N., 2013. High-throughput work flow for IgG Fc-glycosylation analysis of biotechnological samples. *Analytical Biochemistry* 432 (2), 82-89. doi:10.1016/j.ab.2012.09.032
- Rieger, M.A., Schroeder, T., 2012. Hematopoiesis. *Cold Spring Harbor Perspectives in Biology* 4 (12), a008250. doi:10.1101/cshperspect.a008250
- Robajac, D., Vanhooren, V., Masnikosa, R., Mikovic, Z., Mandic, V., Libert, C., Nedic, O., 2016. Preeclampsia transforms membrane N-glycome in human placenta. *Experimental and Molecular Pathology* 100 (1), 26-30. doi:10.1016/j.yexmp.2015.11.029
- Rorvig, S., Honore, C., Larsson, L.I., Ohlsson, S., Pedersen, C.C., Jacobsen, L.C., Cowland, J.B., Garred, P., Borregaard, N., 2009. Ficolin-1 is present in a highly mobilizable subset of human neutrophil granules and associates with the cell surface after stimulation with fMLP. *Journal of Leukocyte Biology* 86 (6), 1439-1449. doi:10.1189/jlb.1008606
- Rorvig, S., Ostergaard, O., Heegaard, N.H., Borregaard, N., 2013. Proteome profiling of human neutrophil granule subsets, secretory vesicles, and cell membrane: correlation with transcriptome profiling of neutrophil precursors. *Journal of Leukocyte Biology* 94 (4), 711-721. doi:10.1189/jlb.1212619
- Rosati, S., van den Bremer, E.T., Schuurman, J., Parren, P.W., Kamerling, J.P., Heck, A.J., 2013. In-depth qualitative and quantitative analysis of composite glycosylation profiles and

- other micro-heterogeneity on intact monoclonal antibodies by high-resolution native mass spectrometry using a modified Orbitrap. *MAbs* 5 (6), 917-924. doi:10.4161/mabs.26282
- Ruhaak, L.R., Stroble, C., Underwood, M.A., Lebrilla, C.B., 2014. Detection of milk oligosaccharides in plasma of infants. *Analytical and Bioanalytical Chemistry* 406 (24), 5775-5784. doi:10.1007/s00216-014-8025-z
- Sadler, J.E., 1998. Biochemistry and genetics of von Willebrand factor. *Annual Review of Biochemistry* 67, 395-424. doi:10.1146/annurev.biochem.67.1.395
- Saito, N., Pulford, K.A., Breton-Gorius, J., Masse, J.M., Mason, D.Y., Cramer, E.M., 1991. Ultrastructural localization of the CD68 macrophage-associated antigen in human blood neutrophils and monocytes. *American Journal of Pathology* 139 (5), 1053-1059.
- Salazar, V.A., Rubin, J., Moussaoui, M., Pulido, D., Nogues, M.V., Venge, P., Boix, E., 2014. Protein post-translational modification in host defense: the antimicrobial mechanism of action of human eosinophil cationic protein native forms. *Febs j* 281 (24), 5432-5446. doi:10.1111/febs.13082
- Sarkar, A., Wintrode, P.L., 2011. Effects of glycosylation on the stability and flexibility of a metastable protein: the human serpin alpha(1)-antitrypsin. *Int J Mass Spectrom* 302 (1-3), 69-75. doi:10.1016/j.ijms.2010.08.003
- Satoma, T., Heiskanen, A., Mikkola, M., Olsson, C., Blomqvist, M., Tiittanen, M., Jaatinen, T., Aitio, O., Olonen, A., Helin, J., Hiltunen, J., Natunen, J., Tuuri, T., Otonkoski, T., Saarinen, J., Laine, J., 2009. The N-glycome of human embryonic stem cells. *BMC Cell Biology* 10, 42. doi:10.1186/1471-2121-10-42
- Schachter, H., 2009. Paucimannose N-glycans in *Caenorhabditis elegans* and *Drosophila melanogaster*. *Carbohydrate Research* 344 (12), 1391-1396. doi:10.1016/j.carres.2009.04.028
- Schachter, H., Boulianne, G., 2011. Life is sweet! A novel role for N-glycans in *Drosophila* lifespan. *Fly (Austin)* 5 (1), 18-24. 3052869

References

- Scholten, A., Mohammed, S., Low, T.Y., Zanivan, S., van Veen, T.A.B., Delanghe, B., Heck, A.J.R., 2011. In-depth Quantitative Cardiac Proteomics Combining Electron Transfer Dissociation and the Metalloendopeptidase Lys-N with the SILAC Mouse. *Molecular & Cellular Proteomics* : MCP 10 (10), O111.008474. doi:10.1074/mcp.O111.008474
- Schuck, F., Wolf, D., Fellgiebel, A., Endres, K., 2016. Increase of alpha-Secretase ADAM10 in Platelets Along Cognitively Healthy Aging. *Journal of Alzheimer's Disease* 50 (3), 817-826. doi:10.3233/jad-150737
- Schumacher, K.N., Dodds, E.D., 2016. A case for protein-level and site-level specificity in glycoproteomic studies of disease. *Glycoconjugate Journal* 33 (3), 377-385. doi:10.1007/s10719-016-9663-5
- Schwarz, F., Aepli, M., 2011. Mechanisms and principles of N-linked protein glycosylation. *Current Opinion in Structural Biology* 21 (5), 576-582. doi:10.1016/j.sbi.2011.08.005
- Scott, D.W., Dunn, T.S., Ballestas, M.E., Litovsky, S.H., Patel, R.P., 2013. Identification of a high-mannose ICAM-1 glycoform: effects of ICAM-1 hypoglycosylation on monocyte adhesion and outside in signaling. *American Journal of Physiology: Cell Physiology* 305 (2), C228-237. doi:10.1152/ajpcell.00116.2013
- Segal, B.H., Leto, T.L., Gallin, J.I., Malech, H.L., Holland, S.M., 2000. Genetic, biochemical, and clinical features of chronic granulomatous disease. *Medicine (Baltimore)* 79 (3), 170-200.
- Sengelov, H., Kjeldsen, L., Borregaard, N., 1993a. Control of exocytosis in early neutrophil activation. *Journal of Immunology* 150 (4), 1535-1543.
- Sengelov, H., Kjeldsen, L., Diamond, M.S., Springer, T.A., Borregaard, N., 1993b. Subcellular localization and dynamics of Mac-1 (alpha m beta 2) in human neutrophils. *Journal of Clinical Investigation* 92 (3), 1467-1476. doi:10.1172/jci116724
- Sethi, M.K., Kim, H., Park, C.K., Baker, M.S., Paik, Y.K., Packer, N.H., Hancock, W.S., Fanayan, S., Thaysen-Andersen, M., 2015. In-depth N-glycome profiling of paired colorectal cancer and non-tumorigenic tissues reveals cancer-, stage- and EGFR-specific protein N-glycosylation. *Glycobiology* 25 (10), 1064-1078. doi:10.1093/glycob/cwv042

- Sethi, M.K., Thaysen-Andersen, M., Smith, J.T., Baker, M.S., Packer, N.H., Hancock, W.S., Fanayan, S., 2014. Comparative N-glycan profiling of colorectal cancer cell lines reveals unique bisecting GlcNAc and α -2,3-linked sialic acid determinants are associated with membrane proteins of the more metastatic/aggressive cell lines. *Journal of Proteome Research* 13 (1), 277-288. doi:10.1021/pr400861m
- Shade, K.T., Platzer, B., Washburn, N., Mani, V., Bartsch, Y.C., Conroy, M., Pagan, J.D., Bosques, C., Mempel, T.R., Fiebiger, E., Anthony, R.M., 2015. A single glycan on IgE is indispensable for initiation of anaphylaxis. *Journal of Experimental Medicine* 212 (4), 457-467. doi:10.1084/jem.20142182
- Shafer, W.M., Hubalek, F., Huang, M., Pohl, J., 1996. Bactericidal activity of a synthetic peptide (CG 117-136) of human lysosomal cathepsin G is dependent on arginine content. *Infection and Immunity* 64 (11), 4842-4845.
- Shafer, W.M., Pohl, J., Onunka, V.C., Bangalore, N., Travis, J., 1991. Human lysosomal cathepsin G and granzyme B share a functionally conserved broad spectrum antibacterial peptide. *Journal of Biological Chemistry* 266 (1), 112-116.
- Shah, P., Wang, X., Yang, W., Toghi Eshghi, S., Sun, S., Hoti, N., Chen, L., Yang, S., Pasay, J., Rubin, A., Zhang, H., 2015. Integrated Proteomic and Glycoproteomic Analyses of Prostate Cancer Cells Reveal Glycoprotein Alteration in Protein Abundance and Glycosylation. *Molecular & Cellular Proteomics* 14 (10), 2753-2763. doi:10.1074/mcp.M115.047928
- Shen, H., Kreisel, D., Goldstein, D.R., 2013. Processes of sterile inflammation. *Journal of Immunology* 191 (6), 2857-2863. doi:10.4049/jimmunol.1301539
- Shihao, C., Jenny, T., Vernon, N.R., Andrew, M.S., Harry, S., 2002. UDP-N-acetylglucosamine: α -3-d-mannoside β -1,2-N-acetylglucosaminyltransferase I and UDP-N-acetylglucosamine: α -6-d-mannoside β -1,2-N-acetylglucosaminyltransferase II in *Caenorhabditis elegans*. *Biochimica et Biophysica Acta (BBA) - General Subjects* 1573 (3), 271279. doi:10.1016/S0304-4165(02)00393-8
- Shin, Y.J., Castilho, A., Dicker, M., Sadio, F., Vavra, U., Grunwald-Gruber, C., Kwon, T.H., Altmann, F., Steinkellner, H., Strasser, R., 2016. Reduced paucimannosidic N-glycan

References

formation by suppression of a specific beta-hexosaminidase from *Nicotiana benthamiana*. *Plant Biotechnol J.* doi:10.1111/pbi.12602

Sica, A., Mantovani, A., 2012. Macrophage plasticity and polarization: in vivo veritas. *Journal of Clinical Investigation* 122 (3), 787-795. doi:10.1172/jci59643

Singh, C., Zampronio, C.G., Creese, A.J., Cooper, H.J., 2012. Higher energy collision dissociation (HCD) product ion-triggered electron transfer dissociation (ETD) mass spectrometry for the analysis of N-linked glycoproteins. *Journal of Proteome Research* 11 (9), 4517-4525. doi:10.1021/pr300257c

Sørensen, O., Arnljots, K., Cowland, J.B., Bainton, D.F., Borregaard, N., 1997. The human antibacterial cathelicidin, hCAP-18, is synthesized in myelocytes and metamyelocytes and localized to specific granules in neutrophils. *Blood* 90 (7), 2796-2803.

Sørensen, O.E., Borregaard, N., 2016. Neutrophil extracellular traps - the dark side of neutrophils. *Journal of Clinical Investigation* 126 (5), 1612-1620. doi:10.1172/JCI84538

Spagnou, S., Miller, A.D., Keller, M., 2004. Lipidic carriers of siRNA: differences in the formulation, cellular uptake, and delivery with plasmid DNA. *Biochemistry* 43 (42), 13348-13356. doi:10.1021/bi048950a

Sperandio, M., 2006. Selectins and glycosyltransferases in leukocyte rolling in vivo. *Febs j* 273 (19), 4377-4389. doi:10.1111/j.1742-4658.2006.05437.x

Stadlmann, J., Pabst, M., Kolarich, D., Kunert, R., Altmann, F., 2008. Analysis of immunoglobulin glycosylation by LC-ESI-MS of glycopeptides and oligosaccharides. *Proteomics* 8 (14), 2858-2871. doi:10.1002/pmic.200700968

Stanley, P., 2011. Golgi glycosylation. *Cold Spring Harbor Perspectives in Biology* 3 (4). doi:10.1101/cshperspect.a005199

Stanley, P., Schachter, H., Taniguchi, N., 2009. N-Glycans, in: Varki, A., Cummings, R.D., Esko, J.D., Freeze, H.H., Stanley, P., Bertozzi, C.R., Hart, G.W., Etzler, M.E. (Eds.), *Essentials of Glycobiology*, 2nd ed. Cold Spring Harbor (NY), New York, pp. 101-114.

- Stavenhagen, K., Hinneburg, H., Thaysen-Andersen, M., Hartmann, L., Varon Silva, D., Fuchser, J., Kaspar, S., Rapp, E., Seeberger, P.H., Kolarich, D., 2013. Quantitative mapping of glycoprotein micro-heterogeneity and macro-heterogeneity: an evaluation of mass spectrometry signal strengths using synthetic peptides and glycopeptides. *Journal of Mass Spectrometry* 48 (6), 627-639. doi:10.1002/jms.3210
- Stavenhagen, K., Kolarich, D., Wuhrer, M., 2015a. Clinical Glycomics Employing Graphitized Carbon Liquid Chromatography-Mass Spectrometry. *Chromatographia* 78 (5-6), 307-320. doi:10.1007/s10337-014-2813-7
- Stavenhagen, K., Plomp, R., Wuhrer, M., 2015b. Site-specific protein N- and O-glycosylation analysis by a C18-porous graphitized carbon-liquid chromatography-electrospray ionization mass spectrometry approach using pronase treated glycopeptides. *Analytical Chemistry*. doi:10.1021/acs.analchem.5b02366
- Stolfa, G., Mondal, N., Zhu, Y., Yu, X., Buffone, A., Jr., Neelamegham, S., 2016. Using CRISPR-Cas9 to quantify the contributions of O-glycans, N-glycans and Glycosphingolipids to human leukocyte-endothelium adhesion. *Scientific Reports* 6, 30392. doi:10.1038/srep30392
- Strasser, R., Bondili, J.S., Schoberer, J., Svoboda, B., Liebminger, E., Glossl, J., Altmann, F., Steinkellner, H., Mach, L., 2007. Enzymatic properties and subcellular localization of Arabidopsis beta-N-acetylhexosaminidases. *Plant Physiology* 145 (1), 5-16. doi:10.1104/pp.107.101162
- Struwe, W.B., Stuckmann, A., Behrens, A.J., Pagel, K., Crispin, M., 2017. Global N-Glycan Site Occupancy of HIV-1 gp120 by Metabolic Engineering and High-Resolution Intact Mass Spectrometry. *ACS Chemical Biology*. doi:10.1021/acschembio.6b00854
- Sugiyama, T., Kohara, H., Noda, M., Nagasawa, T., 2006. Maintenance of the hematopoietic stem cell pool by CXCL12-CXCR4 chemokine signaling in bone marrow stromal cell niches. *Immunity* 25 (6), 977-988. doi:10.1016/j.immuni.2006.10.016
- Sumer-Bayraktar, Z., Grant, O.C., Venkatakrishnan, V., Woods, R.J., Packer, N.H., Thaysen-Andersen, M., 2016. Asn347 glycosylation of corticosteroid-binding globulin fine-tunes the

References

host Immune response by modulating proteolysis by pseudomonas aeruginosa and neutrophil elastase. Journal of Biological Chemistry 291 (34), 17727-17742. doi:10.1074/jbc.M116.735258

Sumer-Bayraktar, Z., Kolarich, D., Campbell, M.P., Ali, S., Packer, N.H., Thaysen-Andersen, M., 2011. N-glycans modulate the function of human corticosteroid-binding globulin. Molecular & Cellular Proteomics : MCP 10 (8). doi:10.1074/mcp.M111.009100

Sumer-Bayraktar, Z., Nguyen-Khuong, T., Jayo, R., Chen, D.D., Ali, S., Packer, N.H., Thaysen-Andersen, M., 2012. Micro- and macroheterogeneity of N-glycosylation yields size and charge isoforms of human sex hormone binding globulin circulating in serum. Proteomics 12 (22), 3315-3327. doi:10.1002/pmic.201200354

Suzuki, J., Maruyama, S., Tamauchi, H., Kuwahara, M., Horiuchi, M., Mizuki, M., Ochi, M., Sawasaki, T., Zhu, J., Yasukawa, M., Yamashita, M., 2016. Gfi1, a transcriptional repressor, inhibits the induction of the T helper type 1 programme in activated CD4 T cells. Immunology 147 (4), 476-487. doi:10.1111/imm.12580

Suzuki, T., 2016. Catabolism of N-glycoproteins in mammalian cells: Molecular mechanisms and genetic disorders related to the processes. Molecular Aspects of Medicine. doi:10.1016/j.mam.2016.05.004

Swamydas, M., Gao, J.L., Break, T.J., Johnson, M.D., Jaeger, M., Rodriguez, C.A., Lim, J.K., Green, N.M., Collar, A.L., Fischer, B.G., Lee, C.C., Perfect, J.R., Alexander, B.D., Kullberg, B.J., Netea, M.G., Murphy, P.M., Lionakis, M.S., 2016. CXCR1-mediated neutrophil degranulation and fungal killing promote Candida clearance and host survival. Science Translational Medicine 8 (322), 322ra310. doi:10.1126/scitranslmed.aac7718

Tadashi, S., Keiichi, Y., Seiji, S., Ken, K., William, J.L., Sadako, I., Yasuo, I., Yasufumi, E., 2002. Endo- β -N-acetylglucosaminidase, an enzyme involved in processing of free oligosaccharides in the cytosol. Proceedings of the National Academy of Sciences 99 (15), 9691-9696. doi:10.1073/pnas.152333599

Taheri, N., Fahlgren, A., Fallman, M., 2016. Yersinia pseudotuberculosis blocks neutrophil degranulation. Infection and Immunity. doi:10.1128/IAI.00760-16

- Tan, B.H., Meinken, C., Bastian, M., Bruns, H., Legaspi, A., Ochoa, M.T., Krutzik, S.R., Bloom, B.R., Ganz, T., Modlin, R.L., Stenger, S., 2006. Macrophages Acquire Neutrophil Granules for Antimicrobial Activity against Intracellular Pathogens. *The Journal of Immunology* 177 (3), 1864-1871. doi:10.4049/jimmunol.177.3.1864
- Tapper, H., Furuya, W., Grinstein, S., 2002. Localized Exocytosis of Primary (Lysosomal) Granules During Phagocytosis: Role of Ca^{2+} -Dependent Tyrosine Phosphorylation and Microtubules. *The Journal of Immunology* 168 (10), 5287-5296. doi:10.4049/jimmunol.168.10.5287
- Tay, J., Levesque, J.P., Winkler, I.G., 2016. Cellular players of hematopoietic stem cell mobilization in the bone marrow niche. *International Journal of Hematology*. doi:10.1007/s12185-016-2162-4
- Thaysen-Andersen, M., Chertova, E., Bergamaschi, C., Moh, E.S., Chertov, O., Roser, J., Sowder, R., Bear, J., Lifson, J., Packer, N.H., Felber, B.K., Pavlakis, G.N., 2015. Recombinant human heterodimeric IL-15 complex displays extensive and reproducible N- and O-linked glycosylation. *Glycoconjugate Journal*. doi:10.1007/s10719-015-9627-1
- Thaysen-Andersen, M., Engholm-Keller, K., Roepstorff, P., 2011. Analysis of Protein Glycosylation and Phosphorylation Using HILIC-MS, Hydrophilic Interaction Liquid Chromatography (HILIC) and Advanced Applications. CRC Press, pp. 551-576.
- Thaysen-Andersen, M., Mysling, S., Hojrup, P., 2009. Site-specific glycoproteomics of N-linked glycopeptides using MALDI-TOF MS: strong correlation between signal strength and glycoform quantities. *Analytical Chemistry* 81 (10), 3933-3943. doi:10.1021/ac900231w
- Thaysen-Andersen, M., Packer, N.H., 2012. Site-specific glycoproteomics confirms that protein structure dictates formation of N-glycan type, core fucosylation and branching. *Glycobiology* 22 (11), 1440-1452. doi:10.1093/glycob/cws110
- Thaysen-Andersen, M., Packer, N.H., 2014. Advances in LC-MS/MS-based glycoproteomics: getting closer to system-wide site-specific mapping of the N- and O-glycoproteome. *Biochimica et Biophysica Acta* 1844 (9), 1437-1452. doi:10.1016/j.bbapap.2014.05.002

References

- Thaysen-Andersen, M., Packer, N.H., Schulz, B.L., 2016. Maturing glycoproteomics technologies provide unique structural insights into the N-glycoproteome and its regulation in health and disease. *Molecular & Cellular Proteomics*. doi:10.1074/mcp.O115.057638
- Theilgaard-Monch, K., Jacobsen, L.C., Borup, R., Rasmussen, T., Bjerregaard, M.D., Nielsen, F.C., Cowland, J.B., Borregaard, N., 2005. The transcriptional program of terminal granulocytic differentiation. *Blood* 105 (4), 1785-1796. doi:10.1182/blood-2004-08-3346
- Tidwell, T., Wechsler, J., Nayak, R.C., Trump, L., Salipante, S.J., Cheng, J.C., Donadieu, J., Glaubach, T., Corey, S.J., Grimes, H.L., Lutzko, C., Cancelas, J.A., Horwitz, M.S., 2014. Neutropenia-associated ELANE mutations disrupting translation initiation produce novel neutrophil elastase isoforms. *Blood* 123 (4), 562-569. doi:10.1182/blood-2013-07-513242
- Tracy, R.P., 2006. The five cardinal signs of inflammation: Calor, Dolor, Rubor, Tumor ... and Penuria (Apologies to Aulus Cornelius Celsus, *De medicina*, c. A.D. 25). *Journals of Gerontology. Series A: Biological Sciences and Medical Sciences* 61 (10), 1051-1052.
- Tretter, V., Altmann, F., Marz, L., 1991. Peptide-N4-(N-acetyl-beta-glucosaminyl)asparagine amidase F cannot release glycans with fucose attached alpha 1----3 to the asparagine-linked N-acetylglucosamine residue. *European Journal of Biochemistry* 199 (3), 647-652.
- Trimble, R.B., Tarentino, A.L., 1991. Identification of distinct endoglycosidase (endo) activities in *Flavobacterium meningosepticum*: endo F1, endo F2, and endo F3. Endo F1 and endo H hydrolyze only high mannose and hybrid glycans. *Journal of Biological Chemistry* 266 (3), 1646-1651.
- Trinidad, J.C., Schoepfer, R., Burlingame, A.L., Medzihradszky, K.F., 2013. N- and O-glycosylation in the murine synaptosome. *Molecular & Cellular Proteomics : MCP* 12 (12), 3474-3488. doi:10.1074/mcp.M113.030007
- Tropak, M.B., Reid, S.P., Guiral, M., Withers, S.G., Mahuran, D., 2004. Pharmacological enhancement of beta-hexosaminidase activity in fibroblasts from adult Tay-Sachs and Sandhoff Patients. *Journal of Biological Chemistry* 279 (14), 13478-13487. doi:10.1074/jbc.M308523200

- Tsai, Y.F., Hwang, T.L., 2015. Neutrophil elastase inhibitors: a patent review and potential applications for inflammatory lung diseases (2010 - 2014). *Expert Opinion on Therapeutic Patents* 25 (10), 1145-1158. doi:10.1517/13543776.2015.1061998
- Van den Steen, P., Rudd, P.M., Dwek, R.A., Opdenakker, G., 1998. Concepts and principles of O-linked glycosylation. *Critical Reviews in Biochemistry and Molecular Biology* 33 (3), 151-208. doi:10.1080/10409239891204198
- van der Meer, J.W., Joosten, L.A., Riksen, N., Netea, M.G., 2015. Trained immunity: A smart way to enhance innate immune defence. *Molecular Immunology* 68 (1), 40-44. doi:10.1016/j.molimm.2015.06.019
- van Heeckeren, A.M., Schluchter, M.D., Drumm, M.L., Davis, P.B., 2004. Role of Cfr genotype in the response to chronic *Pseudomonas aeruginosa* lung infection in mice. *American Journal of Physiology: Lung Cellular and Molecular Physiology* 287 (5), L944-952. doi:10.1152/ajplung.00387.2003
- van Remoortere, A., Bank, C.M., Nyame, A.K., Cummings, R.D., Deelder, A.M., van Die, I., 2003. *Schistosoma mansoni*-infected mice produce antibodies that cross-react with plant, insect, and mammalian glycoproteins and recognize the truncated biantennary n-glycan Man3GlcNAc2-R. *Glycobiology* 13 (3), 217-225. doi:10.1093/glycob/cwg025
- Varki, A., 1998. Factors controlling the glycosylation potential of the Golgi apparatus. *Trends in Cell Biology* 8 (1), 34-40.
- Varki, A., 2017. Biological roles of glycans. *Glycobiology* 27 (1), 3-49. doi:10.1093/glycob/cww086
- Varki, A., Cummings, R.D., Aebi, M., Packer, N.H., Seeberger, P.H., Esko, J.D., Stanley, P., Hart, G., Darvill, A., Kinoshita, T., Prestegard, J.J., Schnaar, R.L., Freeze, H.H., Marth, J.D., Bertozzi, C.R., Etzler, M.E., Frank, M., Vliegenthart, J.F., Lutteke, T., Perez, S., Bolton, E., Rudd, P., Paulson, J., Kanehisa, M., Toukach, P., Aoki-Kinoshita, K.F., Dell, A., Narimatsu, H., York, W., Taniguchi, N., Kornfeld, S., 2015. Symbol nomenclature for graphical representations of glycans. *Glycobiology* 25 (12), 1323-1324. doi:10.1093/glycob/cwv091

References

Varki, A., Etzler, M.E., Cummings, R.D., Esko, J.D., 2009a. Discovery and Classification of Glycan-Binding Proteins, in: Varki, A., Cummings, R.D., Esko, J.D., Freeze, H.H., Stanley, P., Bertozzi, C.R., Hart, G.W., Etzler, M.E. (Eds.), *Essentials of Glycobiology*, 2nd ed, Cold Spring Harbor (NY).

Varki, A., Freeze, H.H., Vacquier, V.D., 2009b. Glycans in Development and Systemic Physiology, in: Varki, A., Cummings, R.D., Esko, J.D., Freeze, H.H., Stanley, P., Bertozzi, C.R., Hart, G.W., Etzler, M.E. (Eds.), *Essentials of Glycobiology*, second ed. Cold Spring Harbor, New York, pp. 531-536.

Varki, A., Sharon, N., 2009. Historical Background and Overview, in: Varki, A., Cummings, R.D., Esko, J.D., Freeze, H.H., Stanley, P., Bertozzi, C.R., Hart, G.W., Etzler, M.E. (Eds.), *Essentials of Glycobiology*, second ed. Cold Spring Harbor, New York, pp. 1-22.

Venkatakrishnan, V., Thaysen-Andersen, M., Chen, S.C., Nevalainen, H., Packer, N.H., 2015. Cystic fibrosis and bacterial colonization define the sputum N-glycosylation phenotype. *Glycobiology* 25 (1), 88-100. doi:10.1093/glycob/cwu092

Vitale, A., Chrispeels, M.J., 1984. Transient N-acetylglucosamine in the biosynthesis of phytohemagglutinin: attachment in the Golgi apparatus and removal in protein bodies. *Journal of Cell Biology* 99 (1 Pt 1), 133-140. PMC2275646

Vreeker, G.C., Wührer, M., 2017. Reversed-phase separation methods for glycan analysis. *Analytical and Bioanalytical Chemistry* 409 (2), 359-378. doi:10.1007/s00216-016-0073-0

Wang, Z., Udeshi, N.D., Slawson, C., Compton, P.D., Sakabe, K., Cheung, W.D., Shabanowitz, J., Hunt, D.F., Hart, G.W., 2010. Extensive crosstalk between O-GlcNAcylation and phosphorylation regulates cytokinesis. *Sci Signal* 3 (104), ra2. doi:10.1126/scisignal.2000526

Warren, L., Fuhrer, J.P., Buck, C.A., 1972. Surface glycoproteins of normal and transformed cells: a difference determined by sialic acid and a growth-dependent sialyl transferase. *Proceedings of the National Academy of Sciences of the United States of America* 69 (7), 1838-1842. PMC426814

- Watorek, W., Halbeek, H., Travis, J., 1993. The isoforms of human neutrophil elastase and cathepsin G differ in their carbohydrate side chain structures. *Bio Chem Hoppe Seyler* 374 (6), 385-393.
- Weerapana, E., Imperiali, B., 2006. Asparagine-linked protein glycosylation: from eukaryotic to prokaryotic systems. *Glycobiology* 16 (6), 91r-101r. doi:10.1093/glycob/cwj099
- Weis, W.I., Drickamer, K., 1996. Structural basis of lectin-carbohydrate recognition. *Annual Review of Biochemistry* 65, 441-473. doi:10.1146/annurev.bi.65.070196.002301
- Wen, T., Rothenberg, M.E., 2016. The Regulatory Function of Eosinophils. *Microbiol Spectr* 4 (5). doi:10.1128/microbiolspec.MCHD-0020-2015
- Wendeler, M., Sandhoff, K., 2009. Hexosaminidase assays. *Glycoconjugate Journal* 26 (8), 945-952. doi:10.1007/s10719-008-9137-5
- Wengner, A.M., Pitchford, S.C., Furze, R.C., Rankin, S.M., 2008. The coordinated action of G-CSF and ELR + CXC chemokines in neutrophil mobilization during acute inflammation. *Blood* 111 (1), 42-49. doi:10.1182/blood-2007-07-099648
- Winchester, B., 2005. Lysosomal metabolism of glycoproteins. *Glycobiology* 15 (6), 1R-15R. doi:10.1093/glycob/cwi041
- Wuhrer, M., Catalina, M.I., Deelder, A.M., Hokke, C.H., 2007. Glycoproteomics based on tandem mass spectrometry of glycopeptides. *Journal of Chromatography. B: Analytical Technologies in the Biomedical and Life Sciences* 849 (1-2), 115-128. doi:10.1016/j.jchromb.2006.09.041
- Wuhrer, M., de Boer, A.R., Deelder, A.M., 2009. Structural glycomics using hydrophilic interaction chromatography (HILIC) with mass spectrometry. *Mass Spectrometry Reviews* 28 (2), 192-206. doi:10.1002/mas.20195
- Wuhrer, M., Deelder, A.M., Hokke, C.H., 2005. Protein glycosylation analysis by liquid chromatography-mass spectrometry. *Journal of Chromatography. B: Analytical Technologies in the Biomedical and Life Sciences* 825 (2), 124-133. doi:10.1016/j.jchromb.2005.01.030

References

- Yagi, H., Saito, T., Yanagisawa, M., Yu, R.K., Kato, K., 2012. Lewis X-carrying N-glycans regulate the proliferation of mouse embryonic neural stem cells via the Notch signaling pathway. *Journal of Biological Chemistry* 287 (29), 24356-24364. doi:10.1074/jbc.M112.365643
- Yang, J., Goetz, D., Li, J.Y., Wang, W., Mori, K., Setlik, D., Du, T., Erdjument-Bromage, H., Tempst, P., Strong, R., Barasch, J., 2002. An iron delivery pathway mediated by a lipocalin. *Molecular Cell* 10 (5), 1045-1056.
- Yang, Y., Barendregt, A., Kamerling, J.P., Heck, A.J., 2013. Analyzing protein micro-heterogeneity in chicken ovalbumin by high-resolution native mass spectrometry exposes qualitatively and semi-quantitatively 59 proteoforms. *Analytical Chemistry* 85 (24), 12037-12045. doi:10.1021/ac403057y
- Yang, Y., Franc, V., Heck, A.J.R., 2017. Glycoproteomics: A Balance between High-Throughput and In-Depth Analysis. *Trends in Biotechnology*. doi:10.1016/j.tibtech.2017.04.010
- Yatim, K.M., Lakkis, F.G., 2015. A brief journey through the immune system. *Clinical Journal of the American Society of Nephrology* 10 (7), 1274-1281. doi:10.2215/cjn.10031014
- Yousefi, S., Simon, H.-U., 2016. NETosis – Does It Really Represent Nature’s “Suicide Bomber”? *Frontiers in Immunology* 7. doi:10.3389/fimmu.2016.00328
- Yu, C.-Y., Mayampurath, A., Zhu, R., Zacharias, L., Song, E., Wang, L., Mechref, Y., Tang, H., 2016. Automated Glycan Sequencing from Tandem Mass Spectra of N-Linked Glycopeptides. *Analytical Chemistry* 88 (11), 5725-5732. doi:10.1021/acs.analchem.5b04858
- Yu, V.W., Scadden, D.T., 2016. Heterogeneity of the bone marrow niche. *Current Opinion in Hematology* 23 (4), 331-338. doi:10.1097/moh.0000000000000265
- Yuen, J., Pluthero, F.G., Douda, D.N., Riedl, M., Cherry, A., Ulanova, M., Kahr, W.H.A., Palaniyar, N., Licht, C., 2016. NETosing Neutrophils Activate Complement Both on Their Own NETs and Bacteria via Alternative and Non-alternative Pathways. *Frontiers in Immunology* 7. doi:10.3389/fimmu.2016.00137

- Zacchi, L.F., Schulz, B.L., 2015. N-glycoprotein macroheterogeneity: biological implications and proteomic characterization. *Glycoconjugate Journal*. doi:10.1007/s10719-015-9641-3
- Zawrotniak, M., Rapala-Kozik, M., 2013. Neutrophil extracellular traps (NETs) - formation and implications. *Acta Biochimica Polonica* 60 (3), 277-284.
- Zhang, W., Cao, P., Chen, S., Spence, A.M., Zhu, S., Staudacher, E., Schachter, H., 2003. Synthesis of paucimannose N-glycans by *Caenorhabditis elegans* requires prior actions of UDP-N-acetyl-D-glucosamine:alpha-3-D-mannoside beta1,2-N-acetylglucosaminyltransferase I, alpha3,6-mannosidase II and a specific membrane-bound beta-N-acetylglucosaminidase. *Biochemical Journal* 372 (Pt 1), 53-64. doi:10.1042/BJ20021931
- Zhou, L., Somasundaram, R., Nederhof, R.F., Dijkstra, G., Faber, K.N., Peppelenbosch, M.P., Fuhler, G.M., 2012. Impact of Human Granulocyte and Monocyte Isolation Procedures on Functional Studies. *Clinical and Vaccine Immunology : CVI* 19 (7), 1065-1074. doi:10.1128/CVI.05715-11
- Zhu, Z., Desaire, H., 2015. Carbohydrates on Proteins: Site-Specific Glycosylation Analysis by Mass Spectrometry. *Annual Review of Analytical Chemistry (Palo Alto, Calif.)* 8, 463-483. doi:10.1146/annurev-anchem-071114-040240
- Ziegler, A., Zaia, J., 2006. Size-exclusion chromatography of heparin oligosaccharides at high and low pressure. *Journal of Chromatography. B: Analytical Technologies in the Biomedical and Life Sciences* 837 (1-2), 76-86. doi:10.1016/j.jchromb.2006.04.013
- Zinchuk, V., Wu, Y., Grossenbacher-Zinchuk, O., 2013. Bridging the gap between qualitative and quantitative colocalization results in fluorescence microscopy studies. *Scientific Reports* 3, 1365. doi:10.1038/srep01365
- Zinchuk, V., Zinchuk, O., Okada, T., 2007. Quantitative colocalization analysis of multicolor confocal immunofluorescence microscopy images: pushing pixels to explore biological phenomena. *Acta Histochem Cytochem* 40 (4), 101-111. doi:10.1267/ahc.07002

References

Zipser, B., Bello-DeOcampo, D., Diestel, S., Tai, M.H., Schmitz, B., 2012. Mannitou monoclonal antibody uniquely recognizes paucimannose, a marker for human cancer, stemness, and inflammation. *Journal of Carbohydrate Chemistry* 31 (4-6), 504-518. doi:10.1080/07328303.2012.661112

Zoega, M., Ravnsborg, T., Hojrup, P., Houen, G., Schou, C., 2012. Proteinase 3 carries small unusual carbohydrates and associates with alpha-defensins. *Journal of Proteomics* 75 (5), 1472-1485. doi:10.1016/j.jprot.2011.11.019

Appendices

Appendix 1: Human ethics approvals

Office of the Deputy Vice-Chancellor
(Research)

Research Office
Research Hub, Building C5C East
Macquarie University
NSW 2109 Australia
T: +61 (2) 9850 4459
<http://www.research.mq.edu.au/>
ABN 90 952 801 237



10 June 2015

Dr Morten Andersen
Macquarie University NSW 2109

Dear Dr Andersen,

Reference No: 5201500409

Title: *White blood cell differentiation and activation markers: Their relationship to diabetic complications*

Thank you for submitting the above application for ethical and scientific review. Your application was considered by the Macquarie University Human Research Ethics Committee (HREC (Medical Sciences)) at its meeting on 28 May 2015, at which further information was requested to be reviewed by the Ethics Secretariat.

The requested information was received with correspondence on 5 June 2015.

I am pleased to advise that ethical and scientific approval has been granted for this project to be conducted at:

- Macquarie University

This research meets the requirements set out in the *National Statement on Ethical Conduct in Human Research* (2007 – Updated March 2014) (the *National Statement*).

This letter constitutes ethical and scientific approval only.

Standard Conditions of Approval:

1. Continuing compliance with the requirements of the *National Statement*, which is available at the following website:

<http://www.nhmrc.gov.au/book/national-statement-ethical-conduct-human-research>

2. This approval is valid for five (5) years, subject to the submission of annual reports. Please submit your reports on the anniversary of the approval for this protocol.

3. All adverse events, including events which might affect the continued ethical and scientific acceptability of the project, must be reported to the HREC within 72 hours.

4. Proposed changes to the protocol must be submitted to the Committee for approval before implementation.

It is the responsibility of the Chief investigator to retain a copy of all documentation related to this project and to forward a copy of this approval letter to all personnel listed on the project.

Should you have any queries regarding your project, please contact the Ethics Secretariat on 9850 4194 or by email ethics.secretariat@mq.edu.au

The HREC (Medical Sciences) Terms of Reference and Standard Operating Procedures are available from the Research Office website at:

http://www.research.mq.edu.au/for/researchers/how_to_obtain_ethics_approval/human_research_ethics

The HREC (Medical Sciences) wishes you every success in your research.

Yours sincerely

Professor Tony Eyers

Chair, Macquarie University Human Research Ethics Committee (Medical Sciences)

This HREC is constituted and operates in accordance with the National Health and Medical Research Council's (NHMRC) *National Statement on Ethical Conduct in Human Research* (2007) and the *CPMP/ICH Note for Guidance on Good Clinical Practice*.

Details of this approval are as follows:

Approval Date: 10 June 2015

The following documentation has been reviewed and approved by the HREC (Medical Sciences):

| Documents reviewed | Version no. | Date |
|---|-------------|-------------------------|
| Macquarie University Prior Review Form (PREF) | 1 | Submitted 30/04/2015 |
| NSW Health Ethics Application Form | 6 | September 2011 |
| RPAH Zone HREC Ethics Approval Letter | | 08/05/2014 |
| Amendment Request to RPAH Zone HREC – Request to Add Personnel | | 24/05/2014 |
| Amendment Approval Letter from RPAH Zone HREC | | 15/07/2014 |
| Correspondence from Dr Andersen responding to the issues raised by the HREC (Medical Sciences) | | Received 05/06/2015 |
| Participant Information and Consent Form (PICF) | 2 | 04/06/2015 |

ADDRESS FOR ALL CORRESPONDENCE
RESEARCH DEVELOPMENT OFFICE
ROYAL PRINCE ALFRED HOSPITAL
CAMPERDOWN NSW 2050



Health
Sydney
Local Health District

TELEPHONE: (02) 9515 6766
FACSIMILE: (02) 9515 7176
EMAIL: lesley.townsend@sswahs.nsw.gov.au
REFERENCE: X14-0074 (Prev X08-0255) & HREC/08/RPAH/431
9.55/JUN14

15 July 2014

A/Professor S McLennan
Department of Endocrinology
Room 361
Blackburn Building, D06
UNIVERSITY OF SYDNEY NSW 2006

Dear Professor McLennan,

Re: Protocol No X14-0074 (Prev X08-0255) & HREC/08/RPAH/431 - "White blood cell differentiation and activation markers: Their relationship to diabetic complications"

The Executive of the Ethics Review Committee, at its meeting of 26 June 2014 considered your correspondence of 24 May 2014 and gave its approval of the following:

- Use of Mass Spectrometry to study the diabetes related changes in plasma and in monocytes and neutrophils isolated from the blood
- Inclusion of Dr M Andersen and Professor N Packer, supervising Mr L Lee and Mr I Loke to perform the Mass Spectrometry studies at the Macquarie University

Yours sincerely,

Lesley Townsend
Executive Officer
Ethics Review Committee (RPAH Zone)



HERC\EXECOR\14-07

Sydney Local Health District
ABN 17 520 269 052
www.slhd.nsw.gov.au

Appendix 2: Biosafety approvals



| Section A | | Biohazard Risk Assessment Form – GMO | |
|--|--|--|---|
| | | Notification Number: 5201500813 Approved 26/10/2015 Exp 26/10/2020 | |
| Department | Chemistry and Biomolecular Sciences | Date: | October 1, 2015 |
| Chief investigator: | Dr Morten Thaysen Andersen | | |
| Contact number/email: | 9850 7487 | | |
| Title of research/practical | Exploring Carbohydrate Enzyme Deficiency and Altered Protein Glycosylation in Disease Mechanisms of Tay Sachs and Sandhoff Disease | | |
| Is additional approval required? | <input type="checkbox"/> Animal Ethics | <input type="checkbox"/> Human Ethics | <input type="checkbox"/> Fieldwork Manager <input checked="" type="checkbox"/> Other (please state) <u>Biosafety IBC – Exempt Dealings</u> |
| Exact location(s) of research: | | | |
| E8C 323 PC2 cell culture laboratory, E8A 220/222 PC2 laboratory, F10A Level 1 Hub 2 and Hub 3 PC2 laboratory, E8A 109 PC2/QC2 laboratory, E8C 320 PC1 laboratory, E8C 326 BMD PC1 laboratory | | | |
| Control measures: E.g. Eliminate by irradiation prior to use, isolation by class II biological safety cabinets, administration by following SWP as below, PPE as listed below. | | | |
| <input type="checkbox"/> Eliminate risk | <input type="checkbox"/> Substitute the hazard | <input checked="" type="checkbox"/> Isolate the hazard | <input checked="" type="checkbox"/> Implement engineering controls <input checked="" type="checkbox"/> Administration (e.g. SWP/Training) <input checked="" type="checkbox"/> PPE |
| Isolation by class II biological safety cabinets Training by experienced personnel, laboratory induction and safe laboratory practice training conducted by experienced and authorised personnel Following good safe operating procedures, good microbiology practices and current biological waste disposal practices Wearing appropriate PPE in accordance to safe operating procedures | | | |
| Supporting documents which must be read in conjunction with this assessment. (e.g. Safe Working Procedures, Safety Data Sheets, Guidelines/Protocols) | | | |
| Safe working procedures: 1) Working with potential human pathogens and known human pathogens in PC2 laboratory 2) Safety Data Sheets | | | |
| What is the type of the biological material? | | | |
| <input checked="" type="checkbox"/> Bacteria | <input type="checkbox"/> Fungus | <input type="checkbox"/> Virus | <input checked="" type="checkbox"/> Cell Line <input type="checkbox"/> Tissue <input type="checkbox"/> Parasite |

| | | | |
|---|--|-----------------------------------|-------------|
| SECTION A | | | |
|  MACQUARIE UNIVERSITY |  Biohazard Risk Assessment Form – NON GMO | Notification Number: NIP041214BHA | |
| Department | Chemistry and Biomolecular Sciences | Date: | 04 Dec 2014 |
| Chief investigator: | Professor Nicolle Packer | | |
| Contact number/email: | 9850 8176 / nicki.packer@mq.edu.au | | |
| Title of research/practical | A study of glycosylation and its changes in healthy and diseased cells and in bacteria and fungi | | |
| Is additional approval required? | Animal Ethics <input checked="" type="checkbox"/> Human Ethics <input checked="" type="checkbox"/> Fieldwork Manager <input type="checkbox"/> Other <input type="checkbox"/> (state) _____ | | |
| Exact location(s) of research: | | | |
| E8A 109 PC2/QC2 laboratory, E8C 320 laboratory, E8C 323 APAF PC2 cell culture laboratory, E8C 326 BMD laboratory, ASAM Level 1 PC2 laboratory, E8C 252 PC2 laboratory (due to complete in February 2015) | | | |
| Control measures: Eliminate risk <input type="checkbox"/> Substitute the hazard <input type="checkbox"/> Isolate the hazard <input checked="" type="checkbox"/> Implement engineering controls <input checked="" type="checkbox"/> Administration <input checked="" type="checkbox"/> (e.g. Training) PPE <input checked="" type="checkbox"/> E.g. Eliminate by irradiation prior to use, isolation by class II biological safety cabinets, administration by following SWP as below, PPE as listed below. | | | |
| Isolation by class II biological safety cabinets Training by experienced personnel, laboratory induction and safe laboratory practice training conducted by experienced and authorised personnel Following good safe operating procedures, good microbiology practices and current biological waste disposal practices Wearing appropriate PPE in accordance to safe operating procedures | | | |
| Supporting documents which must be read in conjunction with this assessment. (e.g. Safe Working Procedures, Safety Data Sheets, Guidelines/Protocols) | | | |
| Safe working procedures: 1) Working with potential human pathogens and known human pathogens in PC2 laboratory 2) Working with peripheral blood in PC2 laboratory Safe work procedure risk assessment: 1) Working with peripheral blood in PC2 laboratory | | | |
| What is the type of the biological material? | | | |
| Bacteria <input checked="" type="checkbox"/> Fungi <input checked="" type="checkbox"/> Virus <input type="checkbox"/> Cell Line <input checked="" type="checkbox"/> Tissue <input checked="" type="checkbox"/> Parasite <input type="checkbox"/> Animal <input type="checkbox"/> Plant <input type="checkbox"/> Soil <input type="checkbox"/> Toxin <input type="checkbox"/> Prions <input type="checkbox"/> Nucleic Acid <input type="checkbox"/> other <input checked="" type="checkbox"/> Peripheral blood cells | | | |
| What is the name of the biological agent? | | | |
| ATCC cell lines Tissue samples from melanoma patients. liver disease patients and tumour samples from patients | | | |

1/28/2017

Macquarie University Student Email and Calendar Mail - 2014 Biosafety Workshop Attendance



MACQUARIE
University

IAN LOKE <ian.loke@students.mq.edu.au>

2014 Biosafety Workshop Attendance

Bio Safety <biosafety@mq.edu.au>
To: IAN LOKE <ian.loke@students.mq.edu.au>

Tue, Aug 16, 2016 at 3:00 PM

Dear Ian,

Thank you for completing the 2014 Macquarie University Institutional Biosafety Workshop. It was noted by the Secretariat that attendance certificates were not distributed that year, however our records do show that you did attend the 2014 Biosafety Workshop.

Biosafety Workshops are required to be repeated every three years.

Please do not hesitate to contact me should you require any further information.

Kind Regards,

Liette